



# Comprehensive Hydrological Study of the Lee County Southeastern Density Reduction / Groundwater Resource (DR/GR) Area

Final Report of the MIKE SHE Model Development and Results



Lee County – Division of Natural Resources  
Ft. Myers, FL 33901

## MIKE SHE

dynamic modelling system for integrated groundwater and surface water resources



September 2009



**Comprehensive Hydrological Study of  
the Lee County Southeastern Density  
Reduction / Groundwater Resource  
(DR/GR) Area.  
Final Report of the MIKE SHE Model  
Development and Results**

100 Second Ave. South,  
Suite 302 North  
Saint Petersburg, FL 33701

Tel: (813) 831-4700  
Fax: (813) 831-4774  
e-mail: [thz@dhi.us](mailto:thz@dhi.us)  
Web: [www.dhi.us](http://www.dhi.us)

|   |   |
|---|---|
| Client<br><br>Dover Kohl and Associates on behalf of Lee County | Client's representative<br><br>Jason King |
|---|---|

|   |             |   |         |          |      |
|---|-------------|---|---------|----------|------|
| Project<br><br>Lee County DR/GR Model Study                                 |             | Project No<br><br>4021.604  |         |          |      |
| Authors<br><br>Marcelo Lago, PhD<br>Kevin Vought, PE<br>Tim Hazlett, PhD    |             | Date<br><br>September 10, 2009  |         |          |      |
|   |             | Approved by<br><br>Tim Hazlett, PhD   |         |          |      |
|   |             |   |         |          |      |
|   |             |   |         |          |      |
|   |             |   |         |          |      |
| Revision  | Description | By  | Checked | Approved | Date |
| Key words<br><br>Lee County<br>Water Resources<br>DR/GR<br>Land use changes |             | Classification<br><br><input type="checkbox"/> Open<br><br><input type="checkbox"/> Internal<br><br><input checked="" type="checkbox"/> Proprietary |         |          |      |

|                                      |              |
|--------------------------------------|--------------|
| Distribution<br><br>Client<br>DHI US | No of copies |
|                                      |              |



© DHI Water and Environment, Inc. 2009

The information contained in this document produced by DHI Water and Environment, Inc. is solely for the use of the Client identified on the cover sheet for the purpose for which it has been prepared and DHI Water and Environment, Inc. undertakes no duty to or accepts any responsibility to any third party who may rely upon this document.

All rights reserved. No section or element of this document may be removed from this document, reproduced, electronically stored or transmitted in any form without the written permission of DHI Water and Environment, Inc.

All hard copies of this document are "UNCONTROLLED DOCUMENTS". The "CONTROLLED" document is held by DHI Water and Environment, Inc.



## Table of Contents

|   |    |
|---|----|
| ACRONYMS AND ABBREVIATIONS .....                | 3  |
| LIST OF TABLES .....                            | 4  |
| LIST OF FIGURES.....                            | 5  |
| EXECUTIVE SUMMARY .....                         | 9  |
| INTRODUCTION.....                               | 14 |
| OBJECTIVES .....                                | 15 |
| EXISTING CONDITIONS MODEL.....                  | 15 |
| Baseline Model .....                            | 16 |
| Local Scale Model .....                         | 20 |
| Climate Data .....                              | 21 |
| Rainfall .....                                  | 21 |
| Evapotranspiration .....                        | 23 |
| Topography.....                                 | 28 |
| Refined Model Topography For LS ECM .....       | 30 |
| Land Use.....                                   | 32 |
| Soils .....                                     | 36 |
| Hydrogeology .....                              | 38 |
| Saturated Zone Model .....                      | 39 |
| Groundwater Boundaries .....                    | 41 |
| Groundwater Withdrawals .....                   | 43 |
| Irrigation .....                                | 45 |
| Agricultural Irrigation .....                   | 47 |
| Urban Irrigation.....                           | 47 |
| Surface Water Model.....                        | 52 |
| ECM Development .....                           | 52 |
| LS ECM Development.....                         | 62 |
| Model Calibration.....                          | 71 |
| Model Improvements .....                        | 71 |
| Water Table Level in Mining Pits.....           | 74 |
| Model Performance at Observation Stations ..... | 75 |
| Water Table Elevation .....                     | 77 |
| Hydroperiod .....                               | 85 |



|   |            |
|---|------------|
| Water Budgets.....  | 89         |
| Surface Water Flow .....  | 93         |
| <b>LAND USE SCENARIOS .....</b>                                       | <b>97</b>  |
| Development of Future Land Use Alternatives .....                     | 97         |
| Initial Conditions.....   | 98         |
| Results .....   | 98         |
| Water Table Plots.....  | 99         |
| Water Table Maps .....  | 112        |
| Hydroperiod Maps .....  | 126        |
| Water Budgets.....  | 138        |
| Surface Water Flows.....  | 149        |
| <b>CONCLUSIONS.....</b>   | <b>151</b> |
| General Findings.....   | 151        |
| Recommendations for the Planning Process.....                         | 152        |
| Model Limitations and Recommended Future Work.....                    | 154        |
| <b>REFERENCES.....</b>  | <b>156</b> |
| <b>APPENDIX A. HYDRAULIC CONDUCTIVITY MAPS.....</b>                   | <b>A1</b>  |
| <b>APPENDIX B. ECM RESULTS AT OBSERVATION STATIONS.....</b>           | <b>B1</b>  |
| <b>APPENDIX C. LS ECM V1 RESULTS AT OBSERVATION STATIONS.....</b>     | <b>C1</b>  |
| <b>APPENDIX D. LAND-USE MAPS FOR LOCAL SCALE MODELS.....</b>          | <b>D1</b>  |
| <b>APPENDIX E. OPEN WATER EVAPORATION AROUND THE DR/GR AREA .....</b> | <b>E1</b>  |
| <b>APPENDIX F. LS ECM V2 RESULTS AT OBSERVATION STATIONS .....</b>    | <b>F1</b>  |
| <b>APPENDIX G. WATER TABLE LEVEL MAPS IN THE DR/GR AREA.....</b>      | <b>G1</b>  |
| <b>APPENDIX H. HYDROPERIOD MAPS IN THE DR/GR AREA.....</b>            | <b>H1</b>  |
| <b>APPENDIX I. WATER BALANCE TABLES AND FIGURES.....</b>              | <b>I1</b>  |
| <b>APPENDIX J. LS ECM V1 CALIBRATION RESULTS .....</b>                | <b>J1</b>  |



## Acronyms and abbreviations

BC: Boundary condition  
BCB: Big Cypress Basin  
BLM: Base Line Model  
DBHYDRO: South Florida Water Management District's corporate environmental database  
DET: (spatially) distributed ET  
DR/GR: Density Reduction/Groundwater Resources  
DSS: Domestic self supply  
ECM: Existing Conditions Model  
ECWCD: East County Water Control District  
EIC: Estero-Imperial River  
ERP: Environmental Resource Permit  
ET: Evapotranspiration  
ETp: Potential Evapotranspiration  
FAS: Floridan Aquifer System  
FCM: Future Conditions Model  
FCRB: Freshwater Caloosahatchee River Basin  
FLUCCS: Florida Land Use, Land Cover Classification System  
ft: feet  
GSE: Ground surface elevation  
IAS: Intermediate Aquifer System  
ICA: Irrigation command area  
KLECE: Kevin L. Erwin Consulting Ecologist, Inc.  
LC: Lee County  
LE: Lake evaporation  
LIDAR: Light Detection and Ranging  
LS: Local scale  
MAE: Mean absolute error  
ME: Mean error  
MIKE 11: Hydraulic component in MIKE SHE  
MIKE SHE: Dynamic modeling system for integrated groundwater and surface water resources  
NEXRAD: Next-Generation Radar  
NRD: Natural Resources Division  
NSM: Natural System Model  
PET: potential ET  
PL: Performance level  
R: Correlation coefficient  
RET: reference ET  
RMSE: Root mean square error  
SAS: Surficial Aquifer System  
SET: station-based ET  
SFWMD: South Florida Water Management District



SWFFS: Southwest Florida Feasibility Study  
TCRB: Tidal Caloosahatchee River Basin  
USGS: United States Geological Survey  
WTE: Water table elevation  
WTP: Water treatment plant

## List of Tables

|  |     |
|--|-----|
| Table 1. DBHYDRO stations with potential ET data for the ECM. ....   | 24  |
| Table 2. Constant ET Parameters. ....  | 26  |
| Table 3. Land use dependent ET Parameters. ....  | 26  |
| Table 4. Land use dependent ET Parameters. ....  | 28  |
| Table 5. MIKE SHE land use categories and corresponding FLUCCS codes. ....   | 33  |
| Table 6. Vegetation-based global parameters used in the ECM and LS ECM. ....   | 34  |
| Table 7. Soil Parameters. ....   | 38  |
| Table 8. Municipal potable water supply well included in the MIKE SHE model. ....  | 45  |
| Table 9. Summary of ICAs defined to represent the water consumption from DSS wells. ....   | 50  |
| Table 10. Mean water table differences in mining pits and lakes from several model runs. ....  | 75  |
| Table 11. Statistical Parameters used for Calibration of the ECM. ....   | 76  |
| Table 12. Number of stations for different performance level ranges. ....  | 76  |
| Table 13. Annual average depth rates of the water balance components from the different versions of LS ECM, different ET data and in two different areas: in the entire DR/GR and in the Mining Pits and shallow water bodies in and around the DR/GR Area. .... | 92  |
| Table 14. Statistical processing of the water table difference maps. ....  | 126 |
| Table 15. Statistical processing of the hydroperiod difference maps. ....  | 132 |
| Table 16. Statistical processing of the model- and KLECE-based hydroperiod-grouped-difference maps. ....   | 133 |
| Table 17. Annual average depth rates of the water balance components for the entire DR/GR Area as predicted from different models. ....  | 139 |
| Table 18. Annual average depth rates of the water balance components for mining pits and lakes around the DR/GR area as predicted from different models. ....  | 144 |
| Table 19. Annual average depth rates of the water balance components in a mining pit area located in the northwest corner of the DR/GR Area in the FCM1. ....  | 146 |
| Table 20. Annual average depth rates of the water balance components in new urban areas. ....  | 148 |
| Table 21. Annual average flow rates at selected pathway locations. ....  | 149 |
| Table 22. Normalized indicators to evaluate the scenario performance. ....   | 153 |

## List of Figures

|  |    |
|--|----|
| Figure 1. Model Domain Areas.....  | 17 |
| Figure 2. Comparison of the SWFFS model, LCBLM, and measured stages. ....  | 18 |
| Figure 3. Location of stations that were used to compare SWFFS model to the LCBLM. ....  | 19 |
| Figure 4. Rainfall Stations and NEXRAD Grid.....   | 22 |
| Figure 5. Comparison of monthly values between the daily rainfall of a DBHYDRO station<br>and the radar rainfall data at the same location. ....       | 23 |
| Figure 6. Potential Evapotranspiration Stations and Thiessen Polygons. ....  | 25 |
| Figure 7. Distributed ET grid around the model domain area. ....   | 27 |
| Figure 8. Model Topography in ECM.....   | 29 |
| Figure 9. Model Topography in the LS ECM. ....   | 31 |
| Figure 10. Existing Conditions Land Use Map.....   | 35 |
| Figure 11. Soils Map. ....   | 37 |
| Figure 12. Geologic Model and Computational Layers along a transect in the DR/GR Area. ....  | 40 |
| Figure 13. Model Boundaries.....   | 42 |
| Figure 14. Municipal potable water supply well locations. ....   | 44 |
| Figure 15. Irrigation Command Areas. ....  | 46 |
| Figure 16. Domestic Self Supply Well Distribution. ....  | 49 |
| Figure 17. Maximum weekly consumption for a DSS well. The total volume includes<br>irrigation and potable water supply.....                            | 52 |
| Figure 18. MIKE 11 Network and Structures in the ECM.....  | 53 |
| Figure 19. Flood coded cells in the ECM.....   | 55 |
| Figure 20. Separated Overland Flow Areas in the ECM.....   | 57 |
| Figure 21. MIKE 11 Time-Varying Boundary Conditions in the ECM. ....   | 59 |
| Figure 22. Tidal Stations. ....  | 61 |
| Figure 23. Mining Pits and Shallow Lakes. ....   | 63 |
| Figure 24. MIKE 11 Network and Structures in the LS ECM.....   | 66 |
| Figure 25. Flood Codes in the LS ECM.....  | 67 |
| Figure 26. Separated Overland Flow Areas in the LS ECM.....  | 68 |
| Figure 27. Drainage system around mining pits with a grayscale shaded relief map of LIDAR<br>topographic data in the background. ....                  | 70 |
| Figure 28. Average water table level map for the DR/GR Area at the end of the dry season as<br>predicted by LS ECM.....                                | 78 |
| Figure 29. Average water table level map for the DR/GR Area at the end of the wet season as<br>predicted by LS ECM.....                                | 79 |
| Figure 30. Transects through the mining pit complex area used to generate the water table<br>level profiles presented from Figure 31 to Figure 34..... | 80 |



Figure 31. Water table level profile along Transect 1 presented in Figure 30 at the end of the dry season. The numbers 5.3 and 8.2 refer to the value in percent of LE - RET used..... 81

Figure 32. Water table level profile along Transect 1 presented in Figure 30 at the end of the wet season. The numbers 5.3 and 8.2 refer to the value in percent of LE - RET used. .... 82

Figure 33. Water table level profile along Transect 2 presented in Figure 30 at the end of the dry season. The numbers 5.3 and 8.2 refer to the value in percent of LE - RET used..... 83

Figure 34. Water table level profile along Transect 2 presented in Figure 30 at the end of the wet season. The numbers 5.3 and 8.2 refer to the value in percent of LE - RET used. .... 84

Figure 35. Hydroperiod map generated based on data created by KLECE from 2007 aerial photos. .... 86

Figure 36. Hydroperiod map obtained from LS ECM. .... 87

Figure 37. Hydroperiod water depth map obtained from LS ECM. .... 88

Figure 38. Annual averaged water balance components in mm/yr for the entire DR/GR Area as predicted by the LS ECM. .... 90

Figure 39. Annual averaged water balance components in mm/yr for the mining pits and other shallow water bodies around the DR/GR Area as predicted by the LS ECM..... 91

Figure 40. Annual averaged flow rates obtained at the river network from the LS ECM. .... 94

Figure 41. Annual averaged flow rates (in ft<sup>3</sup>/s) in the drainage system around mining pits as obtained from the LS ECM. .... 95

Figure 42. Flow rates at some conceptual weirs around mining pits presented on Figure 41. 96

Figure 43. Land use changes in the Future Conditions Model 1 and locations of water table comparison plots. .... 100

Figure 44. Land use changes in the Future Conditions Model 2 and locations of water table comparison plots. .... 101

Figure 45. Land use changes in the Future Conditions Model 3 and locations of water table comparison plots. .... 102

Figure 46. Land use changes in the Future Conditions Model 4 and locations of water table comparison plots. .... 103

Figure 47. Water table elevations at land use change location M1..... 104

Figure 48. Water table elevations at land use change location M2..... 104

Figure 49. Water table elevations at land use change location M3..... 104

Figure 50. Water table elevations at land use change location M4..... 105

Figure 51. Water table elevations at land use change location M5..... 105

Figure 52. Water table elevations at land use change location M6..... 105

Figure 53. Water table elevations at land use change location M7..... 106

Figure 54. Water table elevations at land use change location M8..... 106

Figure 55. Water table elevations at land use change location M9..... 106

Figure 56. Water table elevations at land use change location M10..... 107

Figure 57. Water table elevations at land use change location M11..... 107

|   |     |
|---|-----|
| Figure 58. Water table elevations at land use change location M12.....  | 107 |
| Figure 59. Water table elevations at land use change location M13.....  | 108 |
| Figure 60. Water table elevations at land use change location M14.....  | 108 |
| Figure 61. Water table elevations at land use change location M15.....  | 108 |
| Figure 62. Water table elevations at land use change location M16.....  | 109 |
| Figure 63. Water table elevations at land use change location U1. ....  | 109 |
| Figure 64. Water table elevations at land use change location U2. ....  | 109 |
| Figure 65. Water table elevations at land use change location U3. ....  | 110 |
| Figure 66. Water table elevations at land use change location U4. ....  | 110 |
| Figure 67. Water table elevations at land use change location W1.....   | 110 |
| Figure 68. Water table elevations at land use change location W2.....   | 111 |
| Figure 69. Water table elevations at land use change location W3.....   | 111 |
| Figure 70. Seasonal averaged water table elevation at locations M1, M2 and M3 in FCM1.  | 111 |
| Figure 71. Sketch of the flattening effect on the water table elevation of a mining pit in the presence of a regional gradient.....                             | 112 |
| Figure 72. Difference in dry season water table in FCM1 in relation to the LS ECM (Positive values indicate increase in water table elevation in the FCM1)..... | 114 |
| Figure 73. Difference in wet season water table in FCM1 in relation to the LS ECM (Positive values indicate increase in water table elevation in the FCM1)..... | 115 |
| Figure 74. Difference in dry season water table in FCM2 in relation to the LS ECM (Positive values indicate increase in water table elevation in the FCM2)..... | 116 |
| Figure 75. Difference in wet season water table in FCM2 in relation to the LS ECM (Positive values indicate increase in water table elevation in the FCM2)..... | 117 |
| Figure 76. Difference in dry season water table in FCM3 in relation to the LS ECM (Positive values indicate increase in water table elevation in the FCM3)..... | 118 |
| Figure 77. Difference in wet season water table in FCM3 in relation to the LS ECM (Positive values indicate increase in water table elevation in the FCM3)..... | 119 |
| Figure 78. Difference in dry season water table in FCM4 in relation to the LS ECM (Positive values indicate increase in water table elevation in the FCM4)..... | 120 |
| Figure 79. Difference in wet season water table in FCM4 in relation to the LS ECM (Positive values indicate increase in water table elevation in the FCM4)..... | 121 |
| Figure 80. Water table level profile along Transect 1 presented in Figure 30 at the end of the dry season.....  | 122 |
| Figure 81. Water table level profile along Transect 1 presented in Figure 30 at the end of the wet season. ....   | 123 |
| Figure 82. Water table level profile along Transect 2 presented in Figure 30 at the end of the dry season.....  | 124 |
| Figure 83. Water table level profile along Transect 2 presented in Figure 30 at the end of the wet season. ....   | 125 |



|  |     |
|--|-----|
| Figure 84. Difference in hydroperiod in FCM1 in relation to the LS ECM (Positive values indicate greater duration of water ponding in FCM1).....         | 128 |
| Figure 85. Difference in hydroperiod in FCM2 in relation to the LS ECM (Positive values indicate greater duration of water ponding in FCM2).....         | 129 |
| Figure 86. Difference in hydroperiod in FCM3 in relation to the LS ECM (Positive values indicate greater duration of water ponding in FCM3).....         | 130 |
| Figure 87. Difference in hydroperiod in FCM4 in relation to the LS ECM (Positive values indicate greater duration of water ponding in FCM4).....         | 131 |
| Figure 88. Hydroperiod map generated based on data created by KLECE from 1953 aerial photos. ....  | 135 |
| Figure 89. Mean hydroperiod map differences (existing minus historical) based on data created by KLECE from aerial photos. ....                          | 136 |
| Figure 90. Map of hydroperiod changes after processing the data created by KLECE from aerial photos. ....  | 137 |
| Figure 91. Annual averaged Water Balance Components in the DR/GR Area from all Models. ....  | 140 |
| Figure 92. Seasonal averaged evapotranspiration in the DR/GR Area for all scenarios. ....  | 141 |
| Figure 93. Seasonal averaged net rainfall in the DR/GR Area for all scenarios.....   | 142 |
| Figure 94. Seasonal surface water outflow from the DR/GR Area for all scenarios. ....  | 142 |
| Figure 95. Seasonal groundwater outflow from the DR/GR Area for all scenarios. ....  | 143 |
| Figure 96. Monthly rainfall in the mining pit area (MP) containing site M2 in Figure 43 compared to the averaged monthly rainfall in the DR/GR Area..... | 145 |
| Figure 97. Selected flow comparison locations. ....  | 150 |
| Figure 98. Correlation between the average indicator (score) of each scenario and the land use changes for the DR/GR Area. ....                          | 154 |



## Executive Summary

The Lee County Density Reduction/Groundwater Resource (DR/GR) Area was designated as an area of limited land development to protect sustainable ground-water resources. This study evaluates the effects of land use changes (*e.g.*, urban, agricultural, wetlands, mining, etc.) on the storage and availability of water resources in the area.

In order to understand how land use changes affect the water resource distribution, a comprehensive hydrologic model has been developed to simulate hydrologic and hydraulic conditions for several land use conditions. The MIKE SHE model, developed by DHI, integrates all major hydrologic processes such as rainfall, evapotranspiration (ET), surface water runoff, infiltration, ground-water recharge, ground-water flow, and surface flow through canals. MIKE SHE has been widely used by government agencies and local governments in Florida for water resource management studies and has been identified by Lee County as the best tool available for evaluating the effects of land use change on ground-water resources.

The goal of the Lee County MIKE SHE modeling is to provide the County with a valuable planning aid which quantifies the potential outcomes of water resource balancing efforts. Furthermore, the model results can serve as input for site-specific models for evaluating mining permit applications.

The general approach implemented for this study consisted of developing several MIKE SHE models that simulate the hydrologic and hydraulic response to different land use development conditions in the DR/GR area. The land use conditions evaluated are the conditions that exist today and several future land-use alternatives. A comparative analysis of the results from these models provides quantitative insights into the benefits or stresses caused by specific land use changes on Lee County's water resources.

The Existing Conditions Model (ECM) is a baseline model to which the results of land use alternatives are compared. This model was developed using the most current data available to represent the existing land use conditions. Two scales of models were developed: 1. a large sub-regional scale model covers the entire Lee County area and additional areas to the north, south, and east that are hydraulically connected to the County; and 2. a local-scale model at a higher resolution focusing on the DR/GR area.

Two versions of the ECM were developed as part of this study. The first version is an intermediate version that was immediately updated with more accurate data that became available following its completion. The second version is the update to version one, and serves as the baseline for comparison of land use alternatives.

Observation data for the Existing Conditions Model was obtained from the South Florida Water Management District (SFWMD), Lee County, and the USGS. Some of the initial model development originated from a previously developed MIKE SHE model of the



Southwest Florida Feasibility Study (SWFFS) area. Updates to the SWFFS model input data for the Lee County model include meteorological, land use, irrigation and ground-water withdrawal, and topography.

The Lee County Model represents all the major hydrologic processes in a fully integrated and spatially distributed manner. The surface water model includes an extensive network of primary and secondary canals with many hydraulic structures, natural sloughs, rivers, and lakes. The ground-water model includes the Water Table, Lower Tamiami, and Sandstone aquifers and the Bonita Springs Marl and Upper Peace River confining units. The model simulates distributed irrigation and ground-water withdrawals based on actual well locations and land use maps and estimated rates based on permit data and other information.

As part of the model development, considerable effort was spent improving the representation of certain important features in the model, such as the mining pits and flow ways in the DR/GR area. Furthermore, a number of model parameters, such as overland flow roughness coefficients, hydraulic conductivities and storage parameters of the geologic layers, and subsurface drainage parameters, were tested and varied in order to produce a closer match between model results to observed data.

As part of the calibration process, the Existing Conditions Model results were compared with measured ground-water and surface water data. Since this study focuses on ground-water resources in the DR/GR area, the calibration efforts were prioritized accordingly. Thus, the highest calibration priority was given to the ground-water stations south of the Caloosahatchee River.

The determination of wetland hydroperiods has been an important indicator used in this study. For this evaluation, wetland hydroperiod is defined as the period during which water is above the ground surface. The hydroperiod output of the model, together with the water table elevation and the water balance computation, provides useful insight into the impact of the land use changes on wetland areas.

In order to evaluate the hydrological effects of land use changes in the DR/GR area, four Future Conditions Models (FCMs) were developed. The results of these models were analyzed by using relative measures, such as differences in hydroperiod, water table elevations, and overall water budget.

A natural systems model (NSM) was constructed using the intermediate ECM. The revised topography changed the hydroperiod prediction significantly and the NSM based on that intermediate step was not accurate enough to be useful in the analyses presented in this final report. As such, hydroperiod maps developed by KLECE corresponding to years 1953 and 2007 were used to evaluate how the present developments in the DR/GR Area have affected the water resources, and to evaluate at what extent the model predictions for the future conditions scenarios are going to impact them in the direction of the historical conditions.



The future land use modeling scenarios consist of four alternatives in the DR/GR Area that were provided by Lee County. The land use changes consist of three types: creation of urban areas, expansion or creation of mining pits, and restoration of agricultural lands into wetlands:

- Land use alternative 1 (FCM1) is conceptually similar to Scenario 1 in “Prospects for Southeast Lee County” [Dover, Kohl & Partners, July 2008]. Mining would be limited to already-approved mining pits plus some new pits north of Alico Road near the airport (but with fewer pits than in Scenario 1). A broad westerly flow way to Corkscrew Swamp would be restored southward from the Imperial Marsh.
- Land use alternative 2 (FCM2) is conceptually similar to Scenario 2 in the Dover Kohl report. Mining would be limited to already-approved pits plus a major expansion to the Green Meadows Mine. A broad flow way to Corkscrew Swamp would be restored southward from the east end of Corkscrew Road in Lee County.
- Land use alternative 3 (FCM3) is conceptually similar to Scenario 3 in the Dover Kohl report. Mining would be limited to already-approved pits plus proposed new pits that were in the application process in September 2007, including pits along Corkscrew Road east of the Flint Pen Strand. Both flow ways to Corkscrew Swamp would be restored to whatever extent is still possible after significant portions of each were mined.
- Land use alternative 4 (FCM4) is conceptually similar to an alternative scenario that emerged favorably during public meetings after release of the Dover Kohl report. Mining would be limited to already-approved pits plus a moderate expansion to the Green Meadows Mine. Both flow ways to Corkscrew Swamp would be restored in full.

The extent of the restored areas in all scenarios is less than originally proposed in the Dover Kohl report but would still be a major long-term undertaking for which funding is not currently available. The new urban areas added in the future conditions land use map were exactly the same in all four alternatives. The increase of new mining areas from smallest to largest is: FCM1, FCM4, FCM2, and FCM3. The new mining areas in FCM3 are nearly double the amount of mining areas than in FCM1. The total amount of newly restored areas increases in the order FCM1, FCM2, FCM3 and FCM4.

All land use based parameters in the model were modified to correspond to the new land use types. The irrigation setup in the future conditions model was modified to reflect future land use changes. For example, irrigation areas were removed in areas where the land use was converted from urban or agricultural to mining or wetland areas. The well field configuration of the ECM remained the same in the FCMs, i.e., no wells were added or removed. The groundwater withdrawal rates for public water supply in the last year of available data were repeated for every year in the simulation period for the four future conditions scenarios. The domestic self-supply rates vary according to land use changes.

In order to evaluate the effects of land use changes in the water resources of the DR/GR area, various types of results were generated and compared between the ECM and four future conditions alternatives. Water table elevation maps were created for all land use alternatives for two times of the year: at the end of the dry season (end of May) and at the end of the wet season (end of September). Additionally, water table levels at specific locations (where changes in land use occur) were generated to observe the changes in fluctuations throughout the five-year simulation period. Water budget calculations were extracted for the entire DR/GR to determine which hydrologic components were affected by the different alternatives. Finally, hydroperiod maps and maps of the mean water depth during the hydroperiod were also produced.

From the perspective of water table elevation and hydroperiod, the different scenarios produce changes that in some cases are quite notably distinct from one FCM to another. All of the future condition scenarios show areas where the water level and hydroperiod would decrease with respect to the existing conditions in some areas, while increasing in others. Decreases represent potentially negative impacts to the wetland ecosystems in those areas. The cause of the lower water table level and hydroperiod is the flattening effect of proposed single large mining pits or the combined flattening effect from several mining pits that have a high hydrological connectivity (i.e. via the ground-water).

The model results from the different land use scenarios indicate several concepts that may be useful during the planning process.

- Wetland areas converted from agricultural areas in the future condition alternatives help to increase the water table elevations during the dry season and to extend the period of time that those areas are wet (hydroperiod).
- The conversion of natural and agricultural areas to urban development slightly lowers the water table during the wet season due to the new urban drainage system. The water table in the new urban areas is typically higher at the end of the dry season compared to the existing conditions, which is likely related to a reduction in the ET losses.
- The water budget in all mines and lakes around the DR/GR Area suggests that the annual net rainfall (rainfall minus evaporation) is about zero on average. This is a consequence of the open water evaporation rate, which is commonly higher than the annual ET rate in pre-mined conditions. The model also predicts that the drainage system around some mines produces a positive net surface water outflow from the mines. As a result, the aquifers need to supply water to the mining pits (negative net groundwater recharge) in about the amount that is lost through the drainage system.
- This modeling has indicated, in general, that the annual averaged ET rates from the DR/GR Area would be higher with greater areal coverage of mining pits. The surface water outflow rate (runoff) from the DR/GR Area was lower in all the scenarios compared to the ECM, which is likely related to the greater mining pit coverage.



These results are expected due to the higher ET losses and the lower runoff from mining pits and its effect on the surface water flow in neighboring areas.

- Mining pits cause a flattening in the water table that affects the pre-developed water table gradient. This often implies a decrease in the water table elevation on the up-gradient side of the pits and an increase on the down-gradient side. On the down gradient side, there may also be a decrease in some situations. The most pronounced flattening effect is seen towards the end of the dry season. This also has an effect on the hydroperiod by shortening the up-gradient hydroperiod and increasing (or sometimes also decreasing) the down-gradient hydroperiod. The flattening effect of mine development on the water table is larger in areas with steeper water table gradients, in larger mine pits, and in the case of a number of mining pits that are closer and therefore more hydrologically connected (i.e. via groundwater).

Water budgets, hydroperiod maps, and water elevation maps resulting from the modeling were analyzed for all four FCMs. These maps and numbers were compared to the local scale existing conditions model (LS ECM) results, and the scenarios were ranked according to their impact on natural areas in the DR/GR Area. This comparison revealed that scenarios with higher proportions of restored land areas than mining areas had less negative impact on the overall DR/GR Area. In cases where the areal extent of newly restored land area exceeded the areal extent of new mining areas, there was an overall benefit to the water resources in the DR/GR Area. The scenario that minimizes stress on the current water resources within the DR/GR Area is FCM4. This is followed, from second best to worst, by FCM1, FCM2, and FCM3.



## Introduction

The Lee County Density Reduction/Groundwater Resource (DR/GR) Area was designated as an area of limited land development in an effort to provide a sustainable use of groundwater resources for the County. This study evaluates through the use of a computer model the effect of the land use changes (*e.g.*, urban, agricultural, wetlands, mining, etc.) on the storage and availability of water resources in the area. In order to understand how land use changes affect the water resources distribution, a comprehensive hydrologic model has been developed to simulate hydrologic and hydraulic conditions for several land use conditions. The MIKE SHE model, developed by DHI, is capable of fully integrating all major hydrological processes including: rainfall, evapotranspiration (ET), surface water runoff, infiltration, groundwater recharge, groundwater flow, and surface flow through canals. MIKE SHE has been widely used by government agencies and local governments in Florida for water resources management studies and has been identified by Lee County as a suitable tool for evaluating the effects of land use change on groundwater resources. The goal of the Lee County MIKE SHE modeling is to provide the County with a valuable planning tool which aids in the understanding of the potential outcomes of water resource balancing efforts. Furthermore, the model will generate results that may serve as input for site-specific models for evaluating permit applications.

The general approach implemented for this study consisted of developing several MIKE SHE models that describe the hydrologic and hydraulic response to different land use development conditions in the DR/GR Area. The models represent all the major hydrologic processes in a fully integrated and spatially distributed manner. The land use conditions evaluated are existing and several future alternatives. A comparative analysis of the results from these models is intended to provide a quantitative insight into the benefits or stresses caused by specific land use changes on Lee County's water resources.

This report describes the development and calibration of two Existing Conditions Models (ECMs), one regional (ECM) and one local scale (LS ECM), and the development of four Future Conditions Models (FCMs) based on the LS ECM.

Development of the LS ECM was a multi-step process. The ECM was developed first, which has a resolution of 1500 ft and contains the entire Lee County area. This model was used to extract the LS ECM for the DR/GR Area at a 750-ft resolution and to establish its boundary conditions. The calibration process had been completed early in the development of the LS ECM when much more accurate topographic data became available. The County decided it was in their best interest to utilize the high resolution topographic data to generate a more accurate model, which also included the redefinition of the flow ways. This initially calibrated intermediate step in the development of the final LS ECM is referred to in places as LS ECM V1 in the report. Details about the calibration process for this intermediate model can be found in Appendix J. Results from LS ECM V1 are presented in some discussions regarding the calibration of the final model to demonstrate the sensitivity of the model to the refined topography and flow ways, and to highlight the importance these improvements had in



the ultimate model performance. The final LS ECM is referred to in some graphs and figures as LS ECM V2, but it is otherwise referred to as LS ECM throughout the report.

Another significant change that was implemented in the LS ECM following the introduction of the high resolution topography in the model was the introduction of distributed evapotranspiration (ET) data instead of station based data. Similar to the occasional presentation of output from LS ECM V1, output from other intermediate model development steps is presented to show the sensitivity of the model to the distributed ET data.

This report is organized as follows. The data sources for the model are presented, as well as descriptions of how the data are used by the various model components. Plots that compare the observed data and ECM results for the DR/GR Area are included in the report. The changes in land use for the future scenarios are described in relation to the existing land use, as well as the components of the model that were altered to represent these changes. The final part of the report includes the results that show the effects of the land use changes, i.e., the hydrologic/hydraulic evaluation of the future condition scenarios. Finally, the limitations of the model are stated, as well as recommendations that may improve the accuracy of the results. Several appendices are included which provide more detailed results and additional information on the modeling.

## **Objectives**

The main objective of this study is to quantitatively analyze the benefits or stresses caused by specific land use changes on Lee County's water resources to help the County during the planning process. The land use includes creating new urban areas, wetland areas and mining pits in the DR/GR Area. The effects are evaluated specifically on water balance components, water table elevations and hydroperiods. The study is expected to reveal generalities about the effect of the land use changes, and produce a ranking of the different future condition scenarios tested from a water resources perspective.

## **Existing Conditions Model**

The Existing Conditions Model (ECM) is the base model to which the results of several land use alternatives will be compared. The model was developed using the most current data available to represent the existing land use conditions. The input data for the Existing Conditions Model was obtained from the South Florida Water Management District (SFWMD), the United States Geological Survey (USGS), and from Lee County. Two model scales were developed: 1. a larger scale 1500-ft grid model (ECM) that covers the entire Lee County area and additional areas to the north, south, and east that are hydraulically connected to the County; and 2. a local-scale model (LS ECM) that is a higher resolution model (750-ft grid) focused on the DR/GR Area. The purpose of the larger model is to generate representative boundary conditions at the sub-regional level for the local scale model. All the future land use alternatives were developed at the local scale level using the same boundary conditions and the LS ECM.



## **Baseline Model**

Some of the initial model development originated from a previously developed MIKE SHE model of the Southwest Florida Feasibility Study (SWFFS) area. The SWFFS area consists of four major basins (Tidal Caloosahatchee River, Freshwater Caloosahatchee River, Estero River, and the Big Cypress Basin) and forms part of five counties (Charlotte, Glades, Lee, Henry, and Collier). Figure 1 shows the SWFFS model, ECM, and LS ECM areas. Since the SWFFS model simulates the period of 1995 to 1999, much of the data required updating for use in the Lee County Existing Conditions Model period of 9/1/2002 to 11/1/2007. The SWFFS model hydraulic features are limited to those critical canals, creeks, rivers and sloughs necessary to accurately route surface water flows at a regional scale. Thus, considerable hydraulic detail was added when developing the ECM and LS ECM from other modeling efforts at the sub-regional scale level within the SWFFS area.

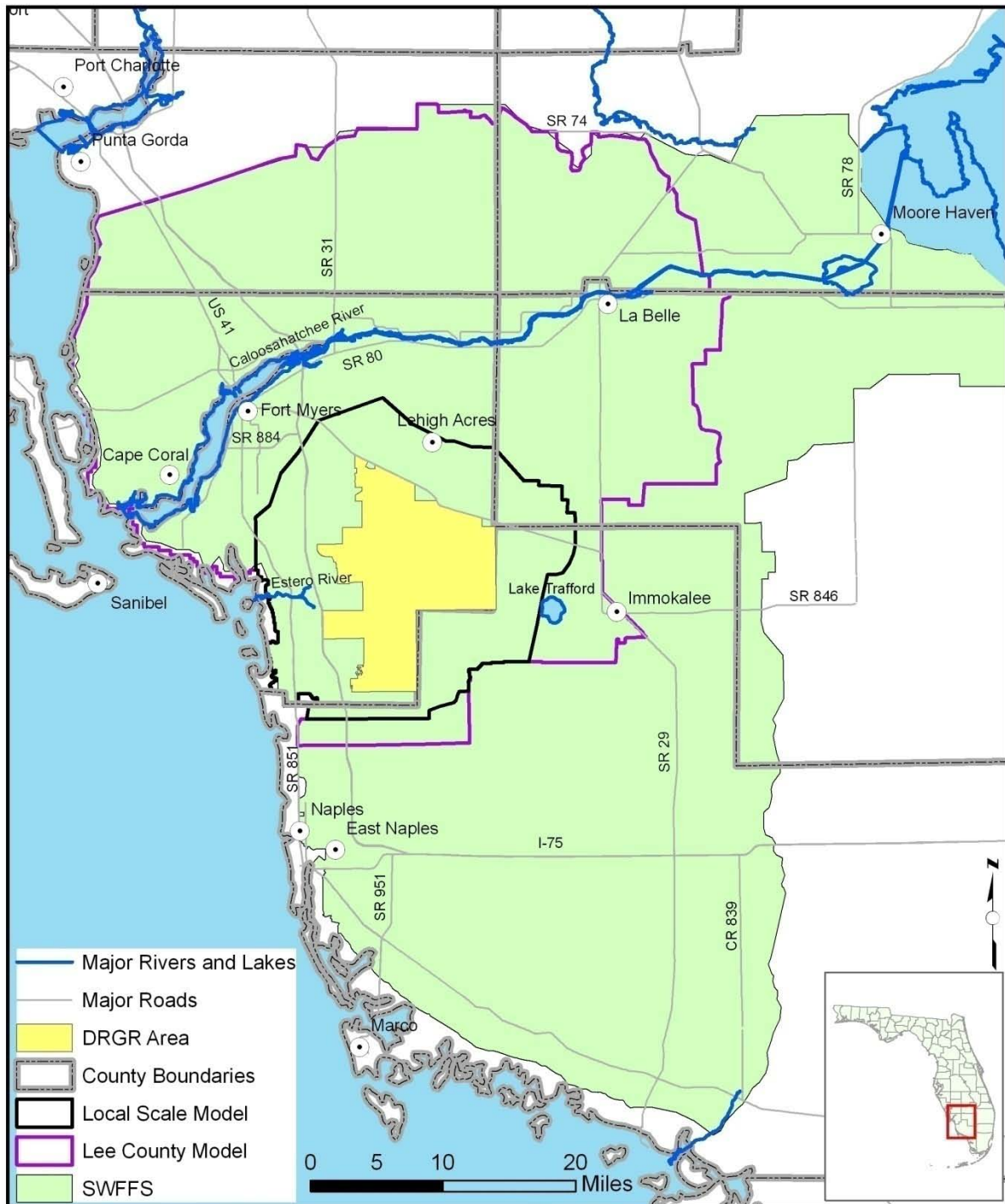


**Figure 1.** Model Domain Areas.

A preliminary comparison of the ECM and the SWFFS model was performed before any updates or improvements were made to the model. This preliminary model is referred to as Lee County Baseline Model (LCBLM). The differences between the SWFFS and the LCBLM are the size of the model domain, canals and structures added or modified from the

Estero-Imperial River (EIC), Big Cypress Basin (BCB), and Tidal Caloosahatchee River Basin (TCRB) sub-regional models, and the boundary conditions. Results of this comparison for two stations, one at Corkscrew and the other at Imperial River, are shown in **Figure 2**. The locations of these stations are shown in **Figure 3**. In general, both models produce similar results for stations within or close to the DR/GR Area. The differences between the simulated and the observed data are addressed during the development and the refinement of the existing conditions model (ECM). The modifications made to the ECM include: update of time-varying data for the period of 2002-2007, extension of the model area further to the south for better boundary representation, and improvements for better calibration performance.

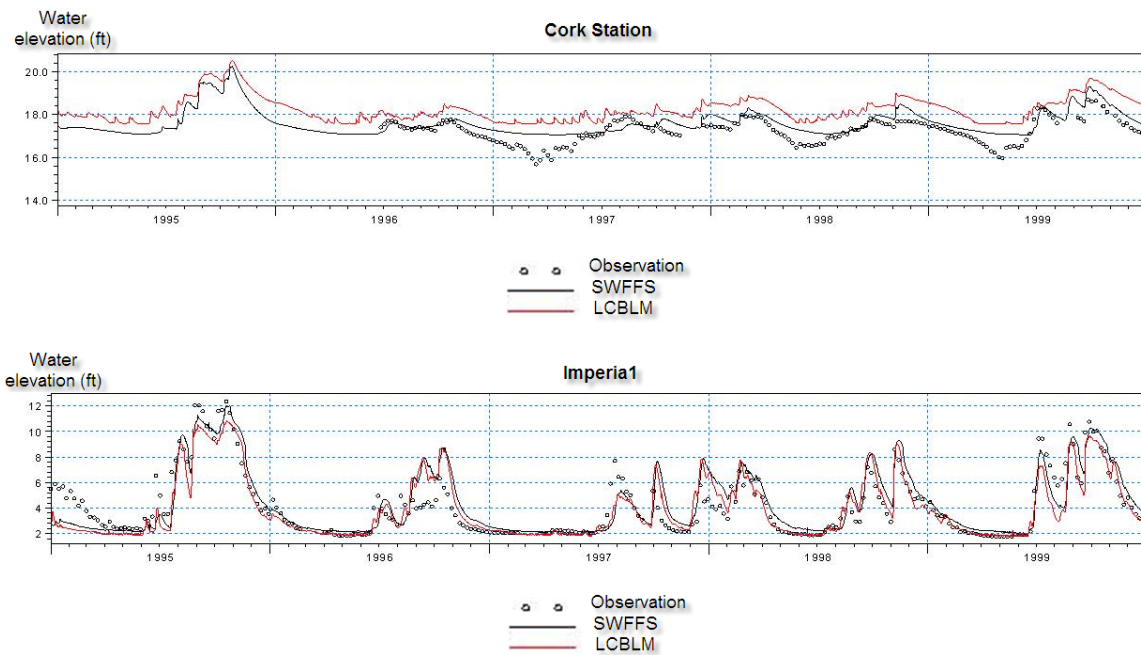


**Figure 2.** Comparison of the SWFFS model, LCBLM, and measured stages.

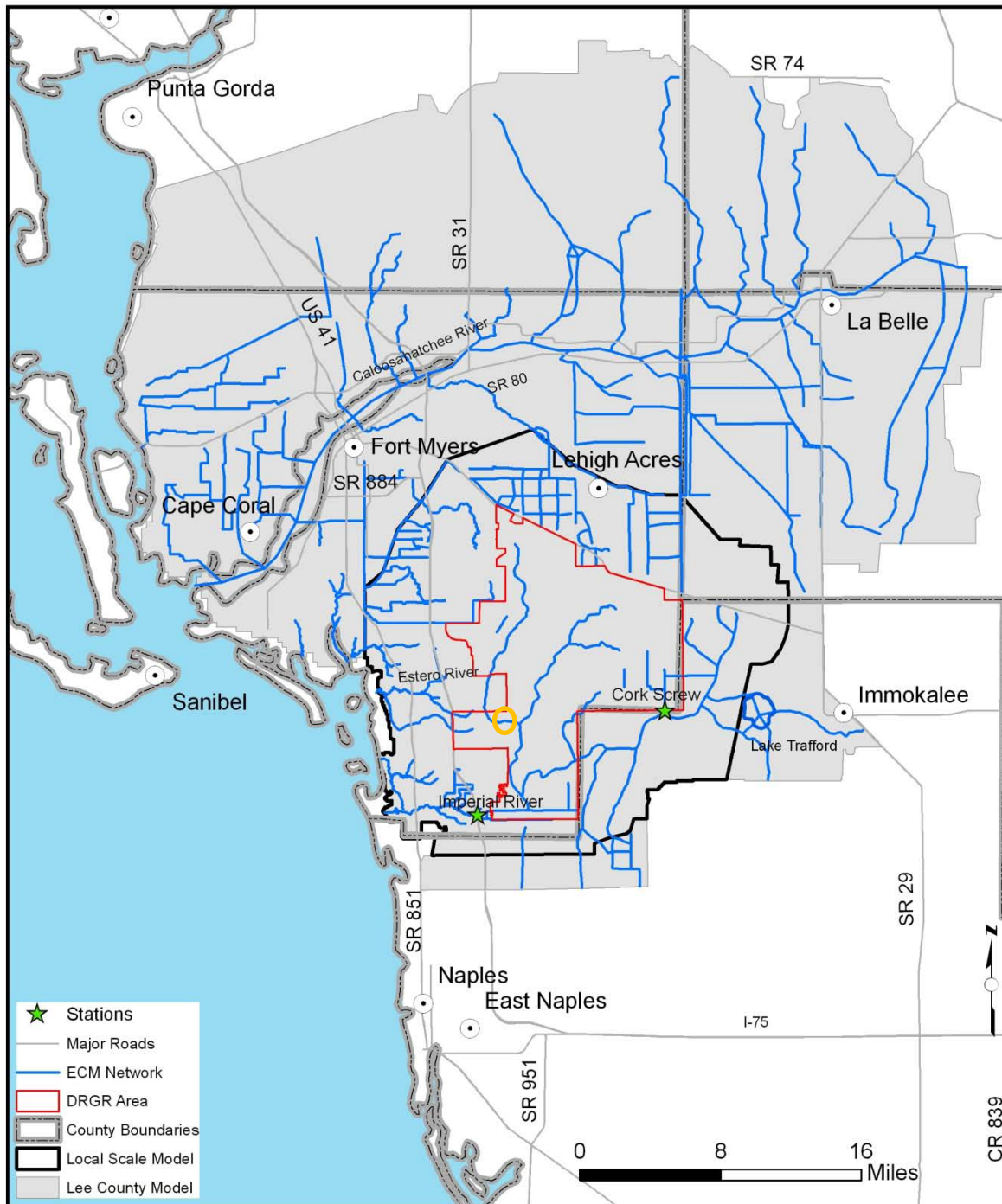


**Figure 3.** Location of stations that were used to compare SWFFS model to the LCBLM.

Note: the connection marked in the southern part of the DR/GR in the figure with the orange circle was adopted from the SWFFS model. However, as shown in the model results (Figure 40), there is not significant flow in that connection on a yearly averaged basis. The water flowing south from the western branch is diverted into the overland flow and collected by the branches that discharge in the Gulf of Mexico. This conceptualization of the surface water flow was improved in additional work described later in this report.



## Local Scale Model

As previously mentioned, a Local Scale Existing Conditions Model (LS ECM) was derived from the Lee County ECM. The purpose of the LS ECM is to zoom into the DR/GR Area at a higher resolution. The LS ECM domain area is shown in previous figures. It covers a somewhat larger extent than the DR/GR Area (approximately 2-6 miles of surrounding area) in order to include all the features modified in future conditions scenarios and to avoid boundary condition effects. The LS ECM has a grid cell size of 750 feet, which is half the size of the original ECM grid size. The total number of grid cells remains approximately the same in both models. The vertical resolution was also increased by splitting the computational layer 3 in the ECM into 2 computational layers. Thus, the LS ECM has four computational layers in total.

The river network for the LS ECM was initially obtained from the ECM network portion that is in the local scale model boundary. A constant head boundary condition is applied by using the time series stage results of the ECM. The time series water levels applied as boundary conditions for the groundwater layers are also extracted from the ECM.

While the initial river network was obtained from the ECM, several significant modifications to the network were made. These modifications are discussed in detail in the Surface Water Model section. Other modifications made to the LS ECM are included in following sections.

The changes introduced in the local scale model make the use of initial conditions extracted from the ECM inappropriate. Thus, a preliminary run of the LS ECM was performed in order to extract the initial conditions from the model results. The model was then initialized using the results of September 1<sup>st</sup>, 2004 from the previous run. The LS ECM simulation period is from September 1<sup>st</sup>, 2001 to November 1<sup>st</sup> 2007.



## Climate Data

The climate data input to the model consists of rainfall and potential evapotranspiration data.

## Rainfall

The rainfall input data was obtained from high resolution radar (NEXRAD) data. The SFWMD provided 15-minute radar rainfall data sets from January 2002 to October 2007. This data set has a spatial resolution of approximately 1.9 km (1.2 miles). The radar rainfall grid in the model domain area is shown in **Figure 4**. Individual time series data for the period from 2005 to 2007 were also provided to correct the data values for some of the pixels.

During the NEXRAD processing, the original data was replaced with the corrected values for the specified pixel locations. The 15-min data was added to obtain daily rainfall values. Finally, the ASCII data was converted to a time varying dfs2 file, the two-dimensional grid format of MIKE SHE. The resulting dfs2 file has a spatial resolution of 1,500 ft and covers the ECM domain area.

The NEXRAD rainfall data was compared to rainfall gage data located around the DR/GR Area. The locations of the stations with available rainfall data in DBHYDRO are also shown on Figure 4. Total daily radar data does not exactly match the daily values measured at the observation stations. The differences are reasonable because the two data sets have a different error range and represent different spatial extents, i.e., radar rainfall data are spatial averaged values from indirect estimations and station data are more exact measurements at a specific location. Thus, the higher error in NEXRAD rainfall data estimation is compensated by capturing the high spatial variability of the rainfall, which is critical when the distance between rainfall stations is large.

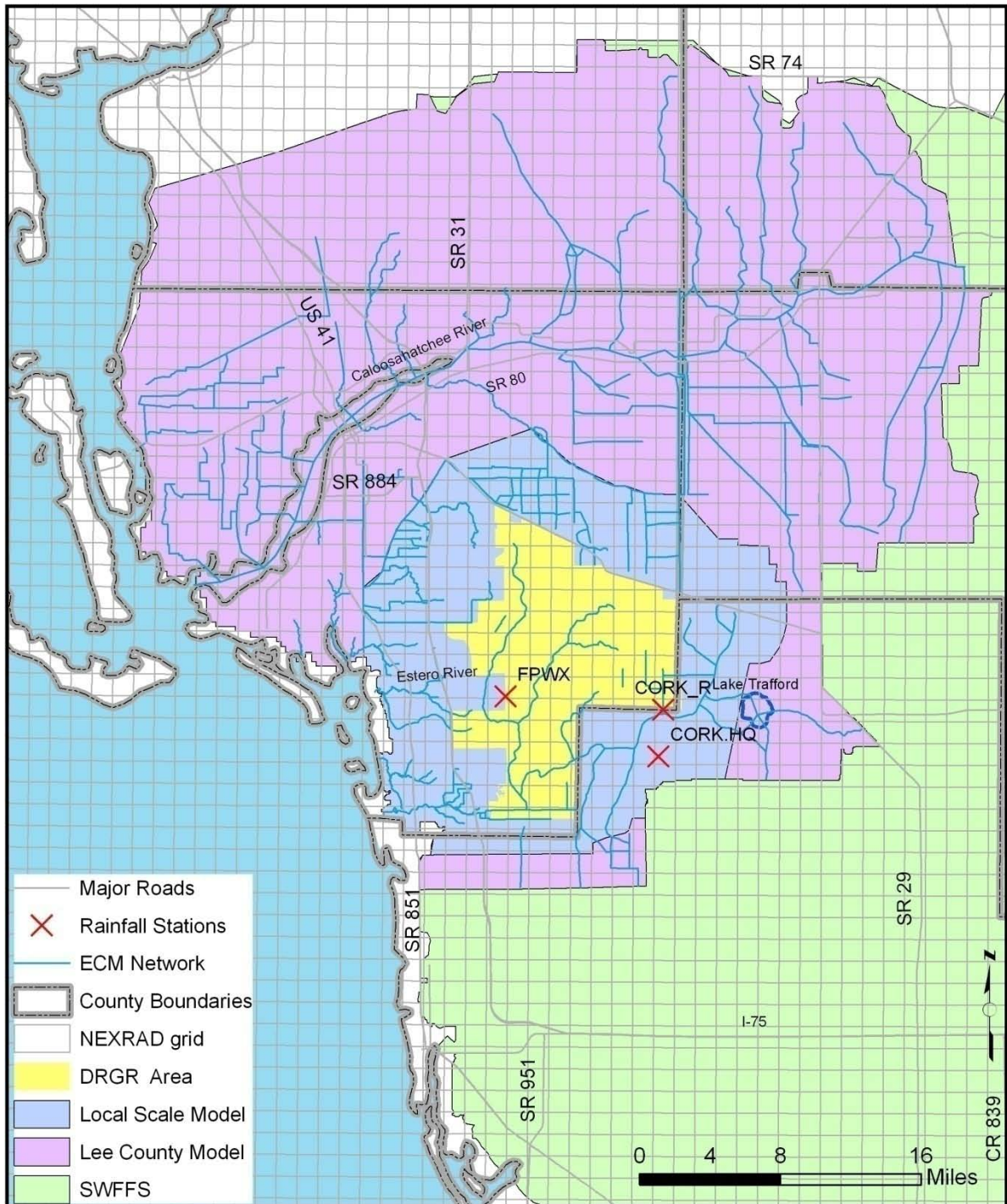


**Figure 4.** Rainfall Stations and NEXRAD Grid.

The differences between NEXRAD and station data sets decrease as the daily values are averaged over a longer period. The relatively good match between monthly cumulative rainfall values from both methods is shown in **Figure 5** at the CORK.HQ station.

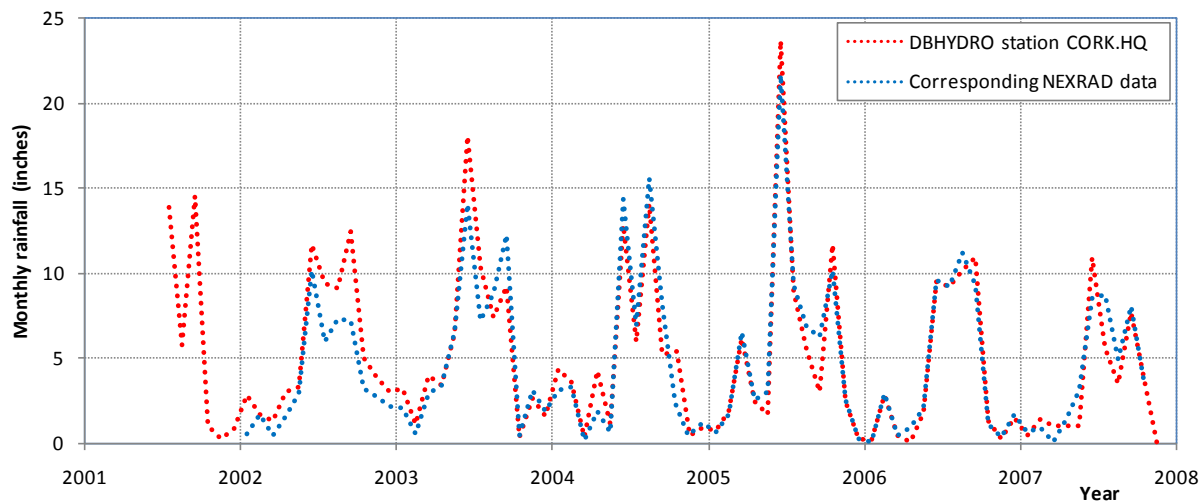


**Figure 5.** Comparison of monthly values between the daily rainfall of a DBHYDRO station and the radar rainfall data at the same location.

## Evapotranspiration

The following sections discuss how this and other ET parameters were used in the ECM and the LS ECM.

### Evapotranspiration in the ECM

The SFWMD defines potential evapotranspiration (ET<sub>p</sub>) as “actual evaporation for lakes, wetlands, and any feature that is wet year-round” (Abtew, 2005). It uses the following equation to estimate ET<sub>p</sub> rates:

$$ET = K_1 \frac{R_s}{\lambda}$$

where ET is daily evapotranspiration from wetland or shallow open water (mm/d),  $R_s$  is solar radiation (MJ/m<sup>2</sup>·d),  $\lambda$  is the latent heat of vaporization (MJ/kg), and  $K_1$  is an empirical coefficient equal to 0.53 mm·m<sup>2</sup>/kg (Abtew, 2005).

ET<sub>p</sub> is a time-varying and spatially distributed input to the MIKE SHE model, like rainfall.

Potential ET rate data from three stations within or near Lee County were extracted from the SFWMD DBHYDRO database. The station data period and locations are presented in **Table 1**. The observed daily ET rates were distributed across the model domain by using a



Thiessen polygon network, as shown in **Figure 6**. A more refined distributed ET was used in the LS ECM as described in the next section.

**Table 1.** DBHYDRO stations with potential ET data for the ECM.

| <b>Dbkey</b> | <b>Station</b> | <b>Start Date</b> | <b>End Date</b> | <b>County</b> |
|--------------|----------------|-------------------|-----------------|---------------|
| OH520        | FPWX           | 1-Jan-01          | 31-Dec-07       | LEE           |
| RW483        | S78W           | 22-Oct-92         | 31-Dec-07       | GLA           |
| RW482        | SILVER         | 6-Dec-00          | 31-Dec-07       | COL           |

In MIKE SHE, actual evapotranspiration (ET<sub>a</sub>) is calculated for every cell of the model using several factors. The calculation of ET<sub>a</sub> uses meteorological and vegetative data to predict the total evapotranspiration and net rainfall after interception of rainfall by the canopy, drainage from the canopy to the soil surface, evaporation from the canopy surface, evaporation from the soil surface, and transpiration, based on soil moisture in the unsaturated root zone (DHI 2008).

The ET processes are split up and modeled in the following order (DHI 2008):

1. a proportion of the rainfall is intercepted by the vegetation canopy, from which part of the water evaporates;
2. the remaining water reaches the soil surface, producing either surface water runoff or percolating to the unsaturated zone;
3. part of the water standing on the soil surface is evaporated;
4. part of the infiltrating water is evaporated from the upper part of the root zone or transpired by the plant roots; and
5. the remainder of the infiltrating water recharges the groundwater in the saturated zone.

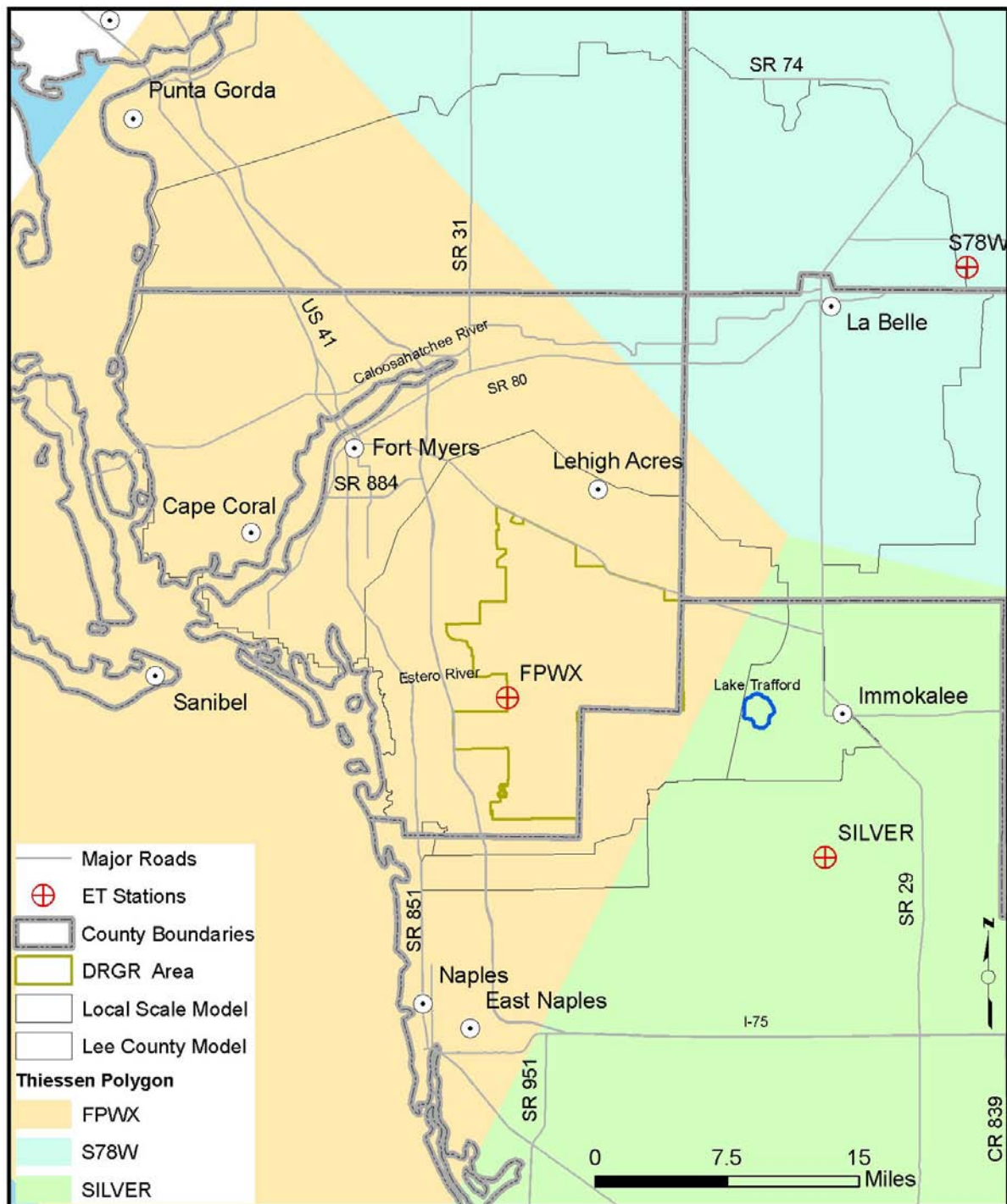


**Figure 6.** Potential Evapotranspiration Stations and Thiessen Polygons.

The ET parameters were divided into two groups: one for land use independent parameters (see **Table 2**) and the other for land use dependent parameters (see **Table 3**) such as leaf area index (LAI) and root depth (Rd).

**Table 2.** Constant ET Parameters.

| Parameter  | value                |
|--|----------------------|
| Canopy interception storage capacity                           | 5 mm                 |
| Growth cycle   | one year             |
| Crop coefficient (Kc)  | 1                    |
| empirical parameter C1   | 0.2                  |
| Kristensen and Jensen empirical parameter C2                   | 0.3                  |
| Kristensen and Jensen empirical parameter C3                   | 20 mm/day            |
| Kristensen and Jensen Root mass distribution parameter (Aroot) | 0.25 m <sup>-1</sup> |

**Table 3.** Land use dependent ET Parameters.

| Land Use/Vegetation  | LAI       | Rd (m)      |
|----------------------|-----------|-------------|
| Citrus               | 4.5       | 1.25        |
| Pasture              | 3 - 4     | 0.75        |
| Sugar Cane & Sod     | 1 - 6     | 0.5 - 1.5   |
| Truck (Row) Crops    | 1.5 - 4.5 | 0.15 - 0.75 |
| Golf Course          | 3         | 0.75        |
| Bare Ground          | 0         | 0           |
| Mesic Flatwood       | 1.5 - 3   | 1.219       |
| Mesic Hammock        | 2.5 - 4   | 1.219       |
| Xeric Flatwood       | 1 - 2     | 1.219       |
| Xeric Hammock        | 2 - 3     | 1.219       |
| Hydric Flatwood      | 1.5 - 3   | 1.219       |
| Hydric Hammock       | 2.5 - 4   | 1.219       |
| Wet Prairie          | 1.5 - 3   | 0.75        |
| Dwarf Cypress        | 1 - 2     | 0.75        |
| Marsh                | 2 - 4     | 0.75        |
| Cypress              | 2 - 4     | 1.524       |
| Swamp Forest         | 3 - 5     | 1.524       |
| Mangrove             | 3 - 4     | 1.824       |
| Water                | 4         | 2.3         |
| Urban Low Density    | 2.5       | 0.6         |
| Urban Medium Density | 2         | 0.6         |
| Urban High Density   | 2         | 0.5         |

Note: LAI = Leaf Area Index, Rd = root depth

### Refined Evapotranspiration in the LS ECM

The USGS recently released spatially distributed ET data for the same 2-km grid as the rainfall distributed data introduced in the model (see grid in **Figure 7**), so this was used to define the ET rates for the model.

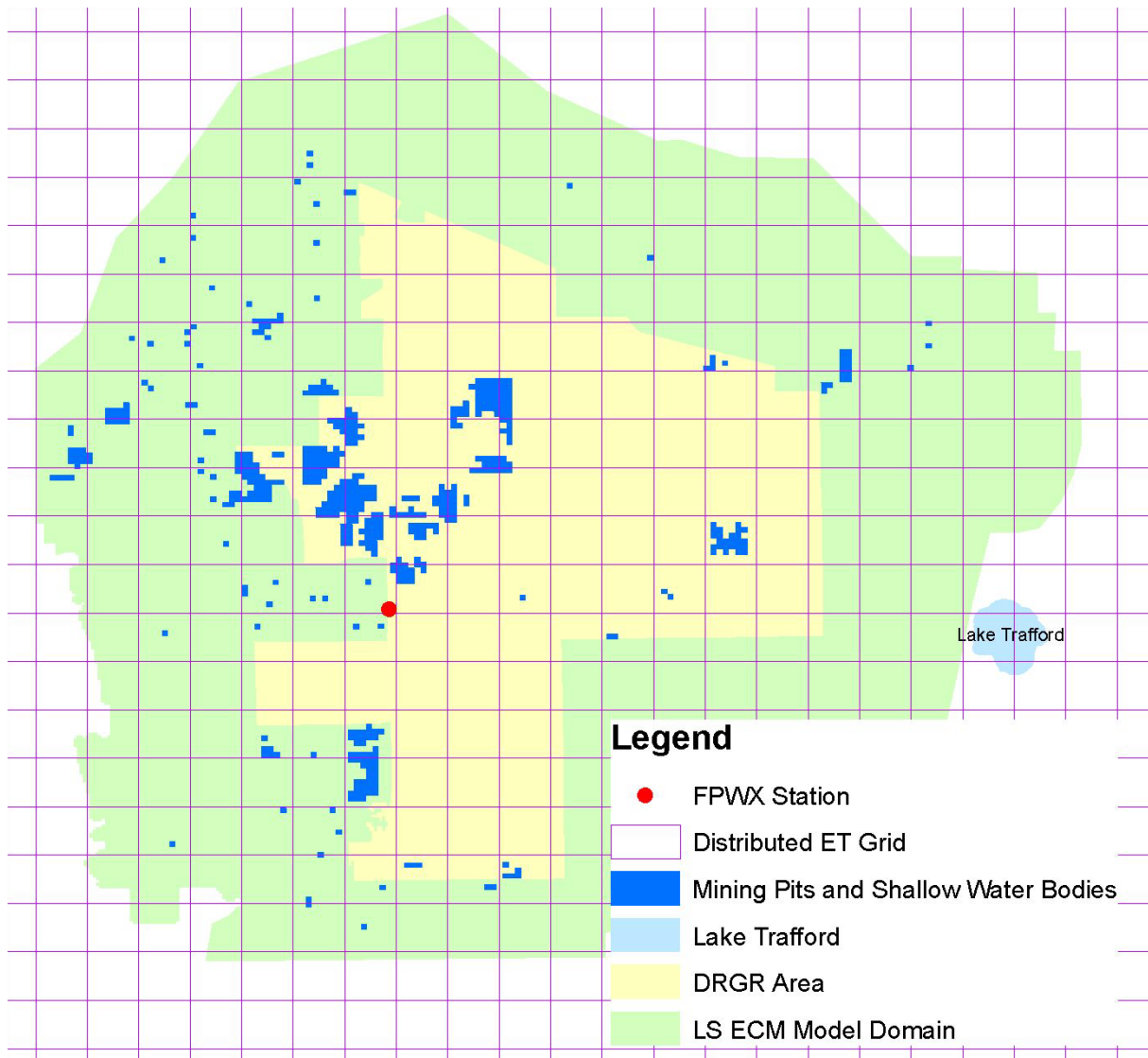


**Figure 7.** Distributed ET grid around the model domain area.

The distributed ET data may have uncertainties since air temperature, relative humidity, and wind speed are interpolated from weather stations [D. Sumner, USGS, personal communication]. The comparison of the distributed ET data and the ET data at station FPWX is presented in Appendix E. The RET approximately reproduce the ET station data on a daily and annual basis.

The value of  $RET + 8.2\%$  was found to provide the best estimate for the lake evaporation in mining pits and other shallow water bodies in the model domain. Additional details are provided in Appendix E. The lake evaporation is considered in the model by assigning a crop coefficient ( $K_c$ ) of 1.082 in the land use classified as water.



The actual evapotranspiration (ETa) is calculated for every cell of the model in the same manor as for the ECM.

The ET parameters were divided into two groups: one for land use independent parameters (see Table 2) and the other for land use dependent parameters (see **Table 4**) such as leaf area index (LAI) and root depth (Rd). Numbers in bold in Table 4 were modified in the LS ECM compared to those used in the ECM.

**Table 4.** Land use dependent ET Parameters.

| Land Use/Vegetation  | LAI       | Rd (m)      |
|----------------------|-----------|-------------|
| Citrus               | 4.5       | 1.25        |
| Pasture              | 3 - 4     | 0.75        |
| Sugar Cane & Sod     | 1 - 6     | 0.5 – 1.5   |
| Truck (Row) Crops    | 1.5 – 4.5 | 0.15 – 0.75 |
| Golf Course          | 3         | 0.75        |
| Bare Ground          | 0         | <b>100</b>  |
| Mesic Flatwood       | 1.5 - 3   | 1.219       |
| Mesic Hammock        | 2.5 - 4   | 1.219       |
| Xeric Flatwood       | 1 - 2     | 1.219       |
| Xeric Hammock        | 2 - 3     | 1.219       |
| Hydric Flatwood      | 1.5 - 3   | 1.219       |
| Hydric Hammock       | 2.5 - 4   | 1.219       |
| Wet Prairie          | 1.5 - 3   | 0.75        |
| Dwarf Cypress        | 1 - 2     | 0.75        |
| Marsh                | 2 - 4     | 0.75        |
| Cypress              | 2 - 4     | 1.524       |
| Swamp Forest         | 3 - 5     | 1.524       |
| Mangrove             | 3 - 4     | 1.824       |
| Water                | <b>0</b>  | 2.3         |
| Urban Low Density    | 2.5       | 0.6         |
| Urban Medium Density | 2         | 0.6         |
| Urban High Density   | 2         | 0.5         |

Note: LAI = Leaf Area Index, Rd = root depth

## Topography

The topography data was obtained from the SFWMD Composite Topography Dataset (SWFFS 2005). This dataset has a cell size of 100 feet and it covers the Lower West Coast part of the South Florida Water Management District. It is composited from multiple sources, which include LIDAR (Light Detection and Ranging) data, aerial/photogrammetric data, and USGS contour and spot-elevation data. This dataset was also used in the SWFFS model. The topography data provided by Lee County does not cover the entire model domain, but it matched the SFWMD when both datasets were overlaid. The original 100-ft raster data was resampled by averaging the elevation values to a 750 ft grid and then converted to a dfs2 file for use in the ECM. The resulting map is displayed in **Figure 8**. This topographic map, however, does not contain the bathymetry of mine pits and other water bodies. These features were incorporated into the topographic map during the model development.

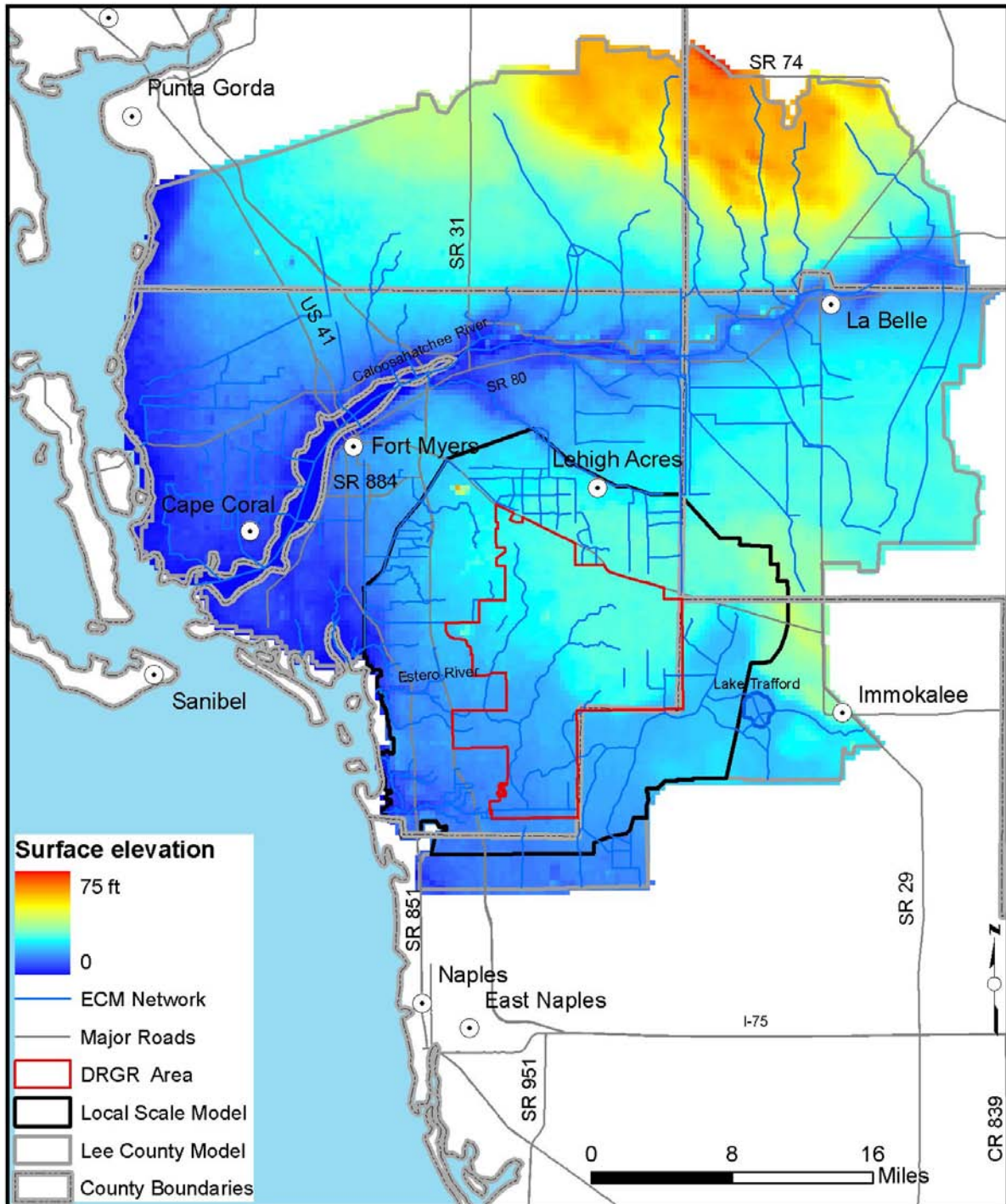


Figure 8. Model Topography in ECM.



## Refined Model Topography For LS ECM

New LIDAR topographic data was flown in 2007 and became available in 2009. This updated topographic data was incorporated into the model after calibration of the first version had been completed. The County's goal in undertaking this update was to improve the accuracy of the model.

The 2007 LIDAR topographic data set was delivered by Lee County in a raster format with a grid size resolution of 5 ft by 5 ft. The data covers only Lee County and it was not available for Collier County areas included in the model domain. Thus, the 5-ft resolution topographic data was averaged in a 750-ft resolution raster file and superimposed on the topographic map previously described in order to build the updated topographic map that covers the entire model domain. **Figure 9** shows the resulting 750-ft surface elevation map. The elevations were decreased in mining pits and lakes in accordance with the conceptualization of the water bodies.

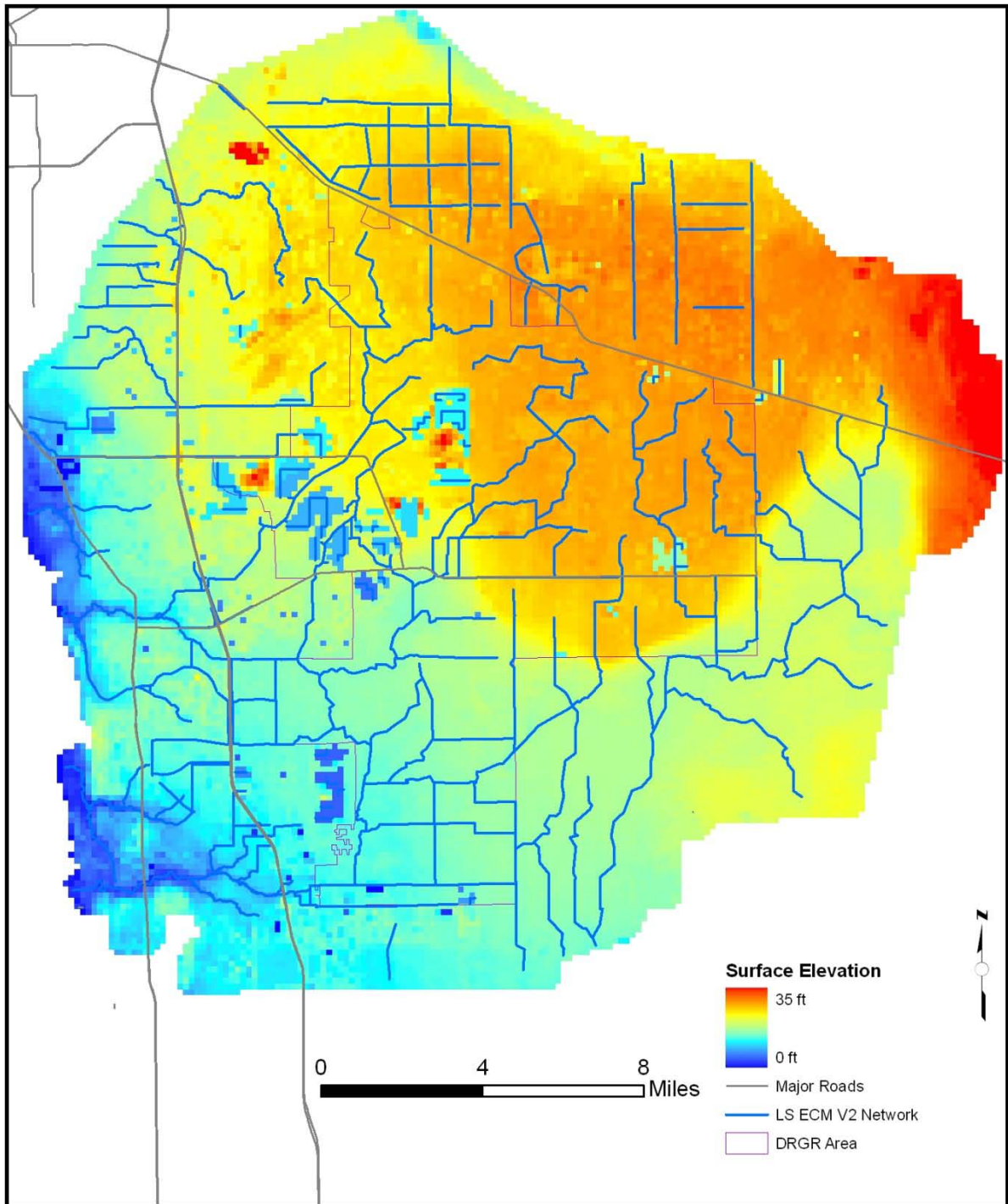


Figure 9. Model Topography in the LS ECM.



## Land Use

This study uses several land use/vegetation maps to represent predevelopment, existing, and future conditions. The existing conditions land use represents the period from 2002 to 2006. The land use data for the ECM was developed from three different sources: the SFWMD, the Southwest Florida Water Management District (SWFWMD), and Kevin L. Erwin Consulting Ecologist, Inc. (KLECE). The SWFWMD 2004 land use data was used to fill in the north western portions of the model domain which are not covered by the SFWMD 2004 land use. The 2007 land use map developed by KLECE, which covers DR/GR areal extent, was superimposed on the 2004 land use data.

The land use categories are based on Florida Land Use, Land Cover Classification System (FLUCCS). The FLUCCS codes for each land use map were grouped in more general MIKE SHE land use categories as shown in **Table 5**. Land use based parameters in the model include overland roughness coefficients, detention storage, drainage parameters, and paved runoff coefficients. The land use parameter values used in the final model are presented in **Table 5**. The land use maps were merged and converted into 750-ft and 1500-ft resolution grid files that cover the entire model domain. The 1500-ft model land use map is shown in **Figure 10**. The 750-ft land use map used in the LS ECM is presented in Appendix D.



**Table 5.** MIKE SHE land use categories and corresponding FLUCCS codes.

| Model Land Use Type  | Model Code | FLUCCS Code  |
|----------------------|------------|--|
| Citrus               | 1          | 220, 221, 222, 223   |
| Pasture              | 2          | 165, 210, 2103, 211, 212, 213, 231, 260, 2603, 261, 262, 263   |
| Sugar Cane & Sod     | 3          | 2156, 242  |
| Truck (Row) Crops    | 5          | 214, 215, 216  |
| Golf Course          | 6          | 182, 1821  |
| Bare Ground          | 7          | 153, 1603, 161, 162, 163 <sup>S</sup> , 181, 2302, 740, 7403, 742 <sup>S</sup> , 743, 744, 747, 8113, 8115, 835  |
| Mesic Flatwood       | 8          | 190, 1903, 191, 194, 310, 3102, 320, 321, 323, 330, 3302, 410, 4103, 411, 414, 429, 435, 440, 4403, 441, 442, 443, 7102, 7202, 741   |
| Mesic Hammock        | 9          | 420, 4203, 422, 423, 426, 427, 4271, 434, 437, 438, 439  |
| Xeric Flatwood       | 10         | 412, 413   |
| Xeric Hammock        | 11         | 322, 421, 432  |
| Hydric Flatwood      | 12         | 4119, 419, 624, 625  |
| Hydric Hammock       | 13         | 329, 424, 425, 428, 433, 610, 6103, 611, 6111, 618   |
| Wet Prairie          | 14         | 643, 6439  |
| Dwarf Cypress        | 15         | 6219   |
| Marsh                | 16         | 6171, 6172, 6403, 641, 6411, 6412, 644, 660  |
| Cypress              | 17         | 620, 6203, 621, 6215, 6216, 6218, 629, 745   |
| Swamp Forest         | 18         | 613, 614, 615, 616, 617, 619, 6191, 626, 628, 630, 6302, 631   |
| Mangrove             | 19         | 612, 642   |
| Water                | 20         | 163 <sup>D</sup> , 166, 184, 254, 5001, 510, 511, 512, 520, 525, 530, 533, 540, 541, 543, 560, 572, 650, 651, 653, 742 <sup>D</sup>  |
| Urban Low Density    | 41         | 110, 1102, 111, 112, 113, 118, 119, 148, 164, 180, 1802, 185, 192, 193, 240, 2403, 241, 243, 245, 246, 247, 250, 2502, 251, 255, 821, 832  |
| Urban Medium Density | 42         | 1009, 120, 1202, 121, 122, 123, 129, 144, 176, 812, 833, 834   |
| Urban High Density   | 43         | 130, 1302, 131, 132, 133, 134, 135, 139, 140, 1402, 141, 1411, 142, 1423, 146, 149, 150, 1503, 151, 152, 154, 155, 156, 159, 160, 170, 1702, 171, 183, 187, 252, 810, 8102, 811, 814, 820, 8202, 830, 8302, 8310 |

**Note:** The conversion is the same for the SFWMD and DR/GR land use maps, except in two FLUCCS codes that were noticed with super indices "S" and "D", respectively.



**Table 6.** Vegetation-based global parameters used in the ECM and LS ECM.

| MSHE Code | Land Use/Vegetation  | OL Manning's (M) | Detention Storage (inches) | Paved Runoff Fraction | Drainage Depth (ft) | Drainage Time Constant (1/day) |
|-----------|----------------------|------------------|----------------------------|-----------------------|---------------------|--------------------------------|
| 1         | Citrus               | 5.88             | 1.0                        | 0                     | 0.5                 | 0.25                           |
| 2         | Pasture              | 7.14             | 1.2                        | 0                     | 0.5                 | 0.25                           |
| 3         | Sugar Cane           | 5.88             | 1.0                        | 0                     | 0.5                 | 0.25                           |
| 5         | Truck Crops          | 5.88             | 1.0                        | 0                     | 0.5                 | 0.25                           |
| 6         | Golf Course          | 7.14             | 1.2                        | 0                     | 1.0                 | 0.25                           |
| 7         | Bare Ground          | 11.36            | 1.2                        | 0                     | 0                   | 0                              |
| 8         | Mesic Flatwood       | 5.00             | 1.2                        | 0                     | 0                   | 0                              |
| 9         | Mesic Hammock        | 3.33             | 1.2                        | 0                     | 0                   | 0                              |
| 10        | Xeric Flatwood       | 10.00            | 1.2                        | 0                     | 0                   | 0                              |
| 11        | Xeric Hammock        | 5.00             | 1.2                        | 0                     | 0                   | 0                              |
| 12        | Hydric Flatwood      | 4.00             | 1.2                        | 0                     | 0                   | 0                              |
| 13        | Hydric Hammock       | 2.50             | 1.2                        | 0                     | 0                   | 0                              |
| 14        | Wet Prairie          | 3.33             | 1.2                        | 0                     | 0                   | 0                              |
| 15        | Dwarf Cypress        | 5.00             | 1.2                        | 0                     | 0                   | 0                              |
| 16        | Marsh                | 2.33             | 1.2                        | 0                     | 0                   | 0                              |
| 17        | Cypress              | 3.33             | 1.2                        | 0                     | 0                   | 0                              |
| 18        | Swamp Forest         | 2.50             | 1.2                        | 0                     | 0                   | 0                              |
| 19        | Mangrove             | 5.00             | 1.2                        | 0                     | 0                   | 0                              |
| 20        | Water                | 16.67            | 1.2                        | 0                     | 0                   | 0                              |
| 41        | Urban Low Density    | 7.14             | 1.0 (0.13)                 | 0.05                  | 0.5 (1.0)           | 0.25 (0.5)                     |
| 42        | Urban Medium Density | 8.33             | 0.4 (0.13)                 | 0.15 (0.22)           | 0.75 (1.0)          | 0.35 (0.5)                     |
| 43        | Urban High Density   | 9.01             | 0.13 (0.13)                | 0.45 (0.70)           | 1.0 (1.0)           | 0.5                            |

Note: OL Manning's M is the reciprocal of the conventional Manning's Roughness Coefficient *n*. Values are shown in parenthesis when used differently in the ECM.

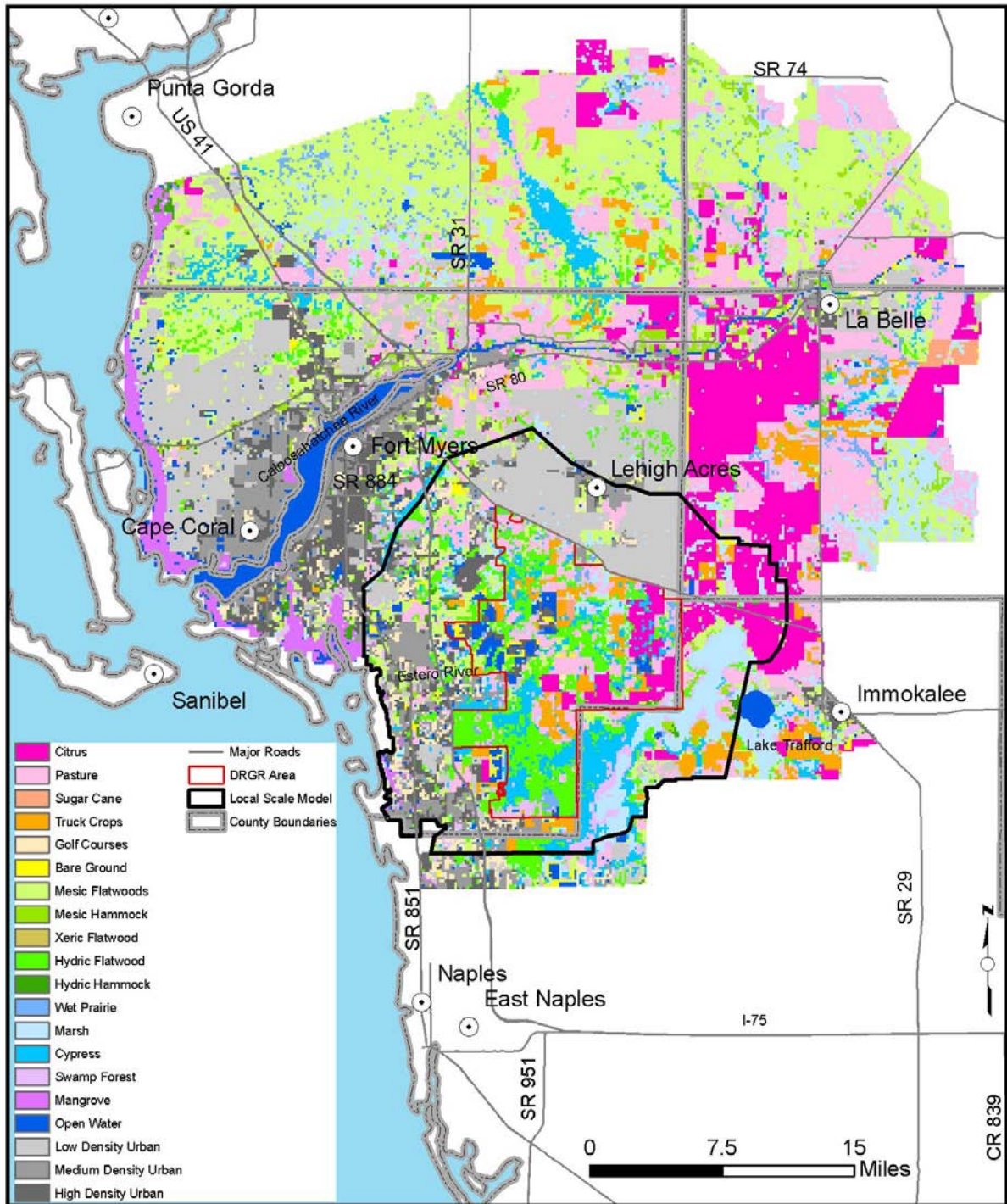


Figure 10. Existing Conditions Land Use Map.



## Soils

The unsaturated zone in South Florida is shallow and the soils are sandy and highly permeable, except in wetlands where a surface deposit of fine-grained sediment may be present. Soil porosities are typically high for sandy soils in South Florida and it has been determined in previous MIKE SHE/MIKE 11 models developed in southwest Florida. Those models use the explicit gravity drainage unsaturated zone option, which does not consider the capillary pressure head term, but it is adequate for long-term regional applications. The texture and properties of soils vary on both local and regional scales. Soil types for the SWFFS area were classified into six different hydrologic response groups, shown in **Figure 11**. This soil classification was based on the predevelopment vegetation map prepared by the SFWMD in 2003, and better represents the conditions of the SWFFS area. The soil classification used in the SWFFS area and associated properties are summarized in **Table 7**.

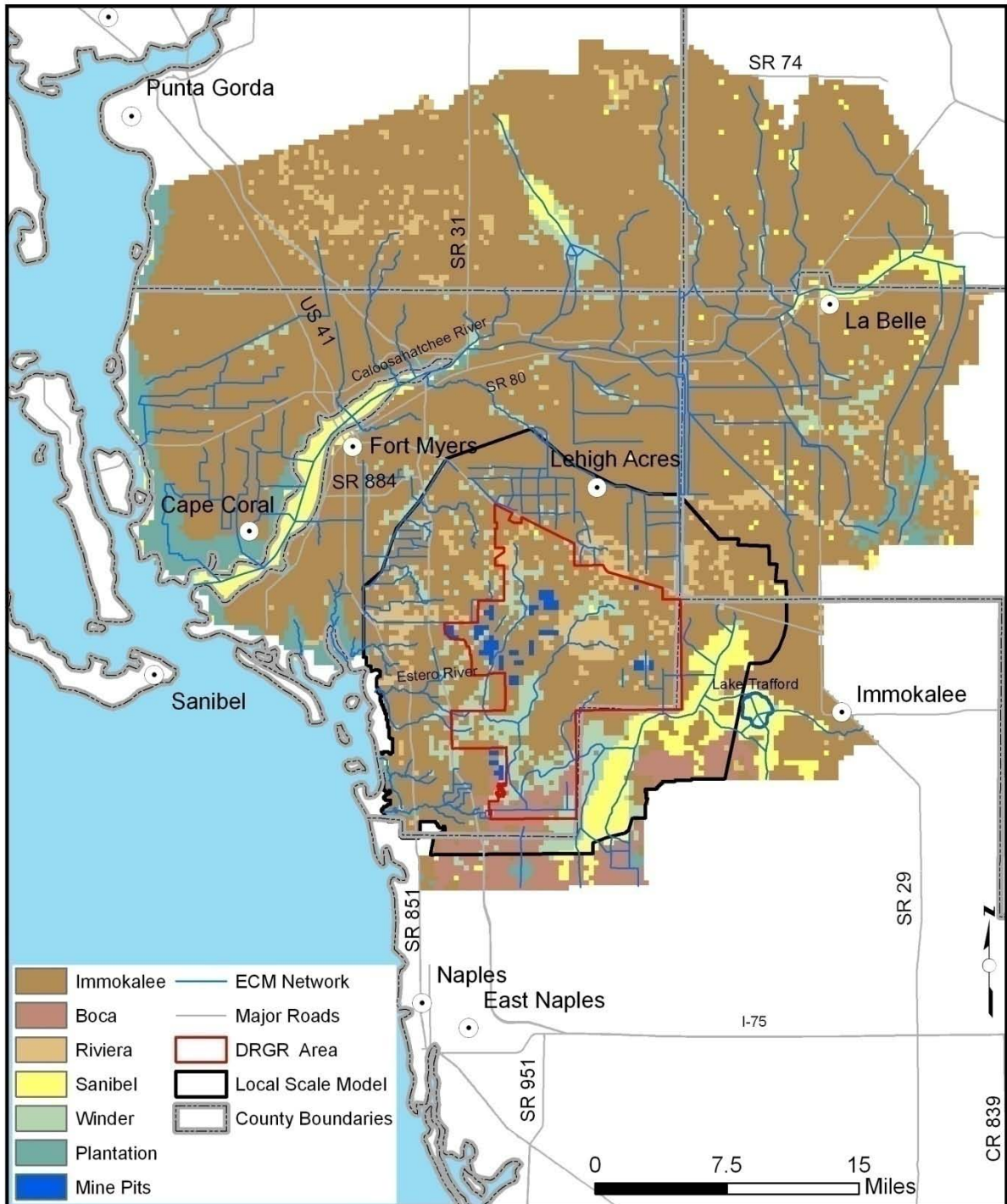


Figure 11. Soils Map.



**Table 7.** Soil Parameters.

| MSHE Code | Soil Type       | Depth interval (m) | Saturated Hydraulic Conductivity Ks (m/s) | Saturated Water Content $\Theta_s$ | Water Content at Field Capacity $\Theta_{fc}$ | Water Content at Wilting Point $\Theta_w$ | Residual Water Content $\Theta_r$ |
|-----------|-----------------|--------------------|---|------------------------------------|---|---|-----------------------------------|
| 1         | Immokalee A1    | (0.0-0.1)          | 2.00E-4                                   | 0.420                              | 0.15  | 0.013                                     | 0.010                             |
|           | Immokalee AE    | (0.1-0.23)         | 1.10E-4                                   | 0.420                              | 0.15  | 0.020                                     | 0.031                             |
|           | Immokalee E1    | (0.23-0.41)        | 8.60E-5                                   | 0.390                              | 0.14  | 0.020                                     | 0.015                             |
|           | Immokalee E2    | (0.41-0.91)        | 1.00E-4                                   | 0.380                              | 0.14  | 0.010                                     | 0.010                             |
|           | Immokalee Bh1   | (0.91-1.27)        | 1.20E-6                                   | 0.380                              | 0.33  | 0.057                                     | 0.031                             |
|           | Immokalee Bh2   | (1.27-1.4)         | 6.10E-6                                   | 0.380                              | 0.28  | 0.050                                     | 0.043                             |
|           | Immokalee Bw/Bh | (1.4-30)           | 7.50E-5                                   | 0.380                              | 0.20  | 0.030                                     | 0.020                             |
| 2         | Boca A          | (0.0-0.08)         | 1.10E-4                                   | 0.487                              | 0.11  | 0.040                                     | 0.029                             |
|           | Boca E1         | (0.08-0.23)        | 9.70E-5                                   | 0.460                              | 0.11  | 0.034                                     | 0.023                             |
|           | Boca E2         | (0.23-0.36)        | 8.00E-5                                   | 0.408                              | 0.09  | 0.024                                     | 0.015                             |
|           | Boca Bw         | (0.36-0.64)        | 5.40E-5                                   | 0.396                              | 0.10  | 0.009                                     | 0.006                             |
|           | Boca Btg        | (0.64-30)          | 8.30E-6                                   | 0.355                              | 0.33  | 0.122                                     | 0.071                             |
| 3         | Riviera Ap      | (0-0.15)           | 3.64E-5                                   | 0.528                              | 0.23  | 0.049                                     | 0.020                             |
|           | Riviera A       | (0.15-0.28)        | 4.20E-5                                   | 0.520                              | 0.22  | 0.047                                     | 0.040                             |
|           | Riviera E1      | (0.28-0.41)        | 5.00E-5                                   | 0.460                              | 0.12  | 0.022                                     | 0.001                             |
|           | Riviera E2      | (0.41-0.64)        | 5.50E-5                                   | 0.400                              | 0.06  | 0.003                                     | 0.001                             |
|           | Riviera Bw      | (0.64-0.74)        | 3.50E-5                                   | 0.380                              | 0.06  | 0.004                                     | 0.001                             |
|           | Riviera Btg     | (0.74-30)          | 2.50E-7                                   | 0.380                              | 0.32  | 0.102                                     | 0.080                             |
| 4         | Sanibel Oa1     | (0-0.12)           | 2.00E-5                                   | 0.752                              | 0.72  | 0.207                                     | 0.200                             |
|           | Sanibel Oa2     | (0.12-0.15)        | 7.80E-5                                   | 0.730                              | 0.69  | 0.205                                     | 0.100                             |
|           | Sanibel A1      | (0.15-0.23)        | 9.40E-5                                   | 0.510                              | 0.39  | 0.025                                     | 0.010                             |
|           | Sanibel A2      | (0.23-0.3)         | 1.70E-4                                   | 0.410                              | 0.17  | 0.013                                     | 0.010                             |
|           | Sanibel C1      | (0.3-0.66)         | 1.40E-4                                   | 0.370                              | 0.09  | 0.013                                     | 0.010                             |
|           | Sanibel C2      | (0.66-30)          | 1.10E-4                                   | 0.380                              | 0.08  | 0.011                                     | 0.010                             |
| 5         | Winder A1       | (0.0-0.08)         | 3.60E-5                                   | 0.374                              | 0.26  | 0.024                                     | 0.014                             |
|           | Winder E        | (0.08-0.33)        | 5.00E-5                                   | 0.370                              | 0.15  | 0.008                                     | 0.004                             |
|           | Winder B/E      | (0.33-0.41)        | 1.60E-6                                   | 0.328                              | 0.23  | 0.048                                     | 0.027                             |
|           | Winder Btg      | (0.41-0.58)        | 7.40E-6                                   | 0.430                              | 0.40  | 0.153                                     | 0.101                             |
|           | Winder BCg      | (0.58-0.74)        | 7.40E-6                                   | 0.340                              | 0.26  | 0.050                                     | 0.028                             |
|           | Winder C1       | (0.74-0.89)        | 1.00E-4                                   | 0.332                              | 0.27  | 0.038                                     | 0.021                             |
|           | Winder C2       | (0.89-1.04)        | 5.00E-6                                   | 0.347                              | 0.23  | 0.042                                     | 0.024                             |
|           | Winder C3       | (0.89-30)          | 1.90E-5                                   | 0.358                              | 0.31  | 0.107                                     | 0.062                             |
| 6         | Plantation Oap  | (0-0.23)           | 1.00E-4                                   | 0.770                              | 0.66  | 0.200                                     | 0.150                             |
|           | Plantation A/E  | (0.23-0.48)        | 8.40E-5                                   | 0.491                              | 0.19  | 0.029                                     | 0.022                             |
|           | Plantation Bw   | (0.48-30)          | 1.20E-4                                   | 0.392                              | 0.10  | 0.003                                     | 0.002                             |

## Hydrogeology

The major hydrogeologic units in southern Florida in descending order are: the Surficial Aquifer System (SAS), the Intermediate Aquifer System (IAS), and the Floridan Aquifer System (FAS). According to Missimer and Martin (2001), Lee County has more individual aquifers with unique hydraulic properties within these systems than any other region in Florida, many of these having high transmissivities. The Water Table Aquifer (SAS), the Sandstone Aquifer (IAS), and the Lower Hawthorn Aquifer (FAS) are the aquifers with the highest production zones for public supply and irrigation. The Lee County MIKE SHE model includes the Water Table Aquifer and the Sandstone Aquifer, but excludes the FAS.

## Saturated Zone Model

The saturated zone groundwater model in MIKE SHE is fully three-dimensional and thus, allows for the spatial distribution of the hydrogeologic unit thickness, horizontal and vertical hydraulic conductivities, and storage parameters. The geologic model can include both geologic layers and geologic lenses. Geologic layers cover the entire model domain whereas lenses exist in only parts of your model area. Both geologic layers and lenses are assigned the geologic parameters mentioned above. The numerical model, i.e. computational layers, is defined by the user to assign an appropriate vertical discretization for the model. The parameters of the layers and lenses that are part of a single computational layer are interpolated into the numerical grid (DHI 2008).

The geologic characterization in the ECM includes essentially the same hydrogeologic units used for the SWFFS model, plus the addition of a conceptual lens to represent the mining pits. The geologic model consists of three geologic layers and three lenses. The geologic layers are the Holocene-Pliocene, the Lower Tamiami and the Peace River Sandstone units, which correspond to the Water Table Aquifer (SAS), Lower Tamiami Aquifer (SAS), and the Sandstone Aquifer (IAS), respectively. The geologic lenses are the Bonita Spring Marl (SAS) and the Upper Peace River (IAS) confining units. The numerical model is divided initially into three computational layers (see **Figure 12**) defined as:

- Computational Layer 1 – Holocene-Pliocene
- Computational Layer 2 – Bonita Spring Marl confining unit + Lower Tamiami Aquifer
- Computational Layer 3 – Upper Peace River confining unit + Sandstone Aquifer.

The Mining Pit conceptual lens in some cases extends down to the upper portion of computational layer 3. The MIKE SHE preprocessing tool converts all the hydrogeological parameters specified for all the geological layers and lenses into the equivalent parameters for the computational layers.

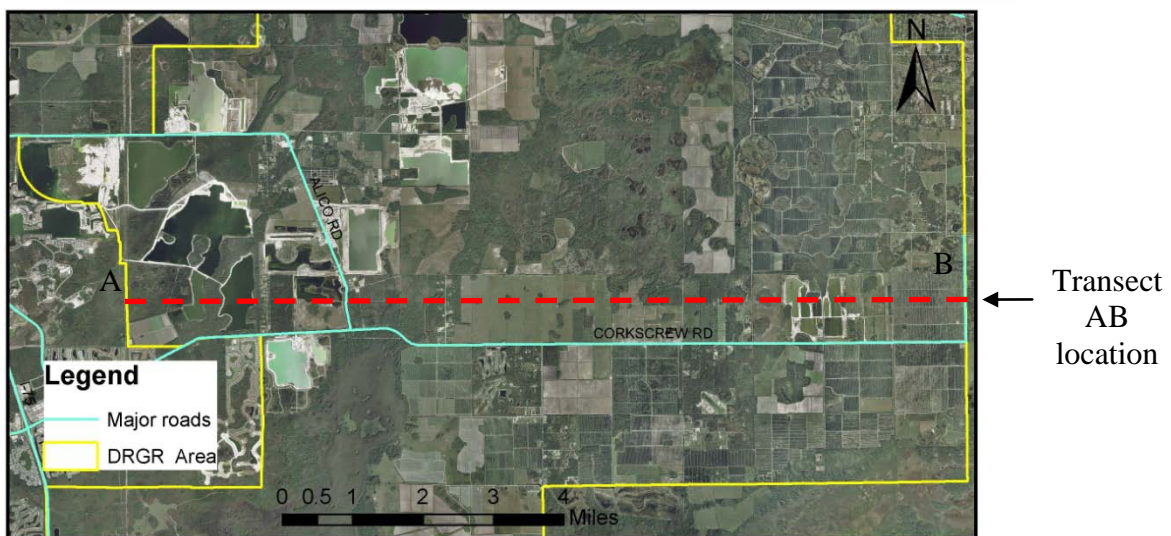
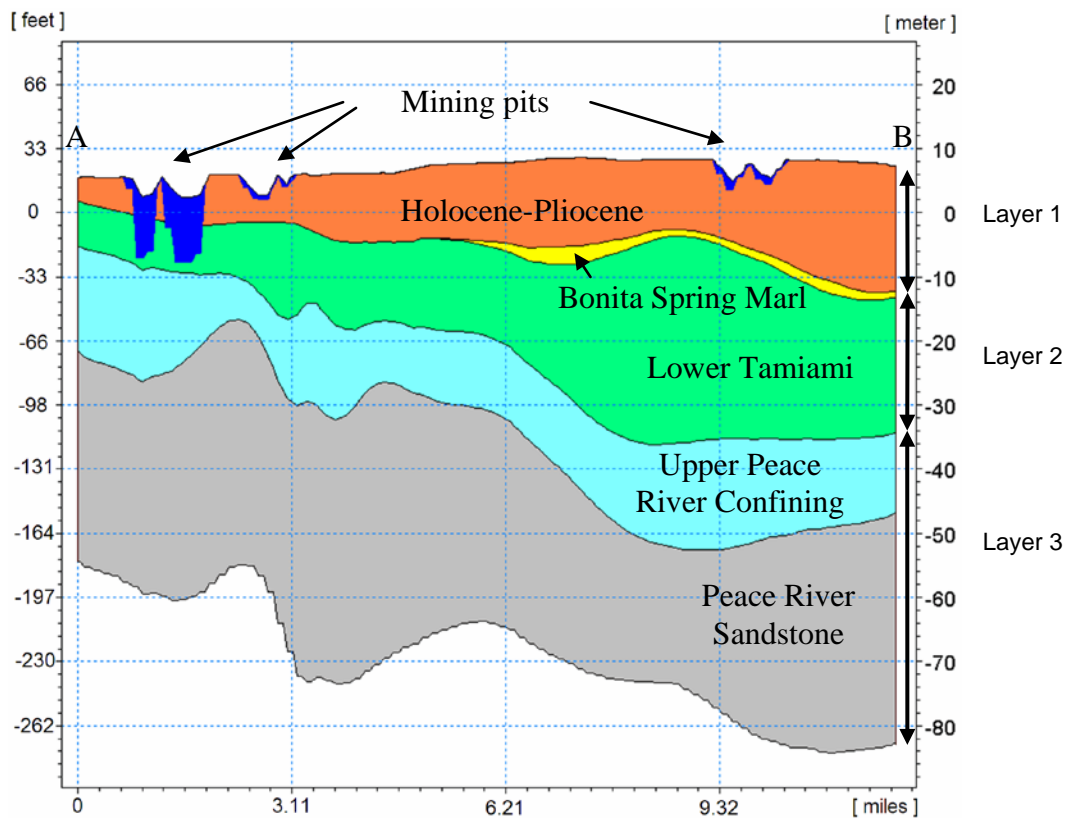


**Figure 12.** Geologic Model and Computational Layers along a transect in the DR/GR Area. **Note:** blue color in above profile corresponds to the extent of the mining pit conceptual lenses and does not include the water above it, which is conceptualized in the overland component of the model.



## Groundwater Boundaries

The Local Scale and Lee County model boundaries are shown in **Figure 13**. The boundary conditions in the groundwater layers at the eastern and southern boundaries were extracted from the SWFFS model results for the 1995-1999 simulation period. The time-varying groundwater heads from the SWFFS were used to calculate the averaged heads for every five Julian days for all simulation years in the three groundwater layers. Those averaged heads for a one year period are extended periodically and used for all the years in the ECM simulation period in order to simulate seasonal changes at the eastern and southern boundaries. The northern and western boundaries coincide with the ones in SWFFS model boundaries and thus, the ECM uses the same type of boundary conditions that was used in the SWFFS model. The northern boundary was set as zero-flux boundary and the western (coastal) boundary was set to a constant head value approximate to the mean sea level elevation (0 m NAVD88).

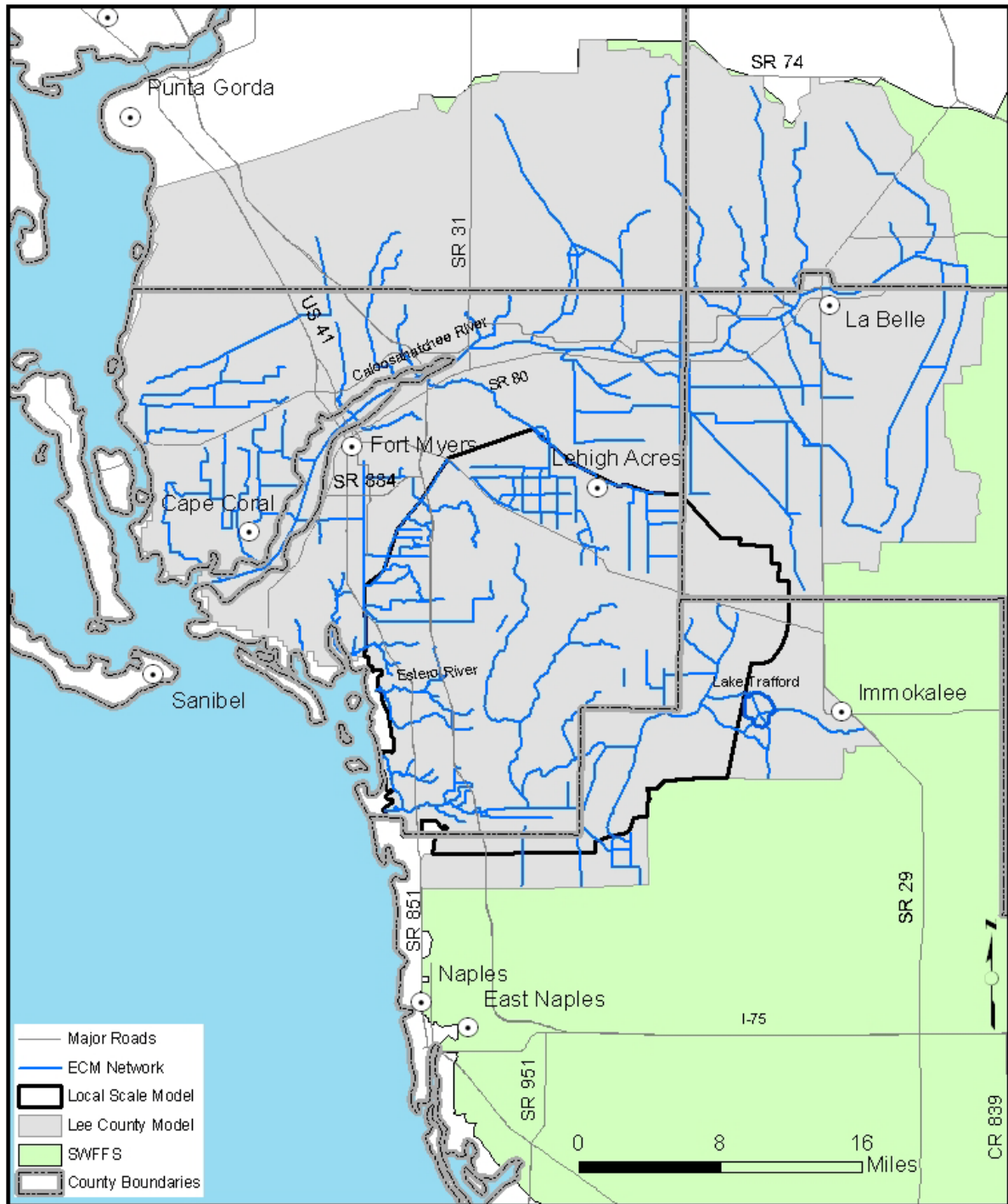


**Figure 13. Model Boundaries.**



## Groundwater Withdrawals

Two types of groundwater extraction wells are included in the model: municipal potable water supply wells and domestic self supply wells. The Pumping Wells Module in MIKE SHE uses a well database in which the location, the depths of the screen interval, and the pumping rates for wells are specified. All of the municipal water supply wells are included in this module. The Irrigation Module, on the other hand, can be used to represent groundwater withdrawals and water from other sources that are applied as irrigation water in the model. The domestic self supply wells are represented in the irrigation module as an irrigation source.

### Municipal Water Supply

Lee County provided the most current locations and depths of the potable water supply wells. This information was used to update the well data from the SWFFS model. The deep wells that extract water from the Hawthorn and Floridan aquifers were not added to the well database since these geological layers are not included in the model.

The pumping wells included in the model are listed in **Table 8** and the well locations are shown in **Figure 14**. The monthly extraction rates were obtained from the SFWMD Public Record Office for the period from year 2000 to 2007. The pumping rates for individual wells were used if it was available. If the data was only available for individual wells, the total rate for the well field was used and a fraction of the total pump rate for each well based on the number of wells in a given well field was applied. There was no data reported for individual wells at two well fields (CCI and GES shown in Table 8) and the total pumping rate was distributed uniformly in each well. For the well labeled as WF, the nominal maximum rate in the permit was applied.

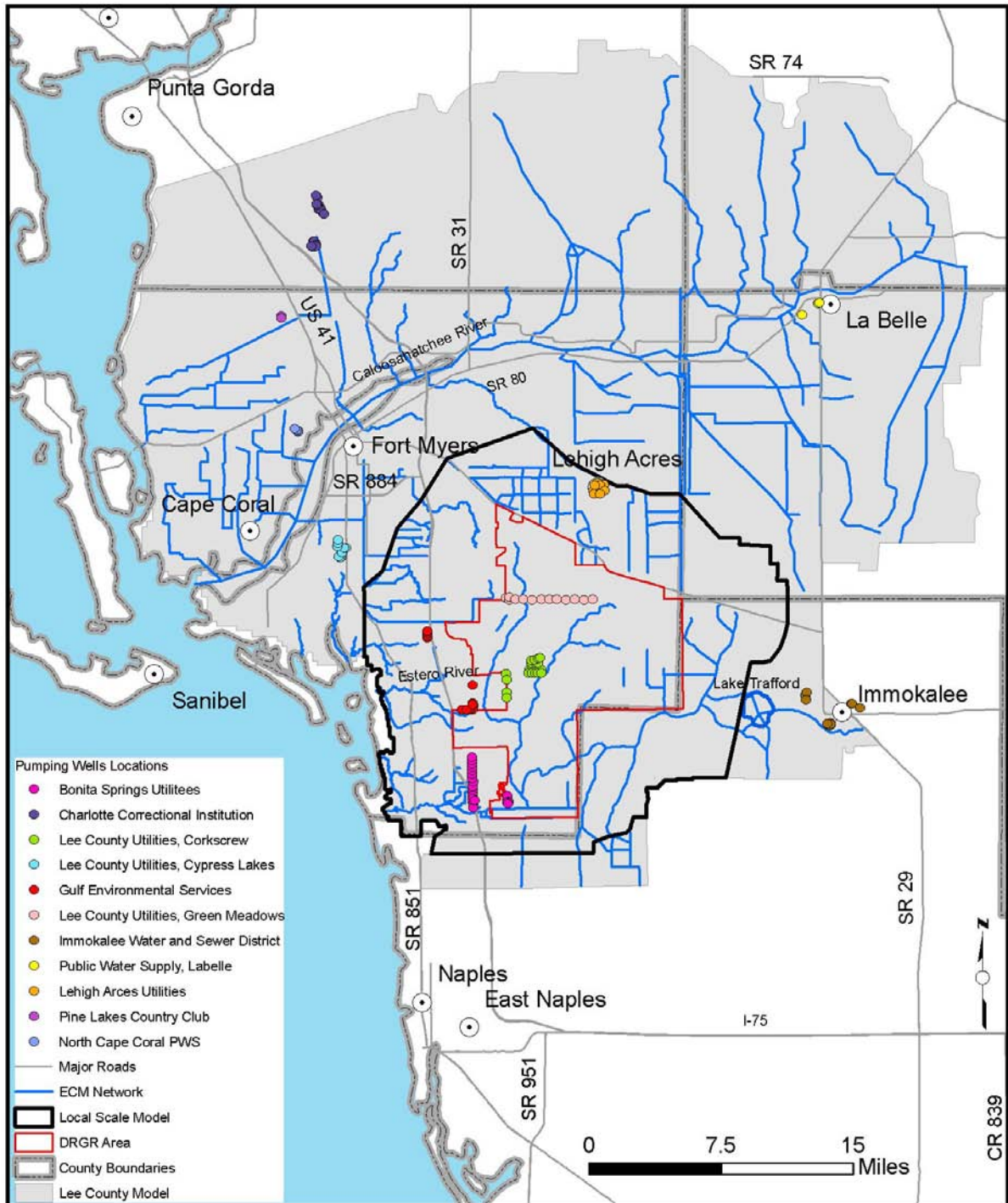


**Figure 14.** Municipal potable water supply well locations.

**Table 8.** Municipal potable water supply well included in the MIKE SHE model.

| Permit Number | Project Name                                   | ID    | Well Numbers  |
|---------------|--|-------|---|
| 08-00047-W    | Charlotte Correctional Institution             | CH-   | 218,219,220,221,222,227,228,229,230,231,1,2,3,4,5,6,7                                     |
| 11-00013-W    | Immokalee Water & Sewer District               | IWSD  | 7,8,9,10,10A,11,12,13,102,103,104,201,202,203,  |
| 26-00105-W    | Public Water Supply, Labelle Wellfield         | LAB   | 5,7,10,11   |
| 36-00003-W    | Lee County Utilities, Green Meadows            | GM-   | 1,1D,2,2A,3,3A,3B,4,4A,5,5A,6,6A,7,7A,8,8A,9,9A,10,10A,11,11A,12,12A,13,13A               |
|               | Lee County Utilities, Corkscrew                | COR   | 2,3,4,5,6,7,8,9,10,11,12,13,14,15,16,18,19,20,21,22,23,24,25D,25S,26D,26S,27D,27S,28D,28S |
|               | Lee County Utilities, Cypress Lakes            | CP-   | 2,3,4,6,7,8,14,15,17  |
| 36-00008-W    | Bonita Springs Utilities                       | BSU   | 1,2,3,4,5,6,7,8,9,10,11,12,13,14,15,16,17,18,19,20,21,22,23,24                            |
| 36-00081-W    | Pine Lakes Country Club                        | PL-   | 1,2   |
| 36-00122-W    | Gulf Environmental Services, Pinewoods         | GES   | 1,2,3,4,5,6,7,8,9,10,11,12,19,22  |
|               | Gulf Environmental Services, Bartow            |       | 13,14,15,16,16A   |
| 36-00152-W    | Waterway Estates, North Cape Coral PWS         | WENCC | 1,2,4,12  |
| 36-00166-W    | Lehigh Acres Utilities, Florida Water Services | LAC   | 1,2,3,4,5,6,7,8,9A,10,19,20,21  |
| 36-02986-W    | Waldee Farm                                    | WF-   | 3   |

### Domestic Self-Supply Wells

The domestic self-supply (DSS) wells were represented in the Irrigation Module. The method used to represent these wells is described below in the urban irrigation section.

### **Irrigation**

The Irrigation Module in MIKE SHE includes two main components: Irrigation Command Areas (ICAs), which is a map that indicates the cells in the model where irrigation is applied, and Irrigation Demand, where the criteria used to start and stop irrigation are specified. For each command area, several sources of irrigation (wells, rivers, external) and types of application (sprinkle, drip, sheet) can be specified. The Irrigation demand is based on “the maximum allowed global deficit” option. Irrigation is activated when the water saturation in the soil is lower than a land-use dependent value between the wilting point and the field capacity of the soil, and it stops when the field capacity is reached. The Irrigation Command Areas for the ECM are shown in **Figure 15**. The ICAs specified in the model are either agricultural or urban areas.

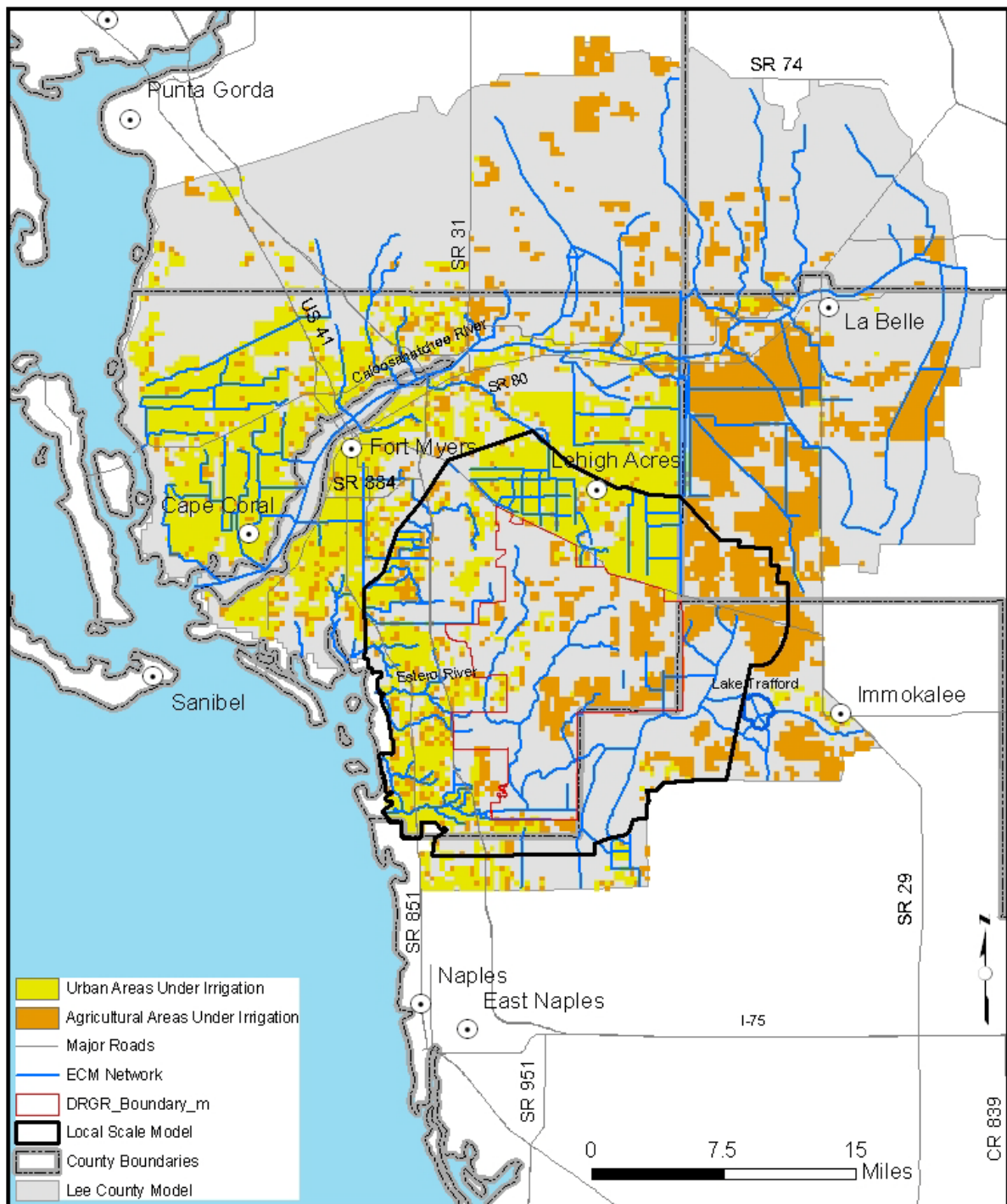


**Figure 15. Irrigation Command Areas.**



Some of the ECM irrigation setup in the model was taken from the SWFFS model. ICAs that rely primarily upon surface water supply from the C-43 Canal were not modified. These areas are mainly located in the Freshwater Caloosahatchee River Basin portion of the model and upstream of the S-79 structure. Some of the irrigation setup was updated to account for land use changes after year 2000. For example, agricultural irrigation was removed from the model or modified in areas where agricultural uses have converted to other uses.

For the LS ECM, the 1,500-ft resolution map with ICA codes was converted to a 750-ft resolution and the maximum pumping rates per cell for shallow well sources were decreased by four, accordingly.

### **Agricultural Irrigation**

For agricultural lands located within and near the DR/GR Area, the most current permit information was obtained from the Florida Water Management Districts Permitting Portal (<http://webapub.sjrwmd.com/agws/permitportal>). For the areas where current or active permits were not available, the most recent (expired) permit was used. The permit information was used to update the source of irrigation (usually one groundwater well with a given screened interval) and the maximum pumping rate allowed. The actual amount of irrigation for a given area at a given model time step depends on the calculated soil moisture content. The soil moisture irrigation criteria differ depending of the type of crop.

Many of the row crop farms utilize flood irrigation methods. The drip irrigation method, in which the water is added directly to the ground surface of the irrigation (ICA) cells, was applied for those areas. Although there is a flood (sheet) irrigation method available in MIKE SHE, it is designed for finer grid scale applications where the flood routing can be more accurately represented. For other types of crops and for urban areas, the sprinkle irrigation method is used. The difference of the water applied as sprinkle (which is incorporated to the rainfall component) and as drip (which is placed on the ground surface) is that the former can have vegetative interception losses.

### **Urban Irrigation**

Domestic Self-Supply (DSS) wells were specified in the model as part of the irrigation processes. This method was selected because irrigation makes up approximately 75 percent of total usage for domestic wells. Lee County provided the location of domestic self supply wells, which was used to determine the number of domestic self supply wells in each 1,500-ft grid cell as shown in **Figure 16**. The County also provided the information of the aquifers used by each DSS well that was processed to assign them an appropriate screen interval. DSS wells were grouped according to location and type of well usage. The green



polygons in Figure 16 show the general area of each group of DSS wells included in the model. The ICAs in the model within each area are the grid cells containing wells.

In Figure 16 the information provided by the County about the DSS wells in the City of Cape Coral did not include all wells. However, a large amount of them are deep wells extracting from the Hawthorn Aquifer (outside the model domain).

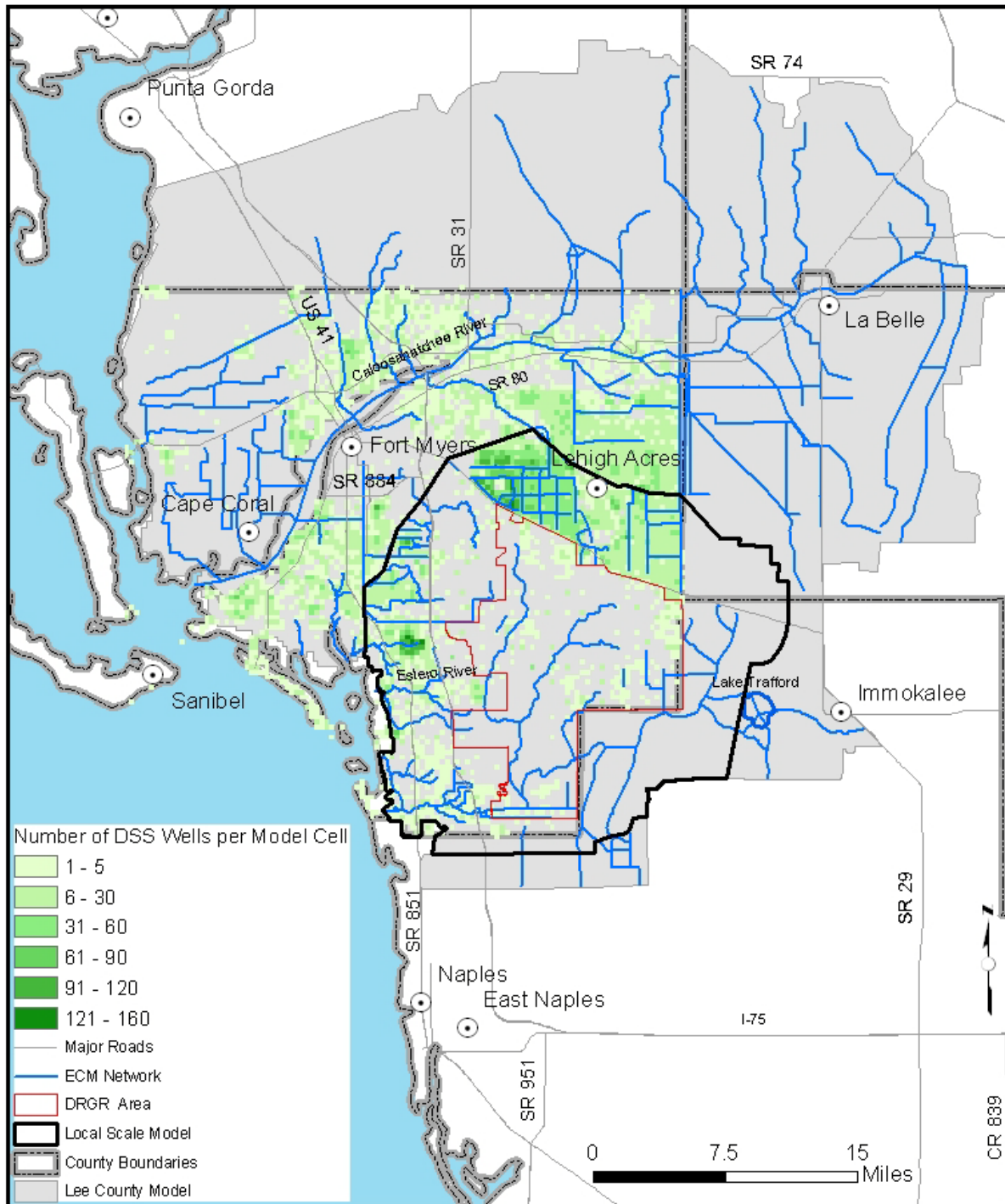


**Figure 16.** Domestic Self Supply Well Distribution.

A detailed description of the domestic self-supply ICAs defined in the model is provided in **Table 9**.



**Table 9.** Summary of ICAs defined to represent the water consumption from DSS wells.

| ICA code | Total No. DSS wells | No. 1,500-ft cells | Include potable? | Well permitting region                           | Most used aquifer | Screen interval (ft) |
|----------|---------------------|--------------------|------------------|--|-------------------|----------------------|
| 545      | 58                  | 3                  | Y                | East Lee County                                  | Sandstone         | 65 - 98              |
| 549      | 108                 | 103                | Y                | Bonita Springs                                   | Sandstone         | 65 - 98              |
| 551      | 7                   | 15                 | Y                | Bonita Springs                                   | Lower Tamiami     | 65 - 98              |
| 557      | 98                  | 1                  | Y                | East Lee County                                  | Sandstone         | 65 - 98              |
| 575      | 135                 | 3                  | Y                | East Lee County                                  | Sandstone         | 65 - 98              |
| 579      | 160                 | 213                | N                | Bonita Springs                                   | Lower Tamiami     | 65 - 98              |
| 602      | 51                  | 4                  | Y                | East Lee County                                  | Sandstone         | 80 - 130             |
| 606      | 89                  | 33                 | Y                | East Lee County                                  | Sandstone         | 65 - 98              |
| 607      | 18                  | 40                 | N                | San Carlos/Estero                                | Sandstone         | 65 - 98              |
| 610      | 279                 | 26                 | N                | East Lee County                                  | Sandstone         | 65 - 98              |
| 612      | 621                 | 116                | N                | San Carlos/Estero and Bonita Springs (Coastline) | Lower Tamiami     | 65 - 98              |
| 626      | 69                  | 39                 | N                | San Carlos/Estero                                | Sandstone         | 65 - 98              |
| 1121     | 44                  | 72                 | N                | Fort Myers                                       | Sandstone         | 65 - 98              |
| 1140     | 47                  | 67                 | N                | North Cape Coral                                 | Lower Tamiami     | 30 - 65              |
| 1158     | 684                 | 18                 | Y                | North Fort Myers                                 | Water Table       | 0 - 35               |
| 1159     | 286                 | 127                | N                | Fort Myers and South Fort Myers                  | Sandstone         | 65 - 98              |
| 1164     | 3184                | 335                | N                | South Fort Myers                                 | Sandstone         | 65 - 98              |
| 1166     | 479                 | 22                 | N                | Six Mile Cypress                                 | Sandstone         | 65 - 98              |
| 1168     | 750                 | 77                 | Y                | Fort Myers                                       | Sandstone         | 80 - 130             |
| 1171     | 1269                | 67                 | N                | Six Mile Cypress                                 | Sandstone         | 80 - 130             |
| 1172     | 2714                | 98                 | Y                | San Carlos/Estero                                | Sandstone         | 80 - 130             |
| 1173     | 863                 | 155                | Y                | North Fort Myers                                 | Mid Hawthorne     | 160 - 230            |
| 1174     | 106                 | 43                 | Y                | Cape Coral                                       | Mid Hawthorne     | 160 - 230            |
| 1175     | 15999               | 379                | Y                | Lehigh Acres                                     | Sandstone         | 80 - 130             |
| 1178     | 1168                | 198                | Y                | East Fort Myers                                  | Sandstone         | 80 - 130             |
| 1179     | 11455               | 674                | Y                | Lehigh Acres                                     | Sandstone         | 80 - 130             |
| 1180     | 366                 | 59                 | Y                | North Fort Myers                                 | Mid Hawthorne     | 160 - 230            |
| 1186     | 708                 | 109                | N                | Cape Coral                                       | Mid Hawthorne     | 160 - 230            |
| 1190     | 381                 | 147                | Y                | Cape Coral                                       | Mid Hawthorne     | 160 - 230            |
| 1193     | 1216                | 118                | Y                | Alva   | Sandstone         | 80 - 130             |
| 1194     | 207                 | 59                 | N                | Cape Coral                                       | Lower Tamiami     | 30 - 65              |

The following assumptions have been made in order to obtain an estimate of the average consumption of a domestic self-supply (DSS) well:

- I. Maximum irrigation water demand is assumed to be 20 gallons per minute per pumping zone, 4 zones per house and each zone operated for 45 minutes per day. The total irrigation rate per house equals  $(20 \times 45 \times 4) = 3,600$  gallons per house per day. Each house irrigates twice weekly; either Wednesday and Saturday, or Thursday and Sunday in accordance with Lee County regulations. Each house applies 75 percent of irrigation water between 12 am and 6 am; and 25 percent between 6 pm and midnight. The irrigation



pumping rate of one average well is then the average of the two possible schedules, which gives the application of the half rate, four times a week.

- II. Potable water demand is assumed to be 100 gallons/per person/per day for uses like cooking, cleaning, and bathing with 3 people per household. The assumed consumption per capita per day is in the range from 100 to 130 reported by (Hammer and Hammer, 2001). The majority of usage (2/3) is assumed to occur in the morning between 6 am and noon while the remainder of usage (1/3) is assumed to occur in the evening between 6 pm and midnight.

Note that the maximum irrigation water demand is equal to or higher than the current irrigation consumption. The current consumption is in general higher during the dry season than during the wet season. The weekly time series for the maximum pumping rate of an average domestic self-supply well obtained from previous assumptions is presented in **Figure 17**. Two cases are considered corresponding to the use of DSS water for all the needs or just for irrigation in areas where the potable water demand is supplied from municipal wells. The weekly period in Figure 17 is then extended over the whole simulation period. The time series created has an average maximum pumping rate from a domestic self-supply well of 1029 gal/day ( $4.51 \times 10^{-5} \text{ m}^3/\text{s}$ ) for irrigation only and of 1329 gal/day ( $5.82 \times 10^{-5} \text{ m}^3/\text{s}$ ) including potable water consumption.

The maximum groundwater extraction rates for each ICA are found by multiplying the appropriate extraction time series (irrigation only or irrigation plus potable supply) for one averaged well by the total number of wells within the ICA. The extraction rate (or demand below this limit) is determined automatically by the model based on the soil moisture content.

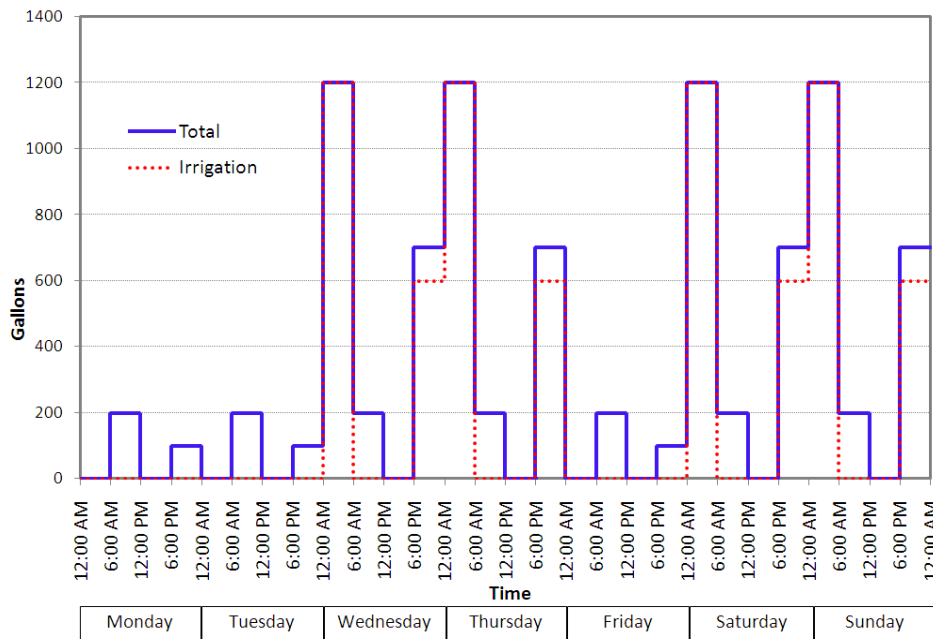


**Figure 17.** Maximum weekly consumption for a DSS well. The total volume includes irrigation and potable water supply.

## Surface Water Model

Surface water is modeled in the overland component of MIKE SHE and in MIKE 11. The Overland Flow component solves the 2-dimensional diffusive wave approximation of the Saint Venant equations and MIKE 11 solves the fully dynamic Saint Venant equations in one dimension. The MIKE SHE overland component routes the surface runoff to the reaches defined in MIKE 11. MIKE SHE also has a drainage component that can route the drainage from urban or agricultural areas to the MIKE 11 canals.

## ECM Development

### MIKE 11 Model

The surface water model includes an extensive network of primary and secondary canals with many hydraulic structures, natural sloughs, rivers, and lakes. The surface water network is modeled using DHI's one-dimensional hydraulic model, MIKE 11. Inputs for the MIKE 11 model consist of the river network path, channel cross-sections, boundary conditions, and bed resistance. Moreover, structures such as culverts, dams, bridges and control gates that may alter river flows and stages are specified as input to the model. The ECM MIKE 11 network and structures is shown in **Figure 18**.

The network was built using the SWFFS canal network as the starting point and adding secondary canals and structures from the EIC, BCB and TCRB sub-regional models to build the BLM. In addition, secondary canals and structures were added or updated from the

ECWCD model. Finally, the structures in Alico and Corkscrew roads were also updated or included based on the information received from Lee County.

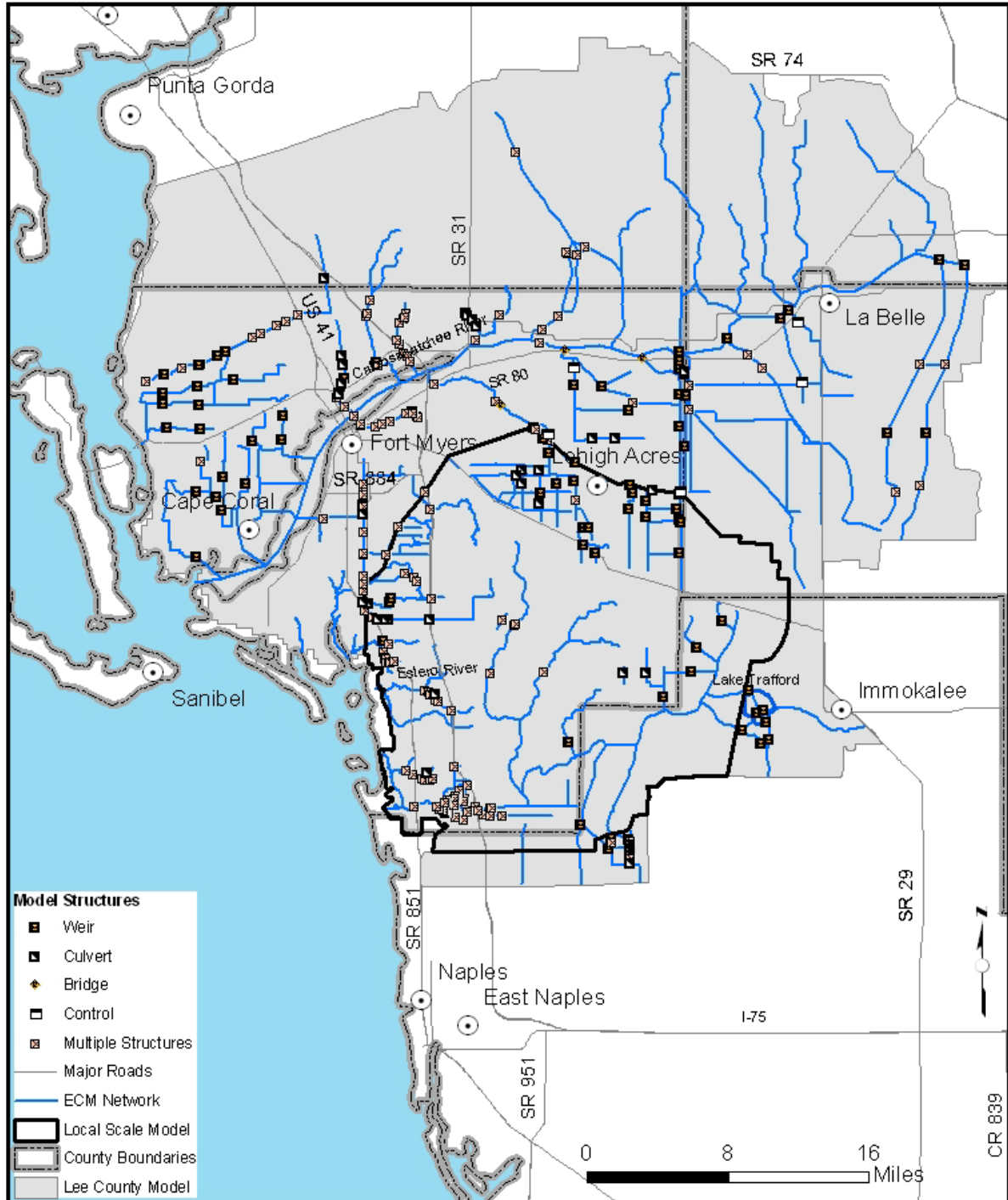


**Figure 18.** MIKE 11 Network and Structures in the ECM.



### MIKE SHE and MIKE 11 Interaction

Water flow is exchanged dynamically between the MIKE 11 hydraulic model and the MIKE SHE hydrologic model. The MIKE 11 canals exchange water with the underlying aquifer, driven by the head gradient and controlled by either the aquifer conductivities or by a river lining leakage coefficient, or a combination of both. Runoff from the MIKE SHE overland surface is driven by topographic gradient and flows into MIKE 11 in places where both the river bank elevations and the water levels are lower than the water elevations in adjacent MIKE SHE cells. MIKE 11 branches also receive water from the drainage component of MIKE SHE.

Flooding from the MIKE 11 rivers, lakes or canals to the overland surface in MIKE SHE is allowed to occur where specified. The flooding method used for the ECM is the flood code mapping option. This method is appropriate for modeling lakes, wide rivers and sloughs. The flood code approach ensures that the volume of water is not double counted in the same spatial location that the branches and the flooded MIKE SHE cells occupy if the extents of the specified flood coded cells are consistent with the cross section widths of the MIKE 11 branches. **Figure 19** shows the flood code map used for the ECM. The flood coded cells are the MIKE SHE cells where the water from MIKE 11 canals is allowed to spill out. The movement of water in flood coded cells along the river direction is controlled by MIKE 11, but this water is also available for all other MIKE SHE processes, such as evaporation, overland flow, and infiltration.

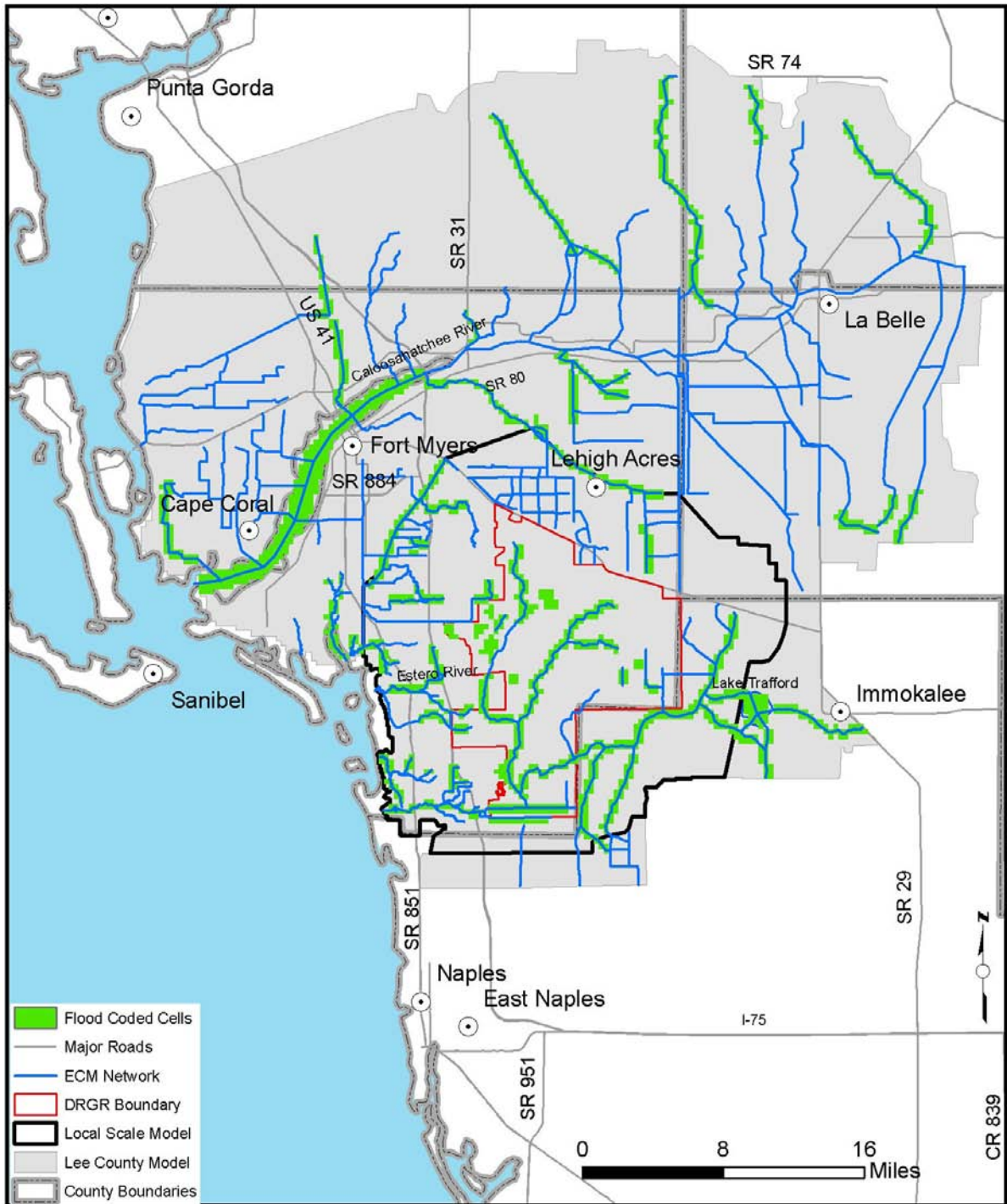


**Figure 19.** Flood coded cells in the ECM.



### Representation of Roads and Berms

Due to the relatively large size of the model cell size (1,500 feet), the elevations of certain features that impede flow between certain areas are not properly represented in the model topography. The separated flow areas are specified in the overland flow module in MIKE SHE to define localized higher topography that would prevent overland flow from naturally occurring from one area to another. For example, an elevated roadway would prevent overland flow except at designated culvert crossings. Another example would include a farm field or mining operation that is bermed on all sides to prevent overland flow from surrounding areas.

Discussions with Lee County staff revealed that Alico and Corkscrew Roads serve as barriers to natural overland flow. Multiple culvert crossings exist along the right-of-ways to allow flow to move towards the south and towards the west. The existing separated overland flow areas defined in the SWFFS model were further subdivided to account for the barriers defined by Alico and Corkscrew Roads. Moreover, additional branches and structures were defined in the MIKE 11 river network to represent the culvert road crossings under these roadways, as stated the previous sections.

Separated flow areas were also defined for the mining pits to represent the surrounding berms. This approach assumes that there is no overland flow between the mine and surrounding properties. In some agricultural or urban areas in the DR/GR Area, separated flow areas were also defined. The separate flow areas map used for the ECM is shown in **Figure 20**.

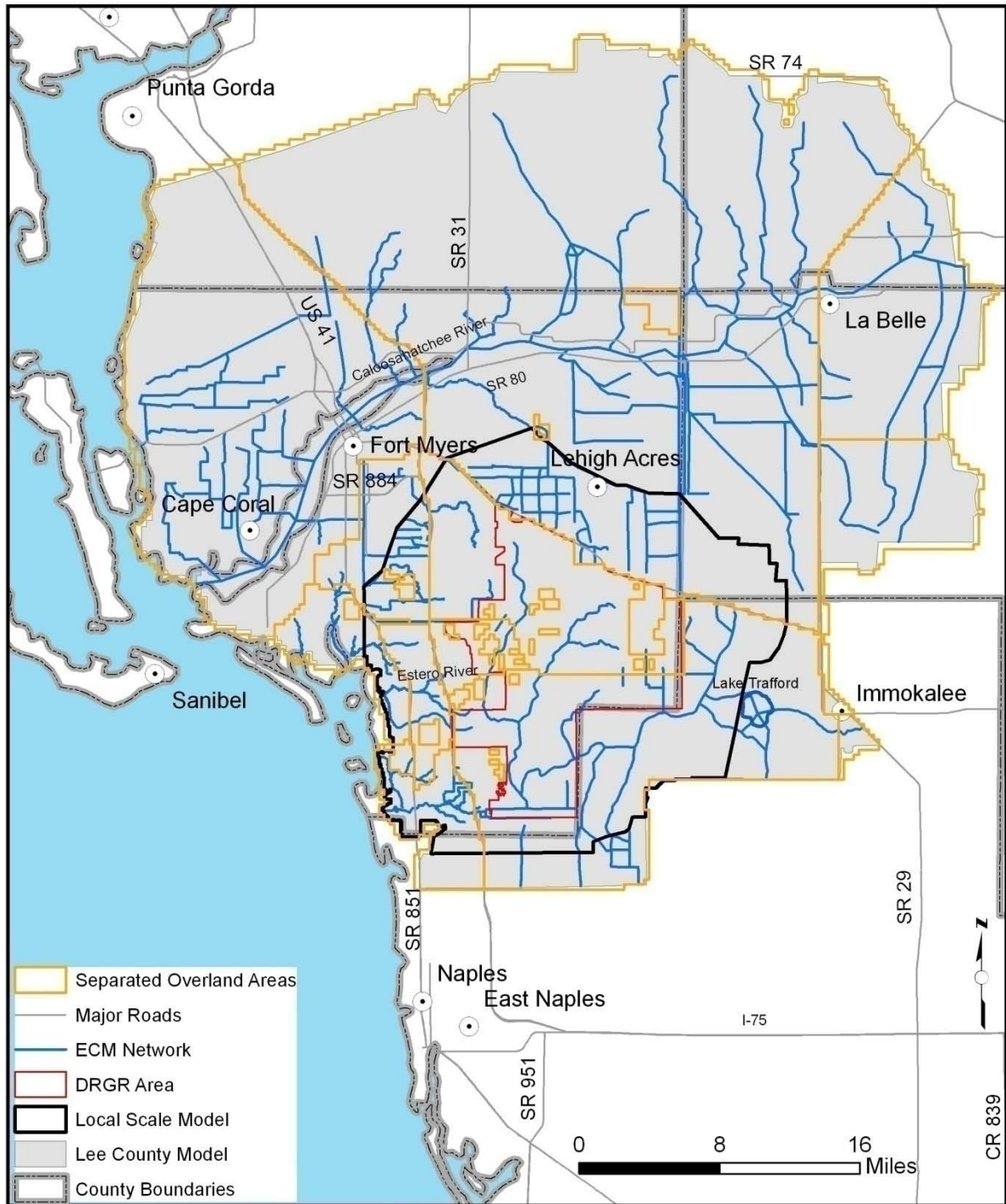


**Figure 20.** Separated Overland Flow Areas in the ECM.

## Representation of Mining Pits

There are several mining pits in and around the DR/GR Area that may alter the water budget in the region. Those mining pits are open water bodies that may have higher ET rates than the pre-developed land. In open water conditions, there is more storage (porosity) than in pre-existing soils, and the amplitude of the changes in the water table level are lower than in subsurface pore water at equal volumetric fluxes from rainfall, ET, infiltration, etc. Moreover, open water bodies represent high hydraulic conductivity areas that flatten the preexisting regional hydraulic gradient and drain upgradient pore water.

The representation of the mining areas includes the following:

- 1) The Environmental Resource Permits (ERPs) for mines require that at least the 25-year three-day (or, in some cases, the 100-year) storm events are contained. In order to represent the berms, a separate flow area was defined at the boundaries of the mining pit areas. The separate flow areas prevent overland flow to or from surrounding areas. The separate flow areas corresponding to mining pits in the ECM are shown in Figure 20.
- 2) Dover, Kohl and Partners provided the depth of the mining pits in and around the DR/GR Area from official records. This information was used to assign the bottom elevation of the conceptual mining pit lens at each corresponding grid cell in the model. This approach, which has been used in other groundwater models (May-Chu and Freyberg, 2008), allows lateral exchange from the mining pit to the adjacent groundwater cells. The mining pit lens is set with a high conductivity ( $K_h = K_v = 1 \text{ m/s} = 2.8 \times 10^5 \text{ ft/day}$ ) and the maximum specific yield ( $S_y = 1$ ), to mimic open water conditions. Some of the deeper mining pits reach the upper part of the Upper Peace River Confining Unit, which is the third computational layer of the model.
- 3) A portion of the mining pits were etched in the model topography to ensure that there is ponded water through the simulation. The portion of the mining pit below the level burned in the topography is represented in the groundwater model as a geological lens.
- 4) After converting the higher resolution land use maps to the model resolution, the maps were modified to ensure that all mining pits were defined using the same code equal to "water". This allows the proper application of land use based parameters for these areas, such as ET parameters to calculate the proper evaporation rate from open water.

## Surface Water Boundaries

Measured water levels and flows were used to define the surface water boundary conditions for the ECM. The surface water time-varying boundaries are shown in **Figure 21**. In MIKE 11, boundary conditions are required at the unconnected ends of all branches. The unlabeled unconnected ends in Figure 21 are set as zero-flux (or closed) boundaries. The eastern boundary of the canal network is located at the S-78 structure in C-43 Canal. The measured discharge at the S-78 structure was specified for this location from DBHYDRO.

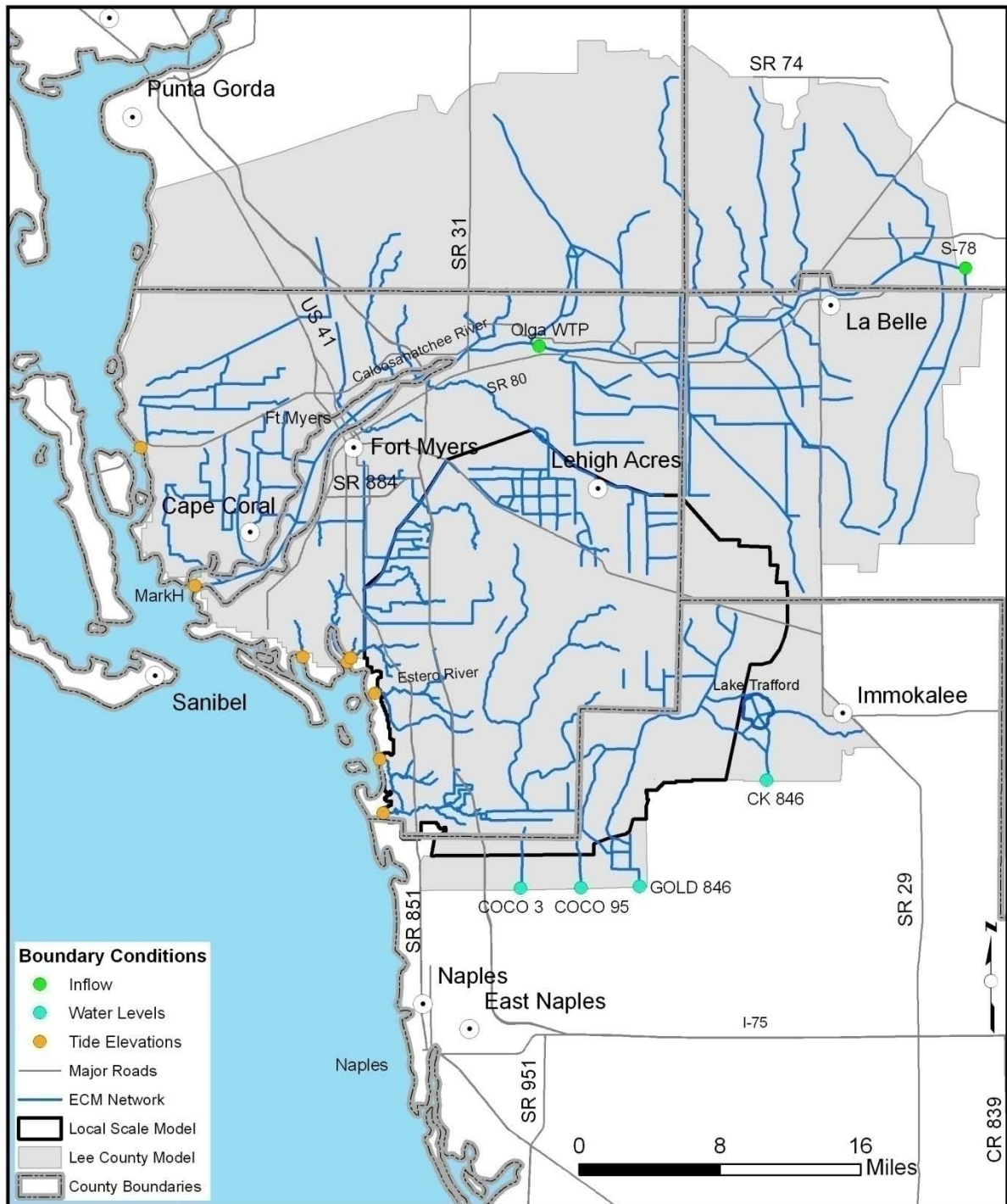


**Figure 21.** MIKE 11 Time-Varying Boundary Conditions in the ECM.

The south-eastern boundaries consist of the Camp Keais Strand at the CR846 crossing and Immokalee Canal at the intersection with SR29. The available stage data from DBHYDRO for the Camp Keais Strand at the CR846 crossing was applied at this location. A closed (no-flow) boundary was specified for the Immokalee Canal.



The ECM area was extended from its original proposed area in order to reduce boundary effects in the southern part of the DR/GR Area. The new southern surface water boundaries consist of the set of downstream ends of canals that drain to the Cocohatchee Canal. The water level time series from Cocohatchee stations were used as the boundary conditions specified at the southern end of these canals.

The Olga Water Treatment Plant (WTP) at Fort Myers was included as a point source intake from the river network, as in the SWFFS model. The original time series data was updated, with the daily data delivered by Howard S. Wegis, at Lee County Utilities, from April 2001 to December 2007.

The hourly tidal water levels from the NOAA (<http://tidesandcurrents.noaa.gov/index.shtml>) Naples station were used for all the west coast boundaries. This station was determined the most suitable tidal station for the western area of the model after a comparison was performed between the available tidal data. The two NOAA stations within or close to the model area that have data available for the entire simulation period are: the Fort Myers station (ID: 8725520), which is approximately 13 miles upstream from the coastline at the Caloosahatchee River, and the Naples station (ID: 8725110), which is approximately 10 miles south of the southern boundary of the model domain (see **Figure 22**). The MARKH station from DBHYDRO, located at the downstream end of the Caloosahatchee River, does not have data available for the entire model simulation period. The average hourly and daily data from the Naples and Fort Myers stations were compared to the daily average data from the MARKH station. The recorded values at this station appear to slightly overestimate the daily averages of the other two stations. There are also some differences between the Fort Myers and Naples stations. First, the oscillations of the hourly time series differ in amplitude and phase. Second, the daily averaged elevation at Fort Myers station is slightly higher in general than at the Naples station. These differences are to be expected since the Fort Myers station is farther upstream from the coastline. Thus, it was determined that the Naples station is more representative of the coastal water levels.

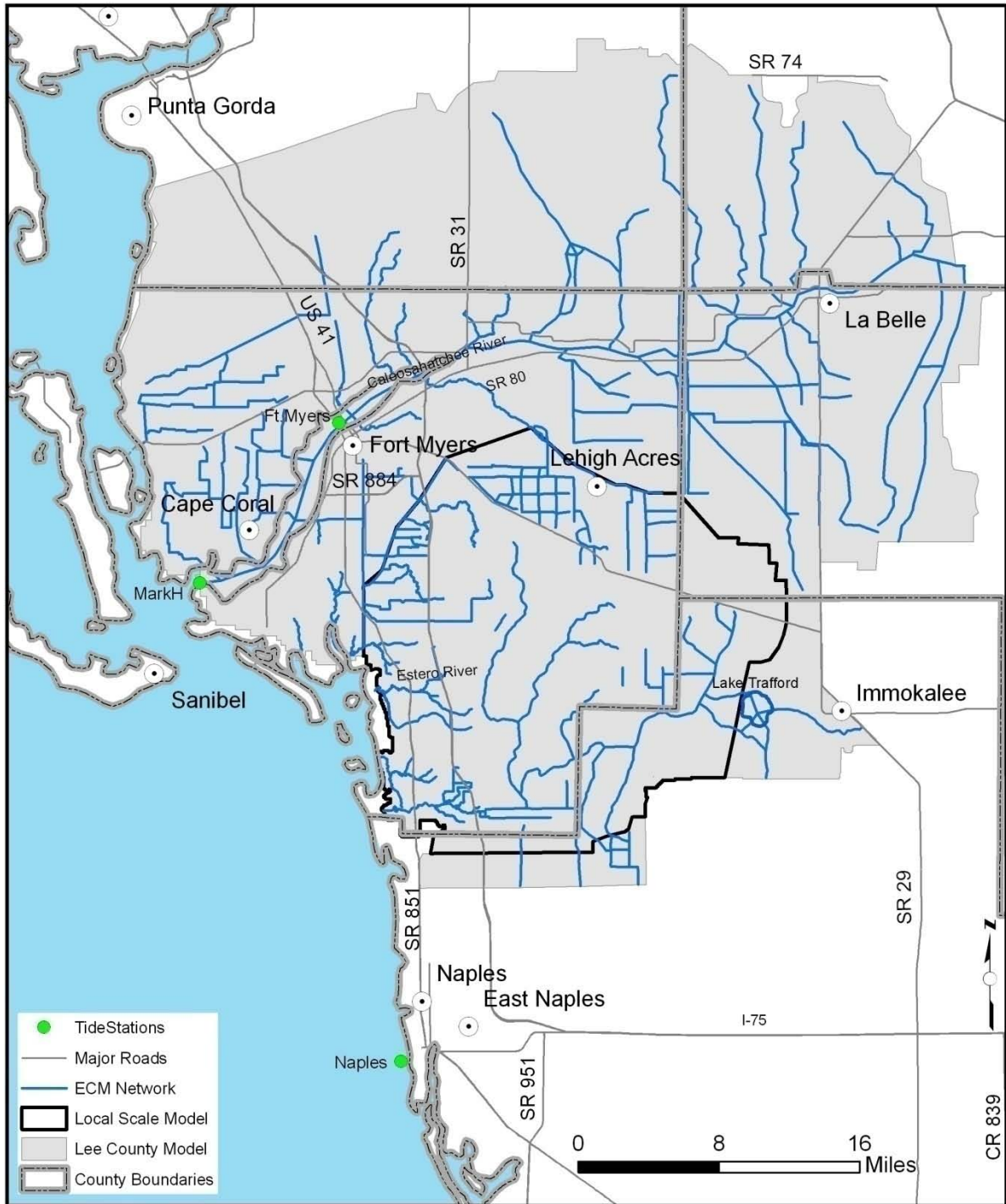


**Figure 22.** Tidal Stations.

## LS ECM Development

Several refinements were made to the surface water component of the LS ECM. Some of the refinements are described below.

- The mining pit coverage was redrawn at 750-ft resolution maps (down from 1500 ft resolution in the ECM) for conceptual lens depth and separated overland flow areas. The separated flow area map with higher resolution was also improved to better represent the road divisions. The drain code map used in the LS ECM was obtained in a similar way as in the ECM from the separated overland flow areas map by setting zero drain codes at mining pits and allowing drainage to the boundaries.
- The 750-ft land use map contains other grid cells classified as water that are not considered as mining pits in the model. Aerial photos reveal in most of those cells well defined open water bodies with sizes from one to several 750-ft grid cells. Those cells are referred to as “shallow lakes” and they were conceptualized in a similar way as mining pit cells. For shallow lakes where the depth was not provided by Dover, Kohl and Partners, a value of 10 ft was assumed.
- The distribution of mining pits and shallow lakes in the LS ECM domain area is shown on **Figure 23**. The representation of the water bodies can be revised in the future, when more information becomes available about the interaction of the water body with the surrounding cells (i.e. presence of berms, drainage system, etc). Also, information about the bathymetry of the water bodies can improve the representation in the model.
- Another improvement in the LS ECM is the representation of contiguous water bodies that are divided by land areas narrower than one grid cell size, like roads for example. As with the ECM, separated overland flow areas were established to prevent communication in the overland component. For the LS ECM, the sheet piling module in the groundwater component was added to the model. Since the separation between the water bodies was less than one grid cell, the model would have shown these water bodies as touching each other without any hydrologic barrier between them. The sheet piling allows for the specification of a hydrologic barrier between these touching water bodies that more closely represents reality. Since mining pits and shallow lakes are represented with a groundwater lens, free communication between contiguous water bodies through the groundwater layer is prevented by introducing conductivity barriers, i.e., artificial sheet pilings. The locations of the flow barriers were found by inspecting aerial photos and assuming the lack of culverts on those divisions. The divisions are shown in Figure 23. A uniform leakage coefficient of  $10^{-4} \text{ sec}^{-1}$  was assumed by considering divisions of 50 ft wide and a typical conductivity of the Holocene-Pliocene geological layer.

Other improvements and refinements to the surface water system in the LS ECM are described in the following sub-sections.

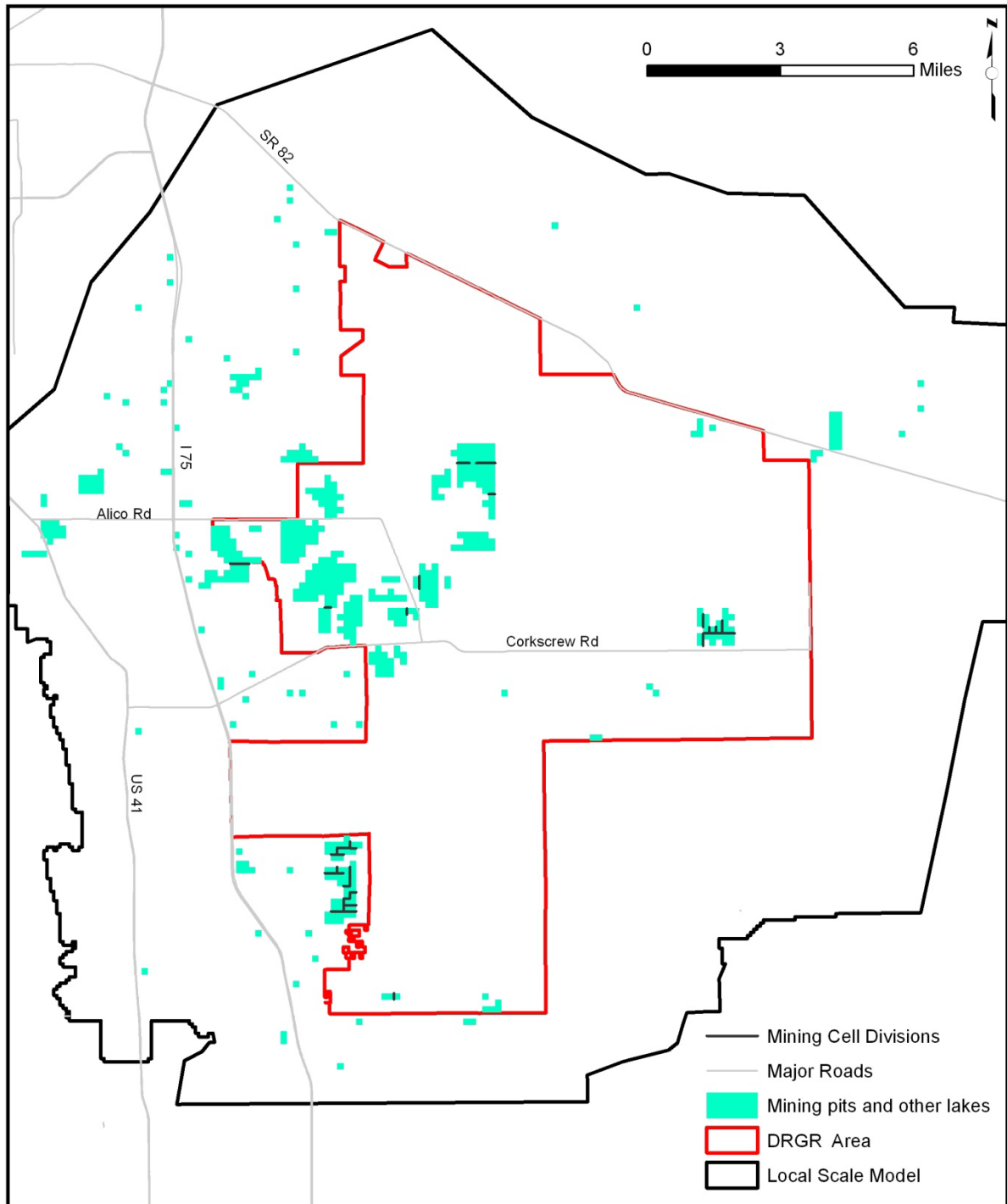


**Figure 23.** Mining Pits and Shallow Lakes.

## Definition of Flow Ways

The inclusion of all the main flow ways in the MIKE 11 component of the model has advantages over using a combination that alternates channel flow and overland flow. MIKE 11 solves the surface water (channelized) flow problem in a more accurate way since it solves the exact equations in smaller time steps and accounts for the channel geometry (or micro-topography). On the other hand, the overland flow component considers two dimensional flow, which is beneficial for wide flow ways (sloughs, lakes, etc) where the flow across the main path (e.g., toward the center of the slough) may be important. The approach followed by DHI to represent the sloughs and lakes in this model is to create a MIKE 11 branch for the slough center flow with a 750-ft wide cross-section and allocate a flood code to allow full interaction with the overland component that controls the 2D surface water flow in the neighboring areas.

The definition of new MIKE 11 branches containing the main flow ways was conducted based on the following information:

1. The 5-ft resolution LIDAR topographic map. In this map, the highs (berms and roads) and lows (canals, creeks and sloughs) are clearly visible. Some bridges are removed from flow ways. However, the existence of some culverts is sometimes difficult to determine from this map.
2. Hydroperiod map from KLECE. Natural flow ways like sloughs are likely present in connected natural areas. High and low hydro-periods are useful to delineate flow path ways in some natural areas.
3. Aerial photos from 2007 (and 2004 outside of the DR/GR). They were useful to delineate pathways particularly where there is not LIDAR topographic data.
4. Notes received from Kevin Hill (dated from 5/27/2008). They were useful to delineate flow ways along and across Corkscrew Road.
5. GIS processing of topographic data. The new LIDAR topographic data was averaged to 100 ft resolution and merged into 100-ft SFWMD data from 2004 in order to “fill the gaps” outside the Lee County areas. The resulting 100-ft resolution topographic file was processed in ArcMap to obtain the flow ways. A similar processing was conducted to a 750-ft resolution topographic map obtained from those two topographic data. The flow path ways obtained in both cases cannot be used directly as the existing flow ways (mainly because of the lower resolution that blur canals and creeks and because this processing does not include the culvert information), but they serve as a guide for the more detailed flow ways delineation conducted visually from the previous information.

The flow ways analysis described above led to a drainage network that was too detailed. That network was later reduced to the coarser MIKE 11 network used in the model.



**Figure 24, Figure 25** and **Figure 26** show the network structures, the flood coded cells and the separate overland areas considered in the new model in conjunction with the new flow ways definition.

ADA Engineering, Inc. [2008] performed some work on the MIKE 11 network in the area between the Estero and Imperial Rivers based on local survey information. The MIKE 11 network of this model was based in part on the MIKE 11 network generated by ADA Engineering, Inc.

While building the MIKE 11 network, considerable effort was made to ensure that all important flow ways were included. However, the network may include flow ways that conduct minimal flow since it is difficult to predict the relevance of all the flow ways considered. Once the network is introduced in the model, the flow rate predicted by the model would allow us to evaluate the importance of each flow way.

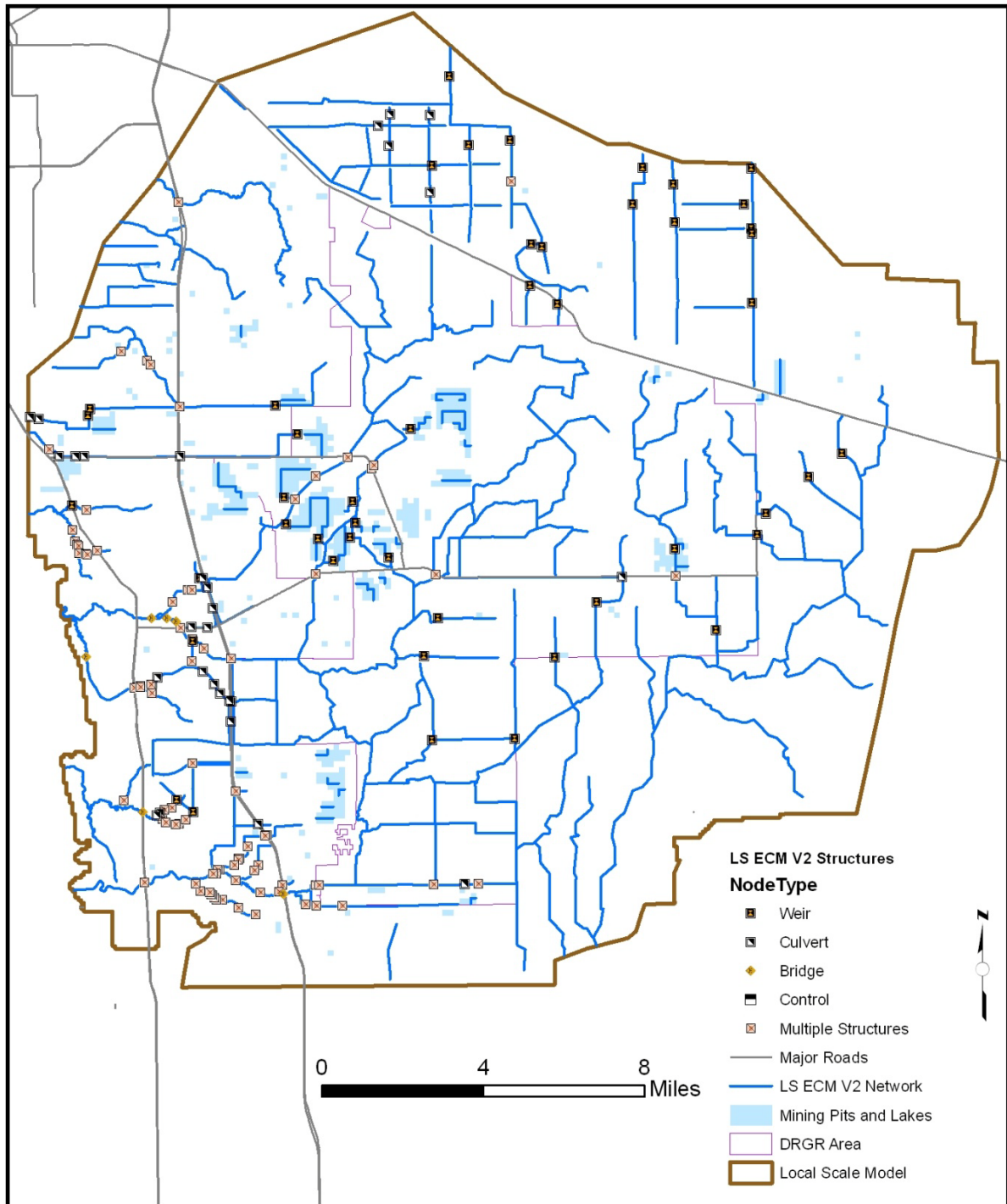


**Figure 24.** MIKE 11 Network and Structures in the LS ECM.

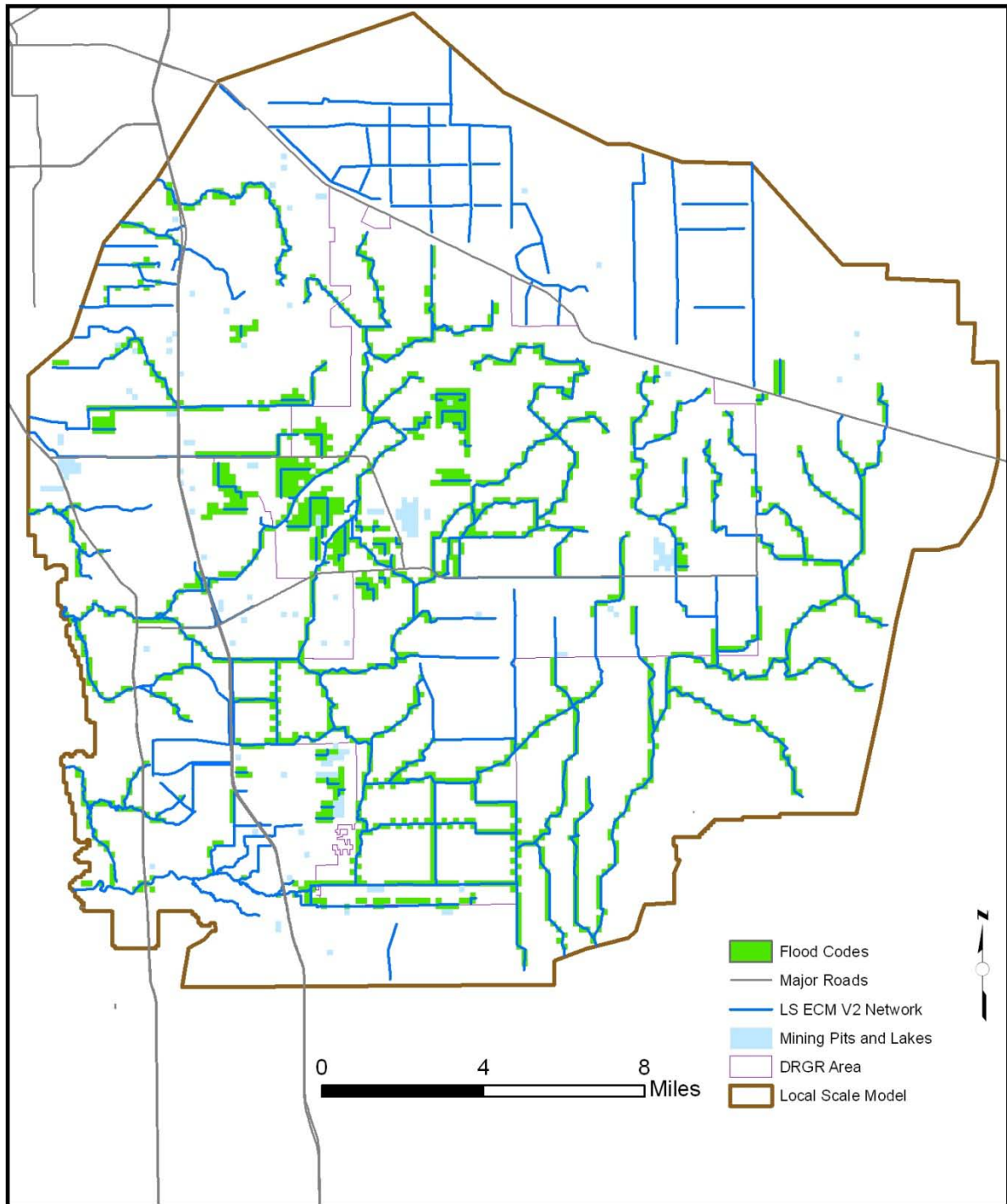


**Figure 25.** Flood Codes in the LS ECM.

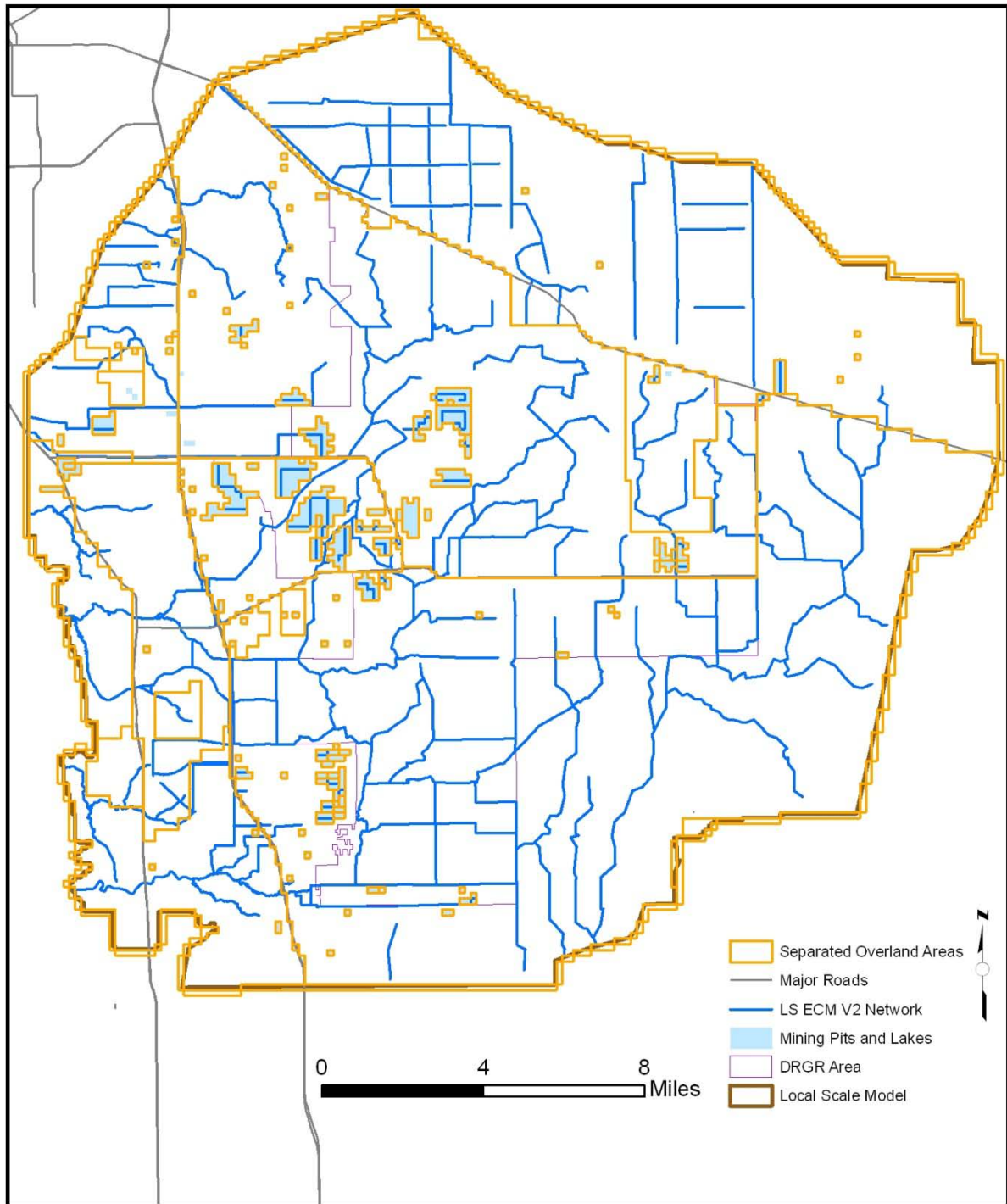


**Figure 26.** Separated Overland Flow Areas in the LS ECM.



### Cross-section Extraction

The cross-section geometry for the MIKE 11 branches was extracted by using the MIKE 11 GIS tool. The 5-ft resolution topographic map was used where available and the SFWMD 100-ft resolution map otherwise. Cross sections were spaced a distance of about two grid cells (~1500 ft). It is recommended to have as many cross-sections as possible to assure a better representation of the channel geometry, but cross-sections spaced less than one grid cell apart may produce instabilities in the model.

In some cases, water in the channel prevented the LIDAR from reaching the channel (or cross-section) bottom. Thus, the cross-sectional geometry of the submerged part was taken from previous surveyed cross-section data. Unfortunately, the LIDAR data was acquired between the months of June and October of 2007 and not at the end of the dry season when the water levels are lower and the bottom of most of the flow ways are dry, which would allow a better estimation of the cross-section geometry from the LIDAR data.

### Drainage around Mining Pits

The initial assumption of bermed mining pits used for the ECM is not always the case as revealed following a visual inspection of the high resolution LIDAR topographic map available for the LS ECM development. The fact that some mining pits may be collecting or releasing water from the nearby areas may be relevant to better account for water levels in the mining pits and the discharge rate of nearby flow ways.

The drainage system conceptualized in the MIKE 11 component around some of the mining pits is shown in **Figure 27**. In cases where the mining pit is not fully bermed, a MIKE 11 branch was included to connect the branch that accounts for the standing water at the mining pit and a nearby flow way. A conceptual weir structure is also included in the connecting branch to provide better control of the elevation above which discharge to or from the mining pit occurs.

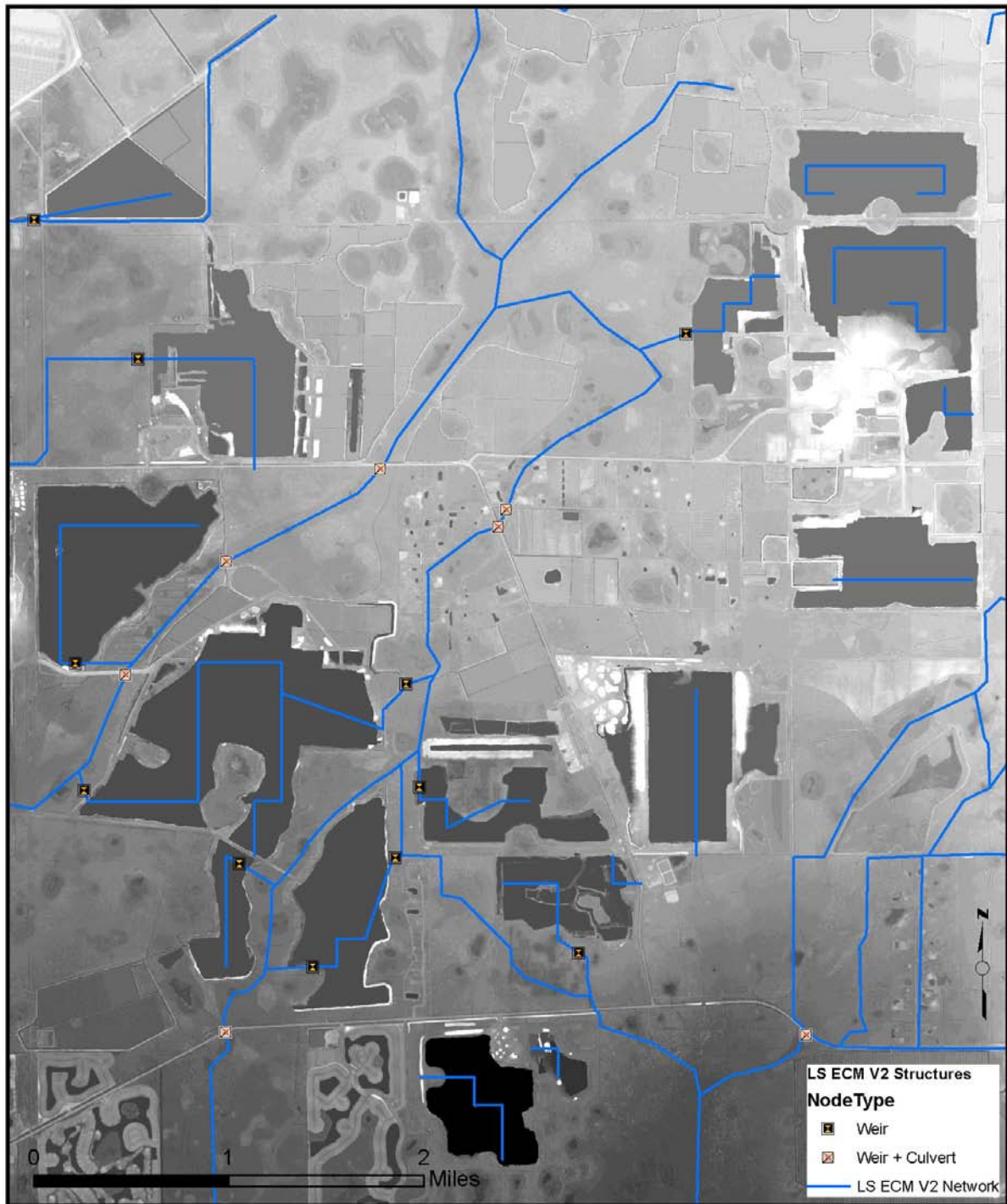


**Figure 27.** Drainage system around mining pits with a grayscale shaded relief map of LIDAR topographic data in the background.

**Note:** Lighter areas in the topographic map represent higher elevations, darker represent lower-lying areas.



## **Model Calibration**

Calibration of the ECM and LS ECM was performed for the period of January 1<sup>st</sup>, 2002 to November 1<sup>st</sup>, 2007. As part of the model development, considerable effort was spent to improve the representation of certain important features in the model, such as the mining pits and flow ways in the DR/GR Area. Furthermore, a number of model parameters, such as overland flow roughness coefficients, hydraulic conductivities and storage parameters of the geological layers, and subsurface drainage parameters, were tested and varied in order to produce a closer match between model results and observed data. The observation time series data consist of stage and flow time series from surface water stations and of water table levels from observation wells. The surface water data was obtained from DBHYDRO and the groundwater data was obtained from Lee County, DBHYDRO, and the USGS. These data were used to compare the model stages, flows, and groundwater heads at the corresponding locations. For the Lee County Model Area there are a total of 143 groundwater monitoring wells, 31 surface water stage and 10 surface flow stations. Due to the time limitations of this project, DHI and Lee County agreed to focus the calibration of the model on the following areas, listed from highest to lowest priority:

1. The DR/GR Area and the Imperial River Basin.
2. The Orange River basin in the area south of Able Canal.
3. The Six Mile Creek Basin in the area west of the DR/GR.
4. The areas north of Caloosahatchee River and east of the S-79 structure in the freshwater Caloosahatchee River basin.

The calibration was focused primarily on the ECM. However, after extracting the higher resolution model (LS ECM), some additional calibration and improvement efforts continued in both models simultaneously.

After including the changes in the LS ECM derived from the new topographic data, some instability appeared in the MIKE 11 network. Instabilities increase the water balance error and may affect the accuracy of the model results. Moreover, further adjustments were required in the model in order to improve performance at stations where performance had decreased. Thus, a limited-time recalibration was conducted for the LS ECM following the update with the high resolution topographic data.

## **Model Improvements**

As part of the model development, considerable effort was spent to improve the representation of certain important features in the model, such as the mining pits and flow ways in the DR/GR Area. Furthermore, a number of model parameters, such as overland flow roughness coefficients, hydraulic conductivities and storage parameters of the geological layers, and subsurface drainage parameters, were tested and varied in order to produce a closer match between model results to observed data.

## ECM

The overall performance of the model was improved by focusing primarily on the DR/GR Area. The most relevant changes in the ECM are summarized below.

- 1) Some cross-sections and structures in the river network were corrected according to previous sub-regional models. Several cross-section shapes were also modified to meet structure geometry and in other cases to follow the topography. The cross-section widths of flooding branches were adjusted to match the MIKE SHE flood codes. The Manning's roughness coefficients and the leakage coefficient were modified in some of the MIKE 11 branches.
- 2) The original overland Manning's  $M$  ( $1/n$ ) global values were modified for Hydric Flatwood (3.33 to 4.0), Marsh (1.67 to 2.33) and Cypress (2.5 to 3.33).
- 3) Additional separated overland flow areas were added to represent flood control features around some agricultural areas in the DR/GR Area. The overland boundary conditions were adjusted in MIKE SHE to represent time-varying conditions.
- 4) Drain depths and time constants for agricultural areas were decreased to 0.5 ft and  $0.25 \text{ day}^{-1}$ , respectively; in order to improve the model performance around the DR/GR Area. The drain code map was adjusted to match the separated overland flow areas map in relevant areas. Drainage was set to zero in mining pits. Drain flow was allowed to flow from agricultural and urban areas to the model boundaries.
- 5) The screen interval and maximum pumping rate in some ICAs were modified based on previous sub-regional models.
- 6) Mining pits were conceptualized as described in a previous section.
- 7) The hydraulic conductivities of the different geological layers and lenses were adjusted during the model refinement process. The conductivities for the different geological layers and lenses were taken initially from the SWFFS model. In this model, the conductivity values were recognized as having high uncertainty and they were considered as calibration parameters (CDM, 2006). During an inspection of the resulting conductivity maps, it was found that there were areas with high vertical conductivities in relation to the horizontal conductivities, which may have resulted from these parameters being calibrated independently. In the ECM, the vertical conductivity for the Water Table Aquifer was limited to a value equal to, or lower than the corresponding horizontal conductivity. Also, conductivities of the two confining lenses and the Sandstone Aquifer were considered isotropic. The isotropy assumption is reasonable because in the model the computational layers 2 and 3 are each composed by one lens and one geological layer (Figure 12). The confining units (represented as lenses) are less permeable than the aquifers (represented as geological

layers). Thus, the conductivity of the lens defines mostly the vertical conductivity of the computational layer and the geological layer conductivity defines the horizontal conductivity. The final conductivity maps obtained after the refining process are illustrated in Appendix A.

- 8) The specific yield in the upper geological layer was changed from 0.2 in most areas to a uniform value of 0.15, as suggested by SFWMD. The results of the model show no significant variation in response to this change.
- 9) The storage coefficient in the three aquifer layers was changed from a distribution with a mean value of approximately  $4 \times 10^{-4} \text{ ft}^{-1}$  to a uniform value of  $10^{-4} \text{ ft}^{-1}$ . Seasonal fluctuations in the groundwater head in deep layers were slightly increased by decreasing this coefficient. The storage coefficient in the model could be decreased further to improve the performance of the model in deeper layers. The minimum possible value of the storage coefficient occurs with negligible porous matrix compressibility. Considering the water compressibility is equal to  $5.3 \times 10^{-5} \text{ atm}^{-1}$  and the porosity is equal to 0.2, the minimum possible storage coefficient value is estimated to be  $3.1 \times 10^{-8} \text{ ft}^{-1}$ .
- 10) A sensitivity test was also performed by splitting the computational layer 3 into two computational layers. With greater vertical resolution (four computational layers), the model took about the same amount of time to run and showed only minor changes in water elevations at observation well stations. Thus, the final ECM has the original three computational layers.

### LS ECM

The numerical instabilities were reduced as much as possible in the LS ECM in order to improve the water budget error and the overall model performance.

Most of the instabilities in the MIKE 11 network were observed where the spacing between cross sections is much lower than the MIKE SHE grid cell size (750 ft). When MIKE SHE grid cells interact with the river network, it chooses the cross section location closer to the grid cell center to discharge the water from the drainage and overland components. If the cross sections are not spaced in one grid cell size or higher, MIKE 11 does not have storage assigned for that cross section and a spike in the stage may occur at that point and time while the water is not redistributed through the MIKE 11 branch. This numerical problem is solved by removing cross sections that are spaced too close to each other.

The maximum pumping rate in a few irrigation command areas (ICAs) was refined. This eliminated unrealistic oscillations in the GW head at those locations. The priority scheme in the irrigation module was changed from “none” to “equal shortage”, which is more appropriate. Moreover, the ICA code (dfs2) file was filtered in order to remove cells with natural land uses (codes from 7 to 20), which are unlikely irrigated in most of their extent.



Branches in some mining pits were removed to improve the model stability. Also, the hydraulic conductivities ( $K_h$  and  $K_v$ ) in the conceptual mining pit lens were reduced from 1 to 0.1 m/s. All "bed only" leakance in MIKE SHE-MIKE 11 links were changed to "Aquifer + bed", which is more realistic.

For fine-tuning specific areas, the procedure followed to improve model performance varied from one site to another. In general, if there was a MIKE 11 branch involved, the model conceptualization of the area and the model parameters were revised. Typically the model conceptualization was changed and some corrections or adjustments were necessary for cross sectional data, flood codes, Manning roughness coefficients, leakage coefficients and conceptual weir elevations. The conductivity in the groundwater layers was typically adjusted in cases without any close MIKE 11 branches.

The option of "checking water levels before routing" for the case of the paved-area runoff coefficient was enabled to more accurately simulate gravity drainage systems.

### **Water Table Level in Mining Pits**

In order to evaluate the LS ECM performance in mining pits, 62 values of water levels were extracted at different mining pits and lakes in the model domain area from the LIDAR data. Those points correspond to one day of year 2007, in accordance to the LIDAR flight date. The possible flight dates for those locations were June 18, 28 and 29; August 4, 5, and 6; and August 22, 23, and 24.

The mean water table differences between observed values and model predictions at those 62 locations in mining pits and lakes is presented in **Table 10** as computed from different model tests.

- A first intermediate test of the model (identified as LS ECM V1) overpredicts the water table levels on average in mining pits and lakes by 1.0 ft.
  - This step in the calibration process preceded the introduction of the refined topography or the distributed ET data.
- A second intermediate test of the LS ECM (marked with \*\*) caused an improvement in the first result of 0.3 ft (mean difference of 0.7 ft).
  - This step uses the refined topographic map, revised flow ways conceptualized in MIKE 11 and drainage in some mining pits. Also uses the same station based ET as the ECM.
- A third intermediate test of the LS ECM (marked with \*) caused an improvement of 0.4 ft compared to the second result (mean difference of 0.3 ft).
  - This step was modified with the new distributed reference ET (RET) data.

- The final version of the model (LS ECM) caused an improvement of 0.3 ft compared to the third step. This gives a net improvement of 1.0 ft, leaving a mean water table difference in mining pits of 0.0 ft. A zero mean difference does not mean that the water levels from the model are exact in all mining pits and lakes, but on average, the over- and under-predictions balance out.
  - In the final version, lake evaporation was modified to a value of RET + 8.0% to be applied in open water cells of the model.

This sequence reveals the importance of the different changes introduced in the model regarding the average water table levels predicted in mining pits, for which the inclusion of the distributed RET and a higher lake evaporation each had about the same impact as the changes caused by the inclusion of the new topography.

In the third test simulation of the model (LS ECM\*), which differs from the early version (LS ECM\*\*) due to adjustments during the recalibration, the average water table level differences in mining pits and lakes is less than 0.1 ft (using the absolute differences) for the two lake evaporation values considered of RET + 8.2% and RET + 5.3%, as shown in Table 10. In the final version of the model (LS ECM), obtained after further adjustments, the mean difference (D) is still below 0.1 ft, and the mean absolute difference (DA) is slightly lower than in previous versions.

**Table 10.** Mean water table differences in mining pits and lakes from several model runs.

| Model     | ET  | LE – ET<br>(% of ET) | D<br>( ft ) | DA<br>( ft ) |
|-----------|-----|----------------------|-------------|--------------|
| LS ECM V1 | SET | 0                    | -1.04       | 2.68         |
| LS ECM**  | SET | 0                    | -0.7        | ---          |
|           | RET | 0                    | -0.3        | ---          |
|           | RET | 8.0                  | 0.02        | 1.68         |
| LS ECM *  | RET | 5.3                  | -0.06       | 1.67         |
|           | RET | 8.2                  | 0.01        | 1.66         |
| LS ECM    | RET | 8.2                  | -0.07       | 1.65         |

Note: “D” stands for mean difference between LIDAR elevation and water level from the model and “DA” for the mean of the absolute differences. The early version of LS ECM is marked with “\*\*” and the preliminary-report version of LS ECM is marked with an “\*”. See text for details.

### Model Performance at Observation Stations

In order to evaluate the model, the performance metrics for groundwater and surface water observation stations were established. The statistical parameters and equations are shown in **Table 11**. Detailed tables and figures with the results at observation stations are presented in Appendix B for the ECM and in Appendix F for the LS ECM. In **Table 12**, the number of stations in three performance level ranges are summarized for different types of observation stations. These metrics are equivalent to those used in the SWFFS regional model for the groundwater stations, but the tolerance levels were reduced for the surface water

stations. A unique indicator of the performance level (PL) per observation station was calculated by averaging the levels of performance (1= high, 2= medium, or 3= low) obtained for each statistical parameter. For example, if the comparison of simulated surface water levels vs. the observed data in a given station results in a correlation value equal to or above 0.8, then the R parameter for this station has a score of 1. The average score for all the parameters in a given station is the PL value for that station.

**Table 11.** Statistical Parameters used for Calibration of the ECM.

| Symbol | Name                    | Formula   |
|--------|-------------------------|---|
| ME     | Mean error              | $\overline{Obs_i - Calc_i} = \frac{1}{n} \sum_{i=1}^n (Obs_i - Calc_i)$   |
| MAE    | Mean Absolute Error     | $\overline{ Obs_i - Calc_i } = \frac{1}{n} \sum_{i=1}^n  Obs_i - Calc_i $   |
| RMSE   | Root Mean Square Error  | $\sqrt{\overline{(Obs_i - Calc_i)^2}} = \sqrt{\frac{1}{n} \sum_{i=1}^n (Obs_i - Calc_i)^2}$   |
| R      | Correlation Coefficient | $\frac{\sigma_{oc}^2}{\sigma_o \sigma_c}$ $\sigma_{oc}^2 = \overline{(Obs_i - \overline{Obs_i})(Calc_i - \overline{Calc_i})}$ $\sigma_o^2 = \overline{(Obs_i - \overline{Obs_i})^2} \quad \sigma_c^2 = \overline{(Calc_i - \overline{Calc_i})^2}$ |

**Table 12.** Number of stations for different performance level ranges.

| Type of observation point    | Model -> | LS ECM             |         |         |
|------------------------------|----------|--------------------|---------|---------|
|                              | PL ->    | 1.0-1.5            | 1.6-2.4 | 2.5-3.0 |
|                              | Total    | Number of stations |         |         |
| Mining Pits                  | 62       | 22                 | 24      | 16      |
| Shallow Wells (Layer=1)      | 82       | 48                 | 30      | 4       |
| Intermediate Wells (Layer=2) | 10       | 6                  | 3       | 1       |
| Deep Wells (Layer=3,4)       | 6        | 0                  | 2       | 4       |
| Surface Water                | 23       | 8                  | 14      | 1       |

Note: "PL" stands for average performance level.

For stations where the model was underperforming, a visual inspection of the model results versus the observed data was conducted. This inspection was used to identify potential outliers in the observation files and other possible causes for the differences. Finally, the



average hydroperiod information received from KLECE for the DR/GR Area was utilized to perform a comparative evaluation of the hydroperiod predicted by the model within the DR/GR Area and to adjust the parameters to improve the model performance.

### **Water Table Elevation**

Water table elevation maps predicted by the model are presented at two times of the year in **Figure 28** and **Figure 29**, corresponding to the end of the dry and wet season, respectively. Water table profiles along two transects in the DR/GR mining complex area (see **Figure 30**) are also presented in **Figure 31** to **Figure 34** at those times of the year for different models.

In the transect plots, the lower water table levels in mining pits and surrounding areas predicted from the LS ECM (identified as V2 in the figures) are noticeable with respect to the levels from the V1 model at the end of the dry and wet seasons. This is in accordance with the average 1-ft overprediction of the V1 model in the water table levels in mining pits that was removed through the calibration process (see Table 10). However, the differences in average water table levels between LE equal to 5.3% or 8.2% higher than RET are small, in correspondence with Table 10.

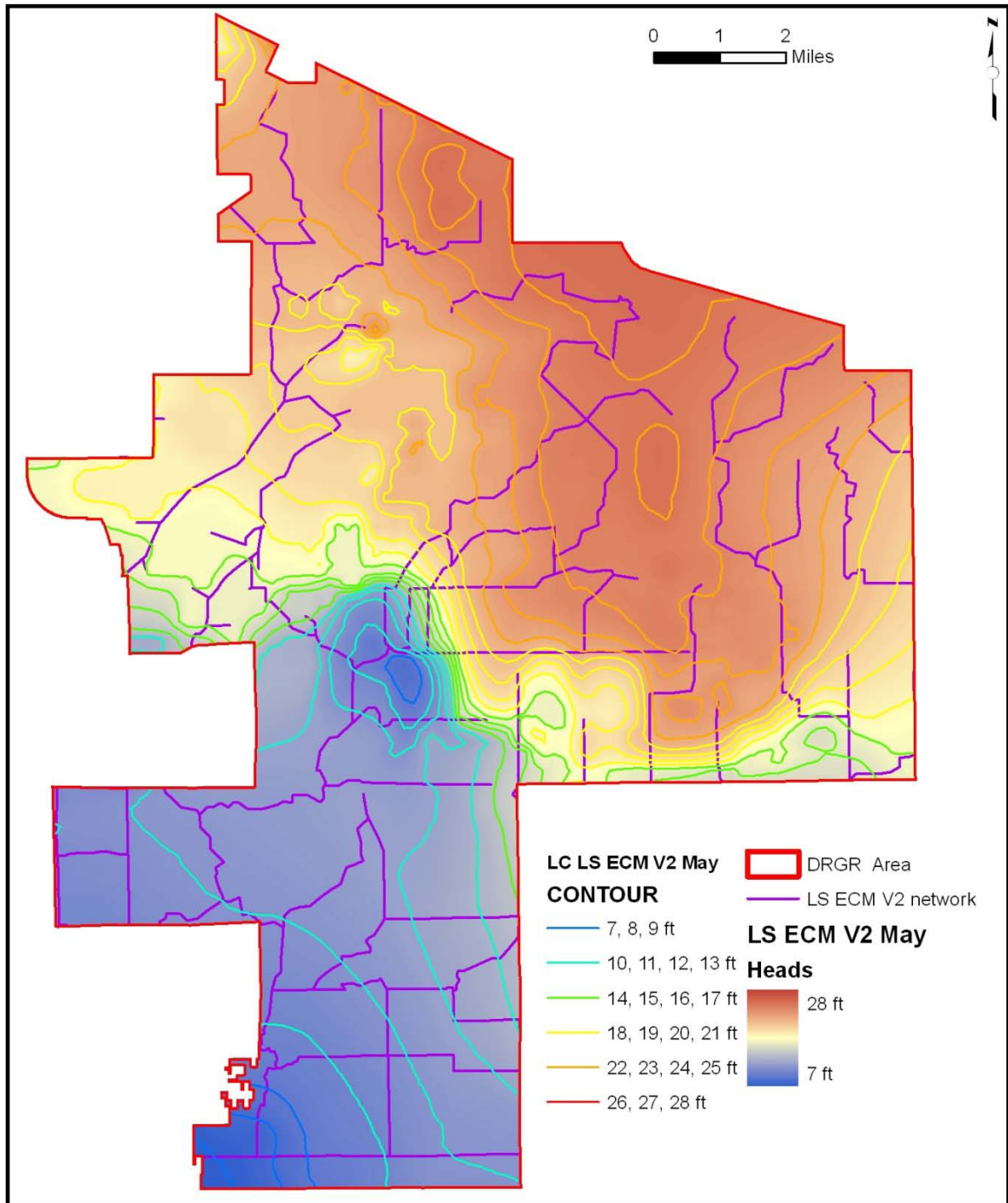


**Figure 28.** Average water table level map for the DR/GR Area at the end of the dry season as predicted by LS ECM.

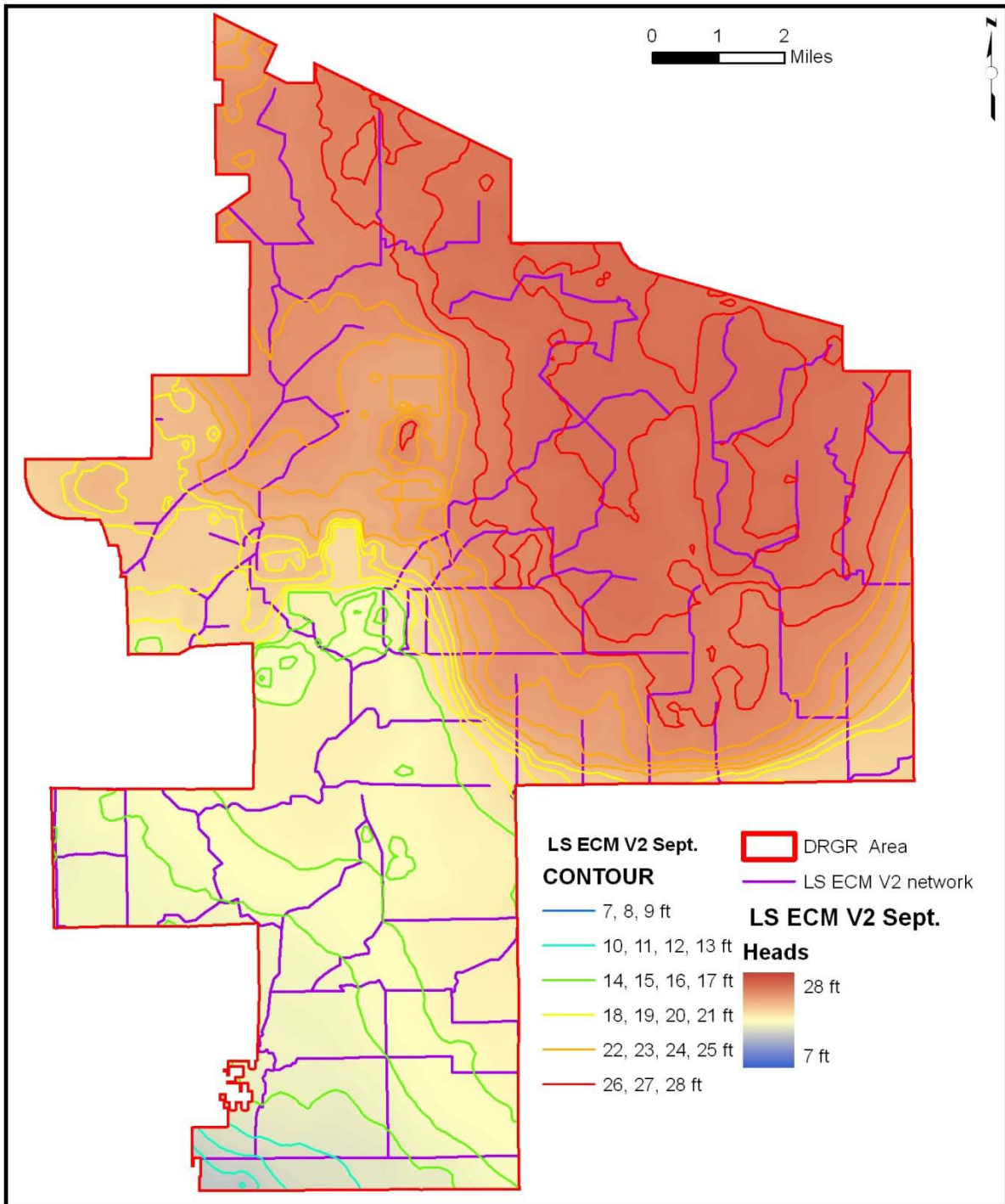


**Figure 29.** Average water table level map for the DR/GR Area at the end of the wet season as predicted by LS ECM.

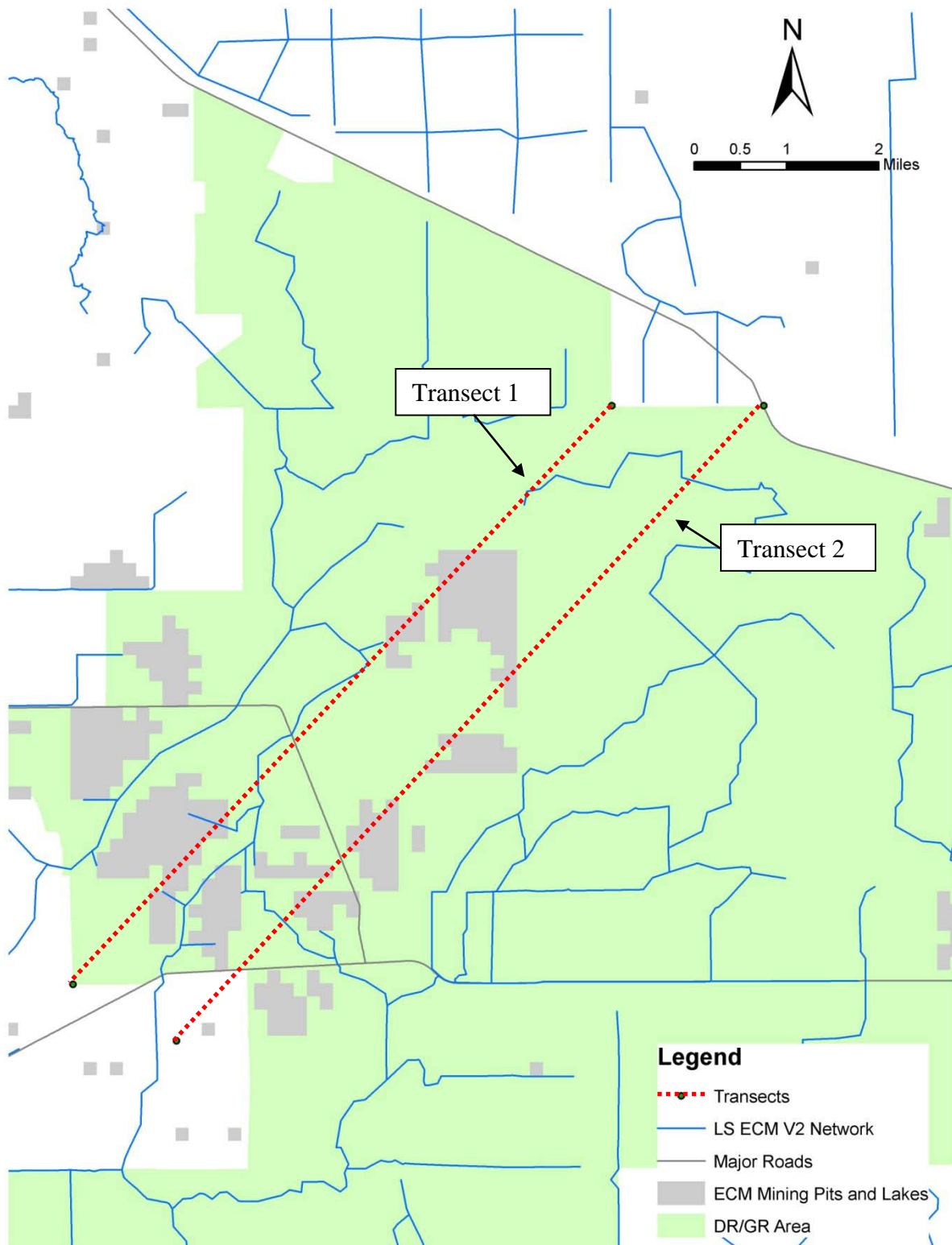


**Figure 30.** Transects through the mining pit complex area used to generate the water table level profiles presented from Figure 31 to Figure 34.

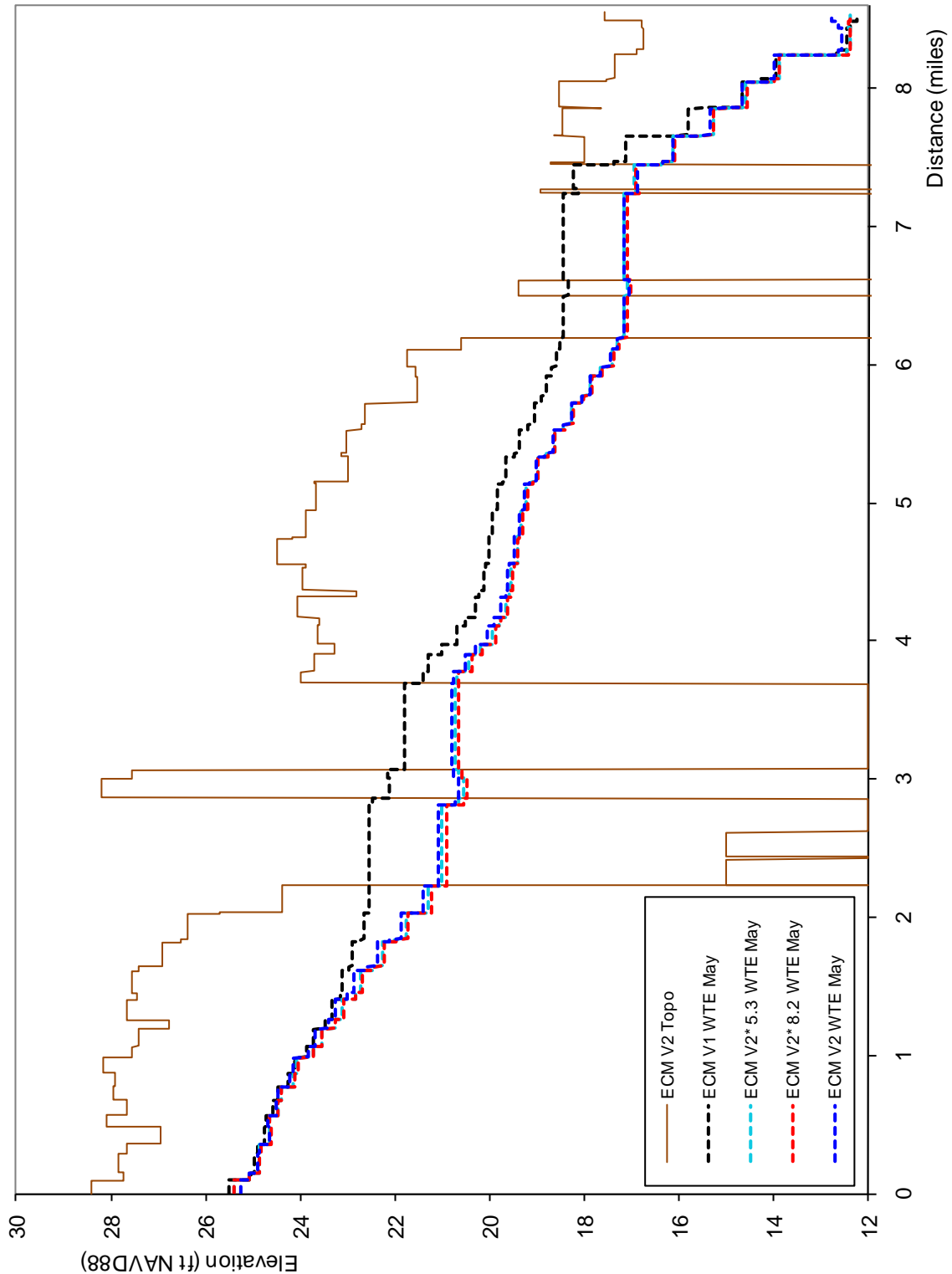


**Figure 31.** Water table level profile along Transect 1 presented in Figure 30 at the end of the dry season. The numbers 5.3 and 8.2 refer to the value in percent of LE - RET used.

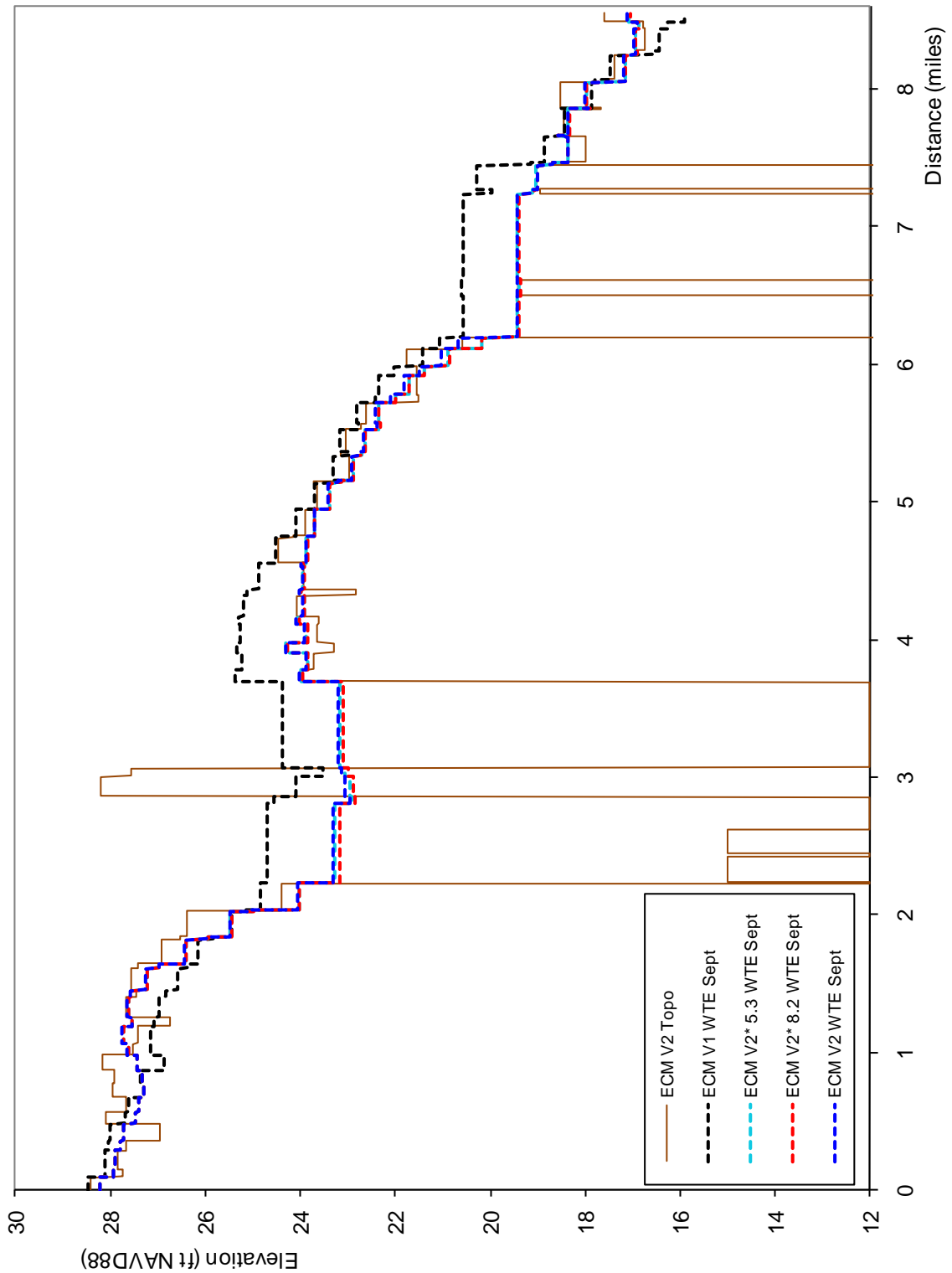


**Figure 32.** Water table level profile along Transect 1 presented in Figure 30 at the end of the wet season. The numbers 5.3 and 8.2 refer to the value in percent of LE - RET used.

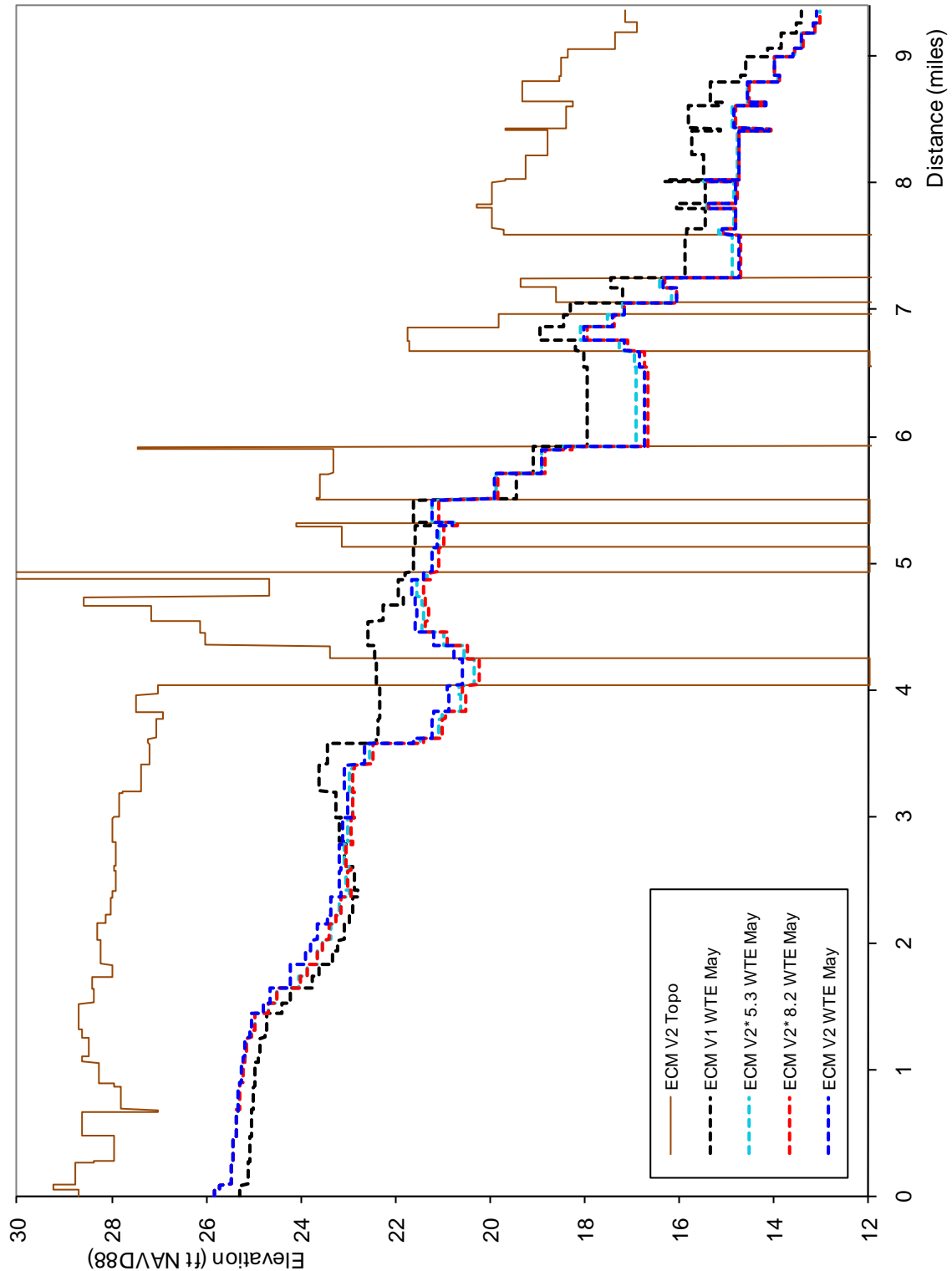


**Figure 33.** Water table level profile along Transect 2 presented in Figure 30 at the end of the dry season. The numbers 5.3 and 8.2 refer to the value in percent of LE - RET used.

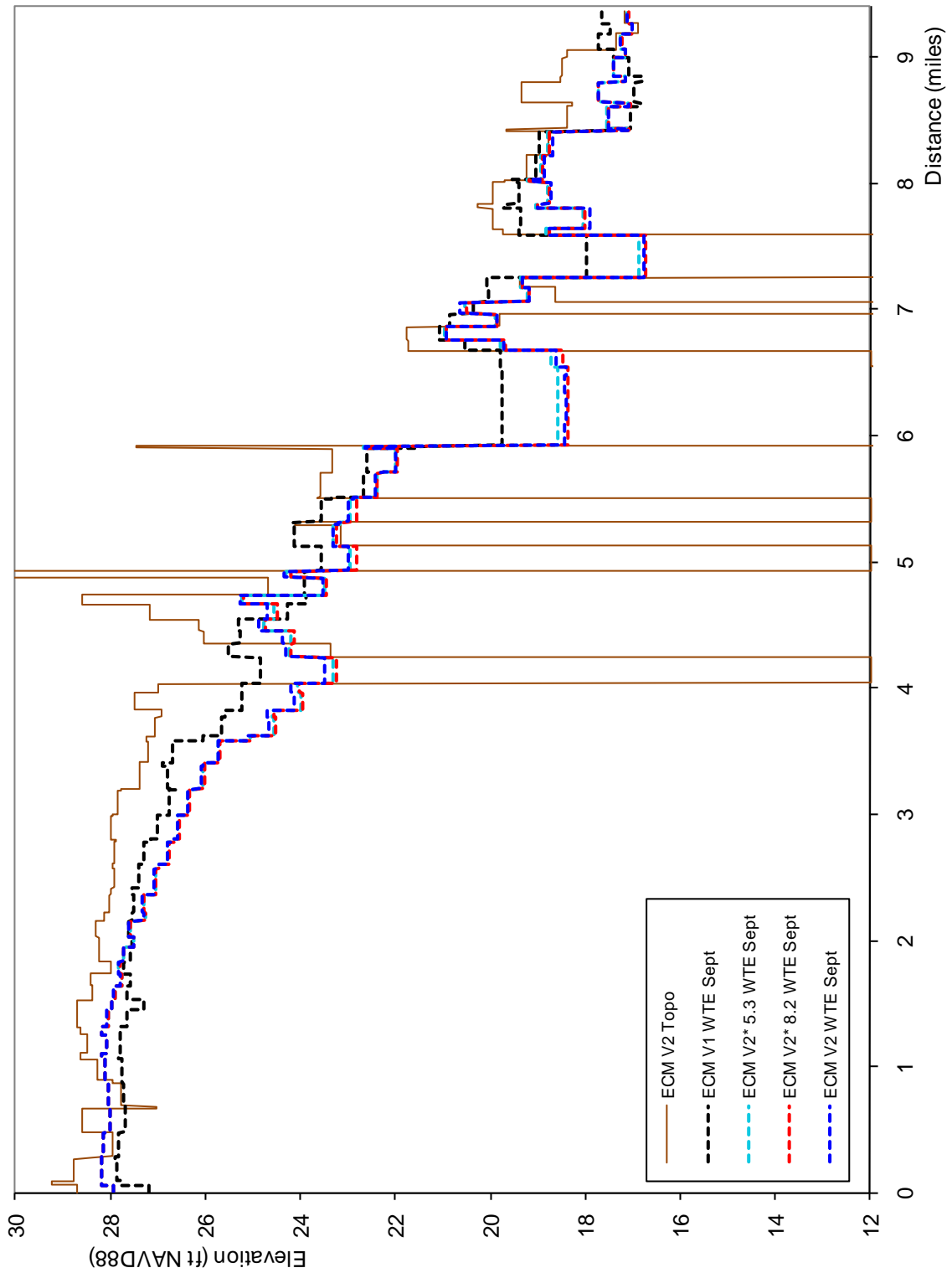


**Figure 34.** Water table level profile along Transect 2 presented in Figure 30 at the end of the wet season. The numbers 5.3 and 8.2 refer to the value in percent of LE - RET used.

## Hydroperiod

The determination of the wetland hydroperiod has been an important indicator used in this study. A wetland hydroperiod has several definitions, but for this evaluation it is defined as the period during which water in the model is at least 1 mm above the topographic surface. The simulated wetland hydroperiod for the DR/GR Area was qualitatively compared with hydroperiod maps generated based on data created by KLECE [2008]. The model follows similar general trends but the comparison is limited due to the coarser resolution of the model in comparison to the map from KLECE data. The scaling limitations are evident when comparing the results of the local higher resolution model hydroperiod map to the KLECE map with higher resolution. Nevertheless, the hydroperiod output of the model together with the water table elevation and the water balance computation provide useful insight into the impact of the land use changes on wetland areas.

The hydroperiod data developed by KLECE is based on the vegetation communities, which have been mapped from GIS data and aerial photographs taken in 2007. This hydroperiod map was generated based on the estimated relationships among vegetation, hydroperiod, and water depth conditions. These are shown in the legend on **Figure 35**. According to KLECE, the estimated water depths and hydroperiods are typical ranges of conditions for unaltered wetland systems in southwest Florida (KLECE 2008). These relationships have not been compared with measured water level data, though. Thus, a quantitative or direct comparison between this hydroperiod map and the one produced by the model is not appropriate.

The hydroperiod map for the DR/GR Area and the corresponding map of mean water depths during the hydroperiod obtained from the model are presented in **Figure 36** and **Figure 37**, respectively. Other related maps can be found in Appendix H.

The hydroperiod map obtained from LS ECM\* does not differ visibly when the lake evaporation changes from RET + 5.3 to RET + 8.2 (see maps in Appendix H). The same applies for the water depth maps during the hydroperiod. Thus, the hydroperiod maps do not show visible sensitivity to that change in lake evaporation.

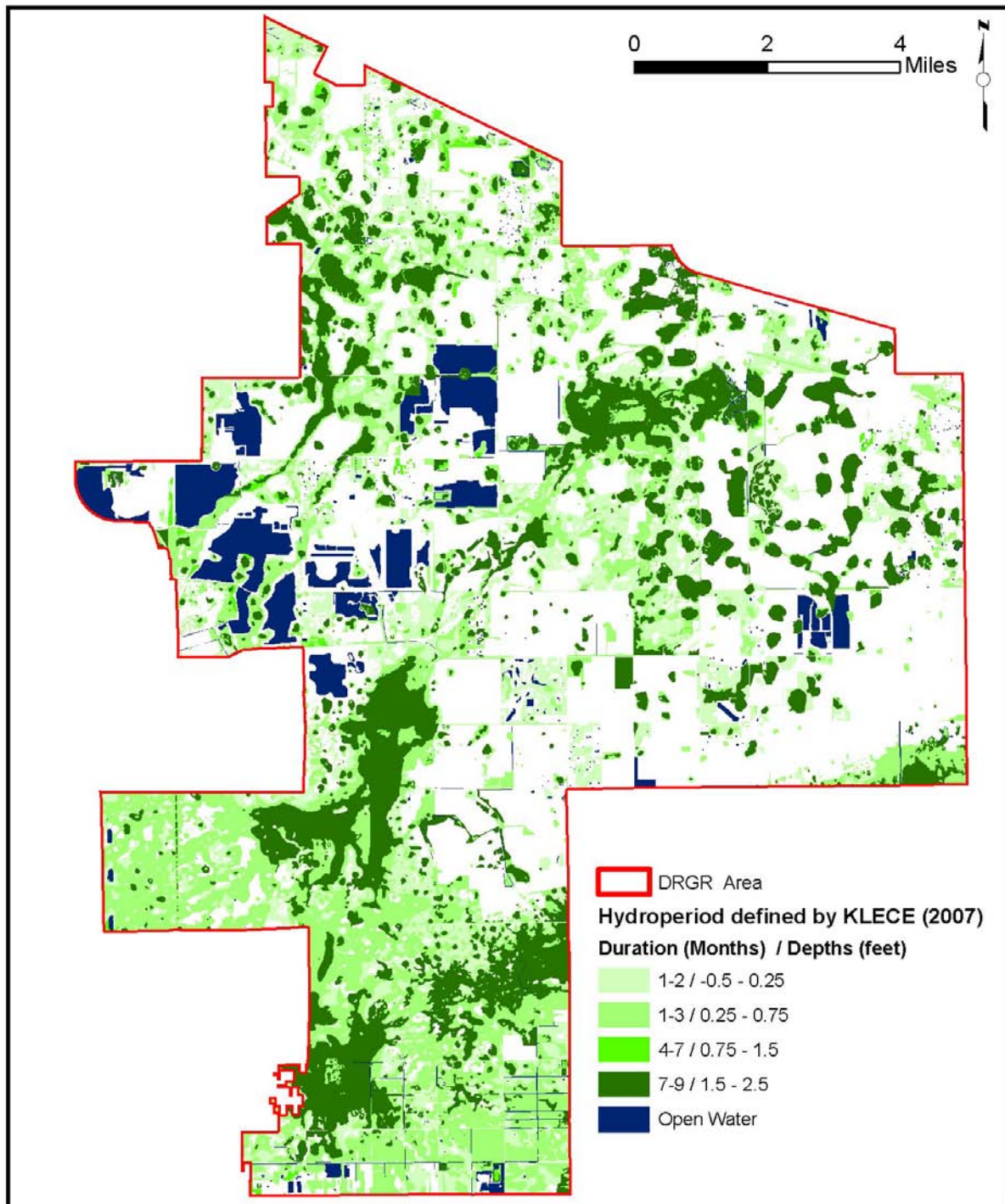


**Figure 35.** Hydroperiod map generated based on data created by KLECE from 2007 aerial photos.

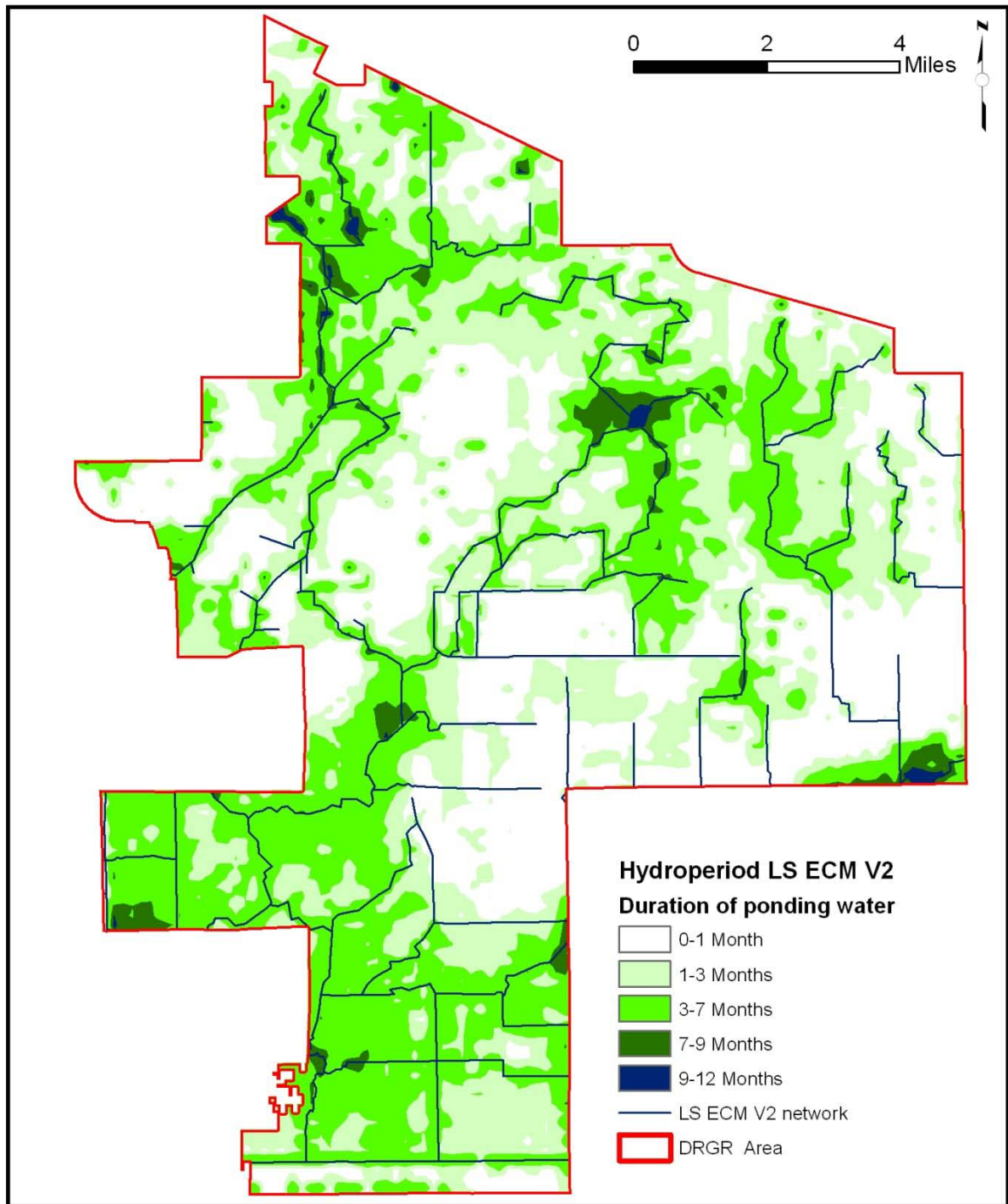
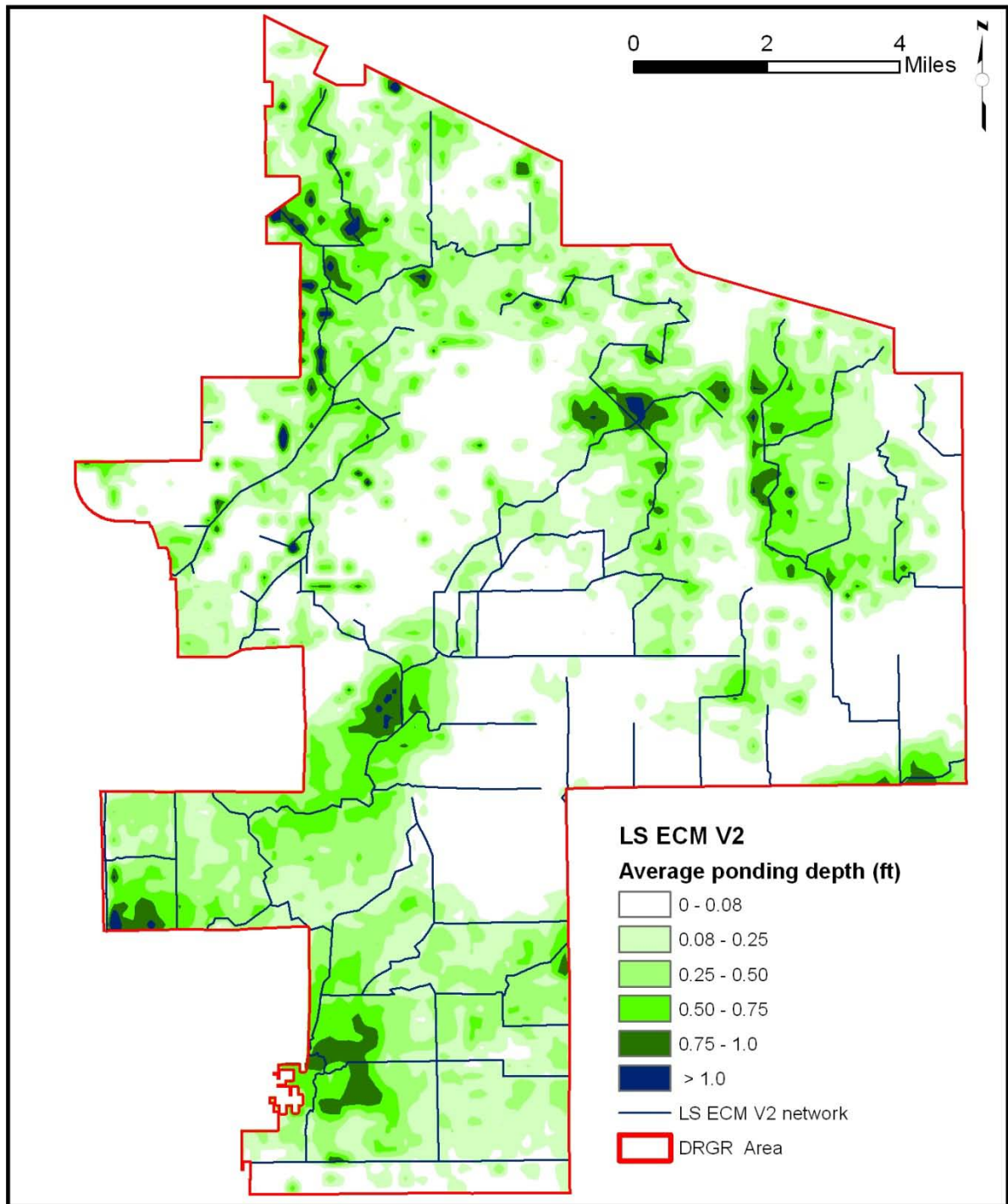


Figure 36. Hydroperiod map obtained from LS ECM.



**Figure 37.** Hydroperiod water depth map obtained from LS ECM.



## Water Budgets

A sketch of annual averaged water balance components obtained from the LS ECM in the entire DR/GR Area and in mining pits and shallow water bodies around the DR/GR area is presented in **Figure 38** and **Figure 39**, respectively. In **Table 13**, the water balance components from the final model and two intermediate models are displayed for comparison of the impact the lake evaporation has on the overall water budgets. All those water balance depth rates reported are annual averaged values for the 5-year period from 2002 to 2006.

Naturally, the increased ET rates in the open water bodies decreases the net rainfall (rainfall minus ET) in these areas. In fact, a lake evaporation of RET + 8.2% produces a net rainfall of zero inches per year in mining pits and lakes. Furthermore, the inclusion of a drainage system in some mining pits causes a net surface water outflow from mining pits and lakes in the model. As a result, the model predicts a negative groundwater outflow from the mining pits and open water bodies.

The overall water budget in the DR/GR area indicates that the higher ET rate and other changes made to the model causes a reduced boundary outflow through the groundwater, overland layers, and also through the rivers.

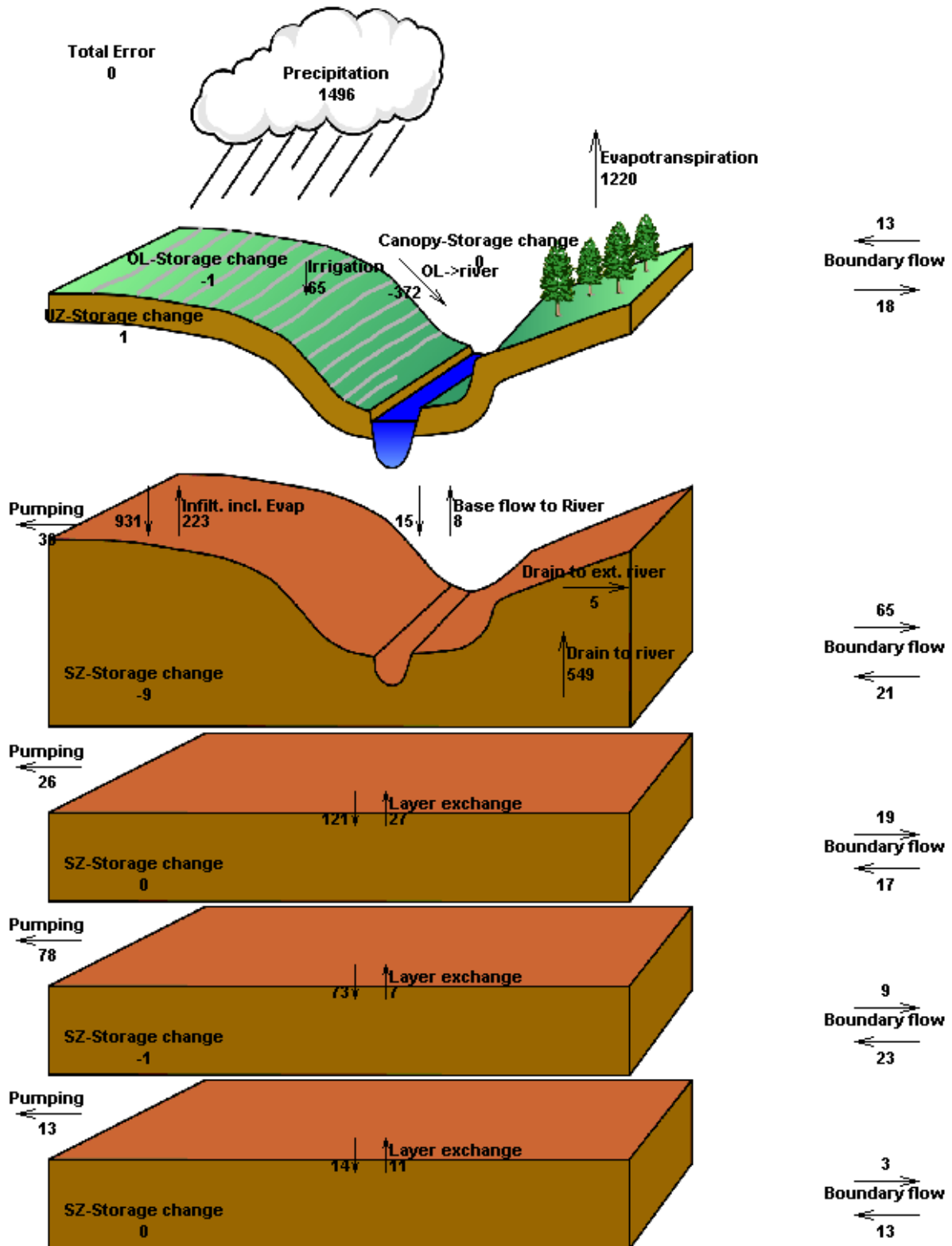


**Figure 38.** Annual averaged water balance components in mm/yr for the entire DR/GR Area as predicted by the LS ECM.

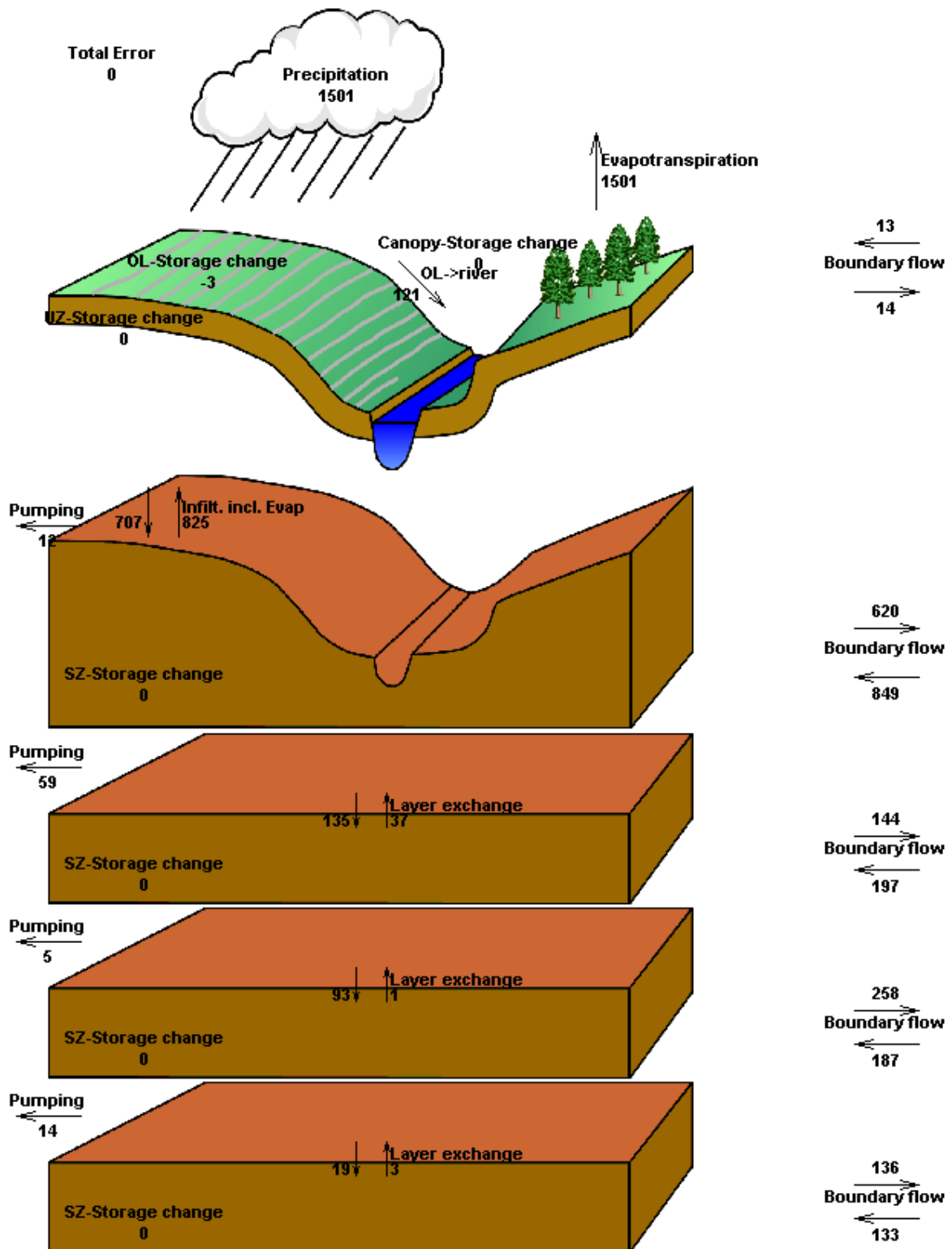


**Figure 39.** Annual averaged water balance components in mm/yr for the mining pits and other shallow water bodies around the DR/GR Area as predicted by the LS ECM.



**Table 13.** Annual average depth rates of the water balance components from the different versions of LS ECM, different ET data and in two different areas: in the entire DR/GR and in the Mining Pits and shallow water bodies in and around the DR/GR Area.

| Depth rates (inches/year)                 | Area                          | DR/GR       |             |             | Mining Pits |             |             |
|---|-------------------------------|-------------|-------------|-------------|-------------|-------------|-------------|
|   | LS ECM version                | ECM*        | ECM*        | ECM         | ECM*        | ECM*        | ECM         |
|   | ET                            | RET         | RET         | RET         | RET         | RET         | RET         |
|   | <b>LE - ET (% of ET)</b>      | <b>5.3</b>  | <b>8.2</b>  | <b>8.2</b>  | <b>5.3</b>  | <b>8.2</b>  | <b>8.2</b>  |
| Rainfall                                  |                               | 58.9        | 58.9        | 58.9        | 59.1        | 59.1        | 59.1        |
| ET  |                               | 48.1        | 48.1        | 48.0        | 57.5        | 59.1        | 59.1        |
| <b>Rainfall - ET (A)</b>                  |                               | <b>10.8</b> | <b>10.7</b> | <b>10.9</b> | <b>1.6</b>  | <b>0.0</b>  | <b>0.0</b>  |
| OL storage change                         |                               | 0.0         | 0.0         | 0.0         | -0.2        | -0.2        | -0.1        |
| UZ Storage change                         |                               | 0.0         | 0.0         | 0.0         | 0.0         | 0.0         | 0.0         |
| Total SZ Storage change (BSZ)             |                               | -0.4        | -0.4        | -0.4        | 0.0         | 0.0         | 0.0         |
| <b>Total storage (B)</b>                  |                               | <b>-0.4</b> | <b>-0.4</b> | <b>-0.4</b> | <b>-0.2</b> | <b>-0.2</b> | <b>-0.2</b> |
| Net OL Boundary outflow (COL)             |                               | 0.1         | 0.1         | 0.2         | 0.0         | 0.0         | 0.0         |
| Drain to Boundary (CDR)                   |                               | 0.0         | 0.0         | 0.0         | 0.0         | 0.0         | 0.0         |
| Net SZ Boundary outflow from SZ1          |                               | 1.7         | 1.7         | 1.7         | -8.0        | -9.0        | -9.0        |
| Net SZ Boundary outflow from SZ2          |                               | 0.0         | 0.0         | 0.1         | -2.1        | -2.2        | -2.1        |
| Net SZ Boundary outflow from SZ3          |                               | -0.6        | -0.6        | -0.5        | 3.0         | 2.9         | 2.8         |
| Net SZ Boundary outflow from SZ4          |                               | -0.4        | -0.4        | -0.4        | 0.2         | 0.1         | 0.1         |
| Net SZ Boundary outflow from all SZ (CSZ) |                               | 0.8         | 0.8         | 0.9         | -7.0        | -8.2        | -8.2        |
| <b>Total Boundary outflow (C)</b>         |                               | <b>0.9</b>  | <b>0.9</b>  | <b>1.1</b>  | <b>-7.0</b> | <b>-8.1</b> | <b>-8.2</b> |
| Pumping from SZ1                          |                               | 1.5         | 1.5         | 1.2         | 0.6         | 0.6         | 0.5         |
| Pumping from SZ2                          |                               | 1.1         | 1.1         | 1.0         | 2.5         | 2.5         | 2.3         |
| Pumping from SZ3                          |                               | 3.3         | 3.3         | 3.1         | 0.2         | 0.2         | 0.2         |
| Pumping from SZ4                          |                               | 0.5         | 0.5         | 0.5         | 0.6         | 0.6         | 0.6         |
| Pumping from all SZ                       |                               | 6.4         | 6.4         | 5.8         | 3.8         | 3.8         | 3.6         |
| Irrigation                                |                               | 3.2         | 3.2         | 2.5         | 0.0         | 0.0         | 0.0         |
| <b>Pumping-Irrigation (D)</b>             |                               | <b>3.2</b>  | <b>3.2</b>  | <b>3.2</b>  | <b>3.8</b>  | <b>3.8</b>  | <b>3.6</b>  |
| Infiltration from OL to SZ1               |                               | 27.5        | 27.4        | 27.9        | -3.2        | -4.4        | -4.7        |
| Infiltration from SZ1 to SZ2              |                               | 3.9         | 3.9         | 3.7         | 4.2         | 4.0         | 3.9         |
| Infiltration from SZ2 to SZ3              |                               | 2.8         | 2.8         | 2.6         | 3.8         | 3.8         | 3.6         |
| Infiltration from SZ3 to SZ4              |                               | 0.1         | 0.1         | 0.1         | 0.7         | 0.7         | 0.7         |
| OL->river                                 |                               | -13.7       | -13.6       | -14.7       | 4.9         | 4.5         | 4.8         |
| Drain to river                            |                               | 20.7        | 20.6        | 21.6        | 0.0         | 0.0         | 0.0         |
| Drain to ext. river                       |                               | 0.2         | 0.2         | 0.2         | 0.0         | 0.0         | 0.0         |
| Base flow to River                        |                               | -0.2        | -0.2        | -0.3        | 0.0         | 0.0         | 0.0         |
| <b>Total flow to river (E)</b>            |                               | <b>7.0</b>  | <b>7.0</b>  | <b>6.9</b>  | <b>4.9</b>  | <b>4.5</b>  | <b>4.8</b>  |
| Error (A-B-C-D-E)                         |                               | 0.0         | 0.0         | 0.0         | 0.0         | 0.0         | 0.0         |
| Boundary surface outflow (runoff)         | COL+CDR+E                     | 7.2         | 7.1         | 7.1         | 5.0         | 4.6         | 4.8         |
|   | COL+CDR                       | ---         | ---         | ---         | ---         | ---         | ---         |
| Net groundwater recharge                  | A-(B-BSZ)-(C-CSZ)-E=BSZ+CSZ+D | 3.6         | 3.6         | 3.7         | -3.2        | -4.4        | -4.7        |
|   | A= B+C+D+E                    | ---         | ---         | ---         | ---         | ---         | ---         |

Note: the preliminary version of LS ECM is marked with an “\*”.

## Surface Water Flow

**Figure 40** shows the annual average flow rate in the MIKE 11 network as predicted with the LS ECM from year 2002 to 2006. Primary flow ways are the ones having higher averaged flow rates. The sudden changes in color in the branches primarily indicate the interaction with the overland component of MIKE SHE, i.e., locations where water is flowing between the rivers and the flood plains. The annual average flow map suggests that the MIKE 11 network generated following incorporation of the high resolution LIDAR data into the LS ECM more accurately represents the main flow ways in the DR/GR Area compared to its performance prior to the reanalysis of the flow ways. Further refinement in the network can be conducted by removing branches with negligible flow (that are not visible in Figure 40) and by checking the path and cross section geometry in locations with high interaction with overland flow.

A closer look to the annual average flow rate through the conceptual weirs around mining pits (that were introduced to represent the drainage system) is presented in **Figure 41**. Single sided arrows are used to represent the net flow direction and double sided arrows are used where there are important flows in both directions. The instantaneous flow rates at some of those weirs are plotted in **Figure 42**. According to the model, mining pits with conceptual weirs at locations D and G may serve as reservoirs, collecting water during the rainy season and releasing it early in the dry season. Mining pits with conceptual weirs at locations E-F and I-J may serve to route surface water in the southwest direction. A positive or negative net annual flow rate into a mining pit may indicate whether the specific mining pit is contributing to the groundwater recharge or discharge, respectively. The drainage system around the mining pits is based on LIDAR data elevations and other model assumptions. Observation data to compare and validate those model results were not available at that time.

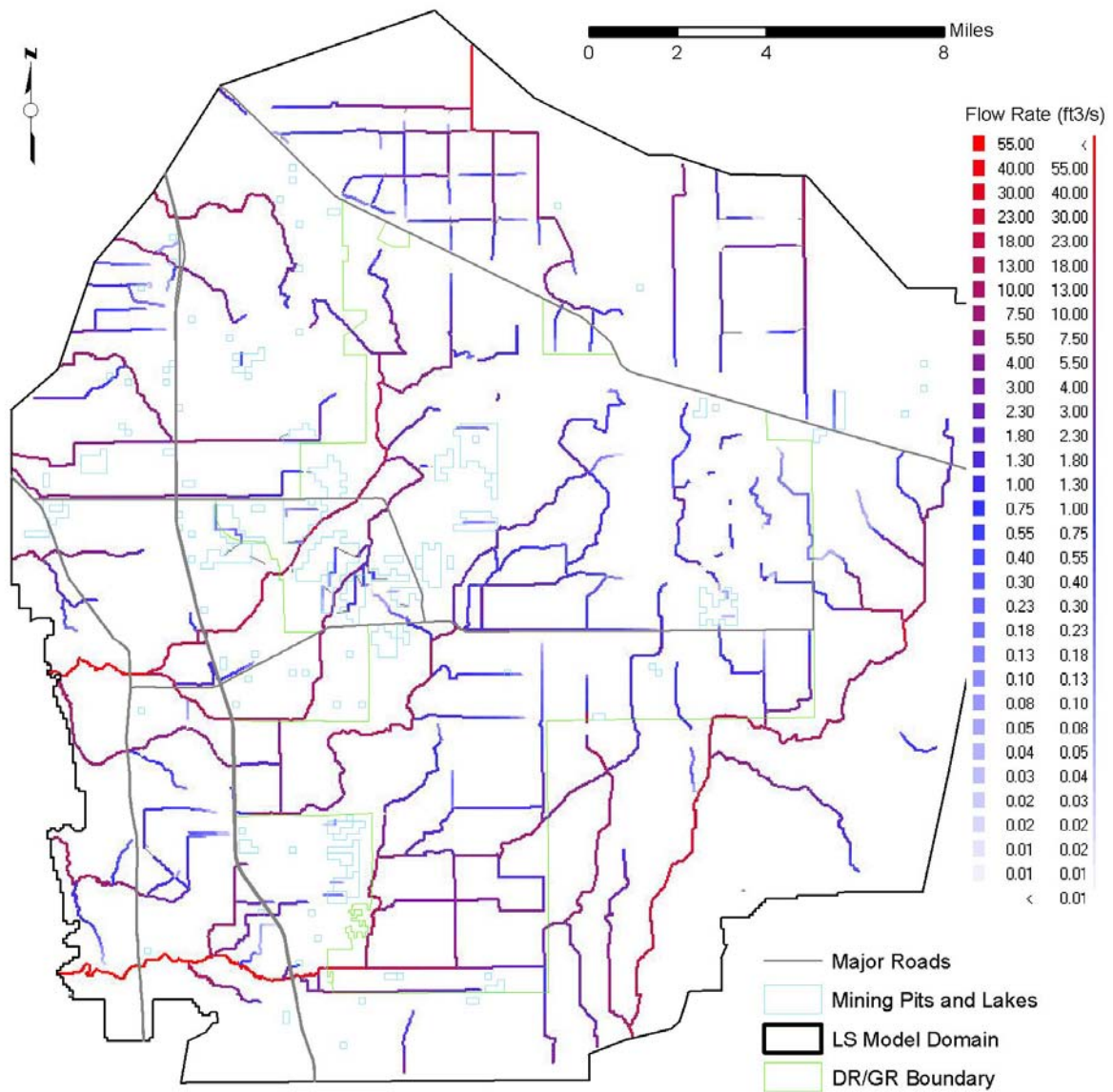


**Figure 40.** Annual averaged flow rates obtained at the river network from the LS ECM.

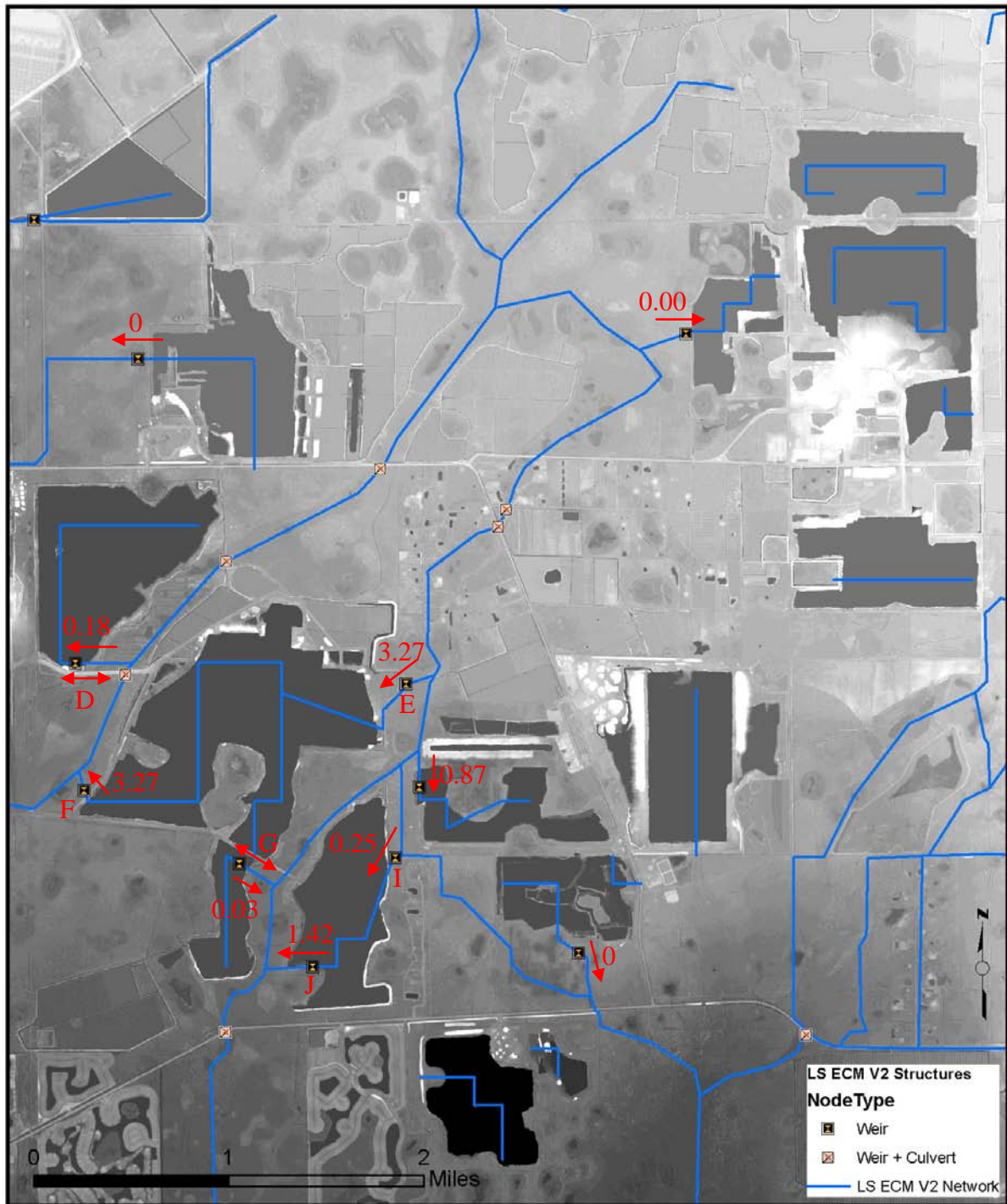


**Figure 41.** Annual averaged flow rates (in ft<sup>3</sup>/s) in the drainage system around mining pits as obtained from the LS ECM.

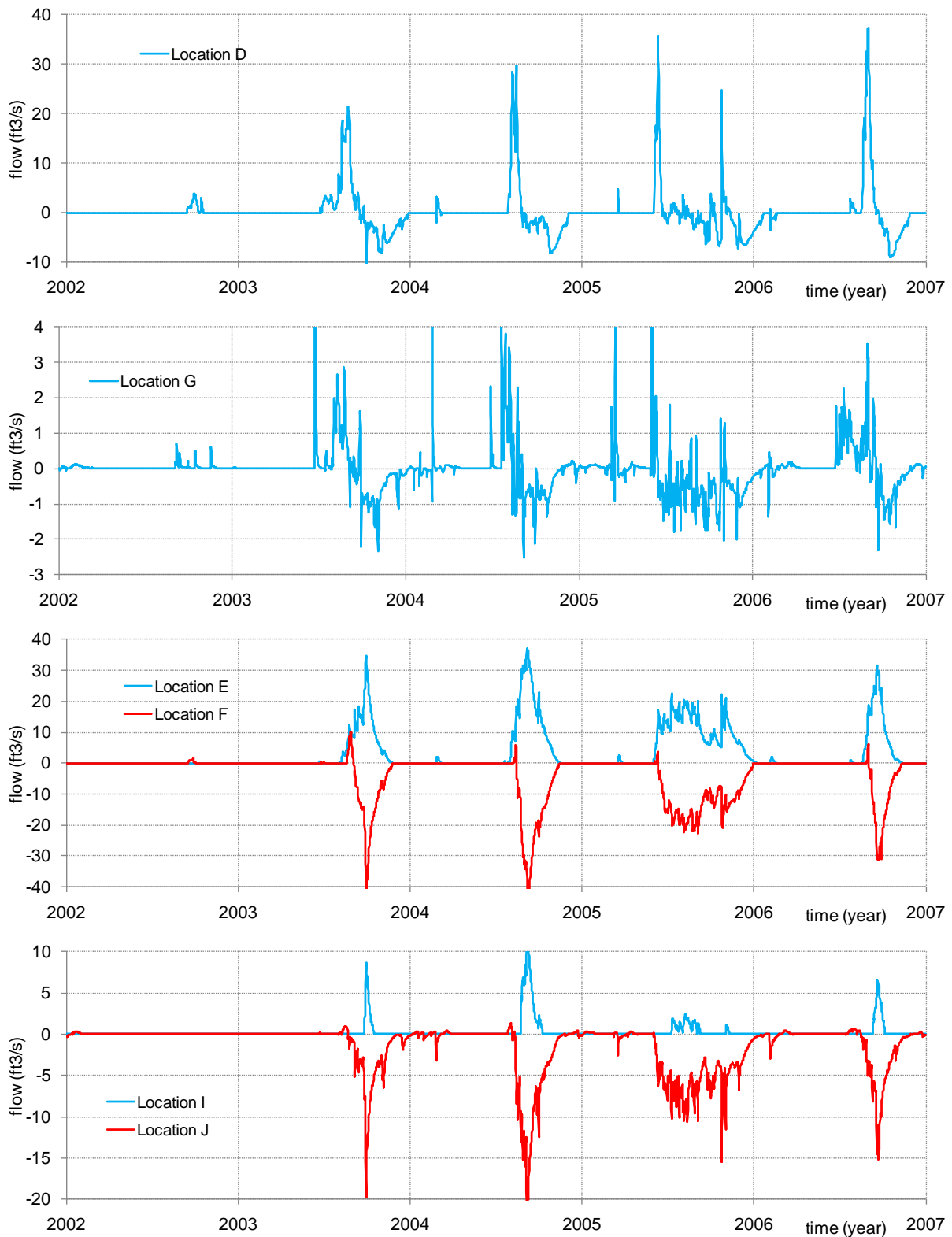


**Figure 42.** Flow rates at some conceptual weirs around mining pits presented on Figure 41.

Note: solid blue and red lines are used when positive flow is toward and away from the mine, respectively.

## Land Use Scenarios

In order to evaluate the hydrological effects of land use changes in the DR/GR Area, four Future Conditions Models (FCMs) were developed. The results of these models were analyzed by using relative measures, such as differences in hydroperiod, water table elevations, and overall water budget.

### Development of Future Land Use Alternatives

The future land use scenarios consist of four alternatives in the DR/GR Area provided by Lee County (see land use maps in Appendix D). The land use changes are of three types: creation of urban areas, expansion or creation of mining pits and restoration of agricultural lands into wetlands. Land use alternative 1 (FCM1) is conceptually similar to Scenario 1 in “Prospects for Southeast Lee County” [Dover, Kohl & Partners, July 2008]. Mining would be limited to already-approved mining pits plus some new pits north of Alico Road near the airport (but fewer pits than in Scenario 1). A broad westerly flow way to Corkscrew Swamp would be restored southward from the Imperial Marsh. Land use alternative 2 (FCM2) is conceptually similar to Scenario 2 in the Dover Kohl report. Mining would be limited to already-approved pits plus a major expansion to the Green Meadows Mine. A broad flow way to Corkscrew Swamp would be restored southward from the east end of Corkscrew Road in Lee County. Land use alternative 3 (FCM3) is conceptually similar to Scenario 3 in the Dover Kohl report. Mining would be limited to already-approved pits plus proposed new pits that were in the application process in September 2007, including pits along Corkscrew Road east of the Flint Pen Strand. Both flow ways to Corkscrew Swamp would be restored to whatever extent is still possible after significant portions of each were mined. Land use alternative 4 (FCM4) is conceptually similar to an alternative scenario that emerged favorably during public meetings after release of the Dover Kohl report. Mining would be limited to already-approved pits plus a moderate expansion to the Green Meadows Mine. Both flow ways to Corkscrew Swamp would be restored in full. The extent of the restored areas in all scenarios is less than originally proposed in the Dover Kohl report.

The new urban areas added in the future conditions land use map were exactly the same in all four alternatives. The increase of new mining areas from smallest mining area to largest mining area is: FCM1, FCM4, FCM2, and FCM3. The mining area in FCM3 is nearly double the amount of mining area in FCM1. The amount of mining area in FCM2 and FCM4 are approximately the same, and these scenarios fall in between FCM3 and FCM1, with respect to mined area. The total amount of newly restored areas increases monotonically from FCM1 to FCM4. FCM3 is a unique case in that its restored areas are imbedded with mining pits. Figures and tables in Appendix D show more details of the land use changes for all scenarios.

All land use based parameters in the model (e.g., overland roughness Manning’s coefficient, detention storage, paved runoff fractions, drainage depths and drainage time constants) were modified to correspond to the new land use maps, but the relationship between land use type and parameters remained consistent with the ECM. The same meteorological and boundary conditions data utilized in the ECM were used in the four FCMs. The irrigation setup

in the future conditions model was modified to reflect future land use changes. For example, irrigation areas were removed in areas where the land use was converted from urban or agricultural to mining or wetland areas. For new urban areas, irrigation was added in those close to the northern DRGR boundary. The monthly groundwater withdrawal rates of the most recent year of available groundwater withdrawal data were repeated for every year in the FCM simulation period (2002-2007). In some cases, the 2007 withdrawal rates were used if available, but in others the 2006 rates were used. The same groundwater withdrawal rates for public water supply were used for the four future conditions scenarios. The domestic self supply rates vary according to land use changes.

## **Initial Conditions**

Special effort was conducted to obtain initial conditions that are representative of “average” or “steady state” conditions in the LS FCMs, as in the final version of the LS ECM. The SFWMD technical staff recommends a warming period of several months in the model (including an entire rainy season) in order to make the model results independent of the initial condition assumed. However, in the DR/GR model, there are two slow processes that need more than one year in order to remove the long term “drift” caused by assuming inaccurate initial conditions. They are the head in the deepest layer (sandstone aquifer) and the water level in mining pits.

Three to five iterations (running the model for three years and taking the results from September 1, 2004 as initial conditions for the next run) were necessary to assure that the differences in water elevation in mining pits between iterations is less than 10 cm.

Assuming “average” or “steady state” initial conditions in the FCMs means that the model is evaluating the water resources at some time long after the land use changes. In other words, the period of time during which those land use changes are being made are not simulated in the model.

## **Results**

The results shown in this section demonstrate the potential effect of land use alternatives on the water resources of the DR/GR Area. Water table levels at specific locations (where changes in land use occur) were plotted for the different scenarios to compare the water table level changes throughout the five year simulation period. Averaged water table elevation maps were created for all land use alternatives for two times of the year: at the end of the dry season (end of May) and at the end of the wet season (end of September). Hydroperiod maps and maps of the mean water depth during the hydroperiod were also produced for all scenarios. Water table level and hydroperiod map differences between the FCMs and the ECM are also presented.

The water budget for the entire DR/GR Area was calculated to determine what hydrologic components were affected by the different alternatives. Finally, changes in surface water flow were calculated at specific locations for each scenario.

## Water Table Plots

**Figure 43** to **Figure 46** illustrate the specific locations where the changes in water table elevation were compared for all land use alternatives throughout the 5-year simulation period. The water table elevation plots are shown in **Figure 47** to **Figure 69**. The following results arise from those comparative plots:

- In all the locations converted to mining pits (M2, M6, M7, M8, M12, and M15), the seasonal amplitude of the water table oscillation is reduced, which is an expected consequence of increased open-water storage in mining pits.
- The model results in locations M1, M2 and M3 (see **Figure 70**) predict that the mine is acting like a groundwater reservoir, i.e., releasing water (collected during the rainy season) into the aquifers during the dry season. As a result, the seasonal amplitude of the water table oscillation around the mine pit is reduced, and particularly, the water table level during the dry season is higher. This effect is an expected consequence of the higher open-water storage than in the neighboring porous media. In the Water Budget section, further analysis of this proposed mine is conducted by computing the water balance components.
- Locations M4, M5, M6 and M7 are upstream of a mining pit complex in the DR/GR Area, and locations M8, M9 and M10 are downstream. As predicted by the model, larger and more closely spaced mining pits in the FCM create a larger flattening effect over the regional water table gradient. Specifically, the dry-season water table level decreases up gradient and increases down gradient. This effect was also observed on a smaller scale around single mining pits in locations with steeper slopes at locations M11 and M13. The areal extent of zones with lower and higher water table levels can be seen in the maps presented in the following section.
- In two of the three locations converted to wetlands (W2 and W3), the dry-season water table elevation increases. In the case of location W3, that increase is higher when it is close to new mining pits (in FCM3).
- Most of the new urban locations (U1, U2, and U3) showed a slight decrease in the wet-season water table elevation, which is likely a consequence of the new urban drainage. An increase in the dry-season water table elevation is observed in most of the new urban locations (U1, U3, and U4), which is likely related to a reduction in the ET losses (see more details in the water budget section).

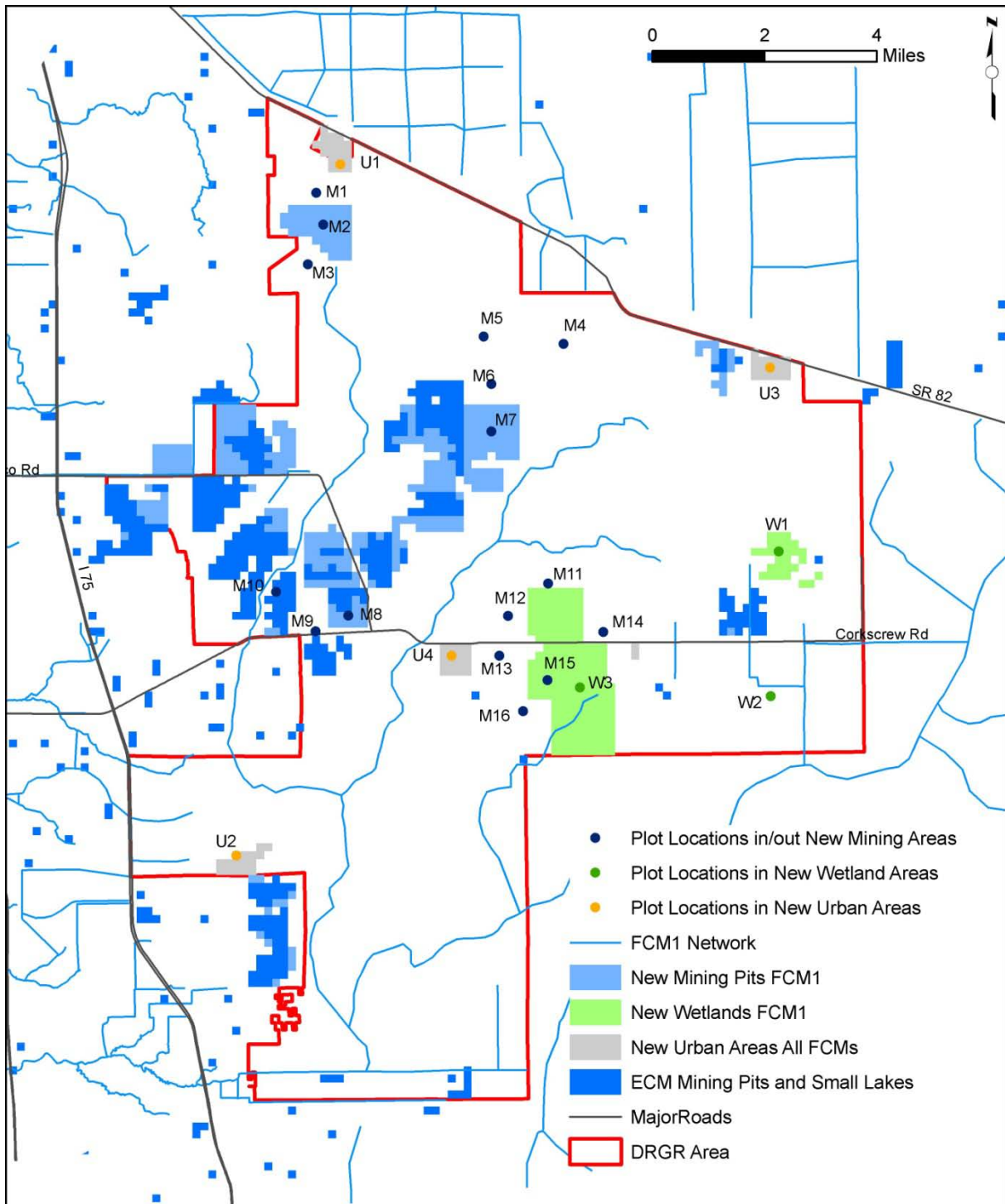


**Figure 43.** Land use changes in the Future Conditions Model 1 and locations of water table comparison plots.

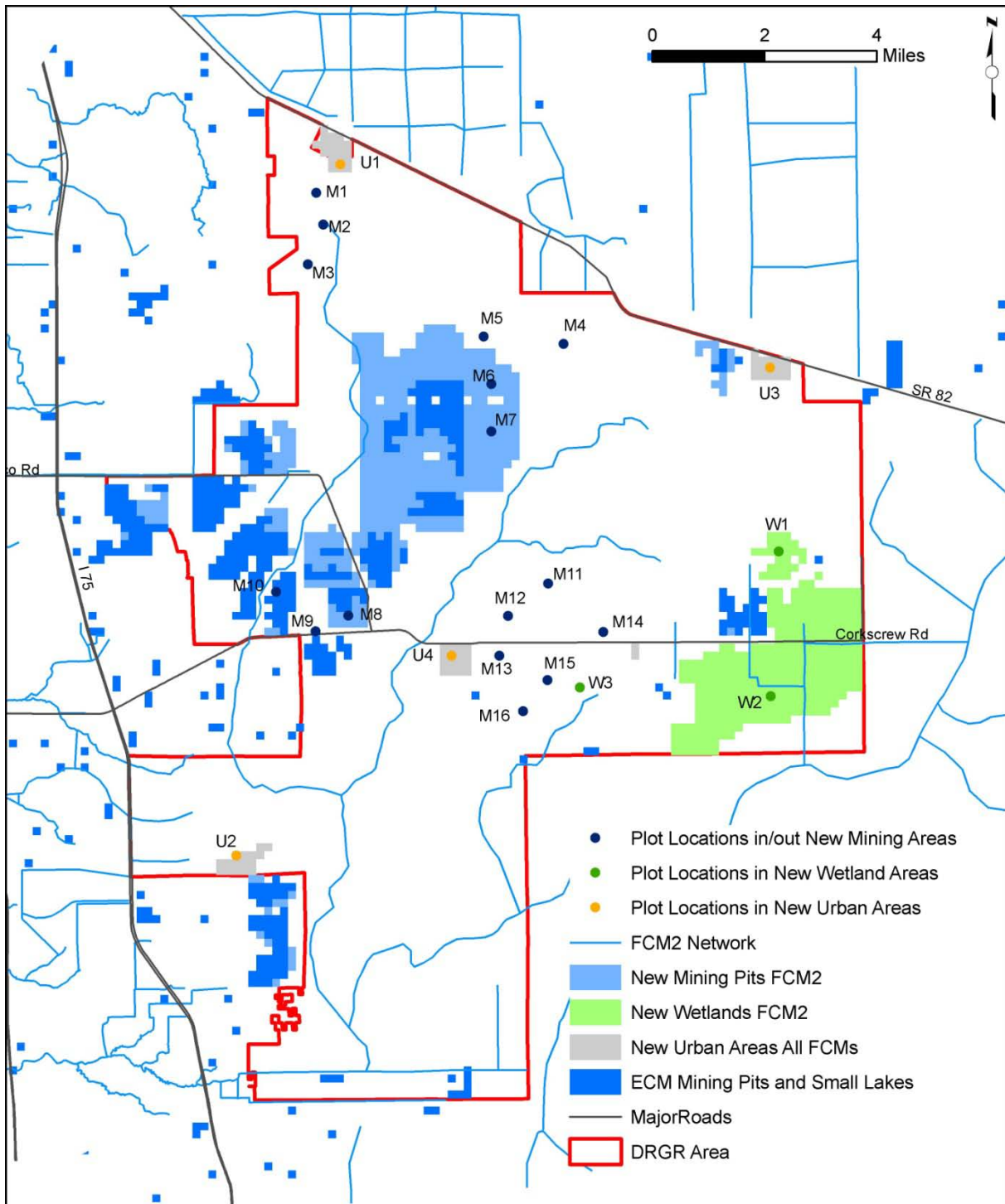


**Figure 44.** Land use changes in the Future Conditions Model 2 and locations of water table comparison plots.

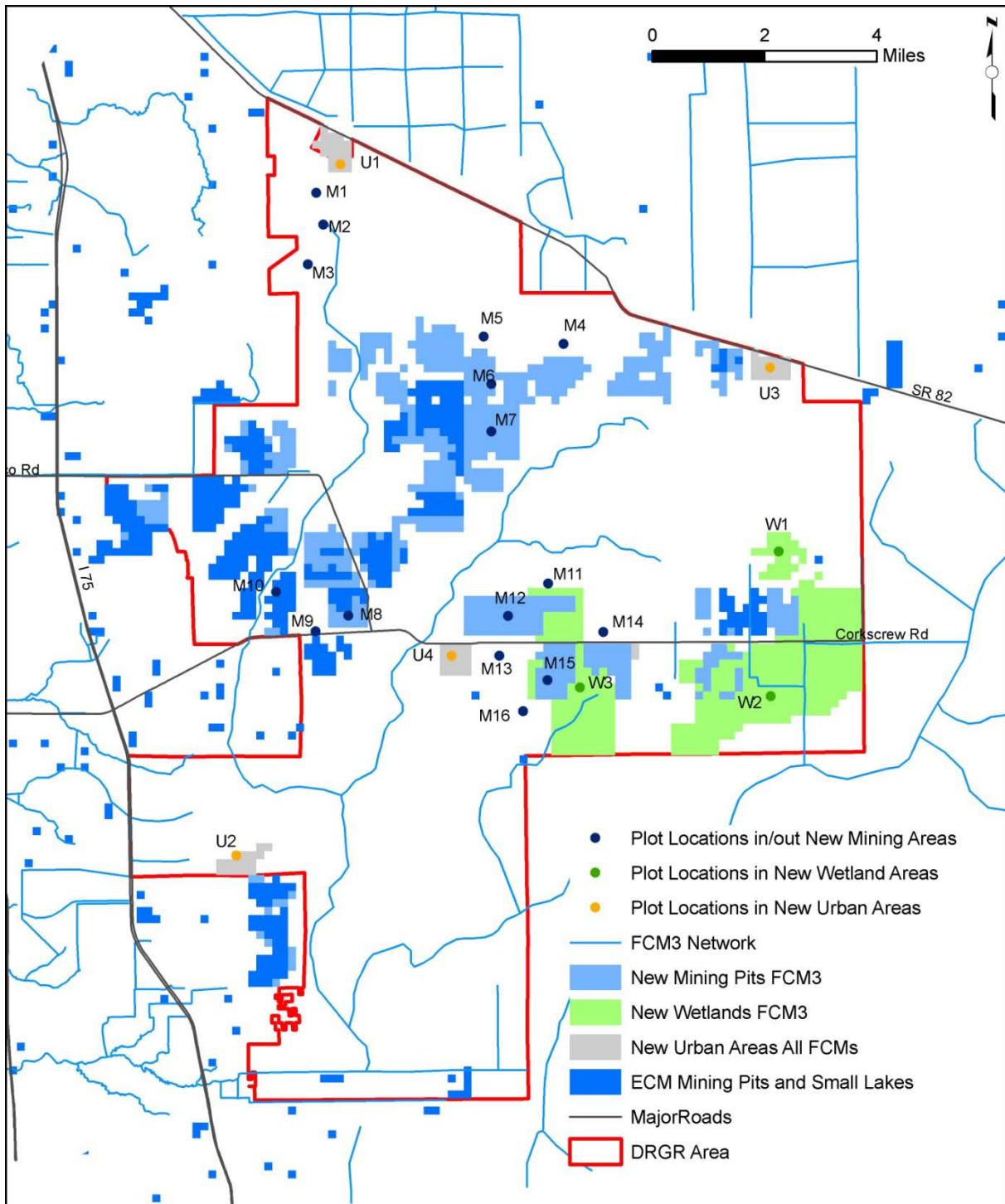


**Figure 45.** Land use changes in the Future Conditions Model 3 and locations of water table comparison plots.

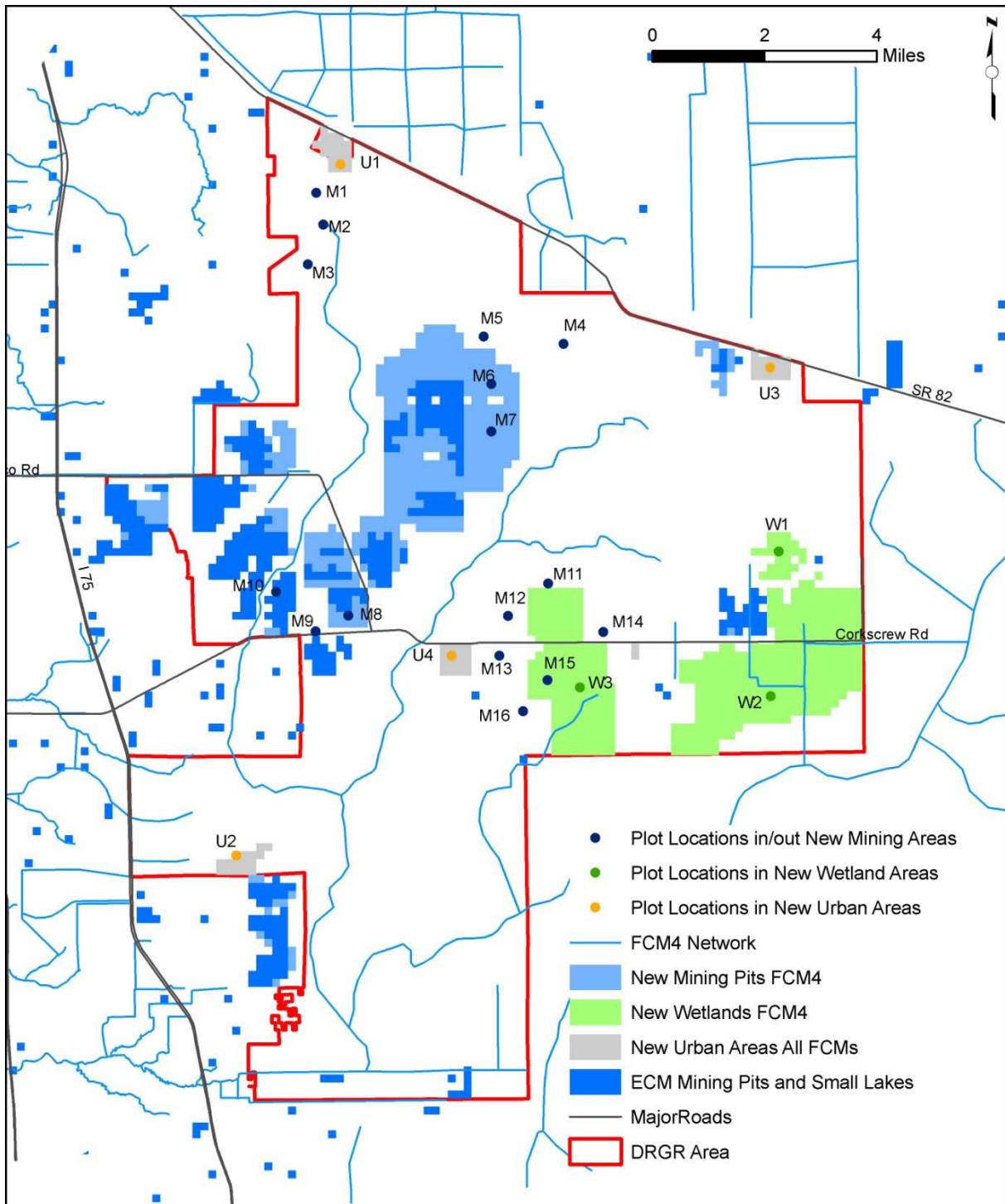


**Figure 46.** Land use changes in the Future Conditions Model 4 and locations of water table comparison plots.

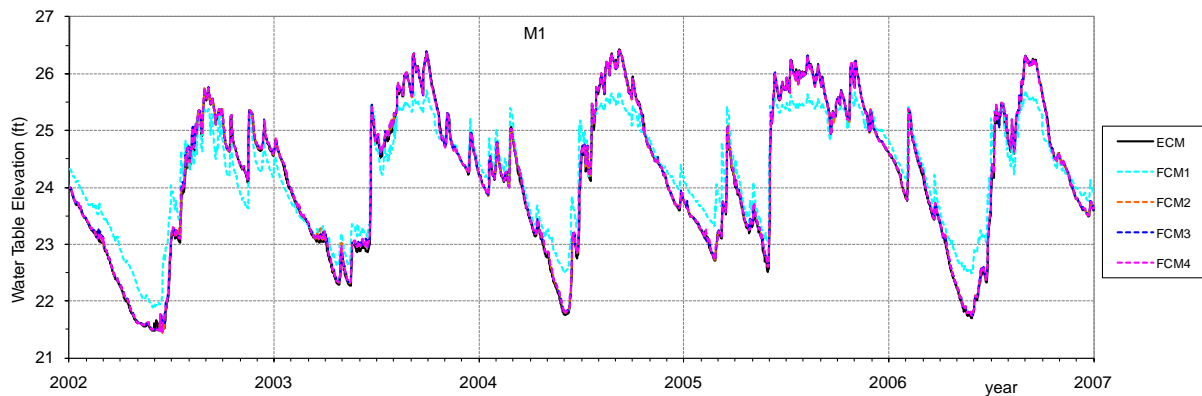


**Figure 47.** Water table elevations at land use change location M1.

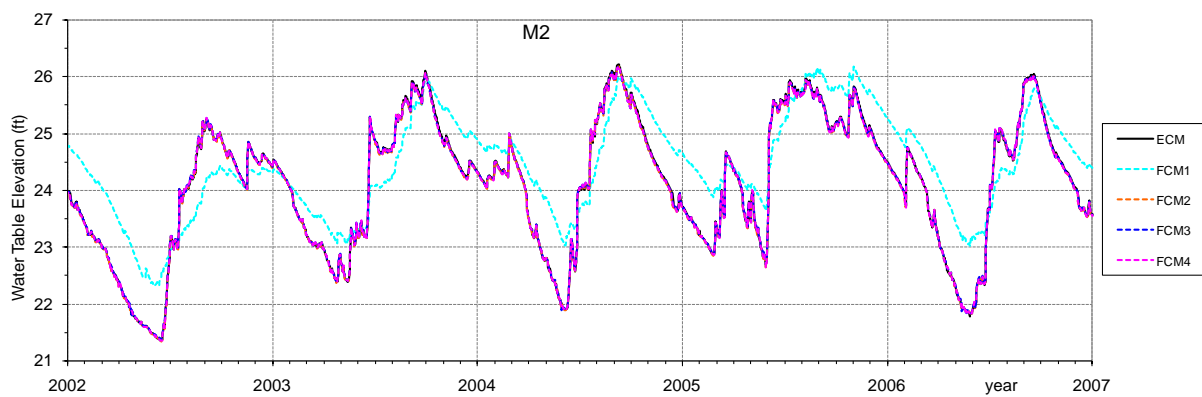


**Figure 48.** Water table elevations at land use change location M2.

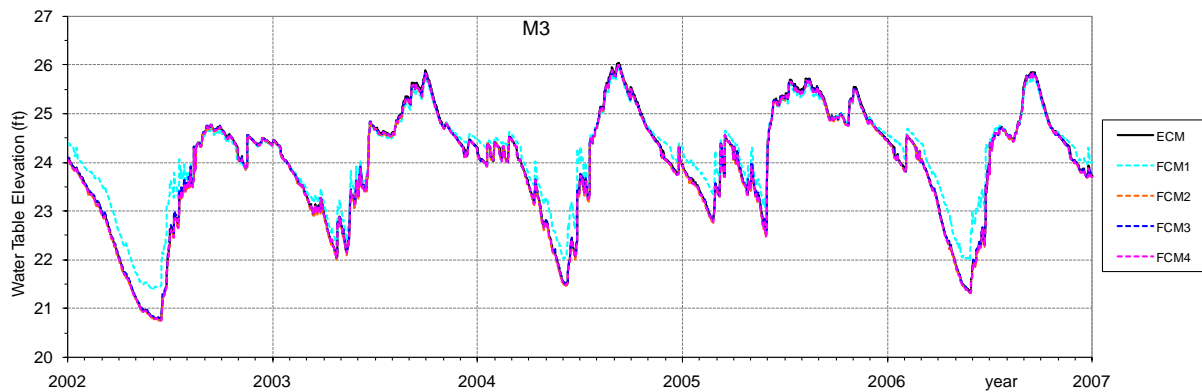


**Figure 49.** Water table elevations at land use change location M3.

**Note:** Locations M1 and M3 are close to a new mining pit included in FCM1 and location M2 is inside it. The model predicts that this mining pit recharges the groundwater such that the water table elevation (WTE) in neighboring areas increases during dry periods compared to the ECM. WTE oscillation in location M2 shows a reduction in the seasonal amplitude when located in a mining pit. The corresponding seasonal averaged plots are shown in Figure 70.

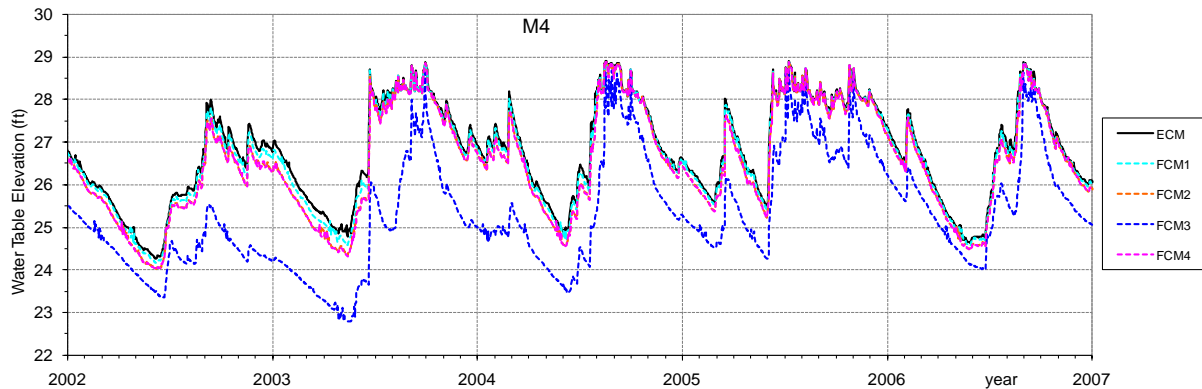


**Figure 50.** Water table elevations at land use change location M4.

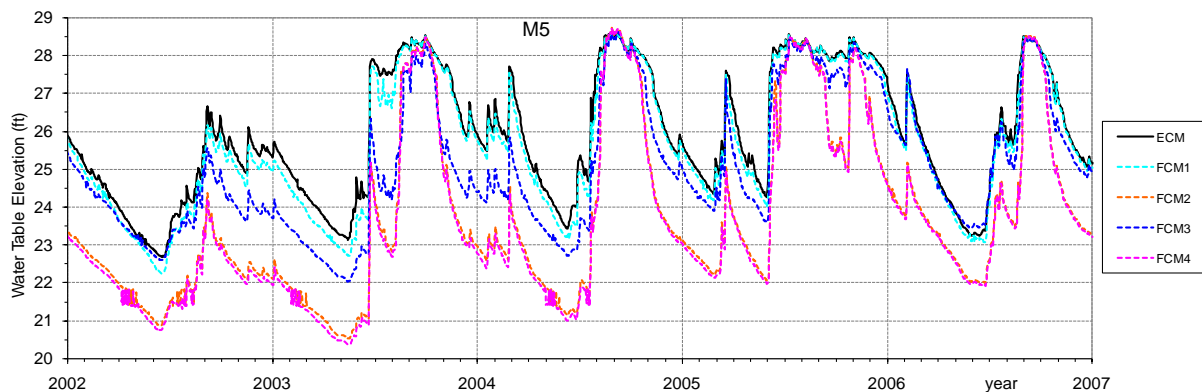


**Figure 51.** Water table elevations at land use change location M5.

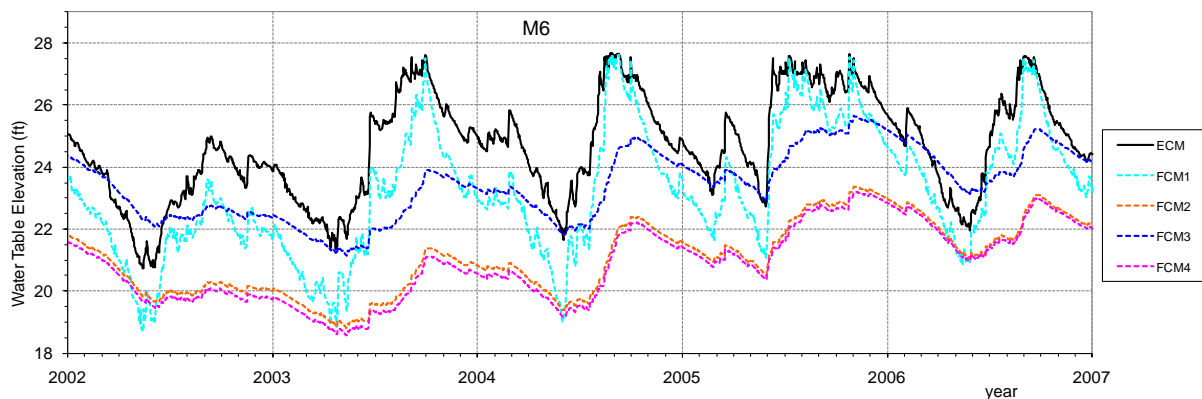


**Figure 52.** Water table elevations at land use change location M6.

**Note:** Locations M4, M5, M6 and M7 show that the new mining pit area in the FCMs generally causes a WTE decrease in the northern–central part of the DR/GR Area. This area is up gradient of the large mining pit complex area. WTE oscillation in locations M6 and M7 indicate a reduction in the seasonal amplitude when they become part of a mining pit.

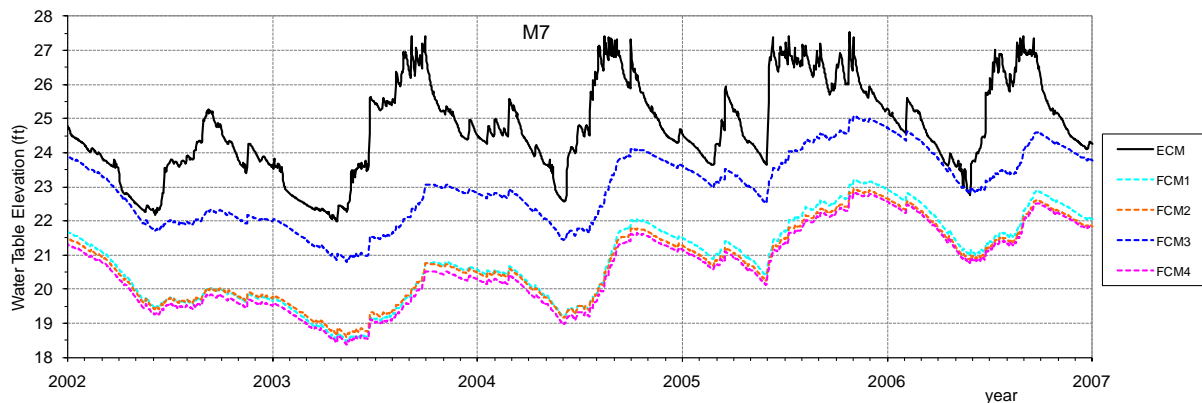


**Figure 53.** Water table elevations at land use change location M7.

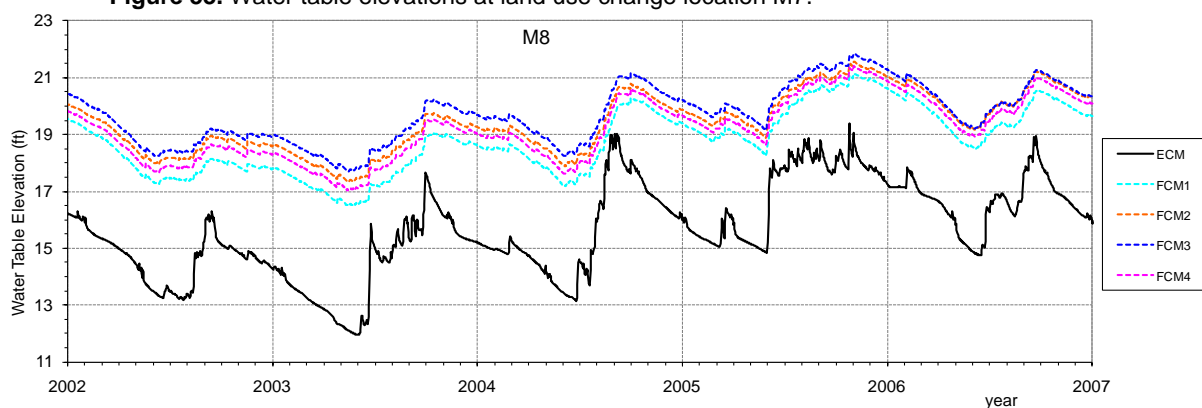


**Figure 54.** Water table elevations at land use change location M8.

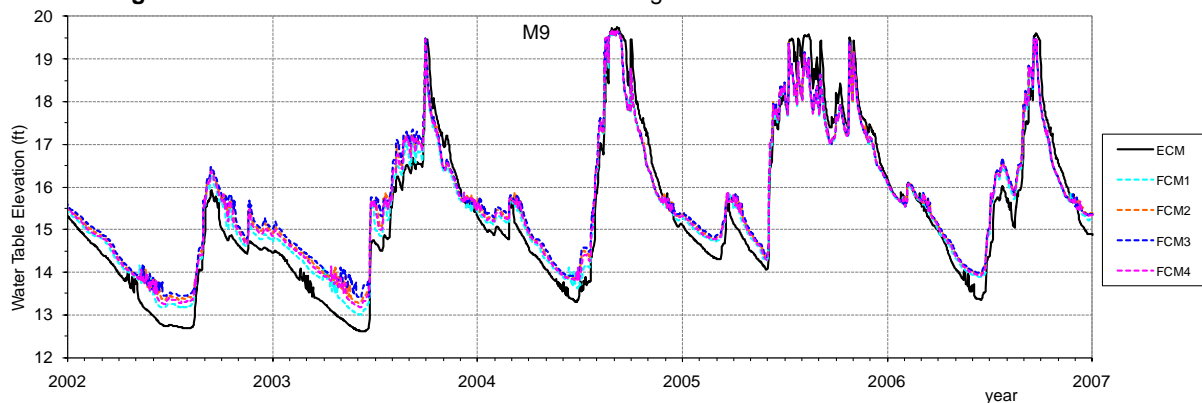


**Figure 55.** Water table elevations at land use change location M9.

Note: Locations M8, M9, and M10 show that the new mining pit area in the FCMs generally cause a WTE increase in the western-central part of the DR/GR Area. This area is down gradient of the large mining pit complex area. The WTE oscillation in location M8 is reduced in seasonal amplitude when it becomes part of a mining pit.

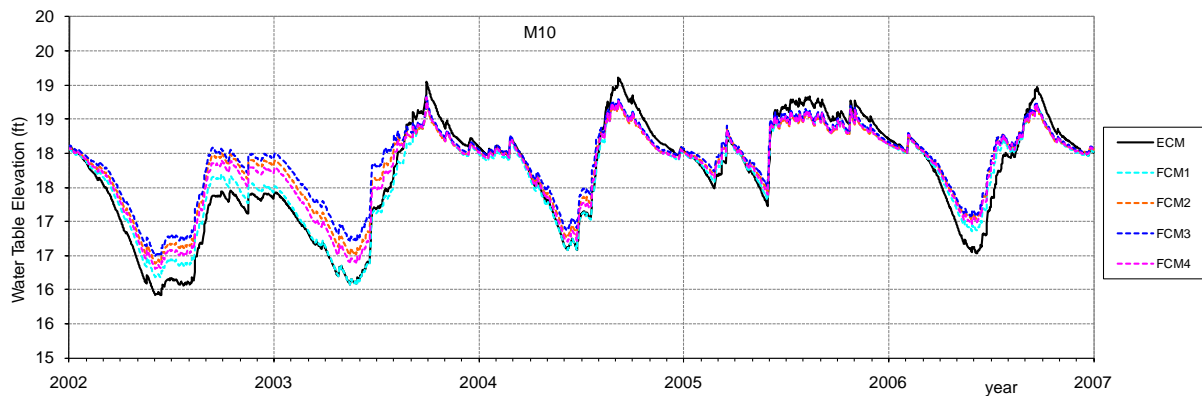


**Figure 56.** Water table elevations at land use change location M10.

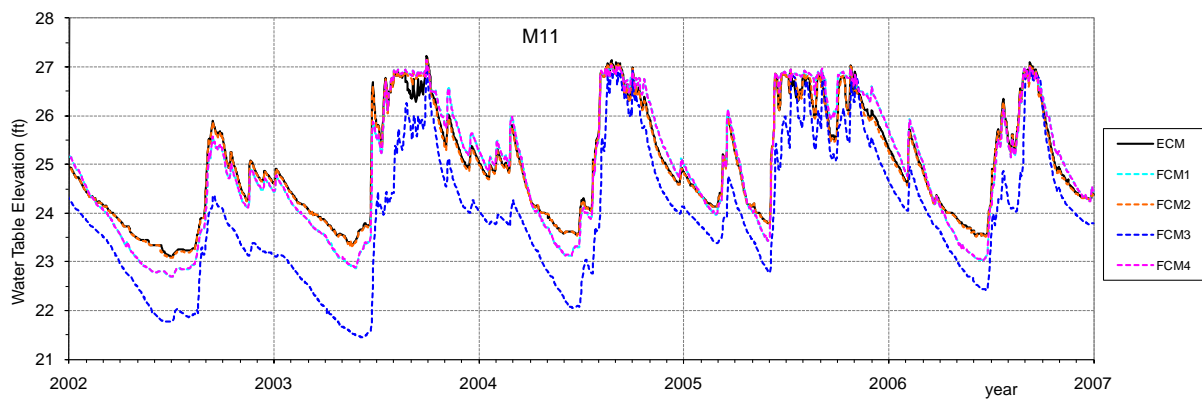


**Figure 57.** Water table elevations at land use change location M11.

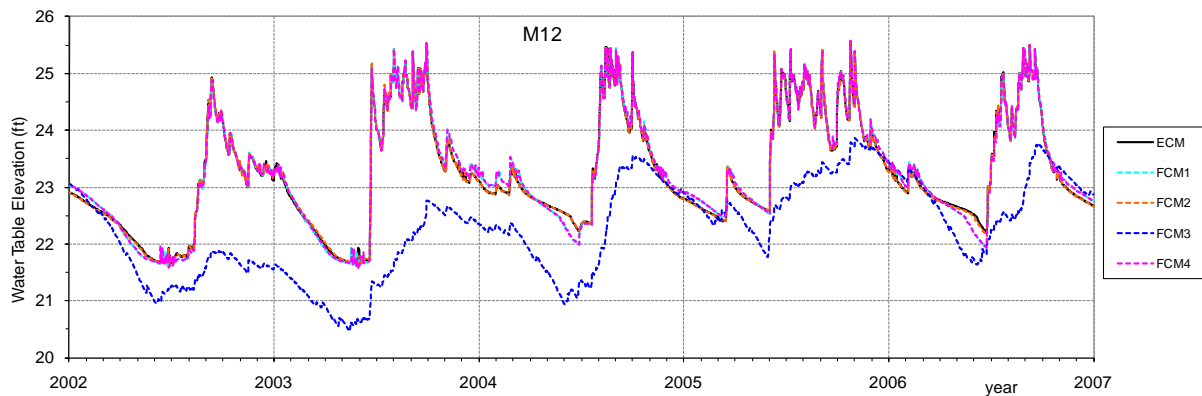


**Figure 58.** Water table elevations at land use change location M12.

Note: Location M11 shows a dry-season WTE oscillation decrease in FCM3. This is likely due to the mining pit down gradient of this location. M12 has a reduction in seasonal WTE oscillation amplitude when it becomes part of the mining pit in FCM3.

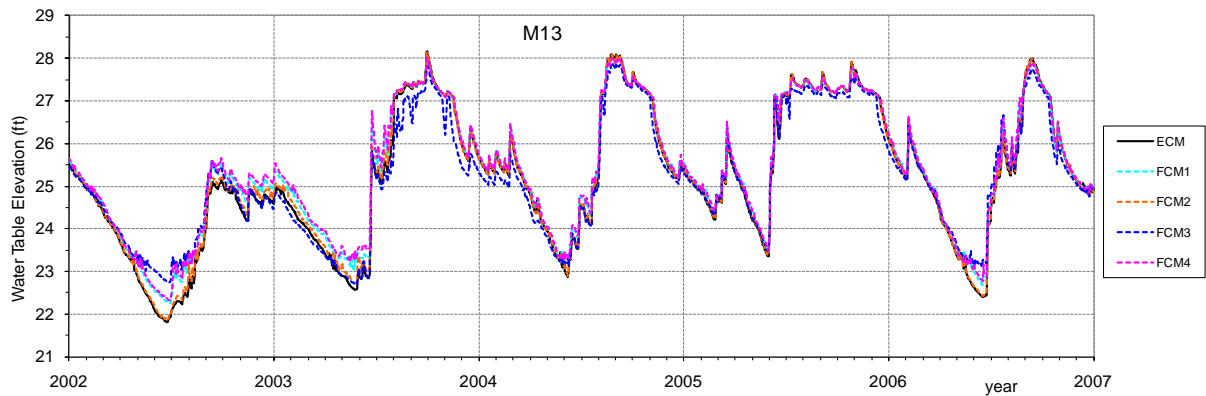


**Figure 59.** Water table elevations at land use change location M13.

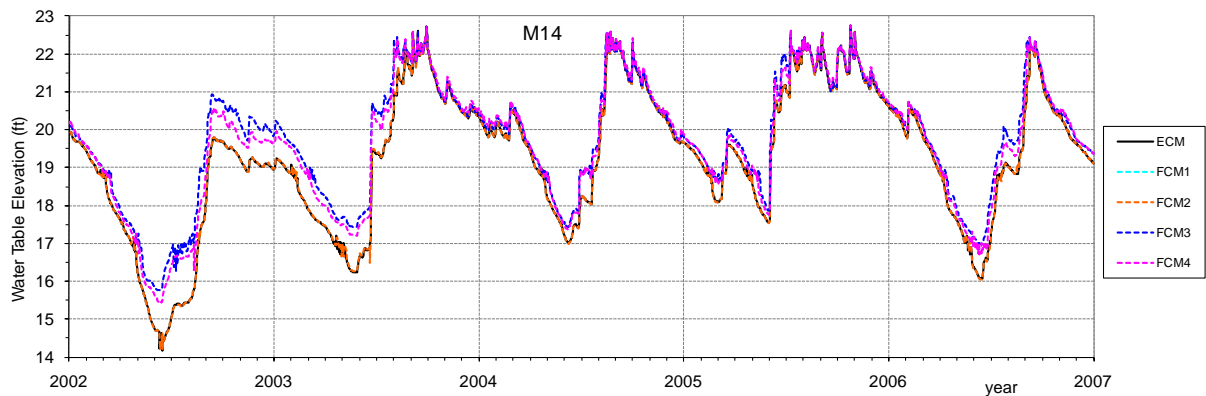


**Figure 60.** Water table elevations at land use change location M14.

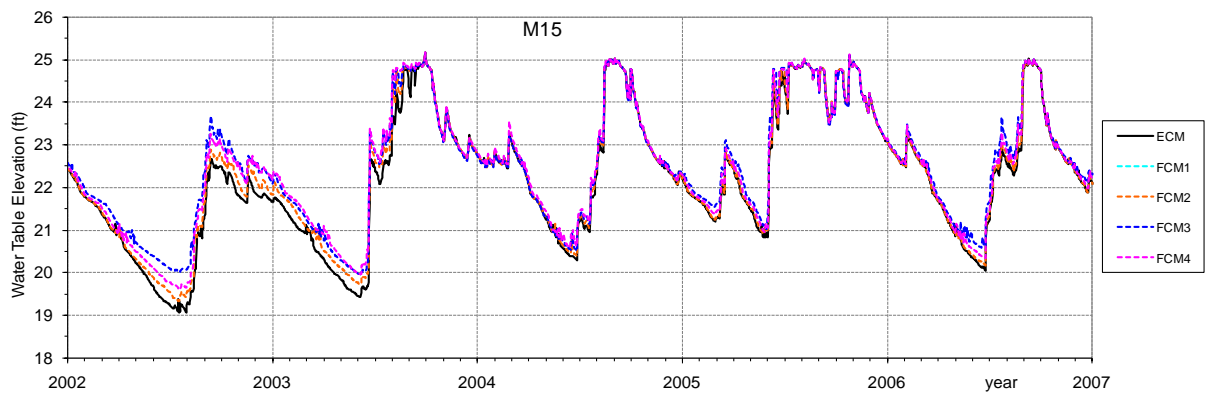


**Figure 61.** Water table elevations at land use change location M15.

**Note:** Locations M13, M14, M15 and M16 show a dry-season WTE increase in FCM3 due to the combined effects of the new mining pit and wetland areas. There is also a dry-season WTE increase in FCM1 and FCM4 due to new wetland areas. M15 shows a reduction of the seasonal oscillation amplitude when it becomes part of the mining pit in FCM3.

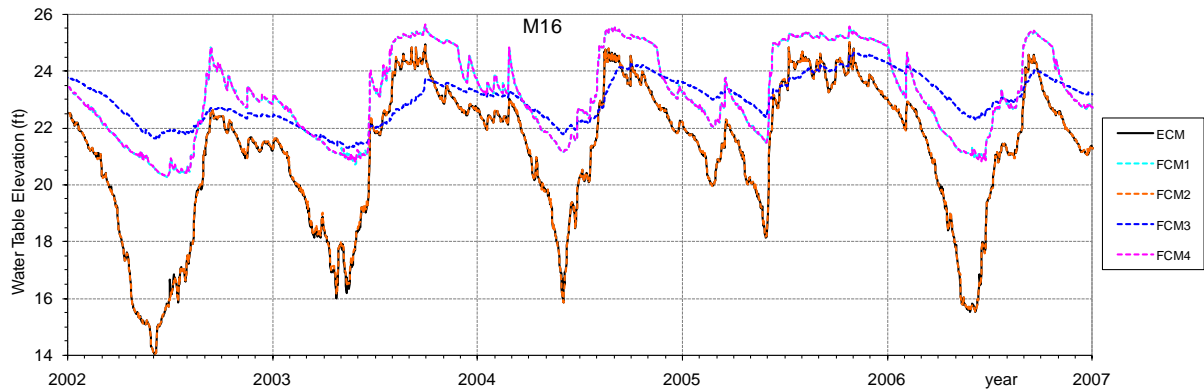


**Figure 62.** Water table elevations at land use change location M16.

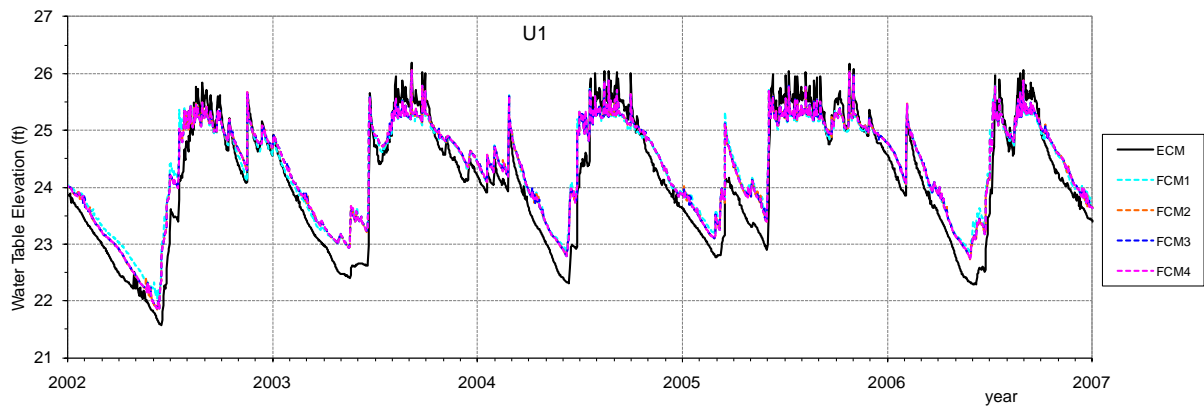


**Figure 63.** Water table elevations at land use change location U1.

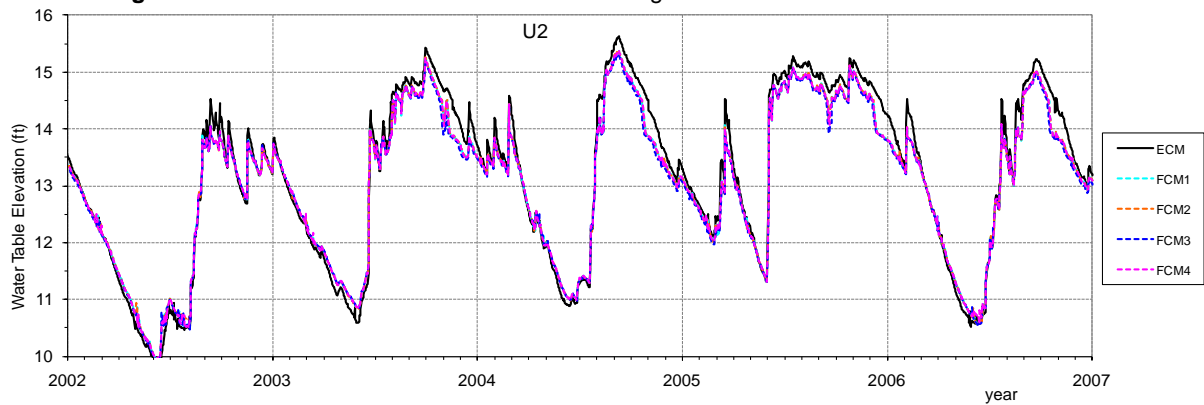


**Figure 64.** Water table elevations at land use change location U2.

Note: Locations U1, U2, and U3 show a decrease in wet-season WTEs, likely due to the new urban area drainage.

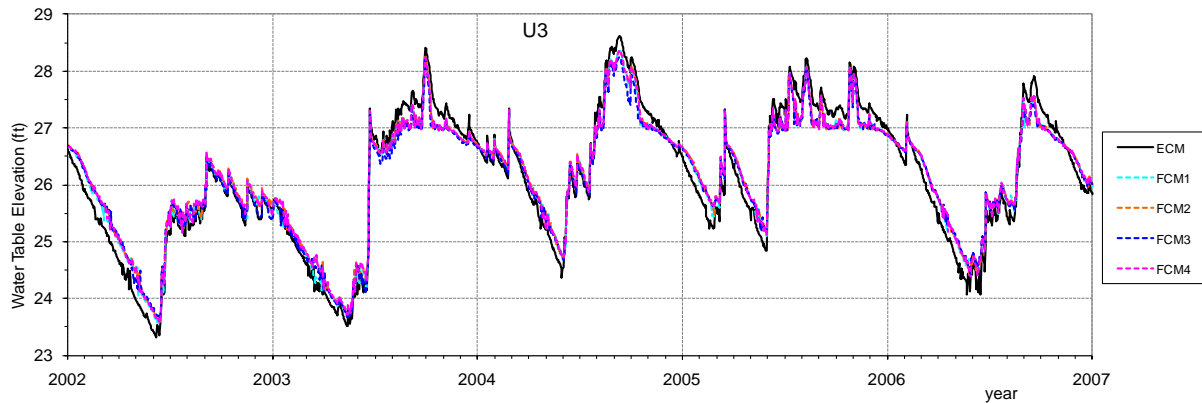


**Figure 65.** Water table elevations at land use change location U3.

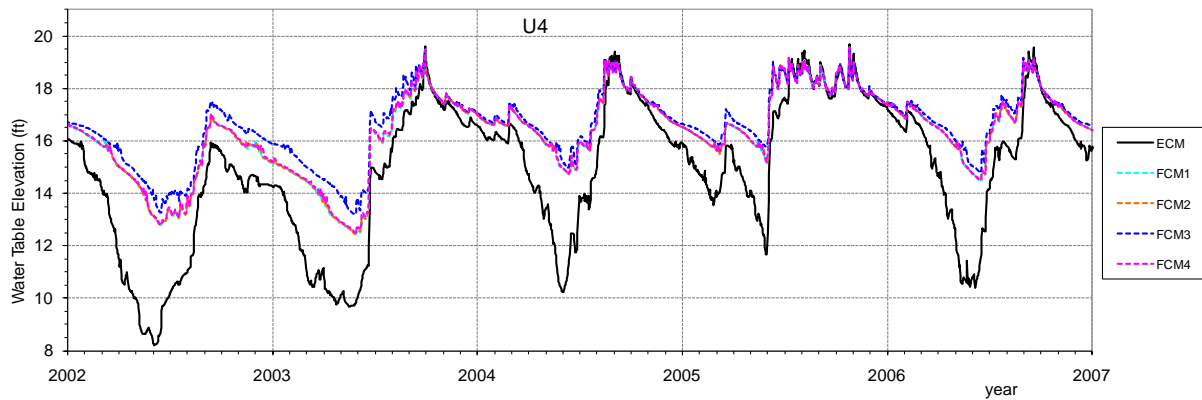


**Figure 66.** Water table elevations at land use change location U4.

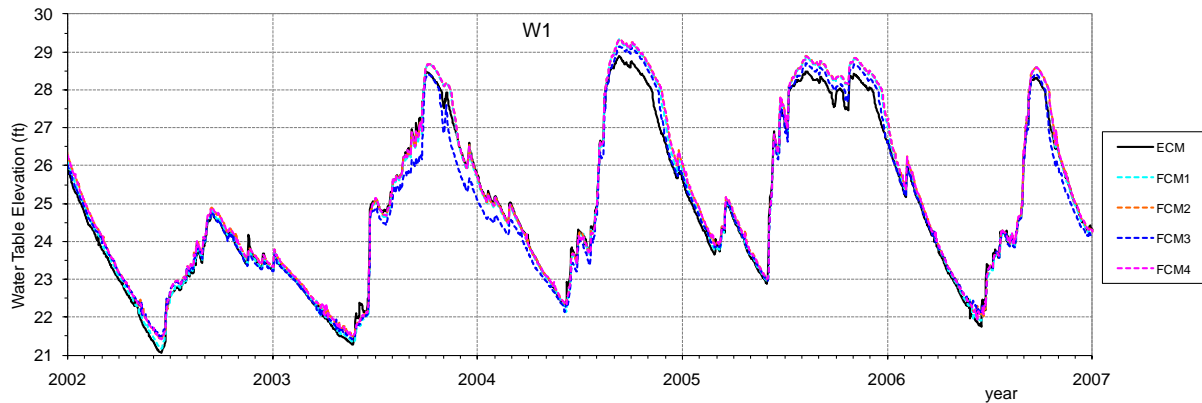


**Figure 67.** Water table elevations at land use change location W1.

**Note:** Locations U1, U3, and U4 show a dry-season WTE increase in all FCMs.. Location W1 shows small WTE differences after the small wetland area was added in all FCMs.

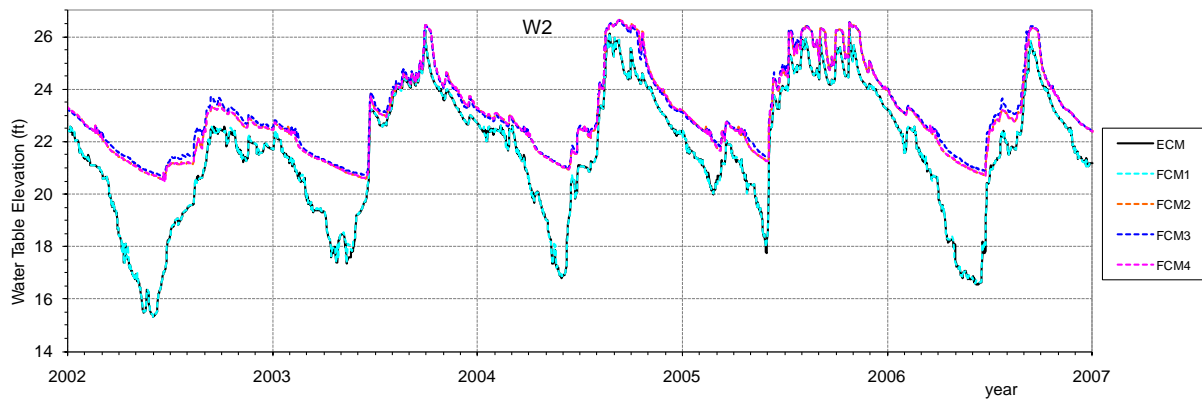


**Figure 68.** Water table elevations at land use change location W2.

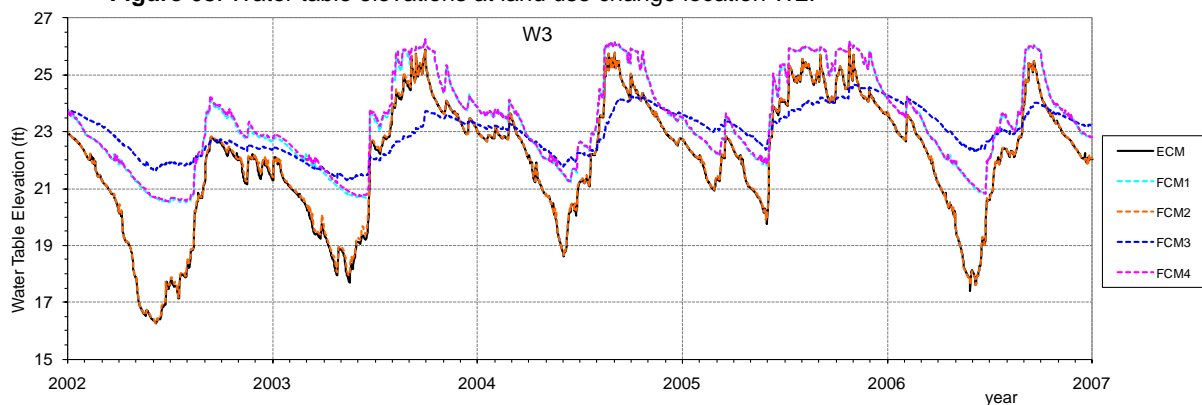


**Figure 69.** Water table elevations at land use change location W3.

Note: Location W2 shows a dry-season WTE increase due to new wetland areas added in FCM2, FCM3, and FCM4. Location W3 shows a dry-season WTE increase due to new wetland areas added in FCM1 and FCM4, and the combination of new mining pit and wetland areas in FCM3.

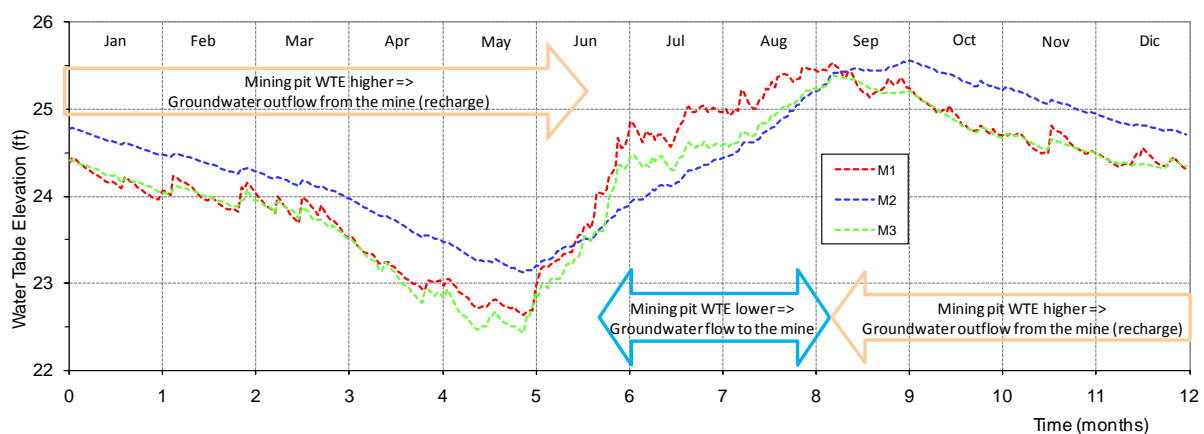


**Figure 70.** Seasonal averaged water table elevation at locations M1, M2 and M3 in FCM1.

## Water Table Maps

Water table elevation maps obtained from all the FCMs are presented in Appendix G. Those maps are extracted from the different models at the end of the dry and the wet season (i.e., the ten last days of May and the ten last days of September, respectively). **Figure 72** to **Figure 79** show water table difference maps for all future condition scenarios in relation to the LS ECM for both the wet and dry seasons.

The most significant changes in the water table are observed in the large mining pit complex of the DR/GR Area. In the future conditions scenarios, the area occupied by mining pits increases, the distance between neighboring mining pits decreases, and they become more hydrologically connected (i.e. via groundwater). Consequently, the water table elevation decreases in up-gradient areas and increases down gradient. The down gradient effect is bigger in the dry season than in the wet season.

A conceptual model of the flattening effect of a single mining pit on the water table elevation is sketched in **Figure 71**. The model predicts that the mine flattens the water table commonly causing a decrease in groundwater levels up gradient with respect to the pre-mining conditions. Down gradient of the mining pits, this effect may produce either an increase or a decrease in groundwater levels, depending on the local hydrologic conditions, the time of the year, etc. These effects in the upstream and downstream areas are more pronounced in the model in areas with steeper topographic slopes and for larger area mine footprints.

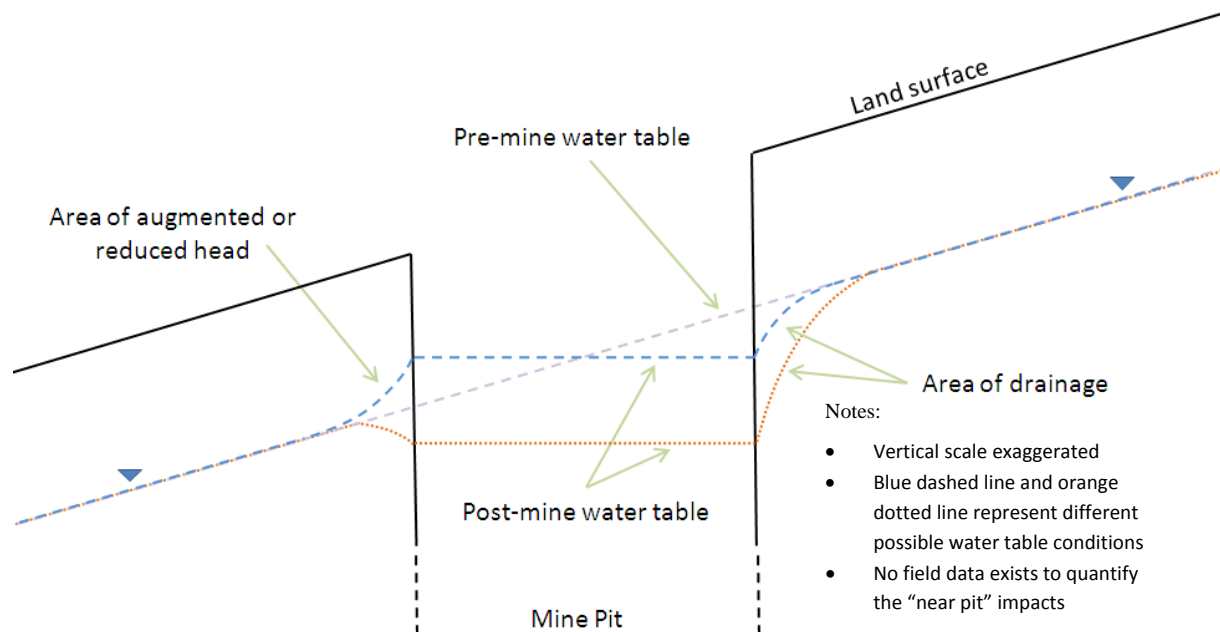


**Figure 71.** Sketch of the flattening effect on the water table elevation of a mining pit in the presence of a regional gradient.

In the case of the large mining pit complex of the DR/GR Area, there are several mines that are hydrologically connected to some extent. The water table profiles from **Figure 80** through **Figure 83** show that the flattening effect in the water table of the entire mining pit complex area becomes more important in the future condition scenarios as the groundwater connectivity between mines increases. In other words, the groundwater connectivity between mines and therefore the flattening effect increases once land between existing pits is also mined.

The flattening effect was also noticeable at a mine proposed in FCM3 at the central part of the DR/GR Area (see Figure 76 and Figure 77). In this case, the mining pit length is smaller than the length of the mining pit complex, but it was located in an area with a steep water table gradient, as can be seen in Figure 28 and Figure 29. The upstream decrease in the WTE is also observed at location M11 presented in Figure 57.

The mine proposed in the FCM1 at the north-western corner of the DR/GR Area does not cause a flattening effect because it is located in a relatively flat area. In this case, the model predicts that the mining pit maintains a higher water table elevation at the end of the dry season around the pit perimeter (see Figure 72). The higher water table elevation here is presented with respect to the LS ECM, where there are not any pits present. This result cannot be extrapolated to mines in other areas in the DR/GR since the rainfall rate in that mine area is much higher than the average rainfall rate in the entire DRGR (see Water Budget section).

The water table in the new wetland areas increases, in general, due to the removal of the drainage system from when it was an agricultural area. Differences in the water table in the new wetland areas are in general greater at the end of the dry season.

The water table in the new urban areas is usually higher at the end of the dry season compared to the existing conditions. This is likely related to a reduction in the ET losses (see more details in the water budget section).

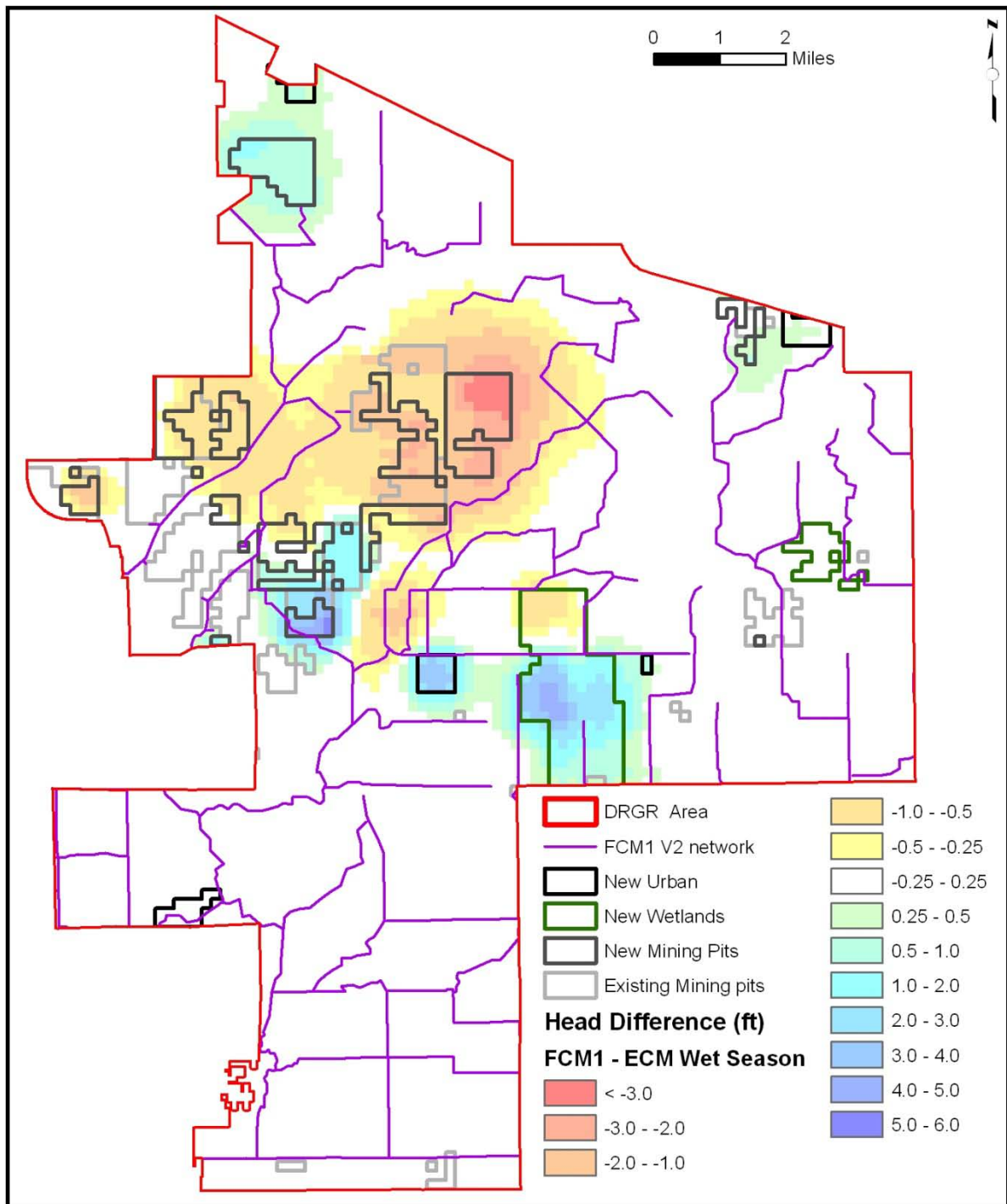


**Figure 72.** Difference in dry season water table in FCM1 in relation to the LS ECM (Positive values indicate increase in water table elevation in the FCM1).

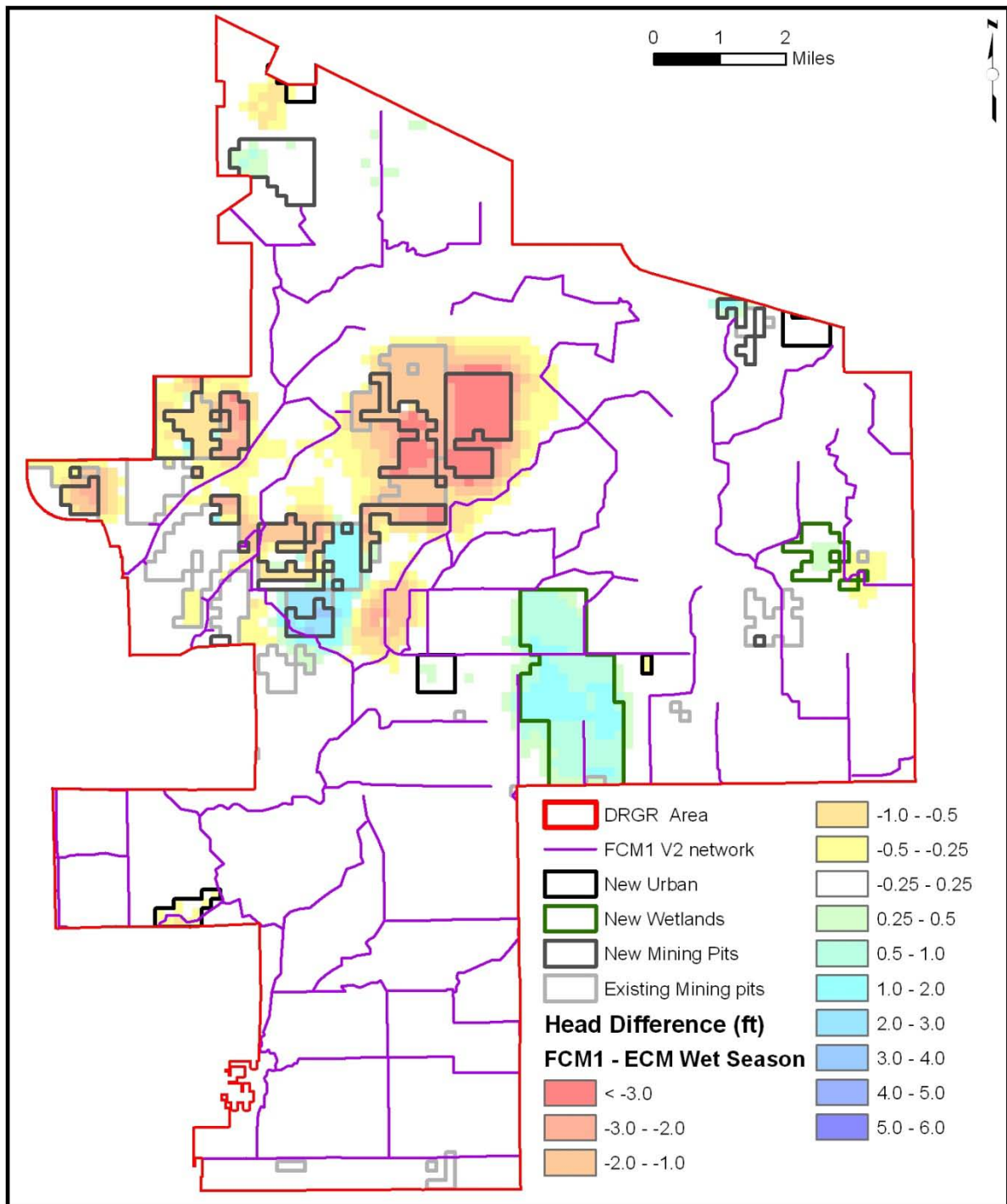


**Figure 73.** Difference in wet season water table in FCM1 in relation to the LS ECM (Positive values indicate increase in water table elevation in the FCM1).

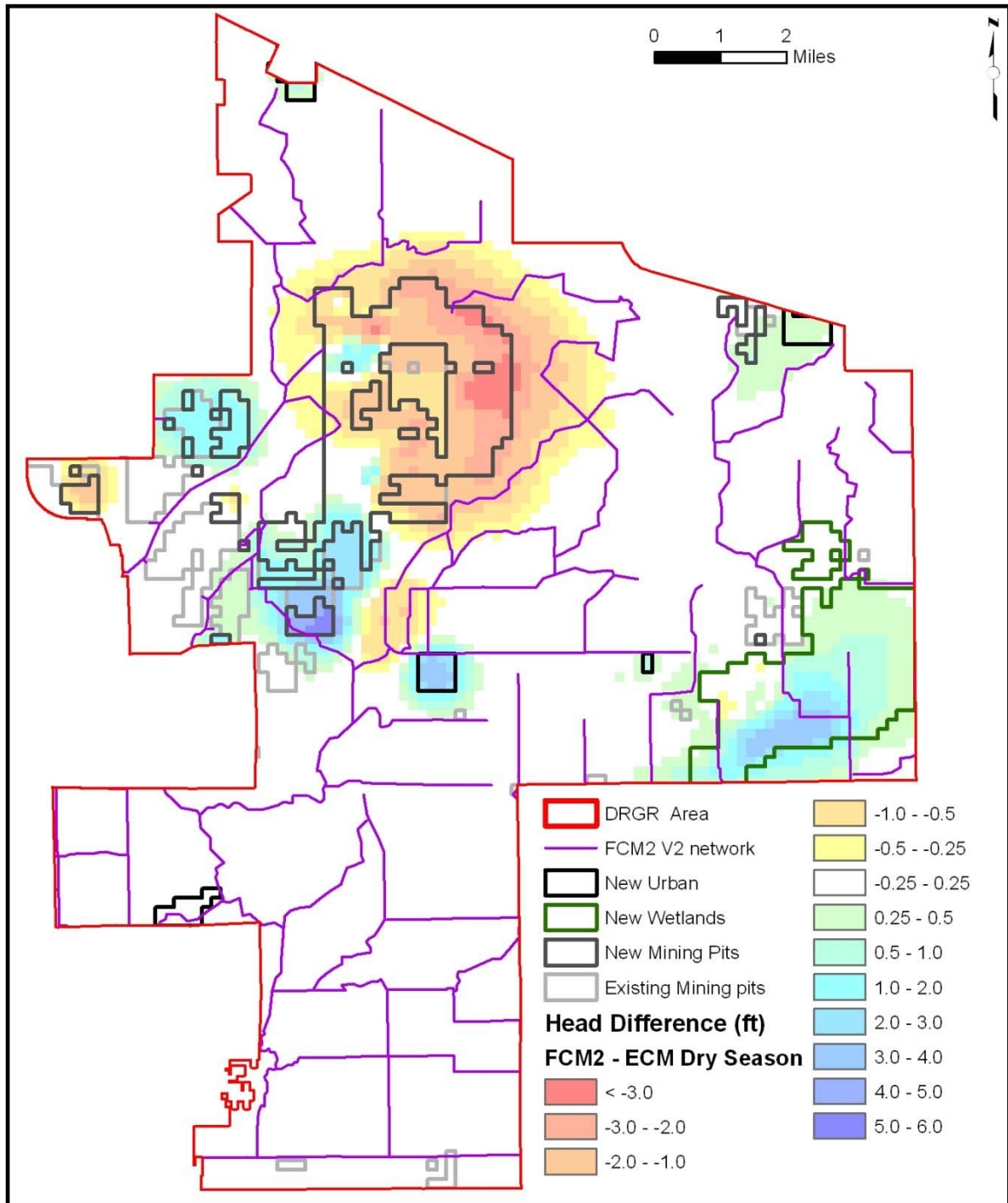


**Figure 74.** Difference in dry season water table in FCM2 in relation to the LS ECM (Positive values indicate increase in water table elevation in the FCM2).

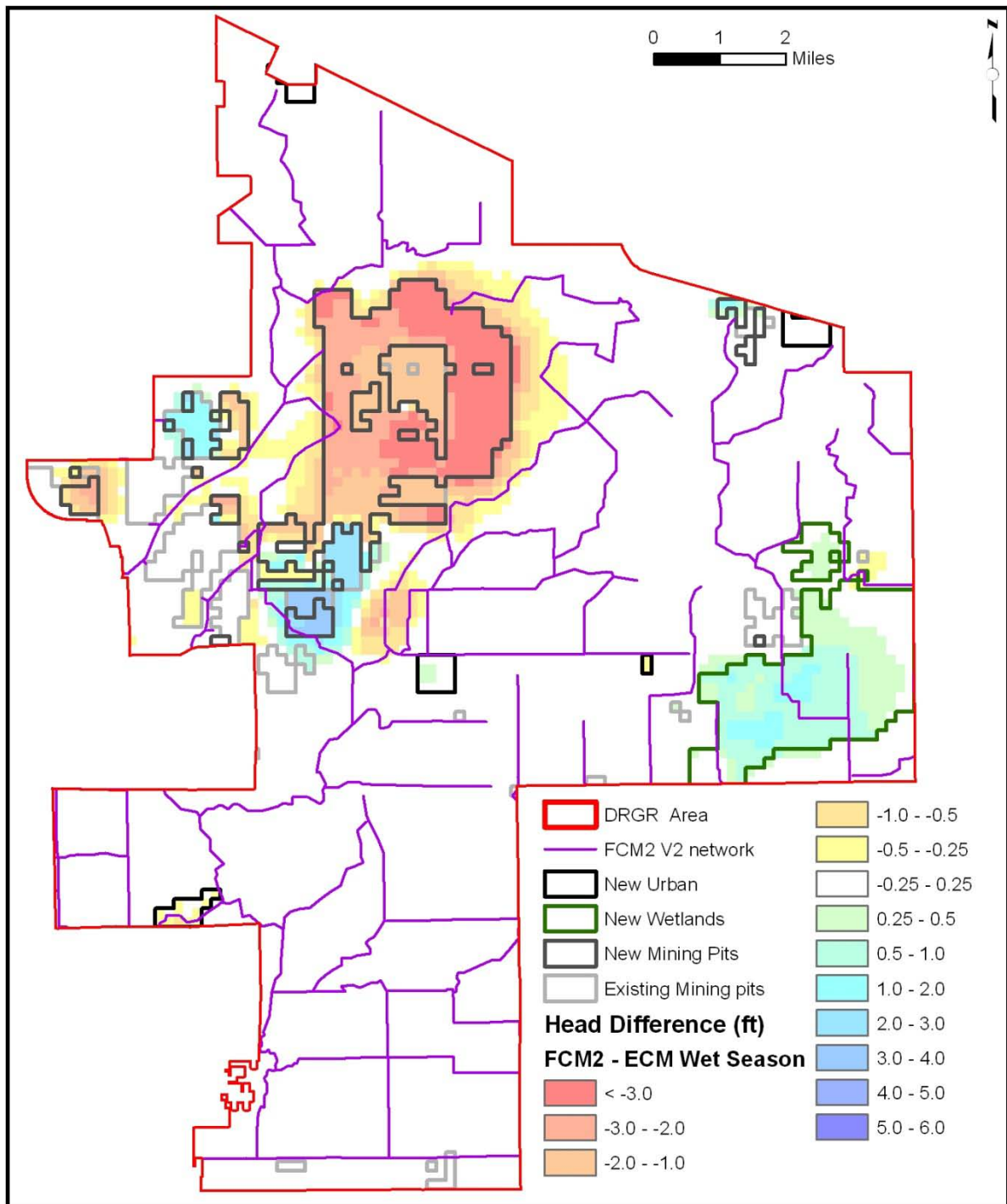


**Figure 75.** Difference in wet season water table in FCM2 in relation to the LS ECM (Positive values indicate increase in water table elevation in the FCM2).

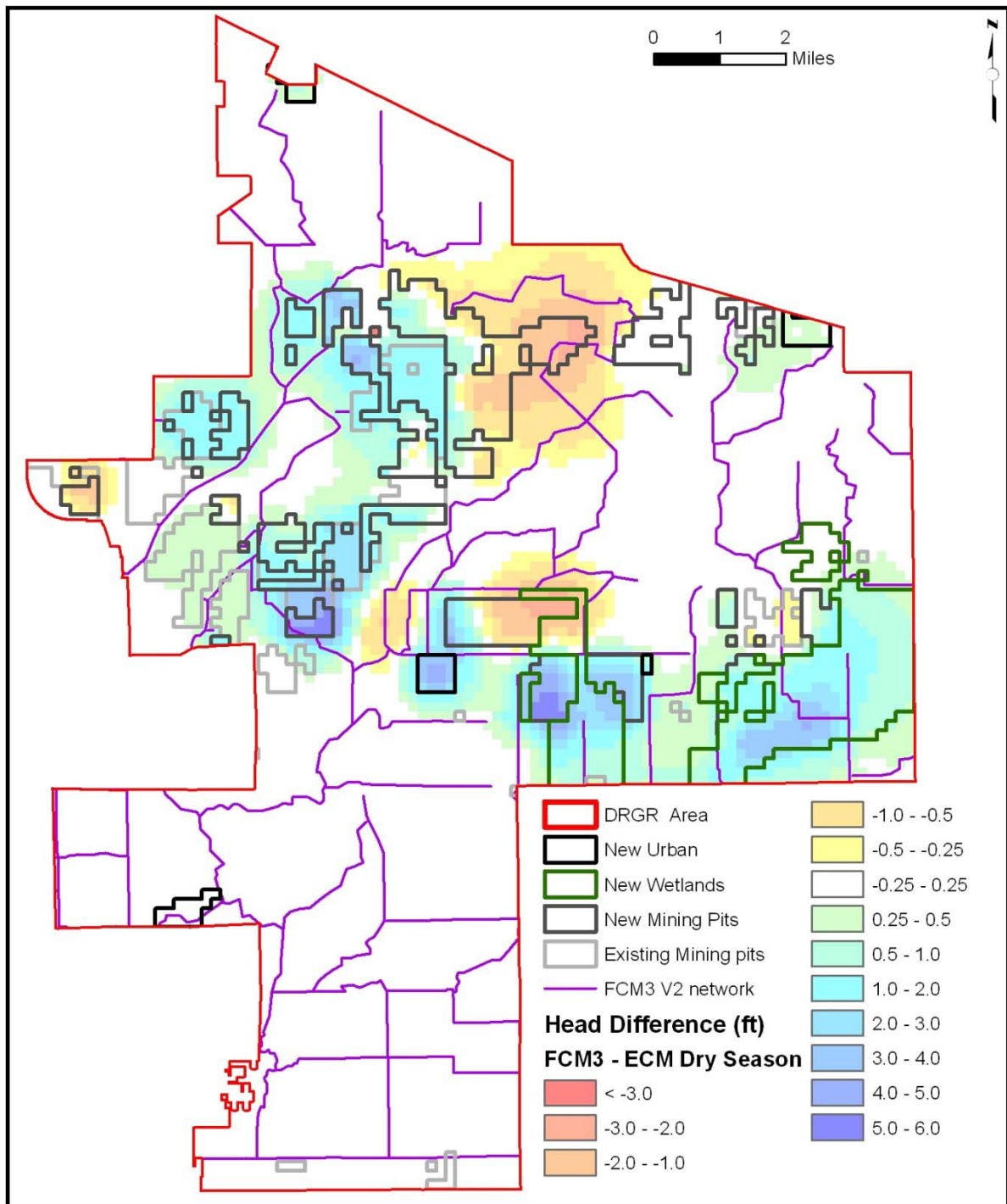


**Figure 76.** Difference in dry season water table in FCM3 in relation to the LS ECM (Positive values indicate increase in water table elevation in the FCM3).

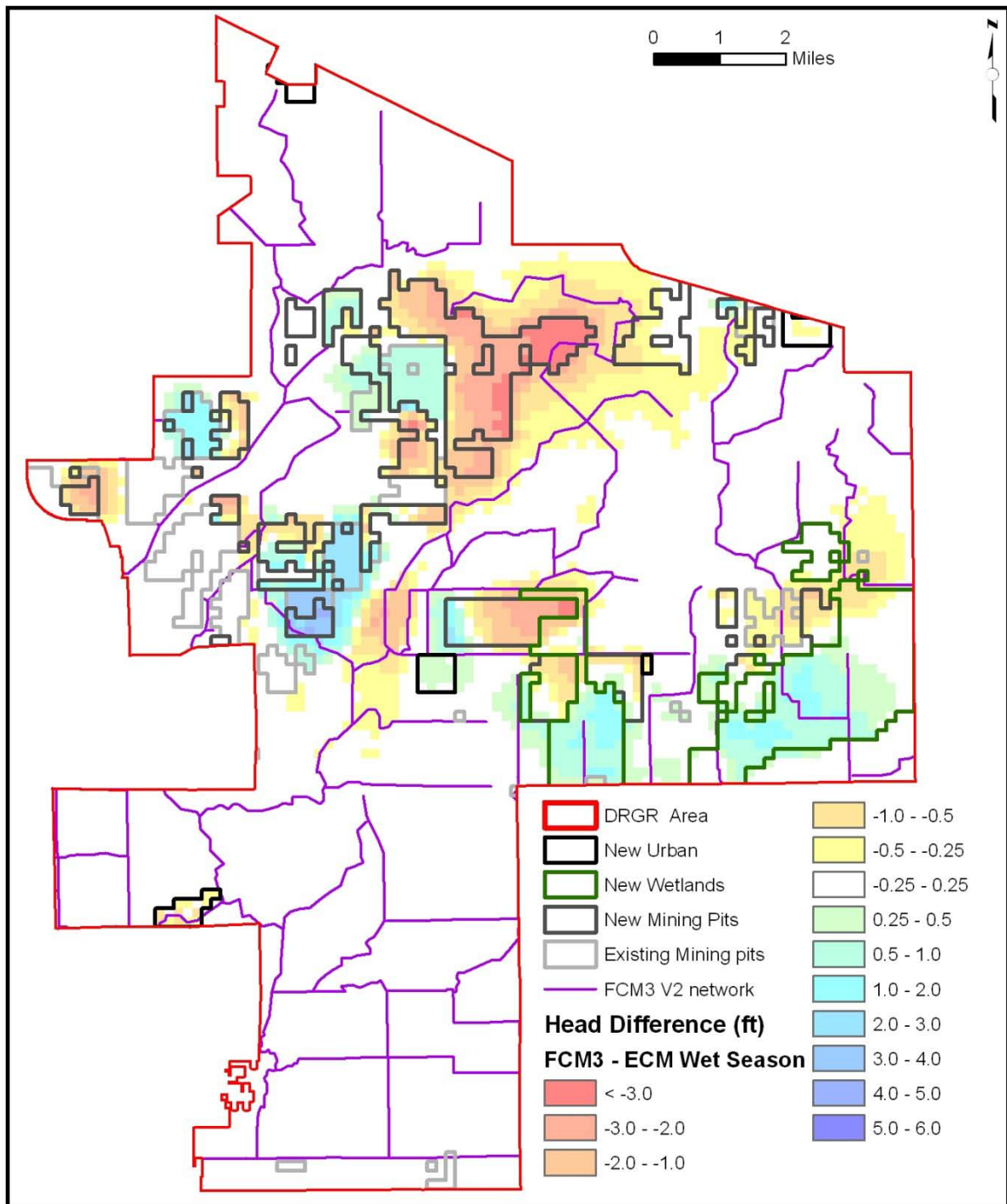


**Figure 77.** Difference in wet season water table in FCM3 in relation to the LS ECM (Positive values indicate increase in water table elevation in the FCM3).

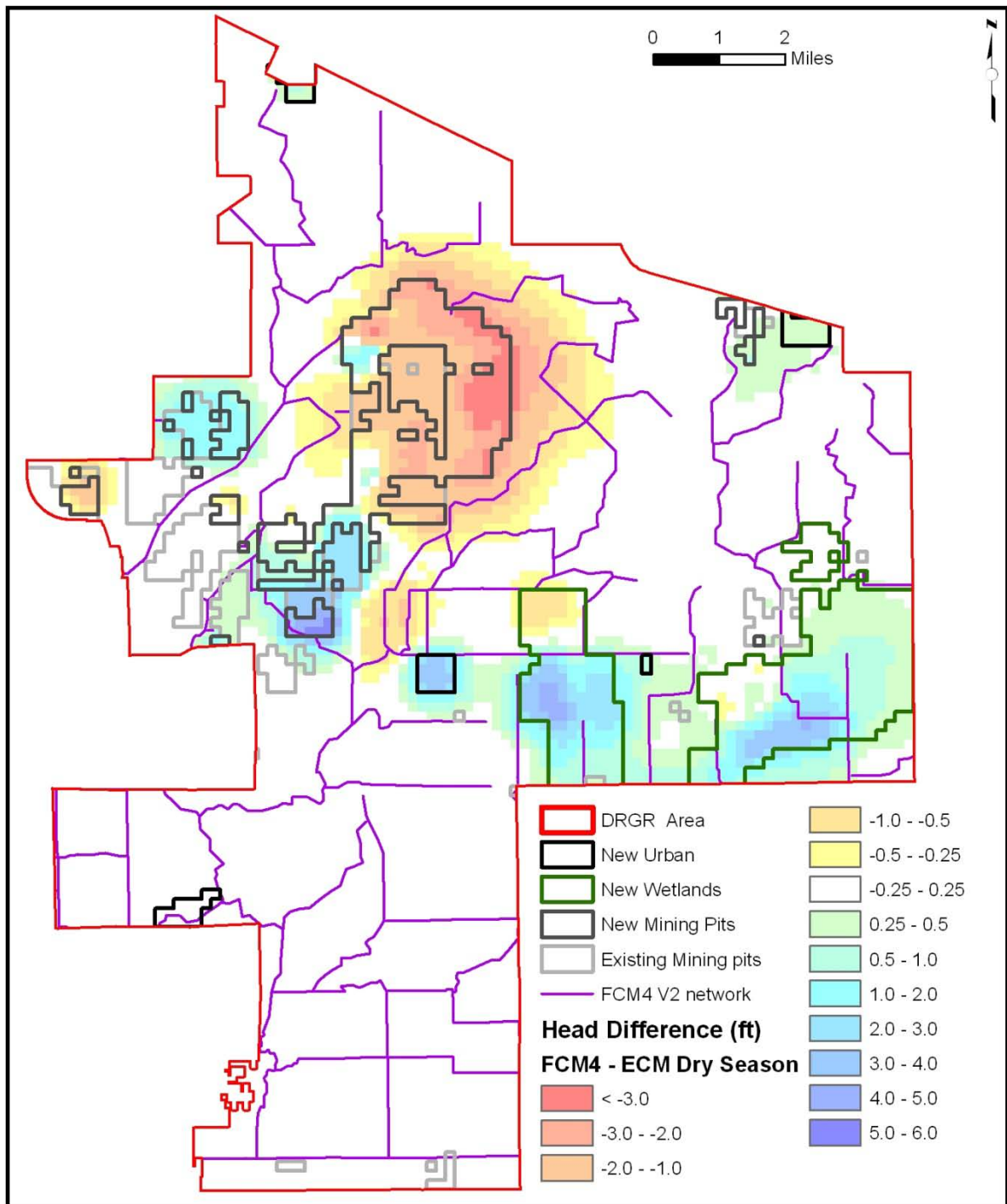


**Figure 78.** Difference in dry season water table in FCM4 in relation to the LS ECM (Positive values indicate increase in water table elevation in the FCM4).

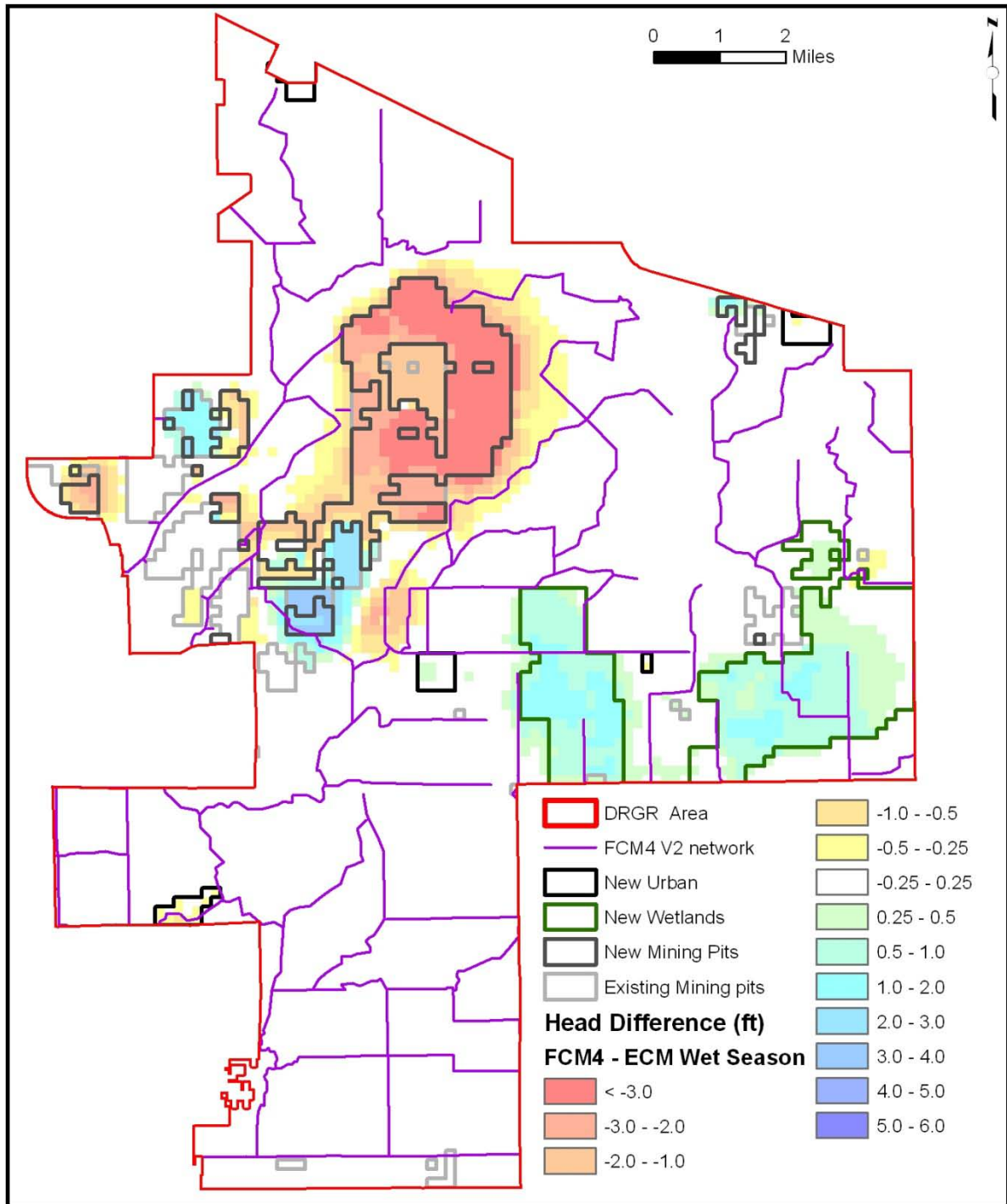


**Figure 79.** Difference in wet season water table in FCM4 in relation to the LS ECM (Positive values indicate increase in water table elevation in the FCM4).

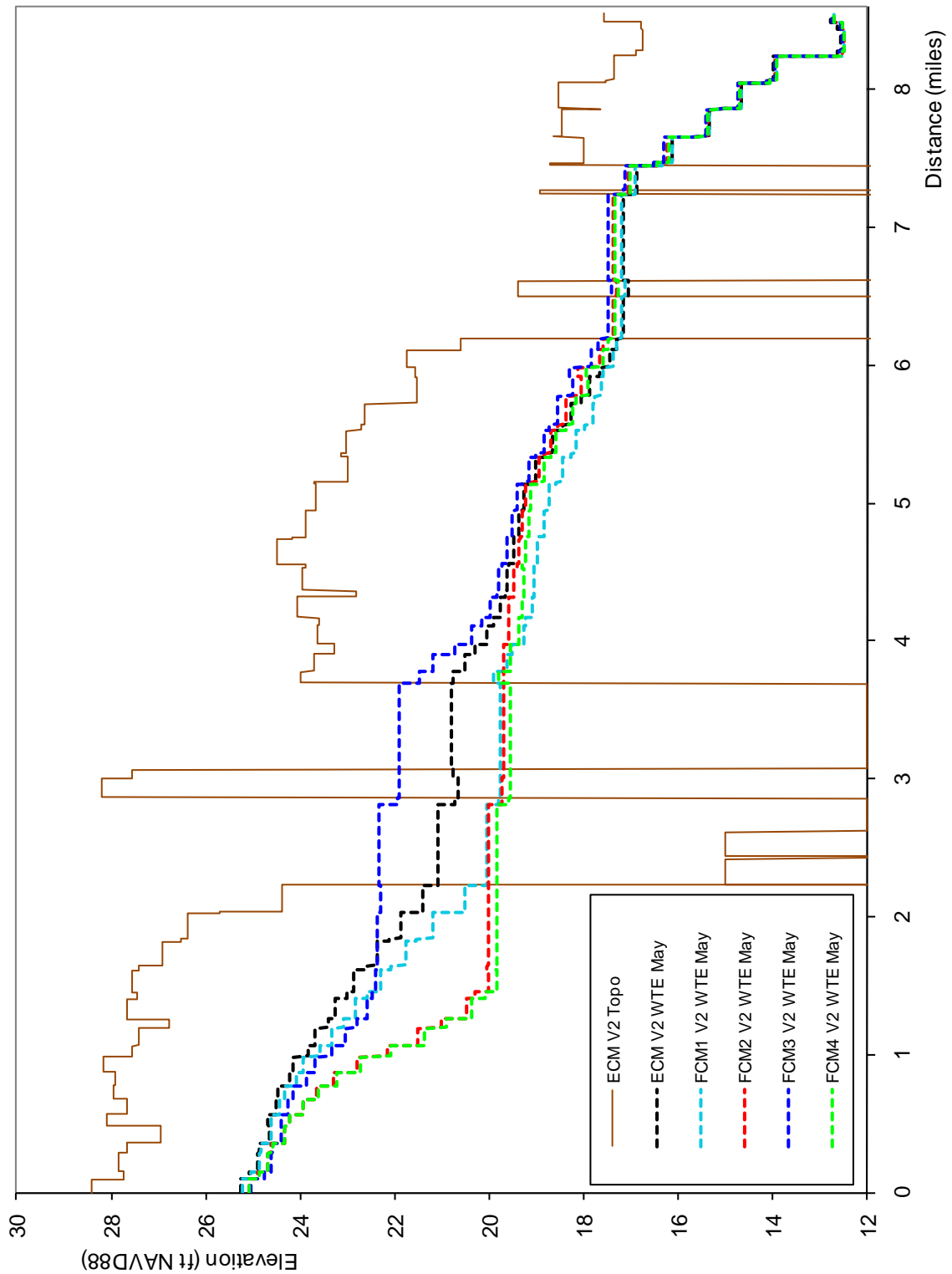


**Figure 80.** Water table level profile along Transect 1 presented in **Figure 30** at the end of the dry season.

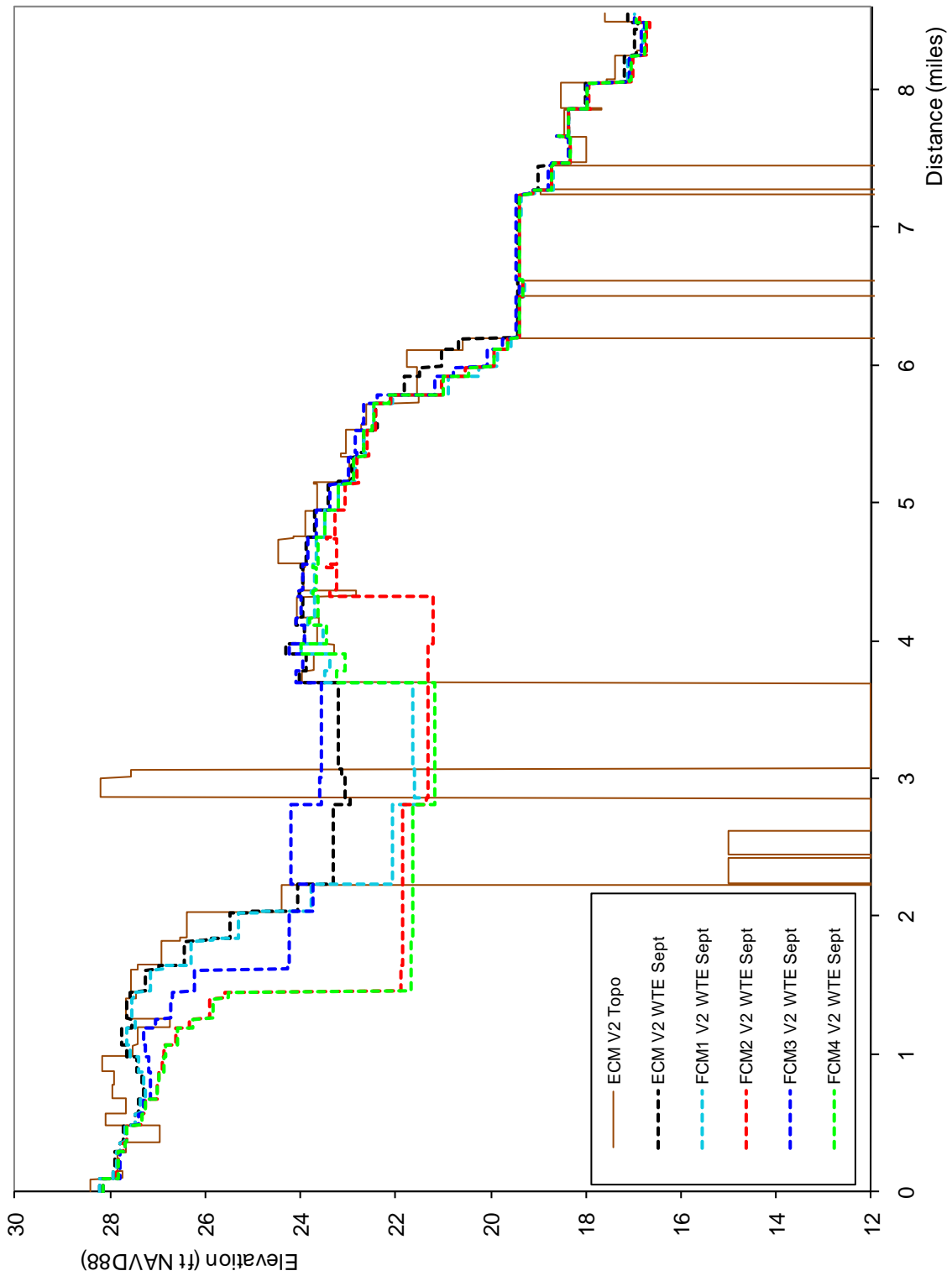


**Figure 81.** Water table level profile along Transect 1 presented in Figure 30 at the end of the wet season.

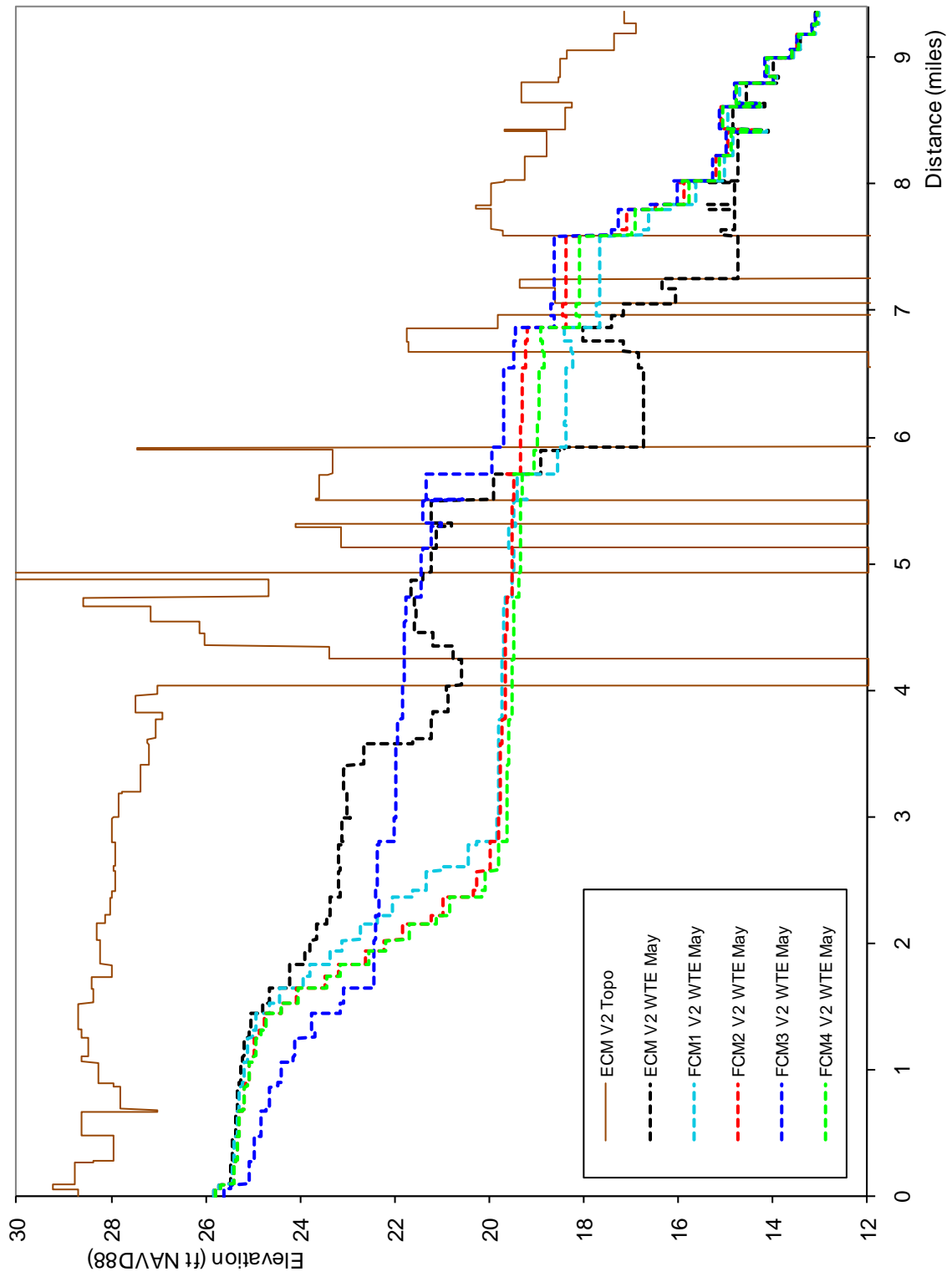


**Figure 82.** Water table level profile along Transect 2 presented in Figure 30 at the end of the dry season.

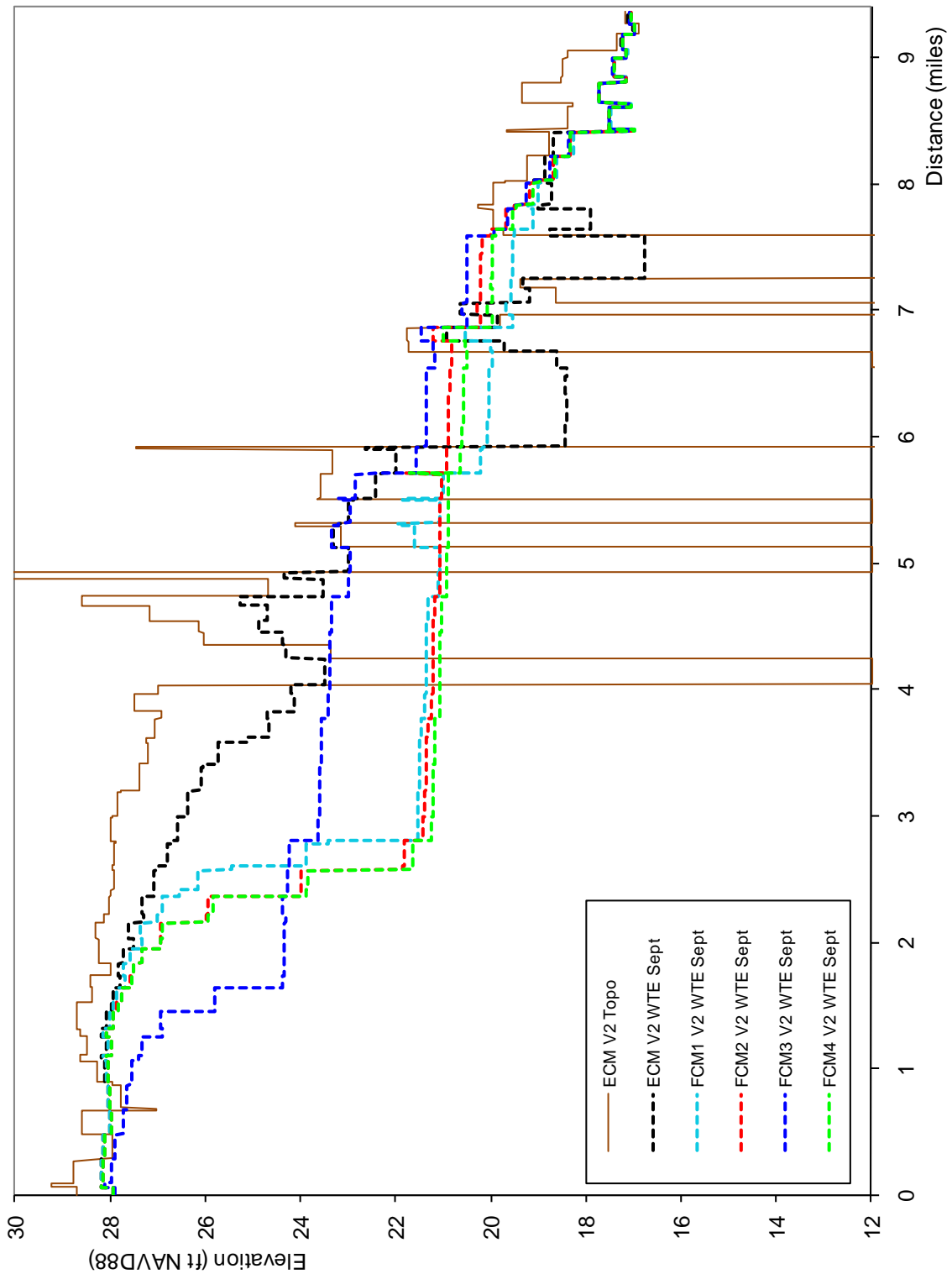


**Figure 83.** Water table level profile along Transect 2 presented in Figure 30 at the end of the wet season.

## Water Table Maps Statistical Analysis

A statistical analysis of the water table difference maps (Figure 72 to Figure 79) was performed by considering grid model cells inside the DR/GR Area that are classified as “natural” land uses (land use codes from 7 to 19). From those grid cells, an average difference was computed. Additionally, the differences were divided into classes matching those shown in the legend of those figures. The number of grid cells that were wetter (positive differences) minus the number of drier grid cells (negative differences) was calculated. The result of this processing is shown in **Table 14**.

The DR/GR Area has been dried out through the years with respect to the predevelopment (natural system) conditions. Thus, it is desirable to increase the water table levels in natural areas inside the DR/GR Area. Consequently, a higher average difference in water table levels (corresponding to wetter conditions at those locations) may be considered a desirable net impact and lower average water table levels could be considered as a negative impact. A higher number of wetter minus drier cells may also be an indication of a desirable net impact. In the former case, the impact is referred to as a net water level change, and in the second case as a net areal extent of wetter conditions. Usually, a net positive impact from a FCM is shown in both water level and areal extent.

According to this statistical processing for natural areas remaining in the DR/GR Area, the dry-season water table elevation differences are highest in the FCM3 and lowest in the FCM1. In the case of the wet-season water table elevation differences, they are highest in the FCM4 and lowest in the FCM3.

**Table 14.** Statistical processing of the water table difference maps.

| FCM Maps   | Statistical parameter                          | FCM1   | FCM2   | FCM3   | FCM4  |
|--|--|--------|--------|--------|-------|
| Water Table Level differences at the end of the dry season (May)       | spatial average (ft)                           | 0.010  | 0.033  | 0.178  | 0.096 |
|  | Number of wetter minus drier 750-ft grid cells | -216   | 16     | 736    | 256   |
| Water Table Level differences at the end of the wet season (September) | spatial average (ft)                           | -0.037 | -0.030 | -0.054 | 0.012 |
|  | Number of wetter minus drier 750-ft grid cells | 82     | 48     | 6      | 372   |

## **Hydroperiod Maps**

Hydroperiod maps obtained from all the FCMs are presented in Appendix H. **Figure 84** through **Figure 87** illustrate the hydroperiod differences between the various scenarios and the existing conditions model (ECM) inside the DR/GR Area. Those maps are a complementary indicator to measure the impact of the land use changes on natural wetland areas.

The hydroperiod results are consistent with water table results previously displayed. The areas that show hydroperiod differences in the Future Condition Models (FCMs) in



general correspond to the areas that show differences in water table elevations at the end of the wet season.

Increasing the areal coverage of mining pits in the large mining pit complex of the DR/GR Area causes differences in the hydroperiod in surrounding areas. In general, the hydroperiod decreases with decreased water table levels up gradient of the mining pits and increases with increased water table levels down gradient of the mining pits. The flow ways north of Corkscrew Road experienced the largest negative effect on hydroperiod in the case of the FCM3.

In general, the hydroperiod increases in restored areas (converted from agricultural to wetland). This is a consequence of removing the drainage system of the agricultural area, which tends to lower the water table during the wet season.

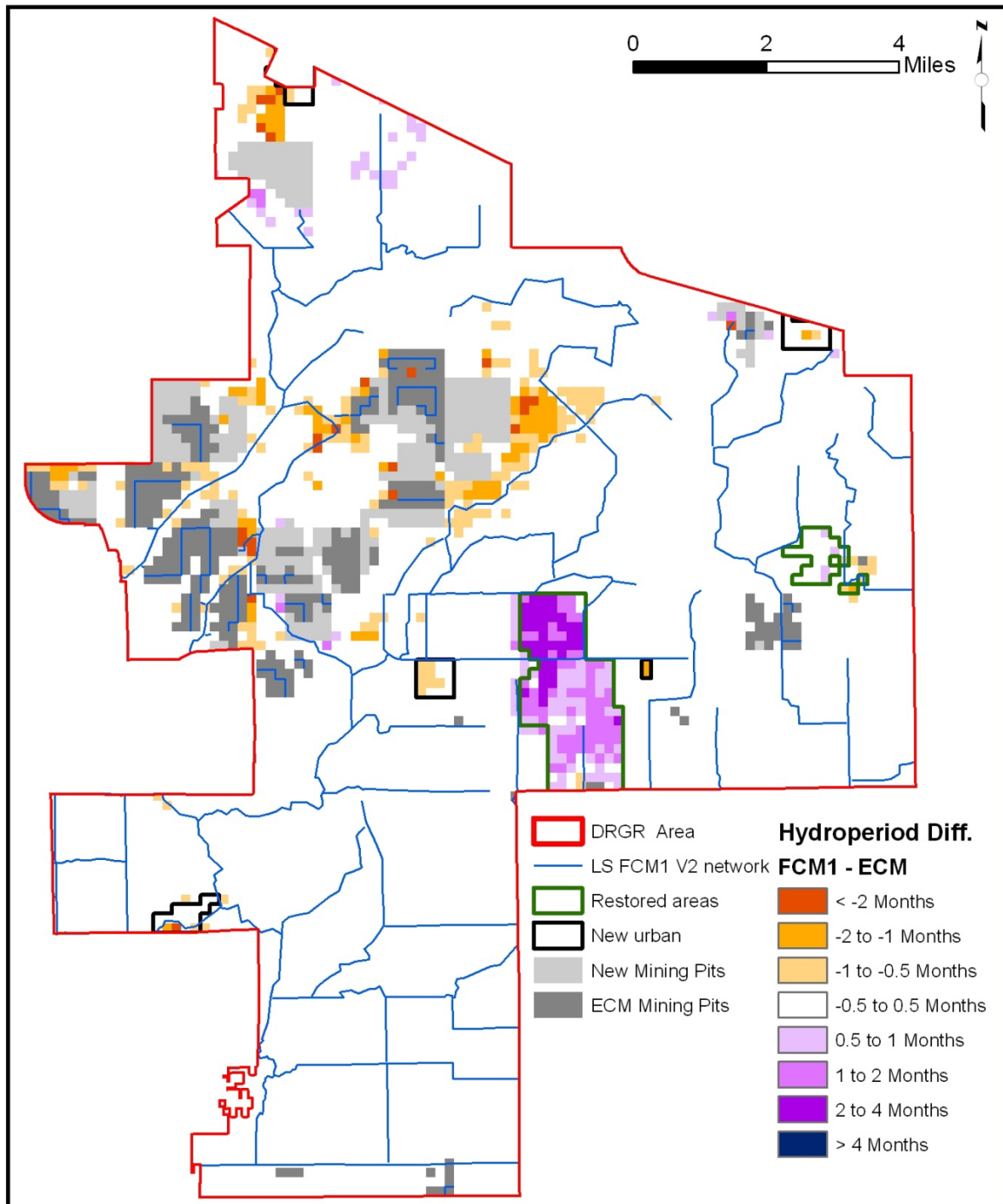


**Figure 84.** Difference in hydroperiod in FCM1 in relation to the LS ECM (Positive values indicate greater duration of water ponding in FCM1).

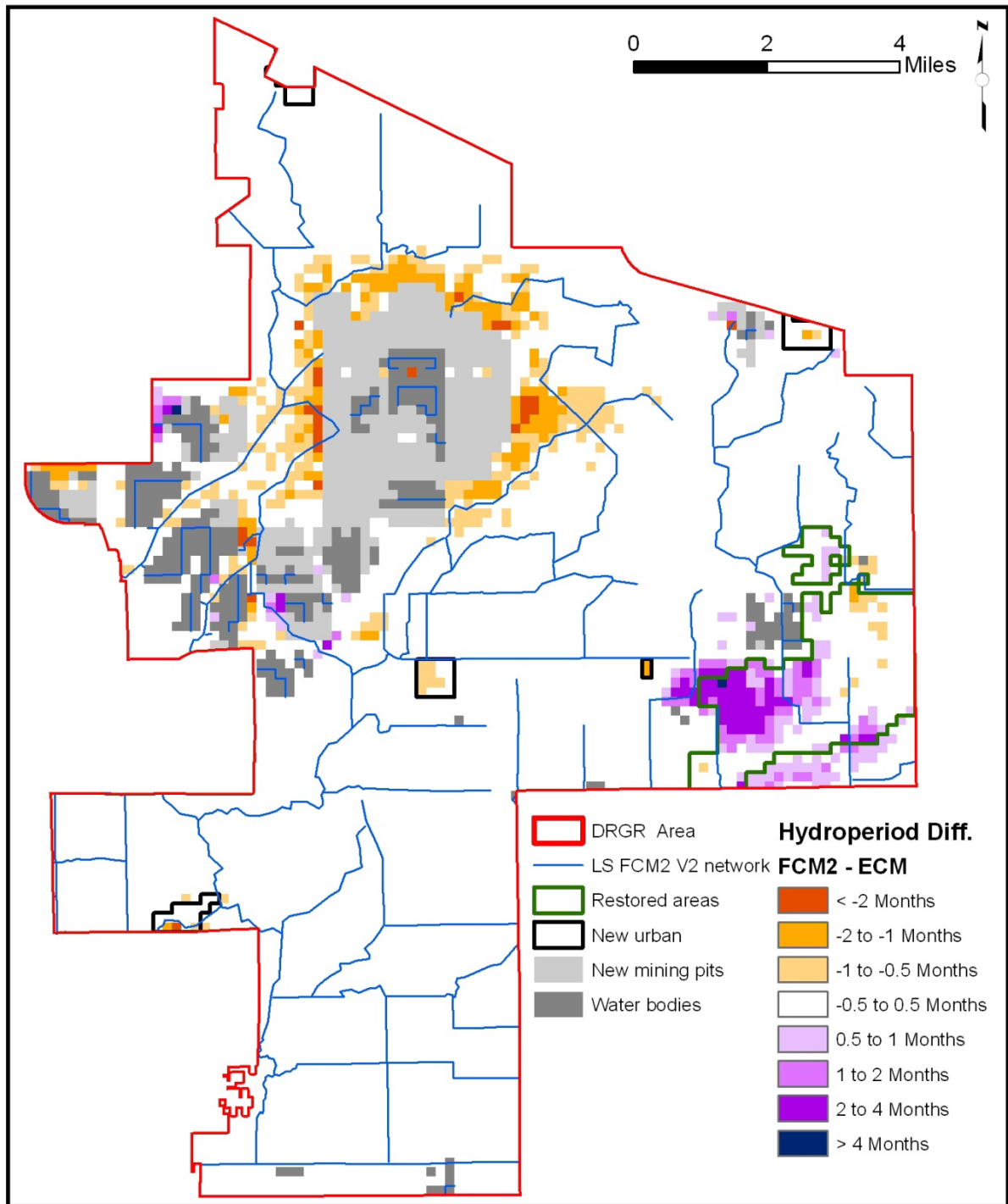


**Figure 85.** Difference in hydroperiod in FCM2 in relation to the LS ECM (Positive values indicate greater duration of water ponding in FCM2).

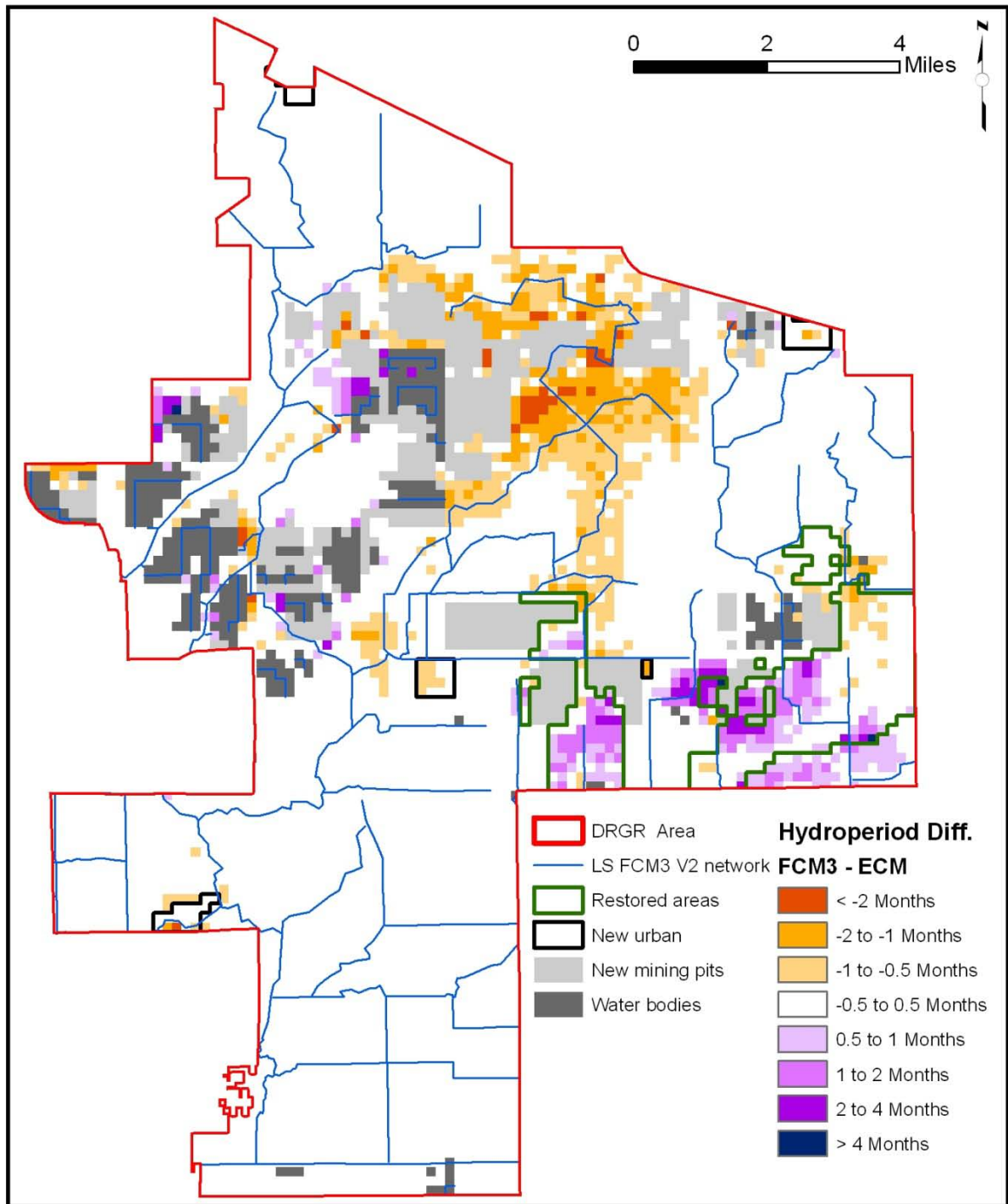


**Figure 86.** Difference in hydroperiod in FCM3 in relation to the LS ECM (Positive values indicate greater duration of water ponding in FCM3).

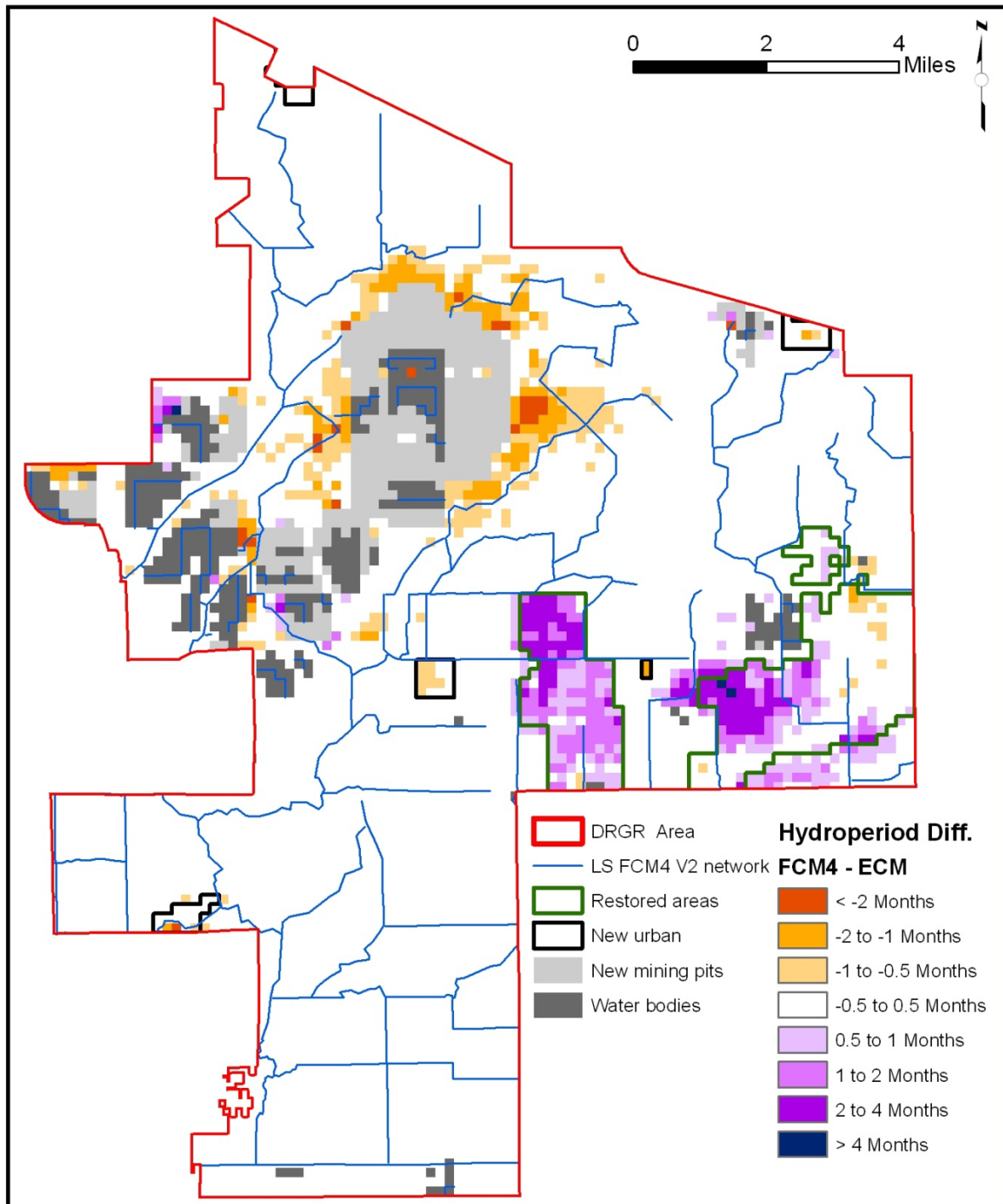


**Figure 87.** Difference in hydroperiod in FCM4 in relation to the LS ECM (Positive values indicate greater duration of water ponding in FCM4).

### Hydroperiod Maps Statistical Analysis

A statistical analysis of the hydroperiod difference maps (Figure 84 to Figure 87) as well as the water depth differences during the hydroperiod (included in Appendix H) was performed by considering grid model cells inside the DR/GR Area that are classified as “natural” land uses (land use codes from 7 to 19). From those grid cells, an average difference was computed. Additionally, the differences were divided into classes matching those shown in the legend of those figures. The number of grid cells that were wetter (positive differences) minus the number of drier grid cells (negative differences) was calculated. The result of this processing is shown in **Table 15**.

An average positive difference in hydroperiod and water depth during the hydroperiod (corresponding to wetter conditions at those locations) may be considered a desirable net impact. A negative average hydroperiod and water depth difference during the hydroperiod could be considered as a negative impact. A higher number of wetter minus drier cells may also be an indication of a desirable net impact. In the former case, the impact is referred to as a net hydroperiod or water depth change, and in the second case as a net areal extent of wetter conditions. Usually, a net positive impact from a FCM is shown in both water level and areal extent.

According to this statistical processing for natural areas remaining in the DR/GR Area, the hydroperiod differences and the water depth differences during the hydroperiod are highest in the FCM4 and lowest in the FCM3.

**Table 15.** Statistical processing of the hydroperiod difference maps.

| FCM Maps                                   | Statistical parameter                          | FCM1  | FCM2  | FCM3  | FCM4 |
|--|--|-------|-------|-------|------|
| Hydroperiod differences                    | spatial average (month)                        | -0.05 | -0.07 | -0.11 | 0.01 |
|  | Number of wetter minus drier 750-ft grid cells | -72   | -214  | -446  | 160  |
| Water depth differences during hydroperiod | spatial average (in)                           | -0.08 | -0.07 | -0.26 | 0.00 |
|  | Number of wetter minus drier 750-ft grid cells | 166   | 136   | -614  | 352  |

### Historic hydroperiod comparison

A natural systems model (NSM) was constructed using the intermediate ECM. This model was intended to be used to help determine future scenarios that most closely returned areas of the DR/GR to their natural states. However, the revised topography changed the hydroperiod prediction significantly and the NSM based on that intermediate step was not accurate enough to be useful for such analyses.

In lieu of the NSM evaluation, a comparison of the hydroperiod maps based on KLECE data for existing conditions (Figure 35) and for the historic conditions (**Figure 88**)



was conducted. For the comparison, the hydroperiod (in the mean of the class interval) from those polygon shape file maps was discretized to 750-ft resolution raster maps.

The map with the difference between the existing and the historical mean hydroperiods is shown in **Figure 89**. From that, a map showing the areas where the hydroperiod was increased or decreased was also obtained as shown in **Figure 90**. The area where the hydroperiod has been decreased from the historical conditions is larger, which indicates the DR/GR Area is drier today than it was in the past.

Unfortunately, a direct comparison between the KLECE data (Figure 89) and the modeled maps (Figure 84 to Figure 87) is not possible since the hydroperiod magnitudes reported by KLECE do not correspond exactly to the hydroperiod magnitudes obtained from the model, as discussed in previous sections.

In order to have a semi-quantitative estimation of how close the FCM hydroperiods are with respect to the historical conditions, the following statistical analysis was conducted. FCM hydroperiod difference maps (Figure 84 to Figure 87) were grouped in three classes as was done in Figure 90, i.e., increased (greater than 0.5 months), decreased (lower than negative 0.5 months) and unchanged (otherwise). Then, the grouped FCM hydroperiod differences in natural area (land use codes from 7 to 19) grid cells in the DR/GR Area were compared with the differences in Figure 89. The results are summarized in **Table 16**.

**Table 16.** Statistical processing of the model- and KLECE-based hydroperiod-grouped-difference maps.

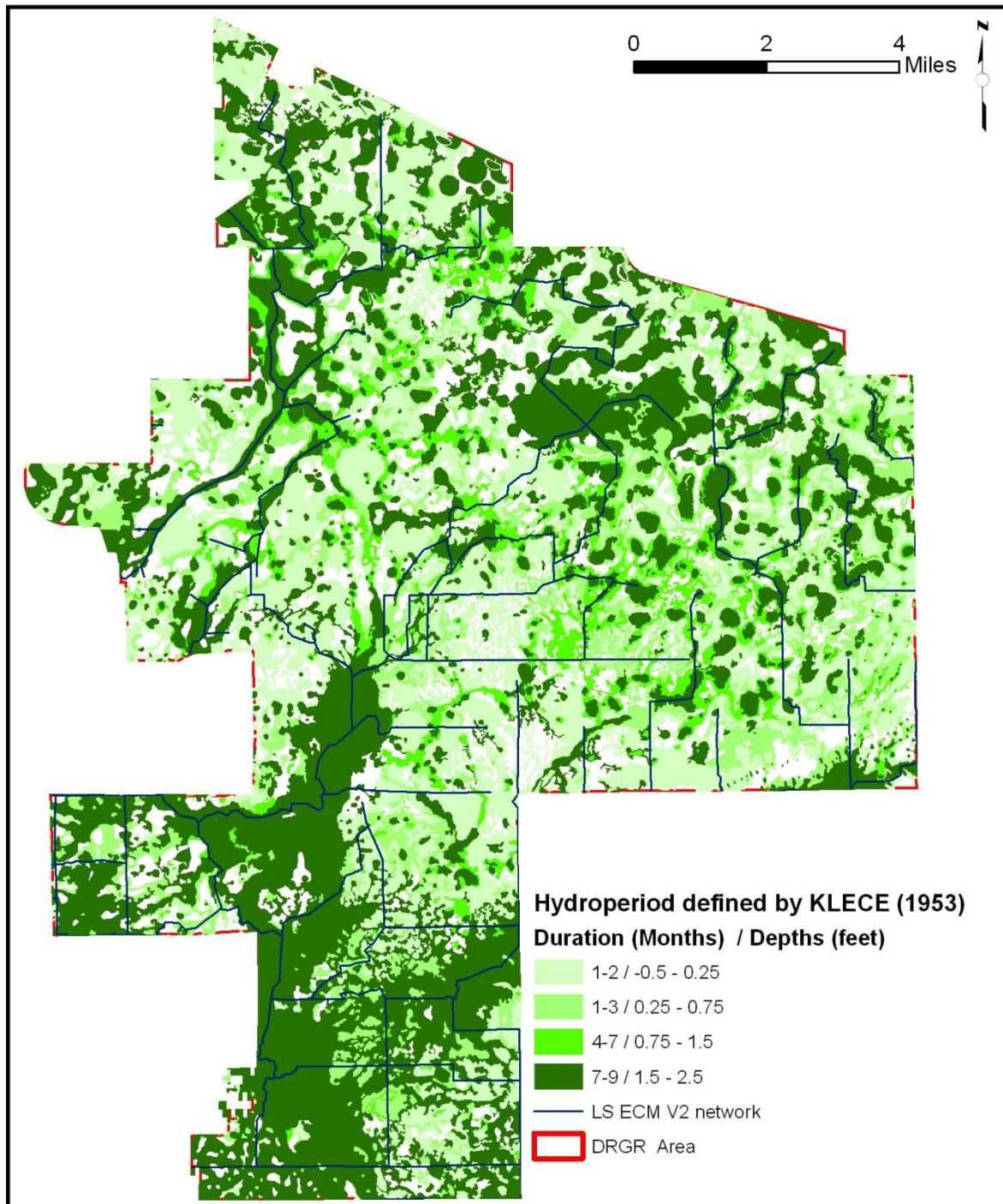
| (1)<br>Existing – historical<br>(based on KLECE)  | (2)<br>FCM – ECM<br>(based on modeling) | (3)<br>FCM – historical<br>(combined) | (4)<br>FCM direction<br>with respect to<br>historical | (5)<br>Number of natural 750-ft grid<br>cells in the DR/GR Area |       |       |       |
|---|---|---------------------------------------|---|---|-------|-------|-------|
|   |   |                                       |   | FCM1  | FCM2  | FCM3  | FCM4  |
| increased   | decreased                               | undefined                             | neutral   | 39  | 37    | 70    | 39    |
| increased   | unchanged                               | increased                             | neutral   | 412   | 410   | 367   | 404   |
| increased   | increased                               | increased                             | neutral   | 35  | 30    | 46    | 64    |
| unchanged   | decreased                               | decreased                             | negative  | 91  | 138   | 223   | 118   |
| unchanged   | unchanged                               | unchanged                             | neutral   | 1355  | 1289  | 1204  | 1319  |
| unchanged   | increased                               | increased                             | neutral   | 53  | 63    | 85    | 100   |
| decreased   | decreased                               | decreased                             | negative  | 96  | 150   | 217   | 146   |
| decreased   | unchanged                               | decreased                             | neutral/negative(*)                                   | 1478  | 1498  | 1477  | 1534  |
| decreased   | increased                               | undefined                             | positive  | 101   | 124   | 153   | 215   |
| Positive- minus negative-<br>direction grid cells |   |                                       | case (*) as neutral                                   | -86   | -164  | -287  | -49   |
|   |   |                                       | case (*) as negative                                  | -1564   | -1662 | -1764 | -1583 |

Table 16 shows the combined hydroperiod difference between future and historical conditions also classified as increased, unchanged and decreased. A class labeled as undefined was added to account for areas with the combination of decreased plus increased where the net result of this combination is unknown.



This table also includes a column to classify the direction of changes in future conditions hydroperiod with respect to the historical conditions (see column (4)). Changes are considered to be in the “negative” direction when the FCM predicts the hydroperiod decreases with respect to the ECM and the existing hydroperiod from KLECE decreases or does not change with respect to the historical. It may be considered to be “neutral” or “negative”, when the FCM predicts no changes in hydroperiod with respect to the ECM and the existing hydroperiod from KLECE decreases with respect to the historical. A change is considered to be in the “positive” direction in this column, when the FCM predicts a hydroperiod increase with respect to the ECM and the existing hydroperiod from KLECE decreases with respect to the historical. Other combinations labeled as “neutral” are assumed to produce no changes in that direction. Even when an increase in the future condition hydroperiod with respect to the ECM may be an indication of some mitigation effort, it is not considered as “positive” in the direction toward the historical conditions, if this occurs in a cell that has the same or higher hydroperiod in the existing conditions with respect to the historical conditions, i.e., increasing the period of the ponded water in an area that already has the historical hydroperiod is not considered “positive”.

An overall measure of the direction of the hydroperiod changes with respect to the historical conditions is computed in the last row of Table 16 by subtracting the number of cells with hydroperiod changes in the “negative” direction (in the “FCM direction with respect to historical” column) to the ones in the “positive” direction (in that same column). Two choices are shown by considering the combination “decreased” in column (1) and “unchanged” in column (2) as “neutral” or “negative”. As a result, FCM3 is the scenario with the highest areal extent where the hydroperiod is shorter than in the historical conditions (i.e. it has the most negative number). FCM1 and FCM4 have the lowest areal extent where the hydroperiod is shorter than in the historical conditions (i.e. their results are closest to positive values in the last row of the table).



**Figure 88.** Hydroperiod map generated based on data created by KLECE from 1953 aerial photos.

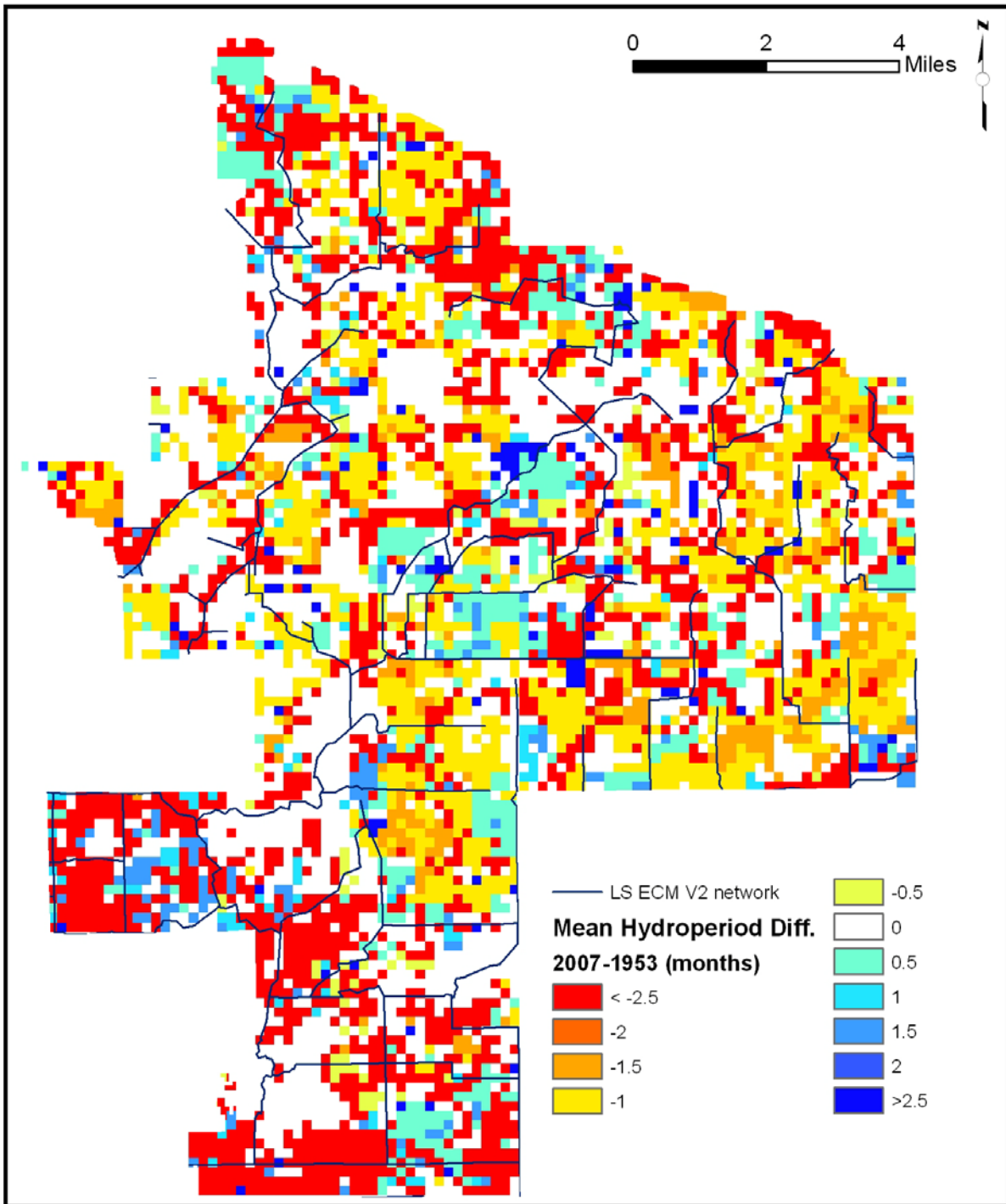


**Figure 89.** Mean hydroperiod map differences (existing minus historical) based on data created by KLECE from aerial photos.

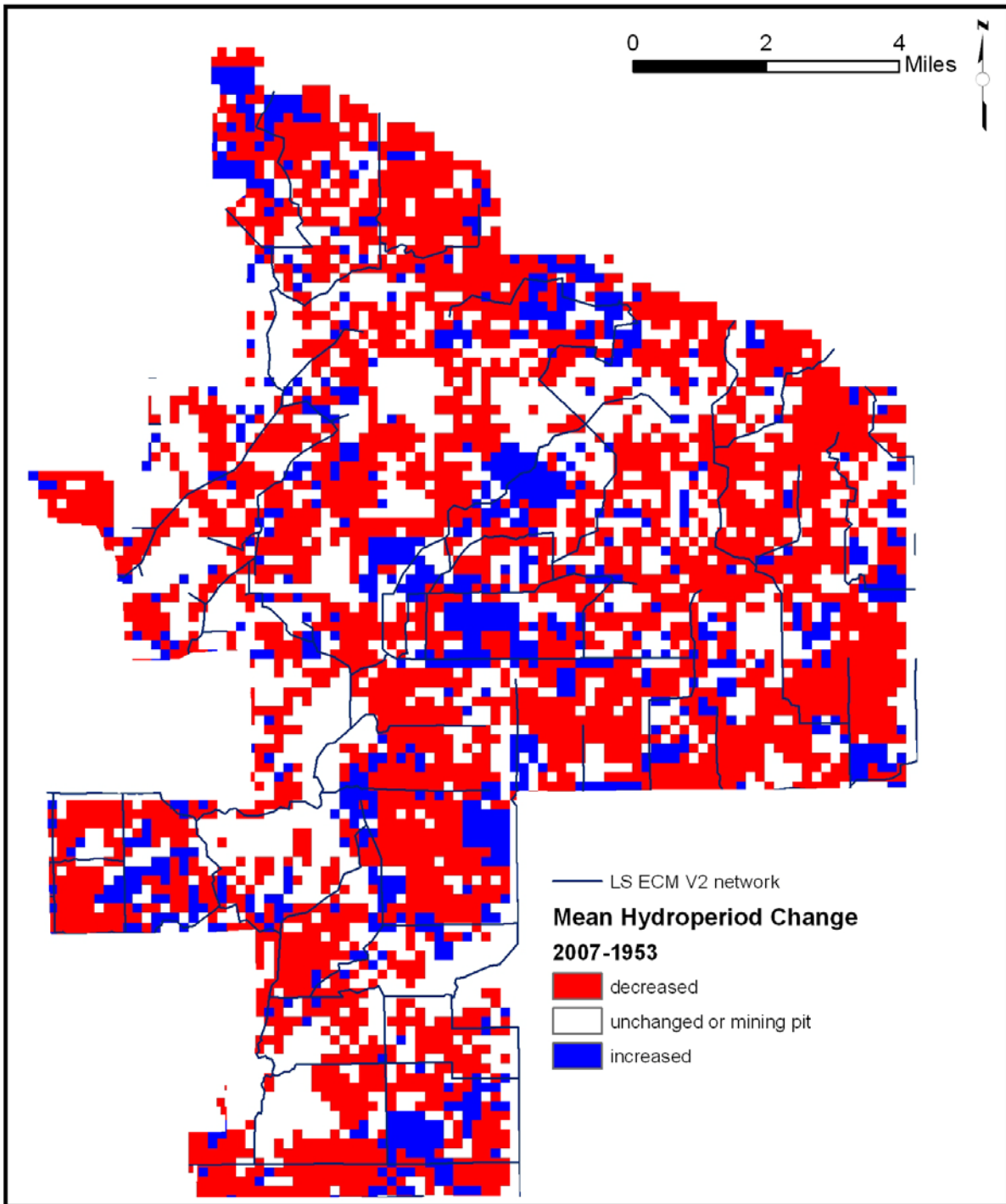


**Figure 90.** Map of hydroperiod changes after processing the data created by KLECE from aerial photos.

## Water Budgets

Water budget calculations conducted for different areas of the models are presented in the following subsections.

### DR/GR Area

A detailed water budget component breakdown for the DR/GR Area is presented in **Table 17**, which are annually averaged for all scenarios. More detailed charts for all the scenarios are included in Appendix I. Some of the main components are plotted as a function of the mining pit areal extent in the DR/GR Area and as a function of the area containing mining pits and natural land use in **Figure 91**. A red line is superimposed to highlight the trend of those depth rates with respect to the mining pit area and the mining pit plus natural areas.

The results from the LS ECM and the FCMs indicate, in general, that increased coverage of mining pits and natural areas in a scenario leads to higher evapotranspiration (ET) rates and, therefore, to lower net rainfall (i.e., rainfall - ET) rates. In other words, higher ET rates are found in scenarios where there is a larger area of water ponded or close to the ground surface (i.e., area of mining pits and wetlands).

The annual-averaged surface water outflow (runoff) rates from the DR/GR Area were about 1.1 inch/year lower for the future scenarios with respect to the LS ECM. The correlation in this case with the mining pit areal extents and with the area containing mining pits and natural land use is not as clear in the plot as in the case of the ET. Decreased runoff when more mining pits are present is expected from the higher open-water storage in mining pits and the subsequent absence of runoff from them. A linear extrapolation of the surface water outflow rates in Figure 91 reaches a value of zero at about 45 % areal extent of mining pit coverage. This may be an indication that the mining pits also reduce the surface water flow in neighboring areas and interrupt pre-developed flow ways.

There is a higher pumping rate assumed in the FCMs of about 0.4 inches/year for the entire DRGR area with respect to the LS ECM. This is about one third of the reduction in the SW outflow rate and may be partially contributing to the SW outflow reduction.

The groundwater outflow from the DR/GR Area (labeled as CSZ in Table 17) is an indicator of groundwater recharge in the DR/GR Area. The model results generally show slightly higher groundwater outflow rates from the DR/GR (about 0.2 inches/year) for the future scenarios with respect to the LS ECM. The correlation in this case with the mining pit areal extents and with the area containing mining pits and natural land use is not as clear in the plot as in the case of the ET.



**Table 17.** Annual average depth rates of the water balance components for the entire DR/GR Area as predicted from different models.

| Depth rates (inches/year)                 |                               | Model | ECM          | FCM1         | FCM2         | FCM3         | FCM4         |
|---|-------------------------------|-------|--------------|--------------|--------------|--------------|--------------|
| Rainfall                                  |                               |       | 58.88        | 58.88        | 58.88        | 58.88        | 58.88        |
| ET  |                               |       | 48.02        | 48.53        | 48.66        | 48.74        | 48.48        |
| <b>Rainfall - ET (A)</b>                  |                               |       | <b>10.86</b> | <b>10.35</b> | <b>10.22</b> | <b>10.14</b> | <b>10.40</b> |
| OL storage change                         |                               |       | -0.03        | -0.03        | 0.01         | -0.11        | 0.02         |
| UZ Storage change                         |                               |       | 0.04         | 0.04         | 0.04         | 0.03         | 0.04         |
| Total SZ Storage change (BSZ)             |                               |       | -0.38        | -0.37        | -0.36        | -0.34        | -0.36        |
| <b>Total storage (B)</b>                  |                               |       | <b>-0.37</b> | <b>-0.36</b> | <b>-0.31</b> | <b>-0.42</b> | <b>-0.31</b> |
| Net OL Boundary outflow (COL)             |                               |       | 0.19         | 0.17         | 0.16         | 0.18         | 0.21         |
| Drain to Boundary (CDR)                   |                               |       | 0.00         | 0.00         | 0.00         | 0.00         | 0.00         |
| Net SZ Boundary outflow from SZ1          |                               |       | 1.74         | 2.00         | 1.80         | 1.75         | 1.81         |
| Net SZ Boundary outflow from SZ2          |                               |       | 0.06         | 0.09         | 0.08         | 0.11         | 0.11         |
| Net SZ Boundary outflow from SZ3          |                               |       | -0.54        | -0.59        | -0.46        | -0.43        | -0.46        |
| Net SZ Boundary outflow from SZ4          |                               |       | -0.38        | -0.41        | -0.36        | -0.34        | -0.35        |
| Net SZ Boundary outflow from all SZ (CSZ) |                               |       | 0.87         | 1.10         | 1.06         | 1.09         | 1.11         |
| <b>Total Boundary outflow (C)</b>         |                               |       | <b>1.06</b>  | <b>1.26</b>  | <b>1.22</b>  | <b>1.26</b>  | <b>1.32</b>  |
| Pumping from SZ1                          |                               |       | 1.18         | 0.99         | 0.86         | 0.68         | 0.75         |
| Pumping from SZ2                          |                               |       | 1.02         | 0.81         | 0.85         | 0.73         | 0.75         |
| Pumping from SZ3                          |                               |       | 3.09         | 3.31         | 2.96         | 2.89         | 2.92         |
| Pumping from SZ4                          |                               |       | 0.50         | 0.57         | 0.57         | 0.56         | 0.57         |
| Pumping from all SZ                       |                               |       | 5.79         | 5.67         | 5.25         | 4.87         | 4.99         |
| Irrigation                                |                               |       | 2.54         | 2.09         | 1.67         | 1.28         | 1.41         |
| <b>Pumping-Irrigation (D)</b>             |                               |       | <b>3.25</b>  | <b>3.58</b>  | <b>3.58</b>  | <b>3.59</b>  | <b>3.58</b>  |
| Infiltration from OL to SZ1               |                               |       | 27.86        | 24.16        | 22.41        | 19.71        | 22.42        |
| Infiltration from SZ1 to SZ2              |                               |       | 3.70         | 3.74         | 3.60         | 3.48         | 3.50         |
| Infiltration from SZ2 to SZ3              |                               |       | 2.63         | 2.84         | 2.69         | 2.65         | 2.65         |
| Infiltration from SZ3 to SZ4              |                               |       | 0.11         | 0.14         | 0.20         | 0.21         | 0.21         |
| OL->river                                 |                               |       | -14.66       | -11.90       | -10.73       | -8.38        | -10.87       |
| Drain to river                            |                               |       | 21.62        | 17.64        | 16.42        | 14.01        | 16.63        |
| Drain to ext. river                       |                               |       | 0.21         | 0.30         | 0.20         | 0.22         | 0.21         |
| Base flow to River                        |                               |       | -0.25        | -0.18        | -0.16        | -0.13        | -0.16        |
| <b>Total flow to river (E)</b>            |                               |       | <b>6.92</b>  | <b>5.86</b>  | <b>5.73</b>  | <b>5.71</b>  | <b>5.81</b>  |
| Error (A-B-C-D-E)                         |                               |       | 0.01         | 0.00         | 0.00         | 0.01         | 0.01         |
| Boundary surface outflow (runoff)         | COL+CDR+E                     |       | 7.11         | 6.03         | 5.89         | 5.88         | 6.02         |
|   | ---                           |       | ---          | ---          | ---          | ---          | ---          |
| Net groundwater recharge                  | A-(B-BSZ)-(C-CSZ)-E=BSZ+CSZ+D |       | 3.73         | 4.30         | 4.27         | 4.33         | 4.33         |
|   | ---                           |       | ---          | ---          | ---          | ---          | ---          |

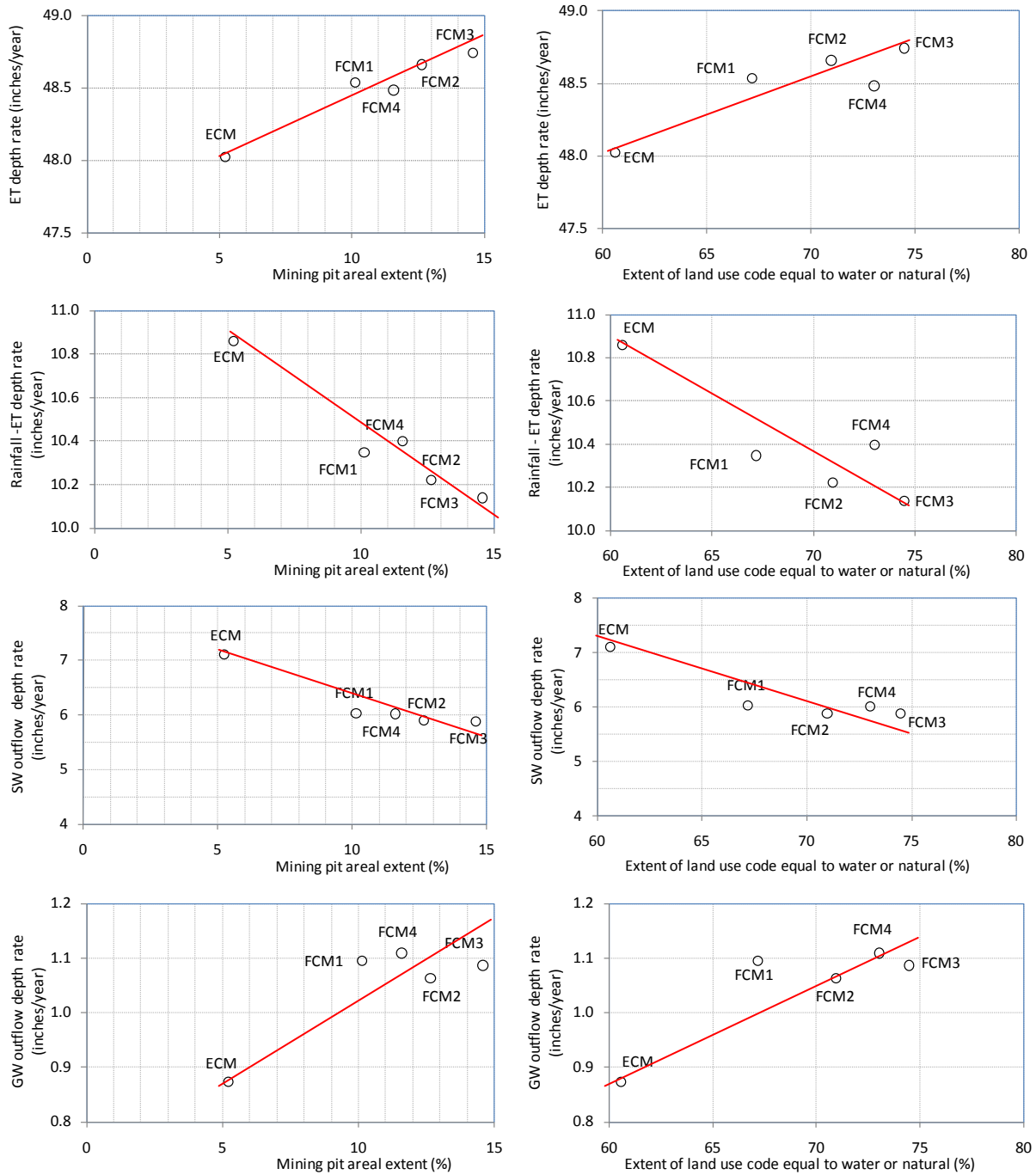


**Figure 91.** Annual averaged Water Balance Components in the DR/GR Area from all Models.

The seasonal oscillation of the main water balance components is shown in **Figure 92** through **Figure 95**. Daily ET rates are higher from April to September due to the higher temperatures. The daily net rainfall rate is positive from mid May to mid October (rainy season), which approximately matches the period of positive surface water outflow from the DR/GR Area. The surface water outflow rate peaks during the months of August and September (late wet season). Groundwater outflows are higher from August to November.

Different land use scenarios show slight differences in seasonal patterns, which cause the differences in the annual averaged values presented in Table 17. ET and groundwater outflow rate differences are lower in the wet months and higher in drier months. Conversely, surface water outflow rate differences are lower in drier months and higher in wet months.

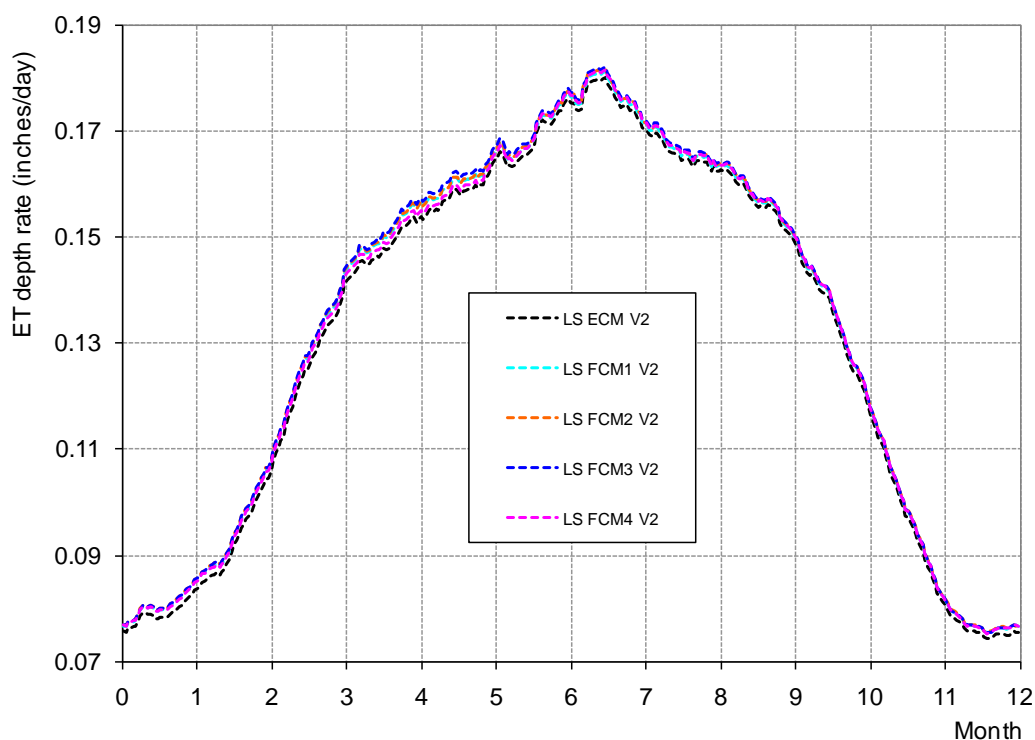


**Figure 92.** Seasonal averaged evapotranspiration in the DR/GR Area for all scenarios.

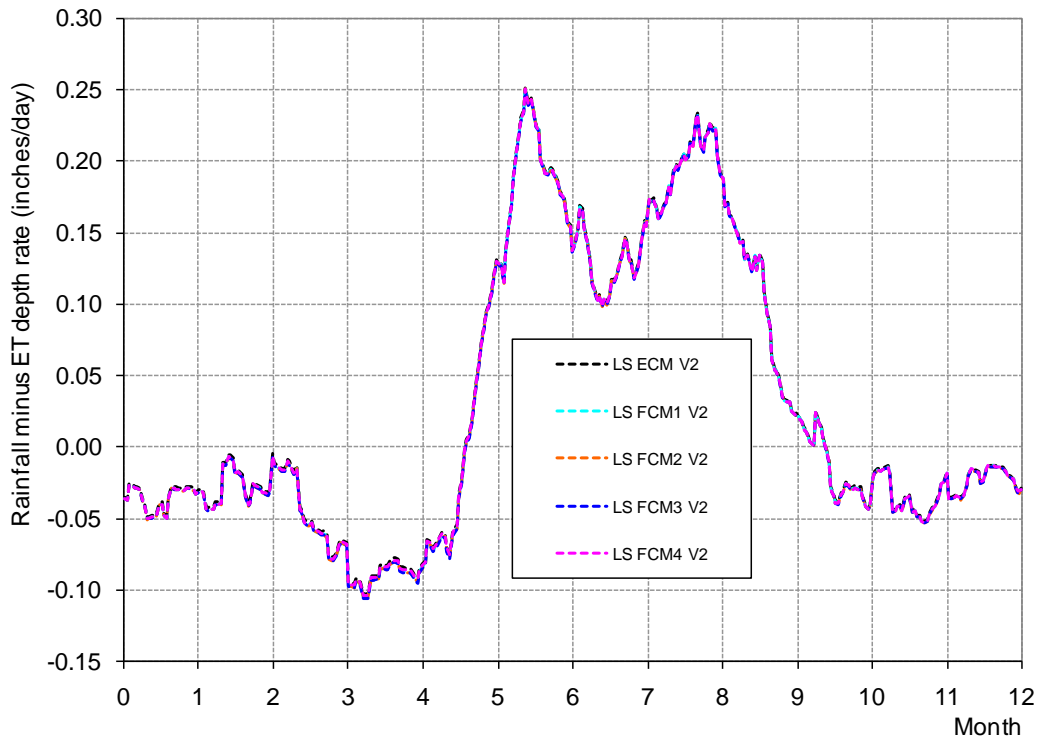


**Figure 93.** Seasonal averaged net rainfall in the DR/GR Area for all scenarios.

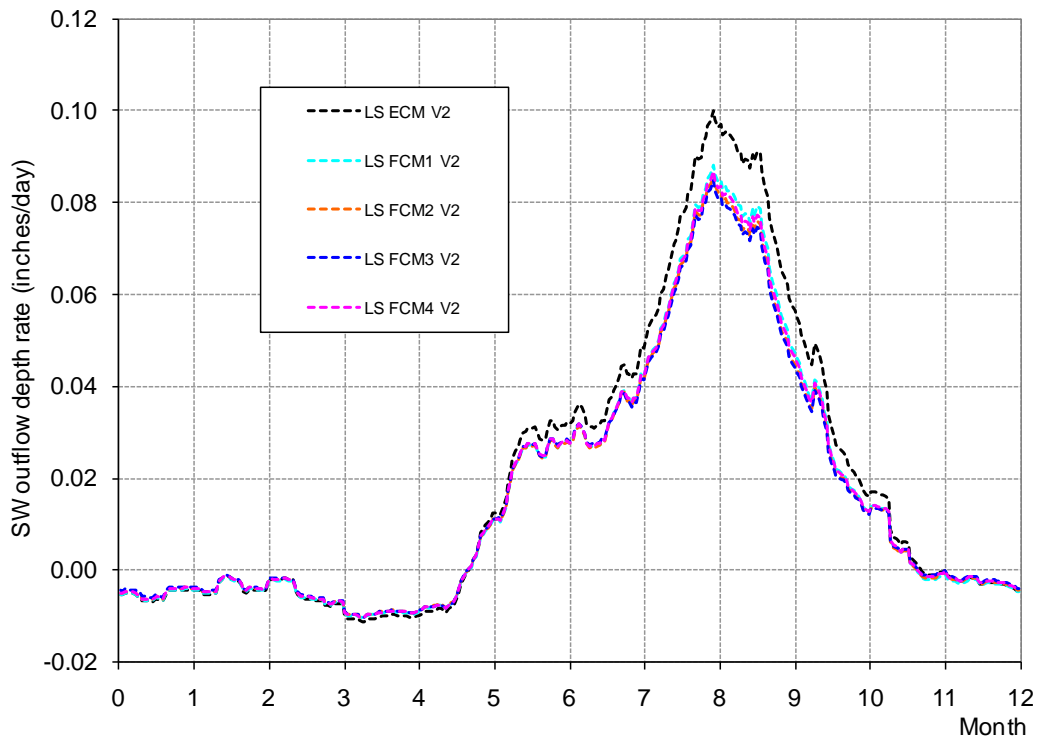


**Figure 94.** Seasonal surface water outflow from the DR/GR Area for all scenarios.

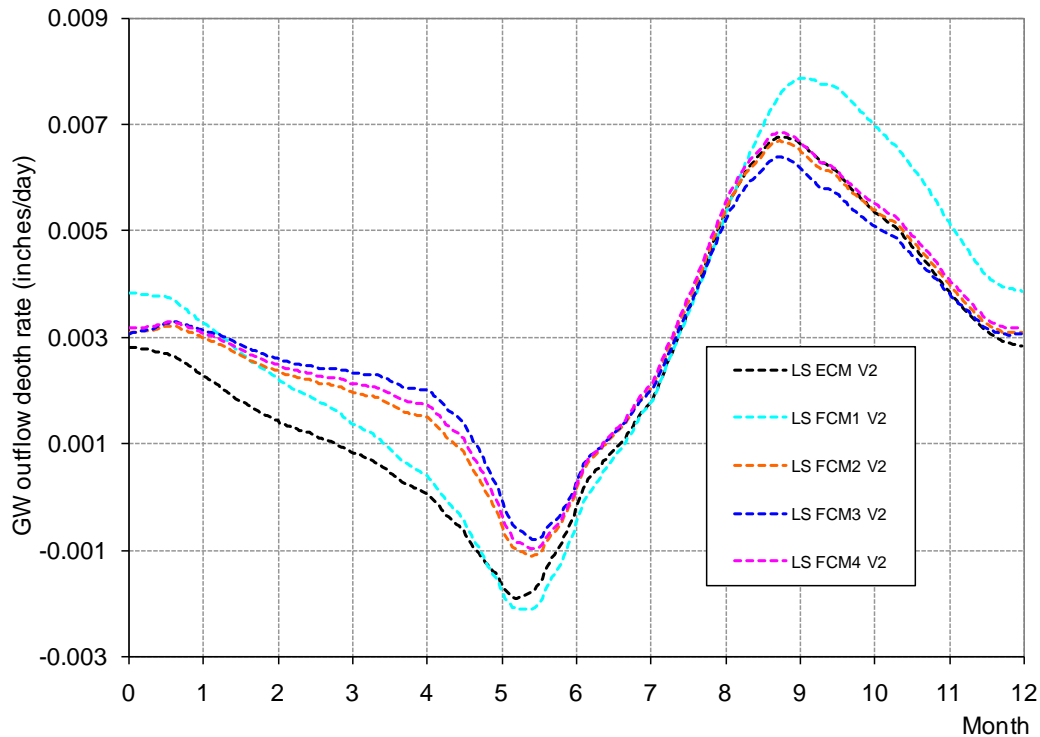


**Figure 95.** Seasonal groundwater outflow from the DR/GR Area for all scenarios.

### Mining Pits and Lakes

A detailed water budget component breakdown for mining pits and shallow water bodies around the DR/GR area is presented in **Table 18**. Notice that the average ET depth rate in the water bodies does not differ significantly from the one in the ECM. Thus, the ET volumetric rate is approximately proportional to the area covered by the water bodies, and this supports the linear correlation between the ET depth rate for the entire DR/GR and the mining pit areal coverage shown previously in Figure 91.

As previously observed when discussing the ECM results in Table 8, the net rainfall (rainfall minus ET) in mining pits and lakes is approximately zero inches per year. Moreover, a positive outflow from the drainage system around mining pits is predicted from the model. As a result, the aquifers need to supply water to the mining pits (negative net groundwater recharge) approximately equal to the amount that is lost through the drainage system (3.8 to 7.0 inches/year).

Observation data, other than the LIDAR, for modeling the drainage system around the mining pits was not available, and there may be inaccuracies. However, if these outflows from mines are verified in the field, the construction of flow barriers (berms, flow structures, etc.) in those locations may reduce the outflow (negative recharge) from the aquifers.



**Table 18.** Annual average depth rates of the water balance components for mining pits and lakes around the DR/GR area as predicted from different models.

| Depth rates (inches/year)                 |                               | Model | ECM   | FCM1   | FCM2  | FCM3  | FCM4   |
|---|-------------------------------|-------|-------|--------|-------|-------|--------|
| Rainfall                                  |                               |       | 59.10 | 59.59  | 59.23 | 58.81 | 59.00  |
| ET  |                               |       | 59.09 | 59.14  | 59.04 | 58.98 | 59.02  |
| <b>Rainfall - ET (A)</b>                  |                               |       | 0.00  | 0.46   | 0.19  | -0.17 | -0.02  |
| OL storage change                         |                               |       | -0.13 | -0.15  | 0.21  | -0.54 | 0.24   |
| UZ Storage change                         |                               |       | 0.00  | 0.00   | 0.00  | 0.00  | 0.00   |
| Total SZ Storage change (BSZ)             |                               |       | -0.02 | -0.02  | -0.01 | -0.03 | -0.01  |
| <b>Total storage (B)</b>                  |                               |       | -0.15 | -0.17  | 0.19  | -0.57 | 0.23   |
| Net OL Boundary outflow (COL)             |                               |       | 0.03  | 0.01   | 0.01  | 0.17  | 0.01   |
| Drain to Boundary (CDR)                   |                               |       | 0.00  | 0.00   | 0.00  | 0.00  | 0.00   |
| Net SZ Boundary outflow from SZ1          |                               |       | -9.02 | -10.89 | -9.75 | -8.10 | -10.18 |
| Net SZ Boundary outflow from SZ2          |                               |       | -2.08 | -0.49  | -0.57 | -0.17 | -0.66  |
| Net SZ Boundary outflow from SZ3          |                               |       | 2.79  | 3.45   | 3.68  | 2.99  | 3.64   |
| Net SZ Boundary outflow from SZ4          |                               |       | 0.10  | 0.41   | 0.74  | 0.35  | 0.63   |
| Net SZ Boundary outflow from all SZ (CSZ) |                               |       | -8.20 | -7.51  | -5.91 | -4.94 | -6.57  |
| <b>Total Boundary outflow (C)</b>         |                               |       | -8.17 | -7.50  | -5.90 | -4.77 | -6.56  |
| Pumping from SZ1                          |                               |       | 0.48  | 0.01   | 0.00  | 0.01  | 0.00   |
| Pumping from SZ2                          |                               |       | 2.33  | 0.67   | 0.83  | 0.74  | 0.90   |
| Pumping from SZ3                          |                               |       | 0.18  | 0.12   | 0.17  | 0.15  | 0.18   |
| Pumping from SZ4                          |                               |       | 0.56  | 0.36   | 0.48  | 0.42  | 0.52   |
| Pumping from all SZ                       |                               |       | 3.55  | 1.16   | 1.49  | 1.32  | 1.60   |
| Irrigation                                |                               |       | 0.00  | 0.00   | 0.00  | 0.00  | 0.00   |
| <b>Pumping-Irrigation (D)</b>             |                               |       | 3.55  | 1.16   | 1.49  | 1.32  | 1.60   |
| Infiltration from OL to SZ1               |                               |       | -4.67 | -6.38  | -4.44 | -3.64 | -4.98  |
| Infiltration from SZ1 to SZ2              |                               |       | 3.87  | 4.50   | 5.31  | 4.45  | 5.20   |
| Infiltration from SZ2 to SZ3              |                               |       | 3.62  | 4.32   | 5.05  | 3.89  | 4.96   |
| Infiltration from SZ3 to SZ4              |                               |       | 0.65  | 0.76   | 1.21  | 0.76  | 1.14   |
| OL->river                                 |                               |       | 4.77  | 6.97   | 4.41  | 3.85  | 4.71   |
| Drain to river                            |                               |       | 0.00  | 0.00   | 0.00  | 0.00  | 0.00   |
| Drain to ext. river                       |                               |       | 0.00  | 0.00   | 0.00  | 0.00  | 0.00   |
| Base flow to River                        |                               |       | 0.00  | 0.00   | 0.00  | 0.00  | 0.00   |
| <b>Total flow to river (E)</b>            |                               |       | 4.77  | 6.97   | 4.41  | 3.85  | 4.71   |
| Error (A-B-C-D-E)                         |                               |       | 0.00  | 0.00   | 0.00  | 0.00  | 0.00   |
| Boundary surface outflow (runoff)         | ---                           |       | ---   | ---    | ---   | ---   | ---    |
|   | COL+CDR                       |       | 0.03  | 0.01   | 0.01  | 0.17  | 0.01   |
| Net groundwater recharge                  | A-(B-BSZ)-(C-CSZ)-E=BSZ+CSZ+D |       | -4.67 | -6.37  | -4.44 | -3.64 | -4.98  |
|   | A= B+C+D+E                    |       | 0.00  | 0.45   | 0.19  | -0.17 | -0.02  |

### Isolated Mine in FCM1

An isolated mine in a relatively flat area located in the northwest corner of the DR/GR Area was considered in future condition model 1 (FCM1). The water table plot in locations M1, M2, and M3, presented in previous sections, showed that the mine is acting like a groundwater reservoir, i.e., releasing water (collected during the rainy season) into the aquifers during the dry season. This may be a unique characteristic of this mine. All the mines in the other scenarios experience too much influence from surrounding mines to determine whether or not they also act as reservoirs.

A water balance calculation was conducted in the proposed mining pit area from the LS ECM and the FCM1 results. The annual averaged rates from 2002 to 2006 are presented in **Table 19**.

The annual averaged net groundwater recharge from that mining pit presented in Table 19 went from -3.7 inches in the ECM to 7.2 inches in the FCM1. This positive increase in the groundwater recharge, however, is accompanied by an increase in the annual ET depth of 10.4 inches and a decrease in the surface water outflow (runoff) of 20.4 inches. In summary, this new proposed mine would increase the groundwater recharge by retaining the pre-mined runoff, but at the cost of losing about half of it as ET.

A comparison between Table 13 and Table 19 reveals that the average annual rainfall in that mining pit area is about 7.4 inches higher than in the entire DR/GR Area and in the entire mining pits and lakes area. The monthly rainfall time series is compared in **Figure 96** for both areas. It is not clear if that higher rainfall rate is due to local climatic conditions or due to the statistical fluctuations expected when analyzing a smaller area. In any case, that mining pit with an annual rainfall that exceeds RET by 19.6% is not representative of the entire DR/GR area where annual rainfall exceeds RET on average by about 8%.

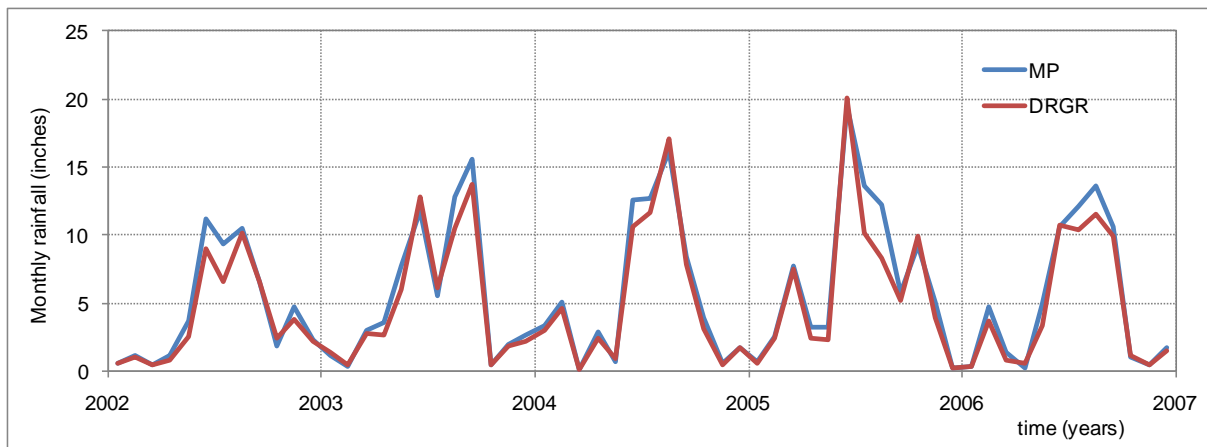


**Figure 96.** Monthly rainfall in the mining pit area (MP) containing site M2 in Figure 43 compared to the averaged monthly rainfall in the DR/GR Area.



**Table 19.** Annual average depth rates of the water balance components in a mining pit area located in the northwest corner of the DR/GR Area in the FCM1.

| Depth rates (inches/year)                 |                               | Model | LS ECM       | LS FCM1     |
|---|-------------------------------|-------|--------------|-------------|
| Rainfall                                  |                               |       | 66.4         | 66.4        |
| ET  |                               |       | 49.8         | 60.1        |
| <b>Rainfall - ET (A)</b>                  |                               |       | <b>16.7</b>  | <b>6.3</b>  |
| OL storage change                         |                               |       | 0.0          | -0.9        |
| UZ Storage change                         |                               |       | 0.0          | 0.0         |
| Total SZ Storage change (BSZ)             |                               |       | -0.3         | -0.1        |
| <b>Total storage (B)</b>                  |                               |       | <b>-0.3</b>  | <b>-1.0</b> |
| Net OL Boundary outflow (COL)             |                               |       | -9.6         | 0.0         |
| Drain to Boundary (CDR)                   |                               |       | 0.0          | 0.0         |
| Net SZ Boundary outflow from SZ1          |                               |       | -4.5         | 6.0         |
| Net SZ Boundary outflow from SZ2          |                               |       | 0.0          | 0.0         |
| Net SZ Boundary outflow from SZ3          |                               |       | 1.3          | 1.4         |
| Net SZ Boundary outflow from SZ4          |                               |       | -0.1         | -0.1        |
| Net SZ Boundary outflow from all SZ (CSZ) |                               |       | -3.4         | 7.3         |
| <b>Total Boundary outflow (C)</b>         |                               |       | <b>-13.0</b> | <b>7.3</b>  |
| Pumping from SZ1                          |                               |       | 0.0          | 0.0         |
| Pumping from SZ2                          |                               |       | 0.0          | 0.0         |
| Pumping from SZ3                          |                               |       | 0.0          | 0.0         |
| Pumping from SZ4                          |                               |       | 0.0          | 0.0         |
| Pumping from all SZ                       |                               |       | 0.0          | 0.0         |
| Irrigation                                |                               |       | 0.0          | 0.0         |
| <b>Pumping-Irrigation (D)</b>             |                               |       | <b>0.0</b>   | <b>0.0</b>  |
| Infiltration from OL to SZ1               |                               |       | 82.2         | 7.2         |
| Infiltration from SZ1 to SZ2              |                               |       | 1.1          | 1.2         |
| Infiltration from SZ2 to SZ3              |                               |       | 1.1          | 1.2         |
| Infiltration from SZ3 to SZ4              |                               |       | -0.2         | -0.2        |
| OL->river                                 |                               |       | -56.0        | 0.0         |
| Drain to river                            |                               |       | 82.2         | 0.0         |
| Drain to ext. river                       |                               |       | 4.5          | 0.0         |
| Base flow to River                        |                               |       | -0.8         | 0.0         |
| <b>Total flow to river (E)</b>            |                               |       | <b>29.9</b>  | <b>0.0</b>  |
| Error (A-B-C-D-E)                         |                               |       | 0.0          | 0.0         |
| Boundary surface outflow (runoff)         | COL+CDR+E                     |       | 20.4         | 0.0         |
|   | ---                           |       | ---          | ---         |
| Net groundwater recharge                  | A-(B-BSZ)-(C-CSZ)-E=BSZ+CSZ+D |       | -3.7         | 7.2         |
|   | A= B+C+D+E                    |       | ---          | 6.3         |



### New Urban Areas

A water budget calculation was performed in four new urban areas corresponding to the sites labeled from U1 through U4 in Figure 43. The comparison of the annual rates between the ECM and the FCMs are presented in **Table 20**. The differences between the scenarios were small, and just the averaged rate from the four scenarios is displayed.

In general, the modeling predicts that new urban areas have lower ET rates with respect to the existing conditions. This is consistent with the low values of LAI and Rd assumed for this land use classification (see Table 4). Moreover, the absence of irrigation systems assumed in the new urban areas at sites U2 and U4, may contribute to the reduction of the ET losses in those areas. The lower actual ET rate is likely the main reason of why the dry-season water table levels in the new urban areas are in general higher than in the ECM.



**Table 20.** Annual average depth rates of the water balance components in new urban areas.

|   | Site  | U1          |              | U2          |              | U3           |               | U4          |             |
|---|-------|-------------|--------------|-------------|--------------|--------------|---------------|-------------|-------------|
| Depth rates (inches/year)                 | Model | ECM         | FCMs         | ECM         | FCMs         | ECM          | FCMs          | ECM         | FCMs        |
| Rainfall                                  |       | 64.6        | 64.6         | 57.5        | 57.5         | 57.5         | 57.5          | 56.2        | 56.2        |
| ET  |       | 46.9        | 45.8         | 47.9        | 41.6         | 52.5         | 43.1          | 52.9        | 35.9        |
| <b>Rainfall - ET (A)</b>                  |       | <b>17.7</b> | <b>18.8</b>  | <b>9.7</b>  | <b>16.0</b>  | <b>5.0</b>   | <b>14.4</b>   | <b>3.2</b>  | <b>20.3</b> |
| OL storage change                         |       | 0.0         | 0.0          | 0.0         | 0.0          | 0.0          | 0.0           | 0.0         | 0.0         |
| UZ Storage change                         |       | -0.1        | 0.0          | 0.1         | 0.0          | 0.0          | 0.1           | 0.0         | 0.0         |
| Total SZ Storage change (BSZ)             |       | -0.4        | -0.3         | -0.2        | -0.2         | -0.5         | -0.6          | -0.3        | -0.2        |
| <b>Total storage (B)</b>                  |       | <b>-0.4</b> | <b>-0.3</b>  | <b>-0.1</b> | <b>-0.1</b>  | <b>-0.5</b>  | <b>-0.4</b>   | <b>-0.3</b> | <b>-0.2</b> |
| Net OL Boundary outflow (COL)             |       | -2.6        | -5.7         | -2.9        | -28.7        | -41.3        | -55.5         | -0.6        | -0.9        |
| Drain to Boundary (CDR)                   |       | 0.0         | 0.0          | 0.0         | 0.0          | 0.0          | 0.0           | 0.0         | 0.0         |
| Net SZ Boundary outflow from SZ1          |       | -5.0        | -3.6         | 8.7         | -14.1        | -24.2        | -39.3         | -9.0        | 0.8         |
| Net SZ Boundary outflow from SZ2          |       | 0.0         | 0.0          | 0.9         | -1.6         | 0.0          | 0.0           | -0.1        | -0.1        |
| Net SZ Boundary outflow from SZ3          |       | 5.7         | -1.6         | 0.9         | 0.9          | -10.3        | -9.5          | 5.5         | 8.4         |
| Net SZ Boundary outflow from SZ4          |       | -0.7        | -1.0         | 0.3         | 0.4          | -0.6         | -0.5          | 1.5         | 1.9         |
| Net SZ Boundary outflow from all SZ (CSZ) |       | 0.0         | -6.2         | 10.8        | -14.4        | -35.1        | -49.2         | -2.1        | 11.1        |
| <b>Total Boundary outflow (C)</b>         |       | <b>-2.6</b> | <b>-11.9</b> | <b>7.9</b>  | <b>-43.1</b> | <b>-76.3</b> | <b>-104.8</b> | <b>-2.7</b> | <b>10.2</b> |
| Pumping from SZ1                          |       | 0.0         | 0.0          | 0.1         | 0.0          | 0.7          | 0.0           | 13.5        | 0.0         |
| Pumping from SZ2                          |       | 0.0         | 0.0          | 0.0         | 0.0          | 0.0          | 0.1           | 0.0         | 0.0         |
| Pumping from SZ3                          |       | 0.4         | 8.1          | 0.0         | 0.0          | 13.5         | 12.5          | 0.0         | 0.0         |
| Pumping from SZ4                          |       | 0.0         | 0.0          | 0.0         | 0.0          | 0.0          | 0.0           | 0.0         | 0.0         |
| Pumping from all SZ                       |       | 0.4         | 8.1          | 0.1         | 0.0          | 14.3         | 12.5          | 13.5        | 0.0         |
| Irrigation                                |       | 0.4         | 8.1          | 0.5         | 0.0          | 7.1          | 5.3           | 13.5        | 0.0         |
| <b>Pumping-Irrigation (D)</b>             |       | <b>0.0</b>  | <b>0.0</b>   | <b>-0.4</b> | <b>0.0</b>   | <b>7.2</b>   | <b>7.2</b>    | <b>0.0</b>  | <b>0.0</b>  |
| Infiltration from OL to SZ1               |       | 20.8        | 32.4         | 100.0       | 339.5        | 53.2         | 75.1          | 17.2        | 21.1        |
| Infiltration from SZ1 to SZ2              |       | 5.3         | 5.4          | 2.1         | -0.2         | 2.6          | 2.5           | 6.9         | 10.2        |
| Infiltration from SZ2 to SZ3              |       | 5.3         | 5.4          | 1.2         | 1.3          | 2.6          | 2.4           | 7.0         | 10.3        |
| Infiltration from SZ3 to SZ4              |       | -0.8        | -1.0         | 0.3         | 0.4          | -0.6         | -0.5          | 1.5         | 1.9         |
| OL->river                                 |       | 0.0         | 0.2          | -87.0       | -294.8       | 0.0          | 0.0           | 0.0         | 0.0         |
| Drain to river                            |       | 0.0         | 0.0          | 90.1        | 323.6        | 0.0          | 0.0           | 6.3         | 10.3        |
| Drain to ext. river                       |       | 20.7        | 30.8         | 0.0         | 32.0         | 74.5         | 112.4         | 0.0         | 0.0         |
| Base flow to River                        |       | 0.0         | 0.0          | -0.8        | -1.5         | 0.0          | 0.0           | -0.1        | -0.1        |
| <b>Total flow to river (E)</b>            |       | <b>20.7</b> | <b>31.0</b>  | <b>2.3</b>  | <b>59.2</b>  | <b>74.5</b>  | <b>112.4</b>  | <b>6.2</b>  | <b>10.2</b> |
| Error (A-B-C-D-E)                         |       | 0.0         | 0.0          | 0.0         | 0.0          | 0.0          | 0.0           | 0.0         | 0.0         |

## Surface Water Flows

**Figure 97** shows a map of locations that were selected for comparison of surface water flow rates among different model scenarios. The annual averaged flow rates presented in **Table 21** show that the flow rate in the main pathways of the DR/GR decreases in the future condition scenarios. This is consistent with the reduction of the total surface outflow rate from the DR/GR Area in the FCMs, as discussed in the previous section.

**Table 21.** Annual average flow rates at selected pathway locations.

| Flow Location | Flow (%) | Flow percentage differences regarding ECM |       |       |      |
|---------------|----------|---|-------|-------|------|
|               | ECM      | FCM1                                      | FCM2  | FCM3  | FCM4 |
| AL            | 18.6     | -4.7                                      | -8.1  | -3.9  | -6.5 |
| CSa           | 22.5     | -9.7                                      | -10.1 | -7.6  | -9.6 |
| CSb           | 3.9      | 0.0                                       | 0.2   | -0.6  | 0.2  |
| CSc           | 4.9      | 0.0                                       | -1.8  | -2.3  | -1.8 |
| CSd           | 55.0     | -7.2                                      | -9.6  | -4.5  | -7.1 |
| I-75a         | 35.6     | -9.1                                      | -9.3  | -10.0 | -9.2 |
| I-75b         | 27.7     | -7.3                                      | -6.8  | -14.6 | -7.8 |
| I-75c         | 13.3     | -2.2                                      | -2.1  | -2.7  | -2.2 |
| I-75d         | 100.0    | -0.6                                      | -0.8  | -2.2  | -0.1 |

Note: A flow of 100 % corresponds to 37.4 ft<sup>3</sup>/s.

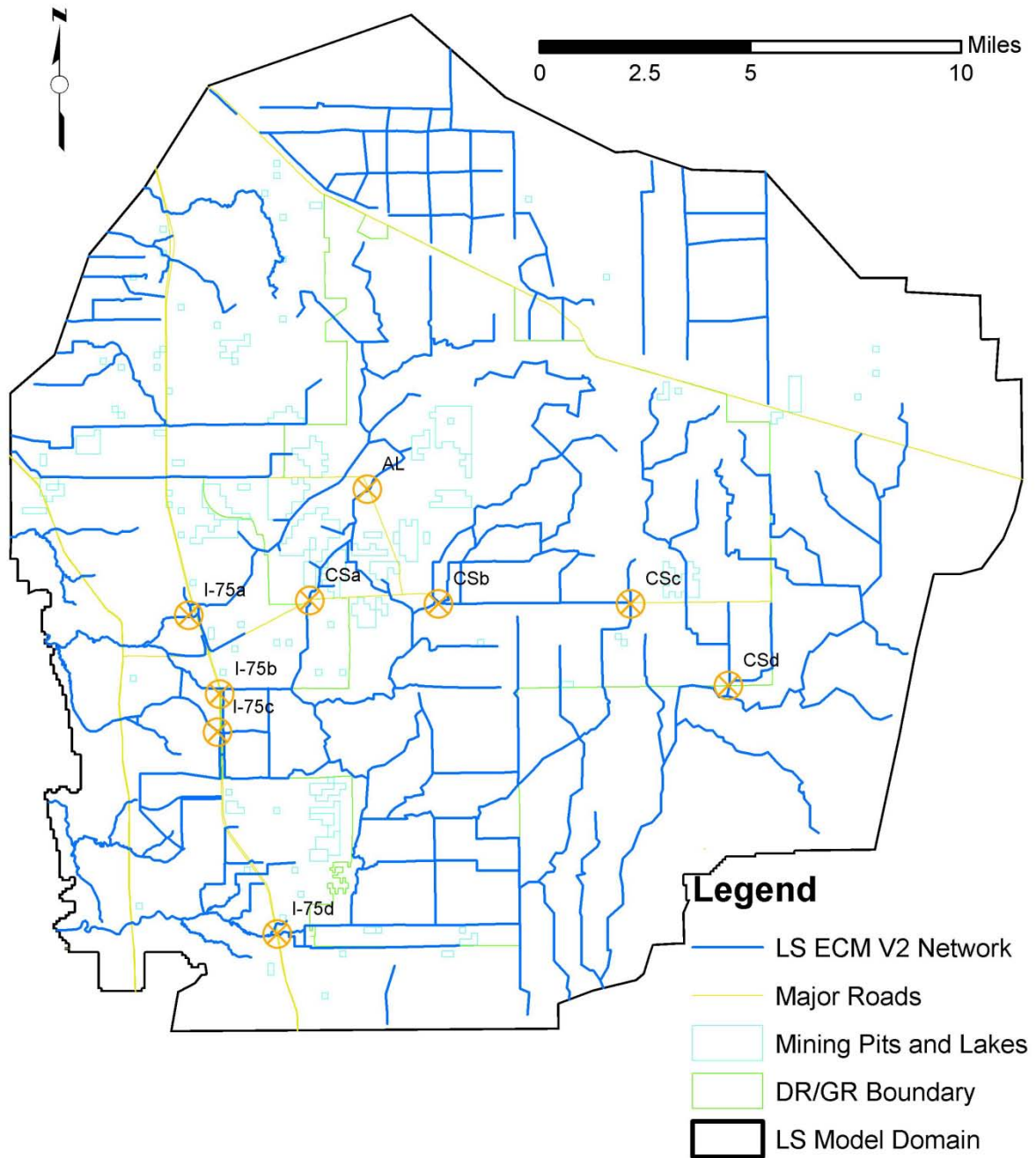


**Figure 97.** Selected flow comparison locations.

## Conclusions

### General Findings

The model results from the different land use scenarios indicate several concepts that may be useful during the planning process.

- Wetland areas converted from agricultural areas in the future condition alternatives help to increase the water table elevations during the dry season and to extend the period of time that those areas are wet (hydroperiod).
- The conversion of natural and agricultural areas to urban development slightly lowers the water table during the wet season due to the new urban drainage system. The water table in the new urban areas is usually higher at the end of the dry season compared to the existing conditions, which is likely related to a reduction in the ET losses.
- The water budget in all mines and lakes around the DR/GR Area suggests that the annual net rainfall (rainfall minus evaporation) is about zero on average. This is a consequence of the open water evaporation rate, which is commonly higher than the annual ET rate in pre-mined conditions. The model also predicts that the drainage system around some mines produces a positive net water outflow from the mines. As a result, the aquifers need to supply water to the mining pits (negative net groundwater recharge) in about the amount that is lost through the drainage system.
- This modeling has indicated, in general, that the annual averaged ET rates from the DR/GR Area would be higher with greater areal coverage of mining pits. The surface water outflow rate (runoff) from the DR/GR Area was lower in all the scenarios compared to the ECM, which is likely related to the greater mining pit coverage. These results are expected due to the higher ET losses and the lower runoff from mining pits and its effect on the surface water flow in neighboring areas.
- Mining pits cause a flattening in the water table that affects the pre-developed water table gradient. This often implies a decrease in the water table elevation on the up-gradient side of the pits and an increase on the down-gradient side. On the down gradient side, there may also be a decrease in some situations. The most pronounced flattening effect is seen towards the end of the dry season. This also has an effect on the hydroperiod by shortening the up-gradient hydroperiod and increasing (or sometimes also decreasing) the down-gradient hydroperiod. The flattening effect of mine development on the water table is larger in areas with steeper water table gradients, in larger mine pits, and in the case of a number of mining pits that are closer and therefore more hydrologically connected (i.e. via groundwater).

The expected qualitative effects of the different land use changes listed above are based on general model predictions generated by this study. In the future, uncertainty associated with these model results can be improved as more field data becomes available. In particular, as groundwater level data near the mining pits becomes available in the future, the model calibration will improve and the results around mining pits will be more representative of observed field data. Furthermore, the combined effect of the land use changes on water table elevation and hydroperiod may vary from one location to another and also from year to year. Thus, it is important to observe the results obtained from the different models at specific areas and times.

### **Recommendations for the Planning Process**

The evaluation of the performance of the four future condition scenarios was based on several performance indicators extracted from the water table, hydroperiod and water budget sections. They are normalized in the interval (0, 1), where “0” represents the driest and “1” the wettest conditions from the four scenarios. The normalized indicators are shown in **Table 22**. The value of the indicator for the LS ECM was also estimated by using a mean difference of zero before normalizing. Water budget indicators for the LS ECM were not considered since they were far from the FCM range. In the case of the groundwater outflow from the ECM, it is not appropriate since it may be affected by the use of a different pumping rate in the FCMs with respect to the LS ECM. An average indicator (or score) for each scenario was computed by assuming a uniform weighting between them. Scenarios that are better for the water resources score higher average indicator values, and scenarios that are worse for the area water resources score lower average indicator values. From the average indicator, the FCM4 is the best scenario due to a variety of factors which includes a smaller number of mining pits compared to the acreage of restored land. These factors actually make FCM4 wetter on average than the LS ECM. Scenario FCM3 is the driest followed by FCM2.

**Table 22.** Normalized indicators to evaluate the scenario performance.

| Section                        | Indicator (normalized)                         | ECM   | FCM1  | FCM2  | FCM3  | FCM4 |
|--------------------------------|--|-------|-------|-------|-------|------|
| Water Table Maps<br>(Table 14) | Dry season water table level mean difference   | -0.06 | 0.00  | 0.14  | 1.00  | 0.51 |
|                                | Wet season water table level mean difference   | 0.82  | 0.26  | 0.37  | 0.00  | 1.00 |
| Hydroperiod maps<br>(Table 15) | Hydroperiod mean difference                    | 0.91  | 0.54  | 0.35  | 0.00  | 1.00 |
|                                | Water depth mean difference during hydroperiod | 1.01  | 0.68  | 0.72  | 0.00  | 1.00 |
| Water Budget<br>(Table 17)     | Annual averaged ET losses                      | ---   | 0.80  | 0.32  | 0.00  | 1.00 |
|                                | Annual averaged GW outflow                     | ---   | 0.71  | 0.00  | 0.50  | 1.00 |
|                                | Average indicator                              | 0.67  | 0.50  | 0.32  | 0.25  | 0.92 |
| Land use Changes               | New mining pit area in DRGR (%)                | 0.00  | 4.90  | 7.42  | 9.35  | 6.35 |
|                                | Restored area in DRGR (%)                      | 0.00  | 3.11  | 5.14  | 6.28  | 7.81 |
|                                | Restored minus new mining pit area in DRGR (%) | 0.00  | -1.79 | -2.28 | -3.07 | 1.46 |

The areal extent of the land use changes is also presented in Table 22 for the new mining pit and restored areas. In **Figure 98**, the average indicator is plotted as a function of the difference between newly restored minus new mining pit area. In this graph, the difference between the newly restored land and new mining pit areas comes from the new mining pit area and restored area rows in Table 22. As the percent of new mining pit area decreases, the resulting difference will be more and more positive. In the graph shown in Figure 98, this will correspond to the data point moving toward the right along the x-axis, which corresponds with an increasing average indicator value (or score) within the known data domain.

The almost perfect correlation in this graph may be helpful for the planning process. This correlation indicates that the restored (mitigated) area should be about equal to the new mining pit area in order to maintain, on average, the water table levels, hydroperiod and water budget in the entire DR/GR area. If the restored areal extent is greater than the new mining pit areal extent (which is the case in FCM4), this relationship suggests that scenario should be wetter than the ECM. The smaller the areal extent of the restored areas with respect to the areal extent of the new mining pit areas, the drier this relationship predicts the scenario to be.

The correlation shown in Figure 98 also enables the estimation of the performance of new scenarios based on one of the four FCMs. The impact of adding new restoration areas or mining pit areas can be quickly estimated from this graph, without a need to develop a new MIKE SHE model. However, these correlations are only valid within the range of values that have been simulated to date. Also, these are only valid for restoration areas or mining pit areas in the vicinity of those modeled to date. Therefore, the new mining pit areas and restored areas should be limited to the locations simulated in the four FCMs, and also in the range of areal extents considered.

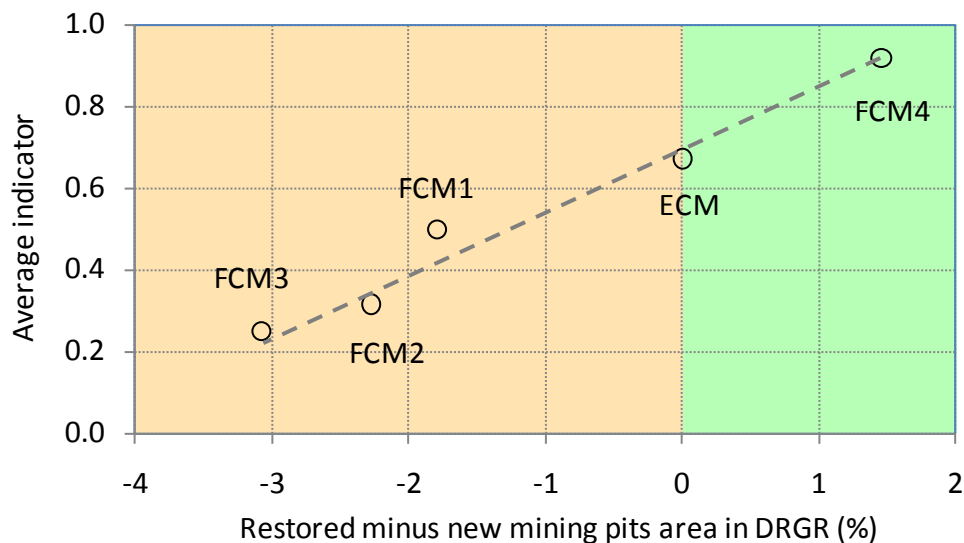


**Figure 98.** Correlation between the average indicator (score) of each scenario and the land use changes for the DR/GR Area.

Another recommendation for the planning process arising from this work is related to where to locate the new mining pits. In order to avoid mining impacts to water table levels and hydroperiods with respect to the current conditions, the flattening effect mentioned above should be minimized. There are two requirements to this, as demonstrated in the modeling results. One is to locate the mining pits in areas with flat topography (and flat water table, assumed to mimic the land surface). The second is to separate the mining pits by some critical distance in order to minimize their hydrologic connectivity. It is acknowledged that both of these requirements may not be achievable due to prior approvals granted for mine pits that are on sloping topography and/or are not adequately separated to minimize hydrologic connectivity. This study did not explore the critical gradient slope or critical spacing between mining pits, though.

### Model Limitations and Recommended Future Work

The MIKE SHE model was developed based on the best available data at the time with a state of the art, fully integrated modeling package. However, as with any other model, there may be some opportunities for improvement.

1. **Revision of pumping data.** Pumping data is a source of uncertainty in all hydrologic models. The pumping rates and the pumping depths are not well known, in general. However, production rates can have a tremendous influence on groundwater heads. In this work, the time to collect that information was limited and its review is recommended in any future work.
2. **Revision of the hydro-geologic data.** The vertical extent of the geologic layers and lenses in the model were extracted from the SWFFS model, as indicated in the project



scope. The hydraulic conductivity, specific yield, and storage coefficient were also taken originally from the same model, and modified during the calibration process. All hydrogeologic parameters could be reviewed from the information available in DBHYDRO.

3. **Inclusion of the Hawthorn Aquifer in the model.** Because of the intensive pumping from the Hawthorn Aquifer and the poor prediction of the heads in the Sandstone Aquifer, the evaluation of the introduction of deeper layers in the model is recommended.
4. **Revision of the drainage system around mining pits.** The drainage system around some mining pits was introduced in the model based on available LIDAR data. However, the incoming and outgoing flows predicted by the model at mining pits could not be verified with observation data. Since those flows are important for the water budget and the surface flow reliability of the model, the review of the drainage system around mining pits is recommended as data become available.

Note that even with the proposed improvements listed above, the model has limitations related to the grid cell size (750 ft). For local studies that require a higher resolution, the construction of a new model with a smaller model domain area and grid cell size is recommended.



## References

- Abtew, W. 1996. *Evapotranspiration measurements and modeling for three wetland systems in South Florida*. Water Resources Bulletin **32** (3), 465-473.
- Abtew, W., Huebner, R.S., and Ciuca V., 2005. *Hydrology of the South Florida Environment*. Chapter 5 in 2005 South Florida Environmental Report.
- ADA Engineering, Inc., 2008. *South Lee County Watershed Plan Update Work Order C-4600000791 WO01-R1 90% Draft Deliverable 1C. Task 1 – Survey Cross Sections and Model Update*. 35 p.
- Allen, R. G., L. S. Periera, D. Raes, and M. Smith. 1998. *Crop evapotranspiration: Guidelines for computing crop requirements*. Irrigation and Drainage Paper No. 56. Rome, Italy: FAO. Available at <http://www.fao.org/docrep/X0490E/X0490E00.htm>
- CDM, 2006. *Southwest Florida Feasibility Study: Hydrologic Model Development – Big Cypress Basin*. Final Report, May 5, 2006.
- DHI, 2008. *MIKE SHE User Manual, Volume II: Reference Guide*.
- Dover, Kohl & Partners, July 2008. *Prospects for Southeast Lee County. Planning for the Density Reduction / Groundwater Resource Area (DR/GR)*.
- Hammer, M. J. and Hammer, M.J. Jr., 2001. *Water and Wastewater Technology Upper Saddle River*: Prentice Hall Fourth Edition.
- Jacobs, J., J. Mecikalski, S. Paech, 2008. *Satellite-based solar radiation, net radiation, and potential and reference evapotranspiration estimates over Florida*. Technical Report July 2008.
- KLECE, 2008. *Ecological Memorandum of The Density Reduction/Ground-water Resource Area (DR/GR)*. Prepared for Dover, Kohl & Partners.
- Lee, T. M., and Swancar, A., 1997. *Influence of evaporation, ground water, and uncertainty in the hydrologic budget of Lake Lucerne, a seepage lake in Polk County, Florida*. U.S. Geological Survey Water-Supply Paper 2439, 61 p.
- May-Chu, T. F. and D. L. Freyberg, 2008. *Simulating a Lake as a High-Conductivity Variably Saturated Porous Medium*, Groundwater 46 (5), pp 688.
- McLane Environmental LLC., May 2007. *Review and Summary of Studies Containing Information Relating to the Density Reduction / Groundwater Resource (DRGR) Lands Southeastern Lee County, Florida*.



Missimer, T. M. and Martin, W. K., 2001. *The Hydrogeology of Lee County, Florida, in Geology and Hydrology of Lee County Florida* by T.M. Missimer and T.M. Scott (editors) Florida Geological Survey Special Publication No. 49.

Sacks, L. A., T. M. Lee, M. J. Radell, 1994. *Comparison of energy-budget evaporation losses from two morphometrically different Florida seepage lakes*. *Journal of Hydrology* **156**, 311-334.

Southwest Florida Feasibility Study Composite topography for SW Florida, 100-ft. (September 2005)

Swancar, A., T. M. Lee, and T. M. O'Hare, 2000. *Hydrogeologic Setting, Water Budget, and Preliminary Analysis of Groundwater Exchange at Lake Starr, a Seepage Lake in Polk County, Florida*. U.S. Geological Survey Water-Resources Investigations Report 00-4030.



## ***APPENDIX A. HYDRAULIC CONDUCTIVITY MAPS***

The conductivity maps for geological layers and lenses are shown from Figure A1 to Figure A7. Those values were based on the SWFFS model maps and they were modified during the calibration process. A logarithm color scale was used and maintained through all the graphs. The conductivity used by the computational layers of the model is computed from those maps.

### **List of Figures**

|  |   |
|--|---|
| Figure A1. Horizontal conductivity map for the Holocene-Pliocene geological layer. ....                                  | 2 |
| Figure A2. Vertical conductivity map for the Holocene-Pliocene geological layer.....                                     | 3 |
| Figure A3. Conductivity map (horizontal and vertical) for the Bonita Spring Marl Confining<br>Unit geological lens.....  | 4 |
| Figure A4. Horizontal conductivity map for the Lower Tamiami geological layer. ....                                      | 5 |
| Figure A5. Vertical conductivity map for the Lower Tamiami geological layer. ....  | 6 |
| Figure A6. Conductivity map (horizontal and vertical) for the Upper Peace River Confining<br>Units geological lens. .... | 7 |
| Figure A7. Conductivity map (horizontal and vertical) for the Upper Peace River Sandstone<br>geological layer. ....      | 8 |

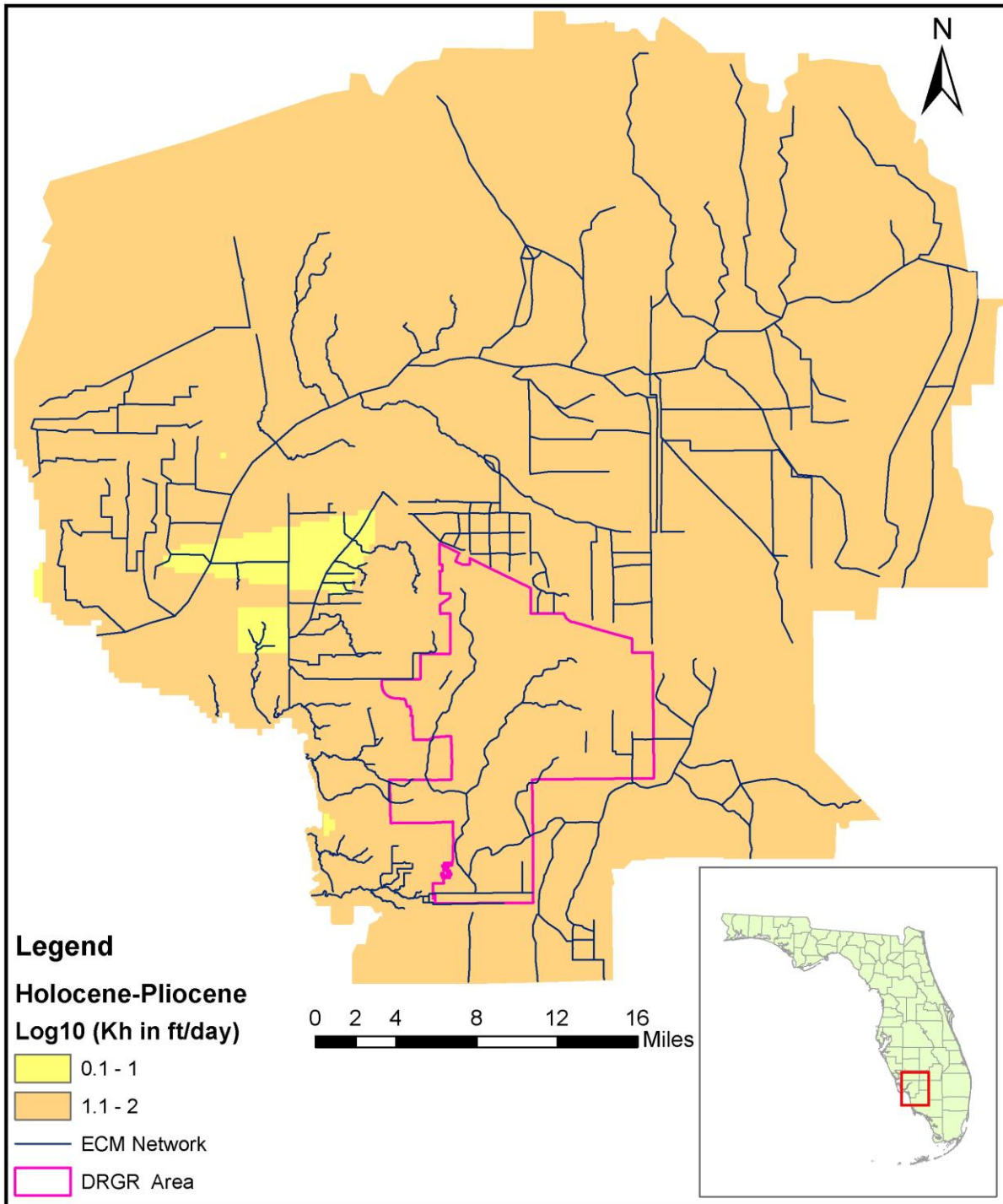


Figure A1. Horizontal conductivity map for the Holocene-Pliocene geological layer.

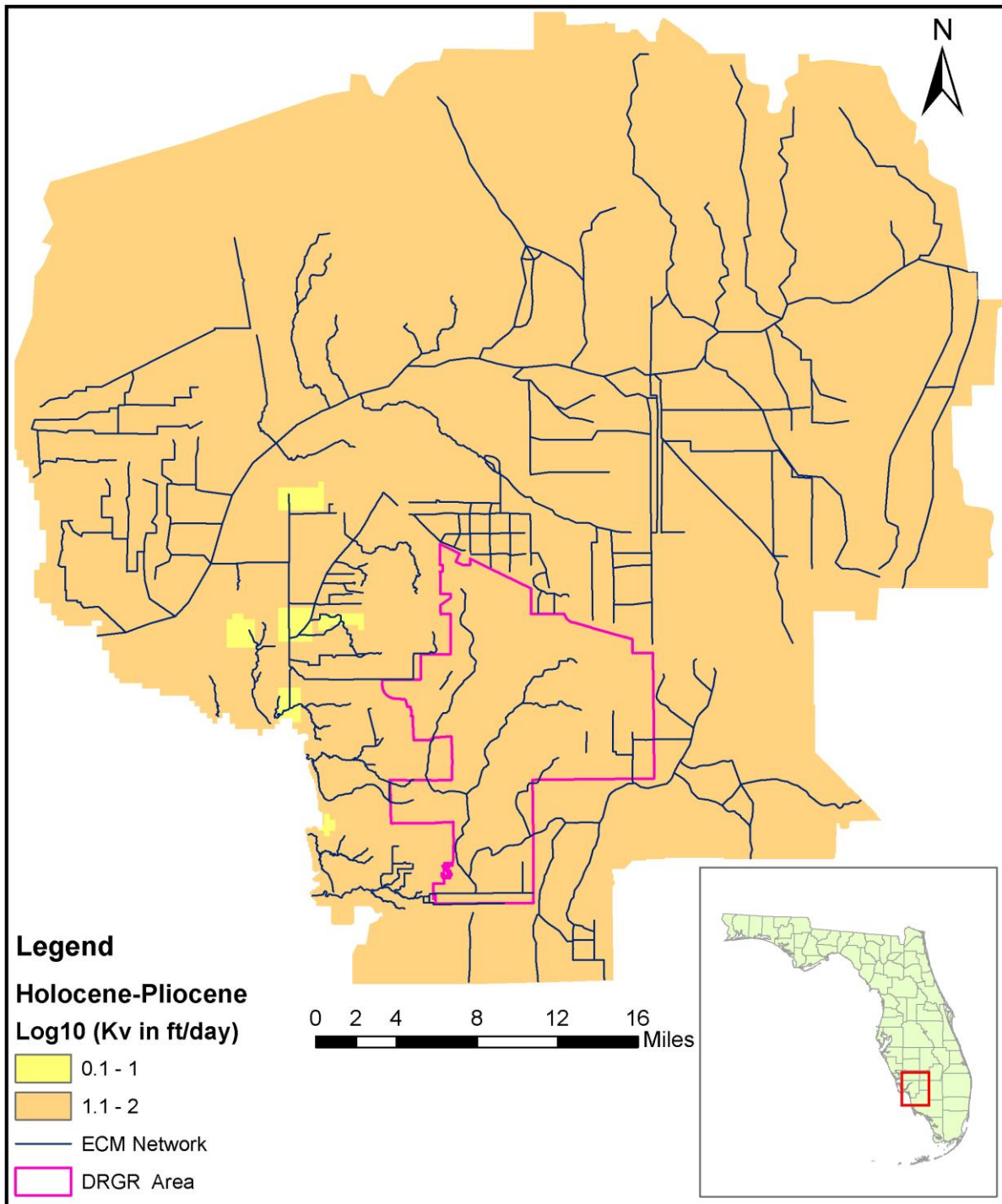


Figure A2. Vertical conductivity map for the Holocene-Pliocene geological layer.

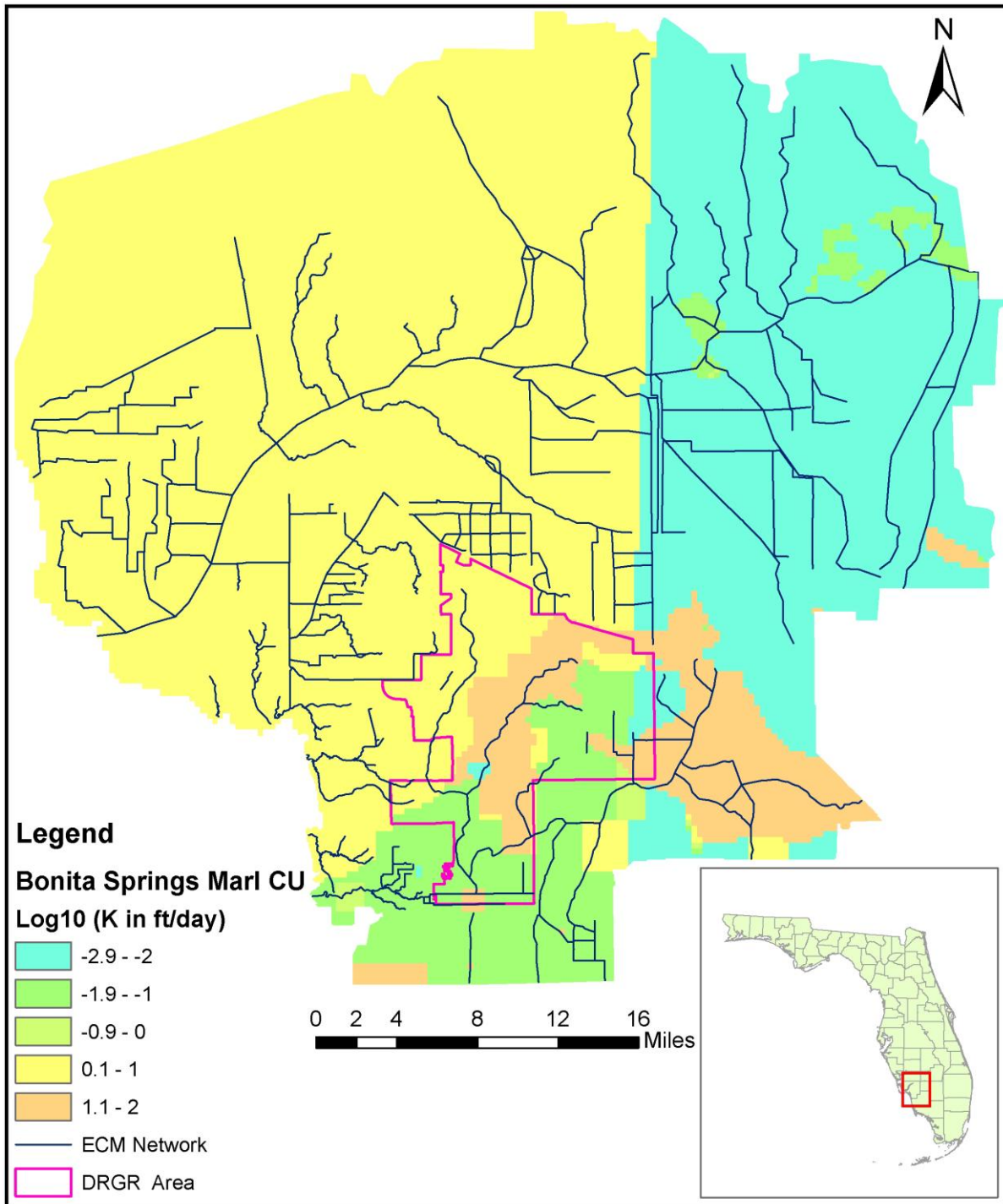


Figure A3. Conductivity map (horizontal and vertical) for the Bonita Spring Marl Confining Unit geological lens.

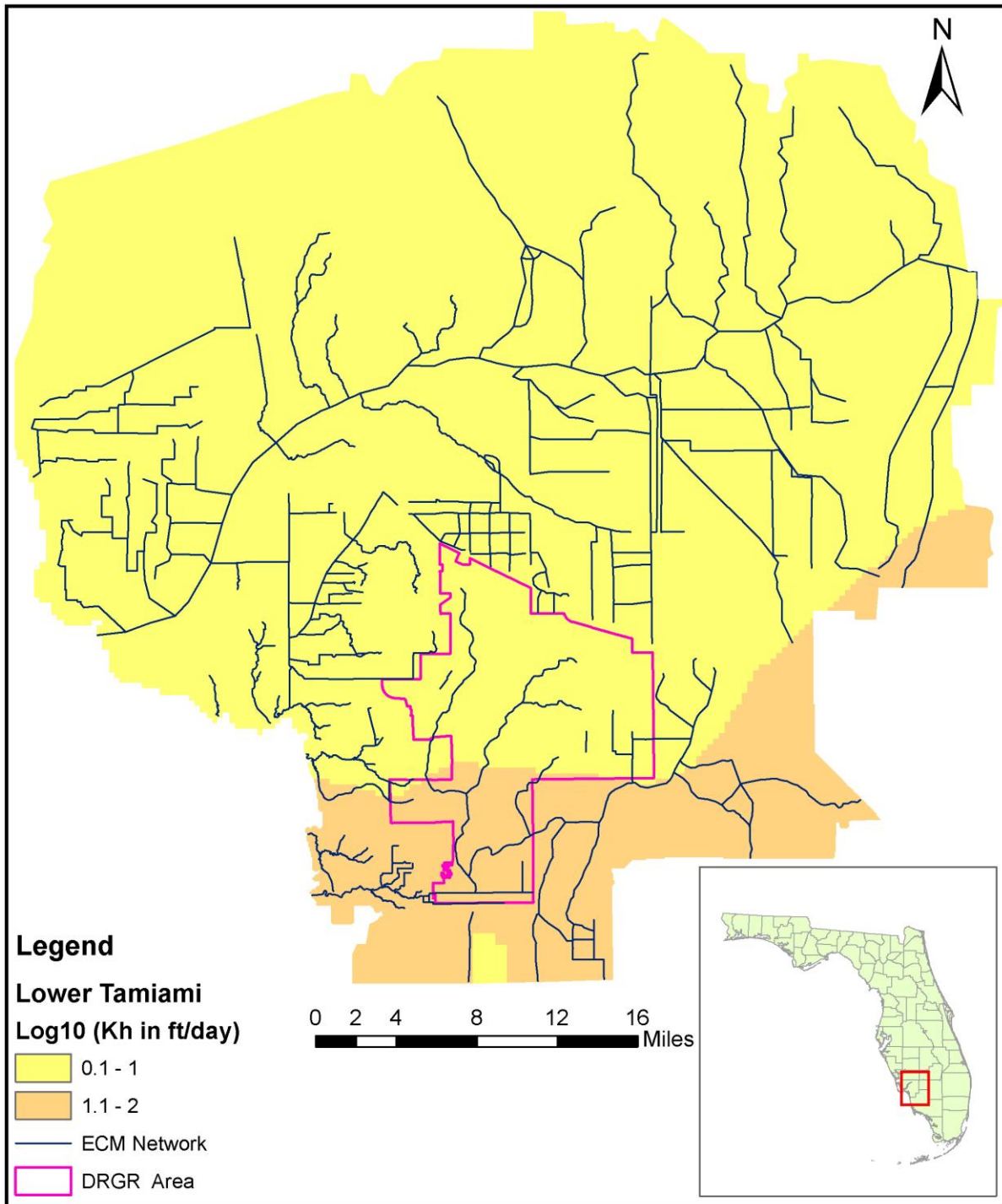


Figure A4. Horizontal conductivity map for the Lower Tamiami geological layer.

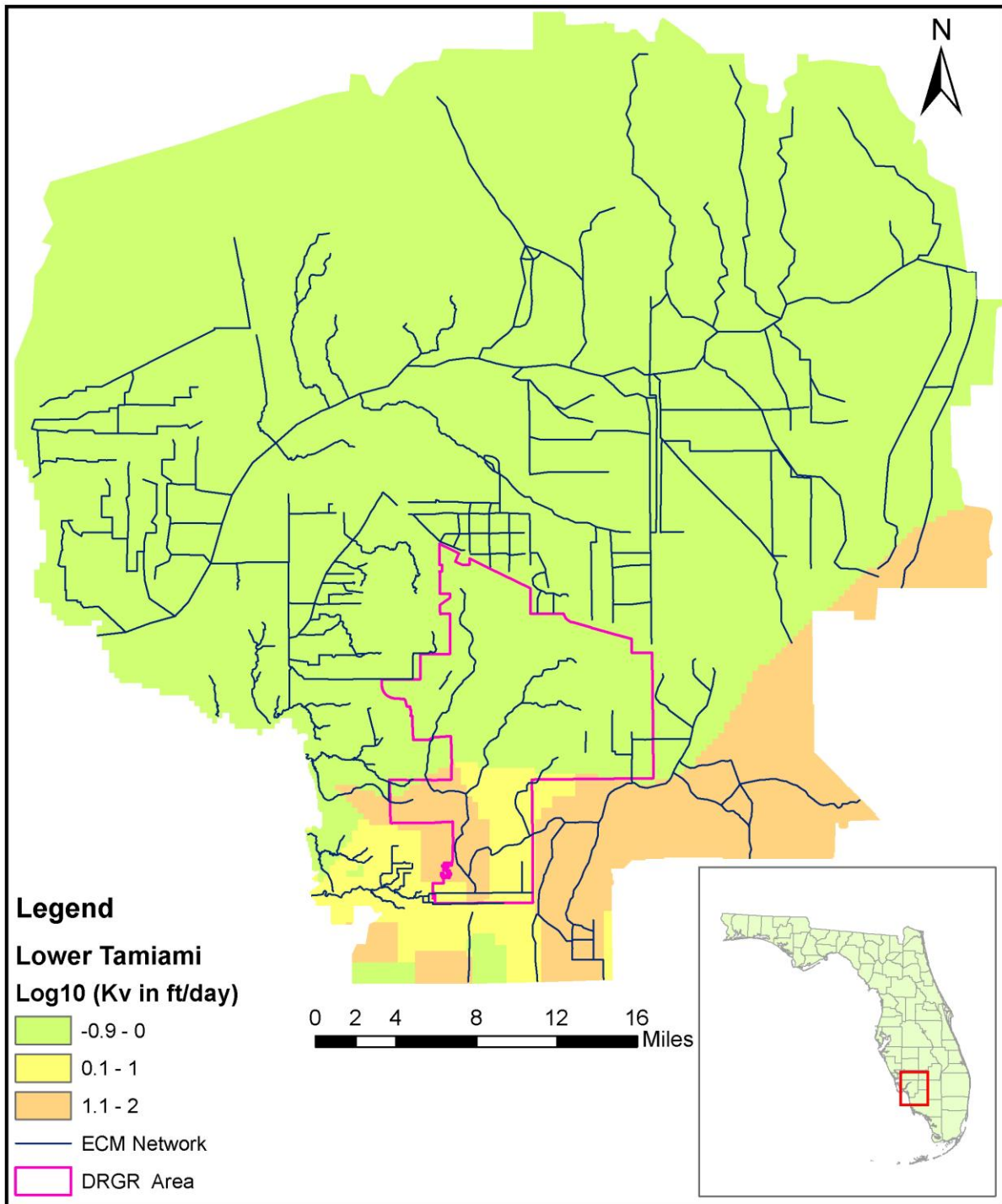


Figure A5. Vertical conductivity map for the Lower Tamiami geological layer.

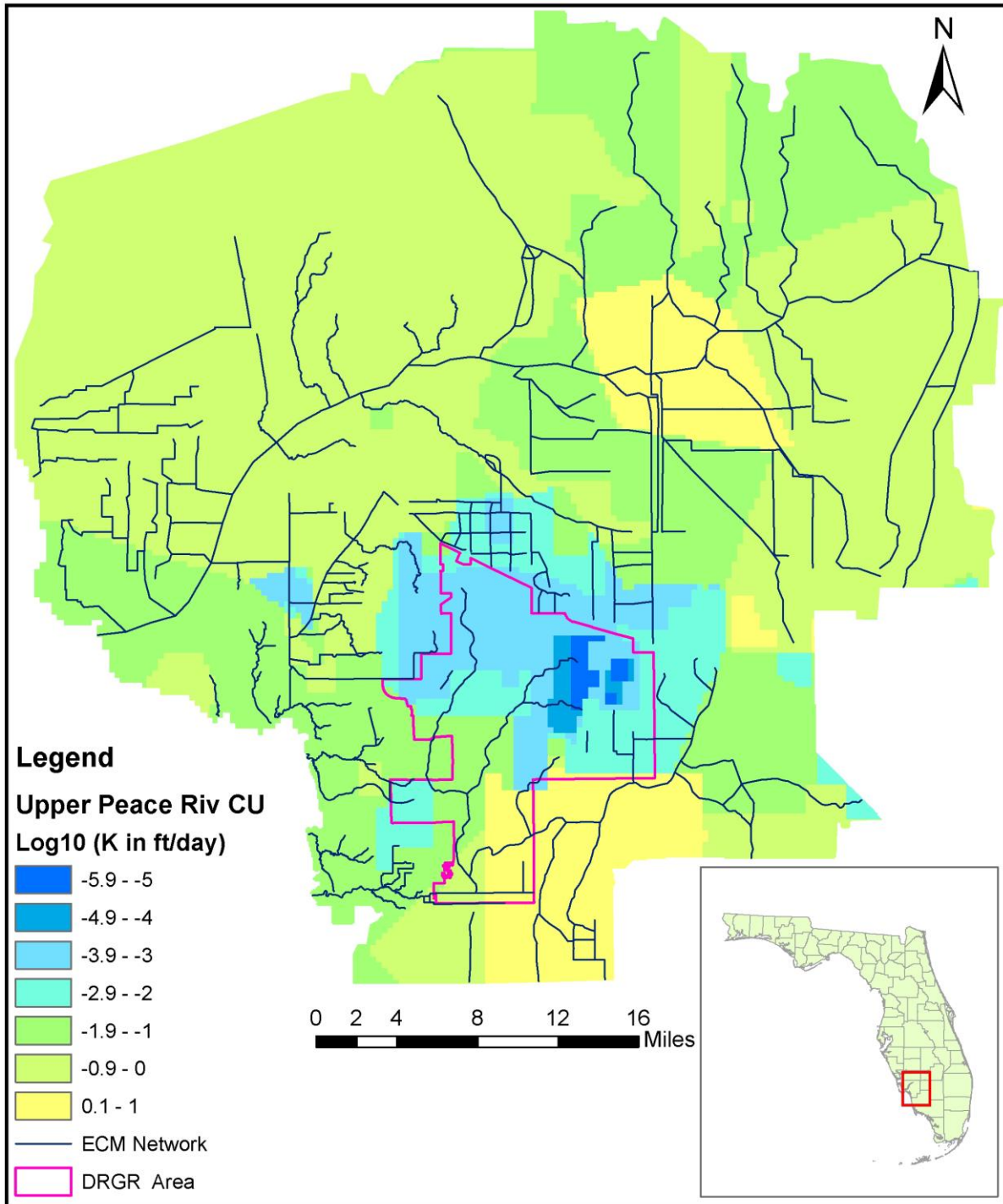


Figure A6. Conductivity map (horizontal and vertical) for the Upper Peace River Confining Units geological lens.

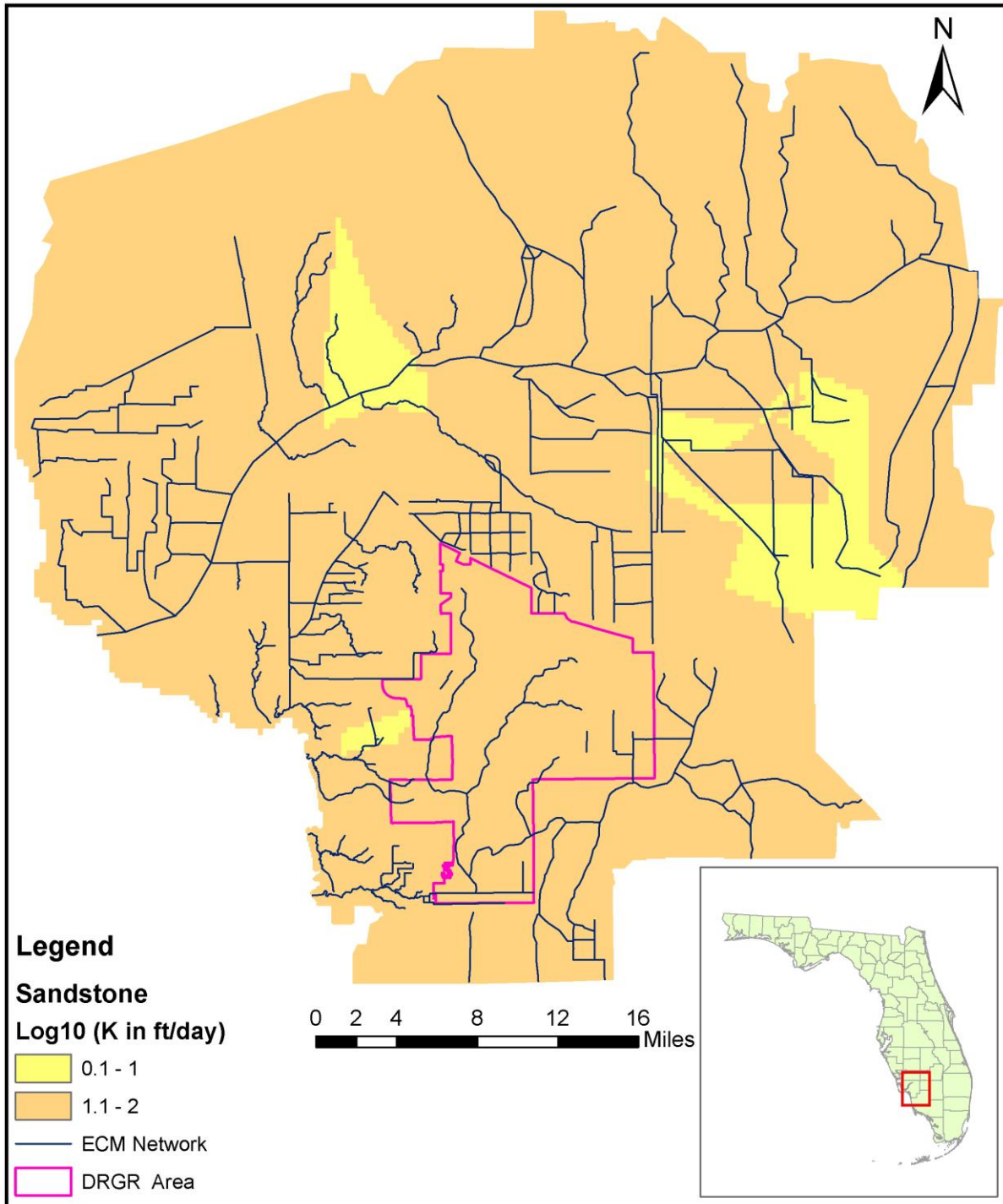


Figure A7. Conductivity map (horizontal and vertical) for the Upper Peace River Sandstone geological layer.



## APPENDIX B. ECM RESULTS AT OBSERVATION STATIONS

All figures and tables related to the results of the Lee County Existing Condition Model (ECM) at observation station locations are presented in this appendix. The appendix was divided in six sections according to the station type and location, as shown in Table B1.

| Station type                       | Location   |                                       |                                 |
|------------------------------------|------------|---------------------------------------|---------------------------------|
|                                    | DR/GR Area | Other south from Caloosahatchee river | North from Caloosahatchee river |
| Surface water                      | B2         |                                       | B5                              |
| Groundwater wells (layers 1 and 2) | B1         | B4                                    | B6                              |
| Ground water wells (layer 3)       | B3         |                                       |                                 |

Table B1. Station type and location covered in each section of the appendix.

After calibration, the model showed the most improvement for the shallow observation wells in the DR/GR Area (Table B2). At the end, 45 of 56 stations fell within the high quality performance range and the other 11 stations in the mid-level range. For surface water stations (Table B3) and other wells (Table B4 and B5) south from the Caloosahatchee River, the model performance was improved in a few stations. In particular, the performance at deep wells in the DR/GR Area is still low in most of the cases. Almost no attention was dedicated to improving the model performance at stations located north of Caloosahatchee River (Table B6 and B7).

### List of sections

|   |    |
|---|----|
| Appendix B1. Shallow groundwater wells in DR/GR Area .....                    | 7  |
| Appendix B2. Surface water stations south from Caloosahatchee .....           | 39 |
| Appendix B3. Groundwater deep wells south from Caloosahatchee .....           | 55 |
| Appendix B4. Other groundwater well stations south of the Caloosahatchee..... | 59 |
| Appendix B5. Surface water stations north from Caloosahatchee .....           | 88 |
| Appendix B6. Groundwater well stations north from Caloosahatchee .....        | 97 |

### List of symbols

GSE: ground surface elevation (topography) in model grid cell;  
 MAE: mean absolute error;  
 ME: mean error;  
 PL: average performance level, which is a number in the range from 1.0 (high) to 3.0 (low);  
 R: Correlation coefficient;  
 RMSE: root mean square error.



## **List of Tables**

|  |    |
|--|----|
| Table B1. Station type and location covered in each section of the appendix. ....  | 1  |
| Table B2. Statistical parameters and level of performance at groundwater shallow monitoring wells (in computational layers 1 and 2) in the DR/GR Area. The green color is used for the highest performance level (1.0, 1.2 and 1.5), yellow for medium (1.8, 2.0, 2.3, 2.5) and orange for low (2.8, 3.0).....                             | 8  |
| Table B3. Statistical parameters and level of performance at surface water stations south of the Caloosahatchee River. The green color indicates the highest performance level (1.0, 1.2 and 1.5), yellow for medium (1.8, 2.0, 2.3, 2.5) and orange for low (2.8, 3.0).....   | 39 |
| Table B4. Statistical parameters and level of performance at deep groundwater monitoring wells (computational layer 3) south of the Caloosahatchee River. The green color indicates the highest performance level (1.0, 1.2 and 1.5), yellow for medium (1.8, 2.0, 2.3, 2.5) and orange for low (2.8, 3.0).....                            | 55 |
| Table B5. Statistical parameters and level of performance at shallow groundwater wells (computational layers 1 and 2) south of the Caloosahatchee River and outside the DR/GR Area. The green color indicates the highest performance level (1.0, 1.2 and 1.5), yellow for medium (1.8, 2.0, 2.3, 2.5) and orange for low (2.8, 3.0). .... | 60 |
| Table B6. Statistical parameters and level of performance at surface water stations north of the Caloosahatchee River. The green color indicates the highest performance level (1.0, 1.2 and 1.5), yellow for medium (1.8, 2.0, 2.3, 2.5) and orange for low (2.8, 3.0).....   | 88 |
| Table B7. Statistical parameters and level of performance at groundwater monitoring wells north of the Caloosahatchee River. The green color indicates the highest performance level (1.0, 1.2 and 1.5), yellow for medium (1.8, 2.0, 2.3, 2.5) and orange for low (2.8, 3.0).....   | 97 |



**List of Figures**

Figure B1. Average performance level at shallow groundwater monitoring wells in the DR/GR Area, before the refinement process..... 9

Figure B2. Average performance level at shallow groundwater monitoring wells in the DR/GR Area, after the refinement process..... 10

Figure B3. Groundwater elevation at wells 40-GW3 and 46A-GW18, after refinement..... 11

Figure B4. Groundwater elevation at wells 49-GW3 and 49-GW6, after refinement..... 12

Figure B5. Groundwater elevation at wells 49-GW7 and 49-GW8, after refinement..... 13

Figure B6. Groundwater elevation at wells 49-GW9 and 49-GW10, after refinement..... 14

Figure B7. Groundwater elevation at wells 49-GW11 and BRM-Lake, after refinement. .... 15

Figure B8. Groundwater elevation at wells BRM-MW1 and BRM-MW2, after refinement. . 16

Figure B9. Groundwater elevation at wells BRM-MW3 and BRM-MW4, after refinement. . 17

Figure B10. Groundwater elevation at wells Corkscrew Swamp and FP2\_GW1, after refinement..... 18

Figure B11. Groundwater elevation at wells FP3\_GW1 and FP4\_GW1, after refinement. .... 19

Figure B12. Groundwater elevation at wells FP5\_GW1 and FP6\_GW1, after refinement. .... 20

Figure B13. Groundwater elevation at wells FP7\_GW1 and FP8\_GW1, after refinement. .... 21

Figure B14. Groundwater elevation at wells FP9\_G and FP10\_G, after refinement. .... 22

Figure B15. Groundwater elevation at wells L-1138 and L-1985, after refinement. .... 23

Figure B16. Groundwater elevation at wells L-2204 and L-5667, after refinement. .... 24

Figure B17. Groundwater elevation at wells L-730 and L-739, after refinement. .... 25

Figure B18. Groundwater elevation at wells MPW02 and MPW03, after refinement. .... 26

Figure B19. Groundwater elevation at wells MPW04 and MPW05, after refinement. .... 27

Figure B20. Groundwater elevation at wells MPW08 and MPW25, after refinement. .... 28

Figure B21. Groundwater elevation at wells MPW27 and MPW28, after refinement. .... 29

Figure B22. Groundwater elevation at wells MPW29 and MPW30, after refinement. .... 30

Figure B23. Groundwater elevation at wells MPW31 and MPW33, after refinement. .... 31

Figure B24. Groundwater elevation at wells MPW34 and MPW35, after refinement. .... 32

Figure B25. Groundwater elevation at wells MPW36 and MPW39, after refinement. .... 33

Figure B26. Groundwater elevation at wells ST1\_G and ST2\_G, after refinement. .... 34

Figure B27. Groundwater elevation at wells ST3\_G and WF1\_G, after refinement. .... 35

Figure B28. Groundwater elevation at wells WF2\_G and WF3\_G, after refinement..... 36

Figure B29. Groundwater elevation at wells WF4\_G and WF5\_G, after refinement..... 37

Figure B30. Groundwater elevation at wells WF6\_G and WF7\_G, after refinement..... 38

Figure B31. Average performance level at surface water monitoring stations south of Caloosahatchee River, after the refinement process..... 40

Figure B32. Stage at stations 10 Mi Canal 8490 and 6 Mi Cypress 1128, after refinement. ... 41



Figure B33. Stage at stations 6 Mi Cypress 3600 and 6 Mi Cypress 7755, after refinement... 42

Figure B34. Stage at stations 6 Mi Cypress 10535 and 6 Mi Cypress 10565, after refinement.  
..... 43

Figure B35. Stage at stations 6 Mi Cypress 14150 and Hendry Creek 768, after refinement.. 44

Figure B36. Stage at stations CorkScrewCan 1174 and CorkTribCan 0, after refinement..... 45

Figure B37. Stage at stations KehlCan 9358 and KehlCan 9479, after refinement. .... 46

Figure B38. Stage at stations Mullock Creek\_2702 and OR Buckingham, after refinement... 47

Figure B39. Stage at station OR Harns Marsh HW and flow at OR Harns Marsh Q, after  
refinement..... 48

Figure B40. Stage at stations S-A-1-HW and S-A-2-HW, after refinement. .... 49

Figure B41. Stage at stations S-HC-1\_HW and S-HC-2\_HW, after refinement. .... 50

Figure B42. Stage at stations S-NM-2\_HW and S-NM-2\_TW, after refinement. .... 51

Figure B43. Flow at stations S-NM-2 Q and S-SF-1 Q, after refinement..... 52

Figure B44. Stage at stations S-SF-1\_HW and S-SF-1\_TW, after refinement. .... 53

Figure B45. Stage at station S-YT-2\_HW, after refinement. .... 54

Figure B46. Average performance level at deep groundwater monitoring wells south of the  
Caloosahatchee River, after the refinement process..... 55

Figure B47. Groundwater elevation at wells L-2192 and L-5649, after refinement. .... 56

Figure B48. Groundwater elevation at wells L-5664 and L-5669R, after refinement..... 57

Figure B49. Groundwater elevation at wells L-5673 and L-5874, after refinement. .... 58

Figure B50. Average performance level at shallow groundwater monitoring wells south of the  
Caloosahatchee River, after the refinement process..... 61

Figure B51. Groundwater elevation at wells 40-GW1 and 40-GW2, after refinement..... 62

Figure B52. Groundwater elevation at wells 40-GW4 and 40-GW5, after refinement..... 63

Figure B53. Groundwater elevation at wells 40-GW6 and 40-GW7, after refinement..... 64

Figure B54. Groundwater elevation at wells 40-GW8 and 40-GW9, after refinement..... 65

Figure B55. Groundwater elevation at wells 40-GW11 and 40-GW12, after refinement..... 66

Figure B56. Groundwater elevation at wells 40-GW13 and 41-GW1, after refinement..... 67

Figure B57. Groundwater elevation at wells 41-GW3 and 41-GW4, after refinement..... 68

Figure B58. Groundwater elevation at wells 41-GW6 and 42-GW1, after refinement..... 69

Figure B59. Groundwater elevation at wells 42-GW2 and 42-GW3, after refinement..... 70

Figure B60. Groundwater elevation at wells 44-GW2 and 44-GW3, after refinement..... 71

Figure B61. Groundwater elevation at wells 45-GW1 and 45-GW2, after refinement..... 72

Figure B62. Groundwater elevation at wells 45-GW3 and 45-GW4, after refinement..... 73

Figure B63. Groundwater elevation at wells 46A-GW3 and 46A-GW4, after refinement..... 74

Figure B64. Groundwater elevation at wells 46A-GW10 and 46A-GW11, after refinement.. 75

Figure B65. Groundwater elevation at wells 46A-GW12 and 46A-GW13, after refinement.. 76



Figure B66. Groundwater elevation at wells 46A-GW14 and 46A-GW15, after refinement.. 77

Figure B67. Groundwater elevation at wells 46A-GW21 and 46A-GW22, after refinement.. 78

Figure B68. Groundwater elevation at wells 46A-GW25 and 46A-GW26, after refinement.. 79

Figure B69. Groundwater elevation at wells 46C-GW1 and 46C-GW2, after refinement. .... 80

Figure B70. Groundwater elevation at wells 46C-GW3 and 46C-GW6, after refinement. .... 81

Figure B71. Groundwater elevation at wells 46C-GW7 and 46C-GW8, after refinement. .... 82

Figure B72. Groundwater elevation at wells 49-GW12 and 49-GW14, after refinement..... 83

Figure B73. Groundwater elevation at wells 49-GW15 and 49L-GW1, after refinement. .... 84

Figure B74. Groundwater elevation at wells HF1\_G and HF2\_G, after refinement..... 85

Figure B75. Groundwater elevation at wells HF3\_G and HF4\_G, after refinement..... 86

Figure B76. Groundwater elevation at well HF7\_G, after refinement. .... 87

Figure B77. Average performance level at surface water monitoring stations north of the Caloosahatchee River, after the refinement process..... 89

Figure B78. Stage at stations Caloosahatchee\_53534 and Gator Slough\_5850, after refinement..... 90

Figure B79. Flow at stations Courtney Q\_7500 and Gator Slough Q\_5910, after refinement. 91

Figure B80. Flow at stations at Hermosa Q\_12500 and Horseshoe Q\_13230, after refinement. .... 92

Figure B81. Flow at station and Meade Q\_2470 and stage at Powell Creek\_4976, after refinement..... 93

Figure B82. Stage at stations S-78 TW and Telegraph Creek\_24691, after refinement. .... 94

Figure B83. Stage at stations S-79 HW and S-79 TW, after refinement..... 95

Figure B84. Flow at stations S-79 Q and San Carlos Q\_4510, after refinement. .... 96

Figure B85. Average performance level at groundwater monitoring wells north of Caloosahatchee River, after the refinement process..... 98

Figure B86. Groundwater elevation at wells 17-GW1 and 17-GW3, after refinement..... 99

Figure B87. Groundwater elevation at wells 17-GW4 and 18-GW1, after refinement..... 100

Figure B88. Groundwater elevation at wells 18-GW2 and 19-GW1, after refinement..... 101

Figure B89. Groundwater elevation at wells 20A-GW1 and 20-GW1, after refinement..... 102

Figure B90. Groundwater elevation at wells 20-GW2 and 20-GW3, after refinement..... 103

Figure B91. Groundwater elevation at wells 21-GW2 and 22-GW1, after refinement..... 104

Figure B92. Groundwater elevation at wells 23-GW1 and 23-GW2, after refinement..... 105

Figure B93. Groundwater elevation at wells 24-GW1 and 24-GW2, after refinement..... 106

Figure B94. Groundwater elevation at wells 26-GW1 and 26-GW2, after refinement..... 107

Figure B95. Groundwater elevation at wells 27O-GW1 and 27-GW1, after refinement..... 108

Figure B96. Groundwater elevation at wells 27-GW2 and 28-GW1, after refinement..... 109

Figure B97. Groundwater elevation at wells 28-GW2 and 29-GW1, after refinement..... 110



Figure B98. Groundwater elevation at wells 29-GW2 and 5-GW4, after refinement..... 111  
Figure B99. Groundwater elevation at wells 5-GW5 and 5-GW6, after refinement..... 112  
Figure B100. Groundwater elevation at wells 5-GW8 and MUSEWELLS, after refinement.  
..... 113



**Appendix B1. Shallow groundwater wells in DR/GR Area**

| Station Name    | Comp. layer | before refinement |          |           |      |            | after refinement |          |           |      |            |
|-----------------|-------------|-------------------|----------|-----------|------|------------|------------------|----------|-----------|------|------------|
|                 |             | ME (ft)           | MAE (ft) | RMSE (ft) | R    | PL         | ME (ft)          | MAE (ft) | RMSE (ft) | R    | PL         |
| 40-GW3          | 1           | -2.08             | 2.10     | 2.36      | 0.72 | <b>2.3</b> | -0.88            | 1.01     | 1.15      | 0.83 | <b>1.3</b> |
| 46A-GW18        | 1           | -2.63             | 2.63     | 2.88      | 0.39 | <b>3.0</b> | -1.12            | 1.23     | 1.43      | 0.79 | <b>1.8</b> |
| 49-GW3          | 1           | -0.42             | 0.63     | 0.83      | 0.43 | <b>1.5</b> | 0.16             | 1.01     | 1.28      | 0.42 | <b>2.0</b> |
| 49-GW6          | 1           | 0.65              | 0.96     | 1.28      | 0.74 | <b>1.3</b> | 0.43             | 1.12     | 1.38      | 0.75 | <b>1.5</b> |
| 49-GW7          | 1           | -0.91             | 1.59     | 1.84      | 0.40 | <b>2.0</b> | 0.42             | 0.91     | 1.34      | 0.56 | <b>1.5</b> |
| 49-GW8          | 1           | 1.82              | 1.82     | 2.19      | 0.18 | <b>2.3</b> | 1.94             | 1.94     | 2.33      | 0.23 | <b>2.3</b> |
| 49-GW9          | 1           | 1.52              | 1.58     | 1.81      | 0.78 | <b>1.8</b> | 1.51             | 1.53     | 1.80      | 0.81 | <b>1.8</b> |
| 49-GW10         | 1           | -0.20             | 0.93     | 1.08      | 0.84 | <b>1.0</b> | -0.14            | 0.83     | 0.98      | 0.85 | <b>1.0</b> |
| 49-GW11         | 1           | 0.48              | 0.95     | 1.26      | 0.88 | <b>1.3</b> | 0.33             | 0.83     | 1.16      | 0.89 | <b>1.0</b> |
| BRM-Lake        | 1           | ---               | ---      | ---       | ---  | ---        | -0.02            | 0.42     | 0.53      | 0.94 | <b>1.0</b> |
| BRM-MW1         | 1           | ---               | ---      | ---       | ---  | ---        | 0.31             | 0.60     | 0.72      | 0.77 | <b>1.0</b> |
| BRM-MW2         | 1           | ---               | ---      | ---       | ---  | ---        | -0.01            | 0.35     | 0.44      | 0.93 | <b>1.0</b> |
| BRM-MW3         | 1           | ---               | ---      | ---       | ---  | ---        | 0.57             | 0.60     | 0.77      | 0.90 | <b>1.0</b> |
| BRM-MW4         | 1           | ---               | ---      | ---       | ---  | ---        | 0.48             | 0.54     | 0.73      | 0.84 | <b>1.0</b> |
| Corkscrew Swamp | 1           | -0.99             | 1.15     | 1.23      | 0.87 | <b>1.3</b> | -0.61            | 1.01     | 1.06      | 0.87 | <b>1.3</b> |
| FP2_GW1         | 1           | -2.82             | 2.82     | 3.09      | 0.81 | <b>2.5</b> | 0.35             | 1.15     | 1.55      | 0.78 | <b>1.5</b> |
| FP3_GW1         | 1           | -0.05             | 0.40     | 0.53      | 0.93 | <b>1.0</b> | 0.31             | 0.65     | 0.80      | 0.83 | <b>1.0</b> |
| FP4_GW1         | 1           | -0.58             | 0.70     | 0.84      | 0.90 | <b>1.0</b> | -0.09            | 0.53     | 0.65      | 0.89 | <b>1.0</b> |
| FP5_GW1         | 1           | -0.68             | 0.80     | 0.97      | 0.89 | <b>1.0</b> | -0.21            | 0.57     | 0.74      | 0.88 | <b>1.0</b> |
| FP6_GW1         | 1           | -0.61             | 0.83     | 1.00      | 0.88 | <b>1.0</b> | -0.27            | 0.77     | 0.97      | 0.86 | <b>1.0</b> |
| FP7_GW1         | 1           | -0.48             | 0.78     | 0.93      | 0.89 | <b>1.0</b> | -0.22            | 0.83     | 1.03      | 0.86 | <b>1.0</b> |
| FP8_GW1         | 1           | -0.40             | 0.71     | 0.87      | 0.89 | <b>1.0</b> | -0.07            | 0.70     | 0.84      | 0.87 | <b>1.0</b> |
| FP9_G           | 1           | -0.49             | 0.78     | 0.94      | 0.88 | <b>1.0</b> | -0.19            | 0.82     | 1.01      | 0.85 | <b>1.0</b> |
| FP10_G          | 1           | -0.69             | 0.82     | 1.01      | 0.87 | <b>1.0</b> | -0.21            | 0.57     | 0.77      | 0.87 | <b>1.0</b> |
| L-1138          | 1           | 0.50              | 0.57     | 0.68      | 0.84 | <b>1.0</b> | -0.56            | 0.92     | 1.10      | 0.80 | <b>1.0</b> |
| L-1985          | 2           | -2.96             | 3.29     | 3.90      | 0.66 | <b>2.8</b> | -0.59            | 2.12     | 2.49      | 0.72 | <b>1.8</b> |
| L-2204          | 2           | -1.05             | 1.06     | 1.21      | 0.84 | <b>1.5</b> | -0.46            | 0.56     | 0.73      | 0.86 | <b>1.0</b> |
| L-5667          | 1           | 0.77              | 0.95     | 1.05      | 0.93 | <b>1.0</b> | 1.26             | 1.44     | 1.56      | 0.92 | <b>1.8</b> |
| L-730           | 2           | 1.45              | 1.45     | 1.53      | 0.85 | <b>1.8</b> | 0.37             | 0.56     | 0.78      | 0.77 | <b>1.0</b> |
| L-739           | 2           | 0.88              | 0.89     | 1.05      | 0.89 | <b>1.0</b> | 0.57             | 0.60     | 0.74      | 0.96 | <b>1.0</b> |
| MPW02           | 1           | ---               | ---      | ---       | ---  | ---        | -0.62            | 0.62     | 0.71      | 0.98 | <b>1.0</b> |
| MPW03           | 1           | ---               | ---      | ---       | ---  | ---        | -0.96            | 0.96     | 0.97      | 0.98 | <b>1.0</b> |
| MPW04           | 1           | ---               | ---      | ---       | ---  | ---        | -0.05            | 0.54     | 0.67      | 0.91 | <b>1.0</b> |
| MPW05           | 1           | ---               | ---      | ---       | ---  | ---        | 0.27             | 0.56     | 0.61      | 0.73 | <b>1.0</b> |
| MPW08           | 1           | ---               | ---      | ---       | ---  | ---        | 0.99             | 0.99     | 1.10      | 0.91 | <b>1.0</b> |
| MPW25           | 1           | ---               | ---      | ---       | ---  | ---        | -0.12            | 0.27     | 0.31      | 0.95 | <b>1.0</b> |
| MPW27           | 1           | ---               | ---      | ---       | ---  | ---        | 0.69             | 0.71     | 1.04      | 0.80 | <b>1.0</b> |
| MPW28           | 1           | ---               | ---      | ---       | ---  | ---        | 1.16             | 1.16     | 1.23      | 0.51 | <b>1.8</b> |
| MPW29           | 1           | ---               | ---      | ---       | ---  | ---        | -0.09            | 0.41     | 0.53      | 0.84 | <b>1.0</b> |
| MPW30           | 1           | ---               | ---      | ---       | ---  | ---        | 0.39             | 0.59     | 0.97      | 0.73 | <b>1.0</b> |



| Station Name | Comp. layer | before refinement |          |           |      |            | after refinement |          |           |      |            |
|--------------|-------------|-------------------|----------|-----------|------|------------|------------------|----------|-----------|------|------------|
|              |             | ME (ft)           | MAE (ft) | RMSE (ft) | R    | PL         | ME (ft)          | MAE (ft) | RMSE (ft) | R    | PL         |
| MPW31        | 1           | ---               | ---      | ---       | ---  | ---        | 0.38             | 0.39     | 0.59      | 0.94 | <b>1.0</b> |
| MPW33        | 1           | ---               | ---      | ---       | ---  | ---        | -0.55            | 1.18     | 1.48      | 0.70 | <b>1.8</b> |
| MPW34        | 1           | ---               | ---      | ---       | ---  | ---        | 0.62             | 0.62     | 0.63      | 0.98 | <b>1.0</b> |
| MPW35        | 1           | ---               | ---      | ---       | ---  | ---        | -1.10            | 1.26     | 1.36      | 0.84 | <b>1.8</b> |
| MPW36        | 1           | ---               | ---      | ---       | ---  | ---        | 0.08             | 0.61     | 0.74      | 0.84 | <b>1.0</b> |
| MPW39        | 1           | ---               | ---      | ---       | ---  | ---        | -1.52            | 2.20     | 2.46      | 0.66 | <b>2.3</b> |
| ST1_G        | 1           | -0.77             | 0.92     | 1.04      | 0.86 | <b>1.0</b> | -0.26            | 0.61     | 0.73      | 0.87 | <b>1.0</b> |
| ST2_G        | 1           | -0.12             | 0.60     | 0.68      | 0.87 | <b>1.0</b> | 0.34             | 0.66     | 0.80      | 0.86 | <b>1.0</b> |
| ST3_G        | 1           | -0.48             | 0.81     | 0.92      | 0.81 | <b>1.0</b> | -0.20            | 0.75     | 0.86      | 0.81 | <b>1.0</b> |
| WF1_G        | 2           | 1.67              | 1.67     | 1.68      | 0.94 | <b>1.8</b> | 0.68             | 0.69     | 0.75      | 0.95 | <b>1.0</b> |
| WF2_G        | 2           | 1.85              | 1.85     | 2.11      | 0.63 | <b>2.0</b> | 1.13             | 1.29     | 1.61      | 0.76 | <b>1.8</b> |
| WF3_G        | 1           | 2.33              | 2.33     | 2.43      | 0.85 | <b>2.3</b> | 1.38             | 1.38     | 1.59      | 0.84 | <b>1.8</b> |
| WF4_G        | 1           | 2.06              | 2.06     | 2.16      | 0.84 | <b>2.3</b> | 0.91             | 1.06     | 1.28      | 0.81 | <b>1.5</b> |
| WF5_G        | 1           | 2.58              | 2.58     | 2.67      | 0.78 | <b>2.5</b> | 0.97             | 1.11     | 1.43      | 0.79 | <b>1.5</b> |
| WF6_G        | 1           | 2.83              | 2.83     | 2.92      | 0.78 | <b>2.5</b> | 0.99             | 1.04     | 1.32      | 0.83 | <b>1.5</b> |
| WF7_G        | 1           | 2.80              | 2.80     | 2.89      | 0.79 | <b>2.5</b> | 1.14             | 1.20     | 1.53      | 0.79 | <b>1.8</b> |

Table B2. Statistical parameters and level of performance at groundwater shallow monitoring wells (in computational layers 1 and 2) in the DR/GR Area. The green color is used for the highest performance level (1.0, 1.2 and 1.5), yellow for medium (1.8, 2.0, 2.3, 2.5) and orange for low (2.8, 3.0).

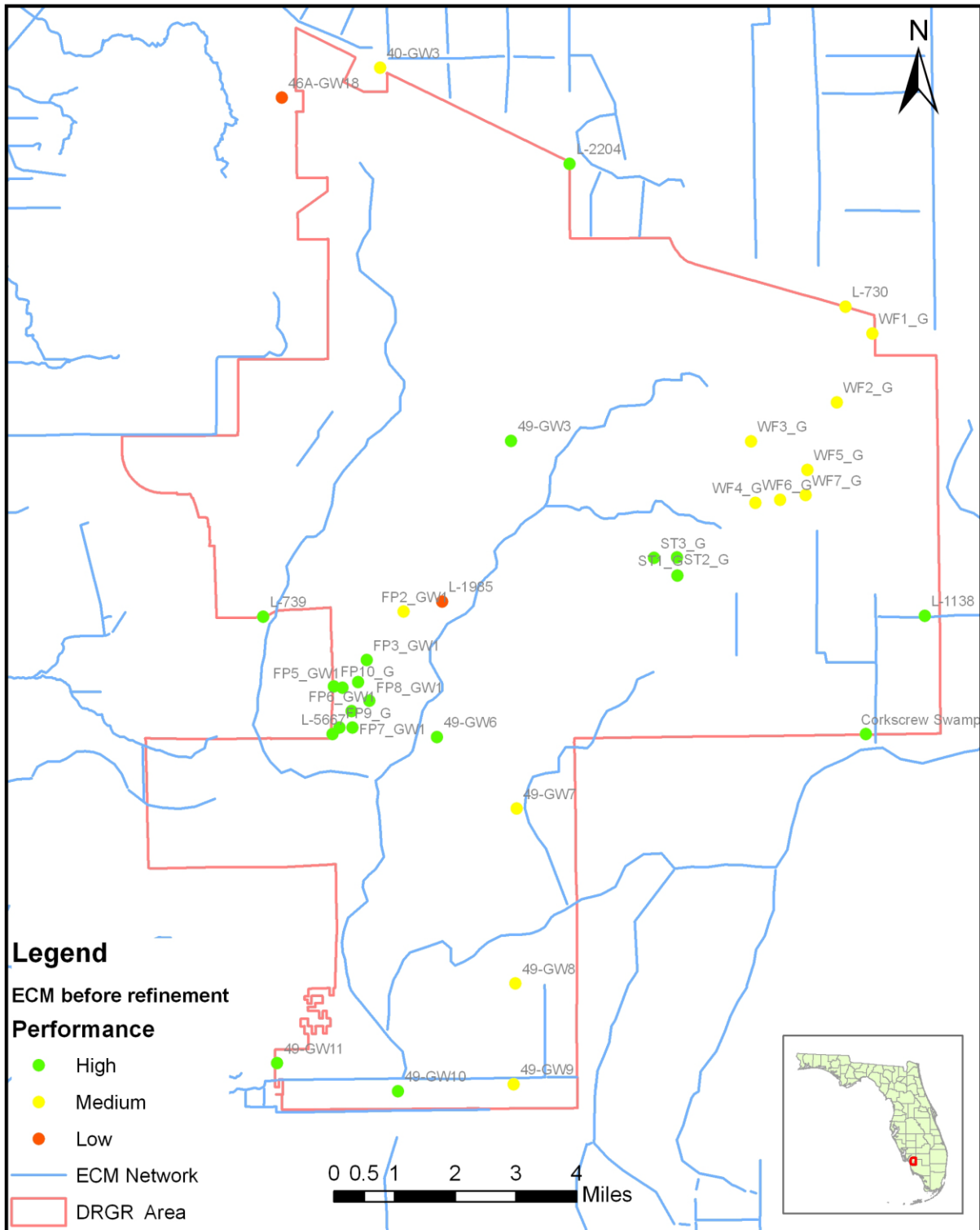


Figure B1. Average performance level at shallow groundwater monitoring wells in the DR/GR Area, before the refinement process.

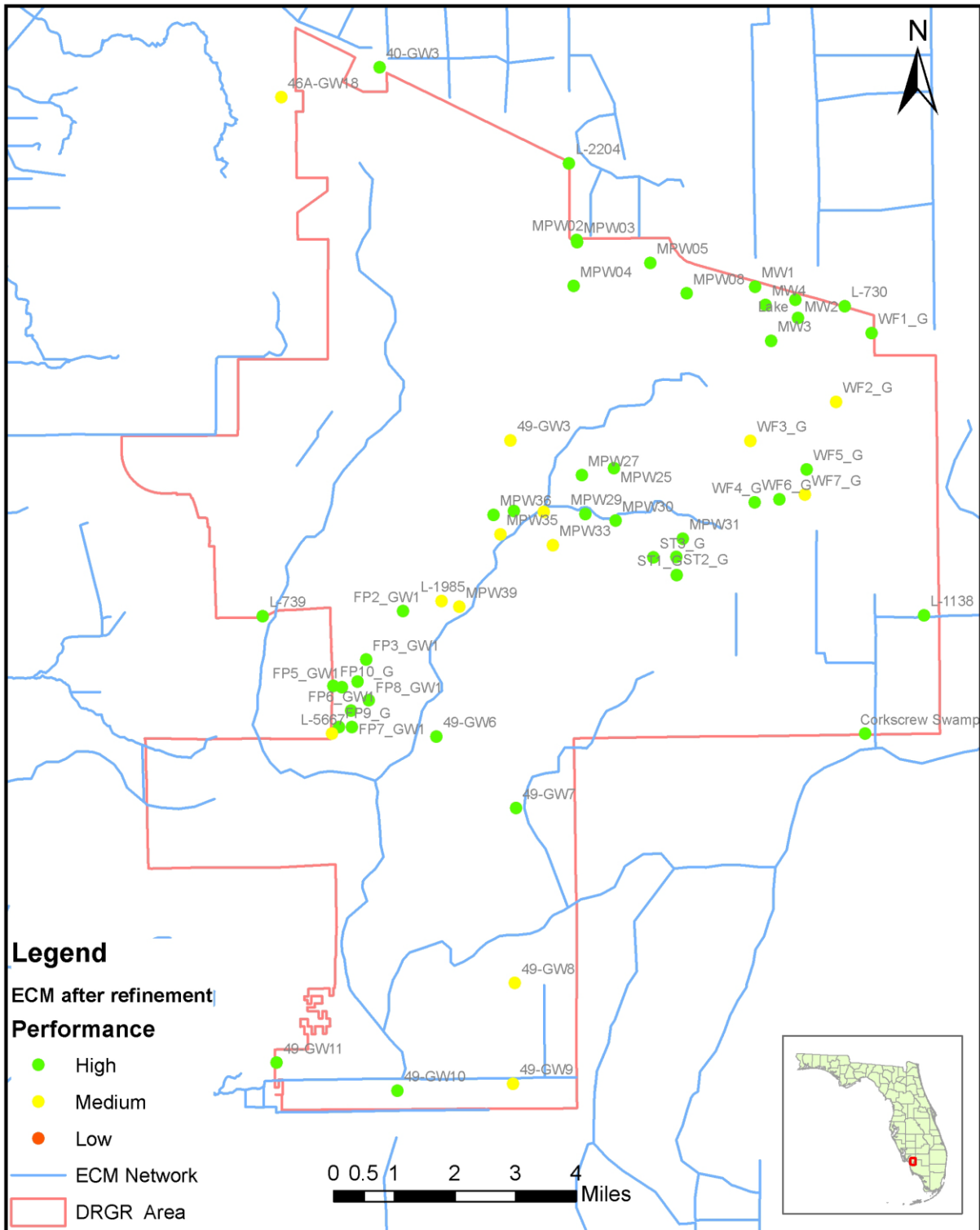
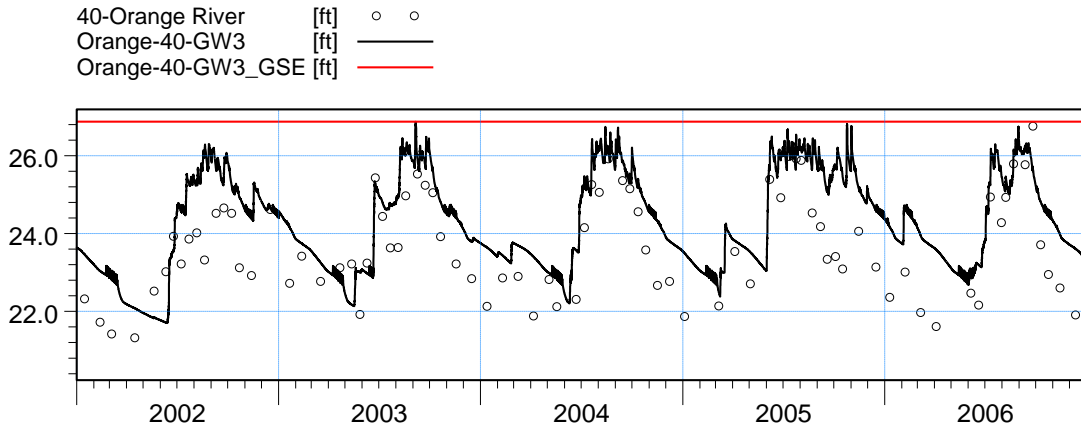
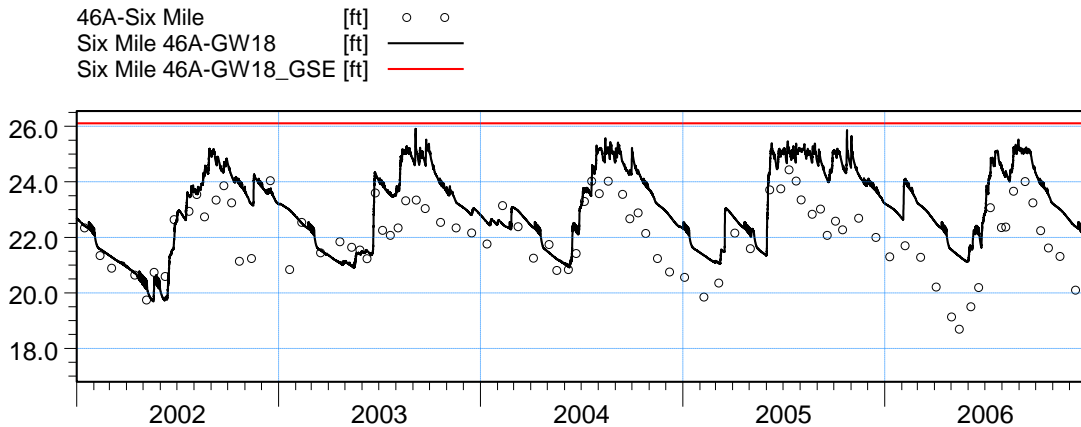


Figure B2. Average performance level at shallow groundwater monitoring wells in the DR/GR Area, after the refinement process.

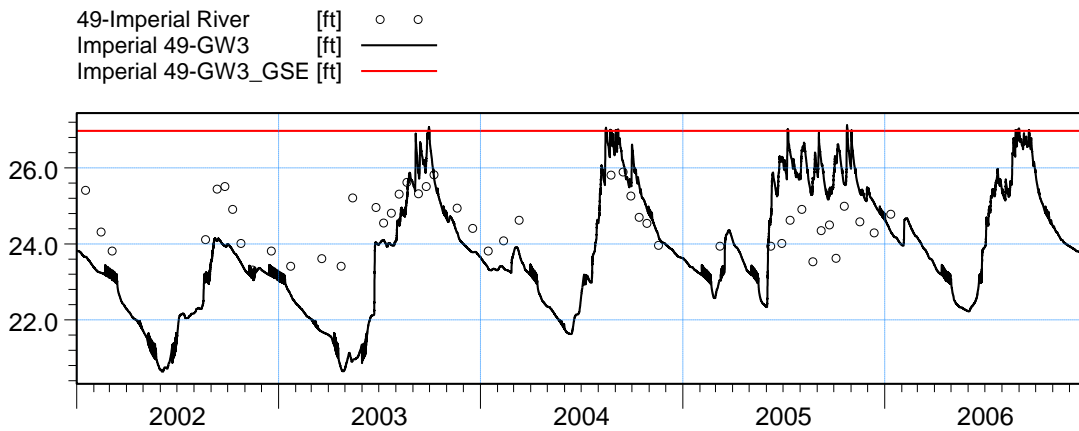


ME=-0.882999  
 MAE=1.00713  
 RMSE=1.15321  
 STDres=0.741757  
 R(Correlation)=0.825504  
 R2(Nash\_Sutcliffe)=0.196999

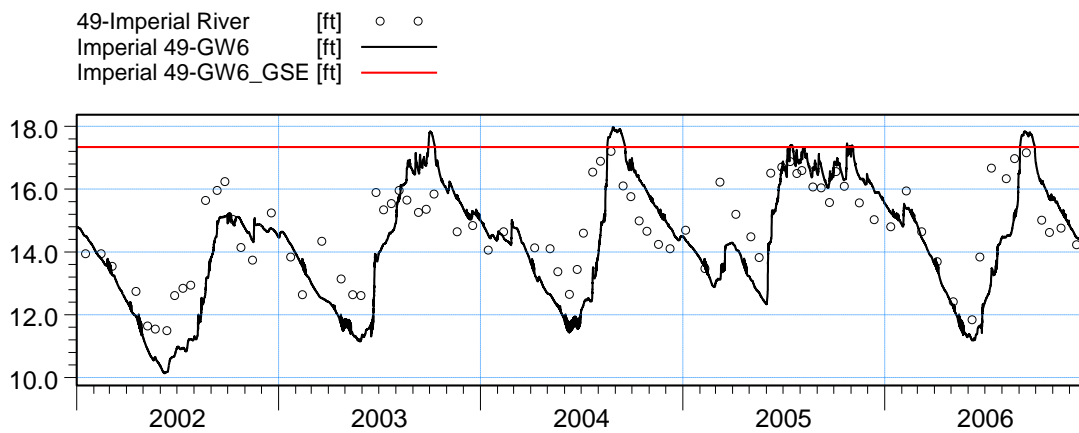


ME=-1.11599  
 MAE=1.22886  
 RMSE=1.42609  
 STDres=0.887872  
 R(Correlation)=0.787101  
 R2(Nash\_Sutcliffe)=-0.266401

Figure B3. Groundwater elevation at wells 40-GW3 and 46A-GW18, after refinement.

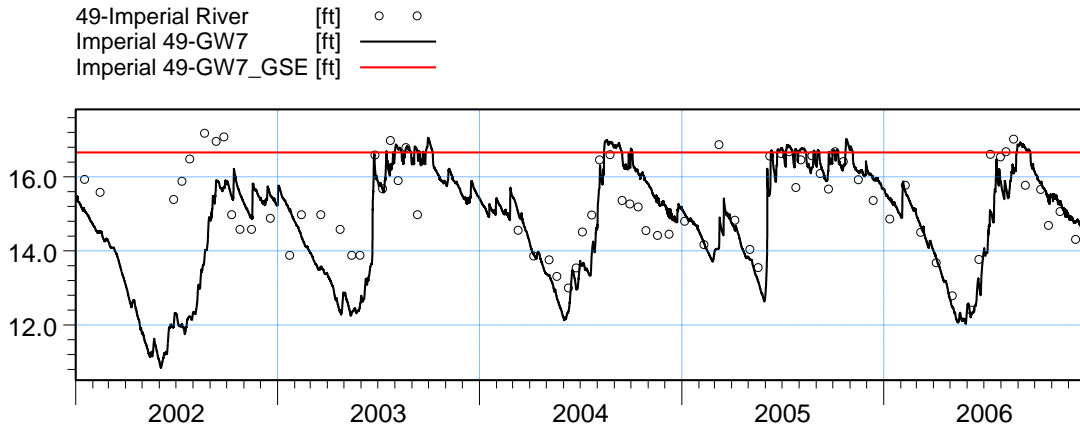


ME=0.156326  
 MAE=1.01293  
 RMSE=1.2819  
 STDres=1.27234  
 R(Correlation)=0.421983  
 R2(Nash\_Sutcliffe)=-2.18317

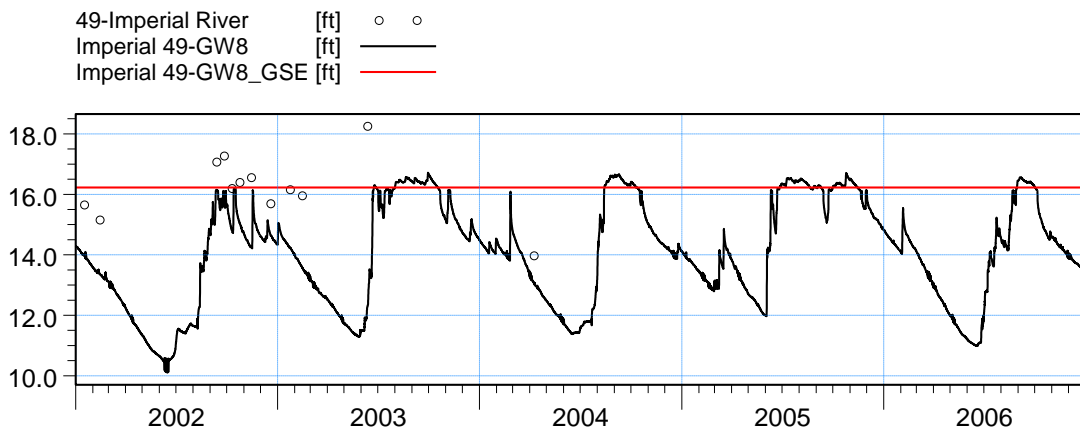


ME=0.432074  
 MAE=1.12157  
 RMSE=1.38237  
 STDres=1.31311  
 R(Correlation)=0.749251  
 R2(Nash\_Sutcliffe)=0.0340635

Figure B4. Groundwater elevation at wells 49-GW3 and 49-GW6, after refinement.

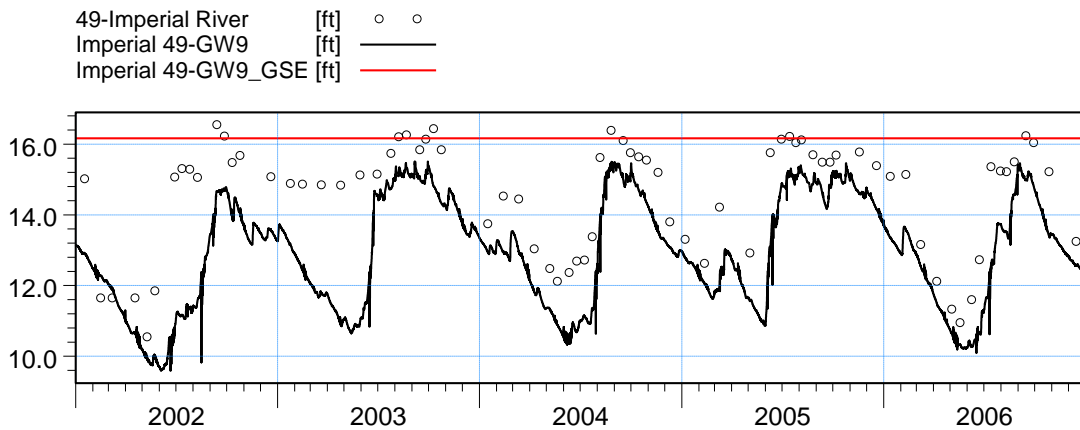


ME=0.415767  
 MAE=0.908725  
 RMSE=1.34047  
 STDres=1.27436  
 R(Correlation)=0.559766  
 R2(Nash\_Sutcliffe)=-0.222682

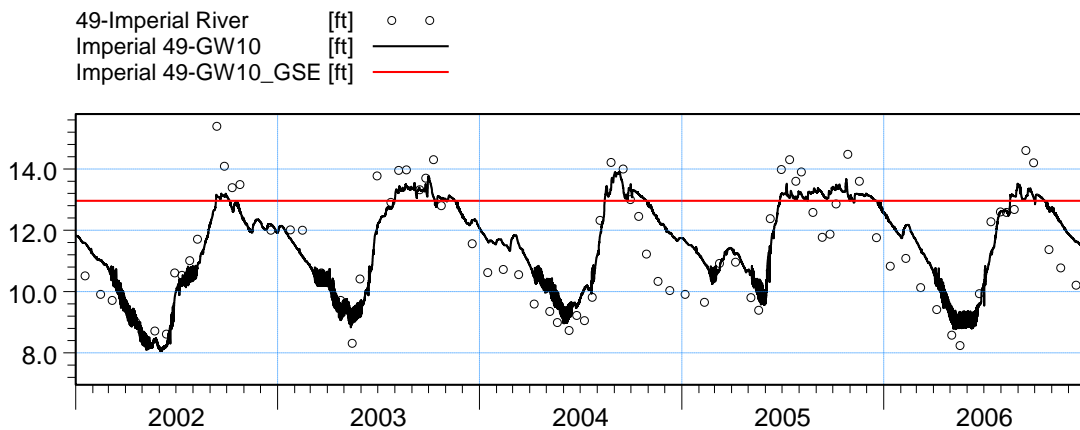


ME=1.94501  
 MAE=1.94501  
 RMSE=2.33323  
 STDres=1.28876  
 R(Correlation)=0.231718  
 R2(Nash\_Sutcliffe)=-4.03885

Figure B5. Groundwater elevation at wells 49-GW7 and 49-GW8, after refinement.

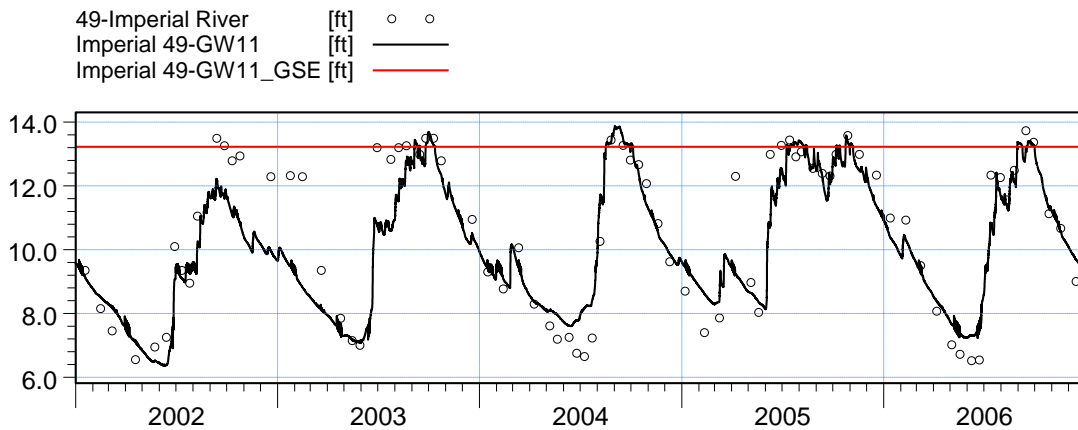


ME=1.51302  
 MAE=1.53448  
 RMSE=1.79901  
 STDres=0.973238  
 R(Correlation)=0.811727  
 R2(Nash\_Sutcliffe)=-0.332736

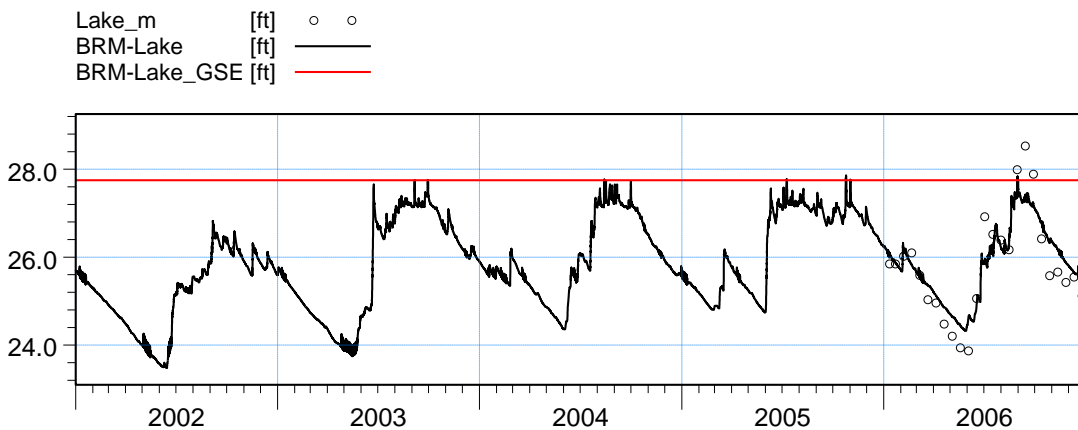


ME=-0.135565  
 MAE=0.832758  
 RMSE=0.982454  
 STDres=0.973056  
 R(Correlation)=0.847408  
 R2(Nash\_Sutcliffe)=0.709231

Figure B6. Groundwater elevation at wells 49-GW9 and 49-GW10, after refinement.

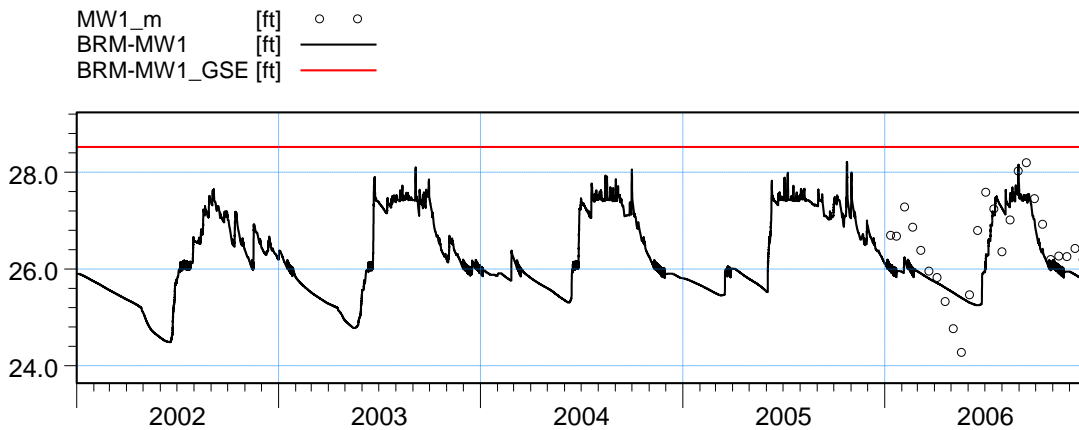


ME=0.326324  
 MAE=0.834825  
 RMSE=1.15569  
 STDres=1.10866  
 R(Correlation)=0.889969  
 R2(Nash\_Sutcliffe)=0.771055

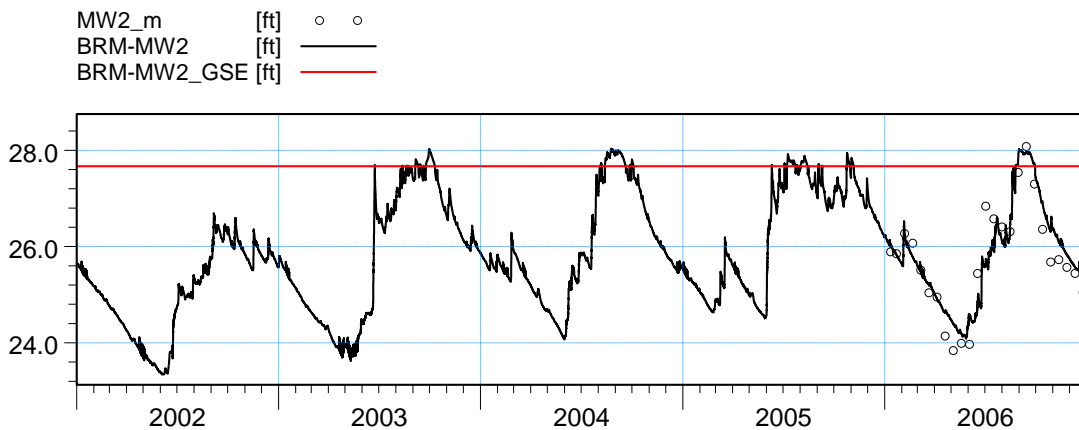


ME=-0.02152  
 MAE=0.415371  
 RMSE=0.533442  
 STDres=0.533008  
 R(Correlation)=0.936396  
 R2(Nash\_Sutcliffe)=0.811934

Figure B7. Groundwater elevation at wells 49-GW11 and BRM-Lake, after refinement.

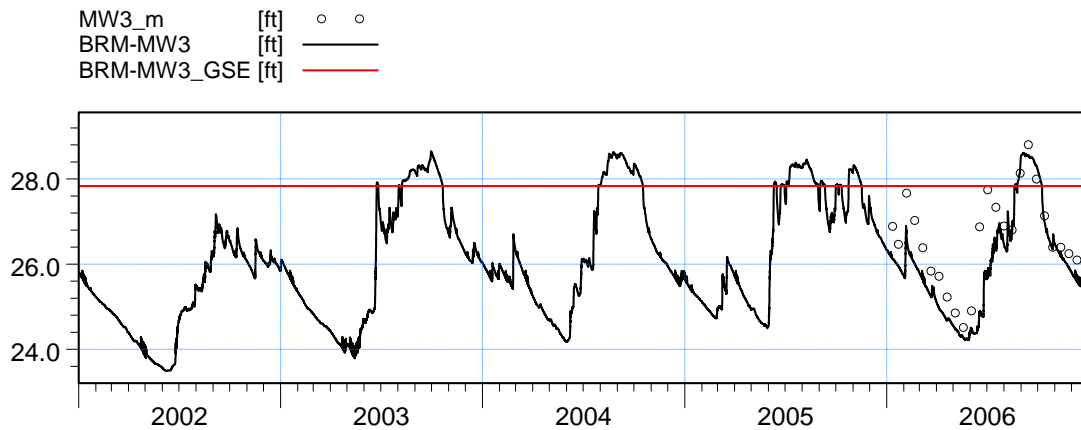


ME=0.314318  
 MAE=0.602899  
 RMSE=0.718454  
 STDres=0.64605  
 R(Correlation)=0.769583  
 R2(Nash\_Sutcliffe)=0.489926

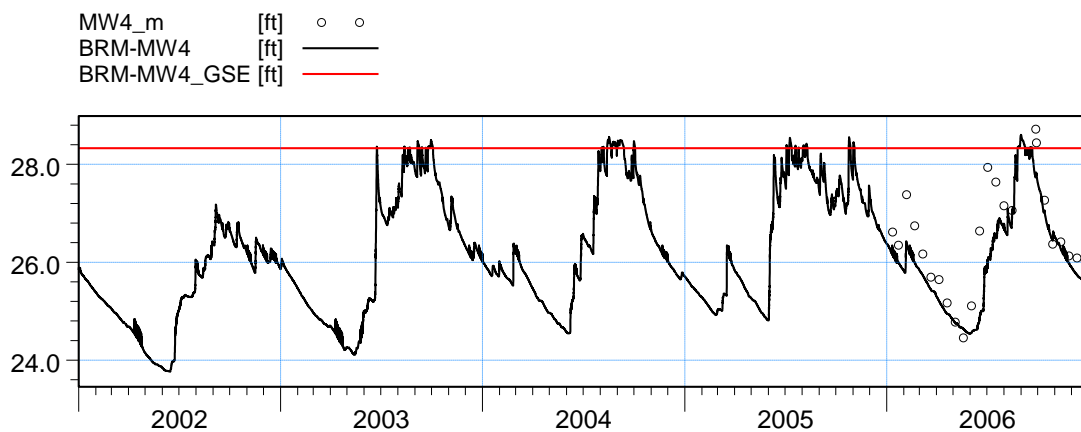


ME=-0.00685231  
 MAE=0.345035  
 RMSE=0.439959  
 STDres=0.439906  
 R(Correlation)=0.926876  
 R2(Nash\_Sutcliffe)=0.85724

Figure B8. Groundwater elevation at wells BRM-MW1 and BRM-MW2, after refinement.

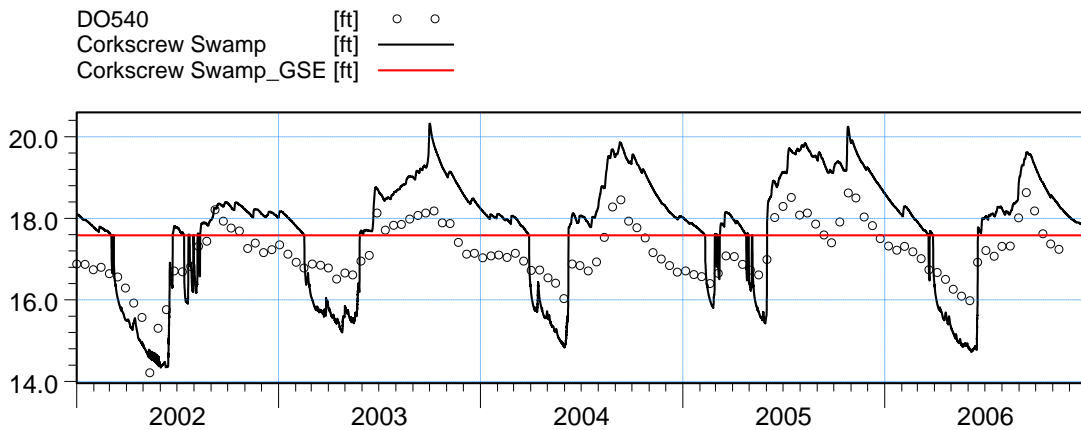


ME=0.574483  
 MAE=0.604515  
 RMSE=0.76845  
 STDres=0.510378  
 R(Correlation)=0.904723  
 R2(Nash\_Sutcliffe)=0.542656

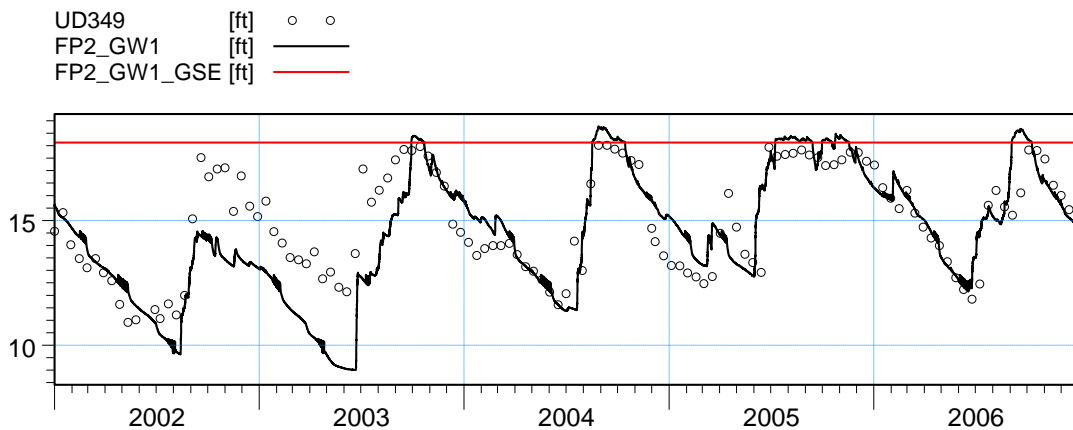


ME=0.484572  
 MAE=0.536979  
 RMSE=0.72577  
 STDres=0.540307  
 R(Correlation)=0.842338  
 R2(Nash\_Sutcliffe)=0.47589

Figure B9. Groundwater elevation at wells BRM-MW3 and BRM-MW4, after refinement.

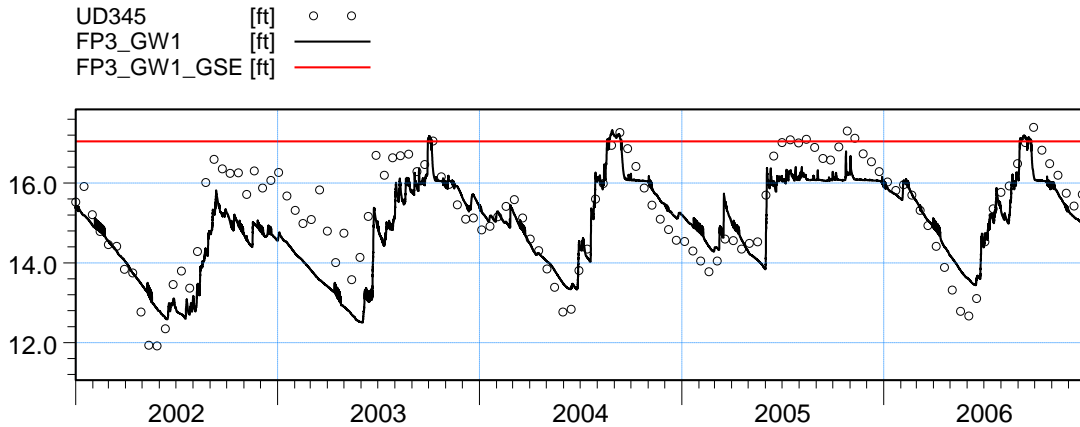


ME=-0.607599  
 MAE=1.00856  
 RMSE=1.06409  
 STDres=0.873567  
 R(Correlation)=0.867188  
 R2(Nash\_Sutcliffe)=-1.26501

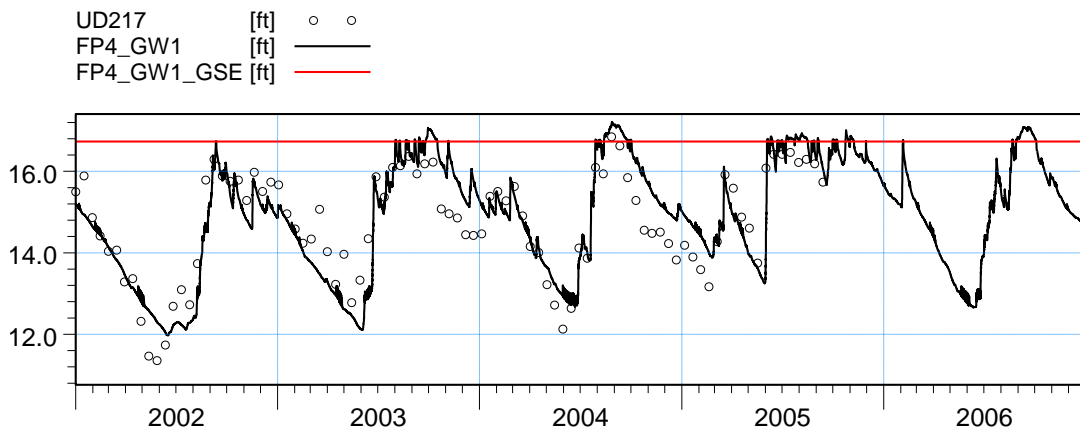


ME=0.350261  
 MAE=1.15321  
 RMSE=1.55363  
 STDres=1.51363  
 R(Correlation)=0.782465  
 R2(Nash\_Sutcliffe)=0.435124

Figure B10. Groundwater elevation at wells Corkscrew Swamp and FP2\_GW1, after refinement.

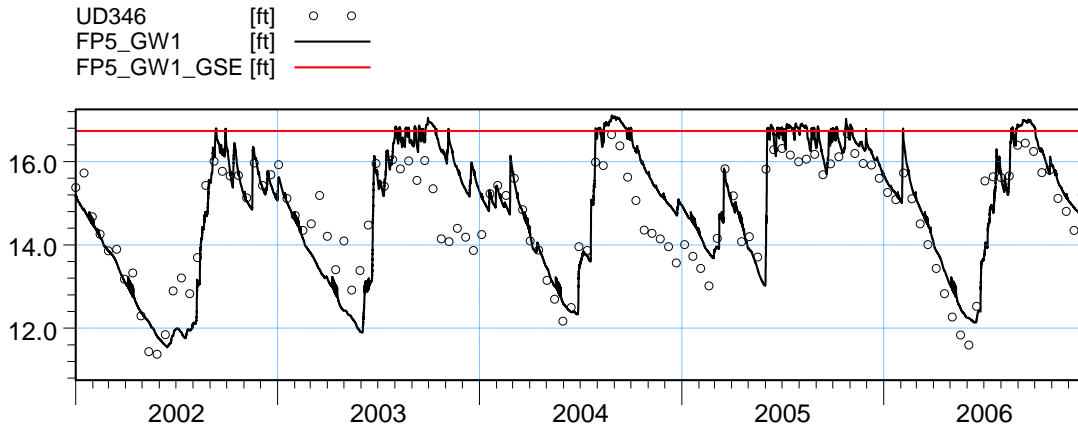


ME=0.314752  
 MAE=0.645675  
 RMSE=0.801417  
 STDres=0.737021  
 R(Correlation)=0.825437  
 R2(Nash\_Sutcliffe)=0.623202

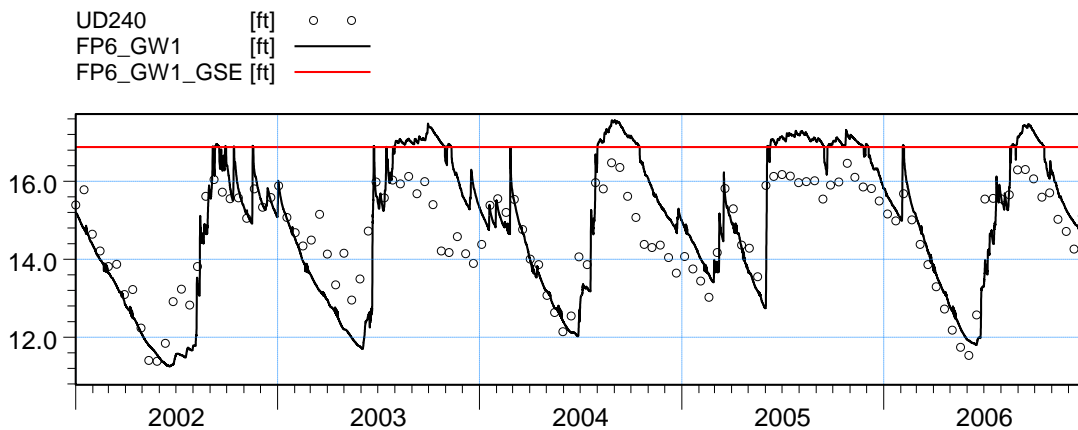


ME=-0.0857351  
 MAE=0.528962  
 RMSE=0.653072  
 STDres=0.64742  
 R(Correlation)=0.8877  
 R2(Nash\_Sutcliffe)=0.754508

Figure B11. Groundwater elevation at wells FP3\_GW1 and FP4\_GW1, after refinement.

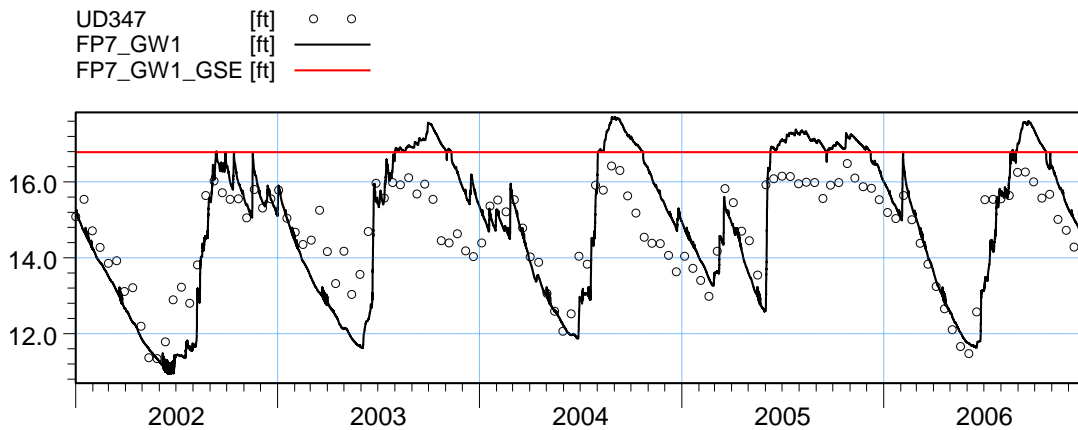


ME=-0.2072  
 MAE=0.570143  
 RMSE=0.737981  
 STDres=0.708296  
 R(Correlation)=0.883512  
 R2(Nash\_Sutcliffe)=0.678304

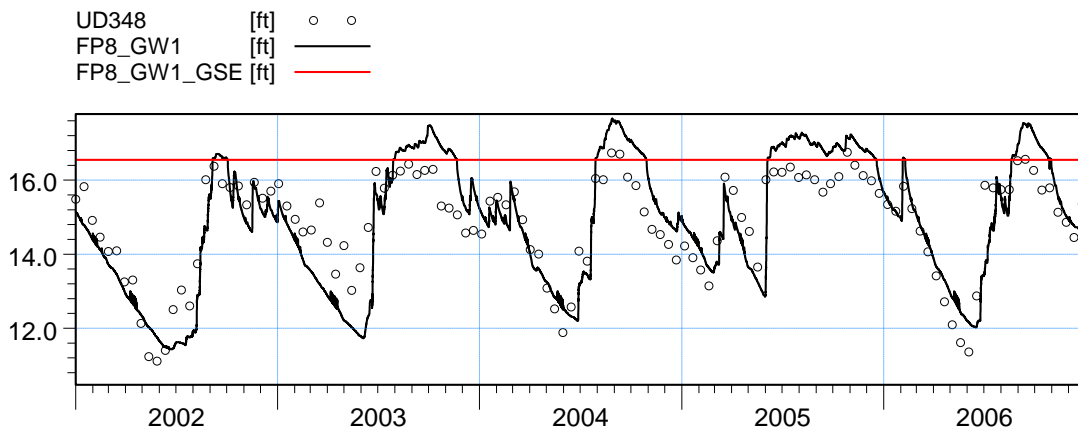


ME=-0.271415  
 MAE=0.769687  
 RMSE=0.969754  
 STDres=0.930997  
 R(Correlation)=0.863877  
 R2(Nash\_Sutcliffe)=0.433794

Figure B12. Groundwater elevation at wells FP5\_GW1 and FP6\_GW1, after refinement.

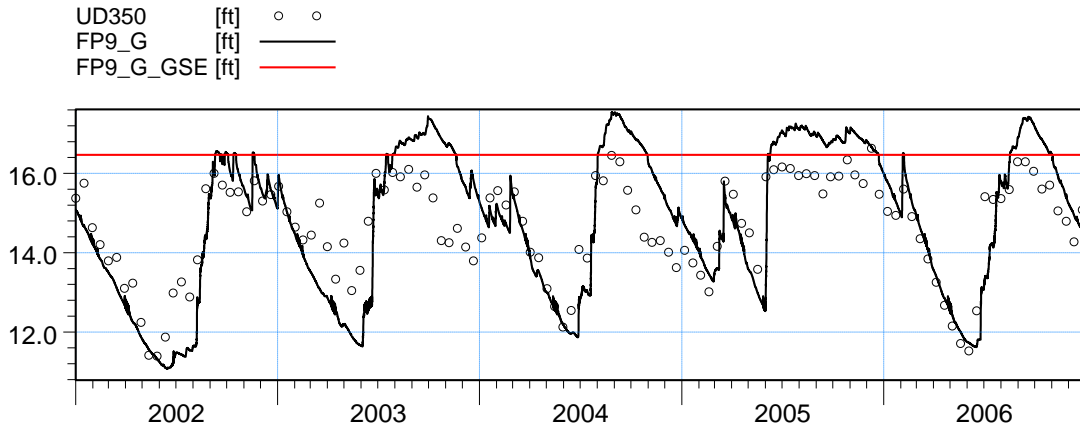


ME=-0.216707  
 MAE=0.834901  
 RMSE=1.02553  
 STDres=1.00238  
 R(Correlation)=0.858039  
 R2(Nash\_Sutcliffe)=0.369256

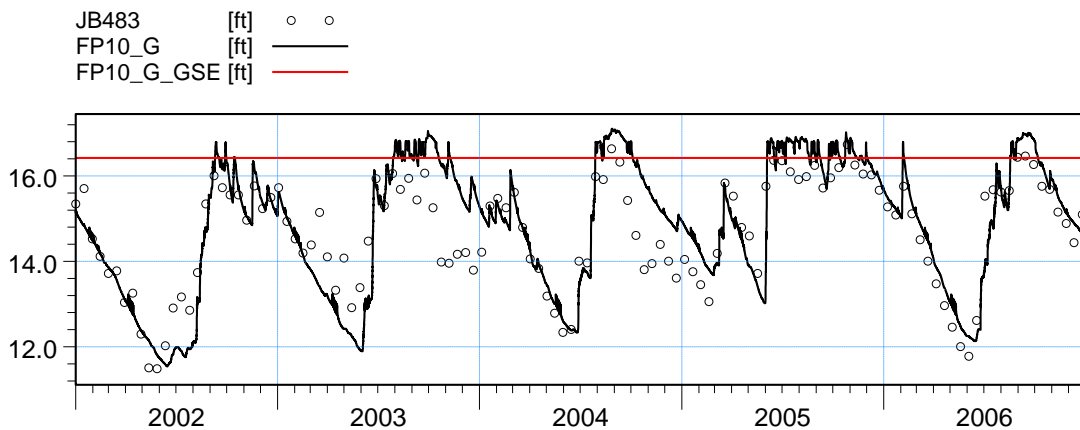


ME=-0.0696309  
 MAE=0.697097  
 RMSE=0.843654  
 STDres=0.840776  
 R(Correlation)=0.873601  
 R2(Nash\_Sutcliffe)=0.634564

Figure B13. Groundwater elevation at wells FP7\_GW1 and FP8\_GW1, after refinement.

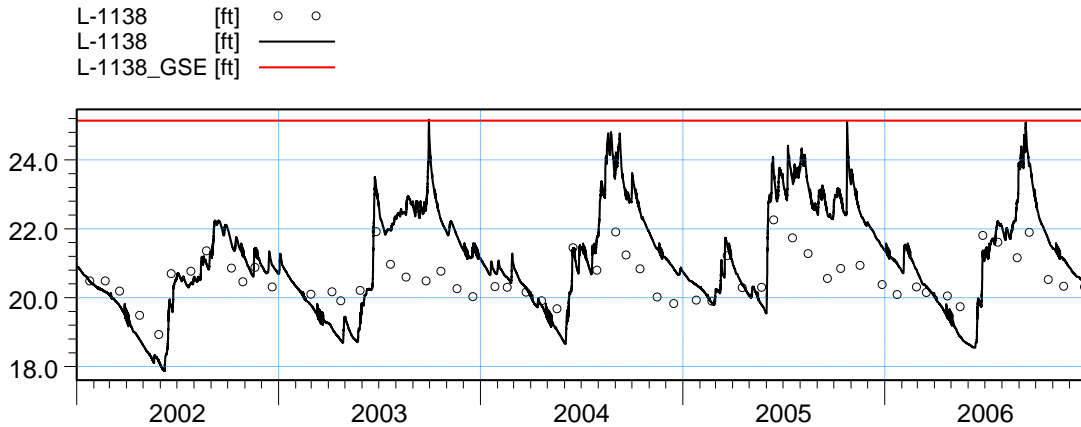


ME=-0.186806  
 MAE=0.815898  
 RMSE=1.00988  
 STDres=0.992448  
 R(Correlation)=0.85299  
 R2(Nash\_Sutcliffe)=0.374568

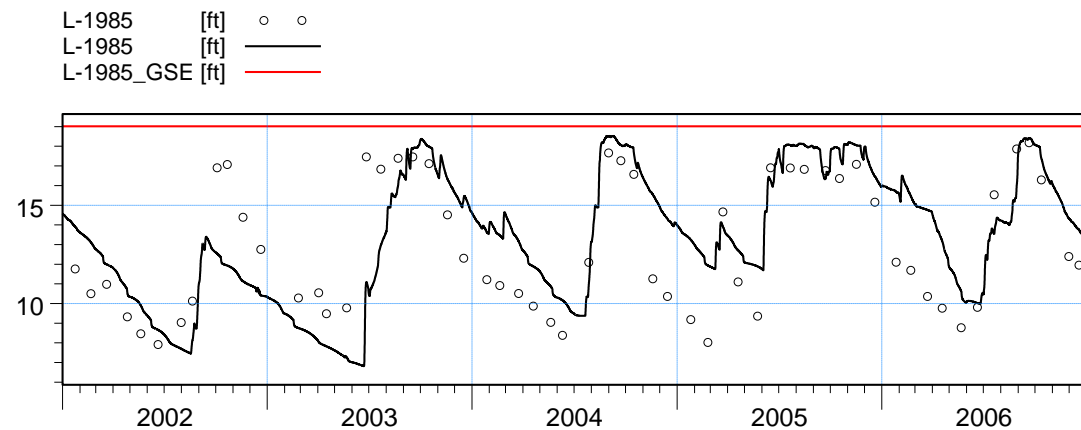


ME=-0.214229  
 MAE=0.57419  
 RMSE=0.765869  
 STDres=0.735297  
 R(Correlation)=0.873809  
 R2(Nash\_Sutcliffe)=0.644985

Figure B14. Groundwater elevation at wells FP9\_G and FP10\_G, after refinement.

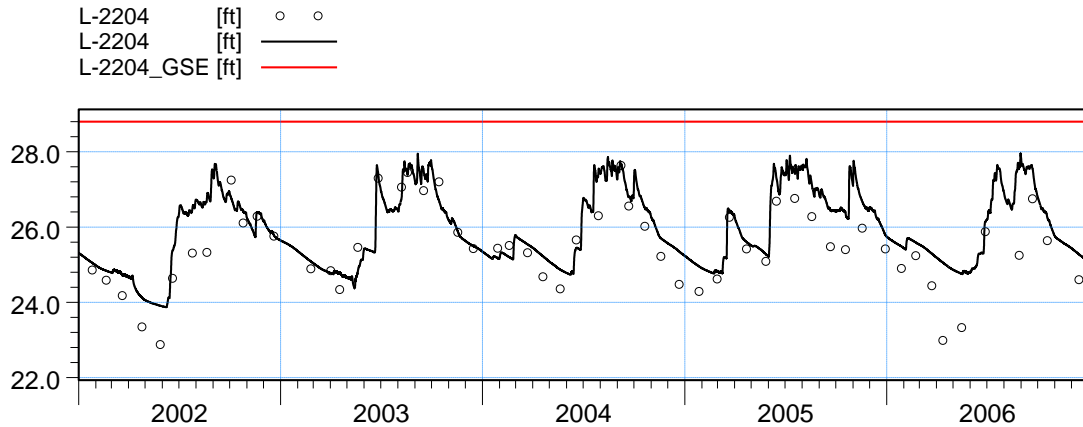


ME=-0.55937  
 MAE=0.919305  
 RMSE=1.09778  
 STDres=0.944581  
 R(Correlation)=0.801927  
 R2(Nash\_Sutcliffe)=-1.67891

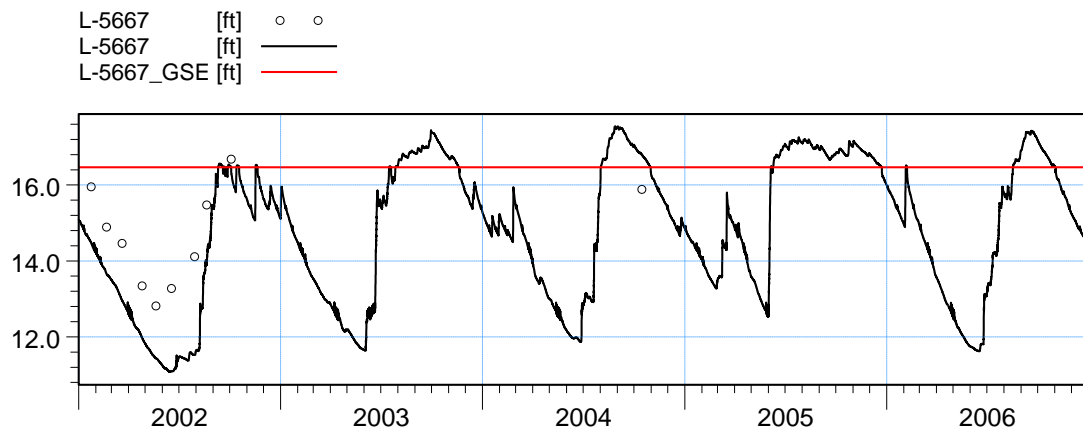


ME=-0.594337  
 MAE=2.12044  
 RMSE=2.49448  
 STDres=2.42265  
 R(Correlation)=0.723383  
 R2(Nash\_Sutcliffe)=0.435711

Figure B15. Groundwater elevation at wells L-1138 and L-1985, after refinement.

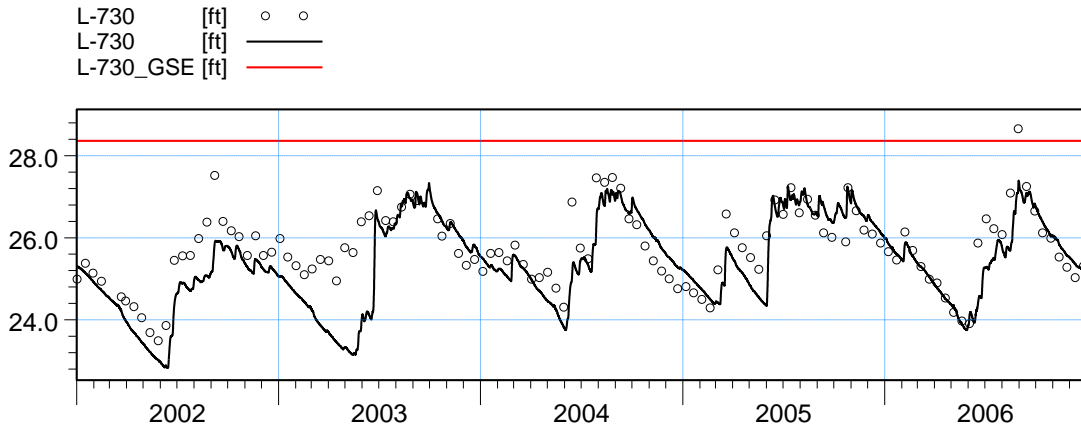


ME=-0.460614  
 MAE=0.55978  
 RMSE=0.728412  
 STDres=0.564287  
 R(Correlation)=0.856813  
 R2(Nash\_Sutcliffe)=0.554528

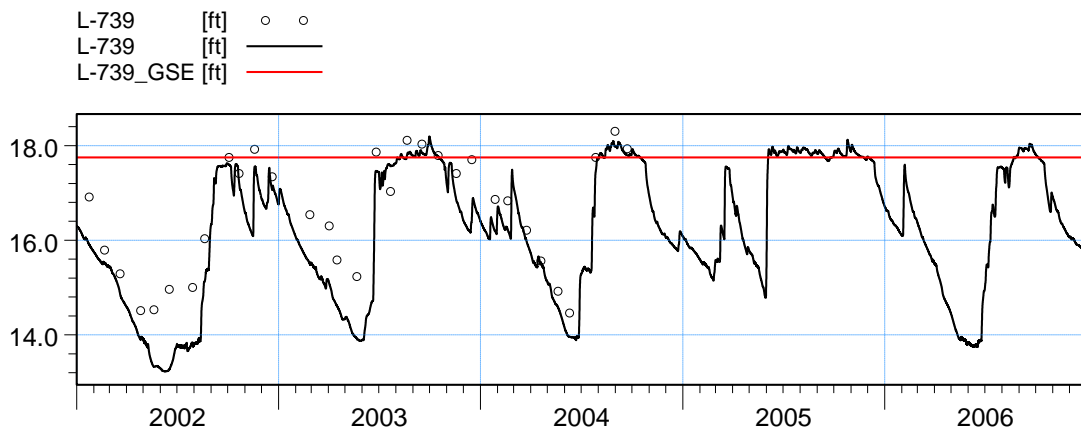


ME=1.26021  
 MAE=1.44235  
 RMSE=1.56118  
 STDres=0.921488  
 R(Correlation)=0.920334  
 R2(Nash\_Sutcliffe)=-0.58526

Figure B16. Groundwater elevation at wells L-2204 and L-5667, after refinement.

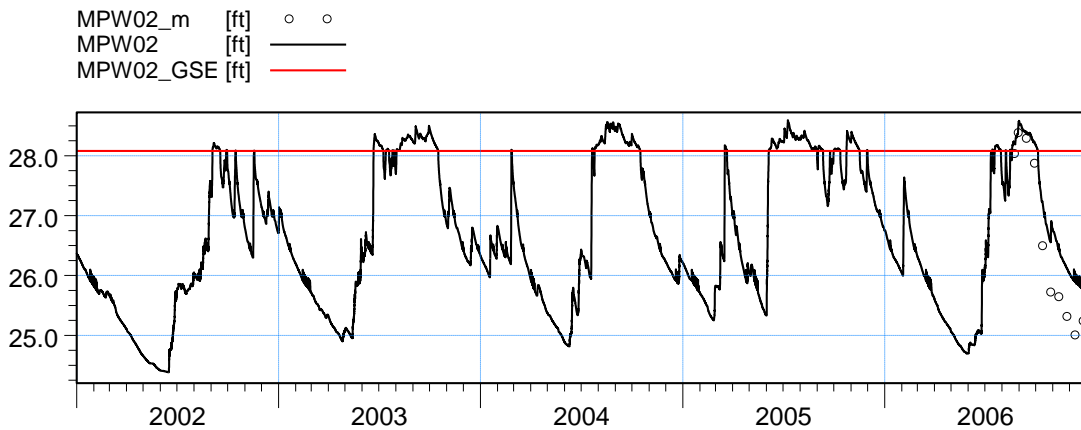


ME=0.367796  
 MAE=0.563437  
 RMSE=0.776566  
 STDres=0.683945  
 R(Correlation)=0.767955  
 R2(Nash\_Sutcliffe)=0.308446

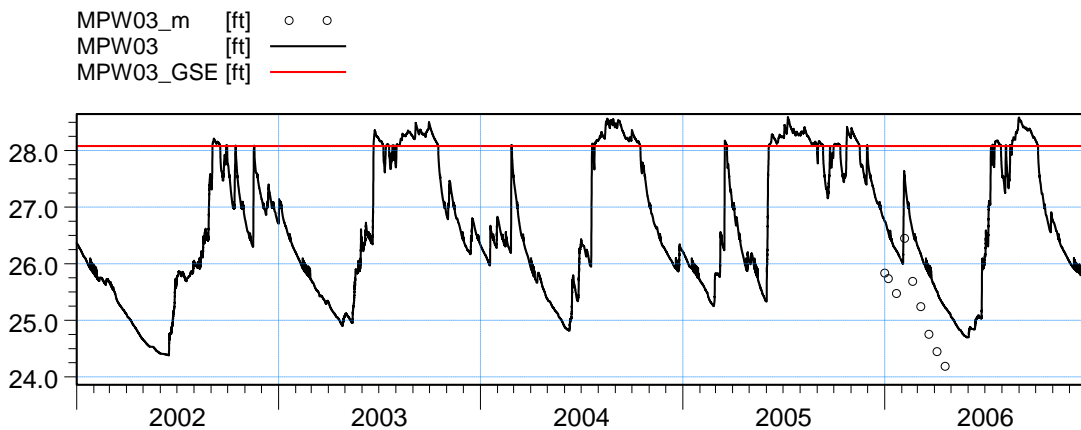


ME=0.569448  
 MAE=0.603136  
 RMSE=0.743453  
 STDres=0.477966  
 R(Correlation)=0.958444  
 R2(Nash\_Sutcliffe)=0.631785

Figure B17. Groundwater elevation at wells L-730 and L-739, after refinement.

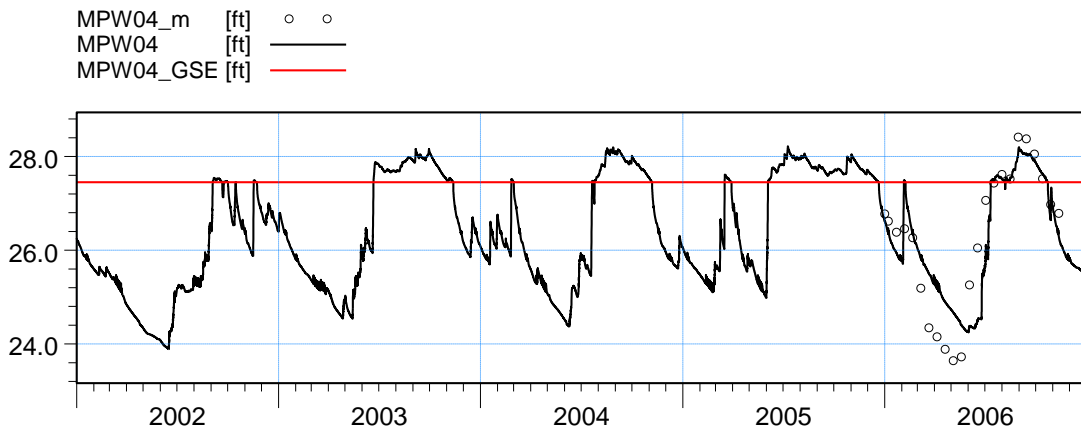


ME=-0.616588  
 MAE=0.620849  
 RMSE=0.709745  
 STDres=0.351508  
 R(Correlation)=0.983144  
 R2(Nash\_Sutcliffe)=0.694746

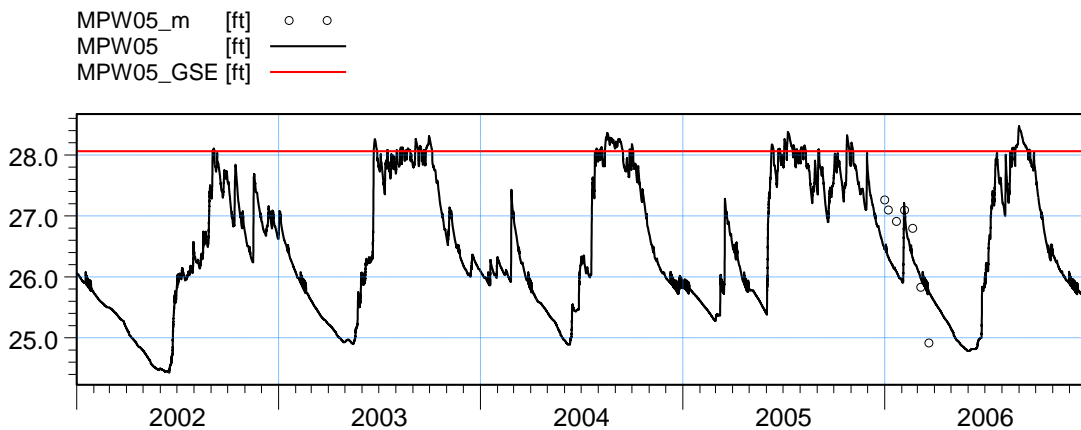


ME=-0.964686  
 MAE=0.964686  
 RMSE=0.972781  
 STDres=0.125238  
 R(Correlation)=0.98205  
 R2(Nash\_Sutcliffe)=-1.46683

Figure B18. Groundwater elevation at wells MPW02 and MPW03, after refinement.

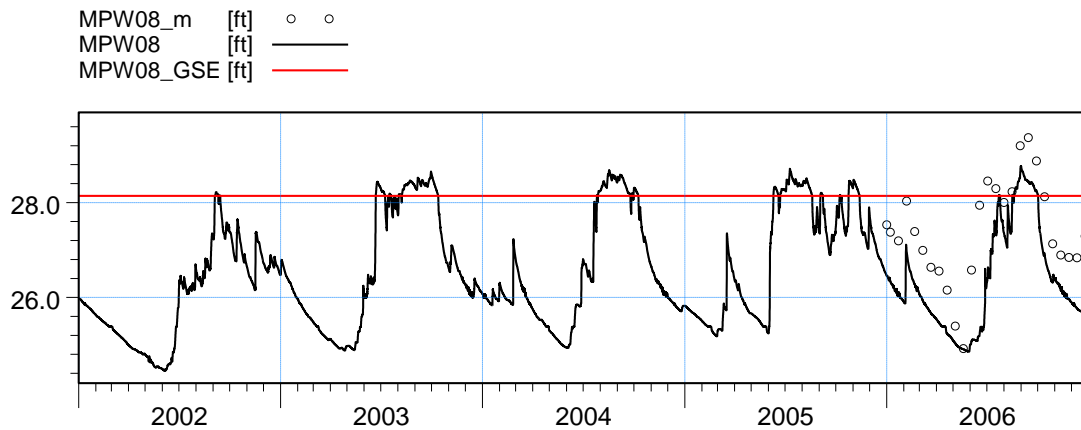


ME=-0.0532552  
 MAE=0.535123  
 RMSE=0.67337  
 STDres=0.67126  
 R(Correlation)=0.907102  
 R2(Nash\_Sutcliffe)=0.810456

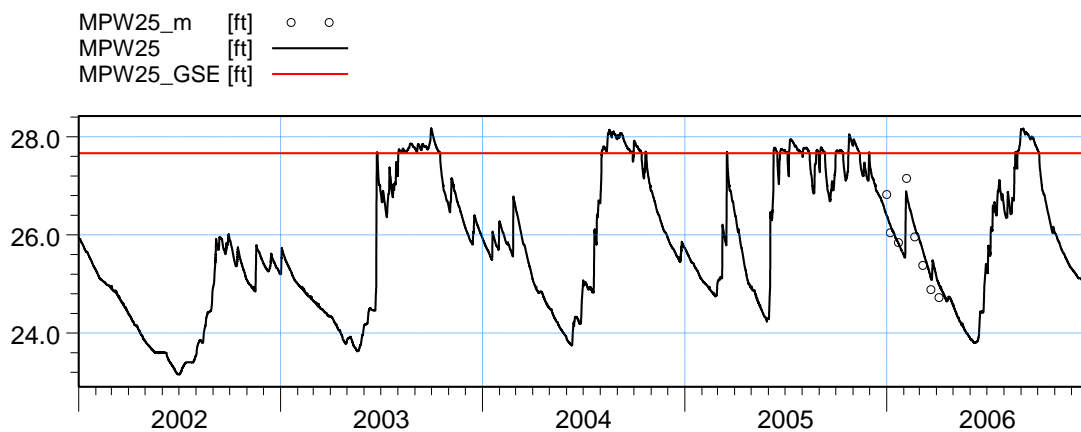


ME=0.266602  
 MAE=0.556511  
 RMSE=0.605915  
 STDres=0.544111  
 R(Correlation)=0.733039  
 R2(Nash\_Sutcliffe)=0.306681

Figure B19. Groundwater elevation at wells MPW04 and MPW05, after refinement.

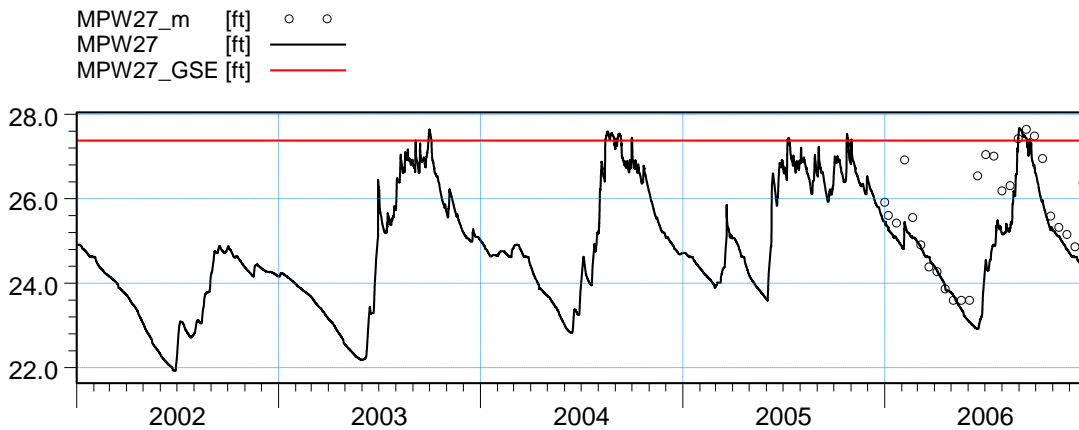


ME=0.990972  
 MAE=0.994096  
 RMSE=1.09613  
 STDres=0.468488  
 R(Correlation)=0.908185  
 R2(Nash\_Sutcliffe)=0.0181446

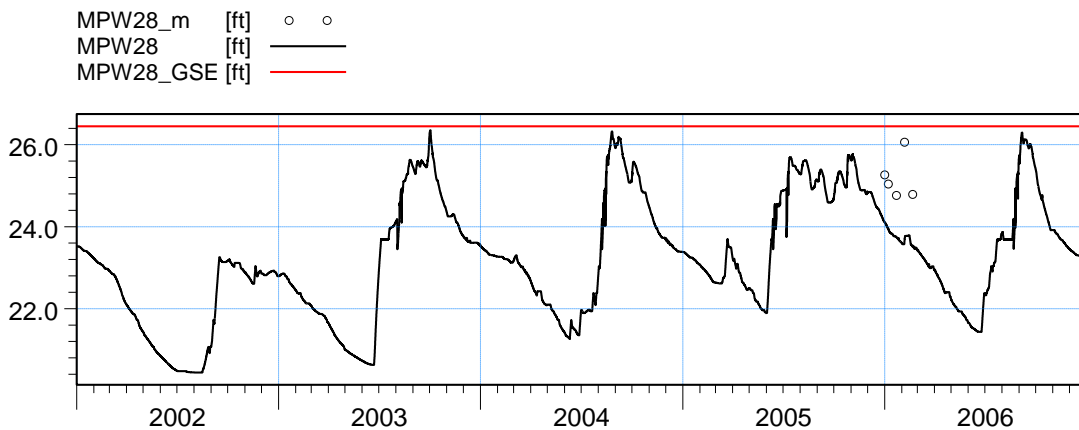


ME=-0.120091  
 MAE=0.26843  
 RMSE=0.310526  
 STDres=0.286364  
 R(Correlation)=0.952225  
 R2(Nash\_Sutcliffe)=0.828998

Figure B20. Groundwater elevation at wells MPW08 and MPW25, after refinement.

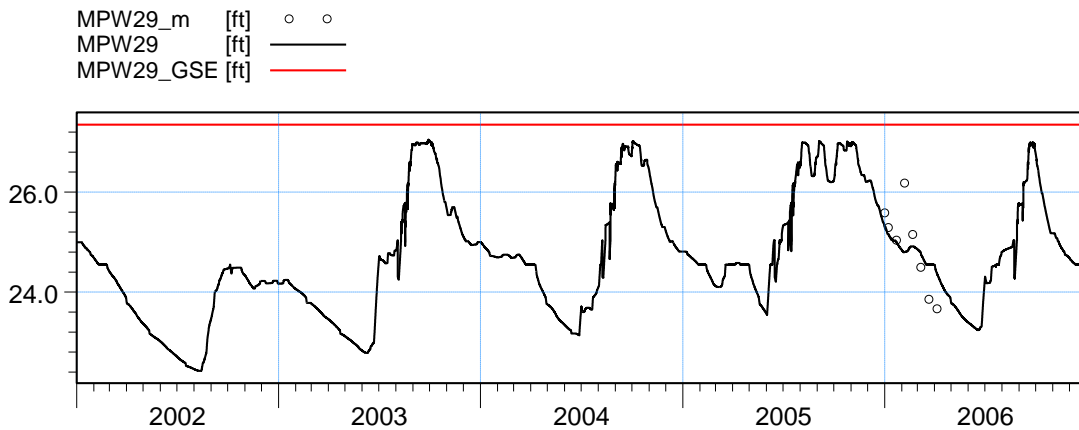


ME=0.692464  
 MAE=0.711822  
 RMSE=1.04325  
 STDres=0.7803  
 R(Correlation)=0.795394  
 R2(Nash\_Sutcliffe)=0.335832

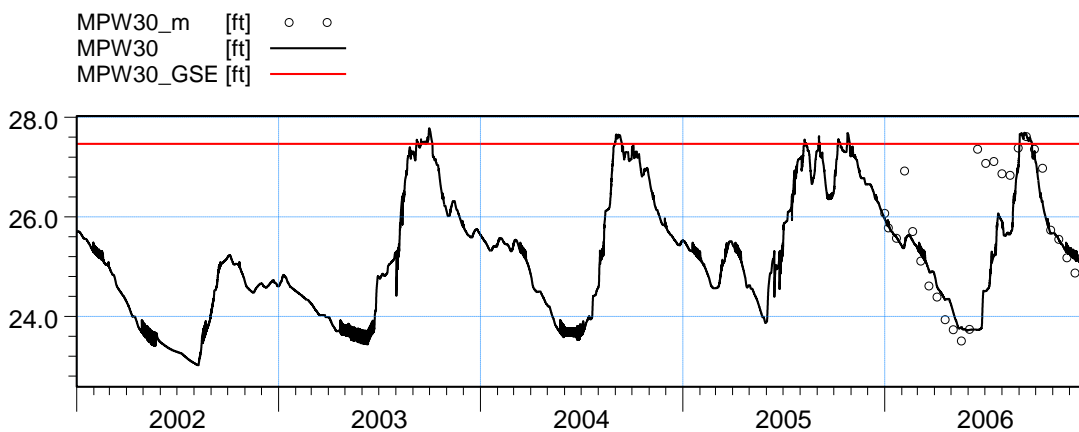


ME=1.16482  
 MAE=1.16482  
 RMSE=1.22787  
 STDres=0.38843  
 R(Correlation)=0.50919  
 R2(Nash\_Sutcliffe)=-6.50899

Figure B21. Groundwater elevation at wells MPW27 and MPW28, after refinement.

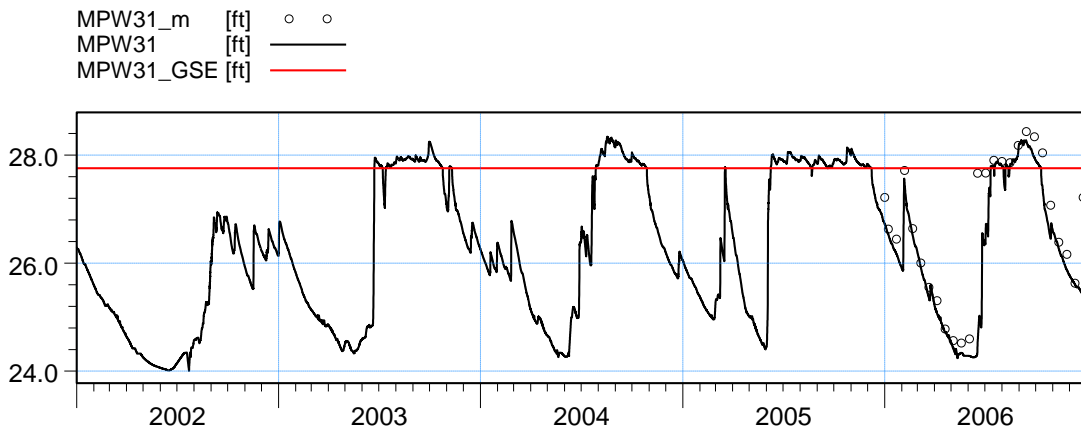


ME=-0.0930842  
 MAE=0.408892  
 RMSE=0.533603  
 STDres=0.525421  
 R(Correlation)=0.844635  
 R2(Nash\_Sutcliffe)=0.485862

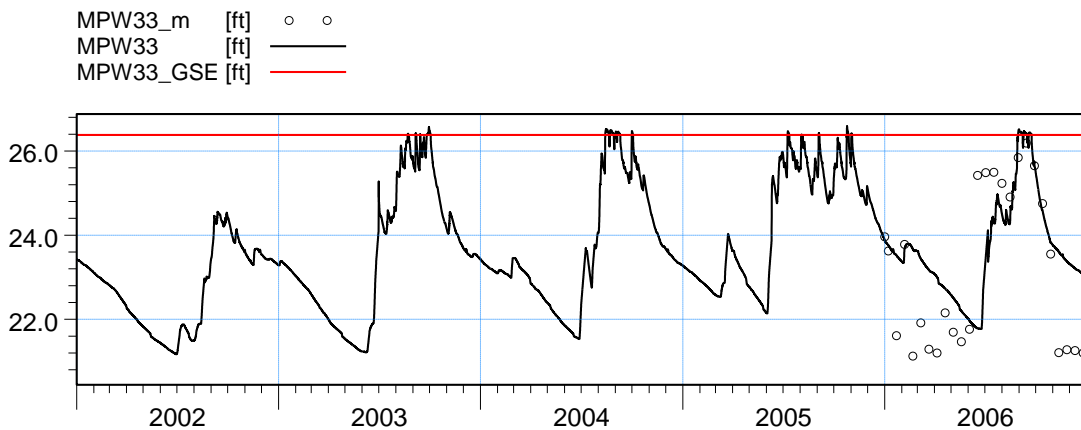


ME=0.386133  
 MAE=0.592821  
 RMSE=0.965849  
 STDres=0.885305  
 R(Correlation)=0.73153  
 R2(Nash\_Sutcliffe)=0.44312

Figure B22. Groundwater elevation at wells MPW29 and MPW30, after refinement.

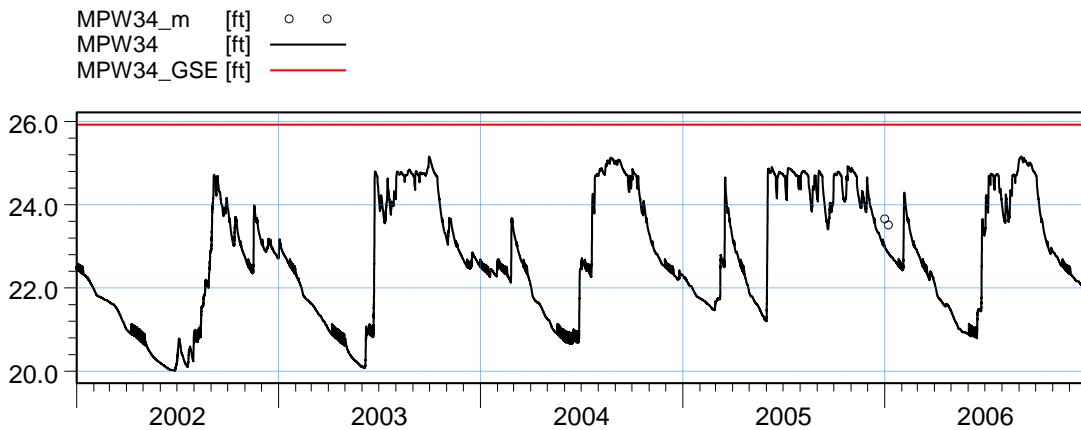


ME=0.380657  
 MAE=0.387031  
 RMSE=0.589928  
 STDres=0.450683  
 R(Correlation)=0.935567  
 R2(Nash\_Sutcliffe)=0.780764

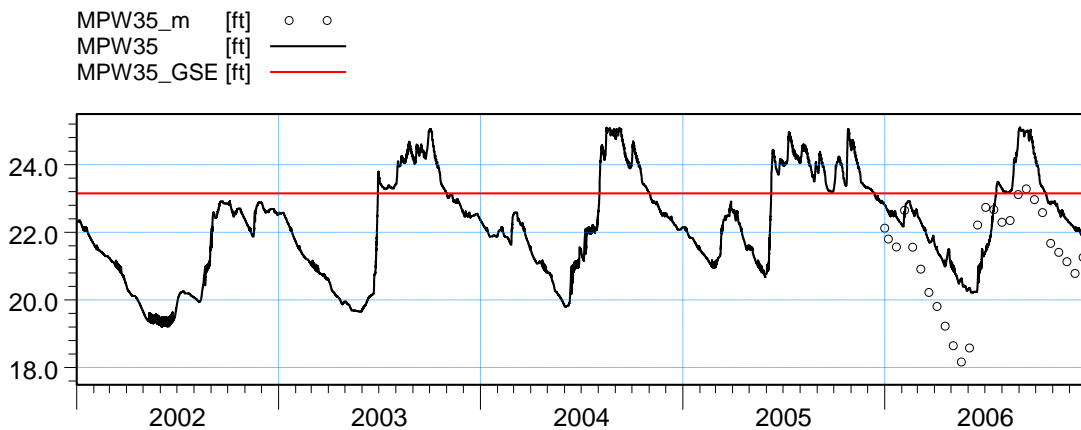


ME=-0.556437  
 MAE=1.18361  
 RMSE=1.48213  
 STDres=1.37371  
 R(Correlation)=0.696321  
 R2(Nash\_Sutcliffe)=0.393506

Figure B23. Groundwater elevation at wells MPW31 and MPW33, after refinement.

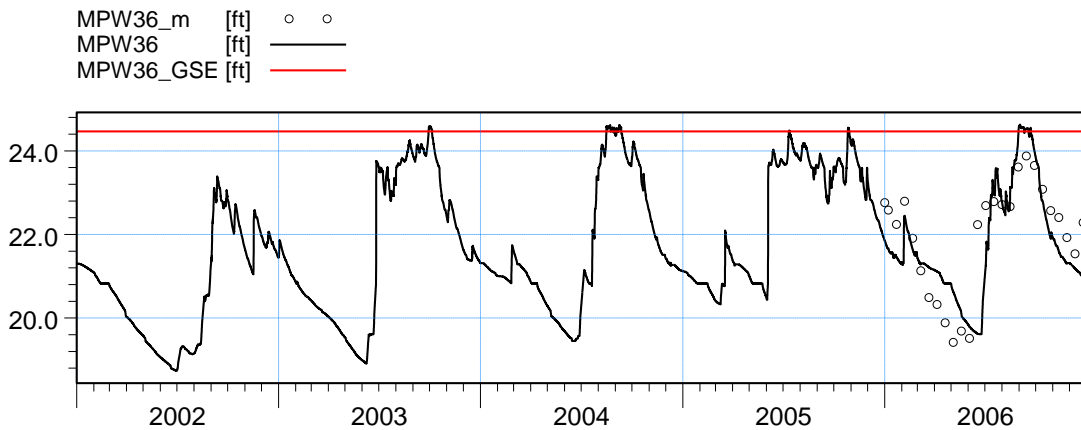


ME=0.624417  
 MAE=0.624417  
 RMSE=0.626974  
 STDres=0.0565652  
 R(Correlation)=0.983537  
 R2(Nash\_Sutcliffe)=-17.5005

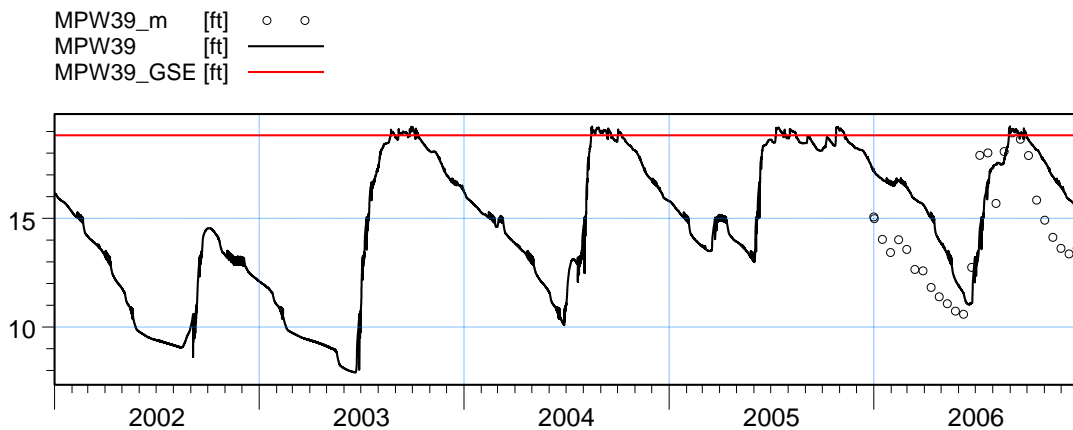


ME=-1.10294  
 MAE=1.25656  
 RMSE=1.36304  
 STDres=0.800865  
 R(Correlation)=0.838832  
 R2(Nash\_Sutcliffe)=0.140964

Figure B24. Groundwater elevation at wells MPW34 and MPW35, after refinement.

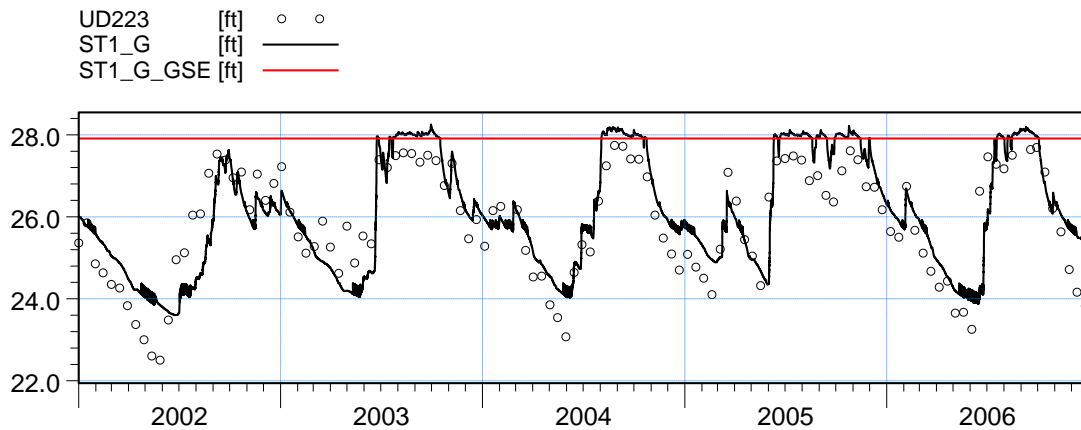


ME=0.0762097  
 MAE=0.607109  
 RMSE=0.741544  
 STDres=0.737618  
 R(Correlation)=0.841994  
 R2(Nash\_Sutcliffe)=0.690066

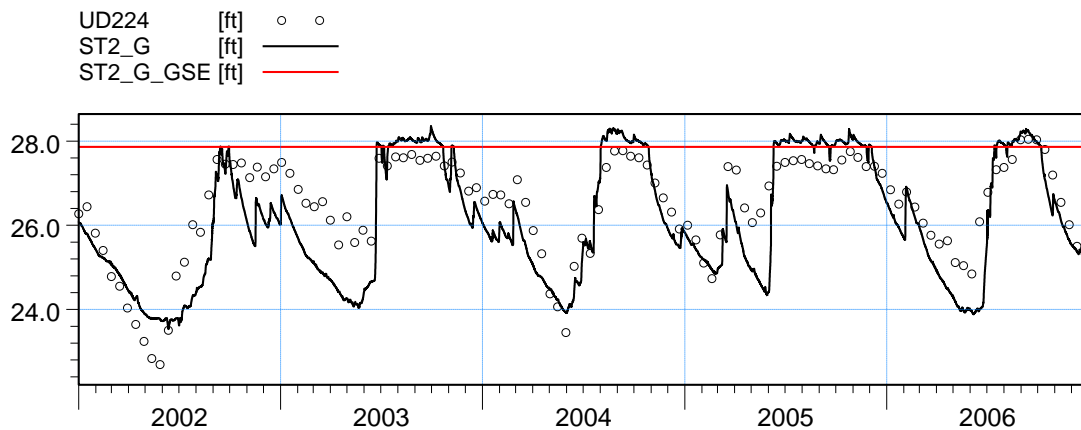


ME=-1.52507  
 MAE=2.19578  
 RMSE=2.45984  
 STDres=1.93002  
 R(Correlation)=0.660331  
 R2(Nash\_Sutcliffe)=0.0300196

Figure B25. Groundwater elevation at wells MPW36 and MPW39, after refinement.

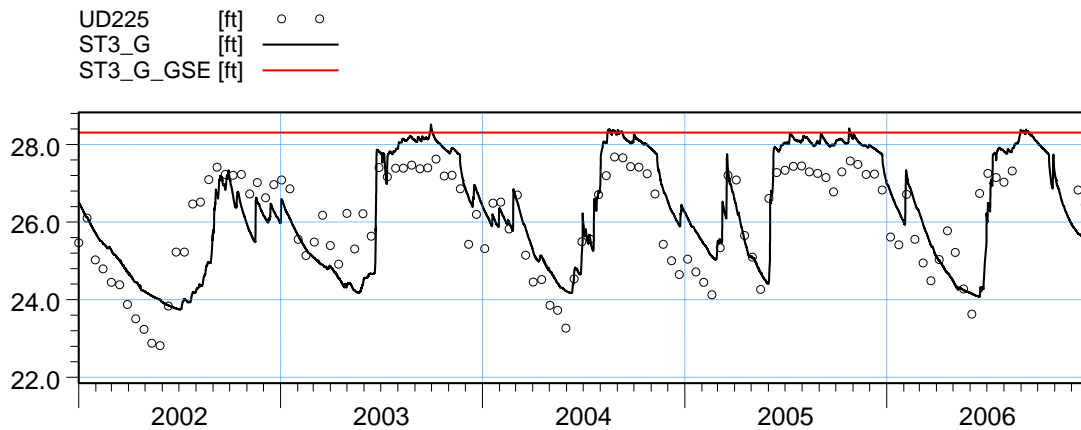


ME=-0.258589  
 MAE=0.610426  
 RMSE=0.731978  
 STDres=0.68478  
 R(Correlation)=0.871193  
 R2(Nash\_Sutcliffe)=0.71066

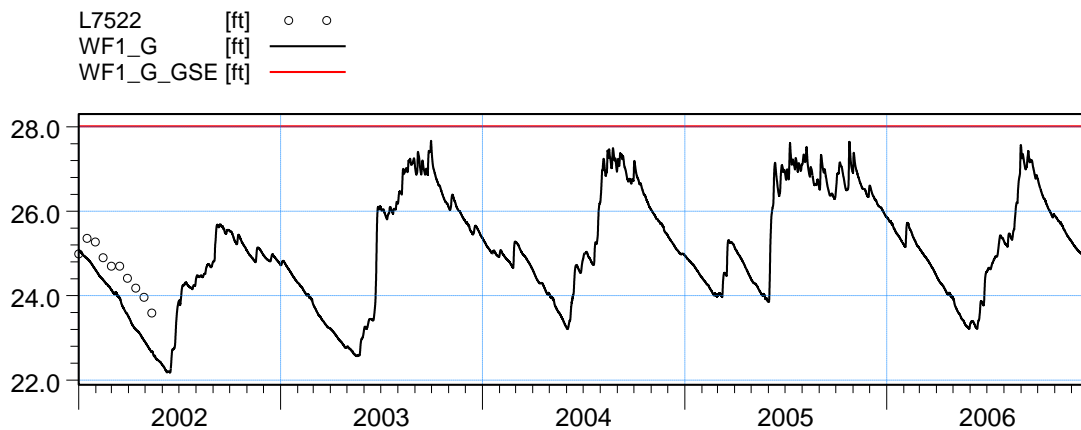


ME=0.336614  
 MAE=0.662502  
 RMSE=0.797297  
 STDres=0.722754  
 R(Correlation)=0.862329  
 R2(Nash\_Sutcliffe)=0.569231

Figure B26. Groundwater elevation at wells ST1\_G and ST2\_G, after refinement.

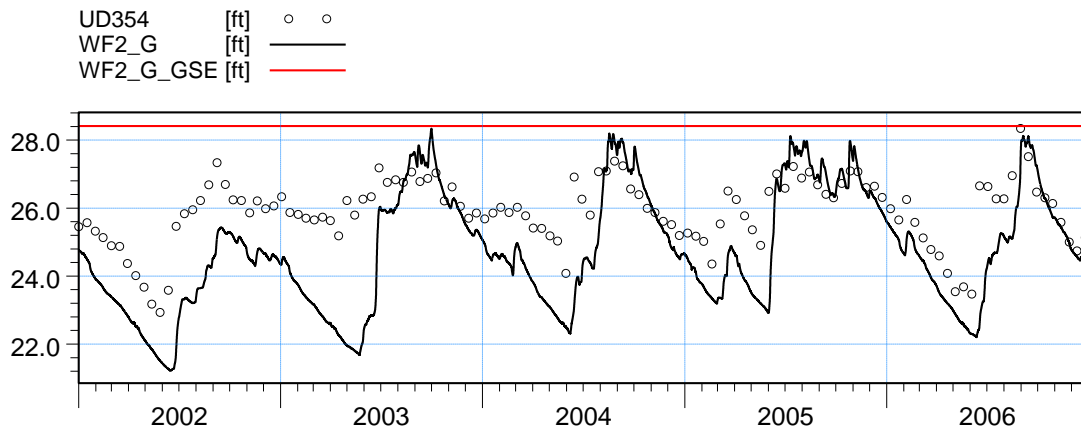


ME=-0.199552  
 MAE=0.752673  
 RMSE=0.864958  
 STDres=0.841624  
 R(Correlation)=0.805634  
 R2(Nash\_Sutcliffe)=0.543968

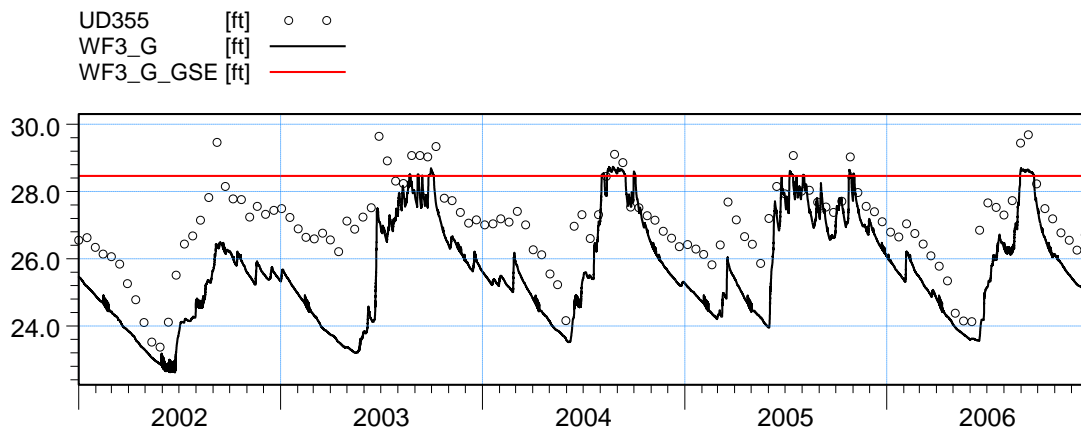


ME=0.683901  
 MAE=0.694185  
 RMSE=0.751569  
 STDres=0.311665  
 R(Correlation)=0.94532  
 R2(Nash\_Sutcliffe)=-1.24606

Figure B27. Groundwater elevation at wells ST3\_G and WF1\_G, after refinement.

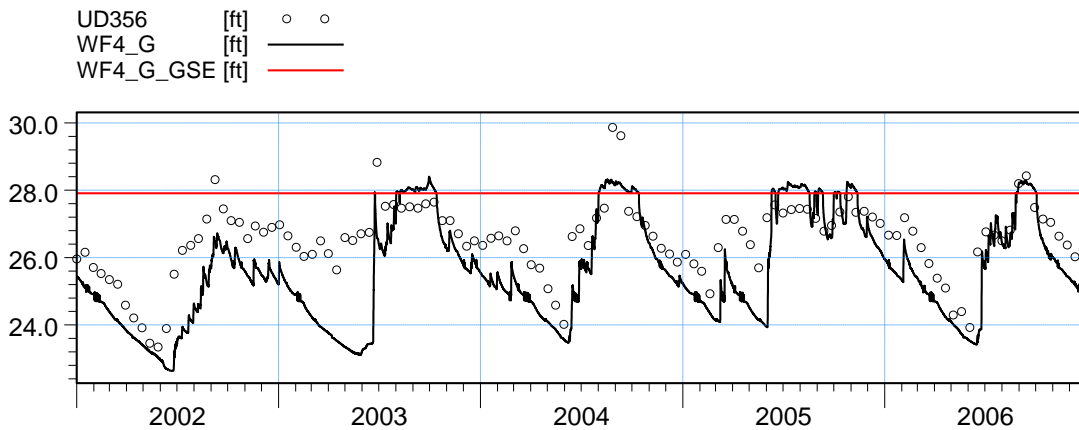


ME=1.13388  
 MAE=1.29008  
 RMSE=1.61327  
 STDres=1.14759  
 R(Correlation)=0.757831  
 R2(Nash\_Sutcliffe)=-1.66004

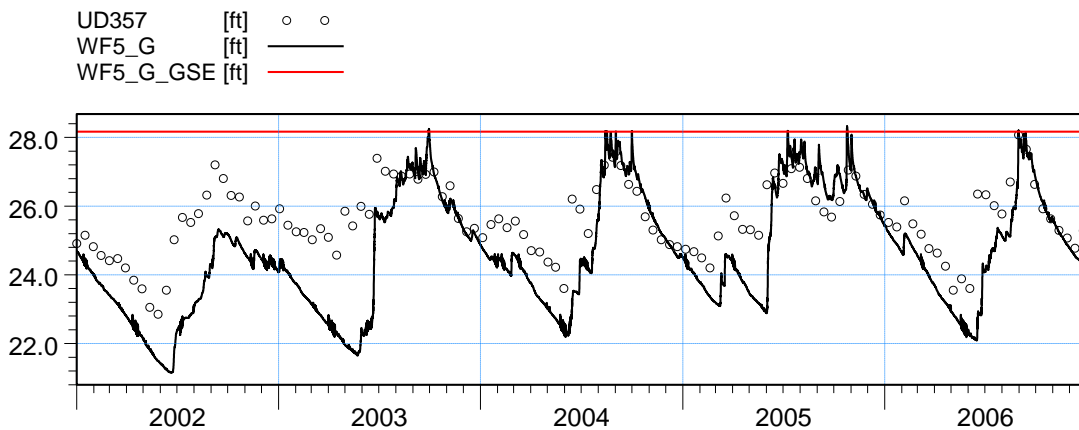


ME=1.3775  
 MAE=1.38444  
 RMSE=1.58922  
 STDres=0.792544  
 R(Correlation)=0.84447  
 R2(Nash\_Sutcliffe)=-0.604467

Figure B28. Groundwater elevation at wells WF2\_G and WF3\_G, after refinement.

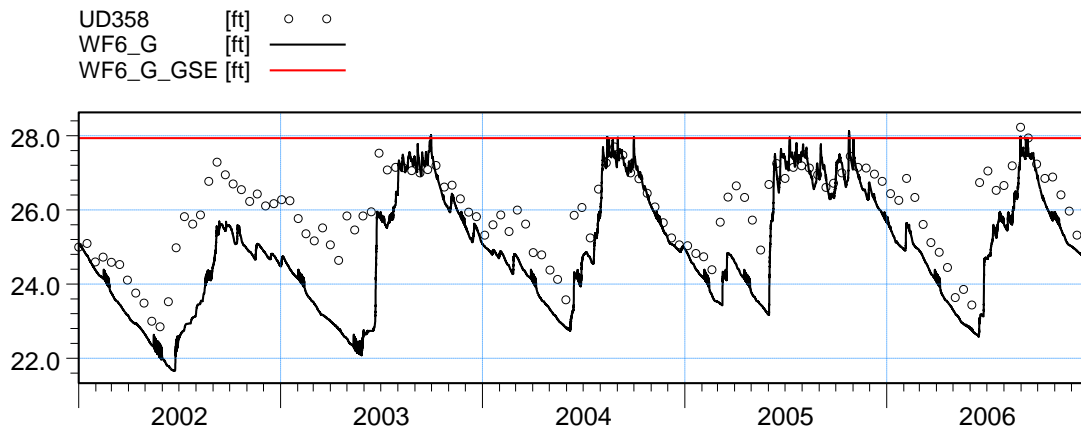


ME=0.908792  
 MAE=1.06321  
 RMSE=1.27764  
 STDres=0.898029  
 R(Correlation)=0.806699  
 R2(Nash\_Sutcliffe)=-0.297008

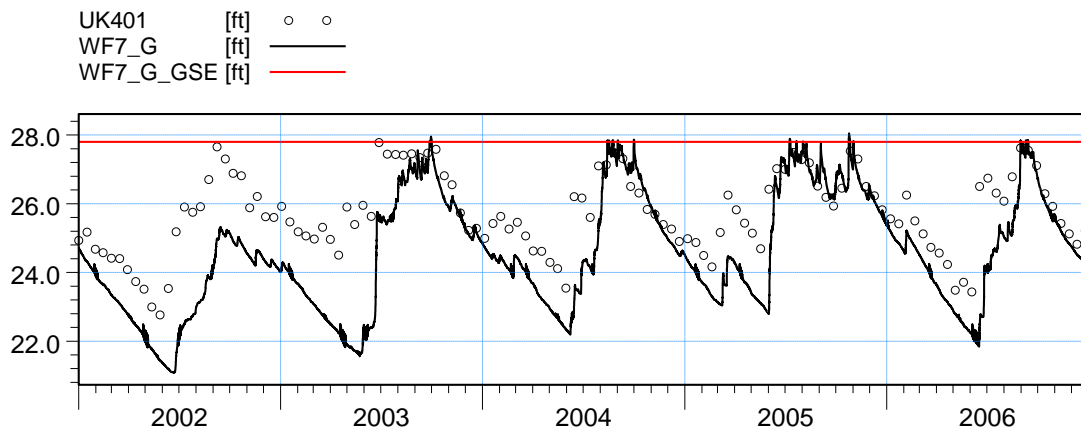


ME=0.966318  
 MAE=1.11034  
 RMSE=1.4315  
 STDres=1.05614  
 R(Correlation)=0.789249  
 R2(Nash\_Sutcliffe)=-0.895795

Figure B29. Groundwater elevation at wells WF4\_G and WF5\_G, after refinement.



ME=0.986615  
 MAE=1.04175  
 RMSE=1.32131  
 STDres=0.878894  
 R(Correlation)=0.825518  
 R2(Nash\_Sutcliffe)=-0.331434



ME=1.13977  
 MAE=1.19621  
 RMSE=1.52914  
 STDres=1.01941  
 R(Correlation)=0.792976  
 R2(Nash\_Sutcliffe)=-0.693257

Figure B30. Groundwater elevation at wells WF6\_G and WF7\_G, after refinement.



**Appendix B2. Surface water stations south from Caloosahatchee**

| Station Name       | before refinement |          |           |      |            | after refinement |          |           |      |            |
|--------------------|-------------------|----------|-----------|------|------------|------------------|----------|-----------|------|------------|
|                    | ME (ft)           | MAE (ft) | RMSE (ft) | R    | PL         | ME (ft)          | MAE (ft) | RMSE (ft) | R    | PL         |
| 10 Mi Canal 8490   | -0.57             | 0.57     | 0.82      | 0.27 | <b>1.5</b> | -0.59            | 0.59     | 0.83      | 0.27 | <b>1.5</b> |
| 6 Mi Cypress 1128  | 1.26              | 1.51     | 1.77      | 0.59 | <b>2.3</b> | 1.36             | 1.57     | 1.81      | 0.61 | <b>2.0</b> |
| 6 Mi Cypress 3600  | 0.49              | 0.70     | 0.77      | 0.62 | <b>1.3</b> | 0.67             | 0.83     | 1.02      | 0.62 | <b>1.8</b> |
| 6 Mi Cypress 7755  | -0.42             | 0.77     | 1.01      | 0.67 | <b>1.5</b> | -0.52            | 0.86     | 1.05      | 0.73 | <b>1.8</b> |
| 6 Mi Cypress 10535 | 1.50              | 1.54     | 1.71      | 0.77 | <b>2.0</b> | 1.56             | 1.62     | 1.80      | 0.73 | <b>2.3</b> |
| 6 Mi Cypress 10565 | 1.38              | 1.39     | 1.51      | 0.85 | <b>1.8</b> | 1.44             | 1.46     | 1.60      | 0.81 | <b>1.8</b> |
| 6 Mi Cypress 14150 | 1.66              | 2.47     | 3.29      | 0.30 | <b>3.0</b> | 1.72             | 2.48     | 3.32      | 0.30 | <b>3.0</b> |
| CorkScrewCan 1174  | -2.01             | 2.03     | 2.26      | 0.83 | <b>2.5</b> | -1.54            | 1.63     | 1.92      | 0.78 | <b>2.3</b> |
| CorkTribCan 0      | ---               | ---      | ---       | ---  | ---        | 0.13             | 1.34     | 1.68      | 0.50 | <b>2.0</b> |
| Hendry Creek 768   | 2.78              | 2.79     | 2.98      | 0.02 | <b>3.0</b> | 2.76             | 2.77     | 2.96      | 0.04 | <b>3.0</b> |
| KehlCan 9358       | 1.18              | 1.75     | 2.19      | 0.73 | <b>2.5</b> | 1.26             | 1.67     | 2.09      | 0.73 | <b>2.5</b> |
| KehlCan 9479       | -0.19             | 0.66     | 0.99      | 0.95 | <b>1.0</b> | 0.03             | 0.76     | 1.08      | 0.93 | <b>1.3</b> |
| Mullock Creek_2702 | 5.24              | 5.24     | 5.25      | 0.63 | <b>2.8</b> | 2.51             | 2.51     | 2.54      | 0.62 | <b>2.8</b> |
| OR Buckingham      | 0.15              | 0.47     | 0.61      | 0.88 | <b>1.0</b> | -0.16            | 0.52     | 0.74      | 0.91 | <b>1.0</b> |
| OR Harns Marsh HW  | 1.71              | 1.77     | 2.01      | 0.90 | <b>2.5</b> | 0.57             | 1.04     | 1.14      | 0.94 | <b>1.5</b> |
| OR Harns Marsh Q   | ---               | ---      | ---       | 0.86 | <b>1.0</b> | ---              | ---      | ---       | 0.92 | <b>1.0</b> |
| S-A-1-HW           | 0.06              | 0.34     | 0.42      | 0.59 | <b>1.5</b> | 0.04             | 0.36     | 0.46      | 0.57 | <b>1.5</b> |
| S-A-2_HW           | -0.46             | 0.49     | 0.56      | 0.84 | <b>1.0</b> | -0.52            | 0.54     | 0.63      | 0.70 | <b>1.3</b> |
| S-HC-1_HW          | -4.86             | 5.01     | 5.17      | -0.1 | <b>3.0</b> | -0.17            | 0.72     | 1.07      | 0.0  | <b>1.8</b> |
| S-HC-2_HW          | -1.20             | 1.20     | 1.38      | 0.46 | <b>2.3</b> | -0.97            | 0.97     | 1.13      | 0.47 | <b>2.3</b> |
| S-NM-2 Q           | ---               | ---      | ---       | 0.48 | <b>3.0</b> | ---              | ---      | ---       | 0.43 | <b>3.0</b> |
| S-NM-2_HW          | -0.03             | 0.18     | 0.24      | 0.61 | <b>1.3</b> | -0.01            | 0.18     | 0.23      | 0.65 | <b>1.3</b> |
| S-NM-2_TW          | 0.82              | 1.01     | 1.13      | 0.60 | <b>2.3</b> | 0.80             | 1.03     | 1.16      | 0.44 | <b>2.0</b> |
| S-SF-1 Q           | ---               | ---      | ---       | 0.83 | <b>1.0</b> | ---              | ---      | ---       | 0.74 | <b>2.0</b> |
| S-SF-1_HW          | 1.29              | 1.29     | 1.30      | 0.91 | <b>1.8</b> | 0.14             | 0.18     | 0.23      | 0.88 | <b>1.0</b> |
| S-SF-1_TW          | -0.04             | 0.28     | 0.37      | 0.52 | <b>1.5</b> | -0.03            | 0.30     | 0.47      | 0.44 | <b>1.5</b> |
| S-YT-2_HW          | 1.16              | 1.26     | 1.46      | 0.72 | <b>2.0</b> | 1.54             | 1.66     | 1.88      | 0.74 | <b>2.3</b> |

Table B3. Statistical parameters and level of performance at surface water stations south of the Caloosahatchee River. The green color indicates the highest performance level (1.0, 1.2 and 1.5), yellow for medium (1.8, 2.0, 2.3, 2.5) and orange for low (2.8, 3.0).

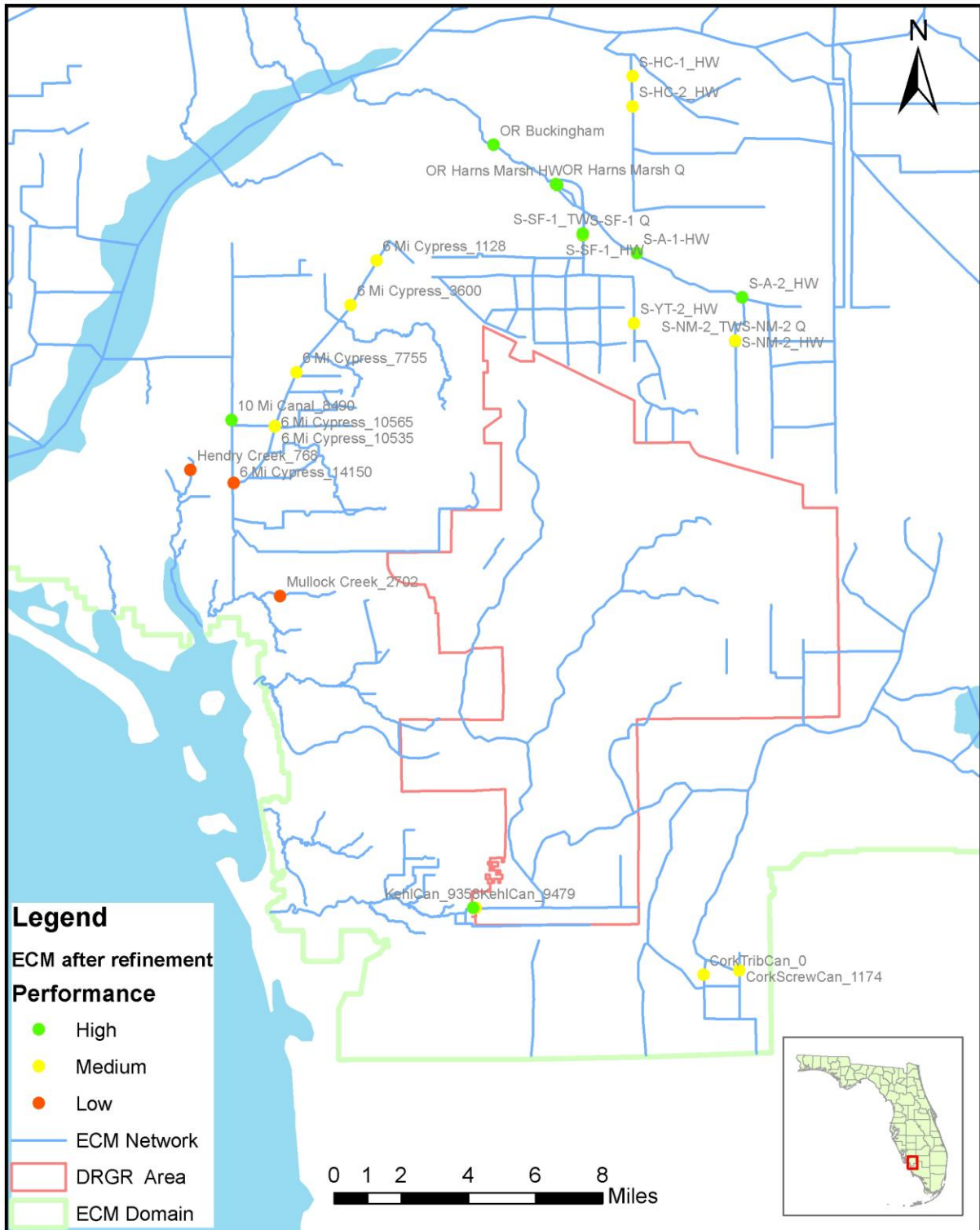
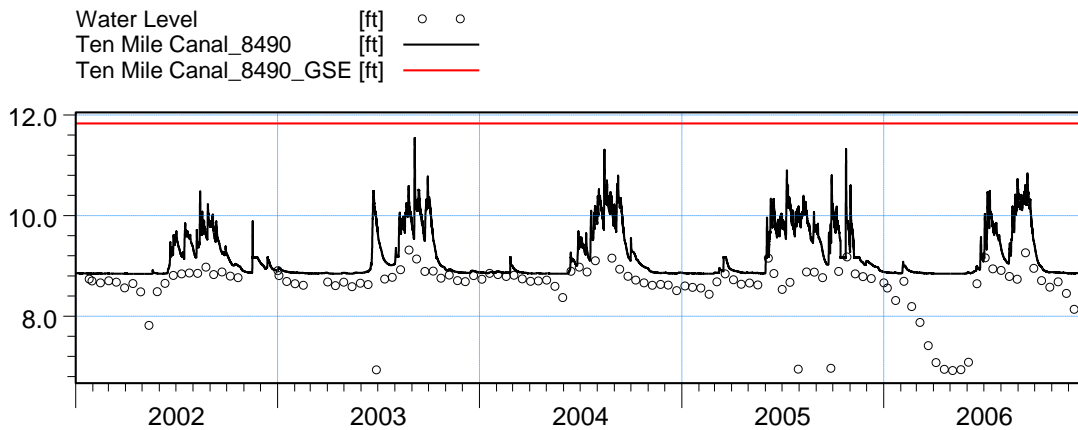
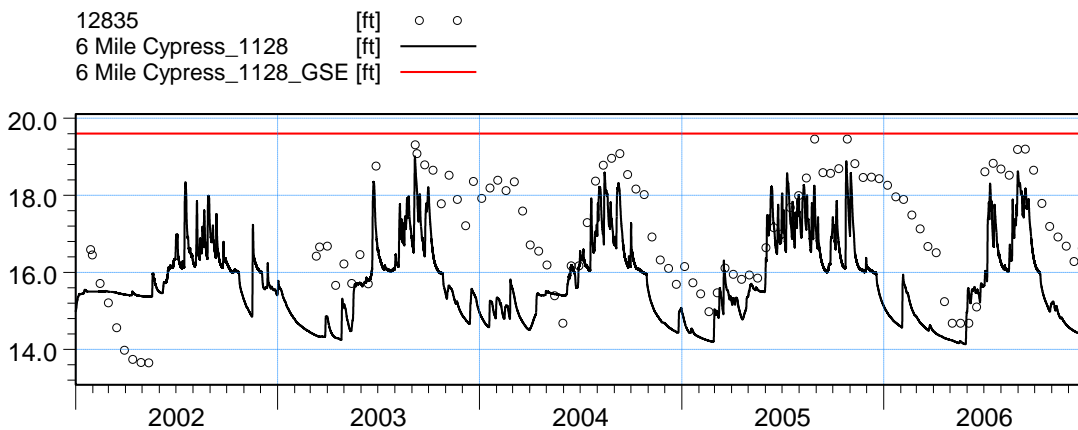


Figure B31. Average performance level at surface water monitoring stations south of Caloosahatchee River, after the refinement process.

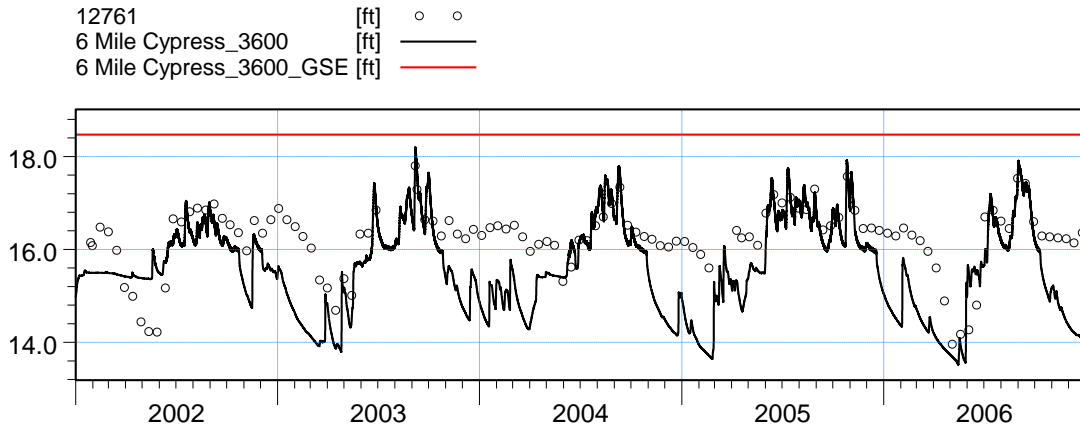


ME=-0.588085  
 MAE=0.588113  
 RMSE=0.83281  
 STDres=0.589685  
 R(Correlation)=0.265991  
 R2(Nash\_Sutcliffe)=-1.52849

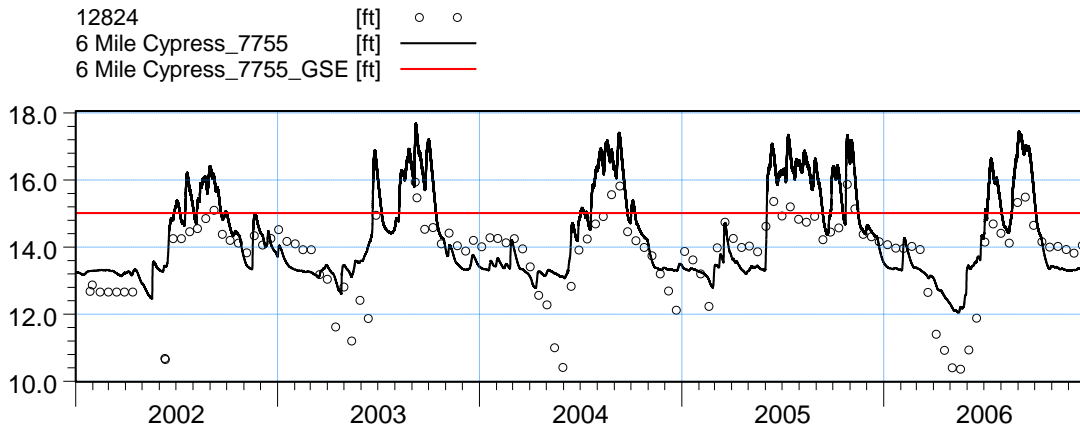


ME=1.36283  
 MAE=1.57469  
 RMSE=1.80997  
 STDres=1.19108  
 R(Correlation)=0.612756  
 R2(Nash\_Sutcliffe)=-0.462988

Figure B32. Stage at stations 10 Mi Canal 8490 and 6 Mi Cypress 1128, after refinement.

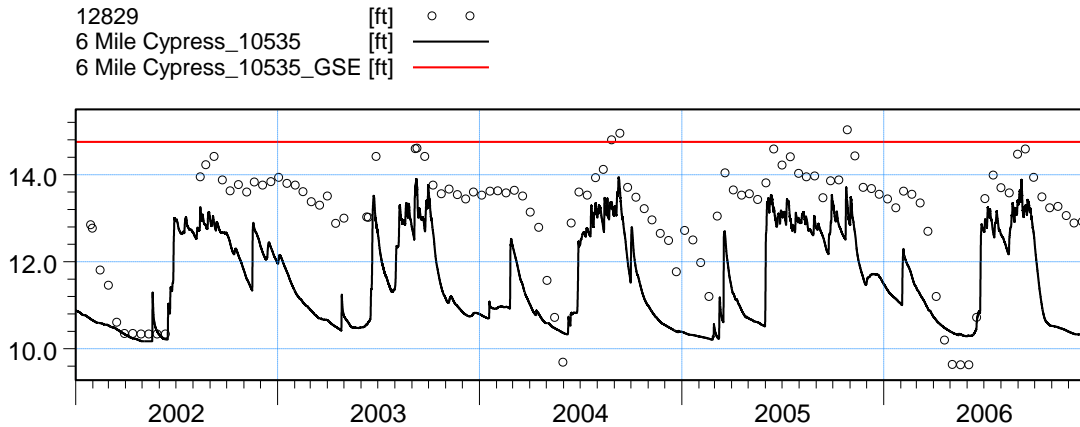


ME=0.672623  
 MAE=0.830582  
 RMSE=1.02426  
 STDres=0.772455  
 R(Correlation)=0.622314  
 R2(Nash\_Sutcliffe)=-0.856346

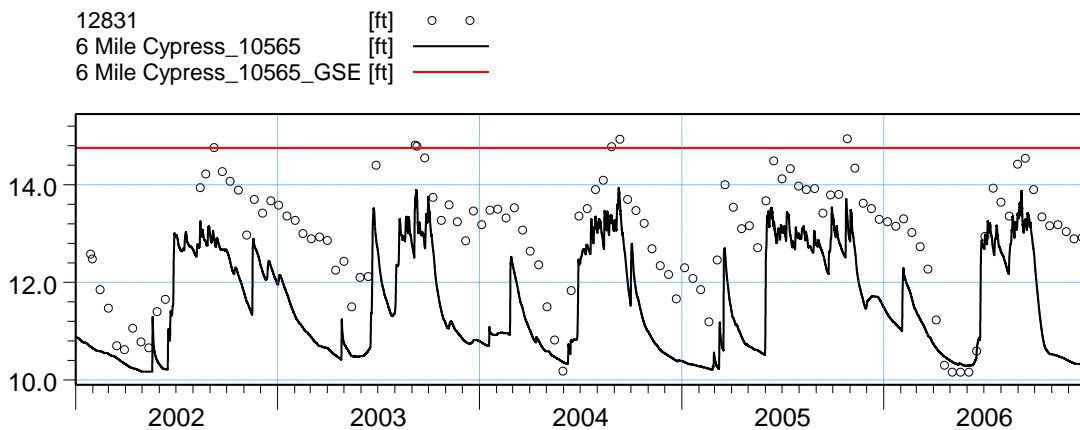


ME=-0.51574  
 MAE=0.864802  
 RMSE=1.04543  
 STDres=0.909366  
 R(Correlation)=0.731534  
 R2(Nash\_Sutcliffe)=0.220577

Figure B33. Stage at stations 6 Mi Cypress 3600 and 6 Mi Cypress 7755, after refinement.

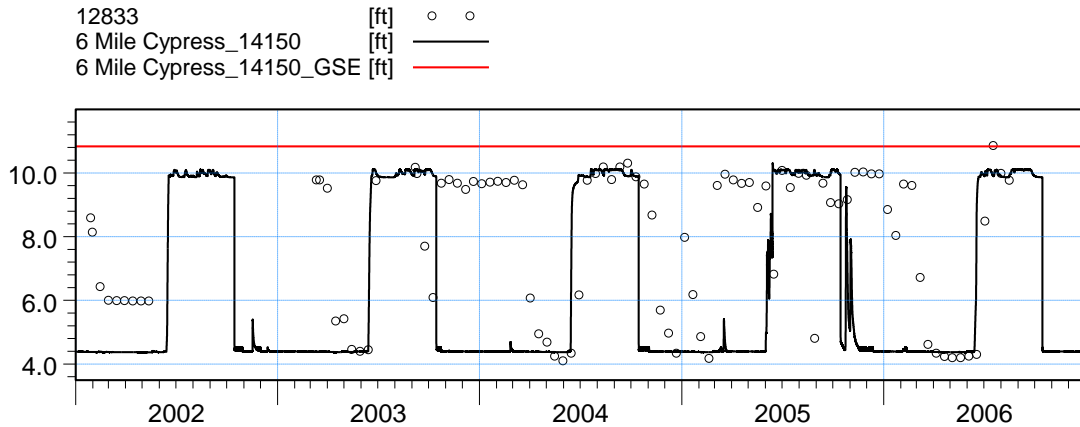


ME=1.56038  
 MAE=1.61927  
 RMSE=1.79889  
 STDres=0.895113  
 R(Correlation)=0.725609  
 R2(Nash\_Sutcliffe)=-0.942251

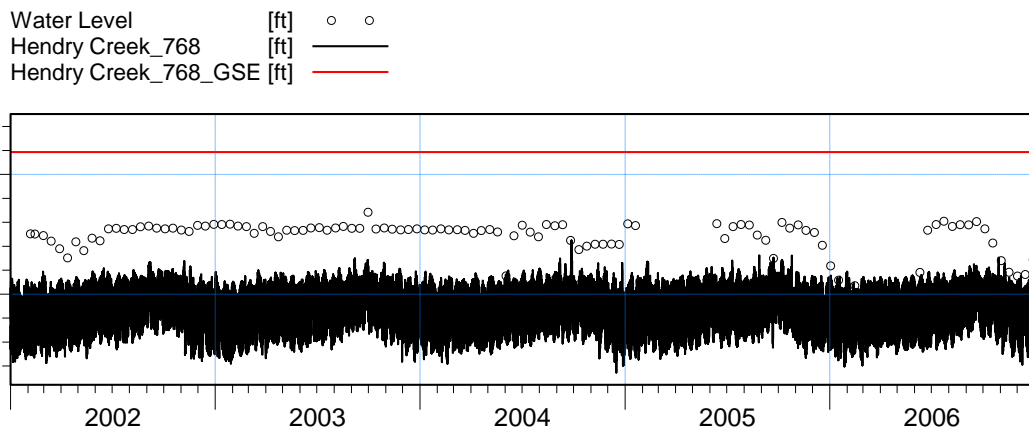


ME=1.43888  
 MAE=1.45631  
 RMSE=1.59616  
 STDres=0.690914  
 R(Correlation)=0.811747  
 R2(Nash\_Sutcliffe)=-0.854769

Figure B34. Stage at stations 6 Mi Cypress 10535 and 6 Mi Cypress 10565, after refinement.

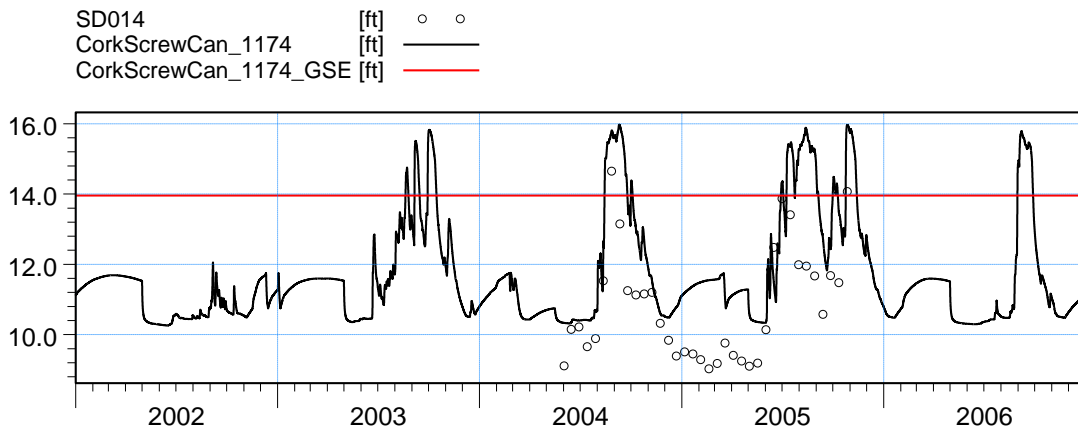


ME=1.71887  
 MAE=2.4831  
 RMSE=3.31772  
 STDres=2.83774  
 R(Correlation)=0.301083  
 R2(Nash\_Sutcliffe)=-1.10748

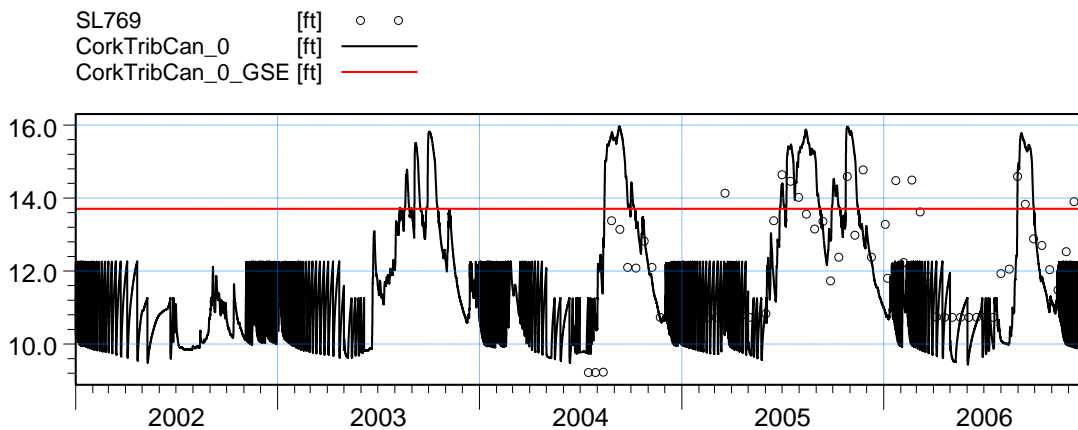


ME=2.76077  
 MAE=2.768  
 RMSE=2.96011  
 STDres=1.06791  
 R(Correlation)=0.0418683  
 R2(Nash\_Sutcliffe)=-11.2114

Figure B35. Stage at stations 6 Mi Cypress 14150 and Hendry Creek 768, after refinement.

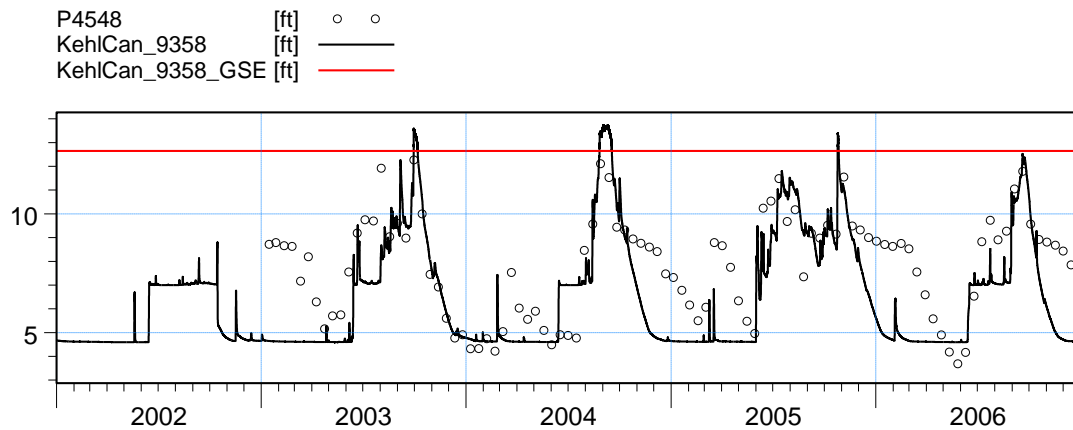


ME=-1.53872  
 MAE=1.62687  
 RMSE=1.92364  
 STDres=1.15445  
 R(Correlation)=0.782989  
 R2(Nash\_Sutcliffe)=-0.587475

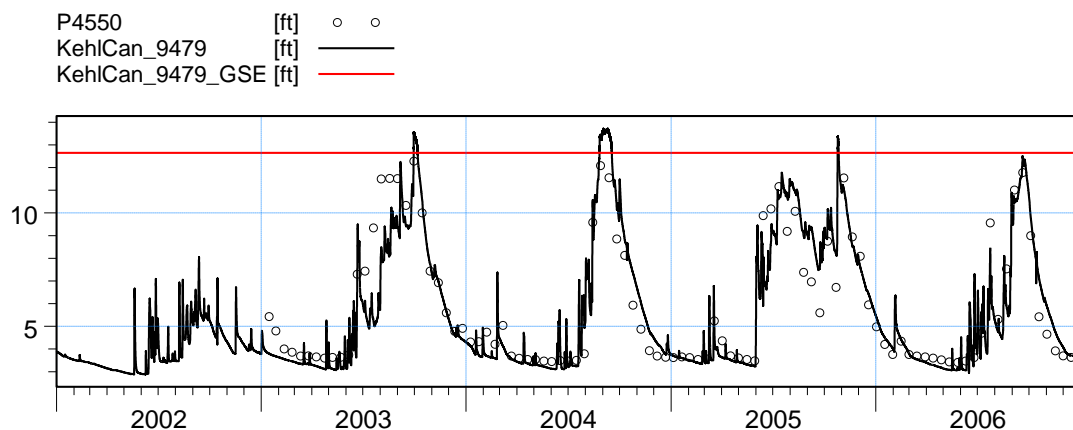


ME=0.135381  
 MAE=1.33816  
 RMSE=1.68236  
 STDres=1.67691  
 R(Correlation)=0.495851  
 R2(Nash\_Sutcliffe)=-0.366319

Figure B36. Stage at stations CorkScrewCan 1174 and CorkTribCan 0, after refinement.

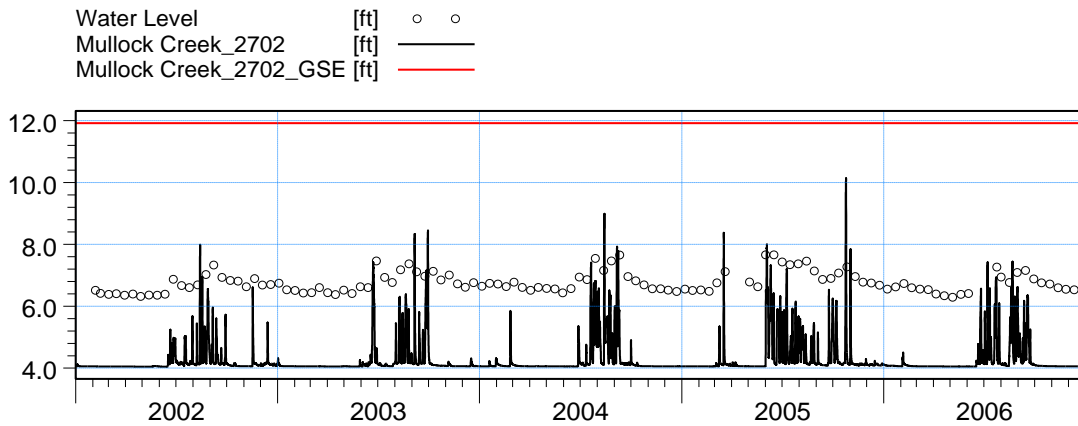


ME=1.25663  
 MAE=1.66719  
 RMSE=2.09345  
 STDres=1.67434  
 R(Correlation)=0.731174  
 R2(Nash\_Sutcliffe)=-0.0161315

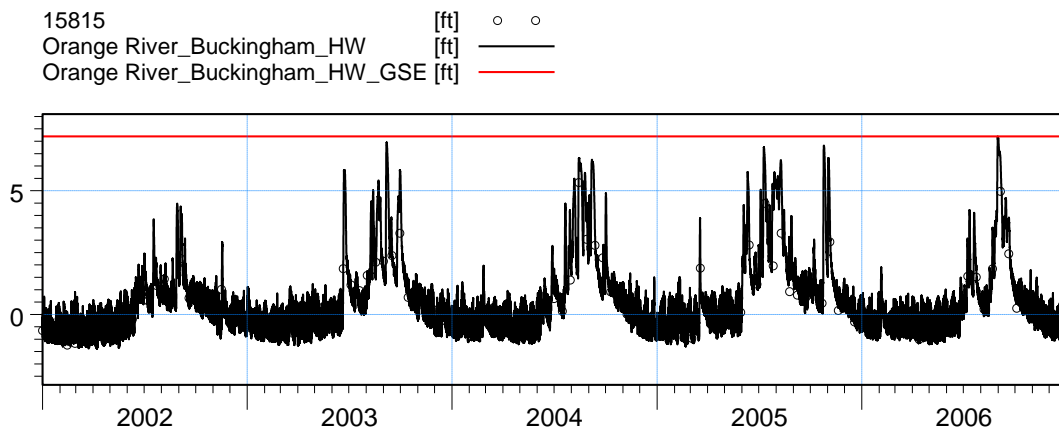


ME=0.0309709  
 MAE=0.763722  
 RMSE=1.07566  
 STDres=1.07522  
 R(Correlation)=0.925463  
 R2(Nash\_Sutcliffe)=0.842275

Figure B37. Stage at stations KehlCan 9358 and KehlCan 9479, after refinement.

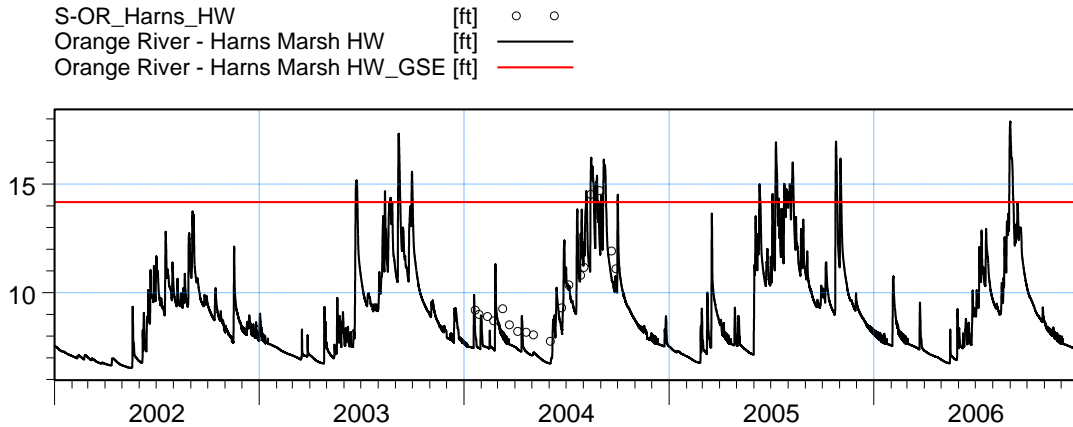


ME=2.50563  
 MAE=2.50992  
 RMSE=2.53893  
 STDres=0.409854  
 R(Correlation)=0.621291  
 R2(Nash\_Sutcliffe)=-51.6848

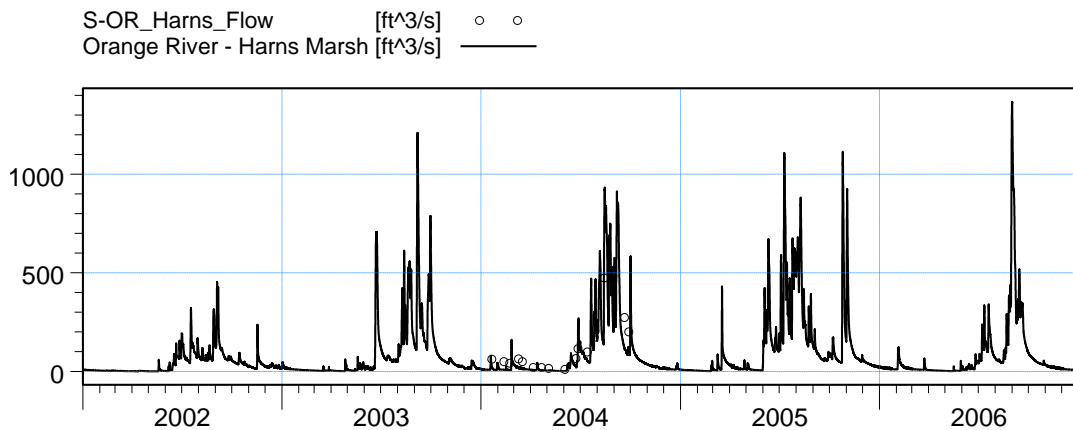


ME=-0.162162  
 MAE=0.518109  
 RMSE=0.736942  
 STDres=0.718879  
 R(Correlation)=0.905109  
 R2(Nash\_Sutcliffe)=0.604474

Figure B38. Stage at stations Mullock Creek\_2702 and OR Buckingham, after refinement.

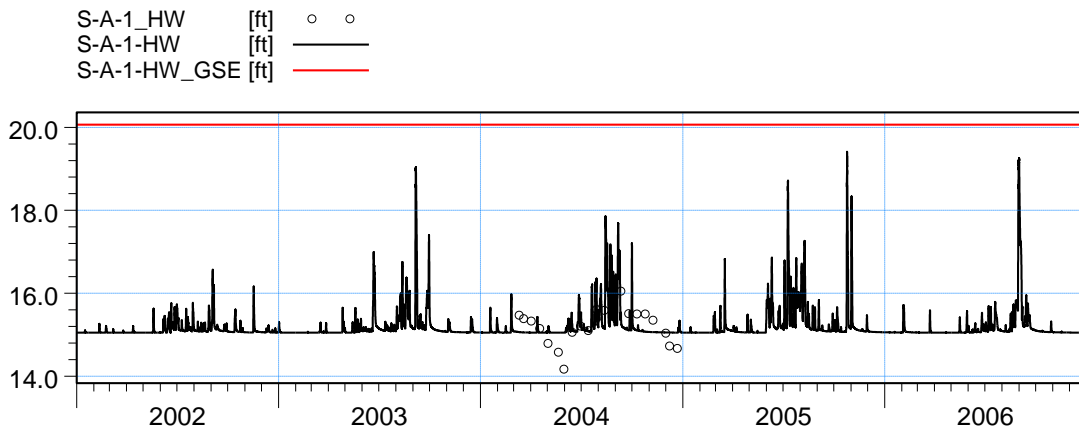


ME=0.56711  
 MAE=1.03529  
 RMSE=1.13885  
 STDres=0.98761  
 R(Correlation)=0.943808  
 R2(Nash\_Sutcliffe)=0.779726

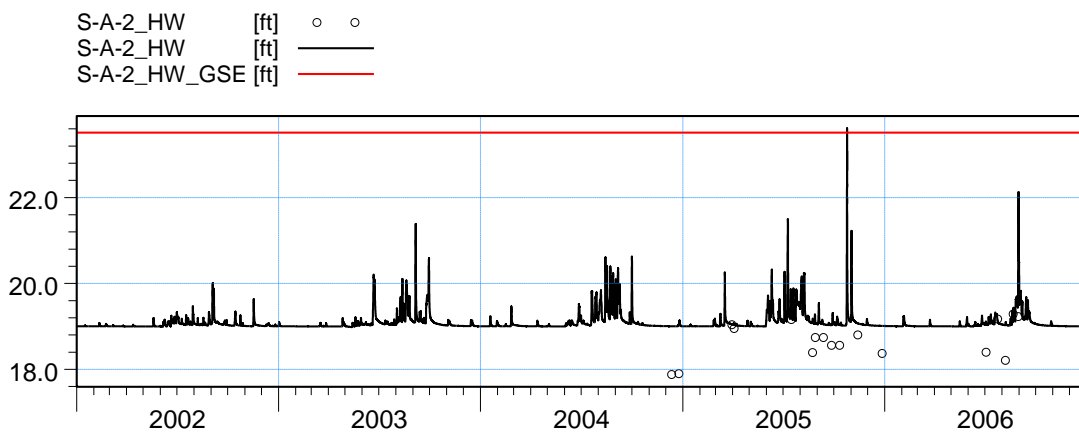


ME=-4.53047  
 MAE=74.7637  
 RMSE=107.167  
 STDres=107.072  
 R(Correlation)=0.918734  
 R2(Nash\_Sutcliffe)=0.616506

Figure B39. Stage at station OR Harns Marsh HW and flow at OR Harns Marsh Q, after refinement.

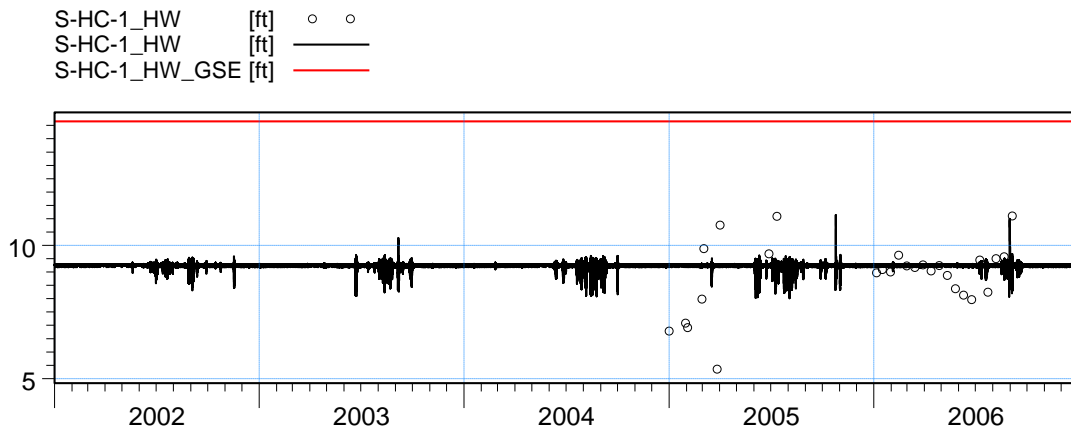


ME=0.0367344  
 MAE=0.364576  
 RMSE=0.456581  
 STDres=0.455101  
 R(Correlation)=0.574239  
 R2(Nash\_Sutcliffe)=0.164268

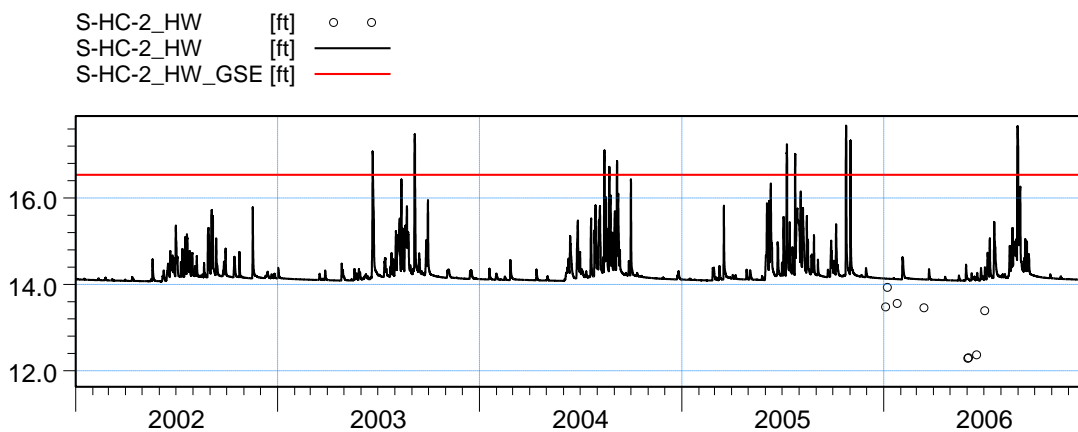


ME=-0.517303  
 MAE=0.542896  
 RMSE=0.630586  
 STDres=0.360606  
 R(Correlation)=0.698681  
 R2(Nash\_Sutcliffe)=-0.613465

Figure B40. Stage at stations S-A-1-HW and S-A-2-HW, after refinement.

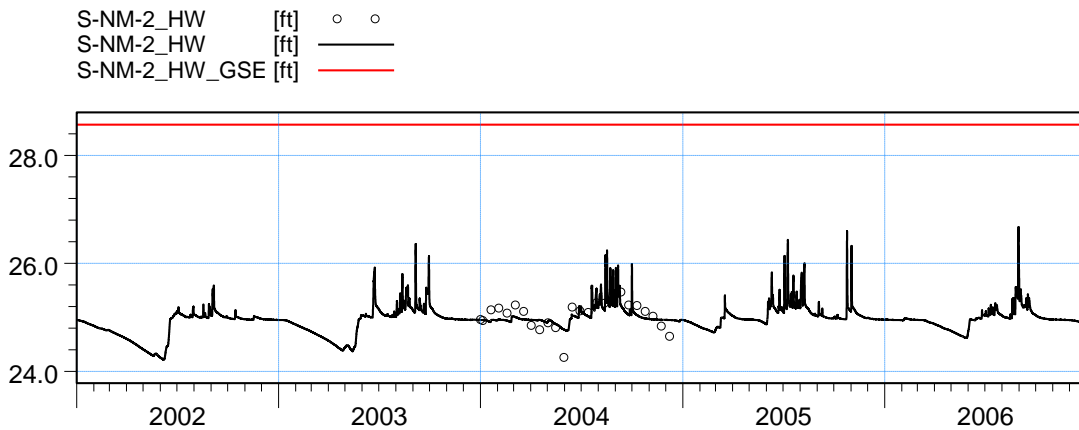


ME=-0.165743  
 MAE=0.721964  
 RMSE=1.07032  
 STDres=1.05741  
 R(Correlation)=-0.0416622  
 R2(Nash\_Sutcliffe)=-0.0494705

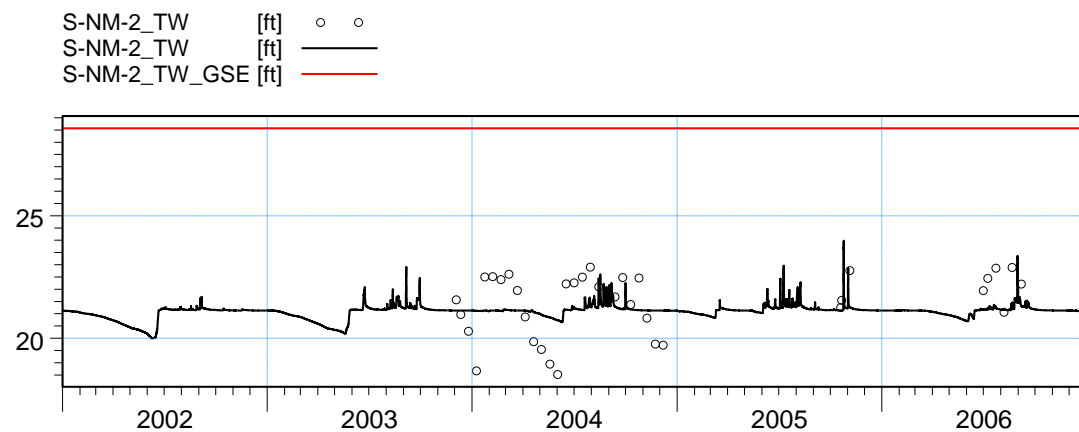


ME=-0.965089  
 MAE=0.967494  
 RMSE=1.12694  
 STDres=0.581899  
 R(Correlation)=0.469869  
 R2(Nash\_Sutcliffe)=-2.05252

Figure B41. Stage at stations S-HC-1\_HW and S-HC-2\_HW, after refinement.

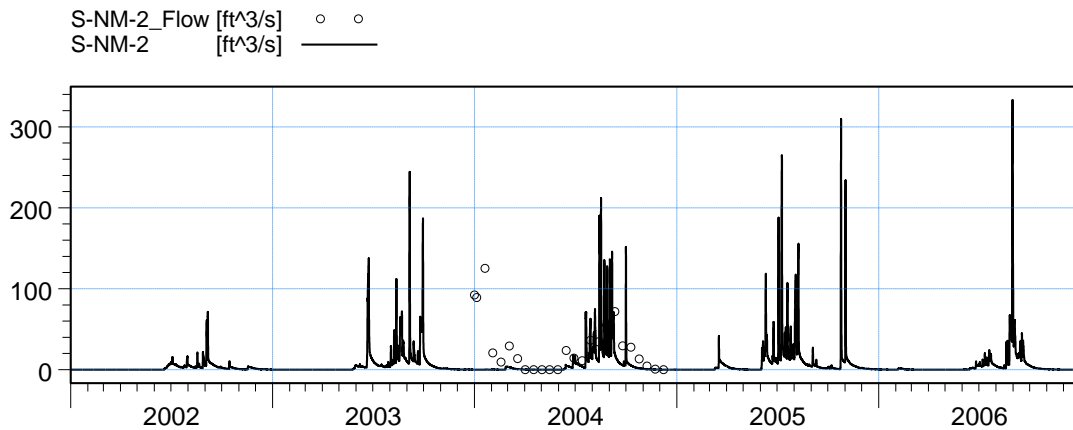


ME=-0.00840827  
 MAE=0.176218  
 RMSE=0.230439  
 STDres=0.230286  
 R(Correlation)=0.649714  
 R2(Nash\_Sutcliffe)=0.420769

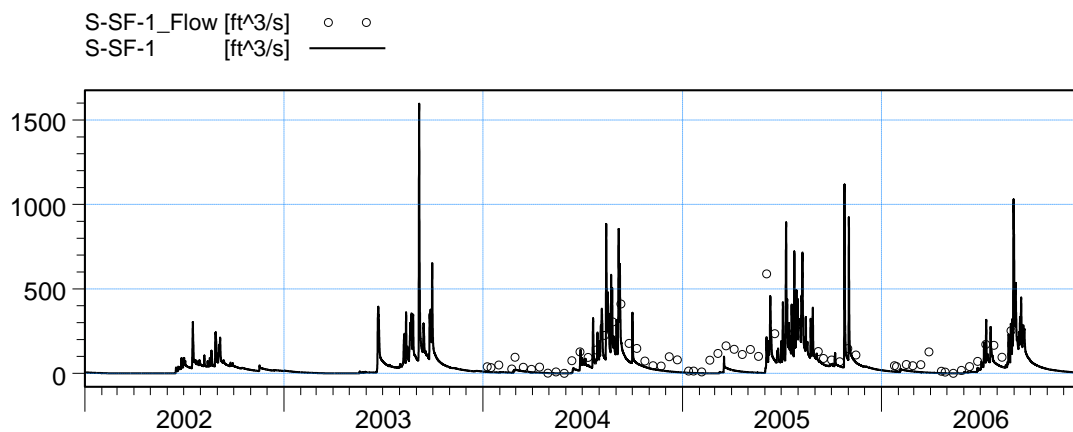


ME=0.799709  
 MAE=1.0344  
 RMSE=1.15746  
 STDres=0.83677  
 R(Correlation)=0.440162  
 R2(Nash\_Sutcliffe)=-0.569621

Figure B42. Stage at stations S-NM-2\_HW and S-NM-2\_TW, after refinement.

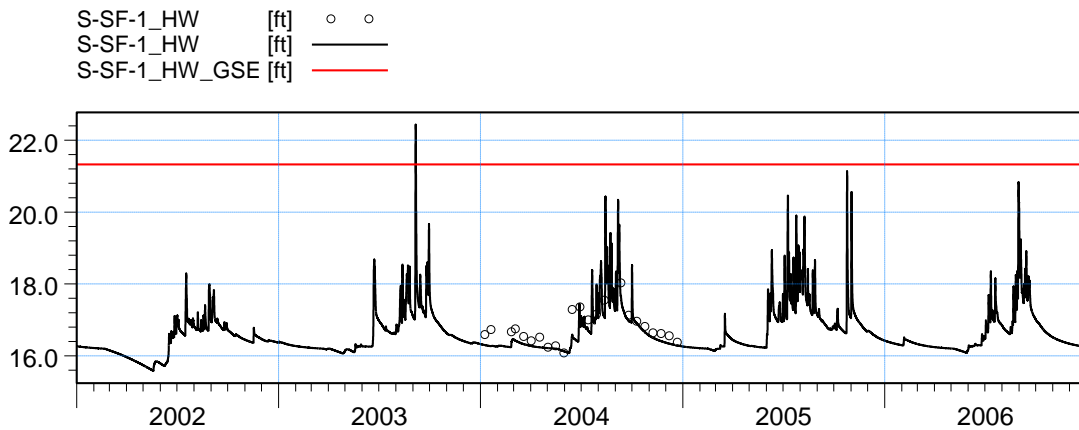


ME=16.7471  
 MAE=20.7897  
 RMSE=35.7248  
 STDres=31.5562  
 R(Correlation)=0.427276  
 R2(Nash\_Sutcliffe)=-0.217012

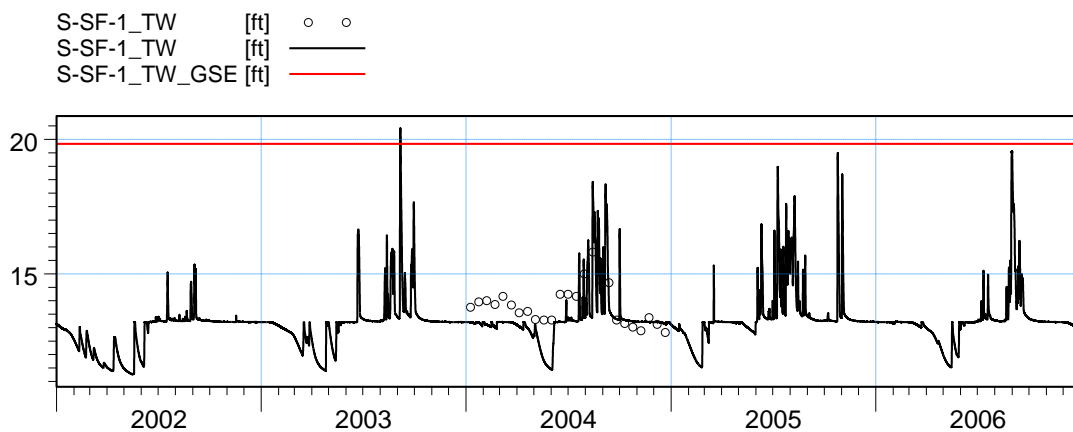


ME=66.218  
 MAE=72.5838  
 RMSE=97.3322  
 STDres=71.3354  
 R(Correlation)=0.742374  
 R2(Nash\_Sutcliffe)=0.119243

Figure B43. Flow at stations S-NM-2 Q and S-SF-1 Q, after refinement.

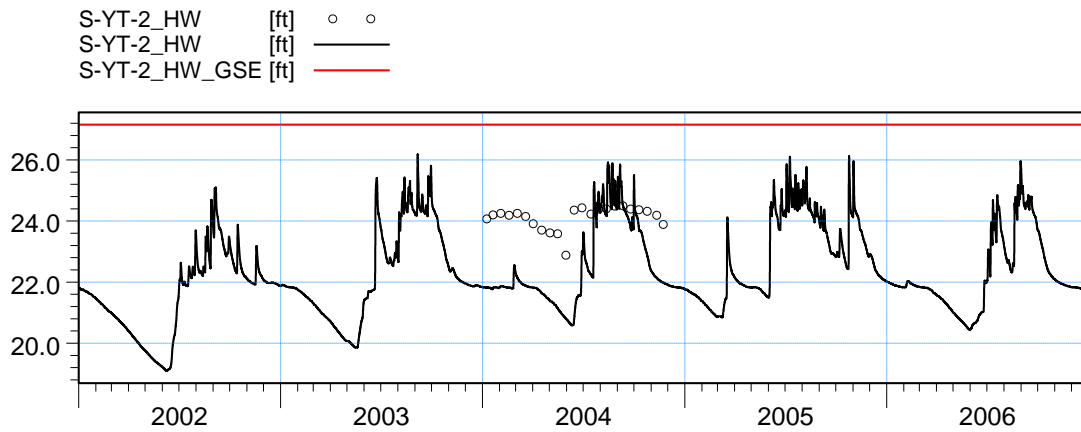


ME=0.14101  
 MAE=0.177881  
 RMSE=0.230141  
 STDres=0.181881  
 R(Correlation)=0.881874  
 R2(Nash\_Sutcliffe)=0.373379



ME=-0.0309521  
 MAE=0.299845  
 RMSE=0.471354  
 STDres=0.470336  
 R(Correlation)=0.441746  
 R2(Nash\_Sutcliffe)=-0.22742

Figure B44. Stage at stations S-SF-1\_HW and S-SF-1\_TW, after refinement.



ME=1.54173  
 MAE=1.65619  
 RMSE=1.87885  
 STDres=1.07384  
 R(Correlation)=0.739977  
 R2(Nash\_Sutcliffe)=-19.2985

Figure B45. Stage at station S-YT-2\_HW, after refinement.

**Appendix B3. Groundwater deep wells south from Caloosahatchee**

| Station Name | before refinement |          |           |       |            | after refinement |          |           |      |            |
|--------------|-------------------|----------|-----------|-------|------------|------------------|----------|-----------|------|------------|
|              | ME (ft)           | MAE (ft) | RMSE (ft) | R     | PL         | ME (ft)          | MAE (ft) | RMSE (ft) | R    | PL         |
| L-2192       | 11.70             | 12.82    | 14.50     | -0.77 | <b>3.0</b> | 1.17             | 4.16     | 5.30      | 0.28 | <b>2.8</b> |
| L-5649       | -0.16             | 3.31     | 3.82      | 0.10  | <b>2.5</b> | -7.52            | 7.52     | 8.17      | 0.67 | <b>2.8</b> |
| L-5664       | -11.39            | 11.39    | 12.07     | 0.67  | <b>2.8</b> | -9.17            | 9.17     | 10.12     | 0.49 | <b>3.0</b> |
| L-5669R      | 1.97              | 2.29     | 2.56      | -0.18 | <b>2.8</b> | -0.25            | 0.57     | 0.69      | 0.77 | <b>1.0</b> |
| L-5673       | -7.63             | 7.72     | 8.80      | -0.22 | <b>3.0</b> | -8.43            | 8.47     | 9.19      | 0.60 | <b>2.8</b> |
| L-5874       | 10.05             | 10.05    | 11.03     | 0.22  | <b>3.0</b> | -3.09            | 3.53     | 4.36      | 0.70 | <b>2.8</b> |

Table B4. Statistical parameters and level of performance at deep groundwater monitoring wells (computational layer 3) south of the Caloosahatchee River. The green color indicates the highest performance level (1.0, 1.2 and 1.5), yellow for medium (1.8, 2.0, 2.3, 2.5) and orange for low (2.8, 3.0).

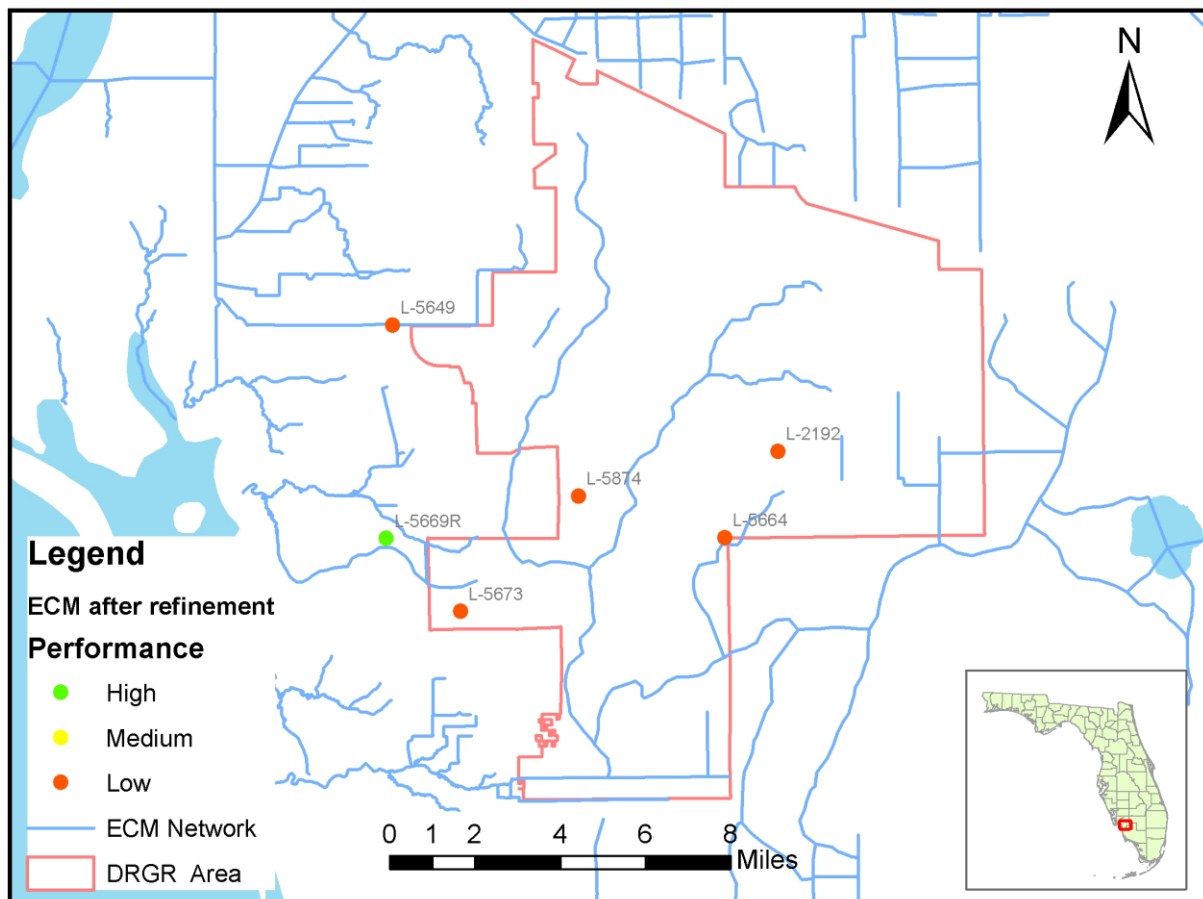
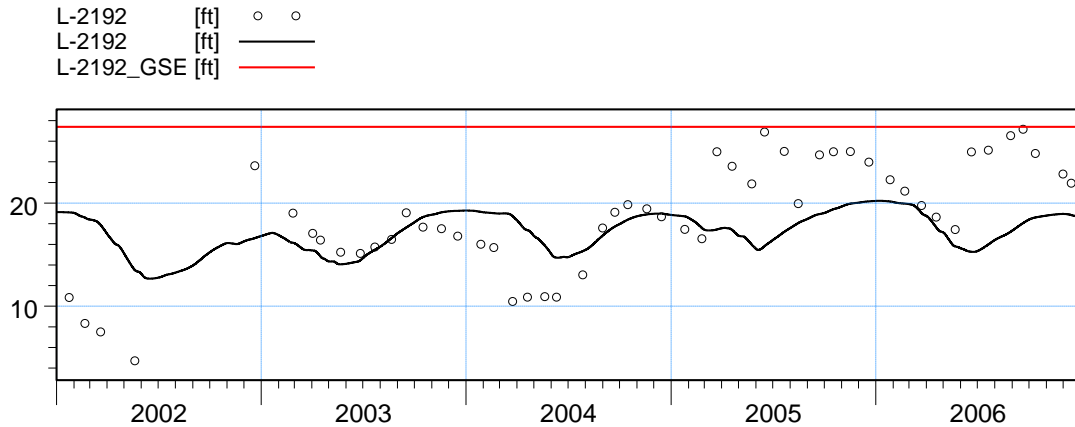
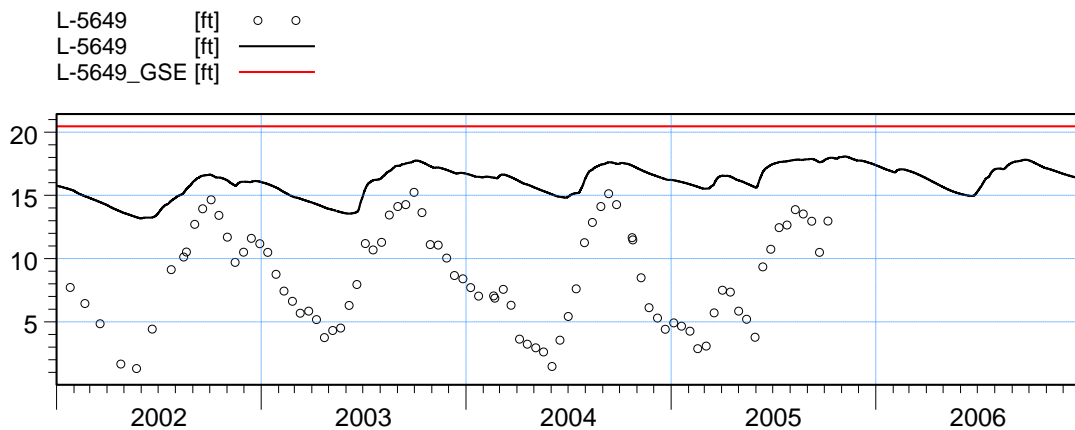


Figure B46. Average performance level at deep groundwater monitoring wells south of the Caloosahatchee River, after the refinement process.

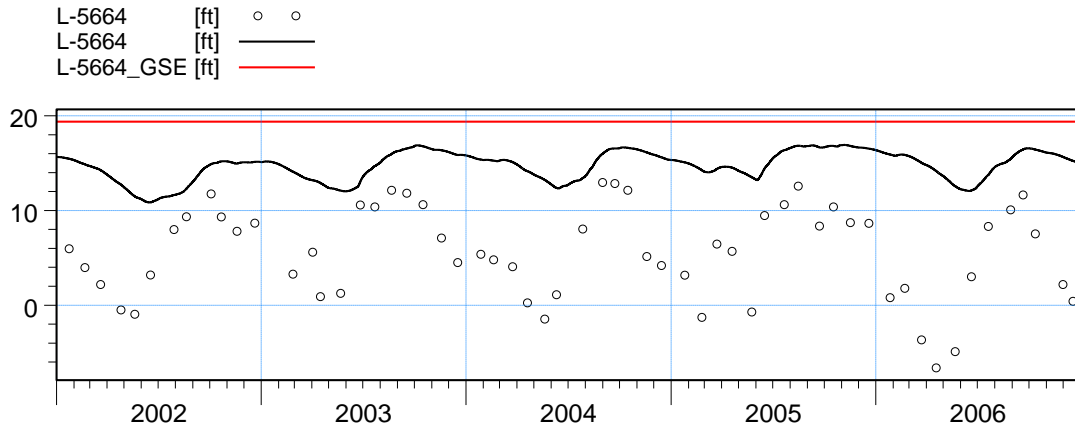


ME=1.16544  
 MAE=4.15687  
 RMSE=5.29633  
 STDres=5.16652  
 R(Correlation)=0.275558  
 R2(Nash\_Sutcliffe)=0.0270882

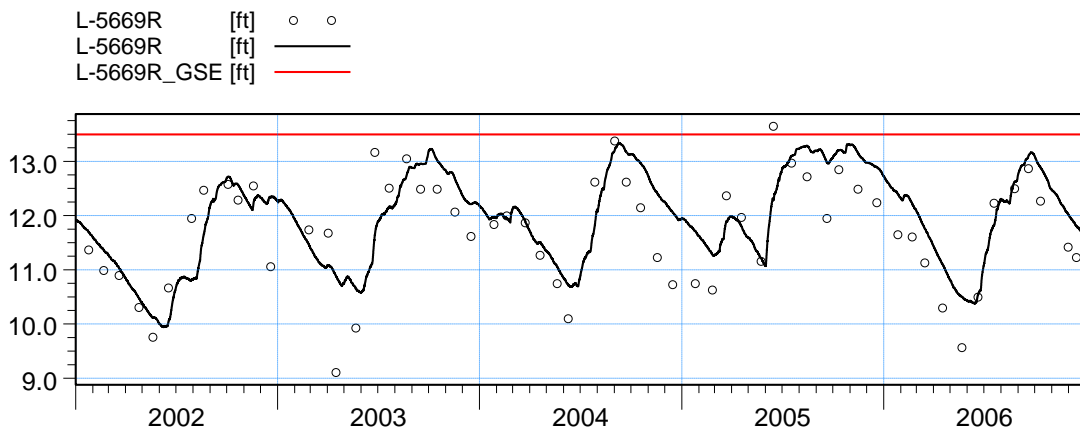


ME=-7.51639  
 MAE=7.51639  
 RMSE=8.16673  
 STDres=3.19365  
 R(Correlation)=0.672583  
 R2(Nash\_Sutcliffe)=-3.57074

Figure B47. Groundwater elevation at wells L-2192 and L-5649, after refinement.

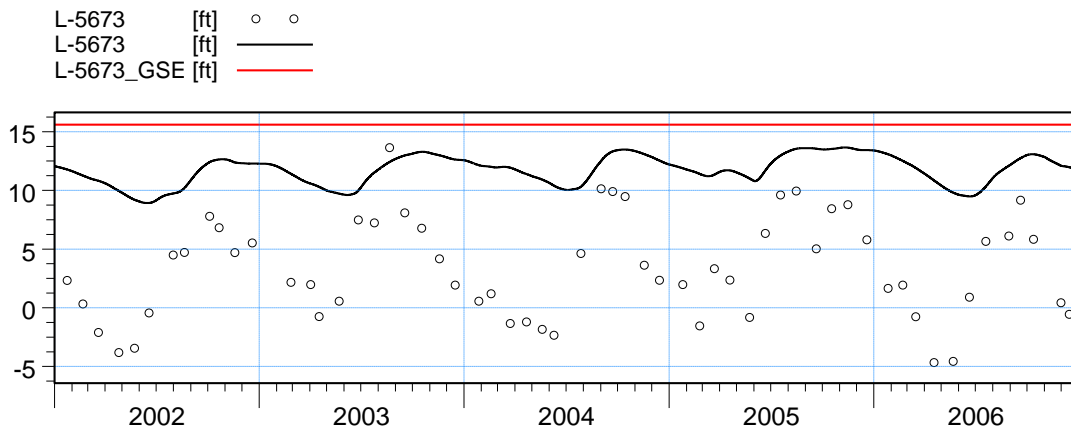


ME=-9.17243  
 MAE=9.17243  
 RMSE=10.1238  
 STDres=4.28469  
 R(Correlation)=0.49174  
 R2(Nash\_Sutcliffe)=-3.38954

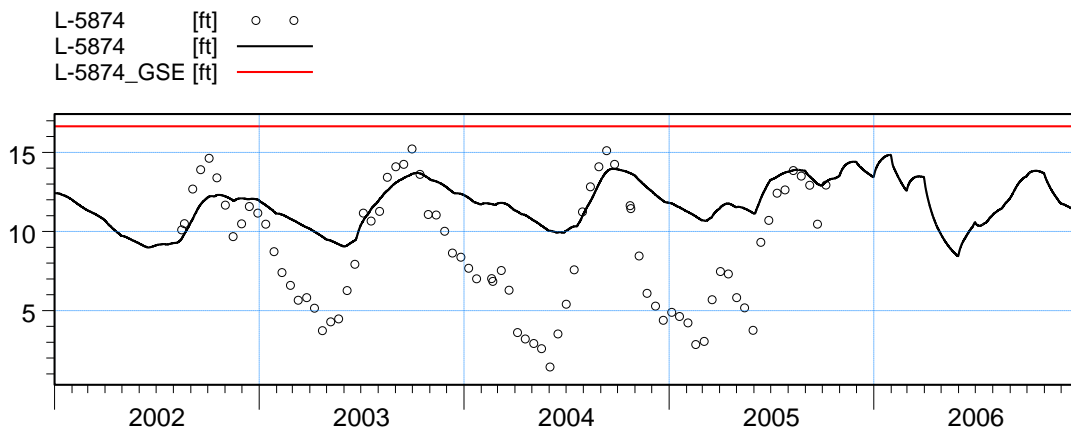


ME=-0.25114  
 MAE=0.567471  
 RMSE=0.68939  
 STDres=0.642018  
 R(Correlation)=0.773239  
 R2(Nash\_Sutcliffe)=0.526848

Figure B48. Groundwater elevation at wells L-5664 and L-5669R, after refinement.



ME=-8.43256  
 MAE=8.47377  
 RMSE=9.19005  
 STDres=3.65362  
 R(Correlation)=0.594992  
 R2(Nash\_Sutcliffe)=-3.65384



ME=-3.08921  
 MAE=3.53472  
 RMSE=4.35997  
 STDres=3.0767  
 R(Correlation)=0.695819  
 R2(Nash\_Sutcliffe)=-0.306047

Figure B49. Groundwater elevation at wells L-5673 and L-5874, after refinement.



**Appendix B4. Other groundwater well stations south of the Caloosahatchee**

| Station Name | Comp. layer | before refinement |          |           |      |            | after refinement |          |           |      |            |
|--------------|-------------|-------------------|----------|-----------|------|------------|------------------|----------|-----------|------|------------|
|              |             | ME (ft)           | MAE (ft) | RMSE (ft) | R    | PL         | ME (ft)          | MAE (ft) | RMSE (ft) | R    | PL         |
| 40-GW1       | 1           | -0.04             | 0.73     | 1.11      | 0.67 | <b>1.3</b> | 0.10             | 0.73     | 1.06      | 0.72 | <b>1.0</b> |
| 40-GW2       | 2           | -3.23             | 3.23     | 3.54      | 0.69 | <b>2.8</b> | 0.59             | 1.28     | 1.71      | 0.42 | <b>2.0</b> |
| 40-GW4       | 2           | 2.88              | 2.88     | 3.04      | 0.79 | <b>2.5</b> | 1.75             | 1.75     | 1.97      | 0.80 | <b>1.8</b> |
| 40-GW5       | 1           | 3.14              | 3.14     | 3.22      | 0.86 | <b>2.5</b> | 1.86             | 1.86     | 2.01      | 0.85 | <b>1.8</b> |
| 40-GW6       | 1           | 0.44              | 1.09     | 1.38      | 0.51 | <b>1.8</b> | 0.77             | 1.28     | 1.68      | 0.44 | <b>2.0</b> |
| 40-GW7       | 1           | -1.32             | 1.35     | 1.71      | 0.62 | <b>2.0</b> | -0.46            | 0.82     | 1.16      | 0.66 | <b>1.3</b> |
| 40-GW8       | 1           | -0.09             | 0.77     | 0.91      | 0.79 | <b>1.0</b> | 0.20             | 0.71     | 0.92      | 0.76 | <b>1.0</b> |
| 40-GW9       | 1           | -3.89             | 3.89     | 3.92      | 0.84 | <b>2.5</b> | -3.79            | 3.79     | 3.83      | 0.86 | <b>2.5</b> |
| 40-GW11      | 1           | -3.90             | 3.90     | 4.08      | 0.79 | <b>2.5</b> | -3.76            | 3.76     | 3.96      | 0.85 | <b>2.5</b> |
| 40-GW12      | 1           | 2.66              | 2.66     | 2.76      | 0.72 | <b>2.5</b> | 1.59             | 1.60     | 1.84      | 0.78 | <b>1.8</b> |
| 40-GW13      | 1           | -0.18             | 0.70     | 0.93      | 0.75 | <b>1.0</b> | -0.22            | 0.69     | 0.90      | 0.80 | <b>1.0</b> |
| 41-GW1       | 1           | -1.05             | 1.14     | 1.43      | 0.50 | <b>2.3</b> | -0.75            | 1.01     | 1.27      | 0.50 | <b>2.0</b> |
| 41-GW3       | 1           | -5.40             | 5.40     | 5.44      | 0.83 | <b>2.5</b> | -4.81            | 4.81     | 4.87      | 0.81 | <b>2.5</b> |
| 41-GW4       | 1           | -1.24             | 1.24     | 1.33      | 0.86 | <b>1.8</b> | -0.85            | 0.85     | 1.00      | 0.81 | <b>1.0</b> |
| 41-GW6       | 1           | 0.80              | 0.95     | 1.17      | 0.75 | <b>1.0</b> | 1.29             | 1.35     | 1.55      | 0.75 | <b>1.8</b> |
| 42-GW1       | 1           | -1.97             | 2.23     | 2.52      | 0.50 | <b>2.8</b> | -2.01            | 2.27     | 2.57      | 0.46 | <b>3.0</b> |
| 42-GW2       | 1           | -2.35             | 2.35     | 2.52      | 0.87 | <b>2.5</b> | -1.95            | 1.95     | 2.09      | 0.86 | <b>1.8</b> |
| 42-GW3       | 1           | -4.50             | 4.50     | 4.54      | 0.54 | <b>2.8</b> | -4.35            | 4.35     | 4.39      | 0.54 | <b>2.8</b> |
| 44-GW2       | 1           | -2.30             | 2.30     | 2.42      | 0.66 | <b>2.5</b> | -1.75            | 1.76     | 1.93      | 0.59 | <b>2.0</b> |
| 44-GW3       | 1           | -0.07             | 1.01     | 1.25      | 0.48 | <b>2.0</b> | 0.02             | 1.03     | 1.30      | 0.46 | <b>2.0</b> |
| 45-GW1       | 1           | -2.98             | 2.98     | 3.06      | 0.53 | <b>2.8</b> | -2.92            | 2.92     | 2.99      | 0.59 | <b>2.8</b> |
| 45-GW2       | 1           | -2.27             | 2.27     | 2.45      | 0.81 | <b>2.3</b> | -2.26            | 2.26     | 2.44      | 0.68 | <b>2.5</b> |
| 45-GW3       | 1           | -3.70             | 3.70     | 3.99      | -0.1 | <b>3.0</b> | -3.60            | 3.60     | 3.92      | 0.0  | <b>3.0</b> |
| 45-GW4       | 1           | 0.51              | 0.62     | 0.88      | 0.62 | <b>1.3</b> | 0.47             | 0.58     | 0.84      | 0.65 | <b>1.3</b> |
| 46A-GW3      | 1           | -2.28             | 2.29     | 2.49      | 0.74 | <b>2.3</b> | -1.48            | 1.54     | 1.74      | 0.76 | <b>1.8</b> |
| 46A-GW4      | 1           | -1.70             | 1.70     | 1.88      | 0.79 | <b>1.8</b> | -0.40            | 1.11     | 1.35      | 0.74 | <b>1.5</b> |
| 46A-GW10     | 1           | -0.17             | 0.52     | 0.73      | 0.82 | <b>1.0</b> | -0.26            | 0.54     | 0.73      | 0.82 | <b>1.0</b> |
| 46A-GW11     | 1           | -1.37             | 1.37     | 1.64      | 0.85 | <b>1.8</b> | -0.91            | 0.91     | 1.02      | 0.93 | <b>1.0</b> |
| 46A-GW12     | 1           | -1.73             | 1.88     | 2.40      | 0.20 | <b>2.3</b> | -1.31            | 1.52     | 1.88      | 0.63 | <b>2.0</b> |
| 46A-GW13     | 1           | -1.64             | 1.64     | 1.74      | 0.90 | <b>1.8</b> | -1.01            | 1.10     | 1.23      | 0.84 | <b>1.5</b> |
| 46A-GW14     | 1           | -0.91             | 1.03     | 1.23      | 0.71 | <b>1.3</b> | -0.82            | 1.10     | 1.26      | 0.61 | <b>1.8</b> |
| 46A-GW15     | 1           | -1.09             | 1.10     | 1.27      | 0.87 | <b>1.8</b> | -0.24            | 0.55     | 0.70      | 0.87 | <b>1.0</b> |
| 46A-GW21     | 1           | -0.96             | 0.99     | 1.21      | 0.79 | <b>1.0</b> | -0.89            | 1.00     | 1.18      | 0.75 | <b>1.0</b> |
| 46A-GW22     | 1           | -1.74             | 1.74     | 1.83      | 0.86 | <b>1.8</b> | -1.29            | 1.34     | 1.48      | 0.84 | <b>1.8</b> |
| 46A-GW25     | 1           | 0.22              | 0.41     | 0.55      | 0.89 | <b>1.0</b> | 0.33             | 0.47     | 0.61      | 0.88 | <b>1.0</b> |
| 46A-GW26     | 1           | -0.88             | 0.91     | 1.05      | 0.78 | <b>1.0</b> | -0.10            | 0.54     | 0.69      | 0.80 | <b>1.0</b> |
| 46C-GW1      | 1           | -2.20             | 2.20     | 2.28      | 0.64 | <b>2.5</b> | -1.96            | 1.98     | 2.10      | 0.60 | <b>2.0</b> |



| Station Name | Comp. layer | before refinement |          |           |      |            | after refinement |          |           |      |            |
|--------------|-------------|-------------------|----------|-----------|------|------------|------------------|----------|-----------|------|------------|
|              |             | ME (ft)           | MAE (ft) | RMSE (ft) | R    | PL         | ME (ft)          | MAE (ft) | RMSE (ft) | R    | PL         |
| 46C-GW2      | 1           | -1.61             | 1.65     | 1.81      | 0.63 | <b>2.0</b> | -1.07            | 1.27     | 1.46      | 0.57 | <b>2.0</b> |
| 46C-GW3      | 1           | -0.99             | 1.01     | 1.22      | 0.39 | <b>1.8</b> | -0.54            | 0.64     | 0.81      | 0.72 | <b>1.0</b> |
| 46C-GW6      | 1           | 5.06              | 5.06     | 5.11      | 0.66 | <b>2.8</b> | 4.45             | 4.45     | 4.48      | 0.75 | <b>2.5</b> |
| 46C-GW7      | 1           | -0.65             | 0.73     | 1.02      | 0.56 | <b>1.3</b> | -0.23            | 0.68     | 0.91      | 0.59 | <b>1.3</b> |
| 46C-GW8      | 1           | 1.50              | 1.50     | 1.62      | 0.85 | <b>1.8</b> | 1.33             | 1.35     | 1.47      | 0.84 | <b>1.8</b> |
| 49-GW12      | 1           | 0.79              | 0.88     | 1.10      | 0.90 | <b>1.0</b> | 0.78             | 0.88     | 1.09      | 0.91 | <b>1.0</b> |
| 49-GW14      | 1           | -0.05             | 0.61     | 0.75      | 0.86 | <b>1.0</b> | -0.05            | 0.59     | 0.73      | 0.87 | <b>1.0</b> |
| 49-GW15      | 1           | 3.41              | 3.41     | 3.50      | 0.52 | <b>2.8</b> | 3.31             | 3.31     | 3.41      | 0.51 | <b>2.8</b> |
| 49L-GW1      | 1           | 0.48              | 0.83     | 1.00      | 0.78 | <b>1.0</b> | 0.26             | 0.71     | 0.94      | 0.77 | <b>1.0</b> |
| HF1_G        | 1           | -4.01             | 4.25     | 5.84      | 0.20 | <b>3.0</b> | -4.25            | 4.41     | 5.96      | 0.28 | <b>3.0</b> |
| HF2_G        | 1           | -0.08             | 0.94     | 1.14      | 0.68 | <b>1.3</b> | -0.32            | 1.08     | 1.28      | 0.72 | <b>1.5</b> |
| HF3_G        | 1           | 2.67              | 2.69     | 3.30      | 0.80 | <b>2.5</b> | 2.27             | 2.32     | 2.69      | 0.80 | <b>2.5</b> |
| HF4_G        | 1           | -1.07             | 1.54     | 1.96      | 0.58 | <b>2.0</b> | -1.39            | 1.80     | 2.22      | 0.61 | <b>2.0</b> |
| HF7_G        | 1           | -1.25             | 1.63     | 2.01      | 0.51 | <b>2.0</b> | -1.40            | 1.70     | 2.09      | 0.57 | <b>2.0</b> |

Table B5. Statistical parameters and level of performance at shallow groundwater wells (computational layers 1 and 2) south of the Caloosahatchee River and outside the DR/GR Area. The green color indicates the highest performance level (1.0, 1.2 and 1.5), yellow for medium (1.8, 2.0, 2.3, 2.5) and orange for low (2.8, 3.0).

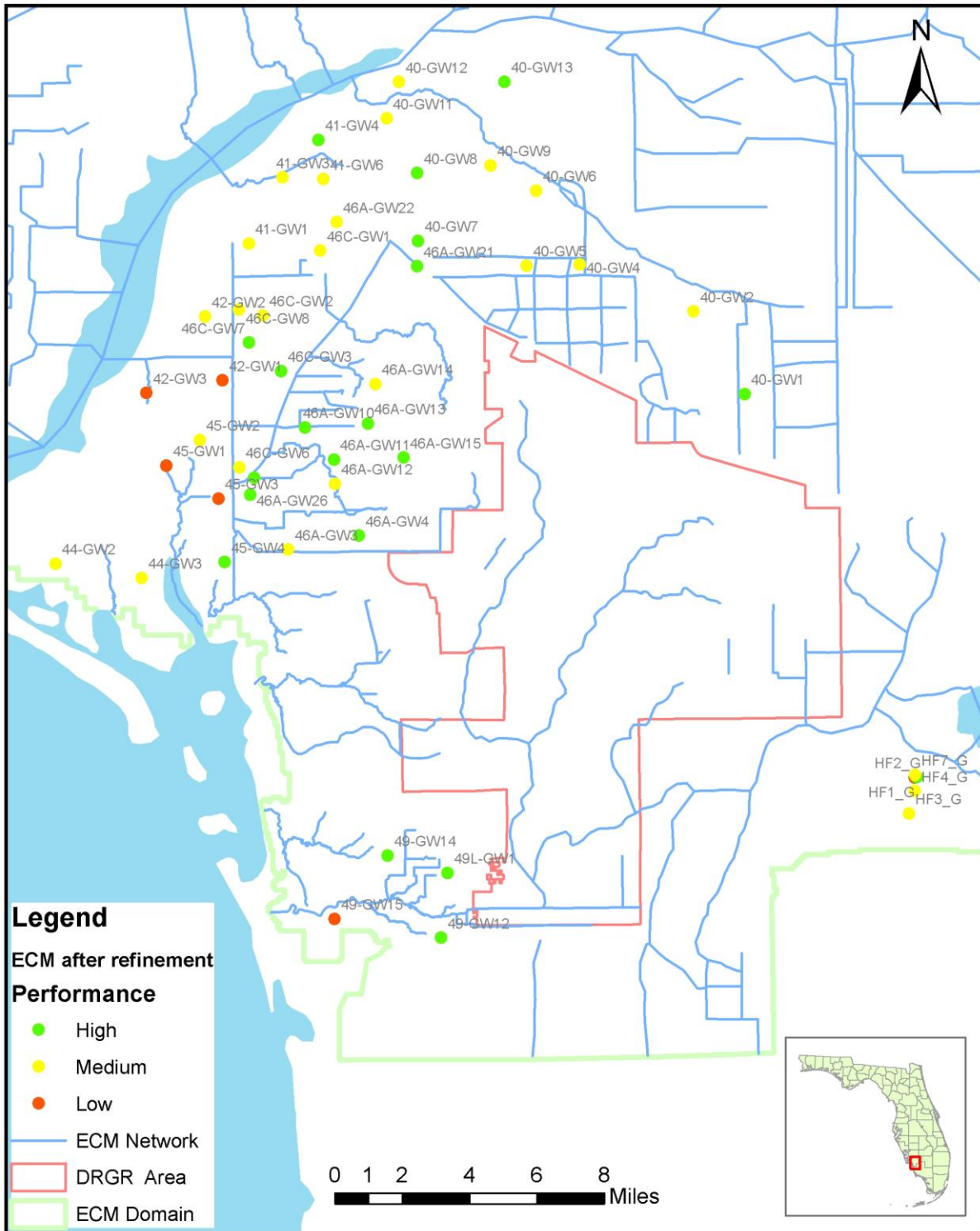
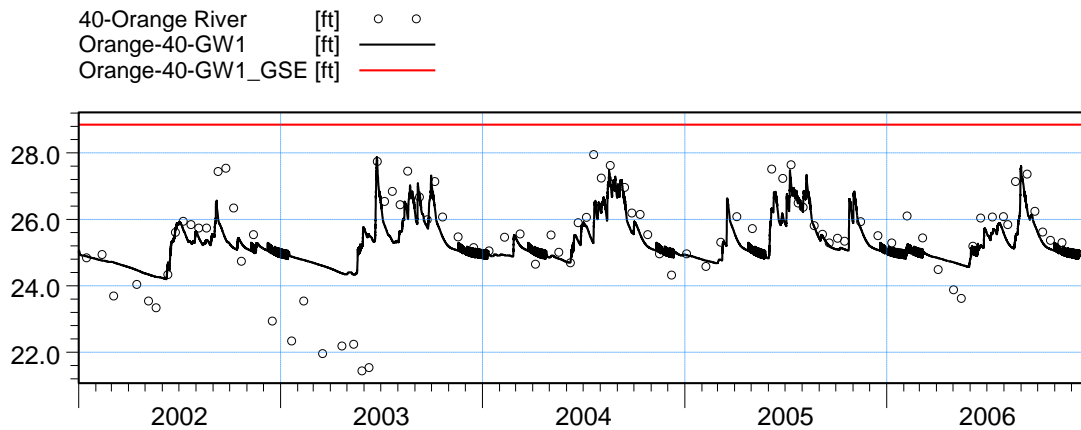
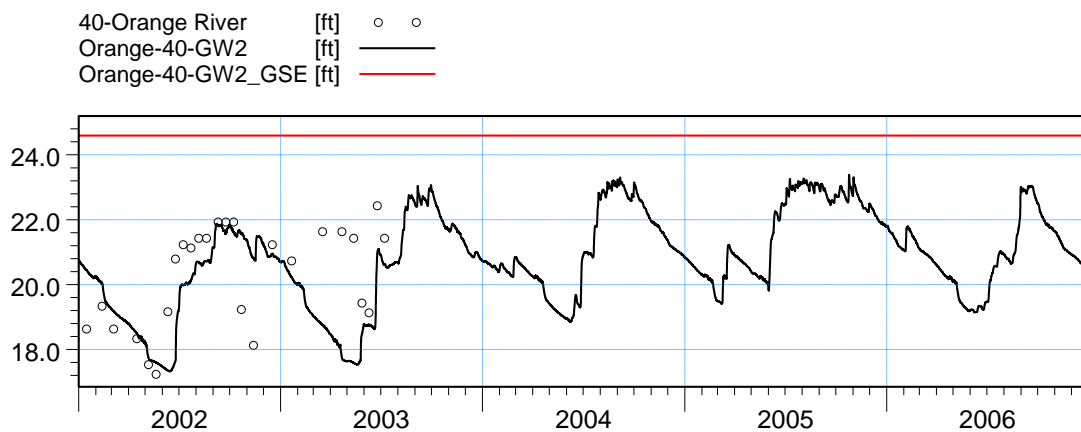


Figure B50. Average performance level at shallow groundwater monitoring wells south of the Caloosahatchee River, after the refinement process.

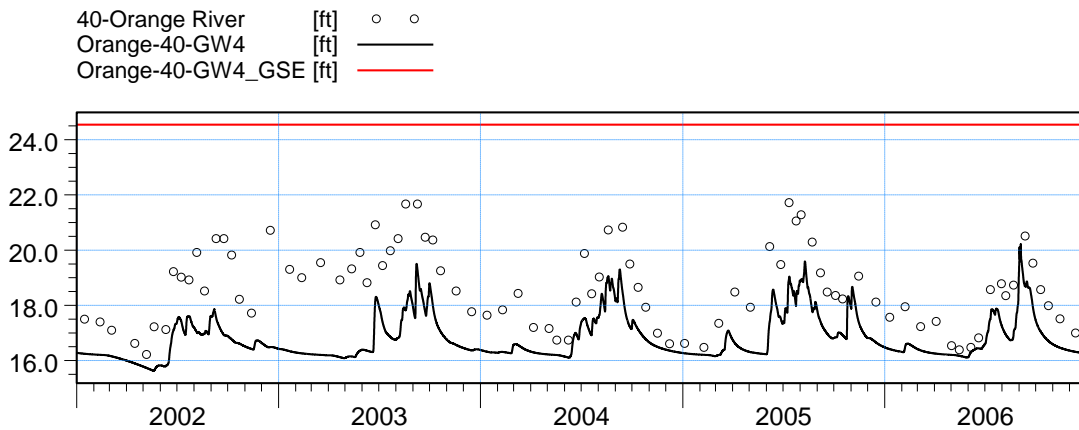


ME=0.0970131  
 MAE=0.725545  
 RMSE=1.0569  
 STDres=1.05243  
 R(Correlation)=0.721884  
 R2(Nash\_Sutcliffe)=0.444446

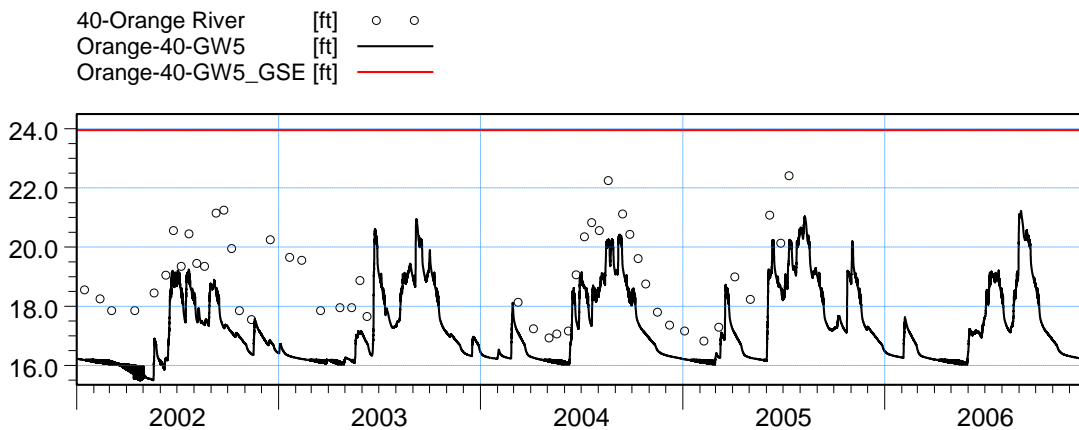


ME=0.594592  
 MAE=1.28016  
 RMSE=1.71354  
 STDres=1.60707  
 R(Correlation)=0.420508  
 R2(Nash\_Sutcliffe)=-0.256598

Figure B51. Groundwater elevation at wells 40-GW1 and 40-GW2, after refinement.

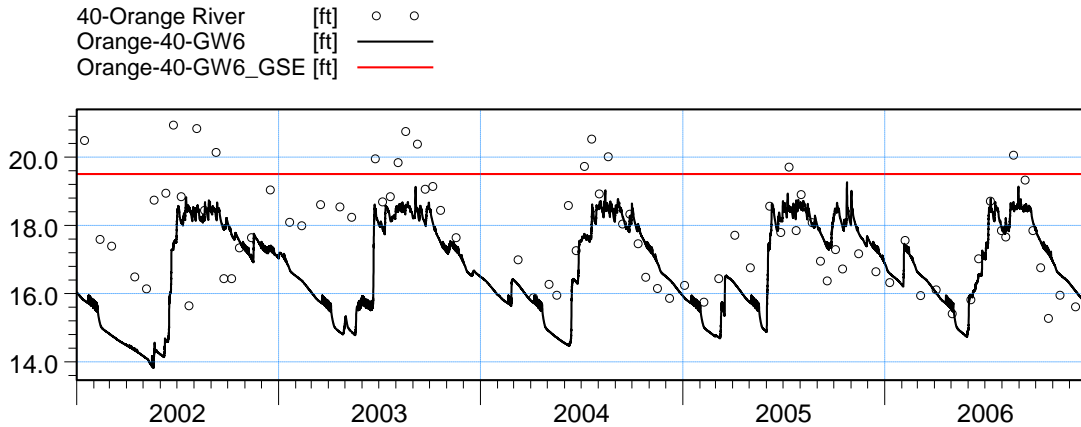


ME=1.75012  
 MAE=1.75012  
 RMSE=1.97403  
 STDres=0.91318  
 R(Correlation)=0.799139  
 R2(Nash\_Sutcliffe)=-0.957346

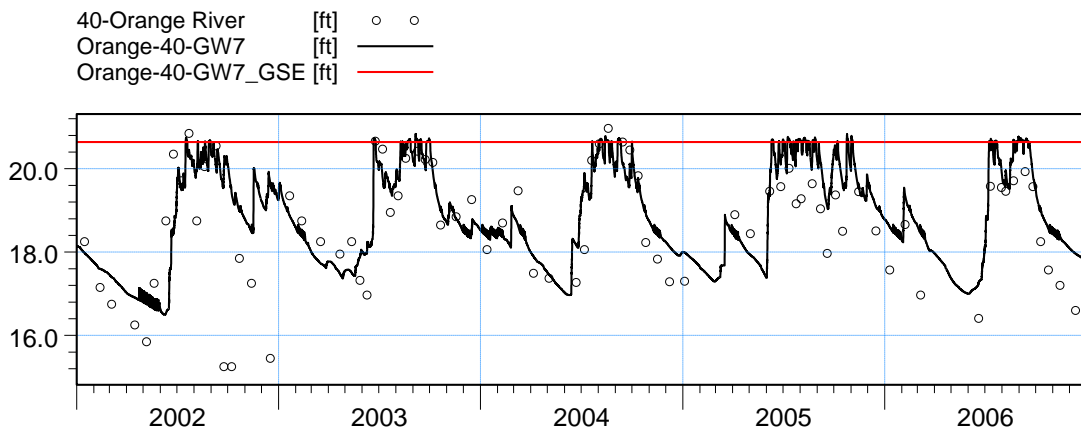


ME=1.85734  
 MAE=1.85734  
 RMSE=2.01195  
 STDres=0.773446  
 R(Correlation)=0.850649  
 R2(Nash\_Sutcliffe)=-0.896539

Figure B52. Groundwater elevation at wells 40-GW4 and 40-GW5, after refinement.

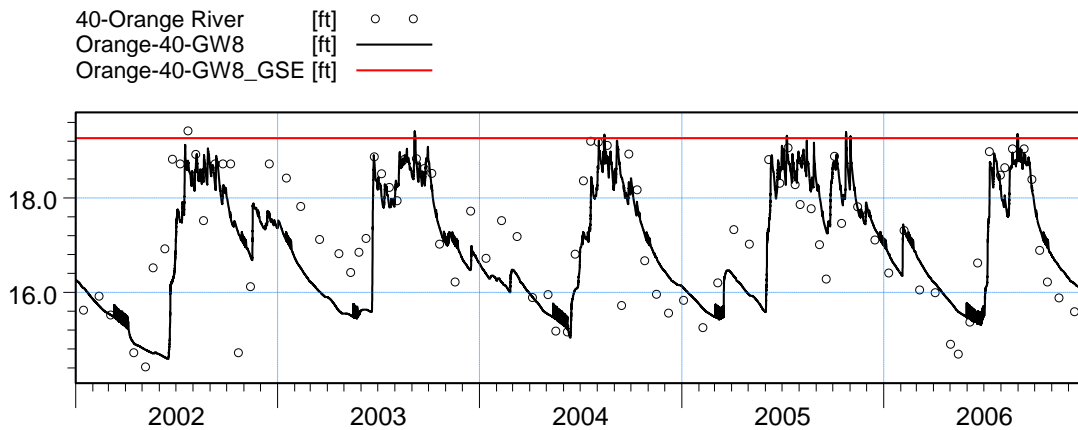


ME=0.766656  
 MAE=1.2815  
 RMSE=1.68055  
 STDres=1.49549  
 R(Correlation)=0.438428  
 R2(Nash\_Sutcliffe)=-0.287443

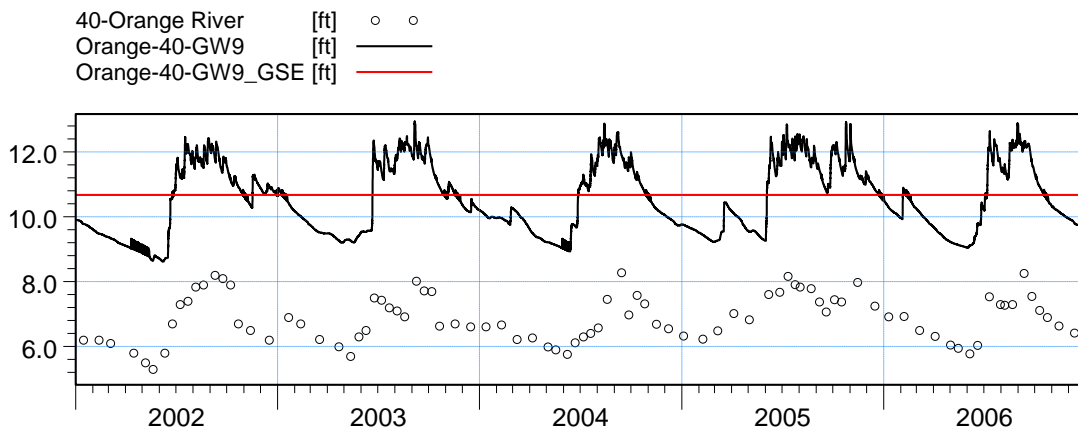


ME=-0.4608  
 MAE=0.819389  
 RMSE=1.16169  
 STDres=1.06639  
 R(Correlation)=0.660026  
 R2(Nash\_Sutcliffe)=0.304081

Figure B53. Groundwater elevation at wells 40-GW6 and 40-GW7, after refinement.

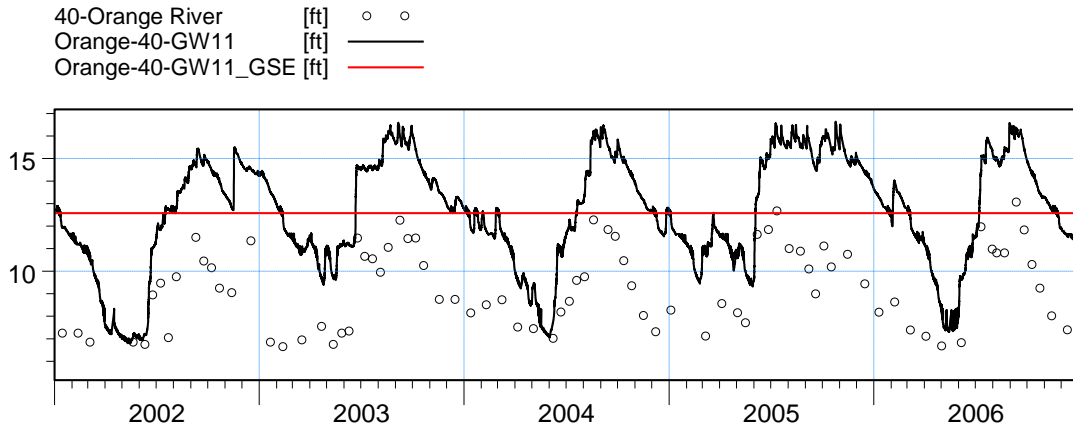


ME=0.195342  
 MAE=0.710861  
 RMSE=0.918747  
 STDres=0.89774  
 R(Correlation)=0.760933  
 R2(Nash\_Sutcliffe)=0.540251

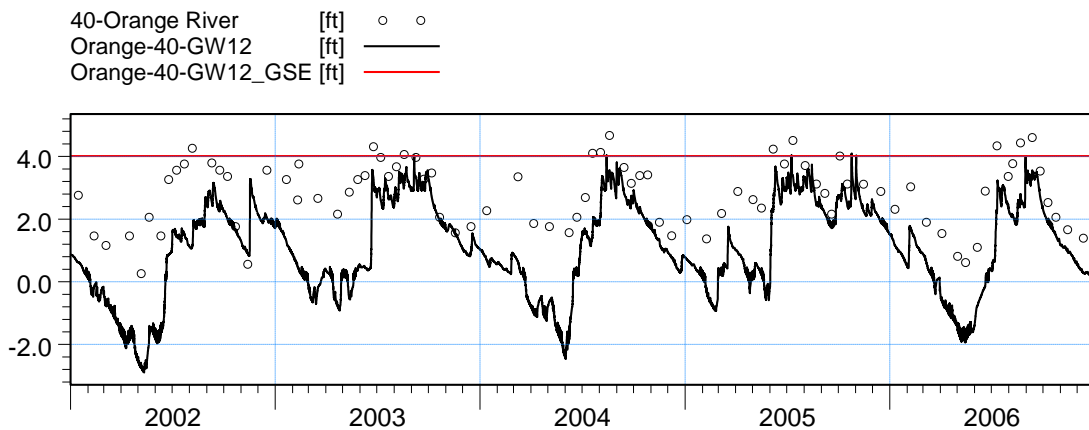


ME=-3.78591  
 MAE=3.78591  
 RMSE=3.83151  
 STDres=0.589347  
 R(Correlation)=0.861901  
 R2(Nash\_Sutcliffe)=-27.07

Figure B54. Groundwater elevation at wells 40-GW8 and 40-GW9, after refinement.

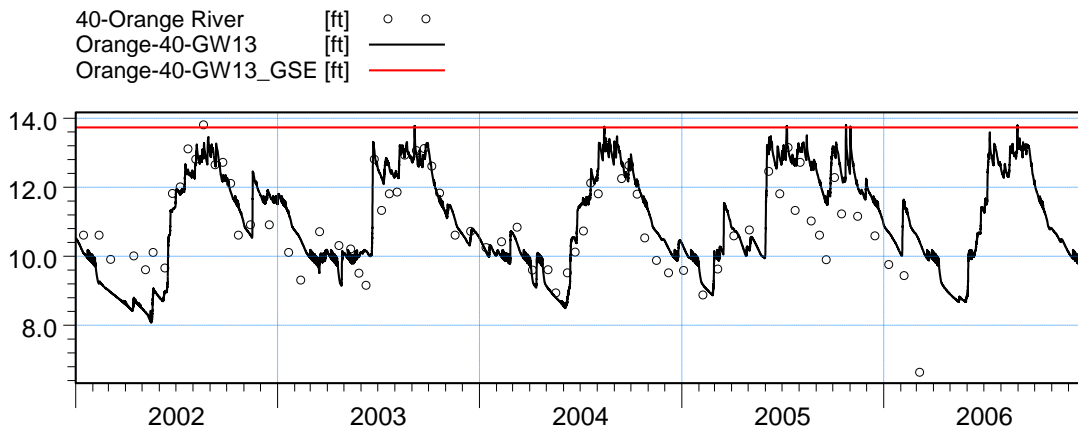


ME=-3.76369  
 MAE=3.76369  
 RMSE=3.96251  
 STDres=1.23941  
 R(Correlation)=0.847367  
 R2(Nash\_Sutcliffe)=-3.85296

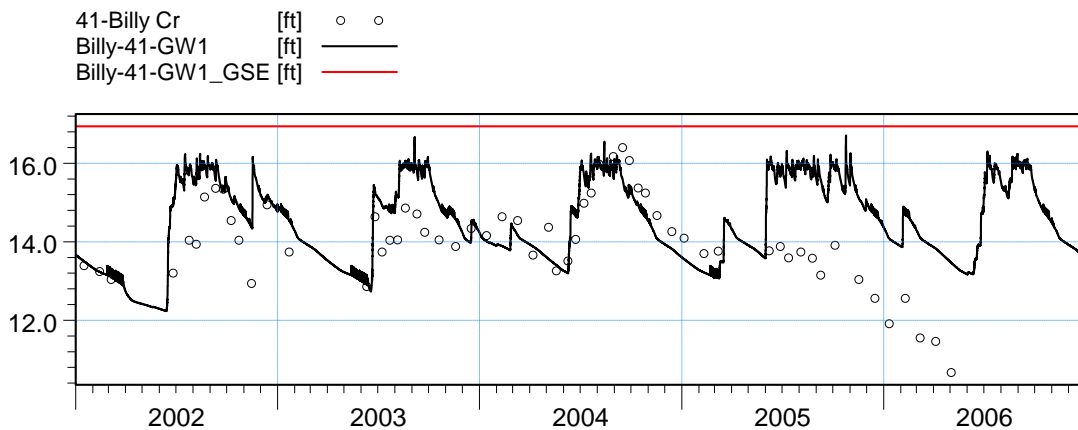


ME=1.58829  
 MAE=1.59612  
 RMSE=1.84348  
 STDres=0.935816  
 R(Correlation)=0.779382  
 R2(Nash\_Sutcliffe)=-2.03272

Figure B55. Groundwater elevation at wells 40-GW11 and 40-GW12, after refinement.

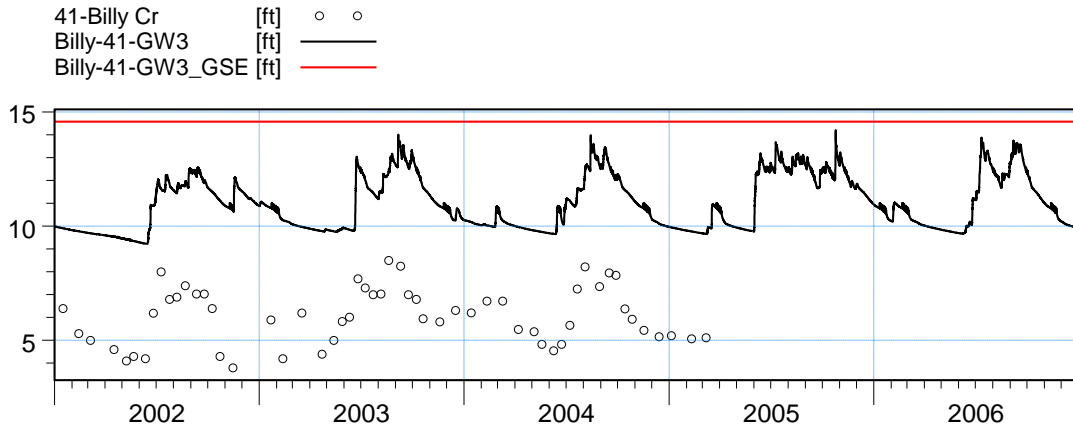


ME=-0.218566  
 MAE=0.688701  
 RMSE=0.897239  
 STDres=0.870211  
 R(Correlation)=0.798248  
 R2(Nash\_Sutcliffe)=0.554485

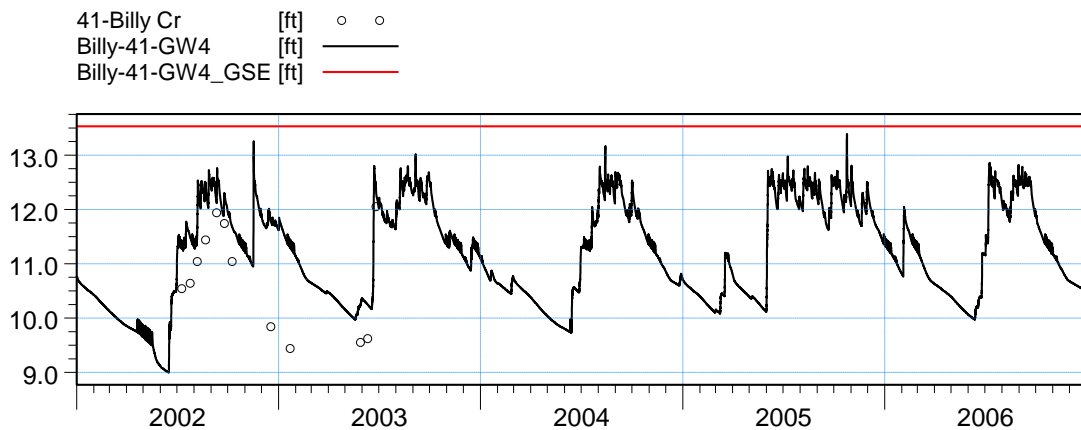


ME=-0.753259  
 MAE=1.01346  
 RMSE=1.27476  
 STDres=1.02841  
 R(Correlation)=0.499287  
 R2(Nash\_Sutcliffe)=-0.353491

Figure B56. Groundwater elevation at wells 40-GW13 and 41-GW1, after refinement.

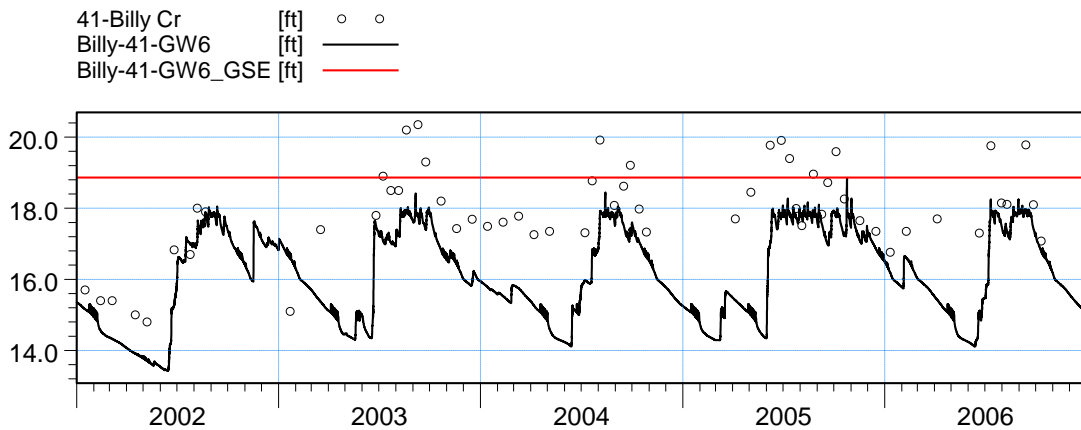


ME=-4.81316  
 MAE=4.81316  
 RMSE=4.86666  
 STDres=0.719614  
 R(Correlation)=0.811224  
 R2(Nash\_Sutcliffe)=-15.0153

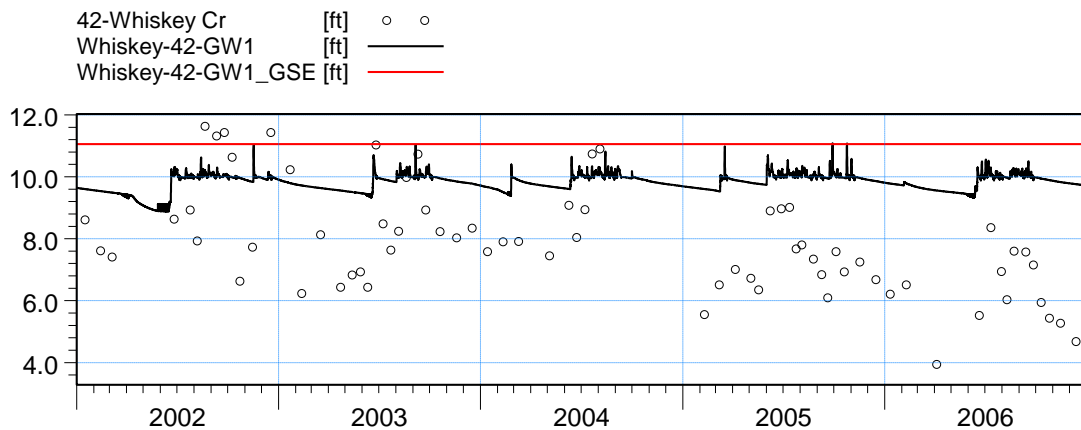


ME=-0.846577  
 MAE=0.846577  
 RMSE=1.00153  
 STDres=0.53514  
 R(Correlation)=0.812151  
 R2(Nash\_Sutcliffe)=-0.198097

Figure B57. Groundwater elevation at wells 41-GW3 and 41-GW4, after refinement.

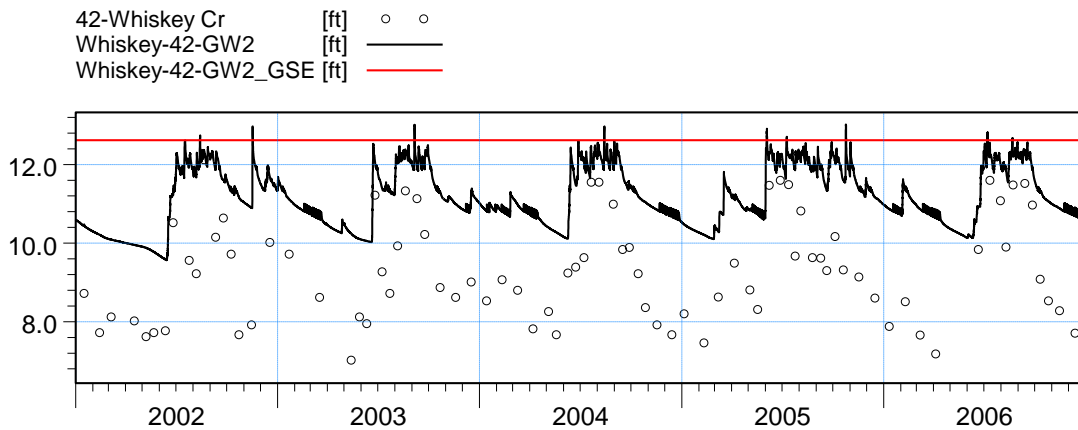


ME=1.28614  
 MAE=1.35425  
 RMSE=1.54834  
 STDres=0.862087  
 R(Correlation)=0.745799  
 R2(Nash\_Sutcliffe)=-0.502367

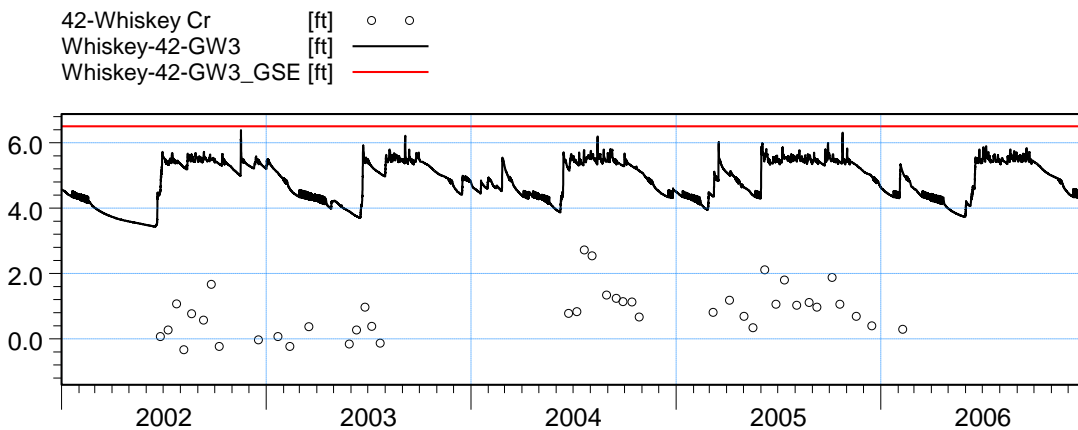


ME=-2.00816  
 MAE=2.27182  
 RMSE=2.56678  
 STDres=1.59864  
 R(Correlation)=0.464516  
 R2(Nash\_Sutcliffe)=-1.31713

Figure B58. Groundwater elevation at wells 41-GW6 and 42-GW1, after refinement.

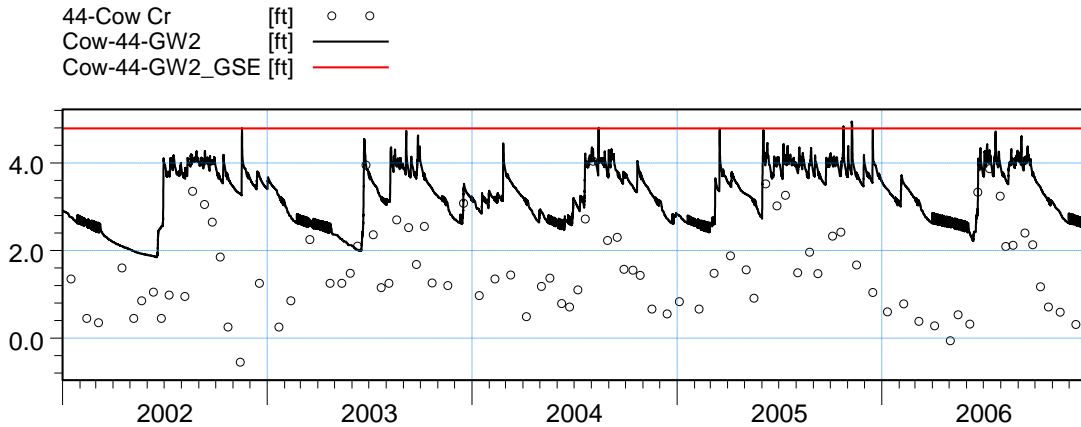


**ME=-1.95297**  
**MAE=1.95297**  
**RMSE=2.09184**  
**STDres=0.749462**  
**R(Correlation)=0.863806**  
**R2(Nash\_Sutcliffe)=-1.62941**

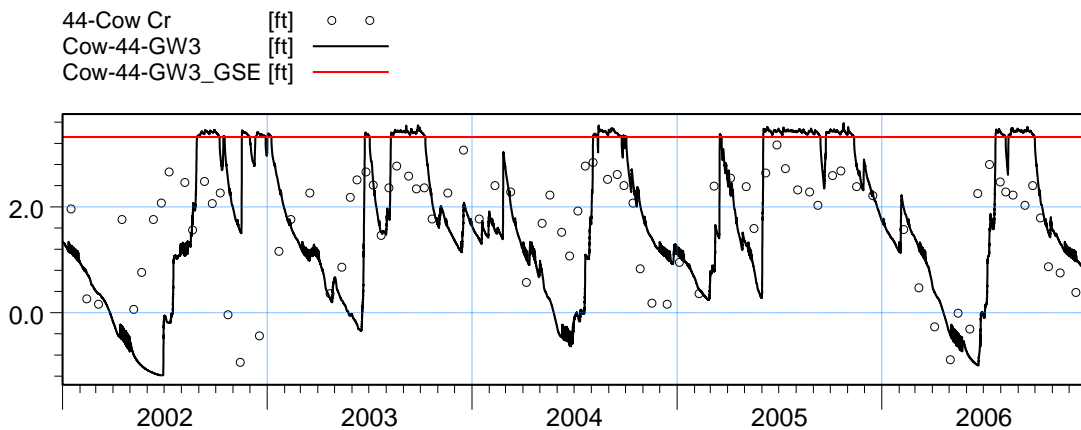


**ME=-4.3535**  
**MAE=4.3535**  
**RMSE=4.39468**  
**STDres=0.600233**  
**R(Correlation)=0.542103**  
**R2(Nash\_Sutcliffe)=-37.5883**

Figure B59. Groundwater elevation at wells 42-GW2 and 42-GW3, after refinement.

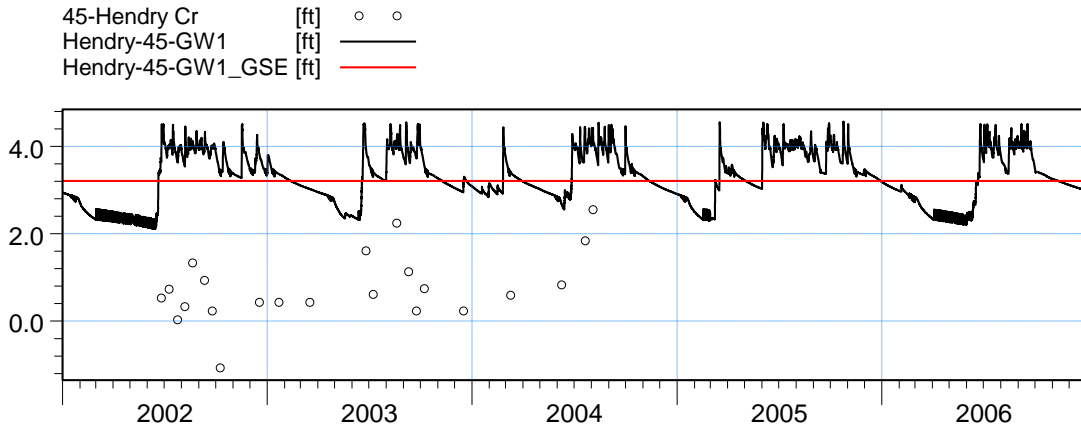


ME=-1.74899  
 MAE=1.75844  
 RMSE=1.92622  
 STDres=0.807058  
 R(Correlation)=0.58604  
 R2(Nash\_Sutcliffe)=-2.75715

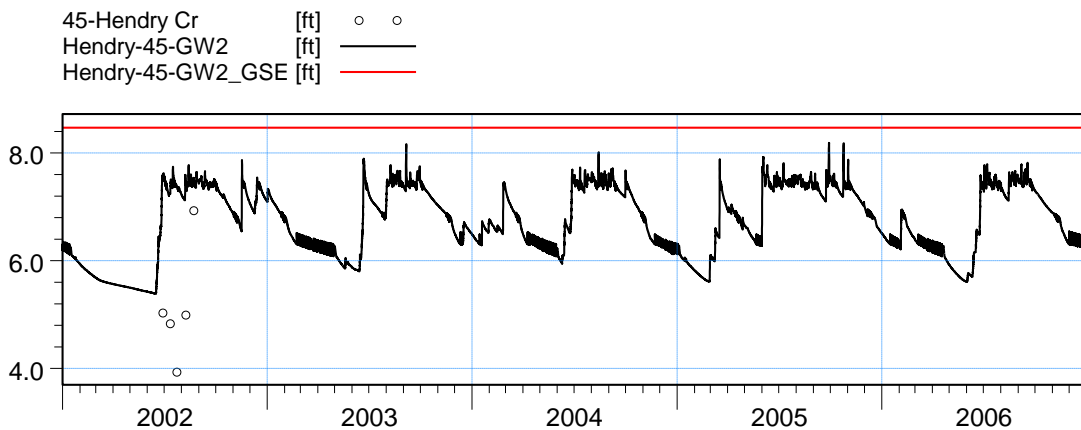


ME=0.0246863  
 MAE=1.031  
 RMSE=1.3038  
 STDres=1.30357  
 R(Correlation)=0.461829  
 R2(Nash\_Sutcliffe)=-0.73173

Figure B60. Groundwater elevation at wells 44-GW2 and 44-GW3, after refinement.

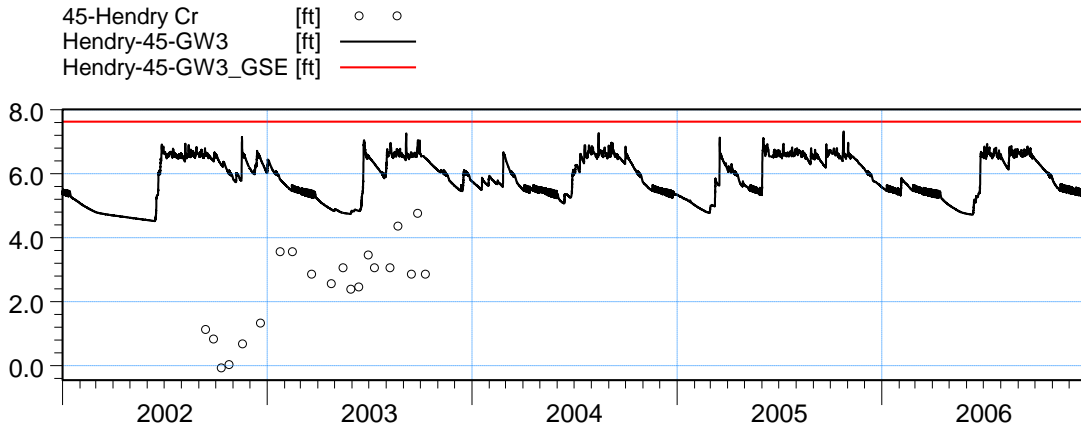


ME=-2.92173  
 MAE=2.92173  
 RMSE=2.98725  
 STDres=0.62221  
 R(Correlation)=0.593932  
 R2(Nash\_Sutcliffe)=-13.9649

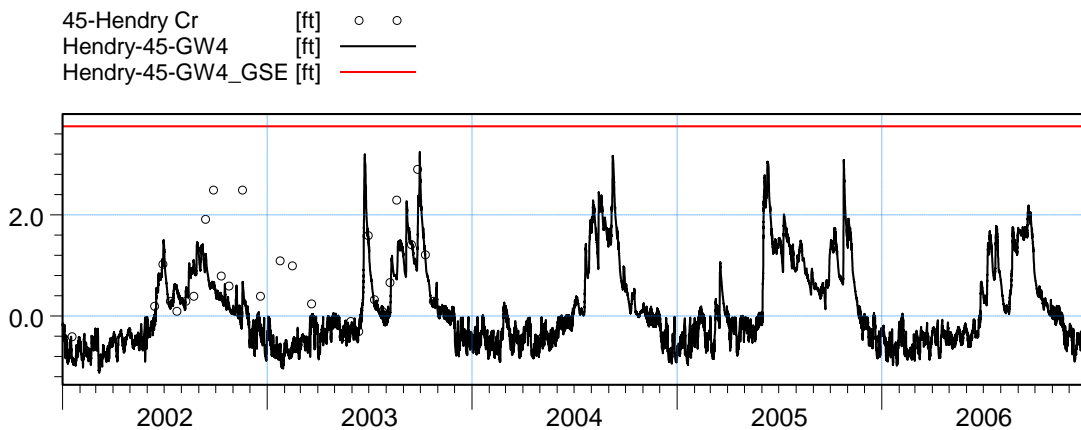


ME=-2.26259  
 MAE=2.26259  
 RMSE=2.44067  
 STDres=0.91517  
 R(Correlation)=0.676543  
 R2(Nash\_Sutcliffe)=-5.20653

Figure B61. Groundwater elevation at wells 45-GW1 and 45-GW2, after refinement.

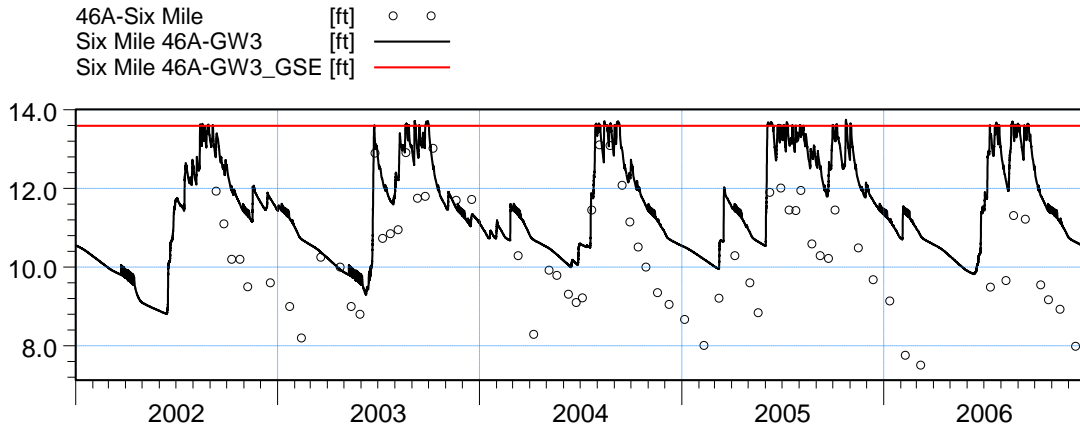


ME=-3.60361  
 MAE=3.60361  
 RMSE=3.91534  
 STDres=1.53098  
 R(Correlation)=-0.0422623  
 R2(Nash\_Sutcliffe)=-7.74402

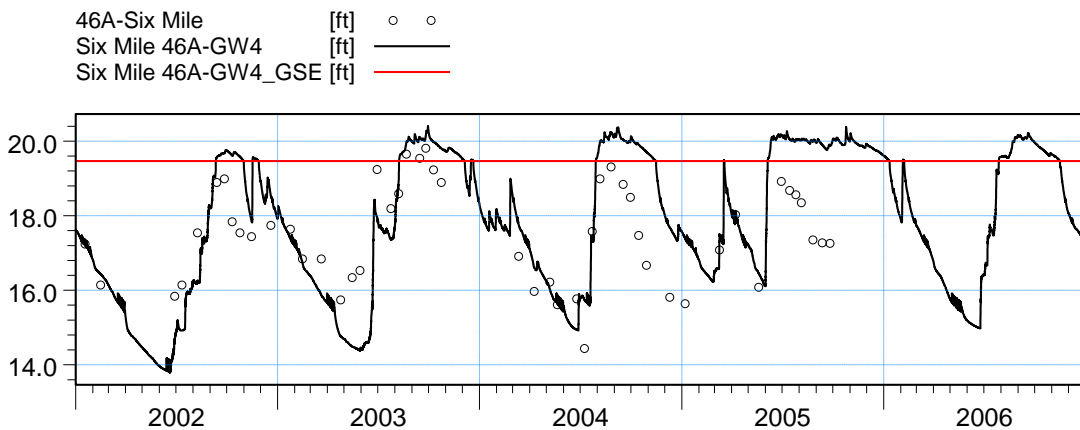


ME=0.474629  
 MAE=0.579963  
 RMSE=0.841582  
 STDres=0.694973  
 R(Correlation)=0.647108  
 R2(Nash\_Sutcliffe)=0.137659

Figure B62. Groundwater elevation at wells 45-GW3 and 45-GW4, after refinement.

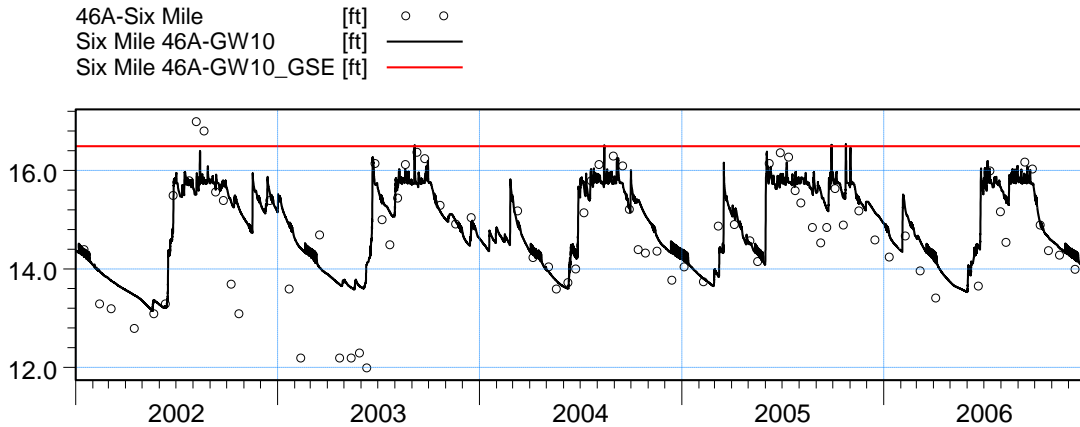


ME=-1.48393  
 MAE=1.54095  
 RMSE=1.74337  
 STDres=0.915035  
 R(Correlation)=0.76008  
 R2(Nash\_Sutcliffe)=-0.548263

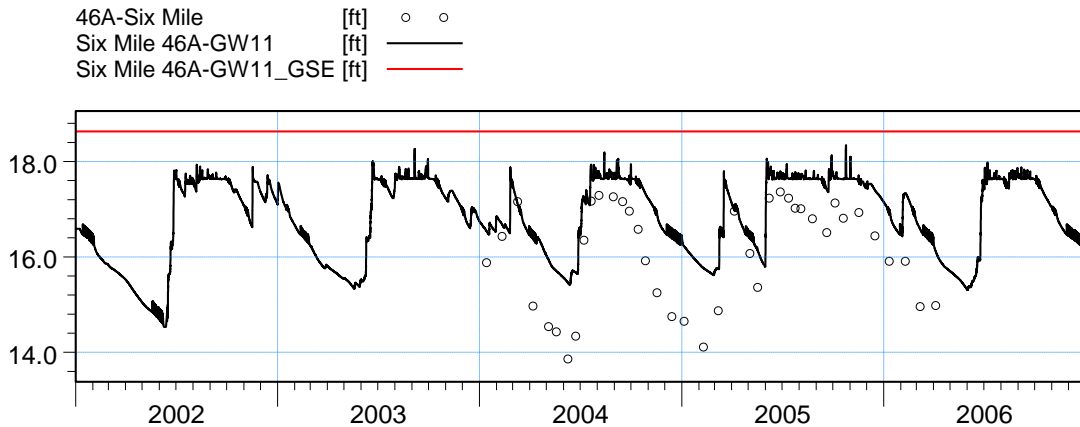


ME=-0.401571  
 MAE=1.1083  
 RMSE=1.35197  
 STDres=1.29095  
 R(Correlation)=0.74141  
 R2(Nash\_Sutcliffe)=-0.0769052

Figure B63. Groundwater elevation at wells 46A-GW3 and 46A-GW4, after refinement.

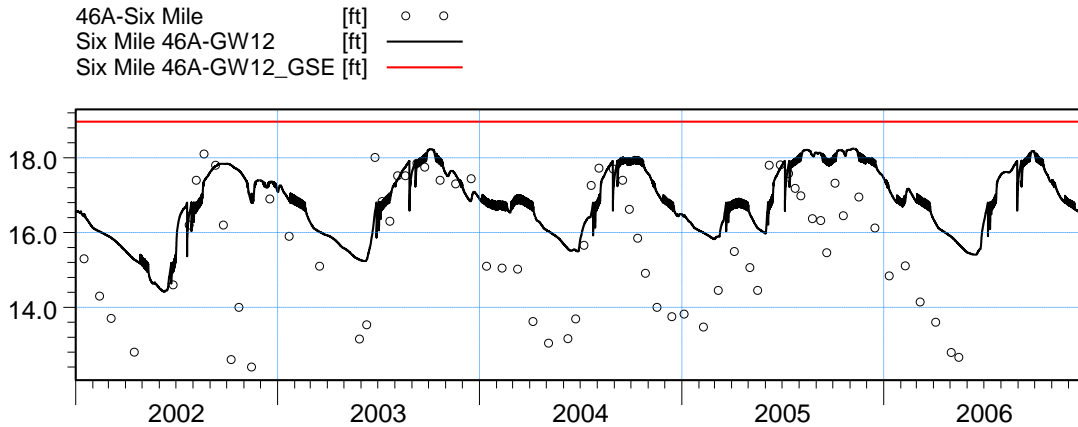


ME=-0.257998  
 MAE=0.539414  
 RMSE=0.728037  
 STDres=0.68079  
 R(Correlation)=0.823544  
 R2(Nash\_Sutcliffe)=0.60551

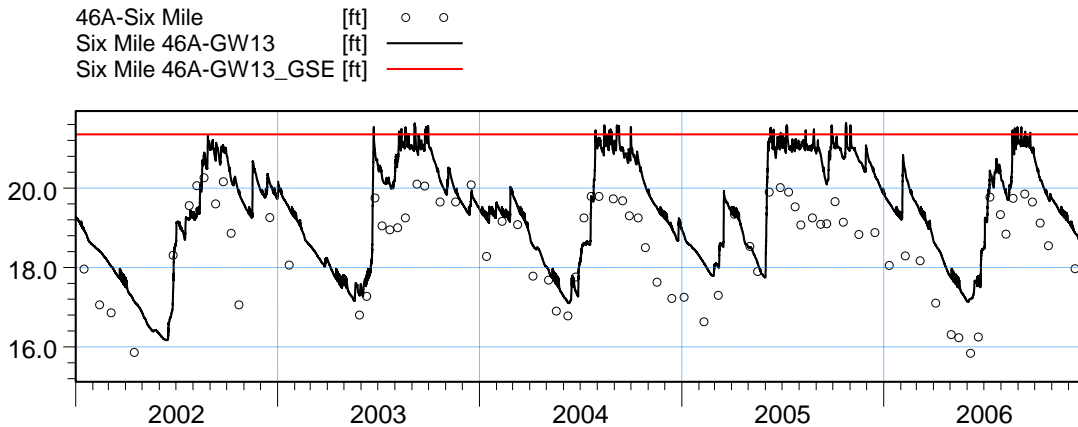


ME=-0.90648  
 MAE=0.908536  
 RMSE=1.02146  
 STDres=0.470824  
 R(Correlation)=0.930029  
 R2(Nash\_Sutcliffe)=0.0921497

Figure B64. Groundwater elevation at wells 46A-GW10 and 46A-GW11, after refinement.

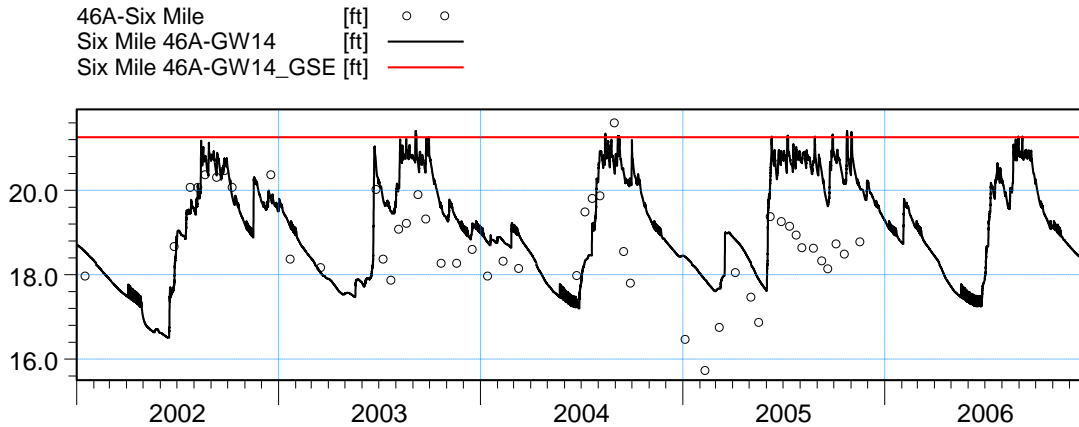


ME=-1.31227  
 MAE=1.5173  
 RMSE=1.87722  
 STDres=1.34235  
 R(Correlation)=0.625454  
 R2(Nash\_Sutcliffe)=-0.219742

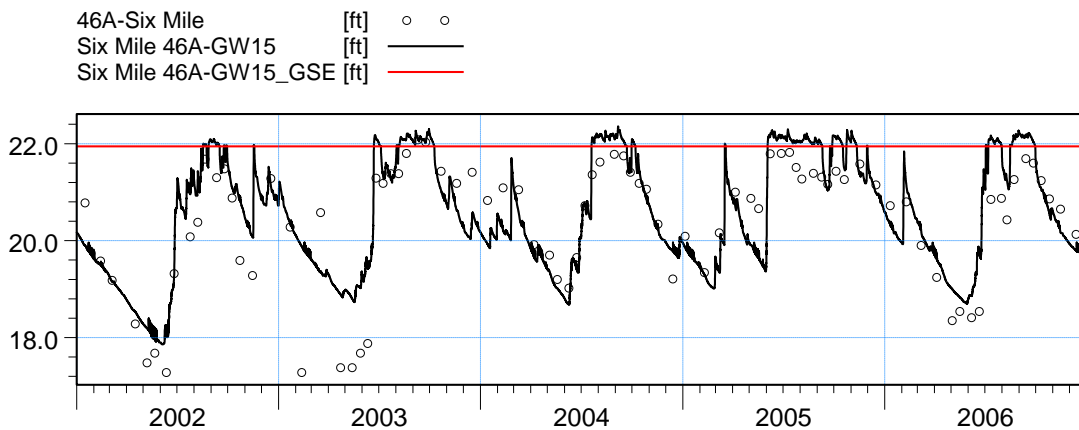


ME=-1.01279  
 MAE=1.10192  
 RMSE=1.23162  
 STDres=0.700824  
 R(Correlation)=0.838718  
 R2(Nash\_Sutcliffe)=-0.0809184

Figure B65. Groundwater elevation at wells 46A-GW12 and 46A-GW13, after refinement.

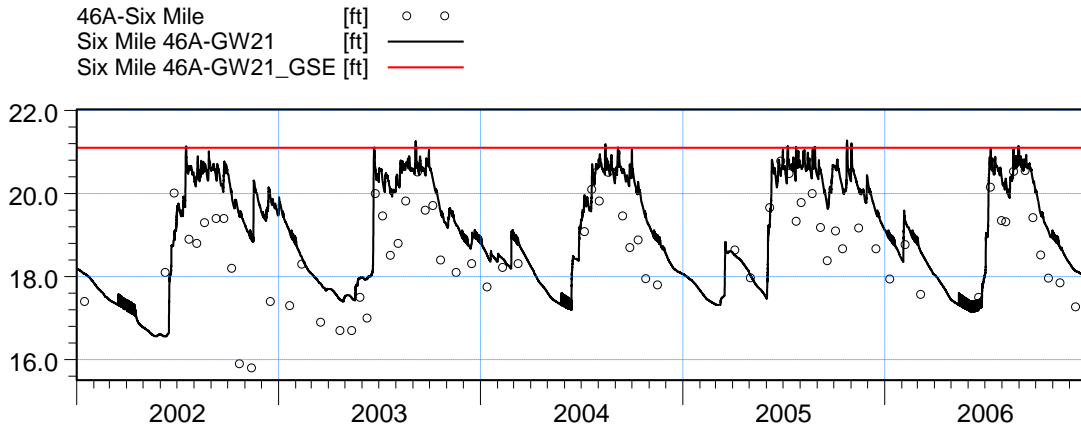


ME=-0.82252  
 MAE=1.09958  
 RMSE=1.2644  
 STDres=0.960301  
 R(Correlation)=0.606887  
 R2(Nash\_Sutcliffe)=-0.267538

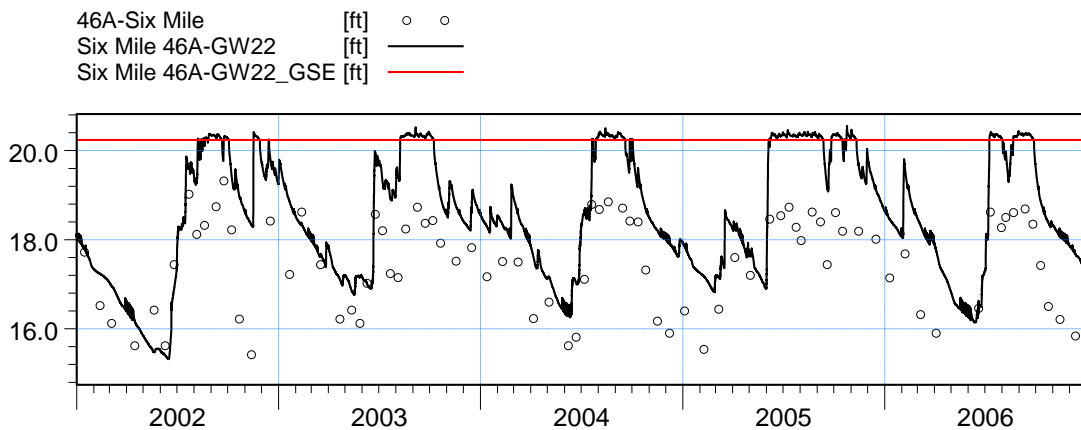


ME=-0.240236  
 MAE=0.54608  
 RMSE=0.699668  
 STDres=0.657132  
 R(Correlation)=0.865684  
 R2(Nash\_Sutcliffe)=0.711119

Figure B66. Groundwater elevation at wells 46A-GW14 and 46A-GW15, after refinement.

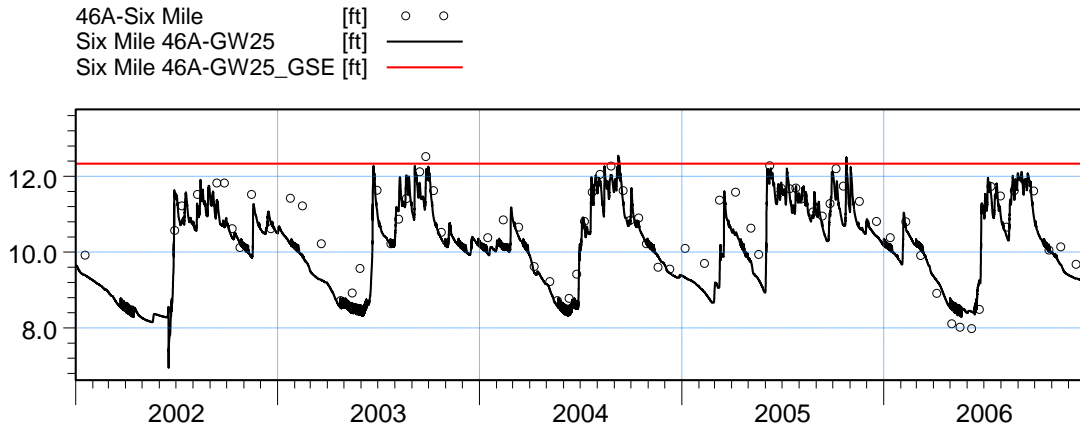


ME=-0.886511  
 MAE=0.999504  
 RMSE=1.18369  
 STDres=0.784358  
 R(Correlation)=0.74948  
 R2(Nash\_Sutcliffe)=-0.0968449

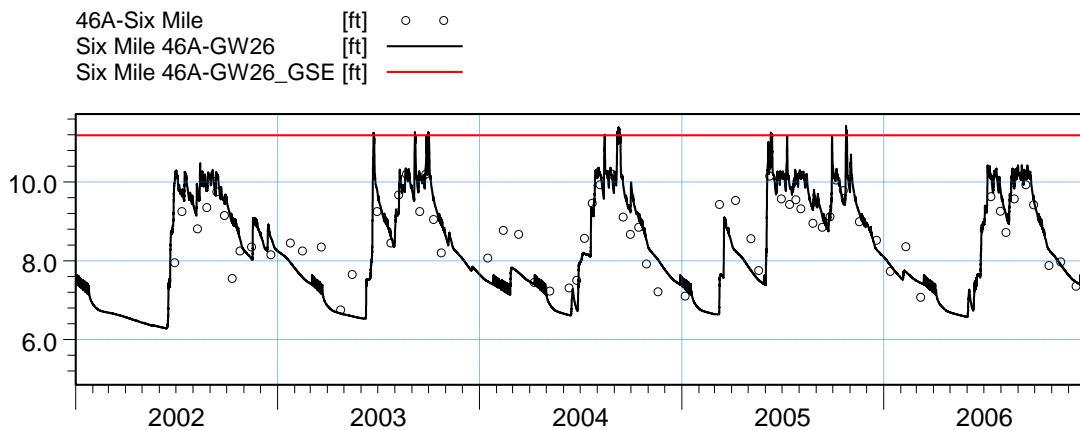


ME=-1.29467  
 MAE=1.34213  
 RMSE=1.48184  
 STDres=0.720896  
 R(Correlation)=0.844312  
 R2(Nash\_Sutcliffe)=-0.989442

Figure B67. Groundwater elevation at wells 46A-GW21 and 46A-GW22, after refinement.

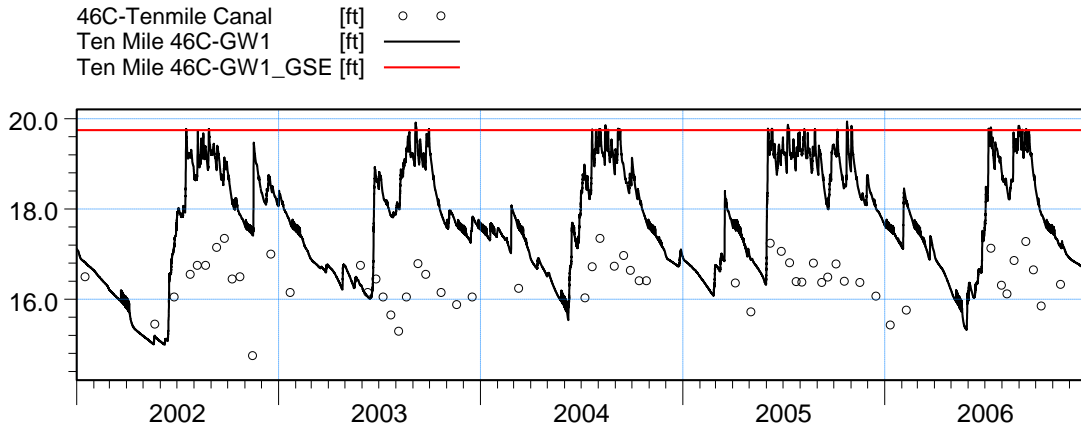


ME=0.327495  
 MAE=0.467464  
 RMSE=0.614234  
 STDres=0.519644  
 R(Correlation)=0.880553  
 R2(Nash\_Sutcliffe)=0.677969

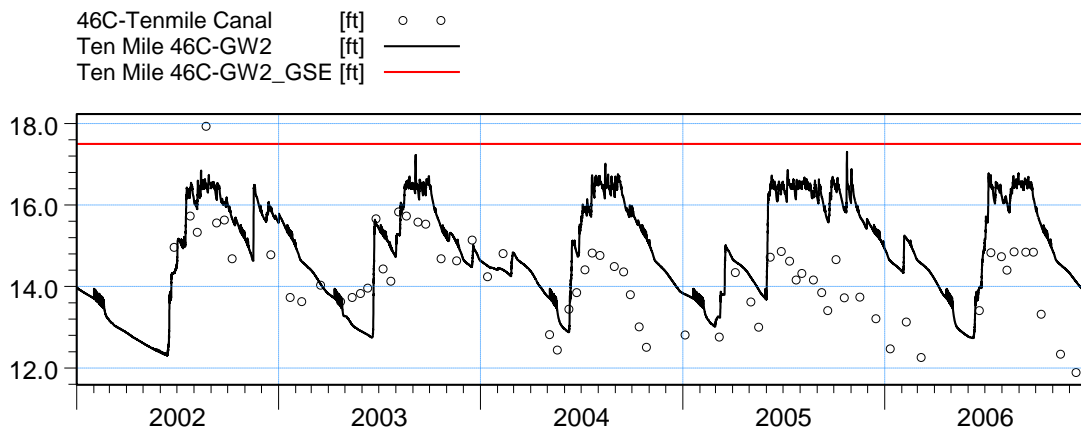


ME=-0.102396  
 MAE=0.539394  
 RMSE=0.693022  
 STDres=0.685415  
 R(Correlation)=0.796653  
 R2(Nash\_Sutcliffe)=0.375777

Figure B68. Groundwater elevation at wells 46A-GW25 and 46A-GW26, after refinement.

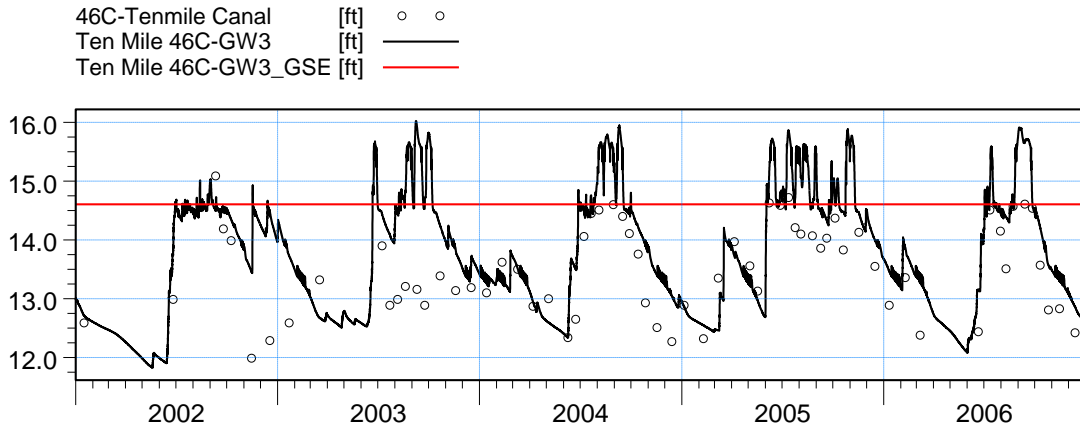


ME=-1.9572  
 MAE=1.98343  
 RMSE=2.09975  
 STDres=0.760458  
 R(Correlation)=0.601877  
 R2(Nash\_Sutcliffe)=-15.5542

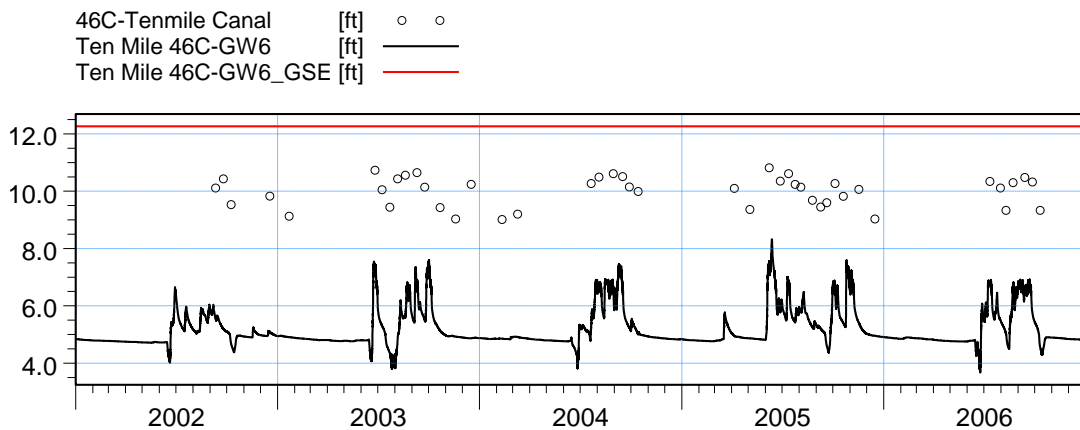


ME=-1.06983  
 MAE=1.26567  
 RMSE=1.45689  
 STDres=0.988927  
 R(Correlation)=0.571981  
 R2(Nash\_Sutcliffe)=-0.925717

Figure B69. Groundwater elevation at wells 46C-GW1 and 46C-GW2, after refinement.

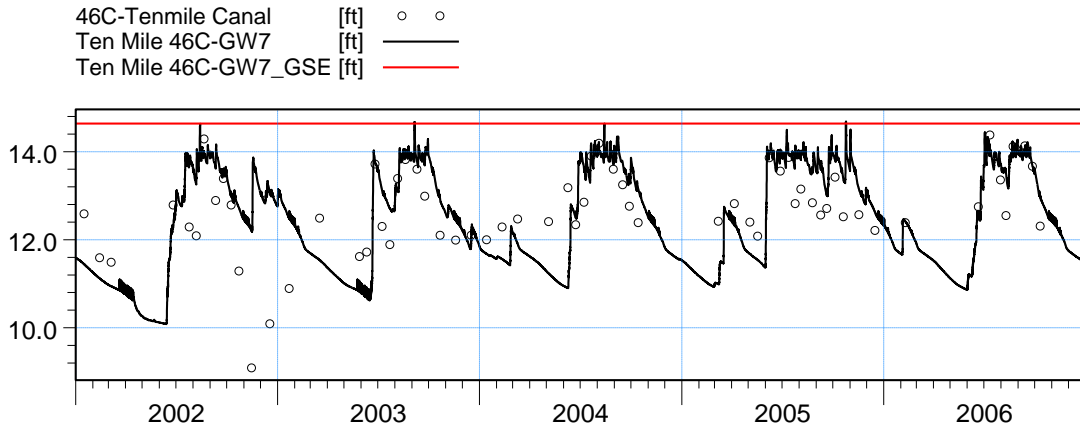


ME=-0.538996  
 MAE=0.64063  
 RMSE=0.811377  
 STDres=0.606478  
 R(Correlation)=0.720363  
 R2(Nash\_Sutcliffe)=-0.121817

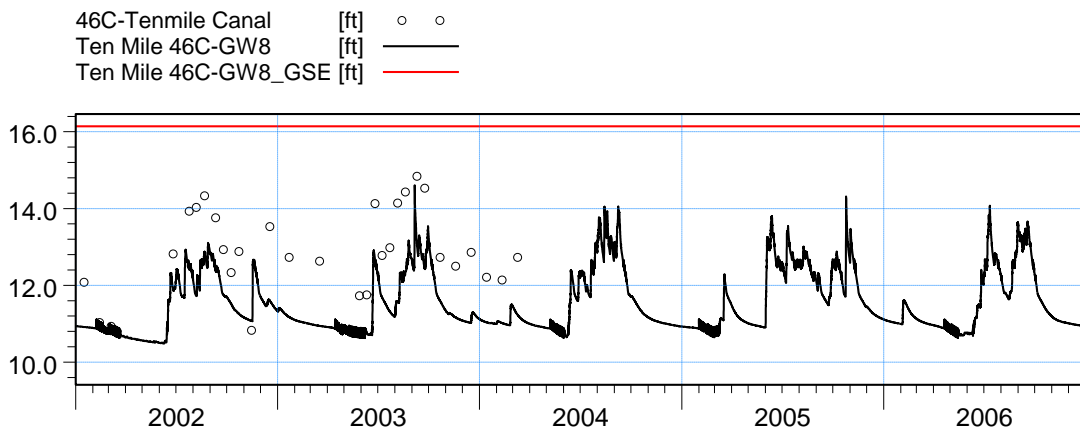


ME=4.45294  
 MAE=4.45294  
 RMSE=4.48236  
 STDres=0.512706  
 R(Correlation)=0.751076  
 R2(Nash\_Sutcliffe)=-76.0102

Figure B70. Groundwater elevation at wells 46C-GW3 and 46C-GW6, after refinement.

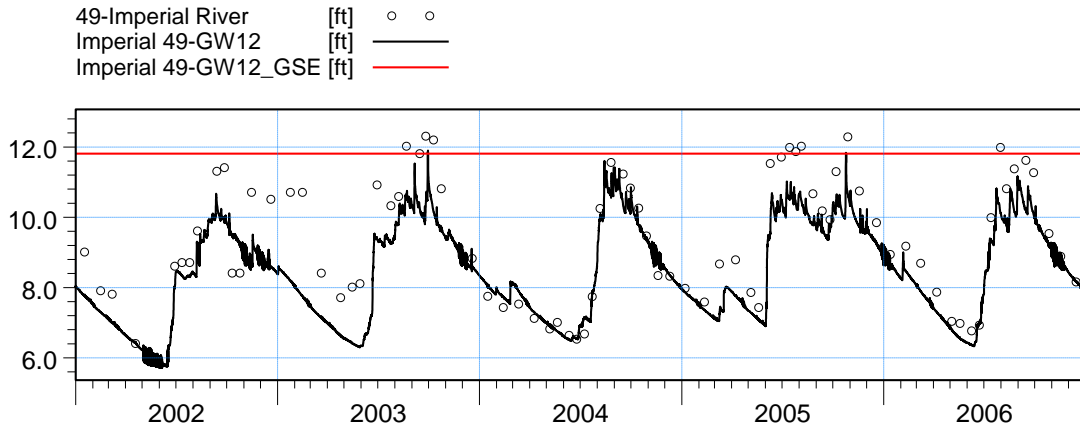


ME=-0.231465  
 MAE=0.682992  
 RMSE=0.910235  
 STDres=0.880313  
 R(Correlation)=0.591169  
 R2(Nash\_Sutcliffe)=0.0643849

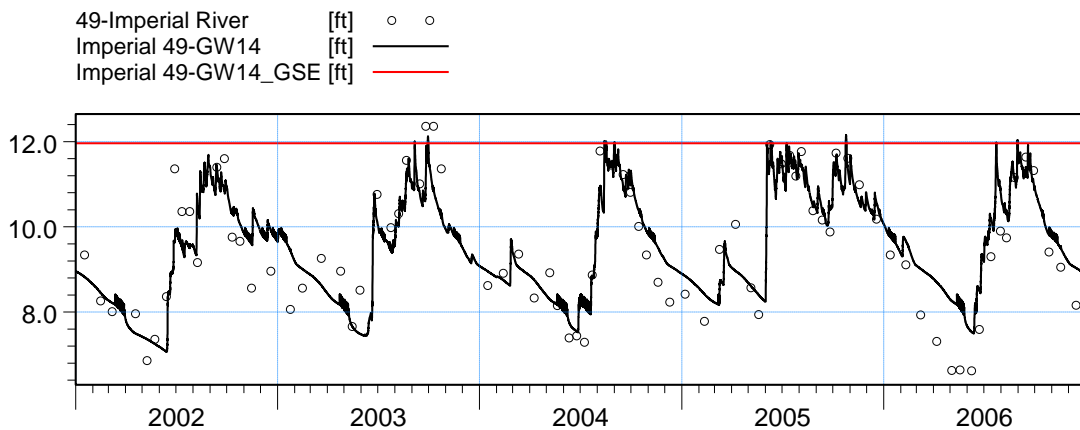


ME=1.33505  
 MAE=1.35153  
 RMSE=1.46781  
 STDres=0.61001  
 R(Correlation)=0.844035  
 R2(Nash\_Sutcliffe)=-0.963631

Figure B71. Groundwater elevation at wells 46C-GW7 and 46C-GW8, after refinement.



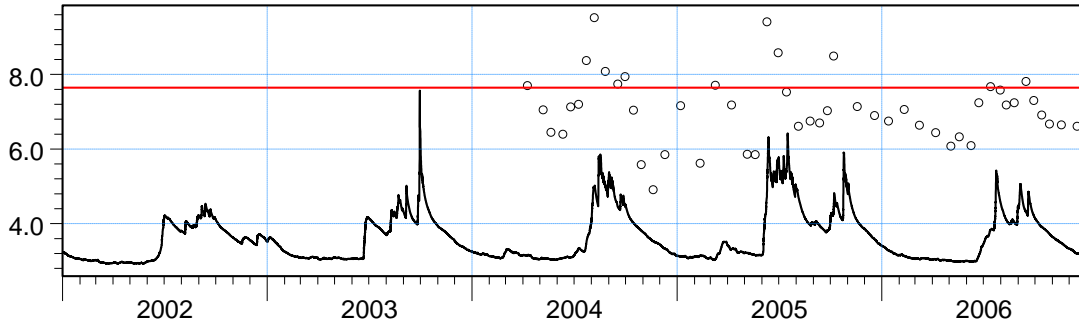
**ME=0.779275**  
**MAE=0.875505**  
**RMSE=1.08619**  
**STDres=0.75666**  
**R(Correlation)=0.906089**  
**R2(Nash\_Sutcliffe)=0.597558**



**ME=-0.0530742**  
**MAE=0.594875**  
**RMSE=0.731879**  
**STDres=0.729952**  
**R(Correlation)=0.873514**  
**R2(Nash\_Sutcliffe)=0.760731**

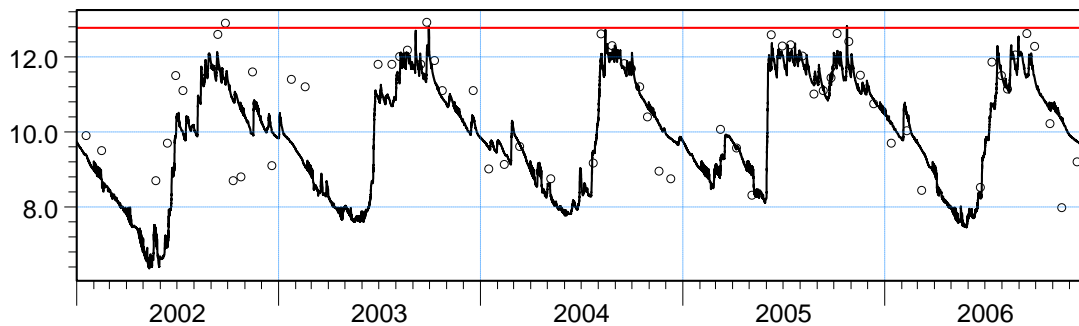
Figure B72. Groundwater elevation at wells 49-GW12 and 49-GW14, after refinement.

49-Imperial River [ft] ○ ○  
 Imperial 49-GW15 [ft] —  
 Imperial 49-GW15\_GSE [ft] —



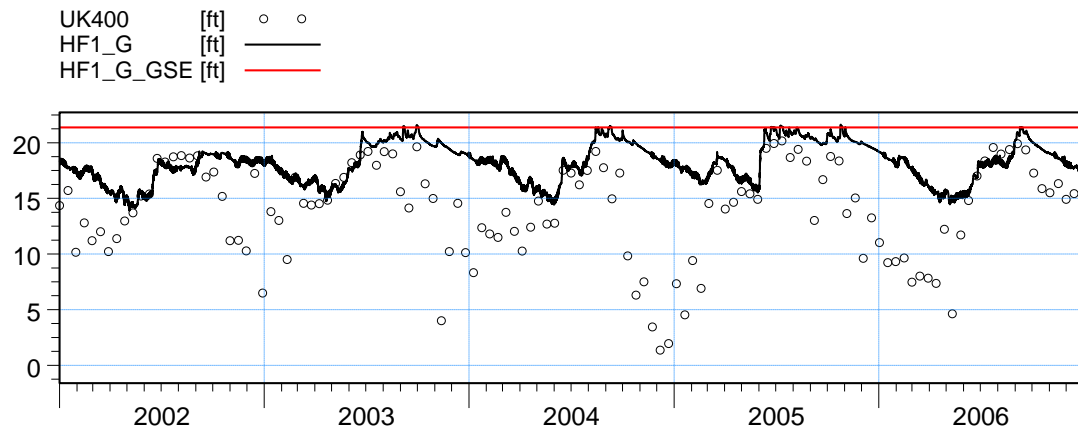
ME=3.31189  
 MAE=3.31189  
 RMSE=3.40843  
 STDres=0.805495  
 R(Correlation)=0.514041  
 R2(Nash\_Sutcliffe)=-13.3098

49L-Leitner Cr [ft] ○ ○  
 Leitner 49L-GW1 [ft] —  
 Leitner 49L-GW1\_GSE [ft] —

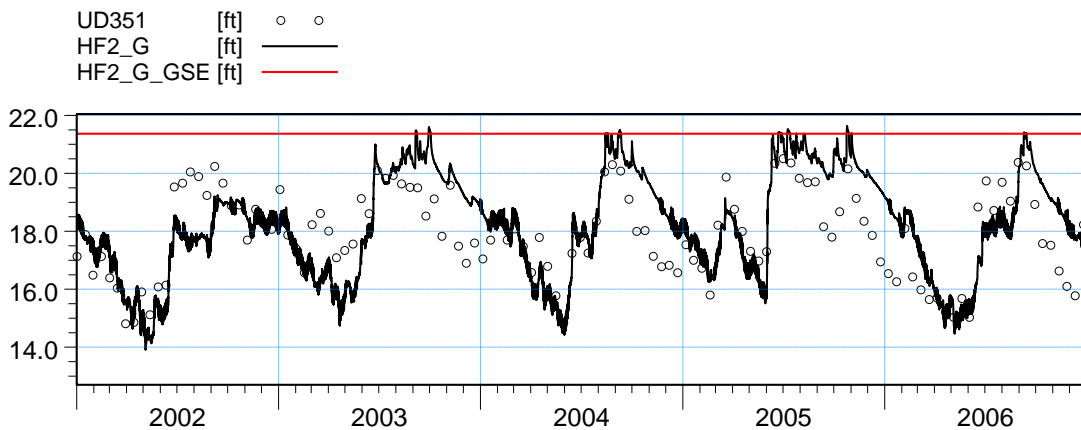


ME=0.260104  
 MAE=0.712718  
 RMSE=0.935974  
 STDres=0.899107  
 R(Correlation)=0.765503  
 R2(Nash\_Sutcliffe)=0.544875

Figure B73. Groundwater elevation at wells 49-GW15 and 49L-GW1, after refinement.

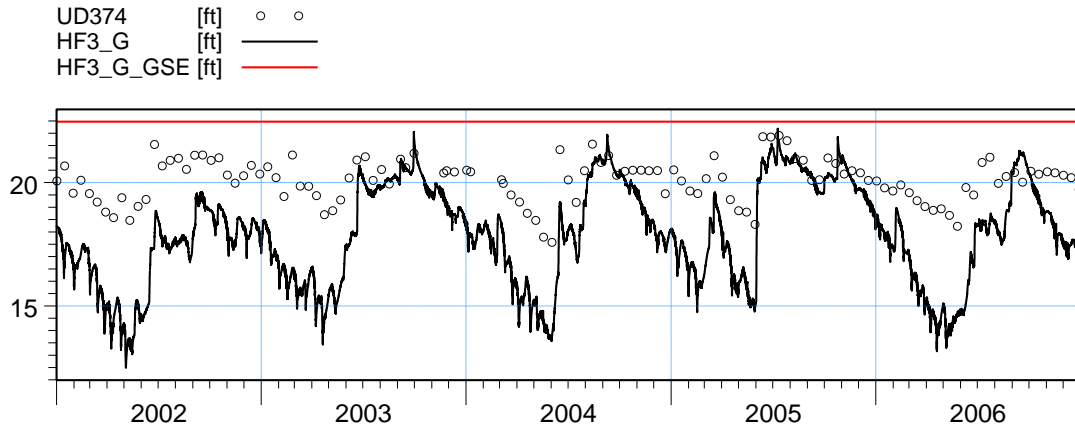


ME=-4.24882  
 MAE=4.40602  
 RMSE=5.95789  
 STDres=4.17659  
 R(Correlation)=0.278698  
 R2(Nash\_Sutcliffe)=-0.910331

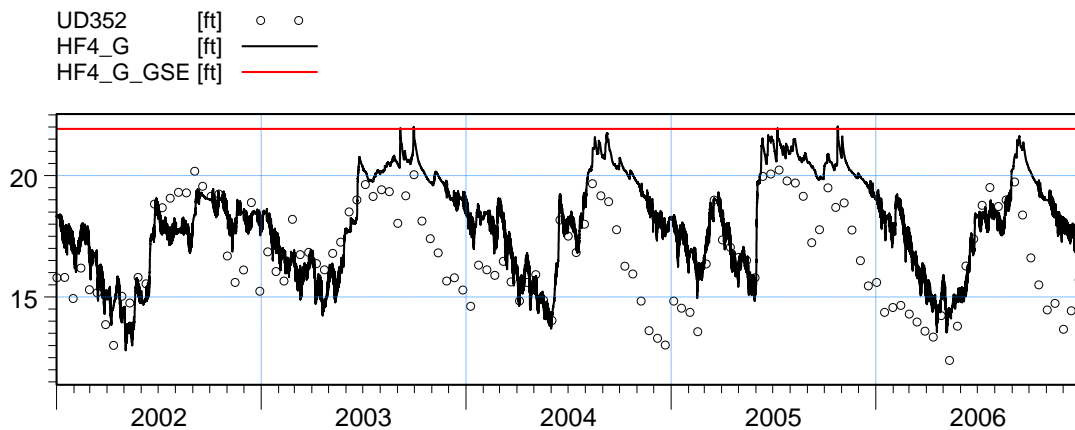


ME=-0.319254  
 MAE=1.07897  
 RMSE=1.2784  
 STDres=1.2379  
 R(Correlation)=0.718473  
 R2(Nash\_Sutcliffe)=0.26918

Figure B74. Groundwater elevation at wells HF1\_G and HF2\_G, after refinement.

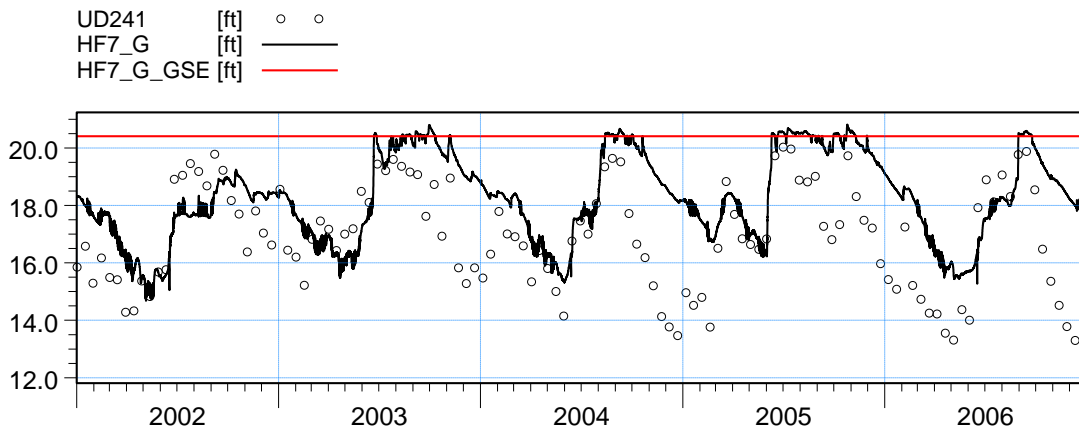


ME=2.27391  
 MAE=2.31589  
 RMSE=2.69184  
 STDres=1.44061  
 R(Correlation)=0.800416  
 R2(Nash\_Sutcliffe)=-8.95032



ME=-1.38548  
 MAE=1.79728  
 RMSE=2.22017  
 STDres=1.73481  
 R(Correlation)=0.614308  
 R2(Nash\_Sutcliffe)=-0.226536

Figure B75. Groundwater elevation at wells HF3\_G and HF4\_G, after refinement.



ME=-1.39891  
 MAE=1.69827  
 RMSE=2.08854  
 STDres=1.55082  
 R(Correlation)=0.574852  
 R2(Nash\_Sutcliffe)=-0.335487

Figure B76. Groundwater elevation at well HF7\_G, after refinement.



**Appendix B5. Surface water stations north from Caloosahatchee**

| Station Name          | before refinement |          |           |      |     | after refinement |          |           |      |     |
|-----------------------|-------------------|----------|-----------|------|-----|------------------|----------|-----------|------|-----|
|                       | ME (ft)           | MAE (ft) | RMSE (ft) | R    | PL  | ME (ft)          | MAE (ft) | RMSE (ft) | R    | PL  |
| Caloosahatchee_53534  | 0.75              | 0.90     | 1.19      | 0.40 | 2.0 | 0.75             | 0.90     | 1.19      | 0.40 | 2.0 |
| Courtney Q_7500       | ---               | ---      | ---       | 0.47 | 3.0 | ---              | ---      | ---       | 0.46 | 3.0 |
| Gator Slough Q_5910   | ---               | ---      | ---       | 0.86 | 1.0 | ---              | ---      | ---       | 0.70 | 2.0 |
| Gator Slough_5850     | 1.04              | 1.46     | 1.63      | 0.87 | 1.8 | 0.50             | 1.66     | 1.88      | 0.84 | 1.8 |
| Hermosa Q_12500       | ---               | ---      | ---       | 0.65 | 2.0 | ---              | ---      | ---       | 0.65 | 2.0 |
| Horseshoe Q_13230     | ---               | ---      | ---       | 0.55 | 3.0 | ---              | ---      | ---       | 0.57 | 3.0 |
| Meade Q_2470          | ---               | ---      | ---       | 0.55 | 3.0 | ---              | ---      | ---       | 0.57 | 3.0 |
| Powell Creek_4976     | -0.93             | 1.15     | 1.46      | 0.46 | 2.3 | -1.03            | 1.18     | 1.49      | 0.45 | 2.3 |
| S-78 TW               | -0.21             | 0.36     | 0.51      | 0.34 | 1.5 | -0.23            | 0.31     | 0.44      | 0.39 | 1.5 |
| S-79 HW               | 0.13              | 0.21     | 0.31      | -0.1 | 1.5 | 0.09             | 0.18     | 0.21      | 0.06 | 1.5 |
| S-79 TW               | 0.13              | 0.44     | 0.56      | 0.60 | 1.3 | 0.15             | 0.42     | 0.54      | 0.60 | 1.5 |
| S-79 Q                | ---               | ---      | ---       | 0.96 | 1.0 | ---              | ---      | ---       | 0.96 | 1.0 |
| San Carlos Q_4510     | ---               | ---      | ---       | 0.46 | 3.0 | ---              | ---      | ---       | 0.46 | 3.0 |
| Telegraph Creek_24691 | 0.66              | 0.85     | 0.97      | 0.58 | 1.8 | 0.69             | 0.83     | 0.94      | 0.58 | 1.8 |

Table B6. Statistical parameters and level of performance at surface water stations north of the Caloosahatchee River. The green color indicates the highest performance level (1.0, 1.2 and 1.5), yellow for medium (1.8, 2.0, 2.3, 2.5) and orange for low (2.8, 3.0).

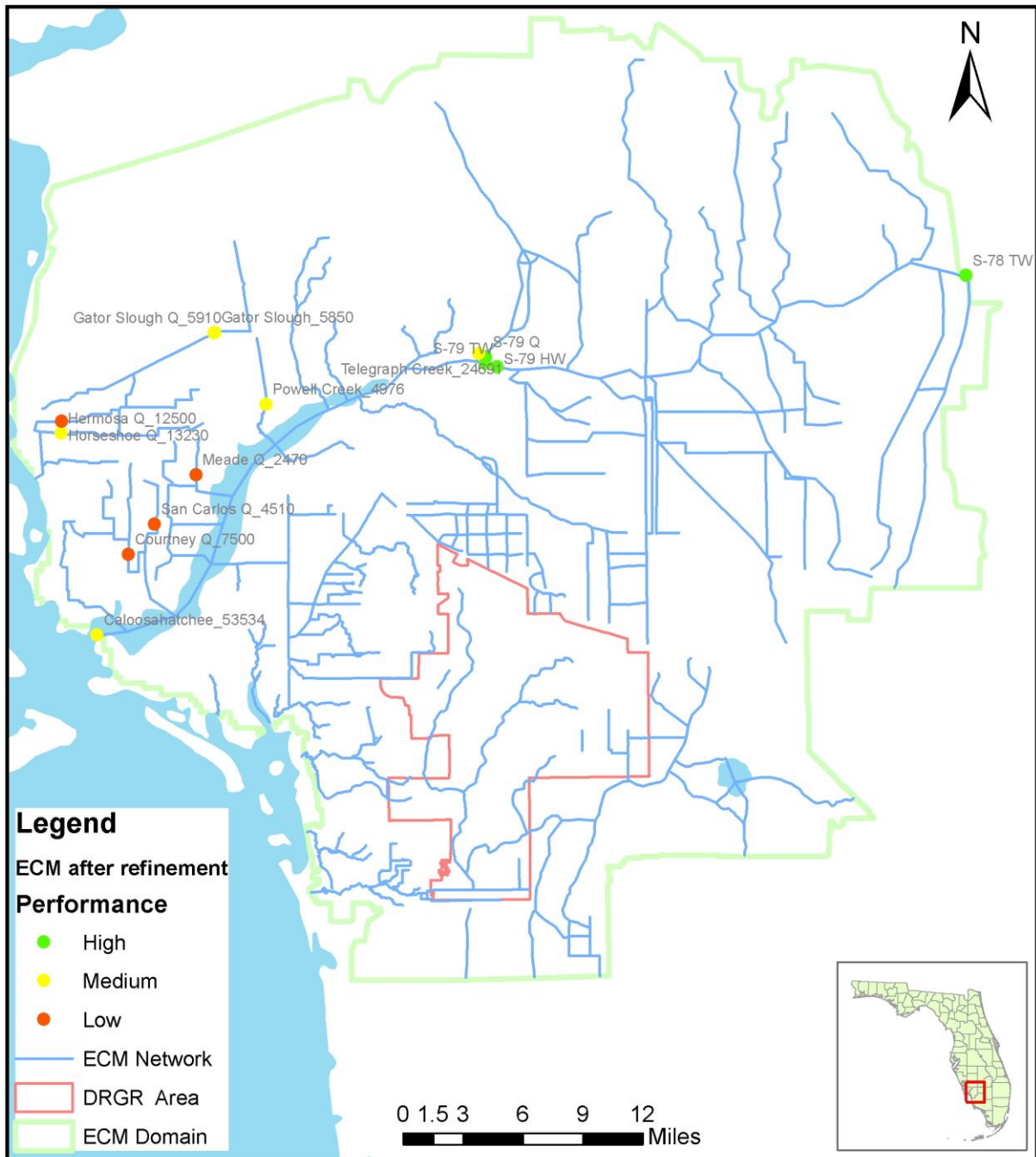
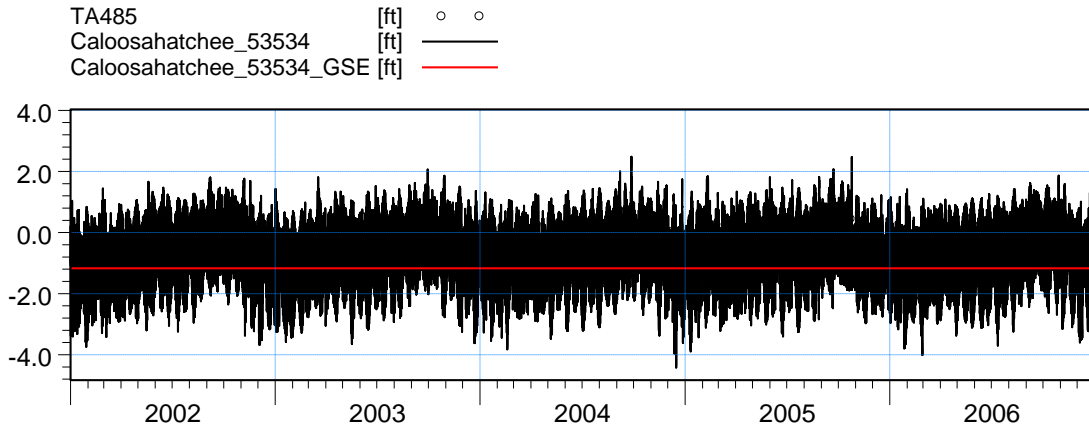
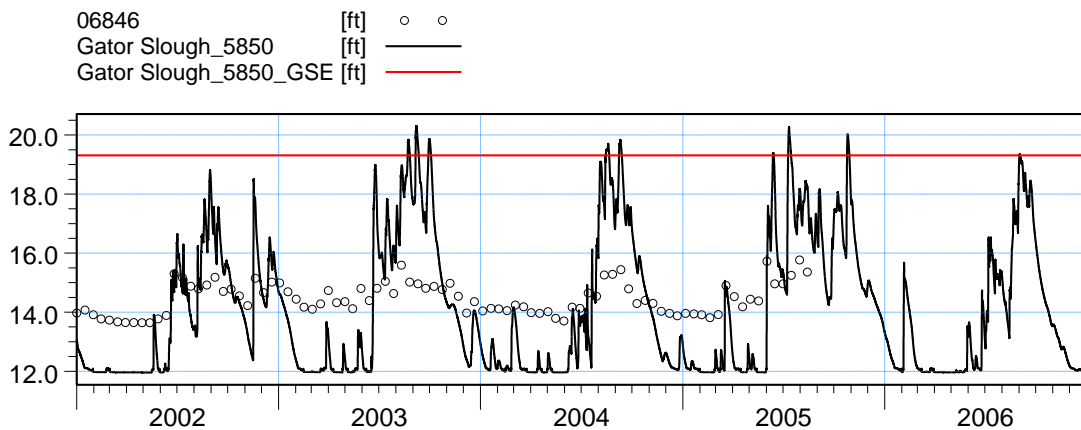


Figure B77. Average performance level at surface water monitoring stations north of the Caloosahatchee River, after the refinement process.

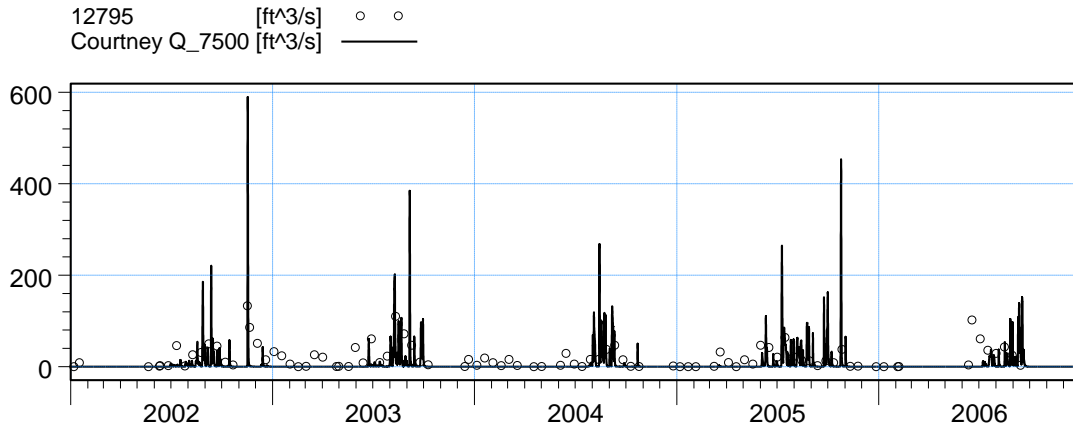


ME=0.751086  
 MAE=0.900596  
 RMSE=1.19164  
 STDres=0.925142  
 R(Correlation)=0.399058  
 R2(Nash\_Sutcliffe)=-9.50492

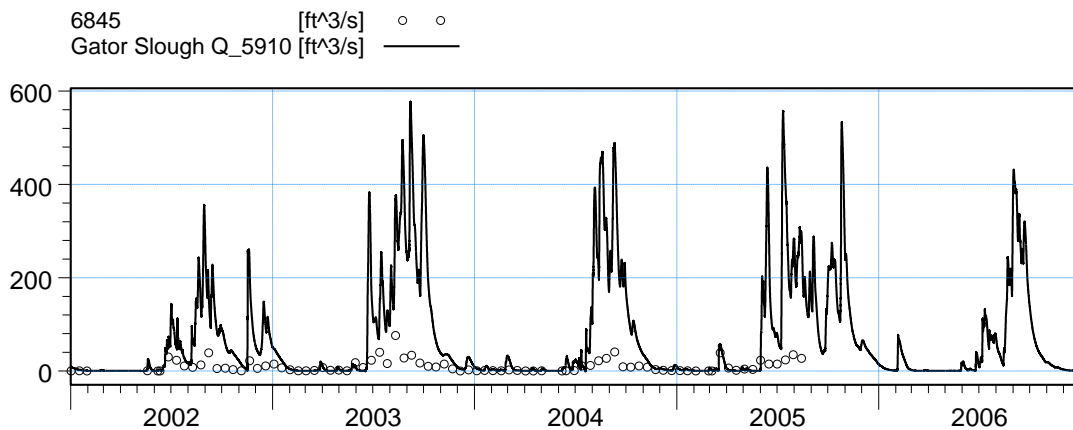


ME=0.497645  
 MAE=1.66397  
 RMSE=1.88178  
 STDres=1.81478  
 R(Correlation)=0.838796  
 R2(Nash\_Sutcliffe)=-9.71579

Figure B78. Stage at stations Caloosahatchee\_53534 and Gator Slough\_5850, after refinement.

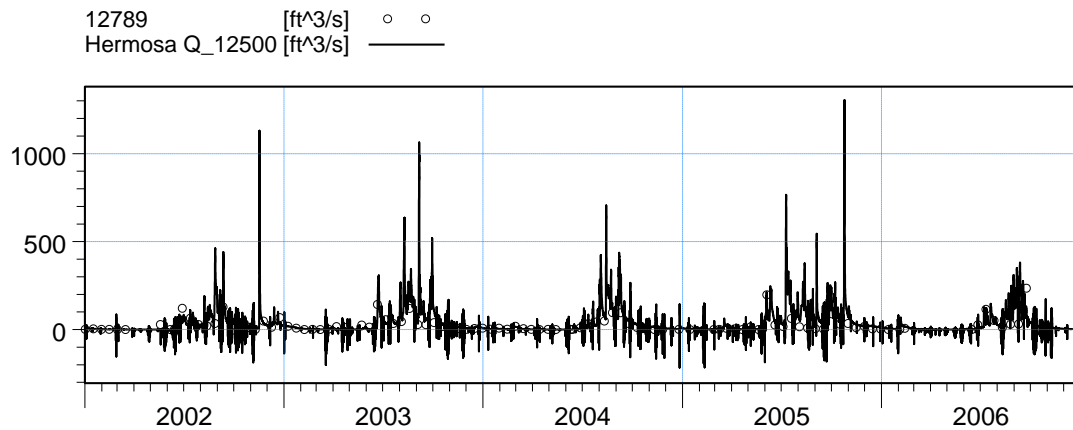


ME=15.2694  
 MAE=20.6338  
 RMSE=32.3936  
 STDres=28.5691  
 R(Correlation)=0.464605  
 R2(Nash\_Sutcliffe)=-0.417753

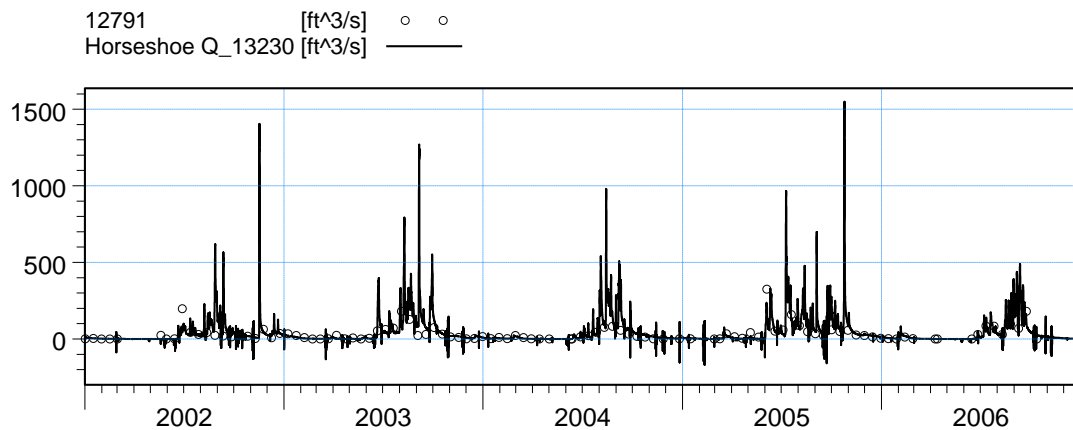


ME=-65.6357  
 MAE=66.5523  
 RMSE=122.748  
 STDres=103.725  
 R(Correlation)=0.703295  
 R2(Nash\_Sutcliffe)=-44.6406

Figure B79. Flow at stations Courtney Q\_7500 and Gator Slough Q\_5910, after refinement.

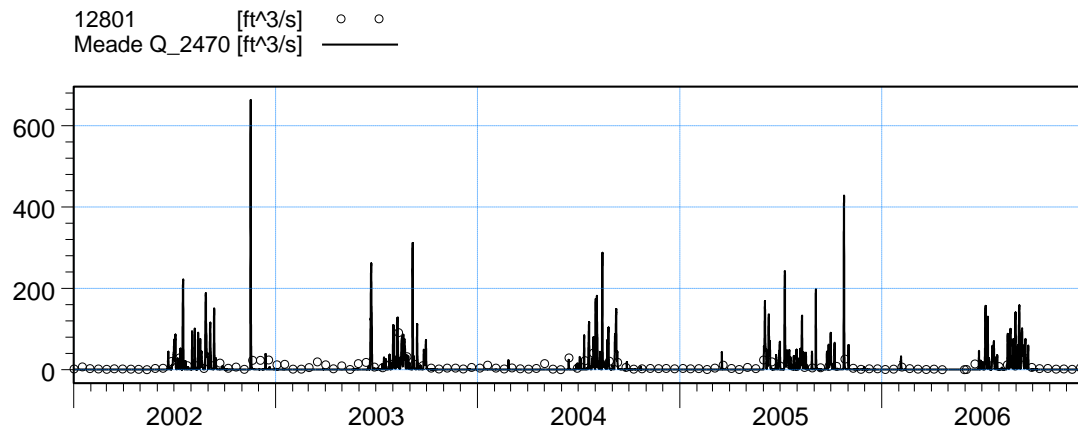


ME=-17.7096  
 MAE=30.712  
 RMSE=61.0575  
 STDres=58.4328  
 R(Correlation)=0.650188  
 R2(Nash\_Sutcliffe)=-0.44612

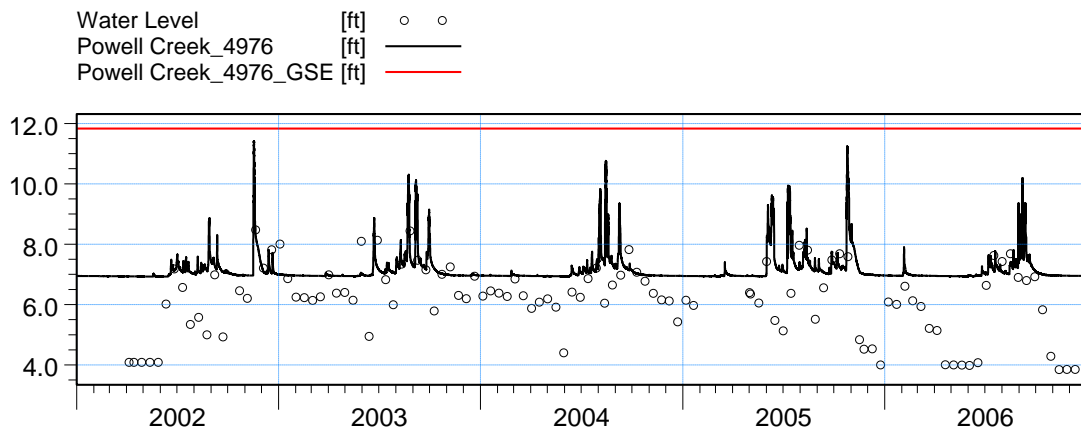


ME=-15.5498  
 MAE=33.2818  
 RMSE=78.5746  
 STDres=77.0206  
 R(Correlation)=0.573977  
 R2(Nash\_Sutcliffe)=-0.924459

Figure B80. Flow at stations at Hermosa Q\_12500 and Horseshoe Q\_13230, after refinement.

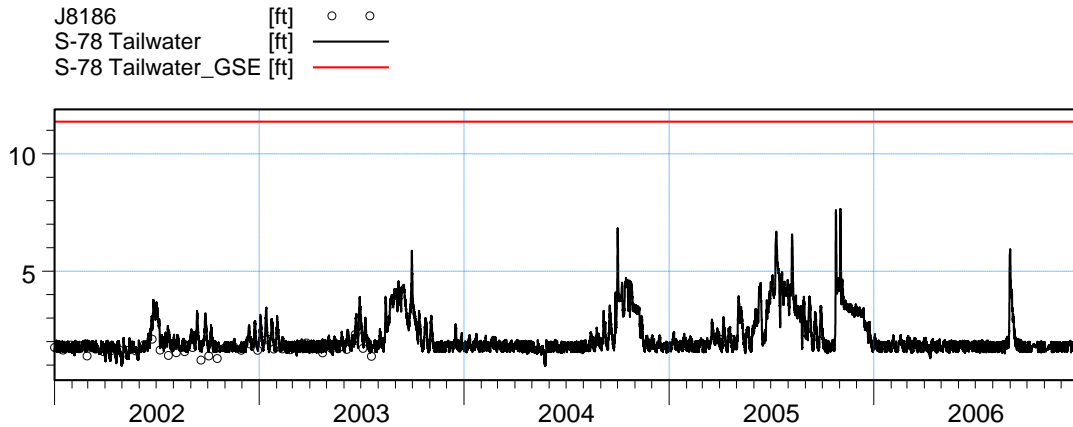


ME=3.02135  
 MAE=8.51831  
 RMSE=19.3577  
 STDres=19.1205  
 R(Correlation)=0.569295  
 R2(Nash\_Sutcliffe)=-0.411272

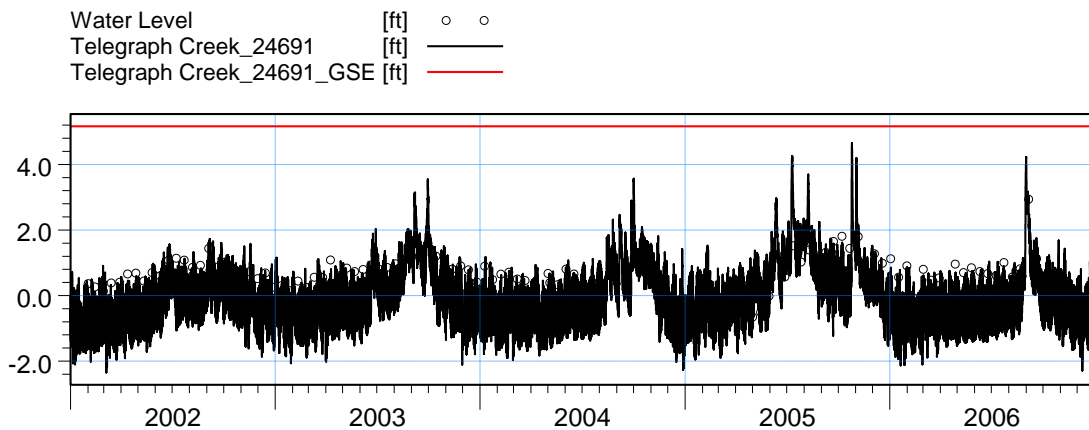


ME=-1.02907  
 MAE=1.18173  
 RMSE=1.49121  
 STDres=1.07922  
 R(Correlation)=0.452534  
 R2(Nash\_Sutcliffe)=-0.527292

Figure B81. Flow at station and Meade Q\_2470 and stage at Powell Creek\_4976, after refinement.

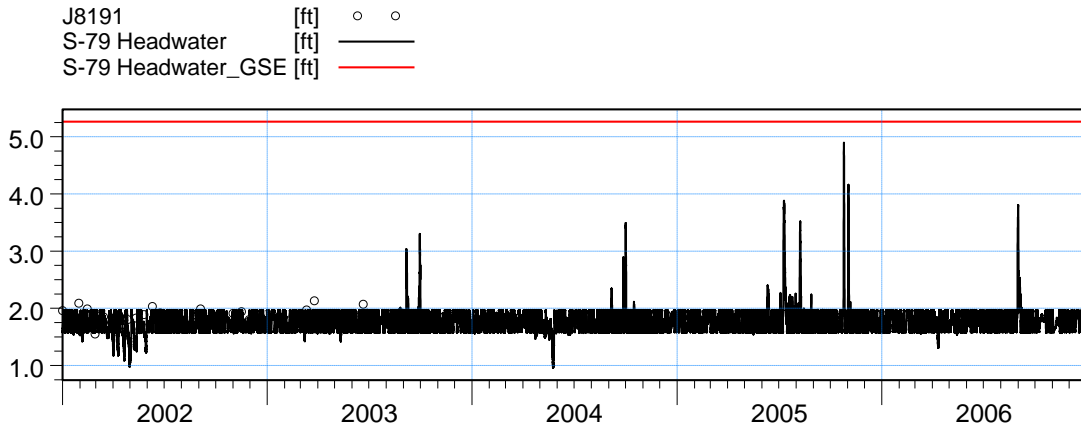


ME=-0.234332  
 MAE=0.30766  
 RMSE=0.438125  
 STDres=0.370192  
 R(Correlation)=0.38914  
 R2(Nash\_Sutcliffe)=-4.17044

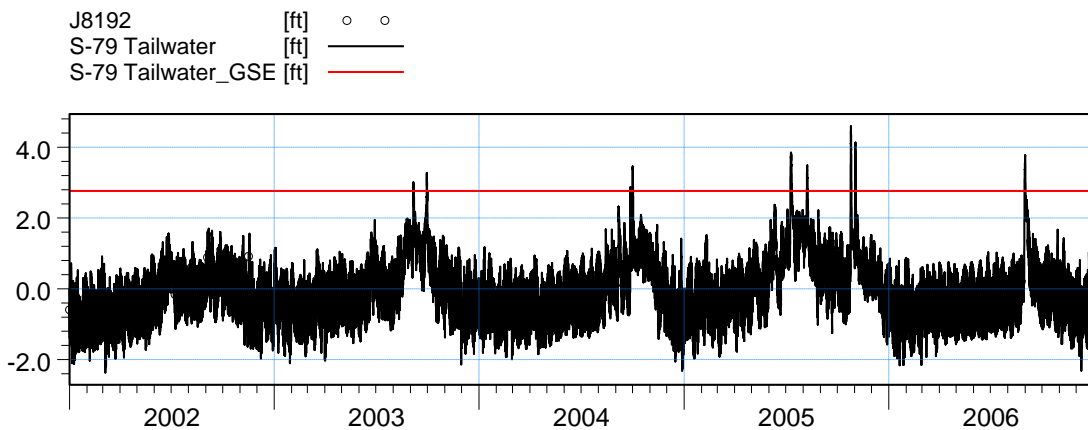


ME=0.686116  
 MAE=0.826173  
 RMSE=0.944604  
 STDres=0.649246  
 R(Correlation)=0.580349  
 R2(Nash\_Sutcliffe)=-2.58816

Figure B82. Stage at stations S-78 TW and Telegraph Creek\_24691, after refinement.

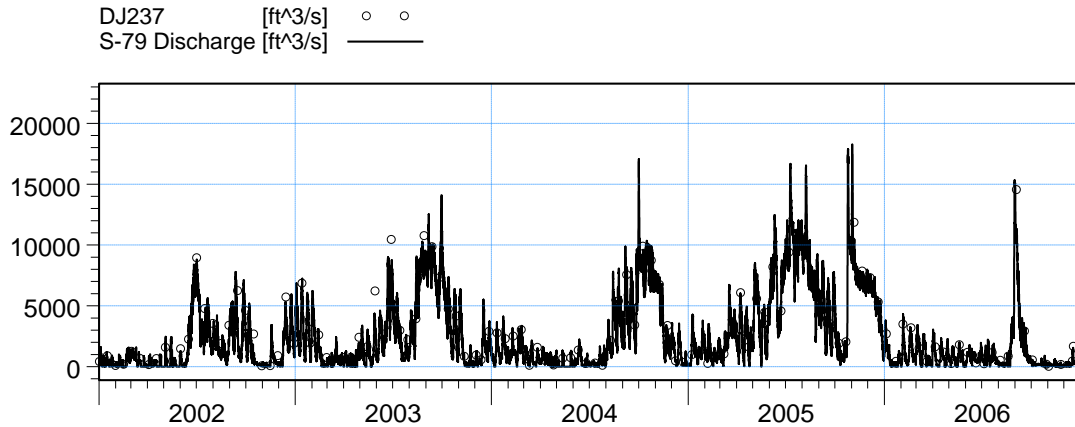


ME=0.0922963  
 MAE=0.175441  
 RMSE=0.214564  
 STDres=0.193698  
 R(Correlation)=0.0611082  
 R2(Nash\_Sutcliffe)=-1.5251

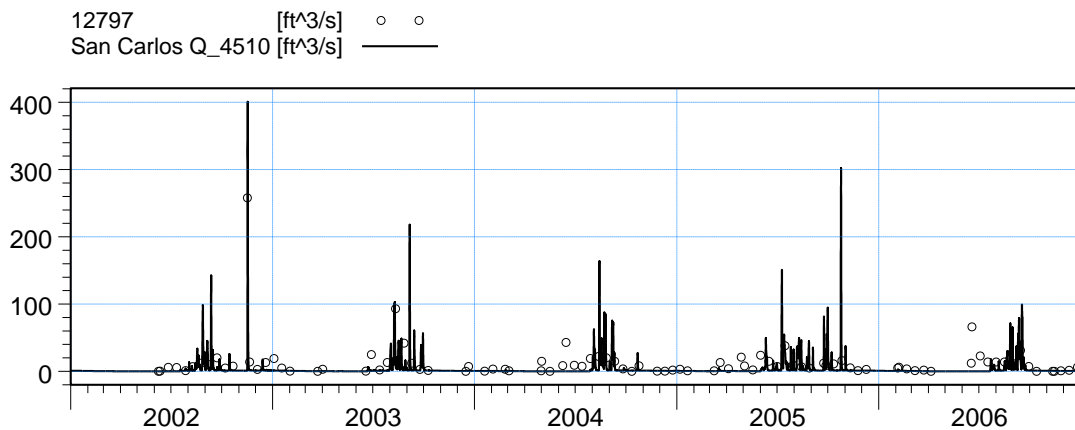


ME=0.152222  
 MAE=0.424678  
 RMSE=0.53888  
 STDres=0.516933  
 R(Correlation)=0.595187  
 R2(Nash\_Sutcliffe)=-0.414306

Figure B83. Stage at stations S-79 HW and S-79 TW, after refinement.



ME=515.611  
MAE=751.188  
RMSE=1107.99  
STDres=980.709  
R(Correlation)=0.95818  
R2(Nash\_Sutcliffe)=0.892242



ME=7.81874  
MAE=10.3527  
RMSE=20.9372  
STDres=19.4225  
R(Correlation)=0.462575  
R2(Nash\_Sutcliffe)=0.0395667

Figure B84. Flow at stations S-79 Q and San Carlos Q\_4510, after refinement.



**Appendix B6. Groundwater well stations north from Caloosahatchee**

| Station Name | before refinement |          |           |       |            | after refinement |          |           |       |            |
|--------------|-------------------|----------|-----------|-------|------------|------------------|----------|-----------|-------|------------|
|              | ME (ft)           | MAE (ft) | RMSE (ft) | R     | PL         | ME (ft)          | MAE (ft) | RMSE (ft) | R     | PL         |
| 17-GW1       | 1.74              | 1.74     | 1.83      | 0.73  | <b>1.8</b> | 1.59             | 1.59     | 1.69      | 0.77  | <b>1.8</b> |
| 17-GW3       | 0.24              | 0.65     | 0.89      | 0.85  | <b>1.0</b> | 0.11             | 0.58     | 0.75      | 0.89  | <b>1.0</b> |
| 17-GW4       | 0.22              | 0.46     | 0.72      | 0.77  | <b>1.0</b> | 0.26             | 0.50     | 0.77      | 0.76  | <b>1.0</b> |
| 18-GW1       | -1.18             | 1.40     | 1.60      | 0.77  | <b>1.8</b> | -0.92            | 1.19     | 1.43      | 0.76  | <b>1.5</b> |
| 18-GW2       | -3.13             | 3.15     | 3.31      | 0.63  | <b>2.8</b> | -2.99            | 3.01     | 3.16      | 0.66  | <b>2.8</b> |
| 19-GW1       | -2.05             | 2.05     | 2.17      | 0.83  | <b>2.3</b> | -1.98            | 1.98     | 2.11      | 0.83  | <b>1.8</b> |
| 20A-GW1      | -0.99             | 1.10     | 1.25      | 0.80  | <b>1.3</b> | -1.31            | 1.38     | 1.53      | 0.80  | <b>1.8</b> |
| 20-GW1       | -1.53             | 1.54     | 1.76      | 0.86  | <b>1.8</b> | -1.48            | 1.49     | 1.70      | 0.86  | <b>1.8</b> |
| 20-GW2       | -1.33             | 1.33     | 1.49      | 0.76  | <b>1.8</b> | -1.32            | 1.32     | 1.47      | 0.77  | <b>1.8</b> |
| 20-GW3       | -1.04             | 1.09     | 1.32      | 0.85  | <b>1.8</b> | -0.87            | 0.96     | 1.18      | 0.84  | <b>1.0</b> |
| 21-GW2       | -1.91             | 1.91     | 1.95      | 0.85  | <b>1.8</b> | -1.91            | 1.91     | 1.96      | 0.85  | <b>1.8</b> |
| 22-GW1       | -2.72             | 2.94     | 4.54      | -0.03 | <b>3.0</b> | -0.69            | 0.99     | 1.21      | 0.74  | <b>1.0</b> |
| 23-GW1       | 0.04              | 3.21     | 4.07      | 0.00  | <b>2.5</b> | -2.08            | 2.08     | 2.38      | 0.51  | <b>2.5</b> |
| 23-GW2       | -4.48             | 4.74     | 7.39      | 0.58  | <b>2.8</b> | -0.03            | 0.46     | 0.62      | 0.65  | <b>1.3</b> |
| 24-GW1       | -0.80             | 1.14     | 1.50      | 0.60  | <b>1.8</b> | -0.75            | 1.12     | 1.46      | 0.61  | <b>1.8</b> |
| 24-GW2       | -0.06             | 0.87     | 1.06      | 0.78  | <b>1.0</b> | -0.01            | 0.83     | 1.01      | 0.79  | <b>1.0</b> |
| 26-GW1       | -5.34             | 5.34     | 5.38      | 0.75  | <b>2.5</b> | -5.59            | 5.59     | 5.63      | 0.69  | <b>2.8</b> |
| 26-GW2       | 1.25              | 1.30     | 1.72      | 0.74  | <b>1.8</b> | 0.15             | 0.93     | 1.23      | 0.72  | <b>1.0</b> |
| 27O-GW1      | 0.30              | 0.84     | 1.00      | 0.66  | <b>1.3</b> | 0.45             | 0.90     | 1.12      | 0.61  | <b>1.3</b> |
| 27-GW1       | -0.59             | 0.72     | 0.87      | 0.74  | <b>1.0</b> | -0.07            | 0.69     | 0.87      | 0.72  | <b>1.0</b> |
| 27-GW2       | 0.18              | 0.89     | 1.20      | 0.40  | <b>1.5</b> | -0.01            | 1.08     | 1.33      | 0.40  | <b>2.0</b> |
| 28-GW1       | 3.08              | 3.08     | 3.32      | 0.63  | <b>2.8</b> | 3.68             | 3.68     | 3.95      | 0.59  | <b>2.8</b> |
| 28-GW2       | -0.27             | 0.84     | 1.04      | 0.71  | <b>1.0</b> | 0.14             | 1.01     | 1.26      | 0.65  | <b>1.8</b> |
| 29-GW1       | -1.97             | 2.19     | 2.73      | 0.01  | <b>2.8</b> | -3.36            | 3.36     | 3.59      | 0.40  | <b>3.0</b> |
| 29-GW2       | -0.37             | 0.66     | 0.91      | 0.83  | <b>1.0</b> | 2.12             | 2.26     | 2.70      | 0.61  | <b>2.8</b> |
| 5-GW4        | -2.78             | 2.81     | 3.11      | 0.32  | <b>3.0</b> | -2.64            | 2.69     | 2.99      | 0.34  | <b>3.0</b> |
| 5-GW5        | -2.20             | 2.20     | 2.34      | 0.57  | <b>2.5</b> | -2.11            | 2.11     | 2.23      | 0.67  | <b>2.5</b> |
| 5-GW6        | -0.66             | 1.10     | 1.41      | -0.25 | <b>2.0</b> | -0.46            | 1.00     | 1.26      | 0.17  | <b>2.0</b> |
| 5-GW8        | -1.99             | 2.01     | 2.27      | 0.69  | <b>2.3</b> | -1.72            | 1.75     | 2.04      | 0.65  | <b>2.0</b> |
| MUSEWELLS    | -4.02             | 4.64     | 6.40      | -0.35 | <b>3.0</b> | -4.74            | 5.29     | 7.01      | -0.31 | <b>3.0</b> |

Table B7. Statistical parameters and level of performance at groundwater monitoring wells north of the Caloosahatchee River. The green color indicates the highest performance level (1.0, 1.2 and 1.5), yellow for medium (1.8, 2.0, 2.3, 2.5) and orange for low (2.8, 3.0).

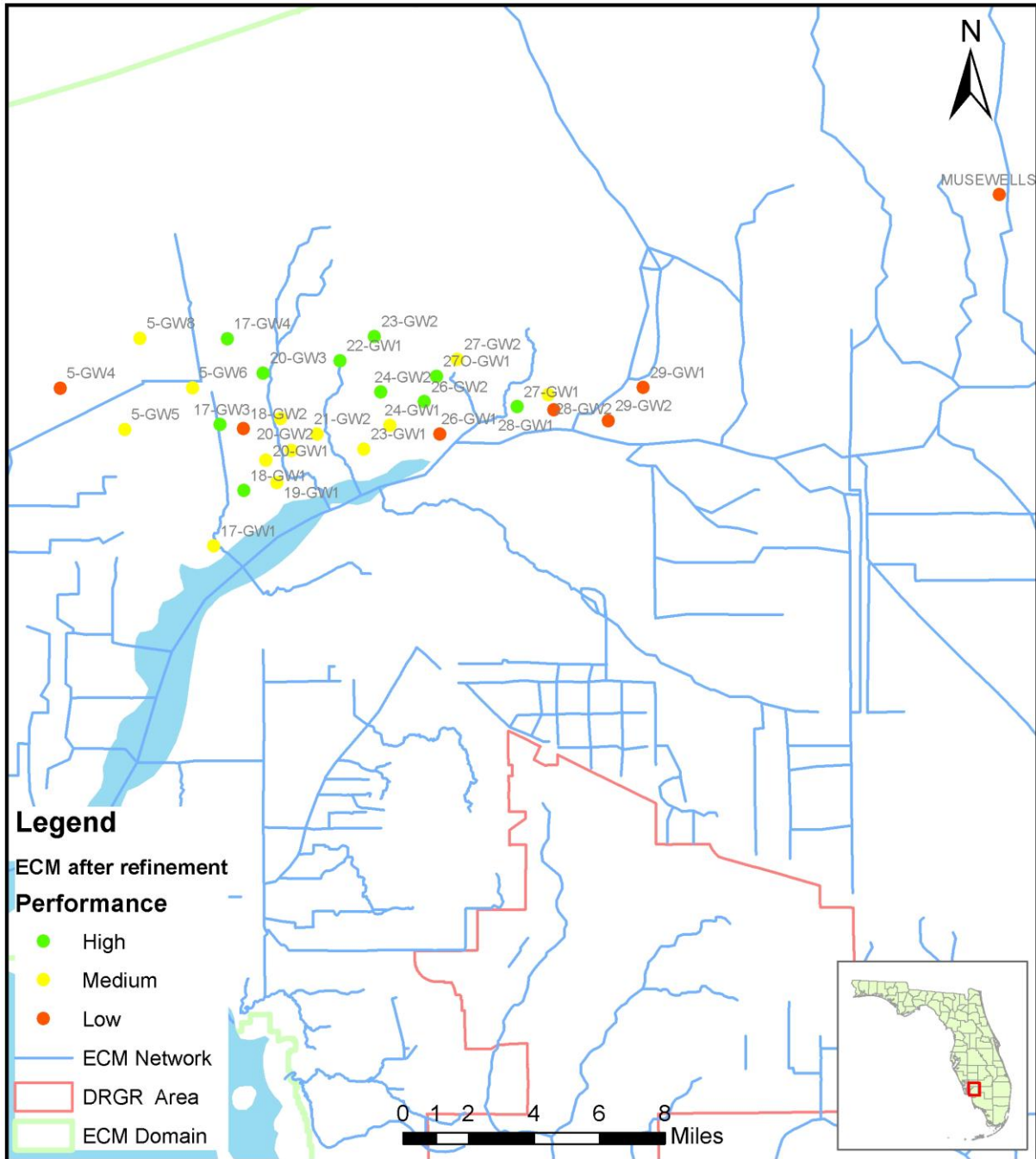
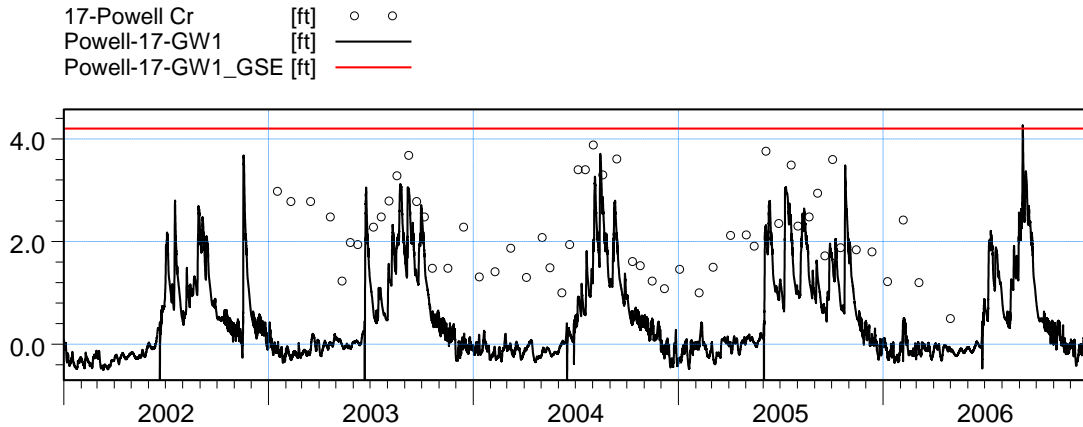
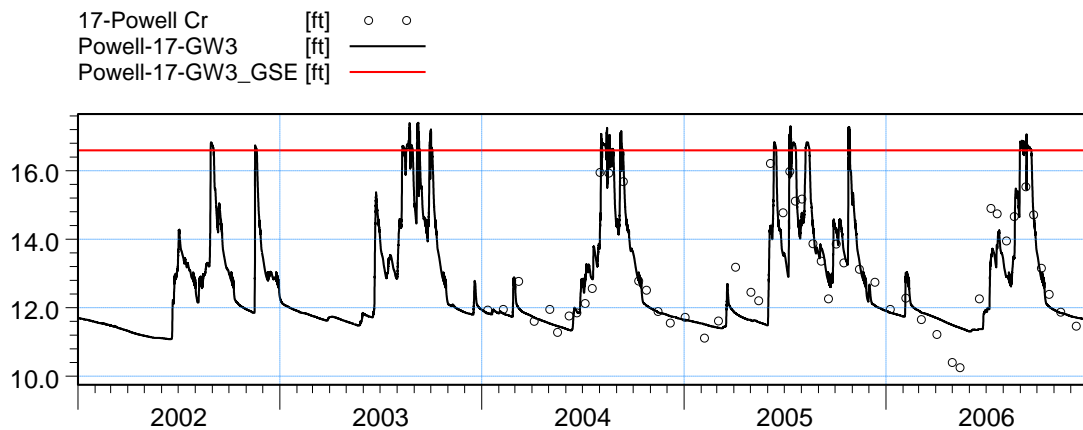


Figure B85. Average performance level at groundwater monitoring wells north of Caloosahatchee River, after the refinement process.

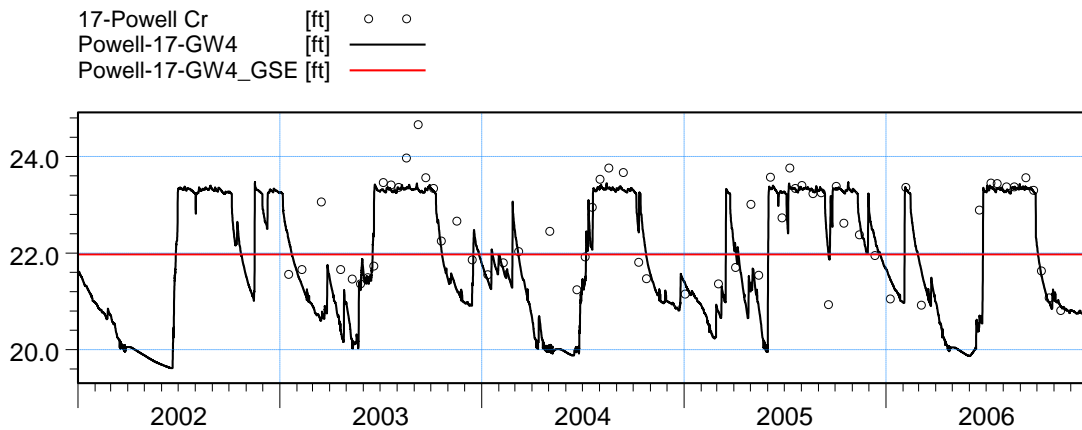


ME=1.58775  
 MAE=1.58775  
 RMSE=1.69191  
 STDres=0.584487  
 R(Correlation)=0.773349  
 R2(Nash\_Sutcliffe)=-2.97405



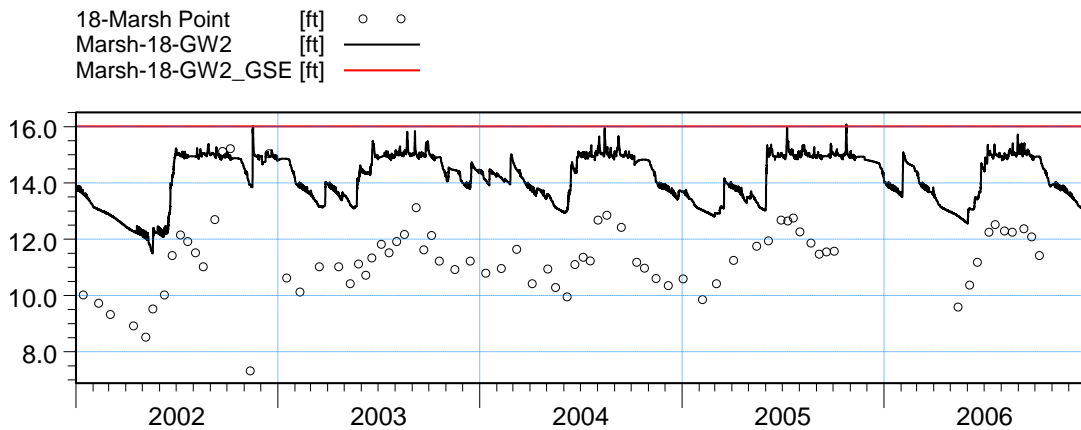
ME=0.109963  
 MAE=0.583  
 RMSE=0.749119  
 STDres=0.741005  
 R(Correlation)=0.885938  
 R2(Nash\_Sutcliffe)=0.771563

Figure B86. Groundwater elevation at wells 17-GW1 and 17-GW3, after refinement.

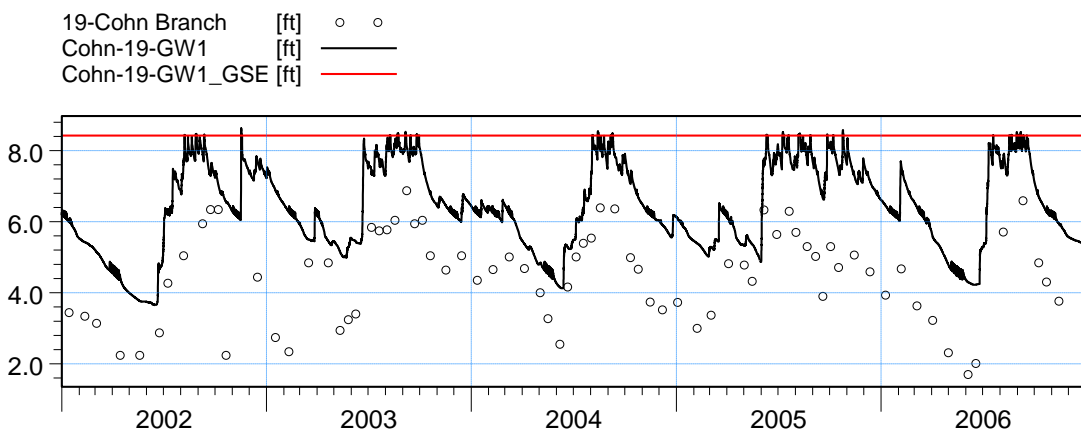


ME=0.263478  
 MAE=0.498786  
 RMSE=0.767094  
 STDres=0.720425  
 R(Correlation)=0.759533  
 R2(Nash\_Sutcliffe)=0.387091

Figure B87. Groundwater elevation at wells 17-GW4 and 18-GW1, after refinement.

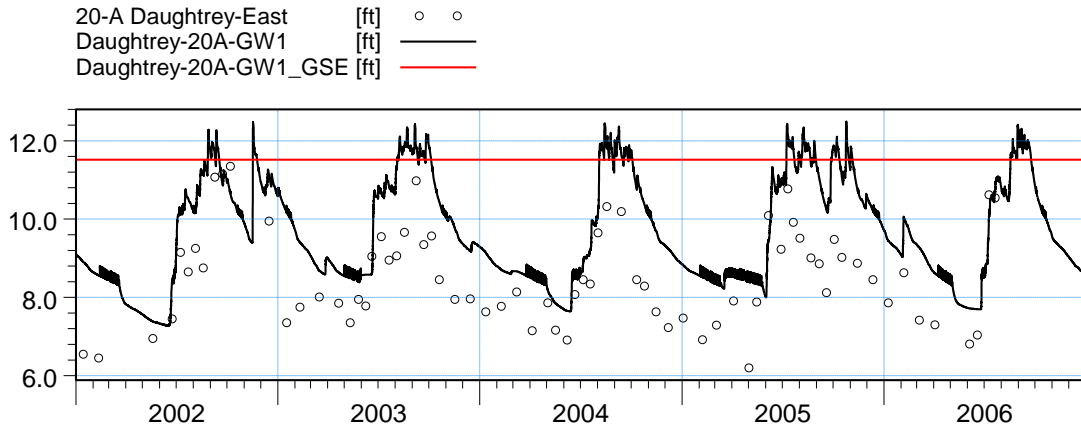


ME=-2.99164  
 MAE=3.00523  
 RMSE=3.16045  
 STDres=1.01907  
 R(Correlation)=0.660179  
 R2(Nash\_Sutcliffe)=-4.42621

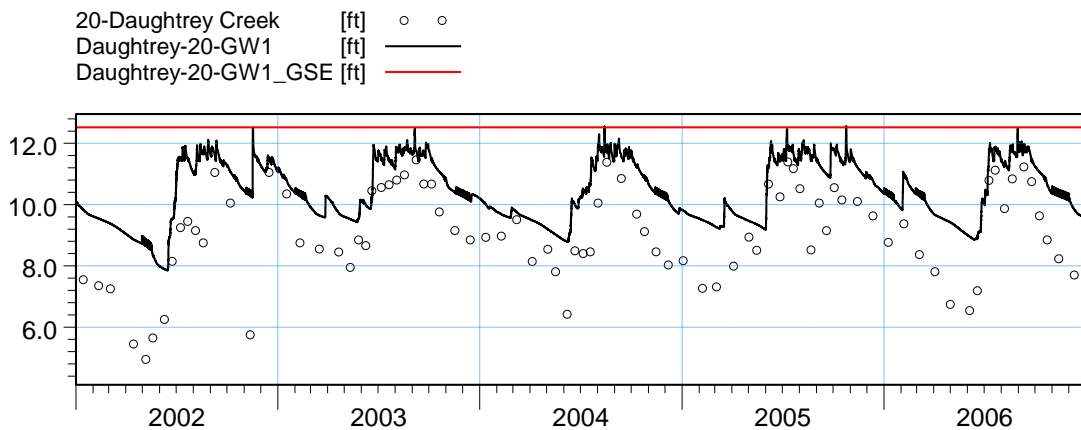


ME=-1.98343  
 MAE=1.98343  
 RMSE=2.11289  
 STDres=0.728228  
 R(Correlation)=0.828452  
 R2(Nash\_Sutcliffe)=-1.72654

Figure B88. Groundwater elevation at wells 18-GW2 and 19-GW1, after refinement.

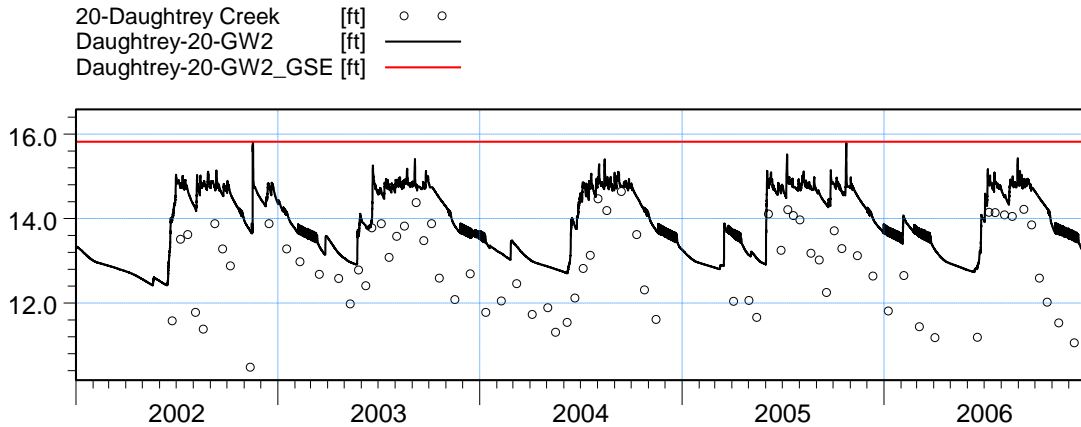


ME=-1.30694  
 MAE=1.37574  
 RMSE=1.53304  
 STDres=0.801309  
 R(Correlation)=0.800392  
 R2(Nash\_Sutcliffe)=-0.535158

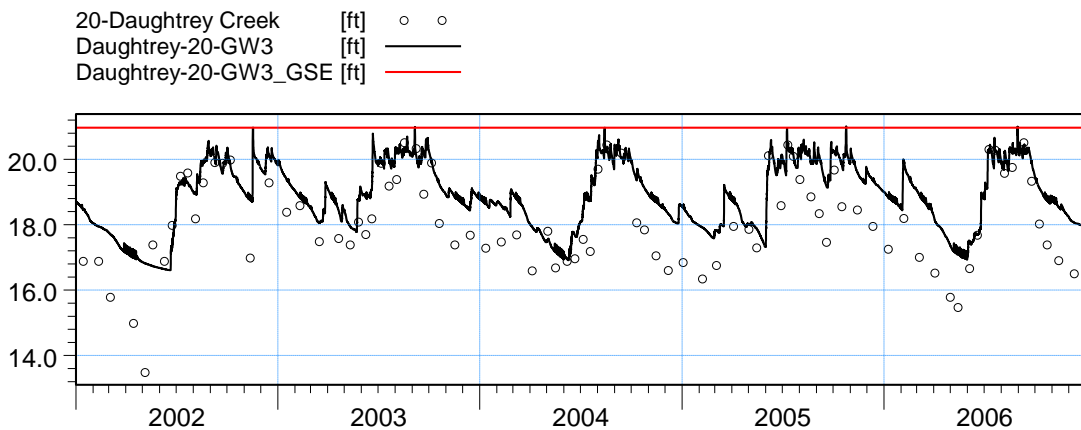


ME=-1.48351  
 MAE=1.49133  
 RMSE=1.70245  
 STDres=0.835183  
 R(Correlation)=0.860013  
 R2(Nash\_Sutcliffe)=-0.248557

Figure B89. Groundwater elevation at wells 20A-GW1 and 20-GW1, after refinement.

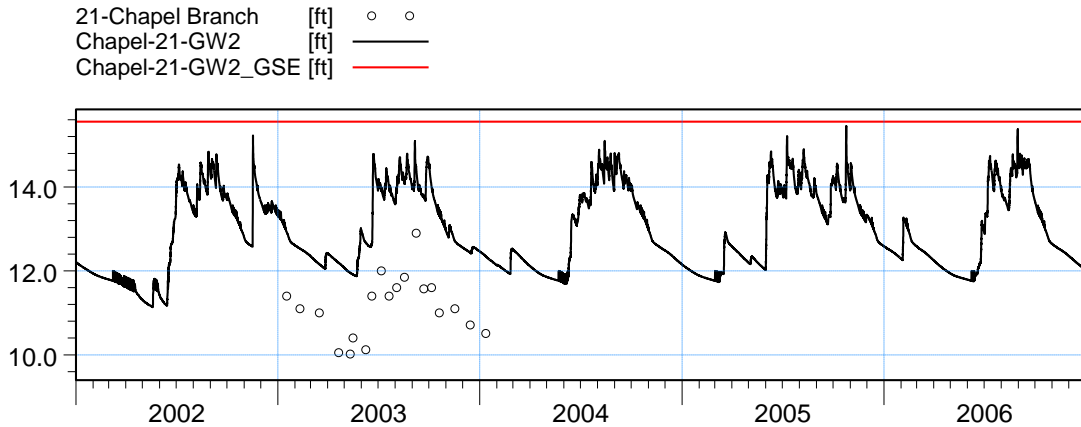


ME=-1.31625  
 MAE=1.31625  
 RMSE=1.4688  
 STDres=0.651806  
 R(Correlation)=0.774508  
 R2(Nash\_Sutcliffe)=-1.10593

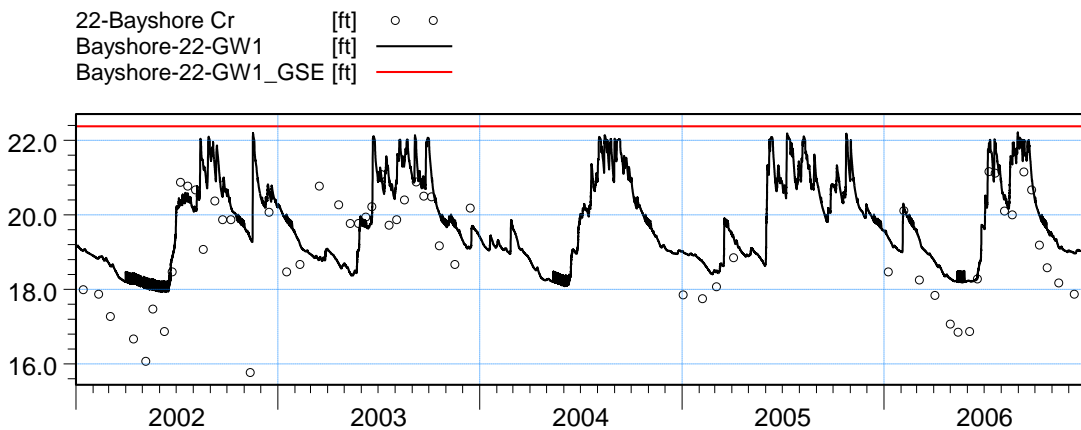


ME=-0.865977  
 MAE=0.960532  
 RMSE=1.18126  
 STDres=0.803404  
 R(Correlation)=0.838509  
 R2(Nash\_Sutcliffe)=0.327749

Figure B90. Groundwater elevation at wells 20-GW2 and 20-GW3, after refinement.

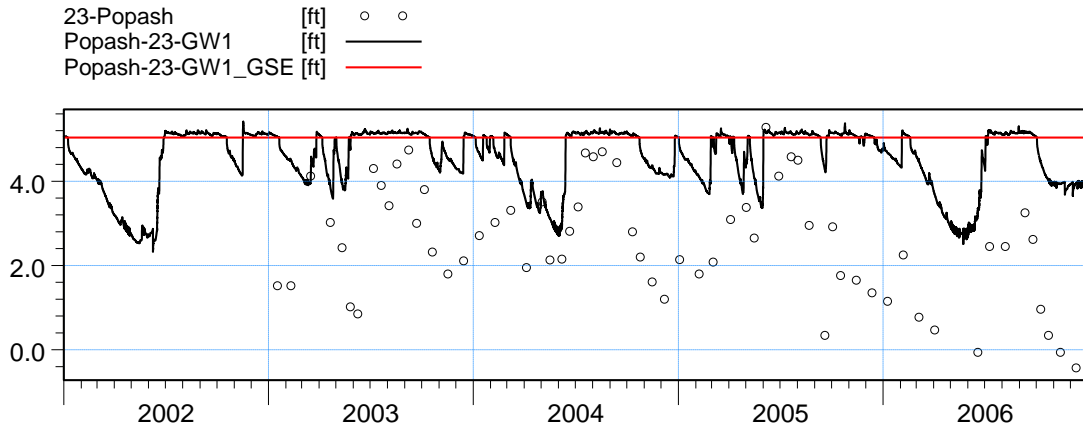


ME=-1.91011  
 MAE=1.91011  
 RMSE=1.95764  
 STDres=0.428773  
 R(Correlation)=0.851248  
 R2(Nash\_Sutcliffe)=-6.42507

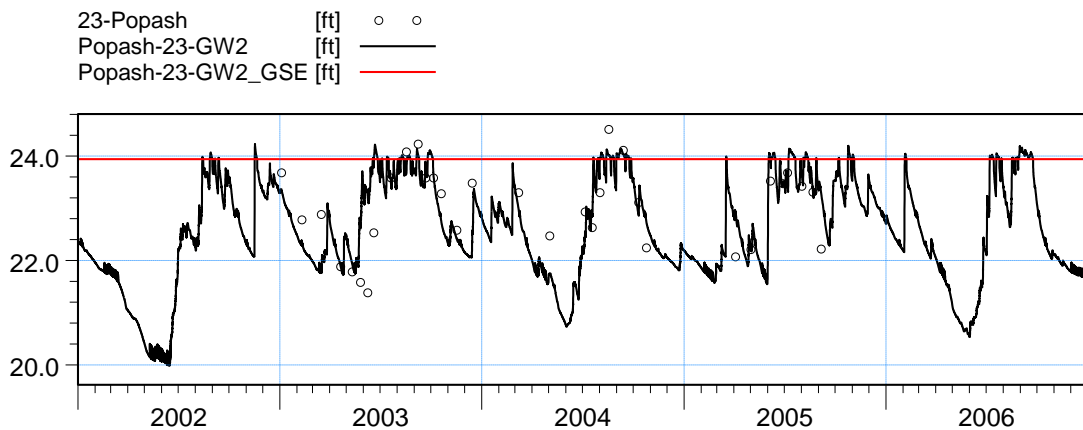


ME=-0.693341  
 MAE=0.986734  
 RMSE=1.20682  
 STDres=0.987767  
 R(Correlation)=0.742392  
 R2(Nash\_Sutcliffe)=0.32956

Figure B91. Groundwater elevation at wells 21-GW2 and 22-GW1, after refinement.

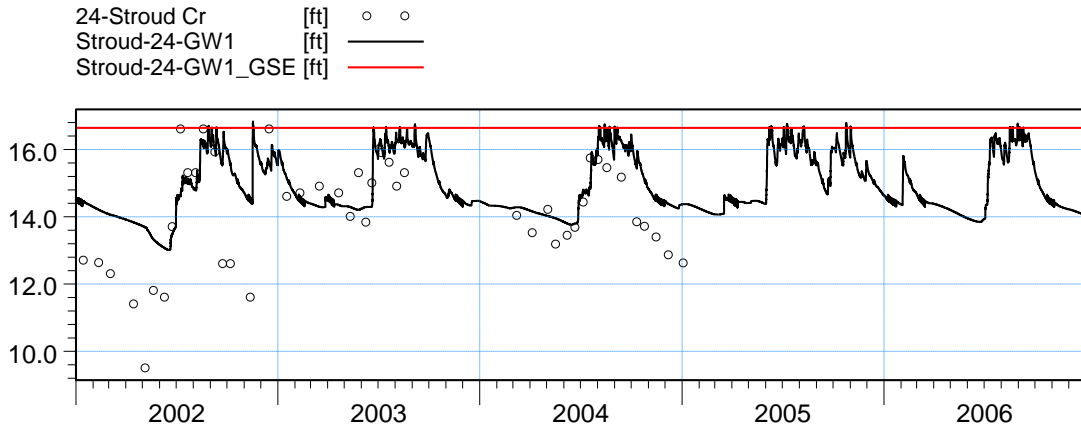


ME=-2.07554  
 MAE=2.08425  
 RMSE=2.38496  
 STDres=1.17481  
 R(Correlation)=0.51019  
 R2(Nash\_Sutcliffe)=-2.07594

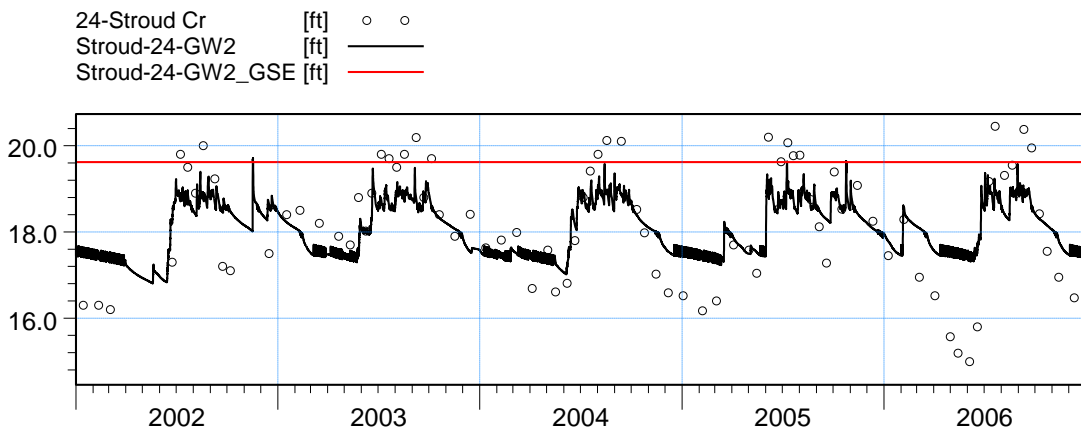


ME=-0.0308459  
 MAE=0.457588  
 RMSE=0.620912  
 STDres=0.620146  
 R(Correlation)=0.646187  
 R2(Nash\_Sutcliffe)=0.3593

Figure B92. Groundwater elevation at wells 23-GW1 and 23-GW2, after refinement.

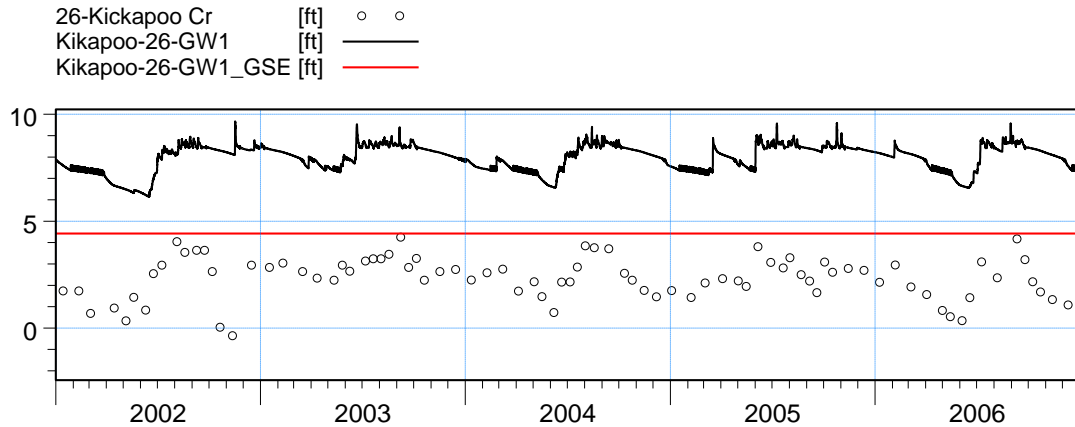


ME=-0.747966  
 MAE=1.11513  
 RMSE=1.45498  
 STDres=1.248  
 R(Correlation)=0.608686  
 R2(Nash\_Sutcliffe)=0.142304

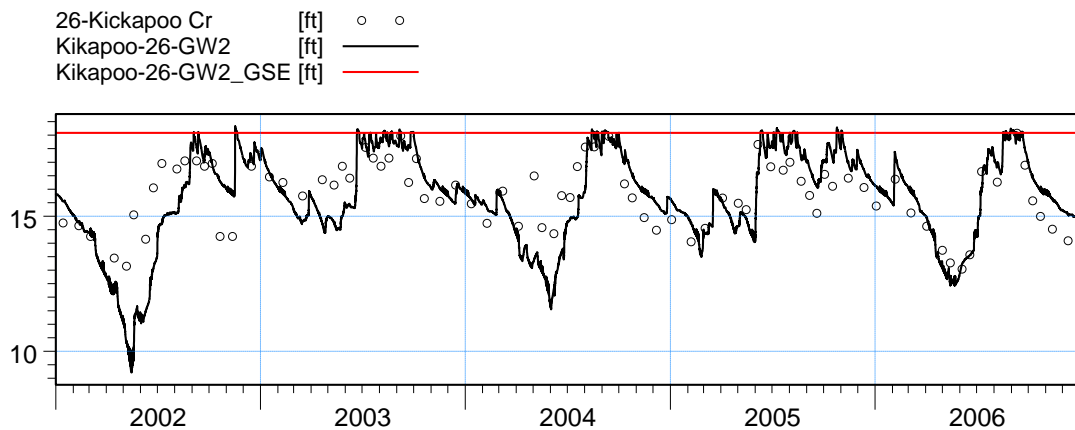


ME=-0.00533193  
 MAE=0.82558  
 RMSE=1.01247  
 STDres=1.01246  
 R(Correlation)=0.794554  
 R2(Nash\_Sutcliffe)=0.474371

Figure B93. Groundwater elevation at wells 24-GW1 and 24-GW2, after refinement.

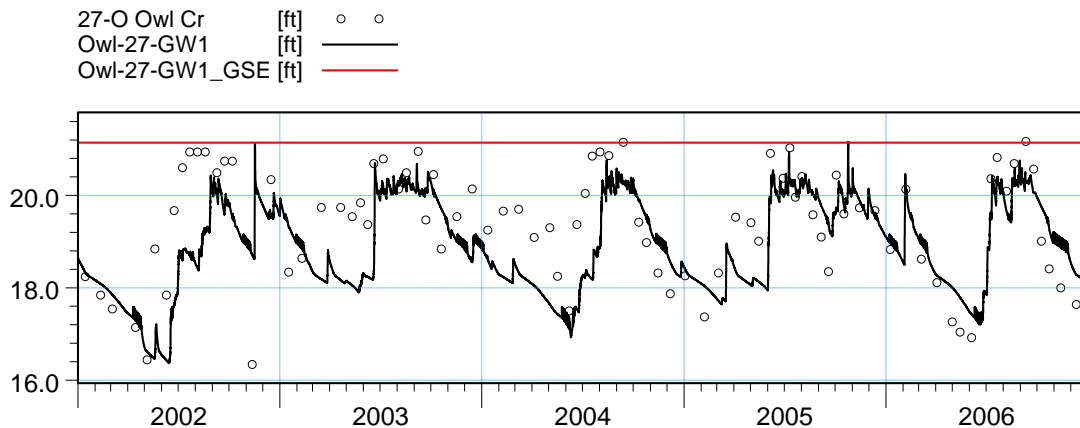


ME=-5.58531  
 MAE=5.58531  
 RMSE=5.63219  
 STDres=0.725187  
 R(Correlation)=0.686331  
 R2(Nash\_Sutcliffe)=-31.0493

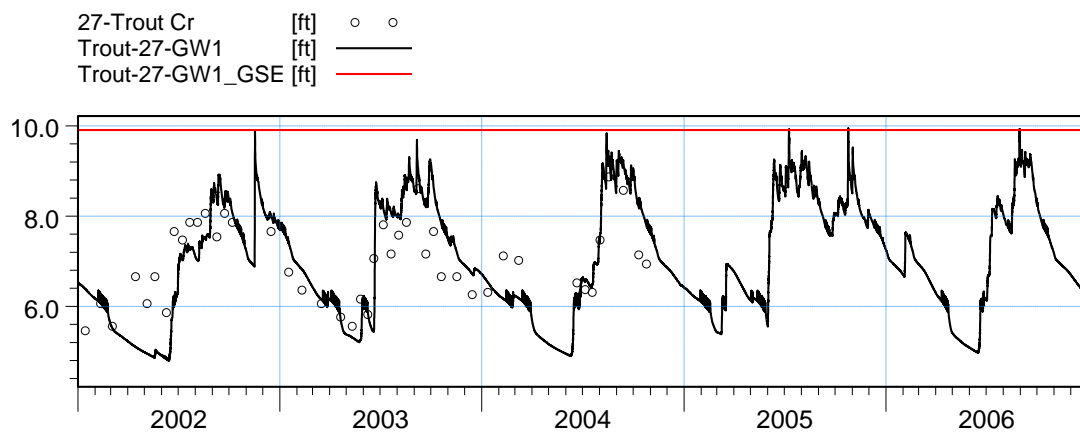


ME=0.152335  
 MAE=0.928914  
 RMSE=1.23436  
 STDres=1.22493  
 R(Correlation)=0.715037  
 R2(Nash\_Sutcliffe)=0.00272002

Figure B94. Groundwater elevation at wells 26-GW1 and 26-GW2, after refinement.

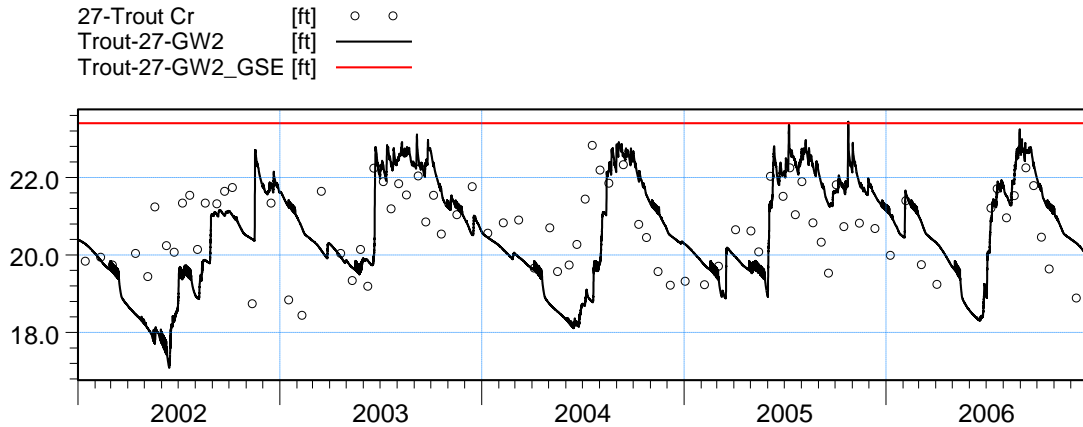


ME=0.445249  
 MAE=0.903019  
 RMSE=1.11705  
 STDres=1.02448  
 R(Correlation)=0.611945  
 R2(Nash\_Sutcliffe)=0.20865

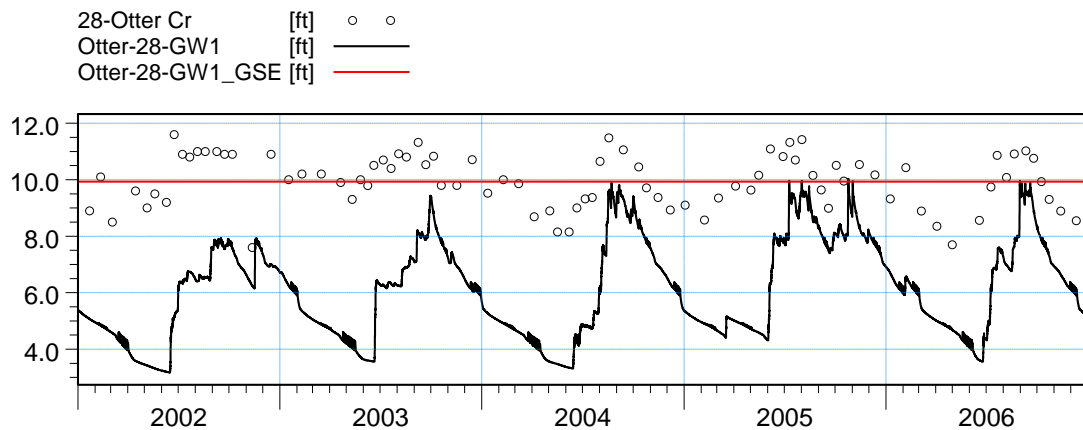


ME=-0.0704249  
 MAE=0.691801  
 RMSE=0.86693  
 STDres=0.864065  
 R(Correlation)=0.719052  
 R2(Nash\_Sutcliffe)=0.0796882

Figure B95. Groundwater elevation at wells 27O-GW1 and 27-GW1, after refinement.

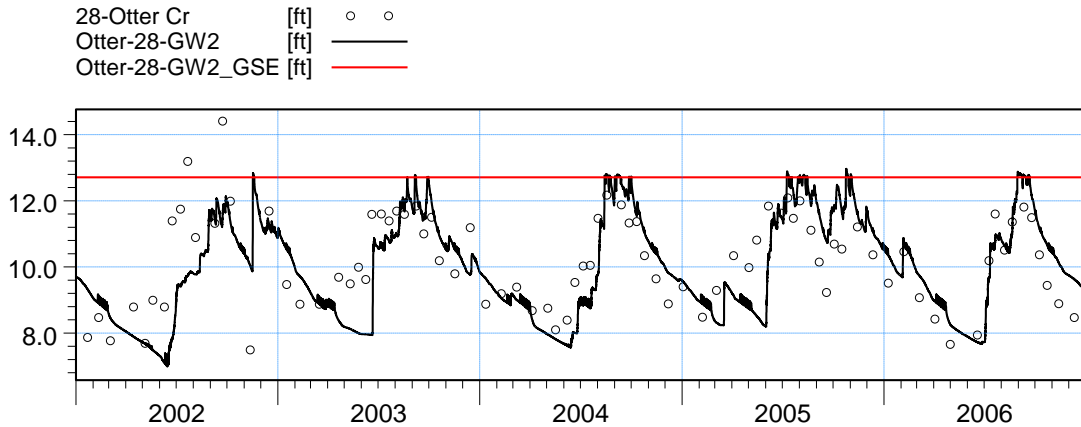


ME=-0.00525769  
 MAE=1.07722  
 RMSE=1.32714  
 STDres=1.32713  
 R(Correlation)=0.395351  
 R2(Nash\_Sutcliffe)=-0.663459

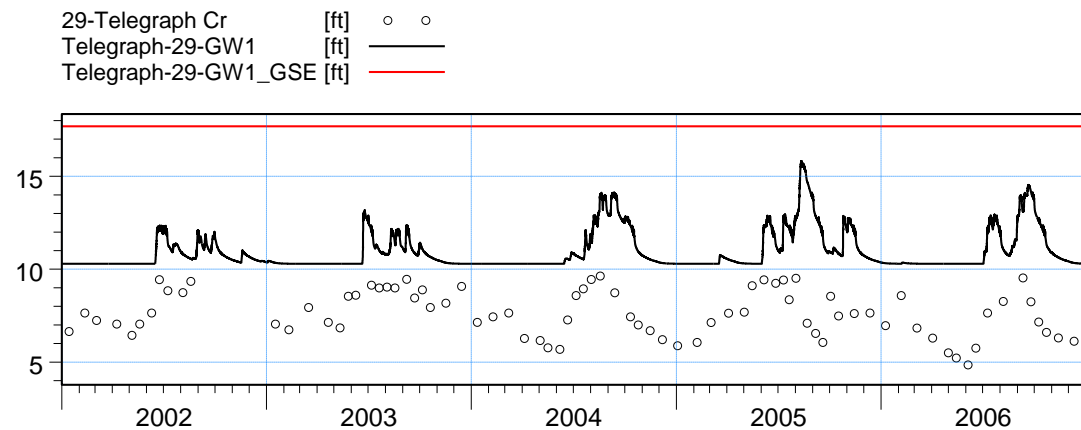


ME=3.67953  
 MAE=3.67953  
 RMSE=3.94838  
 STDres=1.43204  
 R(Correlation)=0.585478  
 R2(Nash\_Sutcliffe)=-16.9481

Figure B96. Groundwater elevation at wells 27-GW2 and 28-GW1, after refinement.

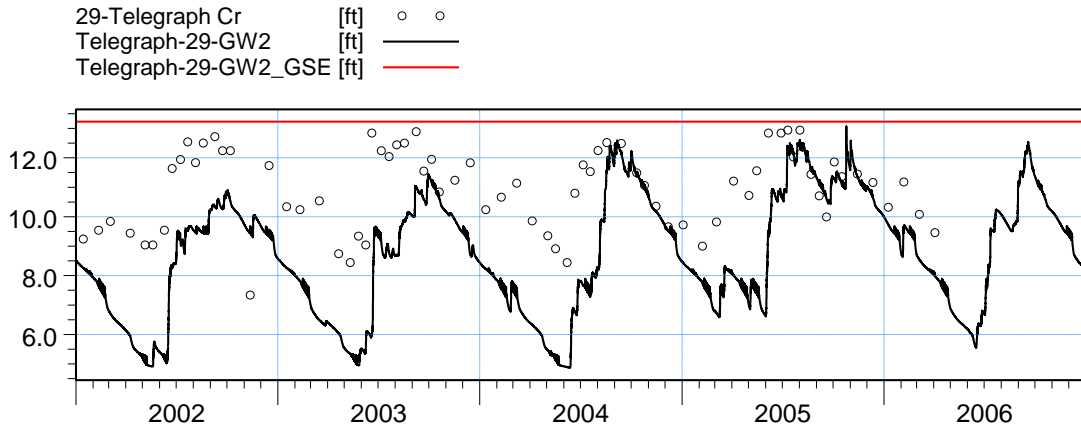


ME=0.135078  
 MAE=1.00713  
 RMSE=1.25811  
 STDres=1.25084  
 R(Correlation)=0.645052  
 R2(Nash\_Sutcliffe)=0.207105

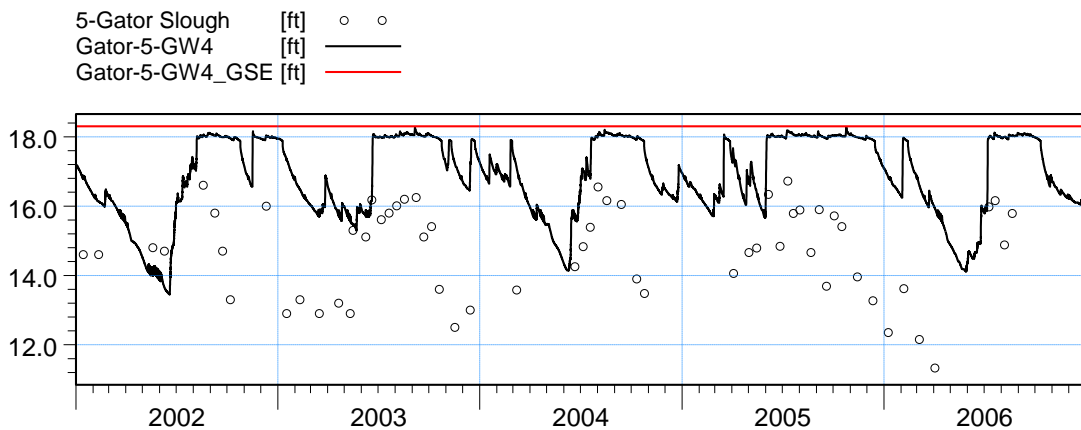


ME=-3.35684  
 MAE=3.35684  
 RMSE=3.59469  
 STDres=1.28586  
 R(Correlation)=0.400213  
 R2(Nash\_Sutcliffe)=-7.25349

Figure B97. Groundwater elevation at wells 28-GW2 and 29-GW1, after refinement.

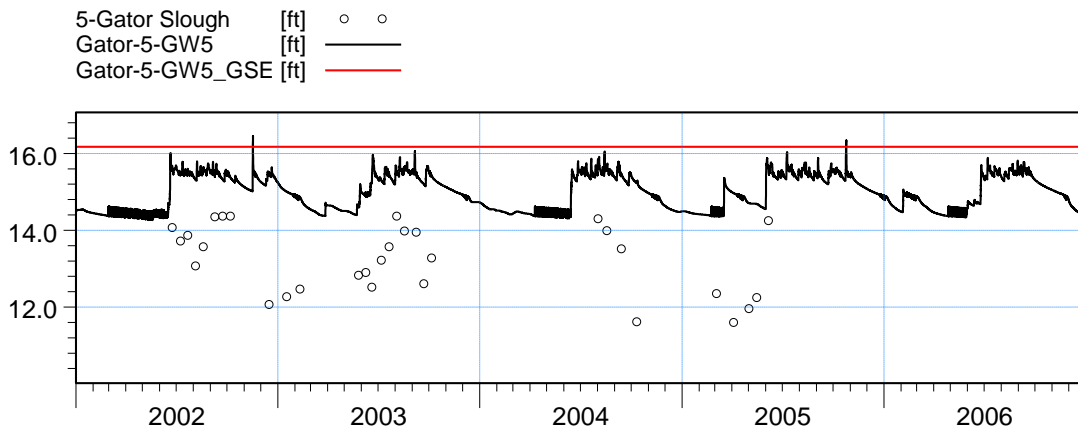


ME=2.12438  
 MAE=2.25942  
 RMSE=2.70105  
 STDres=1.66813  
 R(Correlation)=0.61182  
 R2(Nash\_Sutcliffe)=-2.95651

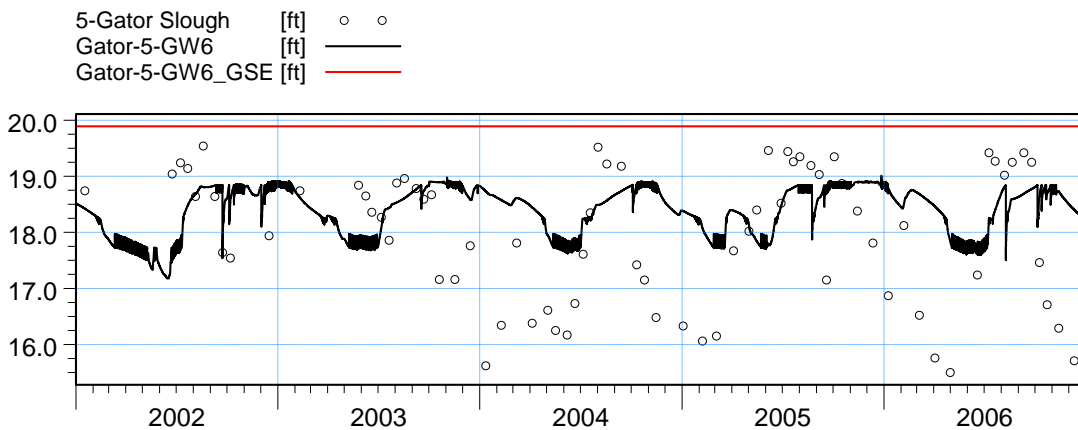


ME=-2.63809  
 MAE=2.69497  
 RMSE=2.99001  
 STDres=1.40736  
 R(Correlation)=0.339797  
 R2(Nash\_Sutcliffe)=-3.78144

Figure B98. Groundwater elevation at wells 29-GW2 and 5-GW4, after refinement.

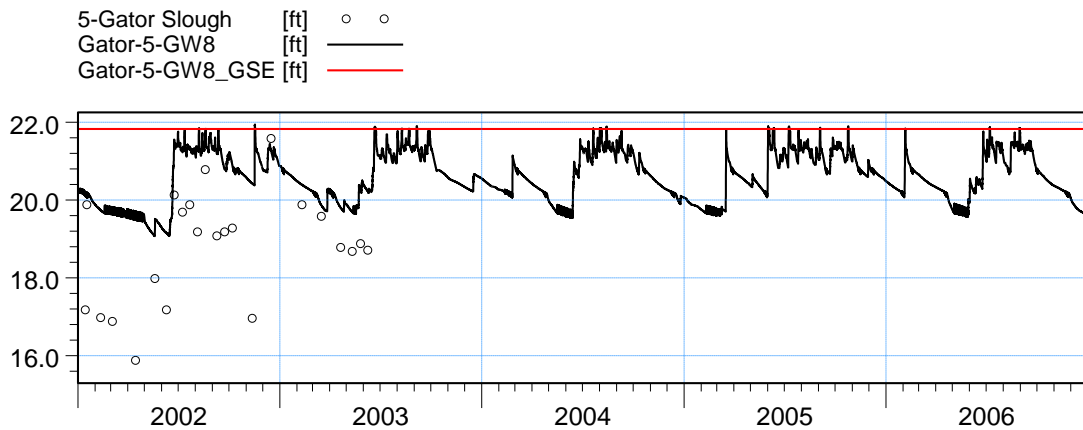


ME=-2.11047  
 MAE=2.11047  
 RMSE=2.23349  
 STDres=0.731026  
 R(Correlation)=0.667842  
 R2(Nash\_Sutcliffe)=-5.01162

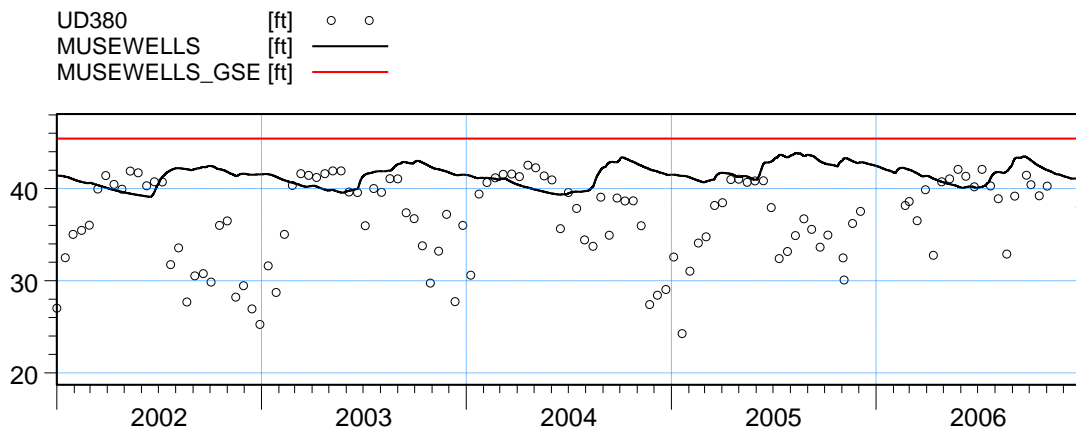


ME=-0.462643  
 MAE=1.0027  
 RMSE=1.26482  
 STDres=1.17717  
 R(Correlation)=0.174678  
 R2(Nash\_Sutcliffe)=-0.149706

Figure B99. Groundwater elevation at wells 5-GW5 and 5-GW6, after refinement.



ME=-1.72184  
 MAE=1.74723  
 RMSE=2.04134  
 STDres=1.09651  
 R(Correlation)=0.647348  
 R2(Nash\_Sutcliffe)=-1.06364



ME=-4.74107  
 MAE=5.29485  
 RMSE=7.01442  
 STDres=5.16956  
 R(Correlation)=-0.313013  
 R2(Nash\_Sutcliffe)=-1.19331

Figure B100. Groundwater elevation at wells 5-GW8 and MUSEWELLS, after refinement.



## ***APPENDIX C. LS ECM RESULTS AT OBSERVATION STATIONS***

All figures and tables related to the results from LS ECM at observation station locations are presented in this appendix. They are compared to the previous results from the ECM inside the LSM domain area, which were presented detailed in Appendix B.

The results from the two different resolution models are similar at most of the observation stations. For 88 stations considered, the average performance index from LS ECM is better in 14 of them and worse in 11.

The meaning of symbols used in this appendix is similar to the ones in other appendixes.

GSE: ground surface elevation;

MAE: mean absolute error;

ME: mean error;

PL: average performance level, which is number in the range from 1.0 (high) to 3.0 (low);

R: Correlation coefficient;

RMSE: root mean square error.

### **List of Tables**

Table C1. Statistical parameters and level of performance at monitoring stations in the LS ECM domain area. The green color indicates the highest performance level (1.0, 1.2 and 1.5), yellow for medium (1.8, 2.0, 2.3, 2.5) and orange for low (2.8, 3.0). ..... 7

**List of Figures**

Figure C1. Average performance level of the ECM results at monitoring stations in the LS ECM domain area..... 8

Figure C2. Average performance level of the LS ECM results at monitoring stations. .... 9

Figure C3. Groundwater elevation at wells 40-GW1 and 40-GW2. The black line corresponds to LS ECM result, and red line to the ECM result. .... 10

Figure C4. Groundwater elevation at wells 40-GW3 and 40-GW4. The black line corresponds to LS ECM result, and red line to the ECM result. .... 11

Figure C5. Groundwater elevation at wells 40-GW5 and 40-GW6. The black line corresponds to LS ECM result, and red line to the ECM result. .... 12

Figure C6. Groundwater elevation at wells 40-GW7 and 46A-GW3. The black line corresponds to LS ECM result, and red line to the ECM result. .... 13

Figure C7. Groundwater elevation at wells 46A-GW4 and 46A-GW10. The black line corresponds to LS ECM result, and red line to the ECM result. .... 14

Figure C8. Groundwater elevation at wells 46A-GW11 and 46A-GW12. The black line corresponds to LS ECM result, and red line to the ECM result. .... 15

Figure C9. Groundwater elevation at wells 46A-GW13 and 46A-GW14. The black line corresponds to LS ECM result, and red line to the ECM result. .... 16

Figure C10. Groundwater elevation at wells 46A-GW15 and 46A-GW18. The black line corresponds to LS ECM result, and red line to the ECM result. .... 17

Figure C11. Groundwater elevation at wells 46A-GW21 and 46A-GW25. The black line corresponds to LS ECM result, and red line to the ECM result. .... 18

Figure C12. Groundwater elevation at wells 46A-GW26 and 49-GW3. The black line corresponds to LS ECM result, and red line to the ECM result. .... 19

Figure C13. Groundwater elevation at wells 49-GW6 and 49-GW7. The black line corresponds to LS ECM result, and red line to the ECM result. .... 20

Figure C14. Groundwater elevation at wells 49-GW8 and 49-GW9. The black line corresponds to LS ECM result, and red line to the ECM result. .... 21

Figure C15. Groundwater elevation at wells 49-GW10 and 49-GW11. The black line corresponds to LS ECM result, and red line to the ECM result. .... 22

Figure C16. Groundwater elevation at wells 49-GW12 and 49-GW14. The black line corresponds to LS ECM result, and red line to the ECM result. .... 23

Figure C17. Groundwater elevation at wells 49-GW15 and 49L-GW1. The black line corresponds to LS ECM result, and red line to the ECM result. .... 24

Figure C18. Groundwater elevation at wells BRM-MW1 and BRM-MW2. The black line corresponds to LS ECM result, and red line to the ECM result. .... 25

Figure C19. Groundwater elevation at wells BRM-MW3 and BRM-MW4. The black line corresponds to LS ECM result, and red line to the ECM result. .... 26

Figure C20. Groundwater elevation at wells BRM-Lake and Corkscrew Swamp. The black line corresponds to LS ECM result, and red line to the ECM result. .... 27



Figure C21. Groundwater elevation at wells FP2\_GW1 and FP3\_GW1. The black line corresponds to LS ECM result, and red line to the ECM result..... 28

Figure C22. Groundwater elevation at wells FP4\_GW1 and FP5\_GW1. The black line corresponds to LS ECM result, and red line to the ECM result..... 29

Figure C23. Groundwater elevation at wells FP6\_GW1 and FP7\_GW1. The black line corresponds to LS ECM result, and red line to the ECM result..... 30

Figure C24. Groundwater elevation at wells FP8\_GW1 and FP9\_G. The black line corresponds to LS ECM result, and red line to the ECM result..... 31

Figure C25. Groundwater elevation at wells FP10\_G and HF1\_G. The black line corresponds to LS ECM result, and red line to the ECM result. .... 32

Figure C26. Groundwater elevation at wells HF2\_G and HF3\_G. The black line corresponds to LS ECM result, and red line to the ECM result. .... 33

Figure C27. Groundwater elevation at wells HF4\_G and HF7\_G. The black line corresponds to LS ECM result, and red line to the ECM result. .... 34

Figure C28. Groundwater elevation at wells L-1138 and L-1985. The black line corresponds to LS ECM result, and red line to the ECM result. .... 35

Figure C29. Groundwater elevation at wells L-2192 and L-2204. The black line corresponds to LS ECM result, and red line to the ECM result. .... 36

Figure C30. Groundwater elevation at wells L-5649 and L-5664. The black line corresponds to LS ECM result, and red line to the ECM result. .... 37

Figure C31. Groundwater elevation at wells L-5667 and L-5669R. The black line corresponds to LS ECM result, and red line to the ECM result. .... 38

Figure C32. Groundwater elevation at wells L-5673 and L-5874. The black line corresponds to LS ECM result, and red line to the ECM result. .... 39

Figure C33. Groundwater elevation at wells L-730 and L-739. The black line corresponds to LS ECM result, and red line to the ECM result. .... 40

Figure C34. Groundwater elevation at wells MPW02 and MPW03. The black line corresponds to LS ECM result, and red line to the ECM result..... 41

Figure C35. Groundwater elevation at wells MPW04 and MPW05. The black line corresponds to LS ECM result, and red line to the ECM result..... 42

Figure C36. Groundwater elevation at wells MPW08 and MPW25. The black line corresponds to LS ECM result, and red line to the ECM result..... 43

Figure C37. Groundwater elevation at wells MPW27 and MPW28. The black line corresponds to LS ECM result, and red line to the ECM result..... 44

Figure C38. Groundwater elevation at wells MPW29 and MPW30. The black line corresponds to LS ECM result, and red line to the ECM result..... 45

Figure C39. Groundwater elevation at wells MPW31 and MPW33. The black line corresponds to LS ECM result, and red line to the ECM result..... 46

Figure C40. Groundwater elevation at wells MPW34 and MPW35. The black line corresponds to LS ECM result, and red line to the ECM result..... 47



|   |    |
|---|----|
| Figure C41. Groundwater elevation at wells MPW36 and MPW39. The black line corresponds to LS ECM result, and red line to the ECM result. ....             | 48 |
| Figure C42. Groundwater elevation at wells ST1_G and ST2_G. The black line corresponds to LS ECM result, and red line to the ECM result. ....             | 49 |
| Figure C43. Groundwater elevation at wells ST3_G and WF1_G. The black line corresponds to LS ECM result, and red line to the ECM result. ....             | 50 |
| Figure C44. Groundwater elevation at wells WF2_G and WF3_G. The black line corresponds to LS ECM result, and red line to the ECM result. ....             | 51 |
| Figure C45. Groundwater elevation at wells WF4_G and WF5_G. The black line corresponds to LS ECM result, and red line to the ECM result. ....             | 52 |
| Figure C46. Groundwater elevation at wells WF6_G and WF7_G. The black line corresponds to LS ECM result, and red line to the ECM result. ....             | 53 |
| Figure C47. Stage at surface stations KehlCan_9358 and KehlCan_9479. The black line corresponds to LS ECM result, and red line to the ECM result. ....    | 54 |
| Figure C48. Stage at surface stations S-SF-1_HW and S-SF-1_TW. The black line corresponds to LS ECM result, and red line to the ECM result. ....          | 55 |
| Figure C49. Flow at surface stations S-SF-1 Q and S-NM-2 Q. The black line corresponds to LS ECM result, and red line to the ECM result. ....             | 56 |
| Figure C50. Stage at surface stations S-NM-2_HW and S-NM-2_TW. The black line corresponds to LS ECM result, and red line to the ECM result. ....          | 57 |
| Figure C51. Stage at surface stations S-YT-2_HW and Mullock Creek_2702. The black line corresponds to LS ECM result, and red line to the ECM result. .... | 58 |



| Station Name    | ECM         |         |          |           |      |     | LS ECM      |         |          |           |      |     |
|-----------------|-------------|---------|----------|-----------|------|-----|-------------|---------|----------|-----------|------|-----|
|                 | Comp. layer | ME (ft) | MAE (ft) | RMSE (ft) | R    | PL  | Comp. layer | ME (ft) | MAE (ft) | RMSE (ft) | R    | PL  |
| 40-GW1          | 1           | 0.10    | 0.73     | 1.06      | 0.72 | 1.0 | 1           | 0.22    | 0.86     | 1.17      | 0.65 | 1.3 |
| 40-GW2          | 2           | 0.59    | 1.28     | 1.71      | 0.42 | 2.0 | 1           | 0.87    | 1.37     | 1.66      | 0.45 | 2.0 |
| 40-GW3          | 1           | -0.88   | 1.01     | 1.15      | 0.83 | 1.3 | 2           | -0.58   | 0.82     | 0.98      | 0.79 | 1.0 |
| 40-GW4          | 2           | 1.75    | 1.75     | 1.97      | 0.80 | 1.8 | 2           | -3.86   | 3.86     | 3.97      | 0.76 | 2.5 |
| 40-GW5          | 1           | 1.86    | 1.86     | 2.01      | 0.85 | 1.8 | 1           | -0.74   | 1.11     | 1.37      | 0.77 | 1.5 |
| 40-GW6          | 1           | 0.77    | 1.28     | 1.68      | 0.44 | 2.0 | 1           | 0.39    | 1.32     | 1.74      | 0.40 | 2.0 |
| 40-GW7          | 1           | -0.46   | 0.82     | 1.16      | 0.66 | 1.3 | 1           | -0.44   | 0.81     | 1.16      | 0.66 | 1.3 |
| 46A-GW3         | 1           | -1.48   | 1.54     | 1.74      | 0.76 | 1.8 | 1           | -1.98   | 1.99     | 2.23      | 0.73 | 1.8 |
| 46A-GW4         | 1           | -0.40   | 1.11     | 1.35      | 0.74 | 1.5 | 1           | -0.52   | 1.12     | 1.36      | 0.74 | 1.5 |
| 46A-GW10        | 1           | -0.26   | 0.54     | 0.73      | 0.82 | 1.0 | 1           | -0.25   | 0.54     | 0.72      | 0.82 | 1.0 |
| 46A-GW11        | 1           | -0.91   | 0.91     | 1.02      | 0.93 | 1.0 | 1           | -1.28   | 1.28     | 1.36      | 0.92 | 1.8 |
| 46A-GW12        | 1           | -1.31   | 1.52     | 1.88      | 0.63 | 2.0 | 1           | -1.68   | 1.79     | 2.10      | 0.69 | 2.0 |
| 46A-GW13        | 1           | -1.01   | 1.10     | 1.23      | 0.84 | 1.5 | 1           | -0.95   | 1.00     | 1.13      | 0.86 | 1.3 |
| 46A-GW14        | 1           | -0.82   | 1.10     | 1.26      | 0.61 | 1.8 | 1           | -0.96   | 1.21     | 1.39      | 0.58 | 1.8 |
| 46A-GW15        | 1           | -0.24   | 0.55     | 0.70      | 0.87 | 1.0 | 1           | -0.47   | 0.58     | 0.79      | 0.89 | 1.0 |
| 46A-GW18        | 1           | -1.12   | 1.23     | 1.43      | 0.79 | 1.8 | 1           | -0.97   | 1.17     | 1.36      | 0.78 | 1.5 |
| 46A-GW21        | 1           | -0.89   | 1.00     | 1.18      | 0.75 | 1.0 | 1           | -1.01   | 1.10     | 1.28      | 0.73 | 1.8 |
| 46A-GW25        | 1           | 0.33    | 0.47     | 0.61      | 0.88 | 1.0 | 1           | 0.12    | 0.49     | 0.63      | 0.82 | 1.0 |
| 46A-GW26        | 1           | -0.10   | 0.54     | 0.69      | 0.80 | 1.0 | 1           | -0.23   | 0.46     | 0.60      | 0.79 | 1.0 |
| 49-GW3          | 1           | 0.16    | 1.01     | 1.28      | 0.42 | 2.0 | 1           | 0.12    | 0.91     | 1.15      | 0.40 | 1.5 |
| 49-GW6          | 1           | 0.43    | 1.12     | 1.38      | 0.75 | 1.5 | 1           | 0.16    | 1.10     | 1.32      | 0.76 | 1.5 |
| 49-GW7          | 1           | 0.42    | 0.91     | 1.34      | 0.56 | 1.5 | 1           | 0.43    | 0.87     | 1.29      | 0.57 | 1.5 |
| 49-GW8          | 1           | 1.94    | 1.94     | 2.33      | 0.23 | 2.3 | 1           | 1.78    | 1.78     | 2.17      | 0.26 | 2.3 |
| 49-GW9          | 1           | 1.51    | 1.53     | 1.80      | 0.81 | 1.8 | 1           | 1.35    | 1.38     | 1.66      | 0.80 | 1.8 |
| 49-GW10         | 1           | -0.14   | 0.83     | 0.98      | 0.85 | 1.0 | 1           | -0.32   | 0.81     | 0.97      | 0.87 | 1.0 |
| 49-GW11         | 1           | 0.33    | 0.83     | 1.16      | 0.89 | 1.0 | 1           | 0.43    | 0.97     | 1.23      | 0.89 | 1.0 |
| 49-GW12         | 1           | 0.78    | 0.88     | 1.09      | 0.91 | 1.0 | 1           | 0.75    | 0.90     | 1.13      | 0.90 | 1.0 |
| 49-GW14         | 1           | -0.05   | 0.59     | 0.73      | 0.87 | 1.0 | 1           | -0.06   | 0.63     | 0.76      | 0.86 | 1.0 |
| 49-GW15         | 1           | 3.31    | 3.31     | 3.41      | 0.51 | 2.8 | 1           | 1.62    | 1.68     | 1.88      | 0.51 | 2.0 |
| 49L-GW1         | 1           | 0.26    | 0.71     | 0.94      | 0.77 | 1.0 | 1           | 0.36    | 0.75     | 0.94      | 0.78 | 1.0 |
| BRM-Lake        | 1           | -0.02   | 0.42     | 0.53      | 0.94 | 1.0 | 1           | 0.15    | 0.38     | 0.51      | 0.94 | 1.0 |
| BRM-MW1         | 1           | 0.31    | 0.60     | 0.72      | 0.77 | 1.0 | 1           | 0.28    | 0.47     | 0.59      | 0.86 | 1.0 |
| BRM-MW2         | 1           | -0.01   | 0.35     | 0.44      | 0.93 | 1.0 | 1           | 0.15    | 0.33     | 0.48      | 0.92 | 1.0 |
| BRM-MW3         | 1           | 0.57    | 0.60     | 0.77      | 0.90 | 1.0 | 1           | 0.85    | 0.85     | 0.99      | 0.91 | 1.0 |
| BRM-MW4         | 1           | 0.48    | 0.54     | 0.73      | 0.84 | 1.0 | 1           | 0.67    | 0.67     | 0.86      | 0.84 | 1.0 |
| Corkscrew Swamp | 1           | -0.61   | 1.01     | 1.06      | 0.87 | 1.3 | 1           | -0.61   | 1.01     | 1.06      | 0.87 | 1.3 |
| FP2_GW1         | 1           | 0.35    | 1.15     | 1.55      | 0.78 | 1.5 | 1           | 0.50    | 1.09     | 1.53      | 0.80 | 1.5 |
| FP3_GW1         | 1           | 0.31    | 0.65     | 0.80      | 0.83 | 1.0 | 1           | 0.28    | 0.60     | 0.73      | 0.86 | 1.0 |
| FP4_GW1         | 1           | -0.09   | 0.53     | 0.65      | 0.89 | 1.0 | 1           | -0.22   | 0.55     | 0.70      | 0.89 | 1.0 |
| FP5_GW1         | 1           | -0.21   | 0.57     | 0.74      | 0.88 | 1.0 | 1           | -0.33   | 0.60     | 0.76      | 0.88 | 1.0 |
| FP6_GW1         | 1           | -0.27   | 0.77     | 0.97      | 0.86 | 1.0 | 1           | -0.41   | 0.76     | 0.94      | 0.87 | 1.0 |
| FP7_GW1         | 1           | -0.22   | 0.83     | 1.03      | 0.86 | 1.0 | 1           | -0.41   | 0.84     | 1.03      | 0.86 | 1.0 |



| Station Name | ECM         |         |          |           |      |     | LS ECM      |         |          |           |      |     |
|--------------|-------------|---------|----------|-----------|------|-----|-------------|---------|----------|-----------|------|-----|
|              | Comp. layer | ME (ft) | MAE (ft) | RMSE (ft) | R    | PL  | Comp. layer | ME (ft) | MAE (ft) | RMSE (ft) | R    | PL  |
| FP8_GW1      | 1           | -0.07   | 0.70     | 0.84      | 0.87 | 1.0 | 1           | -0.27   | 0.70     | 0.85      | 0.88 | 1.0 |
| FP9_G        | 1           | -0.19   | 0.82     | 1.01      | 0.85 | 1.0 | 1           | -0.39   | 0.83     | 1.02      | 0.86 | 1.0 |
| FP10_G       | 1           | -0.21   | 0.57     | 0.77      | 0.87 | 1.0 | 1           | -0.28   | 0.55     | 0.73      | 0.88 | 1.0 |
| HF1_G        | 1           | -4.25   | 4.41     | 5.96      | 0.28 | 3.0 | 1           | -4.28   | 4.43     | 5.98      | 0.27 | 3.0 |
| HF2_G        | 1           | -0.32   | 1.08     | 1.28      | 0.72 | 1.5 | 1           | -0.38   | 1.05     | 1.25      | 0.71 | 1.3 |
| HF3_G        | 1           | 2.27    | 2.32     | 2.69      | 0.80 | 2.5 | 1           | 2.24    | 2.27     | 2.62      | 0.80 | 2.5 |
| HF4_G        | 1           | -1.39   | 1.80     | 2.22      | 0.61 | 2.0 | 1           | -1.38   | 1.79     | 2.21      | 0.62 | 2.0 |
| HF7_G        | 1           | -1.40   | 1.70     | 2.09      | 0.57 | 2.0 | 1           | -1.42   | 1.70     | 2.09      | 0.59 | 2.0 |
| L-1138       | 1           | -0.56   | 0.92     | 1.10      | 0.80 | 1.0 | 1           | -0.29   | 0.78     | 0.89      | 0.81 | 1.0 |
| L-1985       | 2           | -0.59   | 2.12     | 2.49      | 0.72 | 1.8 | 2           | -0.22   | 2.46     | 2.98      | 0.62 | 2.3 |
| L-2192       | 3           | 1.17    | 4.16     | 5.30      | 0.28 | 2.8 | 3           | 0.78    | 4.01     | 5.16      | 0.32 | 2.5 |
| L-2204       | 2           | -0.46   | 0.56     | 0.73      | 0.86 | 1.0 | 2           | -0.70   | 0.76     | 0.92      | 0.87 | 1.0 |
| L-5649       | 3           | -7.52   | 7.52     | 8.17      | 0.67 | 2.8 | 4           | -7.45   | 7.45     | 8.15      | 0.63 | 2.8 |
| L-5664       | 3           | -9.17   | 9.17     | 10.12     | 0.49 | 3.0 | 4           | -9.11   | 9.11     | 10.1      | 0.50 | 2.8 |
| L-5667       | 1           | 1.26    | 1.44     | 1.56      | 0.92 | 1.8 | 1           | 1.09    | 1.29     | 1.39      | 0.93 | 1.8 |
| L-5669R      | 3           | -0.25   | 0.57     | 0.69      | 0.77 | 1.0 | 3           | 0.15    | 0.40     | 0.55      | 0.85 | 1.0 |
| L-5673       | 3           | -8.43   | 8.47     | 9.19      | 0.60 | 2.8 | 3           | -8.21   | 8.26     | 8.98      | 0.63 | 2.8 |
| L-5874       | 3           | -3.09   | 3.53     | 4.36      | 0.70 | 2.8 | 3           | -3.50   | 3.76     | 4.65      | 0.71 | 2.5 |
| L-730        | 2           | 0.37    | 0.56     | 0.78      | 0.77 | 1.0 | 2           | 0.65    | 0.69     | 0.92      | 0.80 | 1.0 |
| L-739        | 2           | 0.57    | 0.60     | 0.74      | 0.96 | 1.0 | 2           | 0.55    | 0.60     | 0.74      | 0.96 | 1.0 |
| MPW02        | 1           | -0.62   | 0.62     | 0.71      | 0.98 | 1.0 | 1           | -0.67   | 0.67     | 0.78      | 0.98 | 1.0 |
| MPW03        | 1           | -0.96   | 0.96     | 0.97      | 0.98 | 1.0 | 1           | -0.98   | 0.98     | 0.99      | 0.99 | 1.0 |
| MPW04        | 1           | -0.05   | 0.54     | 0.67      | 0.91 | 1.0 | 1           | -0.01   | 0.51     | 0.65      | 0.91 | 1.0 |
| MPW05        | 1           | 0.27    | 0.56     | 0.61      | 0.73 | 1.0 | 1           | 0.25    | 0.53     | 0.57      | 0.78 | 1.0 |
| MPW08        | 1           | 0.99    | 0.99     | 1.10      | 0.91 | 1.0 | 1           | 1.06    | 1.07     | 1.15      | 0.92 | 1.5 |
| MPW25        | 1           | -0.12   | 0.27     | 0.31      | 0.95 | 1.0 | 1           | -0.27   | 0.35     | 0.39      | 0.95 | 1.0 |
| MPW27        | 1           | 0.69    | 0.71     | 1.04      | 0.80 | 1.0 | 1           | 0.46    | 0.52     | 0.81      | 0.85 | 1.0 |
| MPW28        | 1           | 1.16    | 1.16     | 1.23      | 0.51 | 1.8 | 1           | 0.95    | 0.95     | 1.00      | 0.77 | 1.0 |
| MPW29        | 1           | -0.09   | 0.41     | 0.53      | 0.84 | 1.0 | 1           | -0.08   | 0.31     | 0.40      | 0.96 | 1.0 |
| MPW30        | 1           | 0.39    | 0.59     | 0.97      | 0.73 | 1.0 | 1           | 0.10    | 0.57     | 0.83      | 0.77 | 1.0 |
| MPW31        | 1           | 0.38    | 0.39     | 0.59      | 0.94 | 1.0 | 1           | 0.25    | 0.30     | 0.48      | 0.95 | 1.0 |
| MPW33        | 1           | -0.55   | 1.18     | 1.48      | 0.70 | 1.8 | 1           | -0.78   | 1.20     | 1.51      | 0.77 | 1.5 |
| MPW34        | 1           | 0.62    | 0.62     | 0.63      | 0.98 | 1.0 | 1           | 0.48    | 0.48     | 0.49      | 0.97 | 1.0 |
| MPW35        | 1           | -1.10   | 1.26     | 1.36      | 0.84 | 1.8 | 1           | -1.01   | 1.06     | 1.24      | 0.90 | 1.5 |
| MPW36        | 1           | 0.08    | 0.61     | 0.74      | 0.84 | 1.0 | 1           | -0.11   | 0.53     | 0.66      | 0.87 | 1.0 |
| MPW39        | 1           | -1.52   | 2.20     | 2.46      | 0.66 | 2.3 | 1           | -1.35   | 2.35     | 2.52      | 0.64 | 2.5 |
| ST1_G        | 1           | -0.26   | 0.61     | 0.73      | 0.87 | 1.0 | 1           | -0.44   | 0.73     | 0.85      | 0.86 | 1.0 |
| ST2_G        | 1           | 0.34    | 0.66     | 0.80      | 0.86 | 1.0 | 1           | 0.05    | 0.61     | 0.73      | 0.86 | 1.0 |
| ST3_G        | 1           | -0.20   | 0.75     | 0.86      | 0.81 | 1.0 | 1           | -0.34   | 0.80     | 0.92      | 0.80 | 1.0 |
| WF1_G        | 2           | 0.68    | 0.69     | 0.75      | 0.95 | 1.0 | 2           | 1.06    | 1.06     | 1.12      | 0.94 | 1.5 |
| WF2_G        | 2           | 1.13    | 1.29     | 1.61      | 0.76 | 1.8 | 2           | 1.31    | 1.39     | 1.73      | 0.77 | 1.8 |
| WF3_G        | 1           | 1.38    | 1.38     | 1.59      | 0.84 | 1.8 | 1           | 1.54    | 1.55     | 1.71      | 0.86 | 1.8 |
| WF4_G        | 1           | 0.91    | 1.06     | 1.28      | 0.81 | 1.5 | 1           | 0.95    | 1.05     | 1.27      | 0.83 | 1.5 |
| WF5_G        | 1           | 0.97    | 1.11     | 1.43      | 0.79 | 1.5 | 1           | 1.03    | 1.08     | 1.40      | 0.81 | 1.8 |
| WF6_G        | 1           | 0.99    | 1.04     | 1.32      | 0.83 | 1.5 | 1           | 0.87    | 0.91     | 1.18      | 0.85 | 1.0 |



| Station Name       | ECM         |         |          |           |      |     | LS ECM      |         |          |           |      |     |
|--------------------|-------------|---------|----------|-----------|------|-----|-------------|---------|----------|-----------|------|-----|
|                    | Comp. layer | ME (ft) | MAE (ft) | RMSE (ft) | R    | PL  | Comp. layer | ME (ft) | MAE (ft) | RMSE (ft) | R    | PL  |
| WF7_G              | 1           | 1.14    | 1.20     | 1.53      | 0.79 | 1.8 | 1           | 1.16    | 1.18     | 1.49      | 0.81 | 1.8 |
| KehlCan 9358       | 0           | 1.26    | 1.67     | 2.09      | 0.73 | 2.5 | 0           | 1.33    | 1.67     | 2.10      | 0.73 | 2.5 |
| KehlCan 9479       | 0           | 0.03    | 0.76     | 1.08      | 0.93 | 1.3 | 0           | 0.10    | 0.72     | 1.06      | 0.92 | 1.3 |
| S-SF-1_HW          | 0           | 0.14    | 0.18     | 0.23      | 0.88 | 1.0 | 0           | 0.23    | 0.28     | 0.32      | 0.83 | 1.0 |
| S-SF-1_Q           | 0           | ---     | ---      | ---       | 0.74 | 2.0 | 0           | ---     | ---      | ---       | 0.71 | 2.0 |
| S-SF-1_TW          | 0           | -0.03   | 0.30     | 0.47      | 0.44 | 1.5 | 0           | -0.03   | 0.31     | 0.48      | 0.43 | 1.5 |
| S-NM-2_HW          | 0           | -0.01   | 0.18     | 0.23      | 0.65 | 1.3 | 0           | 0.00    | 0.19     | 0.24      | 0.61 | 1.3 |
| S-NM-2_Q           | 0           | ---     | ---      | ---       | 0.43 | 3.0 | 0           | ---     | ---      | ---       | 0.41 | 3.0 |
| S-NM-2_TW          | 0           | 0.80    | 1.03     | 1.16      | 0.44 | 2.0 | 0           | 0.80    | 1.04     | 1.16      | 0.43 | 2.3 |
| S-YT-2_HW          | 0           | 1.54    | 1.66     | 1.88      | 0.74 | 2.3 | 0           | 1.63    | 1.74     | 1.97      | 0.76 | 2.5 |
| Mullock Creek 2702 | 0           | 2.51    | 2.51     | 2.54      | 0.62 | 2.8 | 0           | 2.48    | 2.48     | 2.51      | 0.62 | 2.8 |

Table C1. Statistical parameters and level of performance at monitoring stations in the LS ECM domain area. The green color indicates the highest performance level (1.0, 1.2 and 1.5), yellow for medium (1.8, 2.0, 2.3, 2.5) and orange for low (2.8, 3.0).

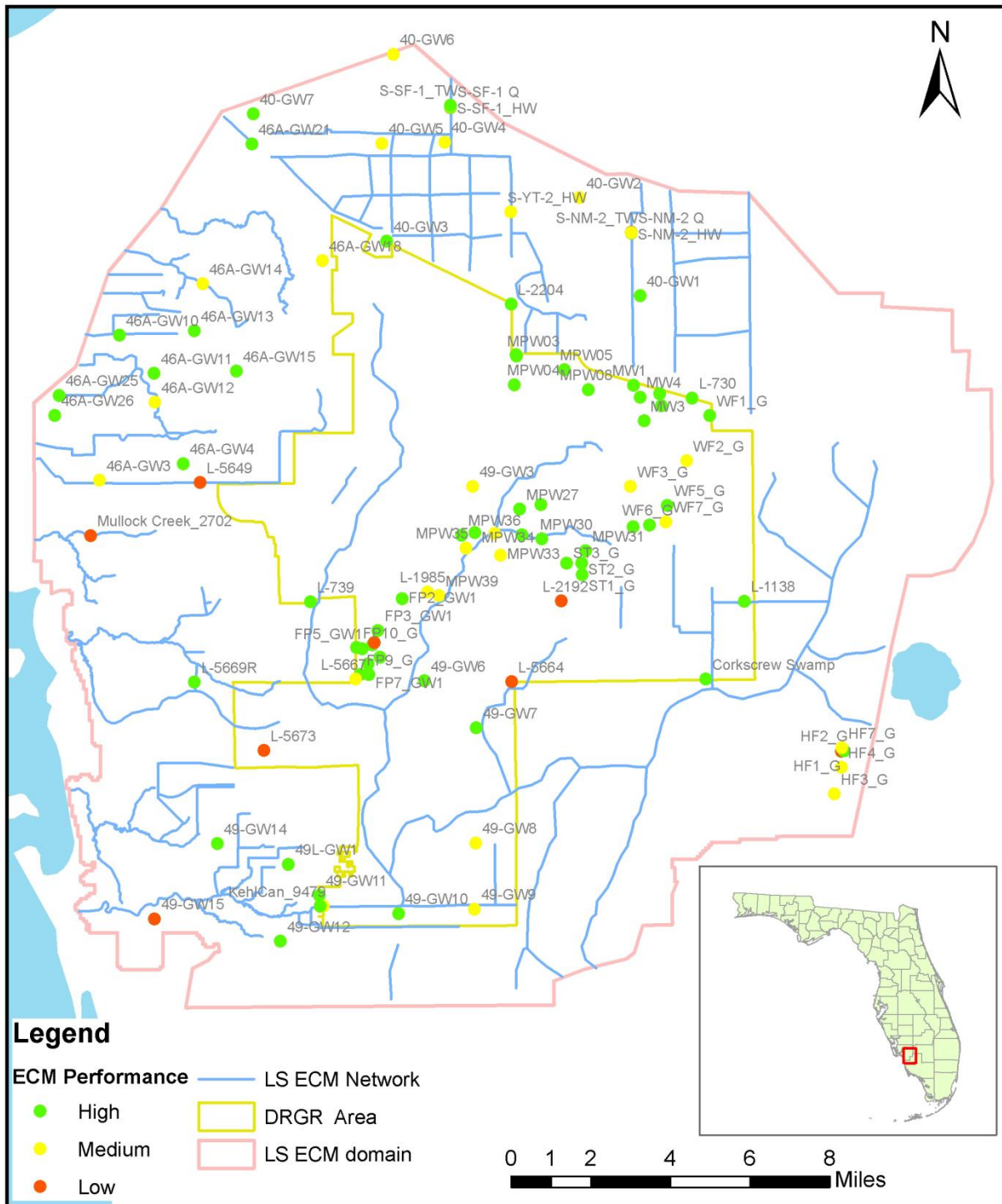


Figure C1. Average performance level of the ECM results at monitoring stations in the LS ECM domain area.

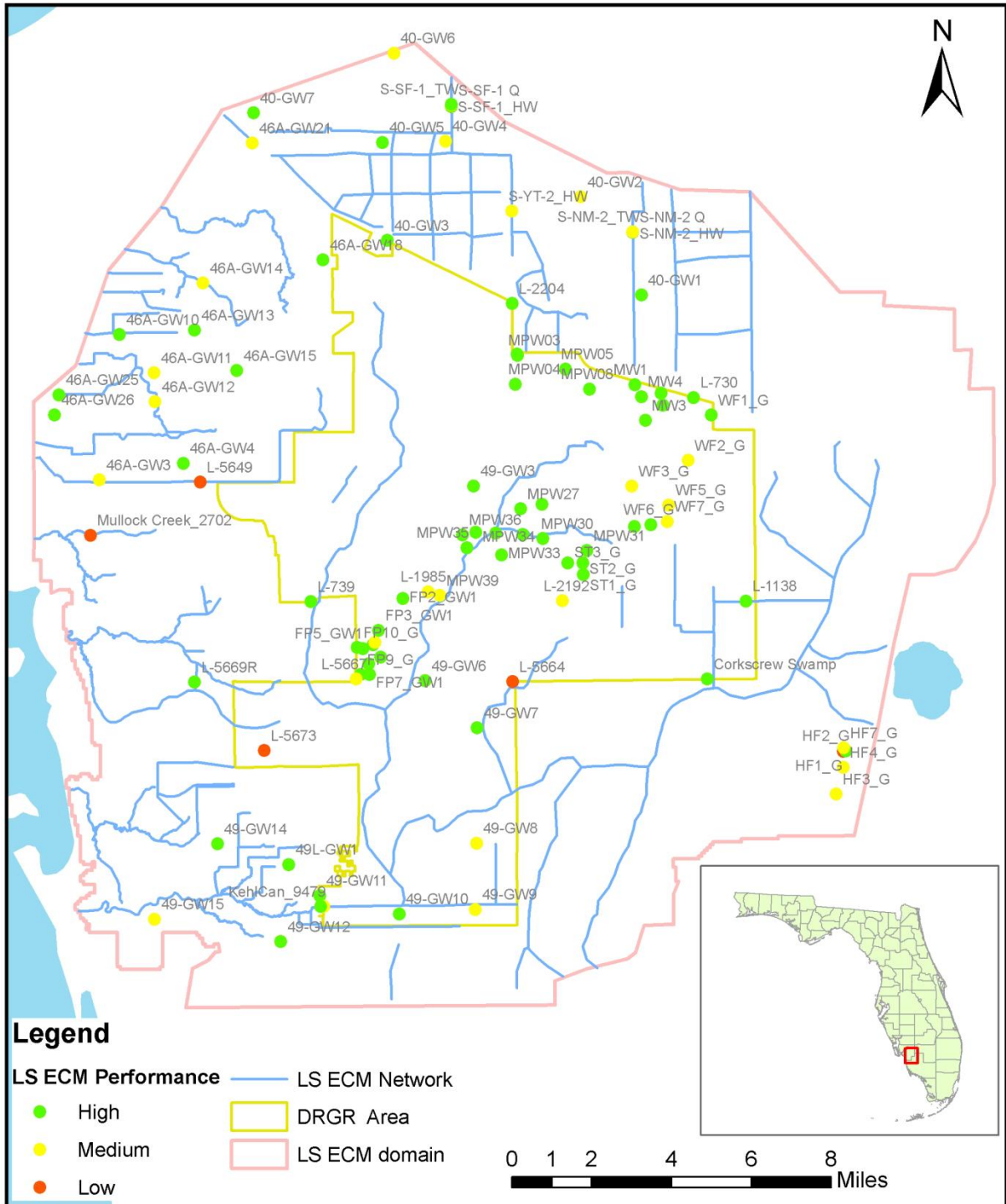
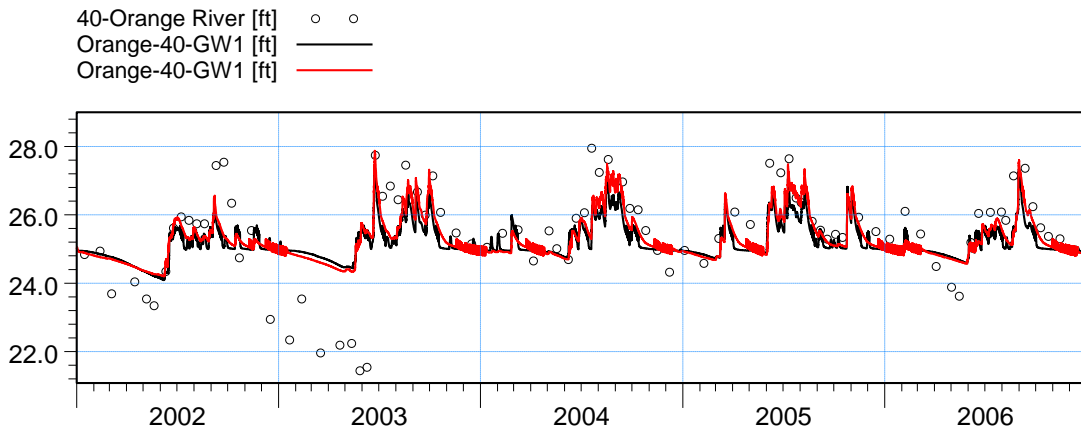
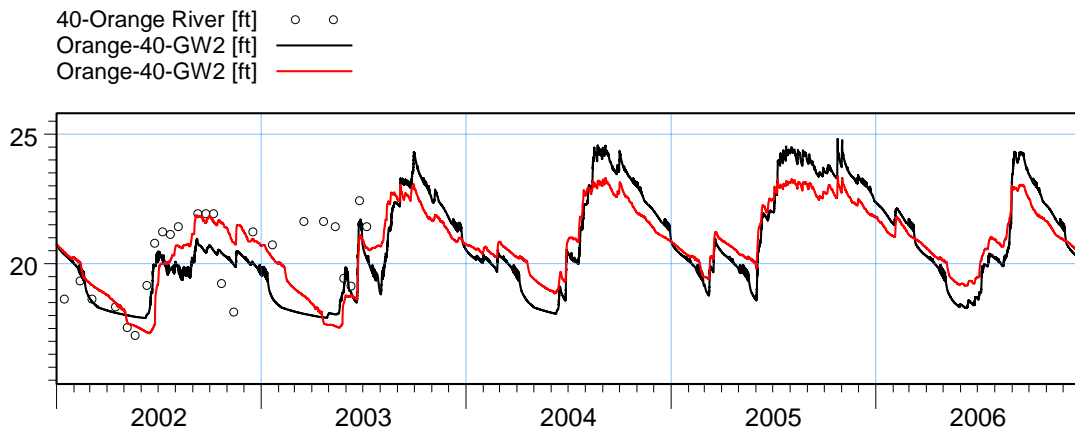


Figure C2. Average performance level of the LS ECM results at monitoring stations.

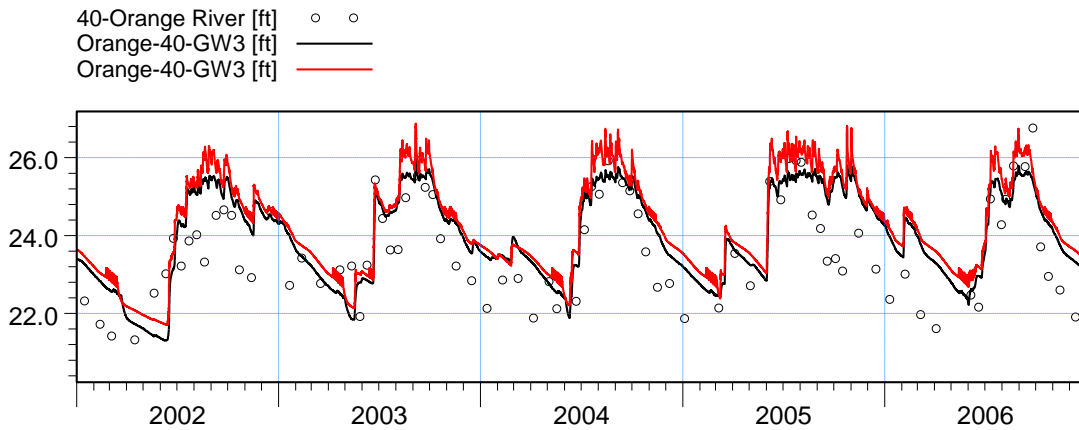


ME=0.215258  
 MAE=0.862872  
 RMSE=1.1701  
 STDres=1.15012  
 R(Correlation)=0.648369  
 R2(Nash\_Sutcliffe)=0.319068

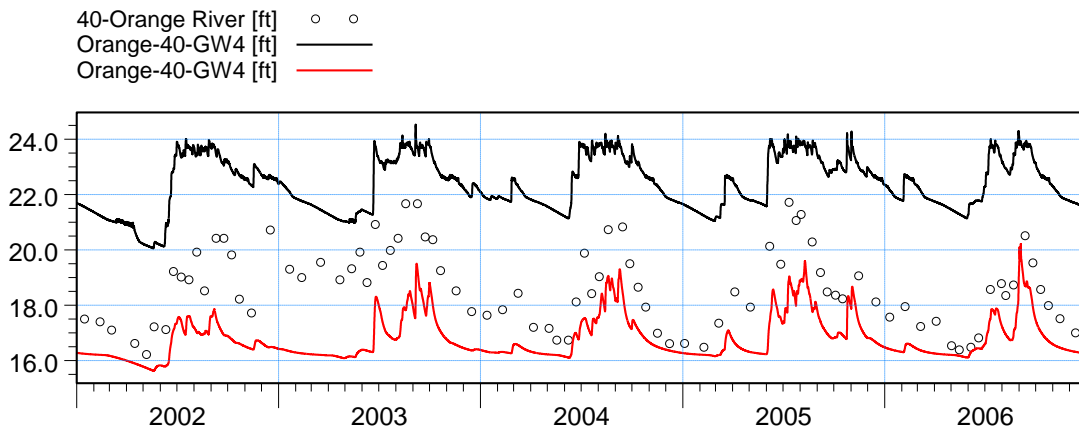


ME=0.868709  
 MAE=1.36943  
 RMSE=1.66372  
 STDres=1.41892  
 R(Correlation)=0.444965  
 R2(Nash\_Sutcliffe)=-0.184595

Figure C3. Groundwater elevation at wells 40-GW1 and 40-GW2. The black line corresponds to LS ECM result, and red line to the ECM result.

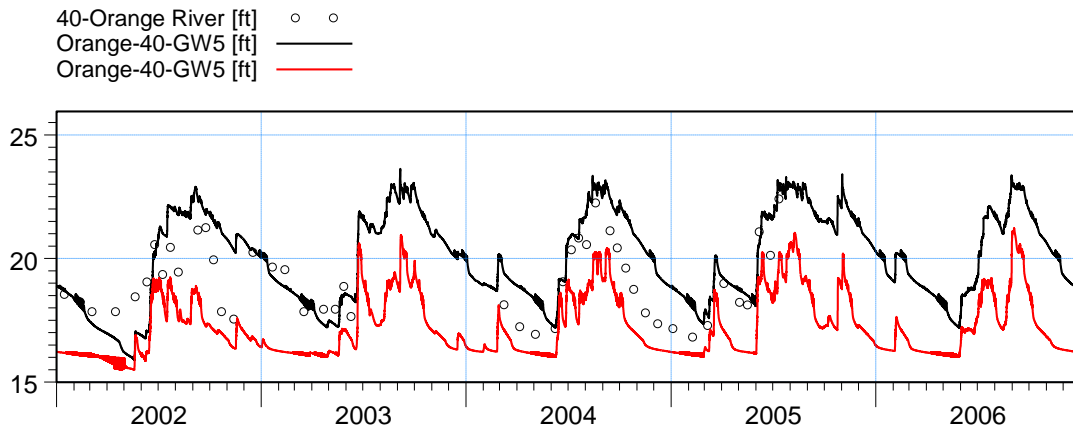


ME=-0.578482  
 MAE=0.817334  
 RMSE=0.983047  
 STDres=0.794821  
 R(Correlation)=0.79182  
 R2(Nash\_Sutcliffe)=0.416489

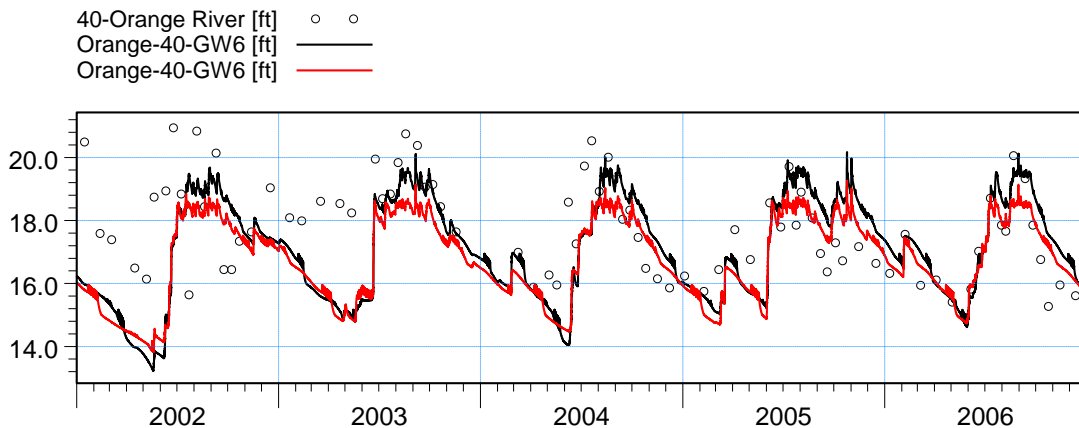


ME=-3.86078  
 MAE=3.86078  
 RMSE=3.97037  
 STDres=0.926404  
 R(Correlation)=0.757352  
 R2(Nash\_Sutcliffe)=-6.91808

Figure C4. Groundwater elevation at wells 40-GW3 and 40-GW4. The black line corresponds to LS ECM result, and red line to the ECM result.

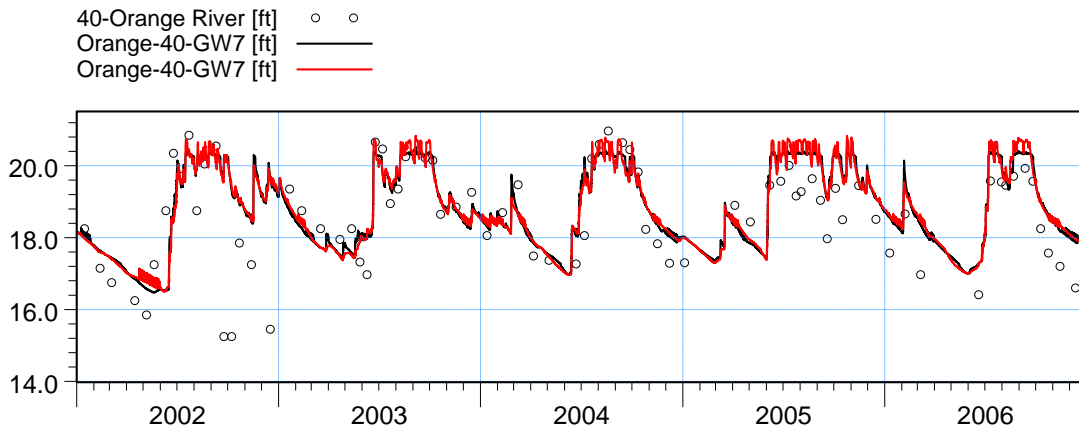


ME=-0.740828  
 MAE=1.11372  
 RMSE=1.37109  
 STDres=1.15372  
 R(Correlation)=0.768068  
 R2(Nash\_Sutcliffe)=0.11923

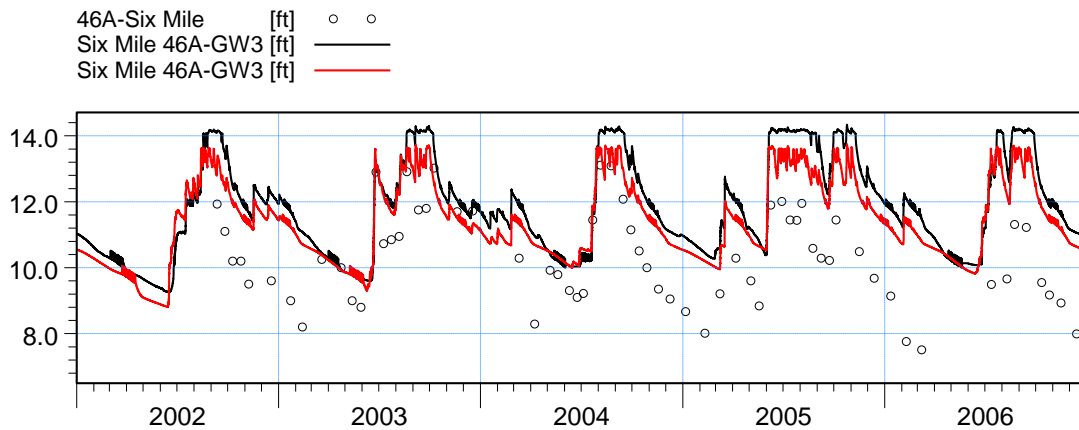


ME=0.392984  
 MAE=1.31909  
 RMSE=1.74118  
 STDres=1.69625  
 R(Correlation)=0.40127  
 R2(Nash\_Sutcliffe)=-0.38201

Figure C5. Groundwater elevation at wells 40-GW5 and 40-GW6. The black line corresponds to LS ECM result, and red line to the ECM result.

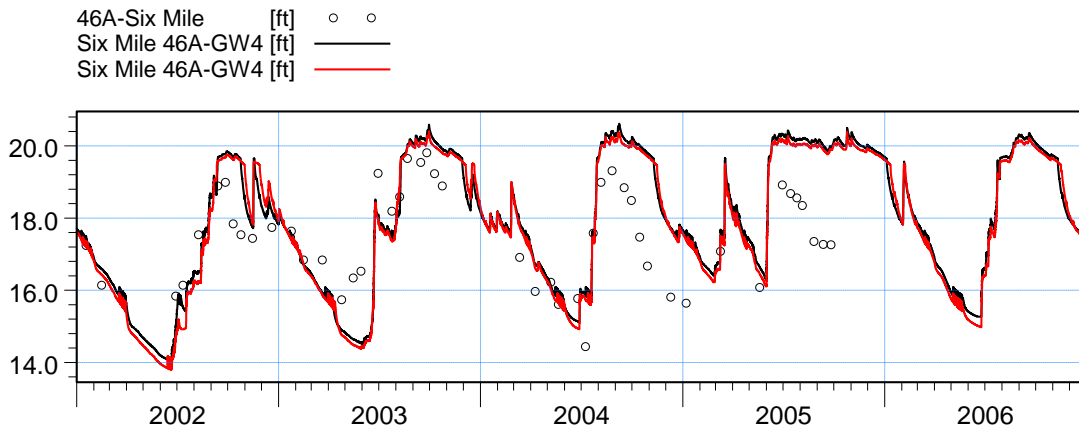


ME=-0.440507  
 MAE=0.80895  
 RMSE=1.15612  
 STDres=1.06891  
 R(Correlation)=0.656994  
 R2(Nash\_Sutcliffe)=0.310736

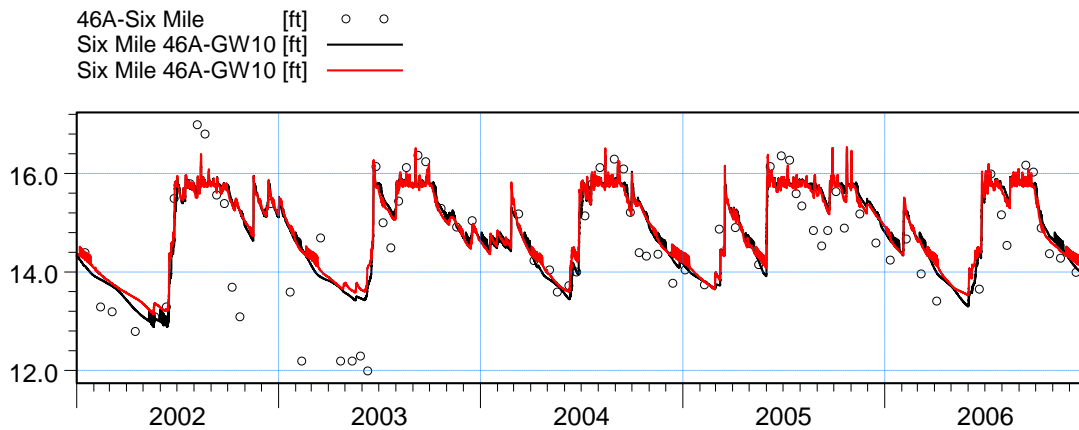


ME=-1.98165  
 MAE=1.9908  
 RMSE=2.23481  
 STDres=1.03317  
 R(Correlation)=0.7254  
 R2(Nash\_Sutcliffe)=-1.54419

Figure C6. Groundwater elevation at wells 40-GW7 and 46A-GW3. The black line corresponds to LS ECM result, and red line to the ECM result.

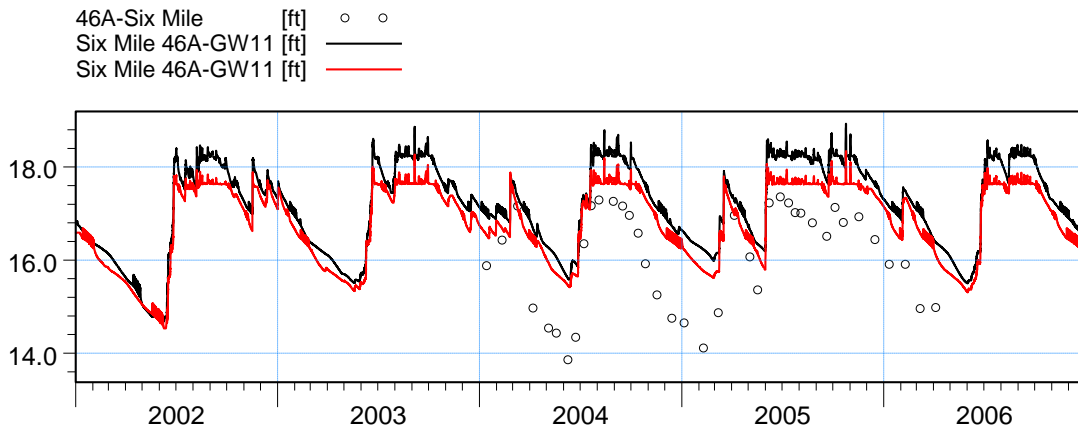


ME=-0.519267  
 MAE=1.11819  
 RMSE=1.361  
 STDres=1.25805  
 R(Correlation)=0.743274  
 R2(Nash\_Sutcliffe)=-0.0913463

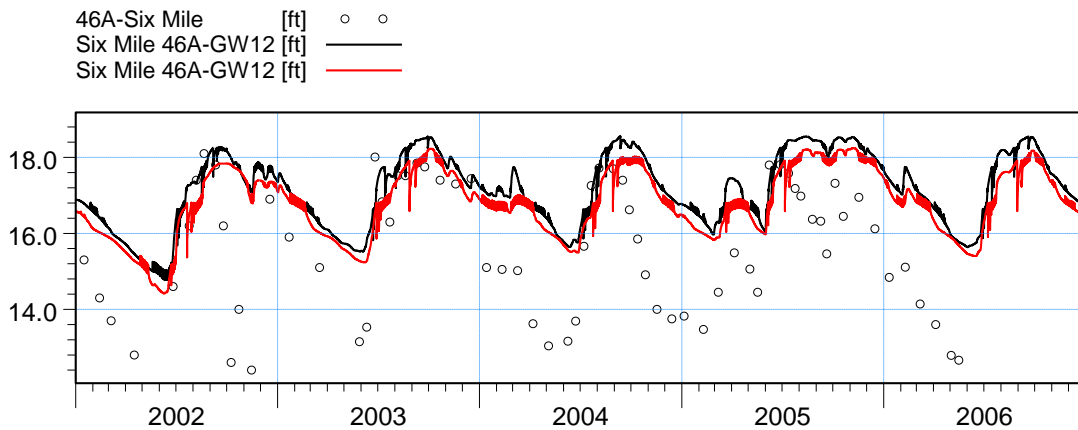


ME=-0.245909  
 MAE=0.536685  
 RMSE=0.719412  
 STDres=0.676078  
 R(Correlation)=0.81567  
 R2(Nash\_Sutcliffe)=0.614801

Figure C7. Groundwater elevation at wells 46A-GW4 and 46A-GW10. The black line corresponds to LS ECM result, and red line to the ECM result.

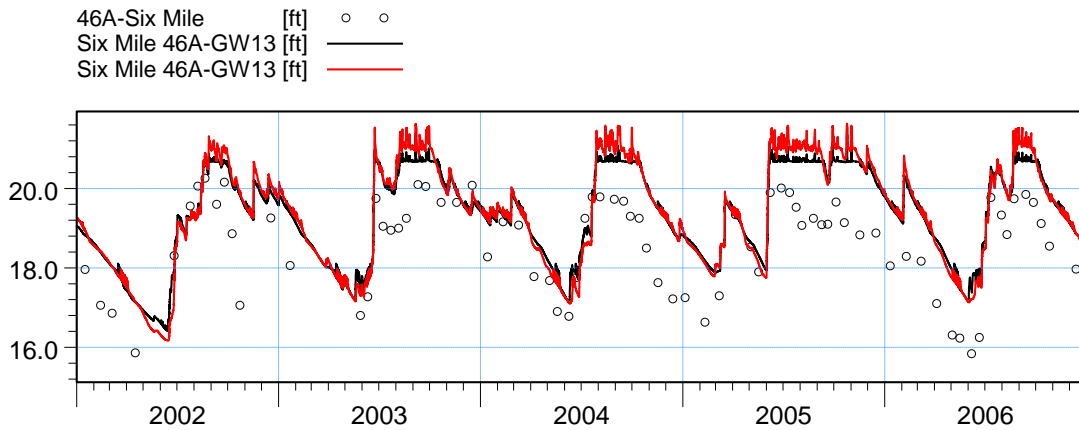


ME=-1.28486  
 MAE=1.28486  
 RMSE=1.35844  
 STDres=0.441026  
 R(Correlation)=0.924647  
 R2(Nash\_Sutcliffe)=-0.605653

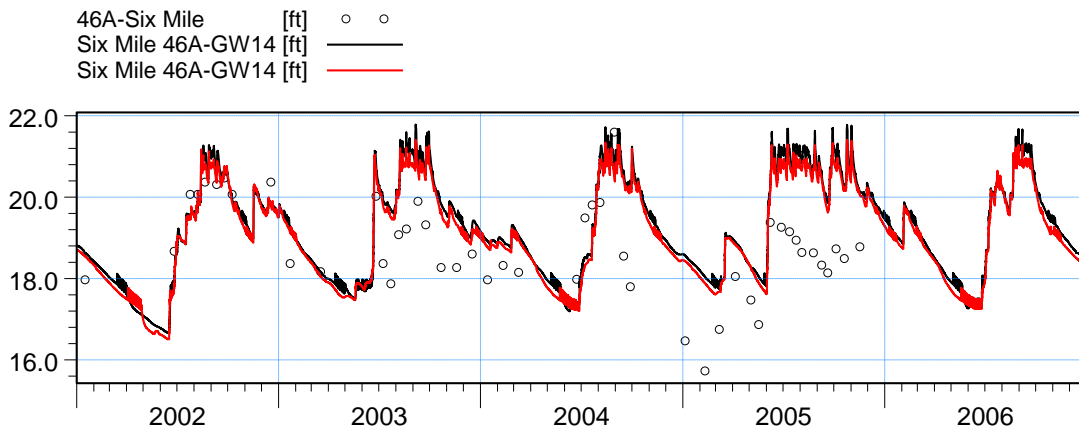


ME=-1.68358  
 MAE=1.78537  
 RMSE=2.10513  
 STDres=1.26378  
 R(Correlation)=0.685096  
 R2(Nash\_Sutcliffe)=-0.533903

Figure C8. Groundwater elevation at wells 46A-GW11 and 46A-GW12. The black line corresponds to LS ECM result, and red line to the ECM result.

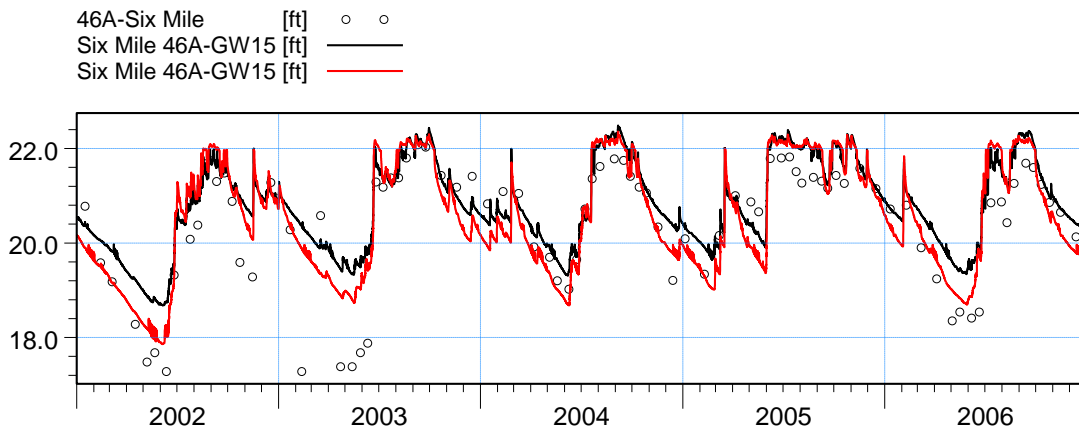


ME=-0.945956  
 MAE=1.00431  
 RMSE=1.13145  
 STDres=0.620771  
 R(Correlation)=0.855919  
 R2(Nash\_Sutcliffe)=0.0877518

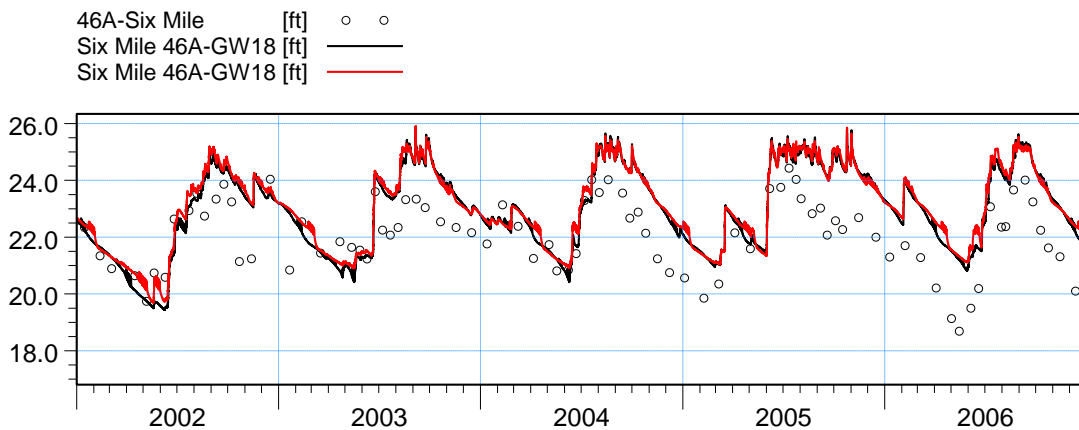


ME=-0.955465  
 MAE=1.20764  
 RMSE=1.38928  
 STDres=1.00856  
 R(Correlation)=0.581027  
 R2(Nash\_Sutcliffe)=-0.530277

Figure C9. Groundwater elevation at wells 46A-GW13 and 46A-GW14. The black line corresponds to LS ECM result, and red line to the ECM result.

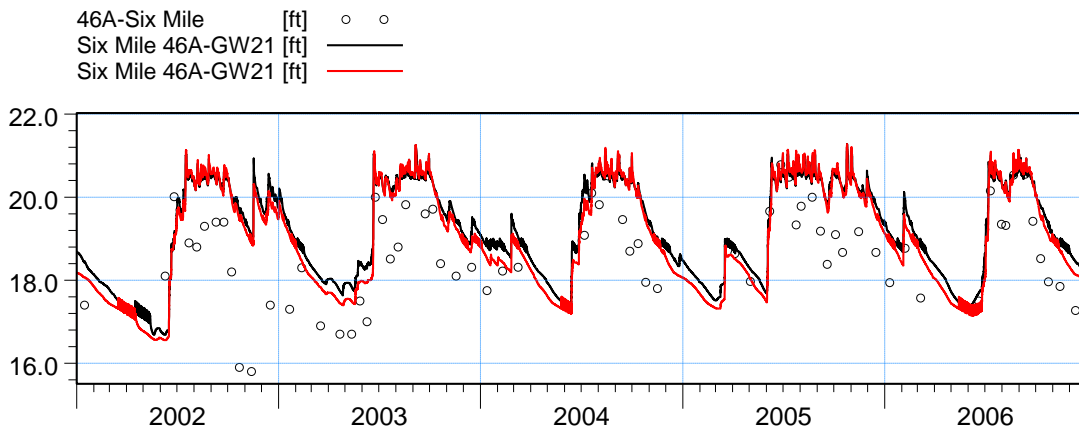


ME=-0.469419  
 MAE=0.577236  
 RMSE=0.78903  
 STDres=0.634204  
 R(Correlation)=0.886484  
 R2(Nash\_Sutcliffe)=0.632615

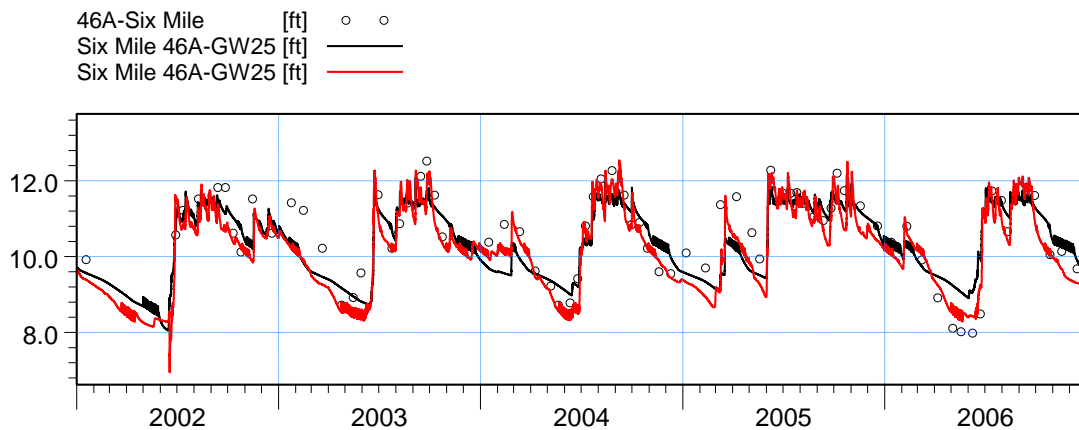


ME=-0.967418  
 MAE=1.17293  
 RMSE=1.35604  
 STDres=0.950241  
 R(Correlation)=0.774985  
 R2(Nash\_Sutcliffe)=-0.145046

Figure C10. Groundwater elevation at wells 46A-GW15 and 46A-GW18. The black line corresponds to LS ECM result, and red line to the ECM result.

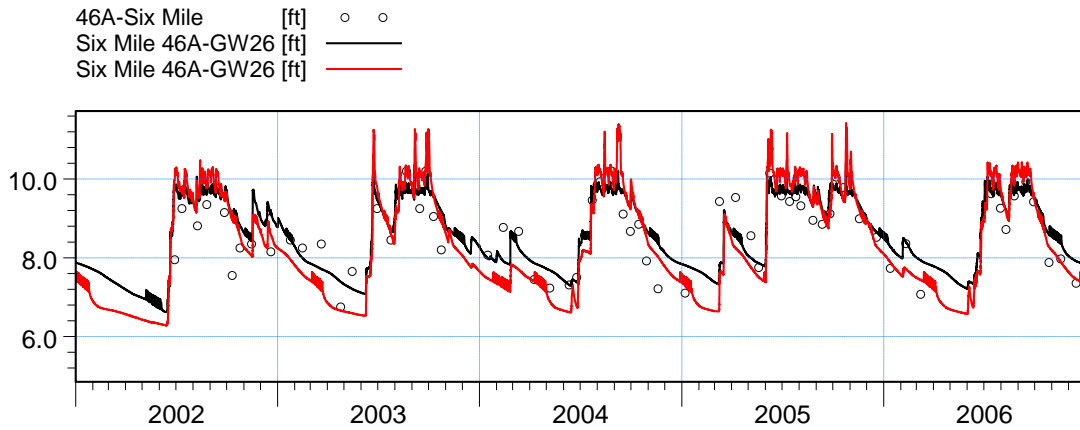


ME=-1.01206  
 MAE=1.10197  
 RMSE=1.2826  
 STDres=0.787898  
 R(Correlation)=0.727294  
 R2(Nash\_Sutcliffe)=-0.287804

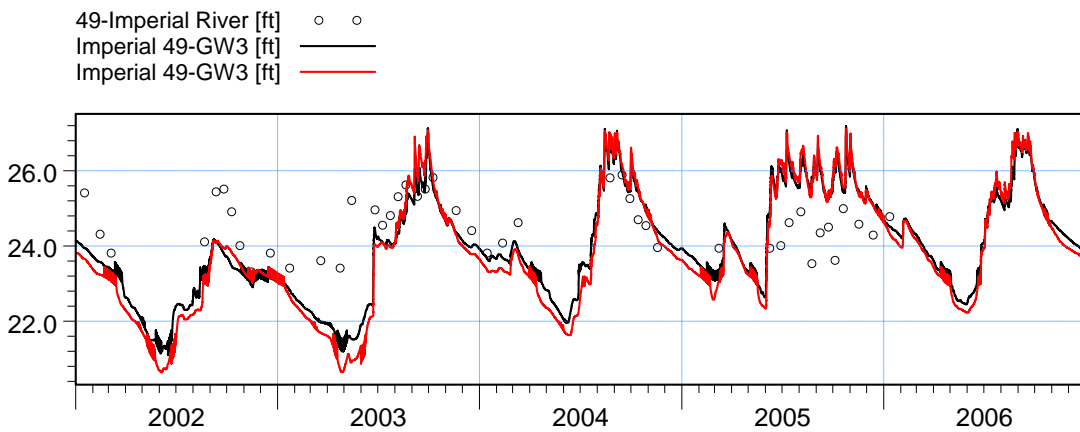


ME=0.123037  
 MAE=0.494223  
 RMSE=0.626604  
 STDres=0.614406  
 R(Correlation)=0.823279  
 R2(Nash\_Sutcliffe)=0.664867

Figure C11. Groundwater elevation at wells 46A-GW21 and 46A-GW25. The black line corresponds to LS ECM result, and red line to the ECM result.

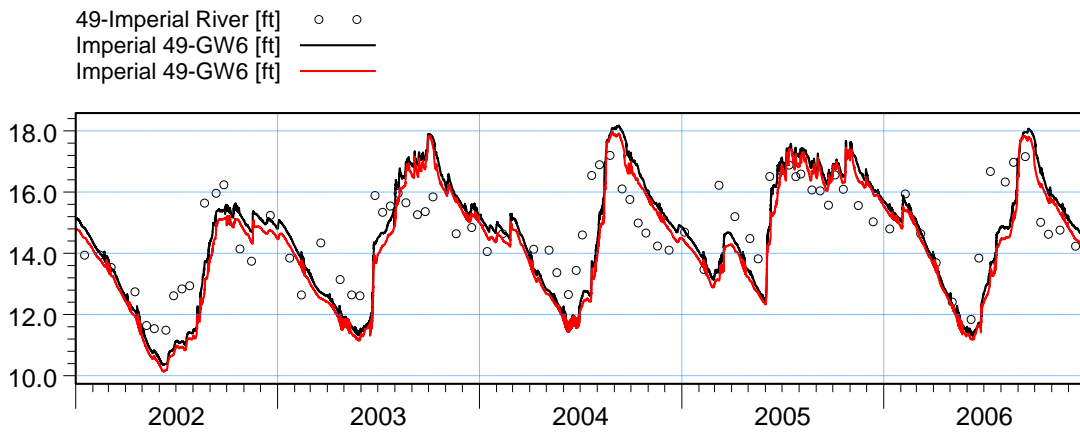


ME=-0.231016  
 MAE=0.459353  
 RMSE=0.597783  
 STDres=0.551341  
 R(Correlation)=0.787018  
 R2(Nash\_Sutcliffe)=0.535556

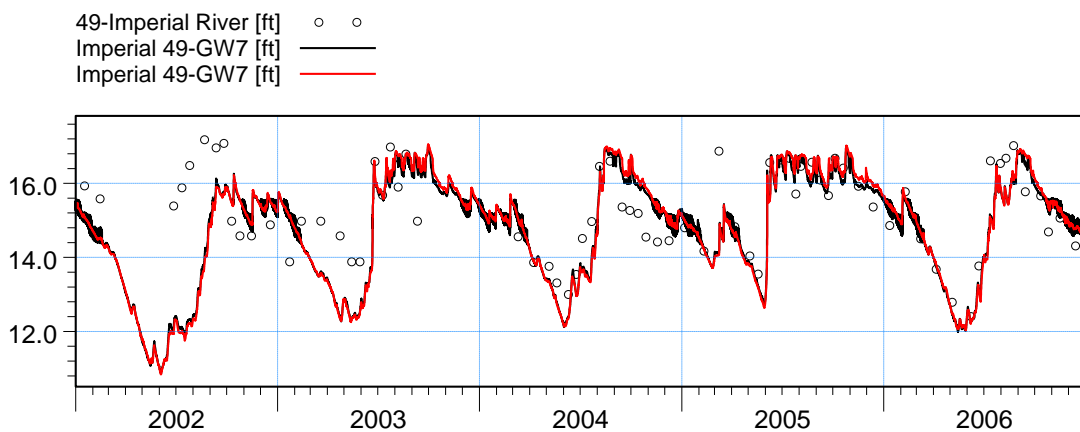


ME=0.120111  
 MAE=0.905135  
 RMSE=1.15059  
 STDres=1.1443  
 R(Correlation)=0.397953  
 R2(Nash\_Sutcliffe)=-1.56442

Figure C12. Groundwater elevation at wells 46A-GW26 and 49-GW3. The black line corresponds to LS ECM result, and red line to the ECM result.

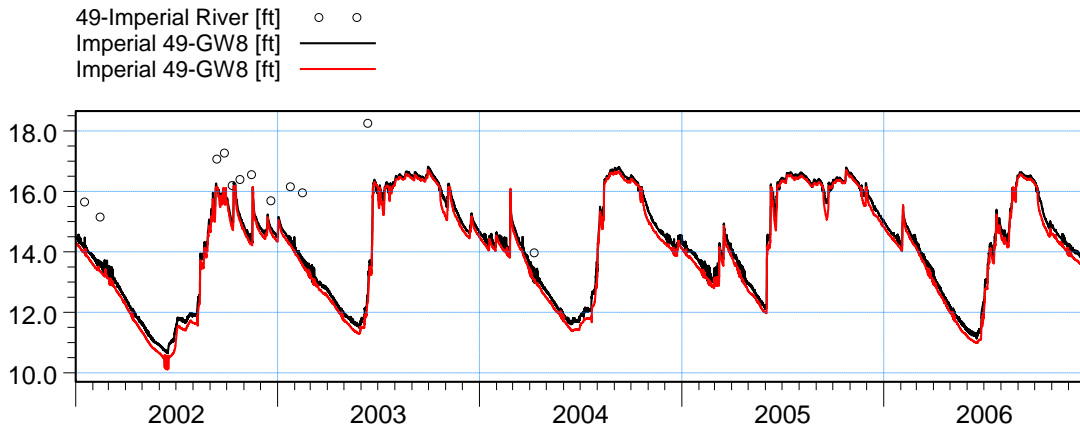


ME=0.15928  
 MAE=1.10072  
 RMSE=1.3201  
 STDres=1.31045  
 R(Correlation)=0.763035  
 R2(Nash\_Sutcliffe)=0.11913

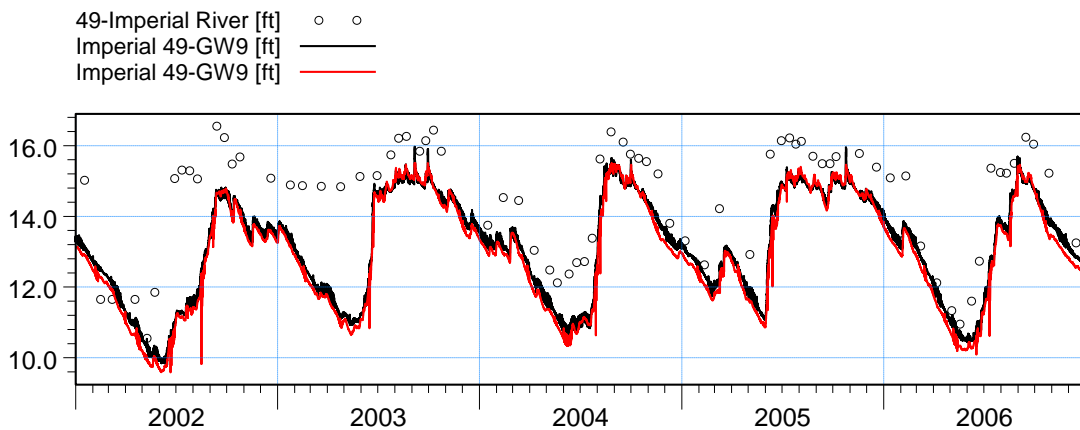


ME=0.427617  
 MAE=0.868823  
 RMSE=1.28836  
 STDres=1.21532  
 R(Correlation)=0.57423  
 R2(Nash\_Sutcliffe)=-0.129474

Figure C13. Groundwater elevation at wells 49-GW6 and 49-GW7. The black line corresponds to LS ECM result, and red line to the ECM result.

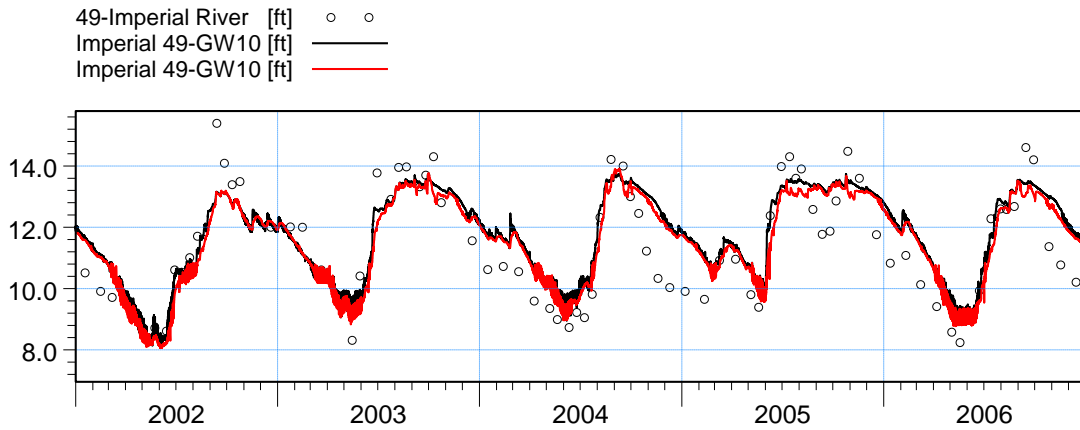


ME=1.78338  
 MAE=1.78338  
 RMSE=2.17374  
 STDres=1.24286  
 R(Correlation)=0.255128  
 R2(Nash\_Sutcliffe)=-3.37353

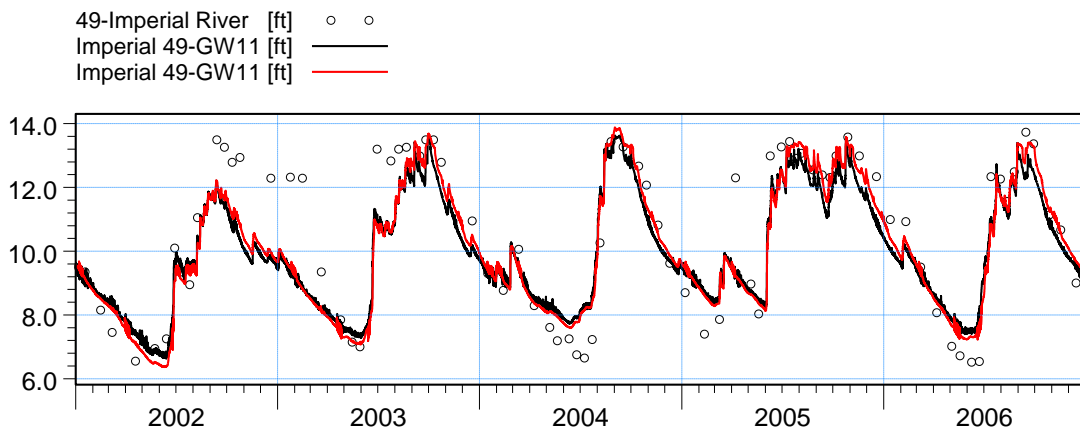


ME=1.34753  
 MAE=1.38006  
 RMSE=1.6551  
 STDres=0.961001  
 R(Correlation)=0.804927  
 R2(Nash\_Sutcliffe)=-0.128044

Figure C14. Groundwater elevation at wells 49-GW8 and 49-GW9. The black line corresponds to LS ECM result, and red line to the ECM result.

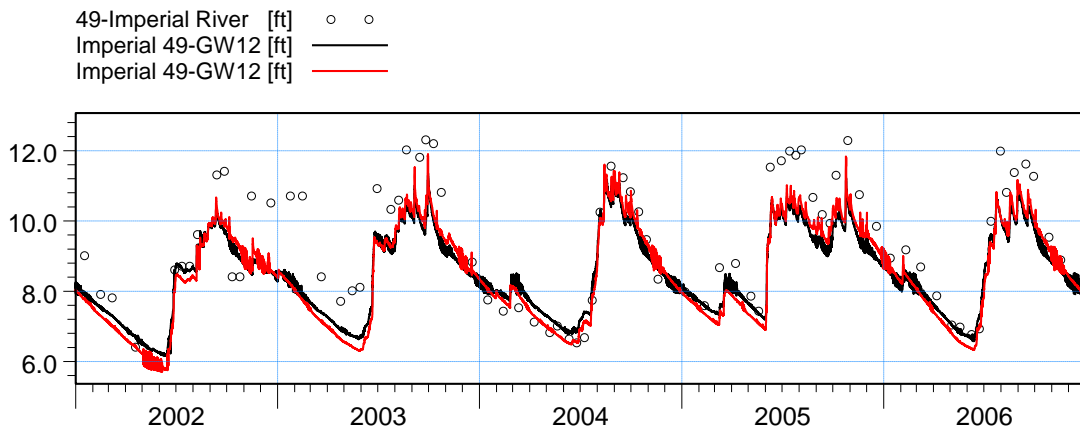


ME=-0.31815  
 MAE=0.809775  
 RMSE=0.974881  
 STDres=0.921506  
 R(Correlation)=0.865945  
 R2(Nash\_Sutcliffe)=0.713697

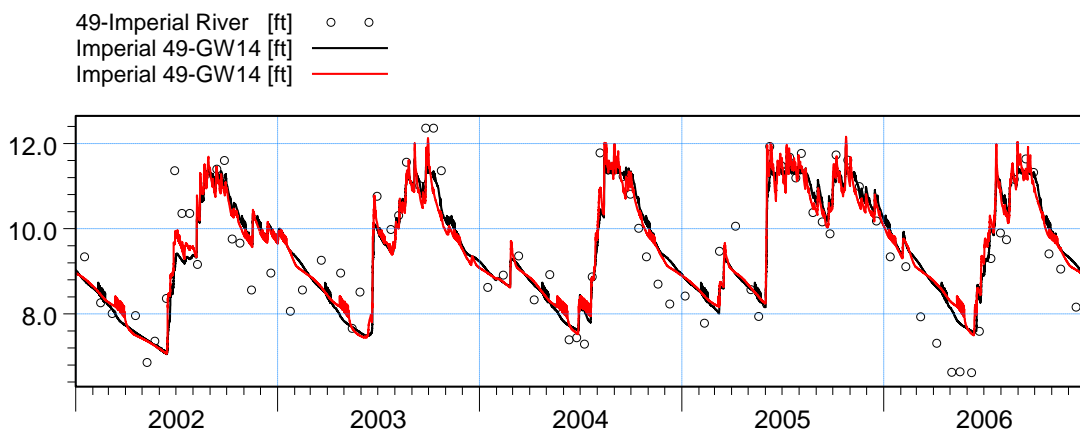


ME=0.432702  
 MAE=0.972423  
 RMSE=1.23268  
 STDres=1.15424  
 R(Correlation)=0.891636  
 R2(Nash\_Sutcliffe)=0.739532

Figure C15. Groundwater elevation at wells 49-GW10 and 49-GW11. The black line corresponds to LS ECM result, and red line to the ECM result.



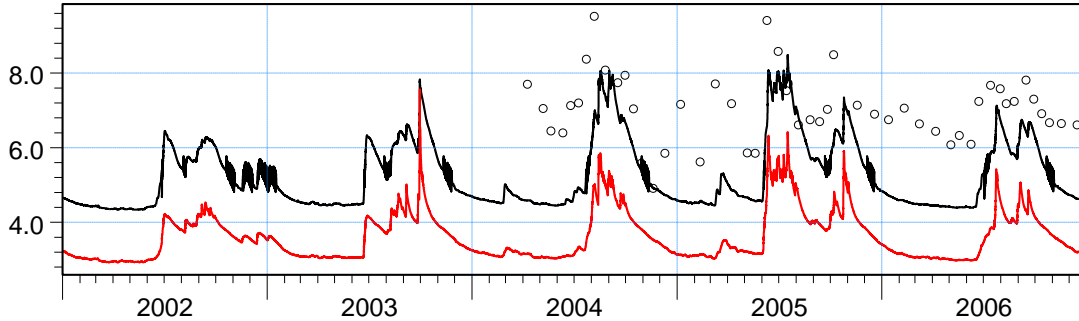
ME=0.747318  
 MAE=0.903635  
 RMSE=1.12611  
 STDres=0.842403  
 R(Correlation)=0.902075  
 R2(Nash\_Sutcliffe)=0.56743



ME=-0.0559433  
 MAE=0.630118  
 RMSE=0.761988  
 STDres=0.759931  
 R(Correlation)=0.861423  
 R2(Nash\_Sutcliffe)=0.740639

Figure C16. Groundwater elevation at wells 49-GW12 and 49-GW14. The black line corresponds to LS ECM result, and red line to the ECM result.

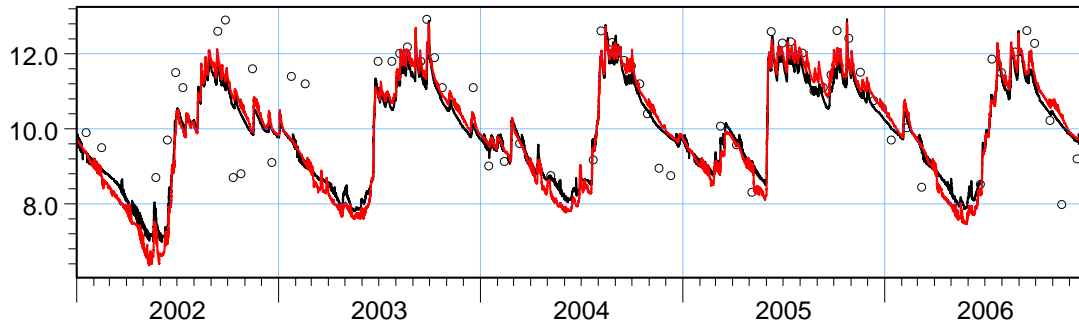
49-Imperial River [ft]    ○ ○  
 Imperial 49-GW15 [ft]    —  
 Imperial 49-GW15 [ft]    —



ME=1.62143  
 MAE=1.68179  
 RMSE=1.87651  
 STDres=0.944593  
 R(Correlation)=0.508067  
 R2(Nash\_Sutcliffe)=-3.33736

Note: differences at 49-GW15 station are likely caused by topography differences between model grid cells.  
 In ECM, GSE = 7.6 ft.  
 In LS ECM, GSE = 10.3 ft.

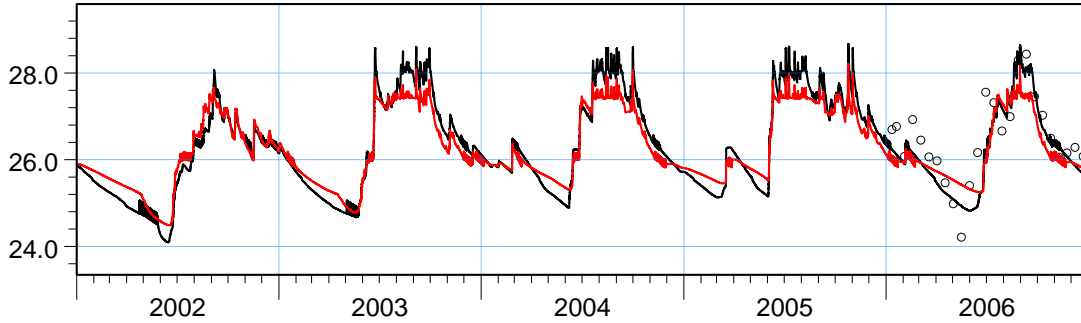
49L-Leitner Cr [ft]    ○ ○  
 Leitner 49L-GW1 [ft]    —  
 Leitner 49L-GW1 [ft]    —



ME=0.356357  
 MAE=0.752029  
 RMSE=0.938772  
 STDres=0.868505  
 R(Correlation)=0.781539  
 R2(Nash\_Sutcliffe)=0.54215

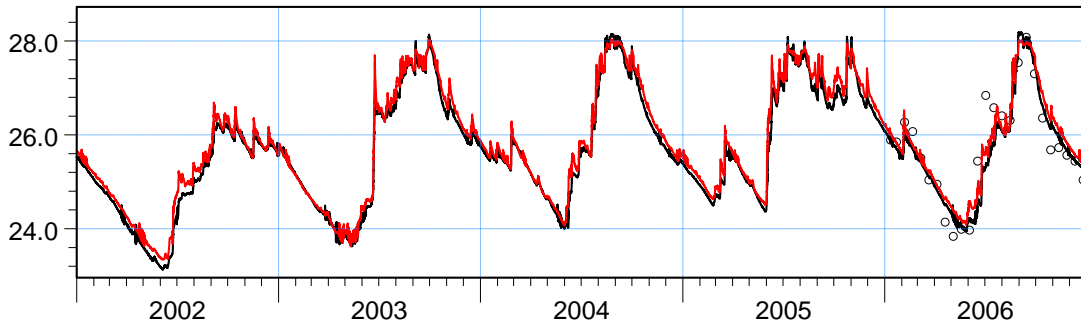
Figure C17. Groundwater elevation at wells 49-GW15 and 49L-GW1. The black line corresponds to LS ECM result, and red line to the ECM result.

MW1\_m [ft]    ○ ○  
 BRM-MW1 [ft]    —  
 BRM-MW1 [ft]    —



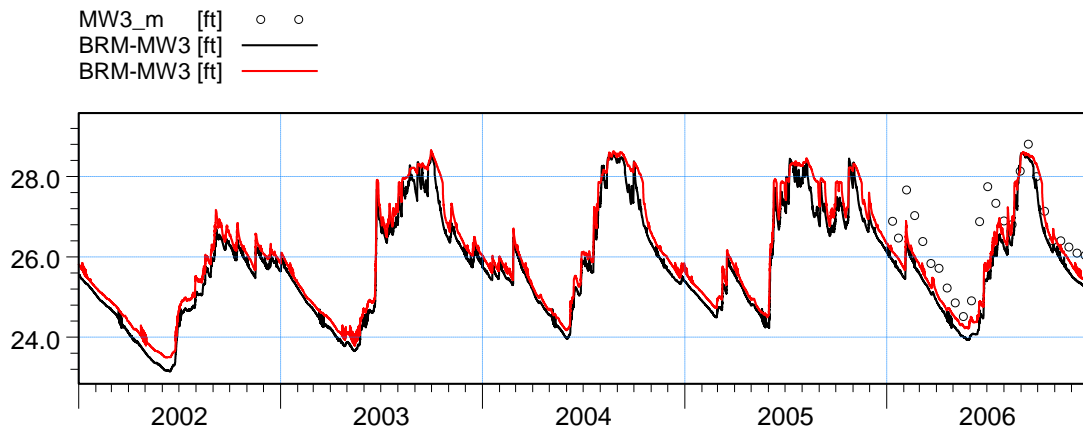
ME=0.286486  
 MAE=0.471358  
 RMSE=0.593058  
 STDres=0.519272  
 R(Correlation)=0.860859  
 R2(Nash\_Sutcliffe)=0.65244

MW2\_m [ft]    ○ ○  
 BRM-MW2 [ft]    —  
 BRM-MW2 [ft]    —

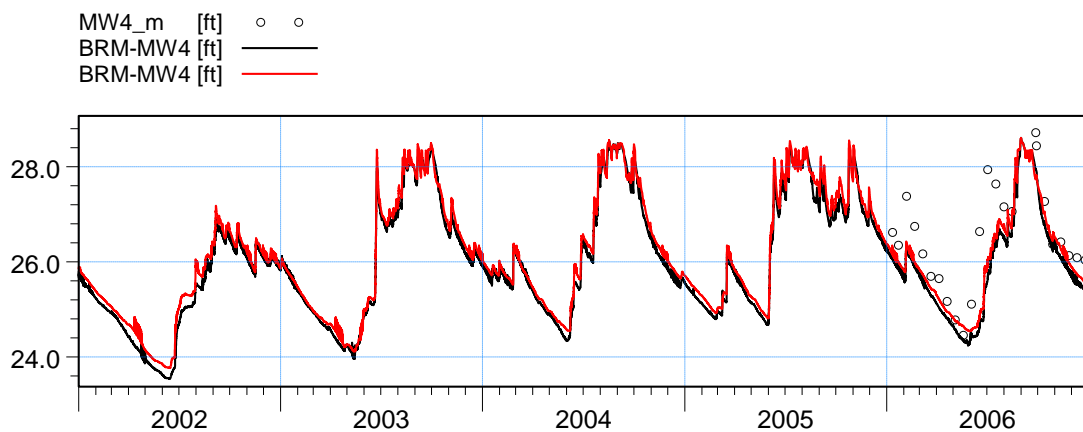


ME=0.146097  
 MAE=0.330765  
 RMSE=0.476677  
 STDres=0.453736  
 R(Correlation)=0.921008  
 R2(Nash\_Sutcliffe)=0.832417

Figure C18. Groundwater elevation at wells BRM-MW1 and BRM-MW2. The black line corresponds to LS ECM result, and red line to the ECM result.

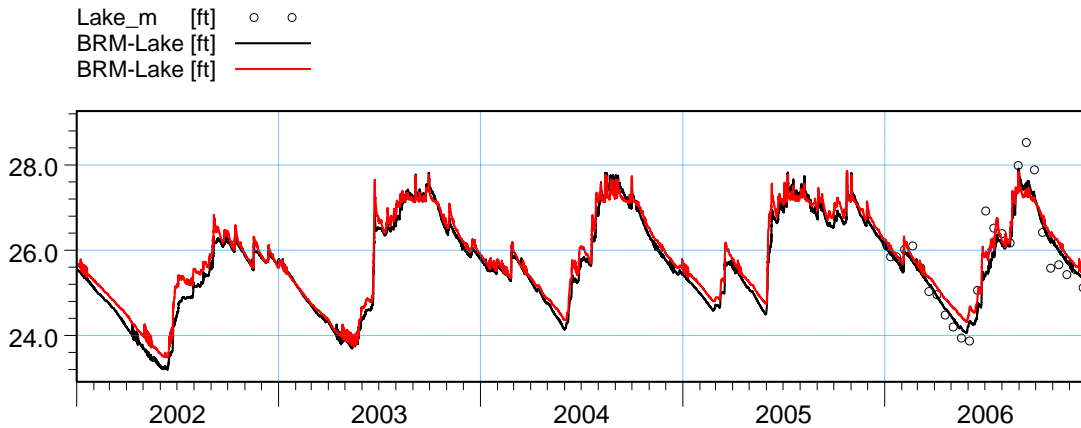


ME=0.849808  
 MAE=0.850054  
 RMSE=0.98661  
 STDres=0.501224  
 R(Correlation)=0.907169  
 R2(Nash\_Sutcliffe)=0.246118

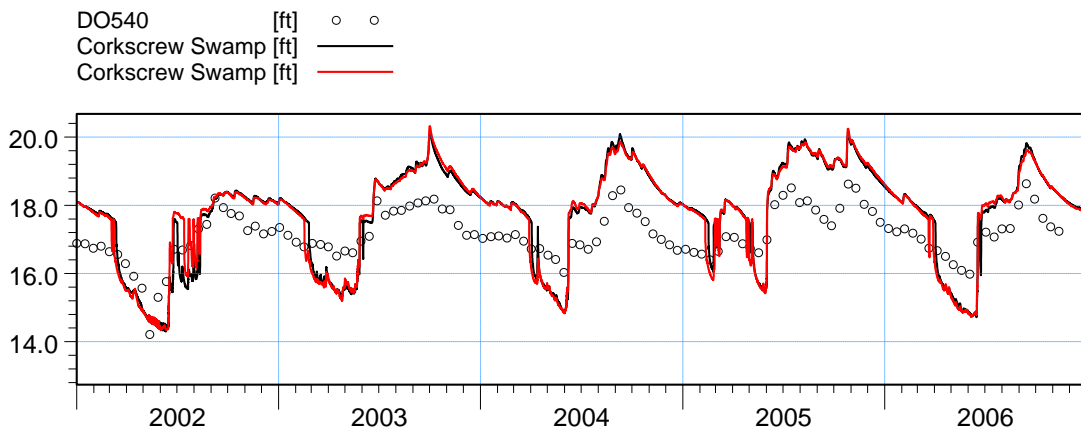


ME=0.668535  
 MAE=0.673313  
 RMSE=0.861776  
 STDres=0.5438  
 R(Correlation)=0.840096  
 R2(Nash\_Sutcliffe)=0.261052

Figure C19. Groundwater elevation at wells BRM-MW3 and BRM-MW4. The black line corresponds to LS ECM result, and red line to the ECM result.

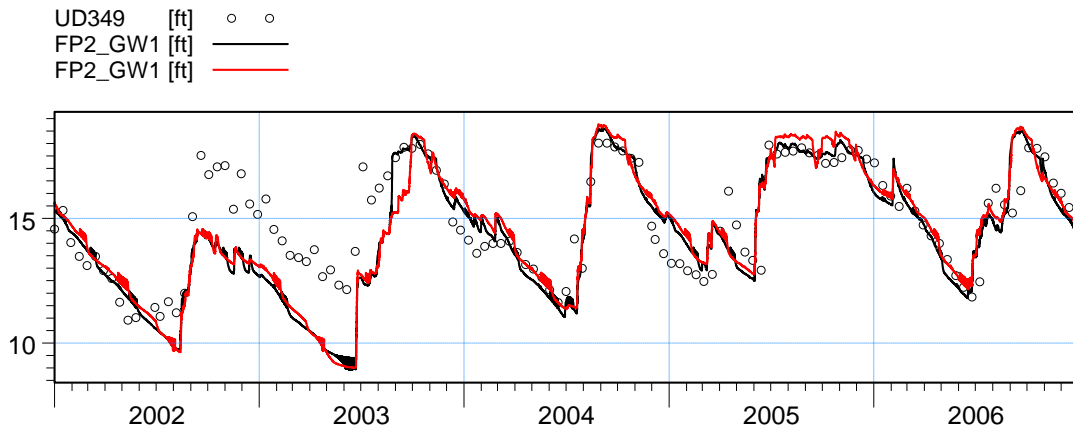


ME=0.145463  
 MAE=0.37675  
 RMSE=0.507723  
 STDres=0.486439  
 R(Correlation)=0.936208  
 R2(Nash\_Sutcliffe)=0.829632

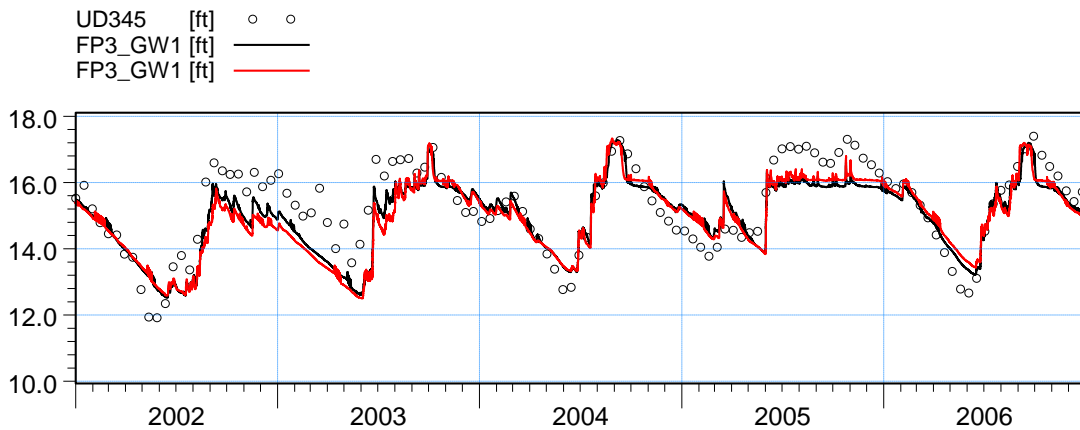


ME=-0.606972  
 MAE=1.00665  
 RMSE=1.05951  
 STDres=0.868422  
 R(Correlation)=0.866191  
 R2(Nash\_Sutcliffe)=-1.24556

Figure C20. Groundwater elevation at wells BRM-Lake and Corkscrew Swamp. The black line corresponds to LS ECM result, and red line to the ECM result.

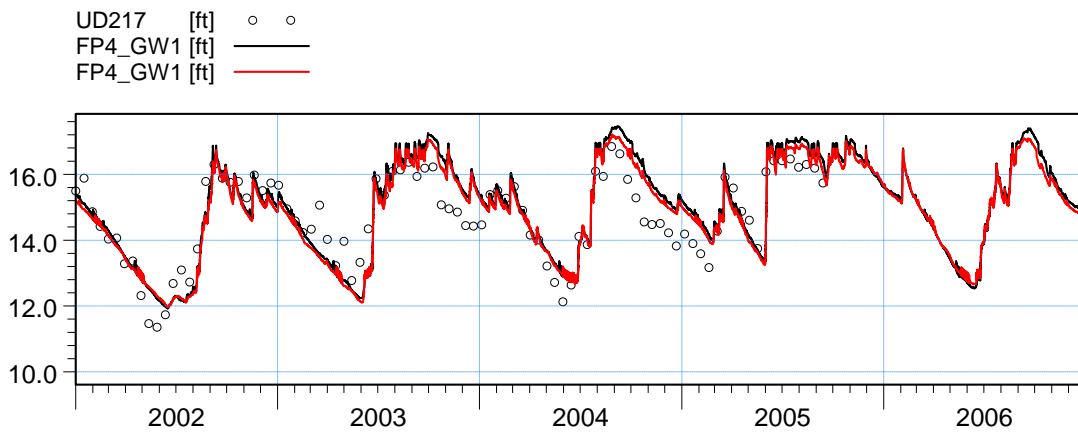


ME=0.50223  
 MAE=1.08661  
 RMSE=1.52592  
 STDres=1.4409  
 R(Correlation)=0.804403  
 R2(Nash\_Sutcliffe)=0.455097

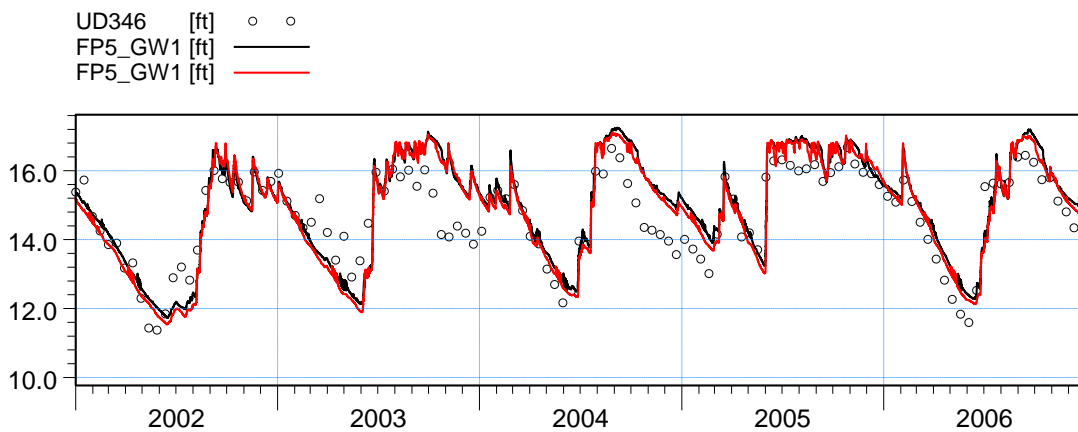


ME=0.27823  
 MAE=0.600786  
 RMSE=0.725598  
 STDres=0.670135  
 R(Correlation)=0.859798  
 R2(Nash\_Sutcliffe)=0.691124

Figure C21. Groundwater elevation at wells FP2\_GW1 and FP3\_GW1. The black line corresponds to LS ECM result, and red line to the ECM result.

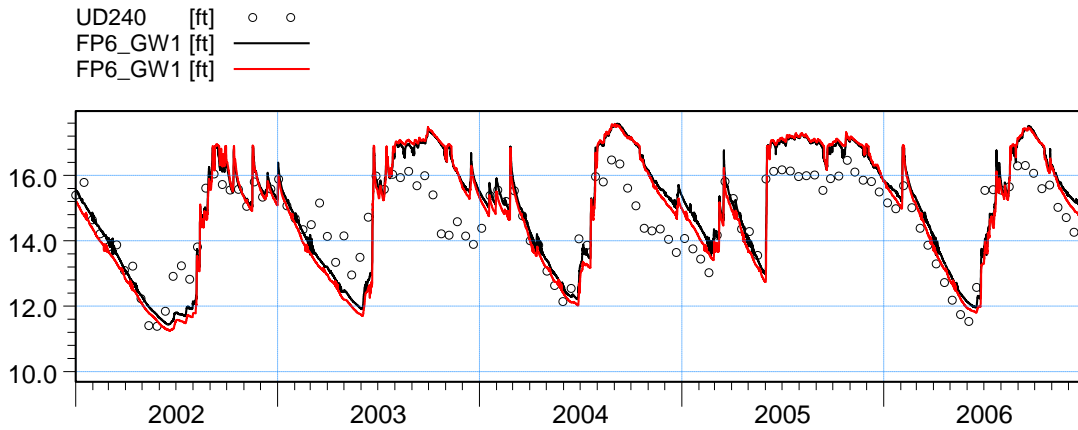


ME=-0.220112  
 MAE=0.554392  
 RMSE=0.698617  
 STDres=0.663036  
 R(Correlation)=0.891076  
 R2(Nash\_Sutcliffe)=0.719073

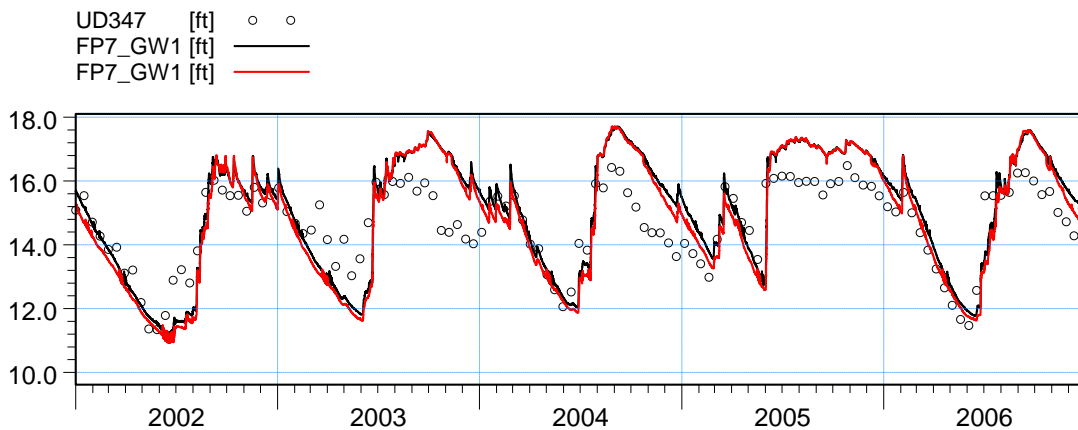


ME=-0.329464  
 MAE=0.596321  
 RMSE=0.764666  
 STDres=0.690049  
 R(Correlation)=0.881118  
 R2(Nash\_Sutcliffe)=0.654618

Figure C22. Groundwater elevation at wells FP4\_GW1 and FP5\_GW1. The black line corresponds to LS ECM result, and red line to the ECM result.

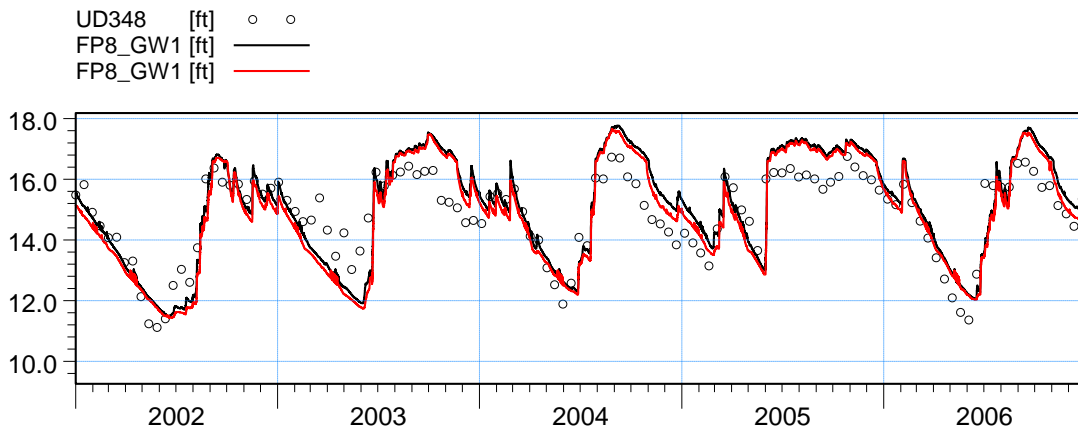


ME=-0.412527  
 MAE=0.756393  
 RMSE=0.941894  
 STDres=0.84675  
 R(Correlation)=0.87017  
 R2(Nash\_Sutcliffe)=0.46586

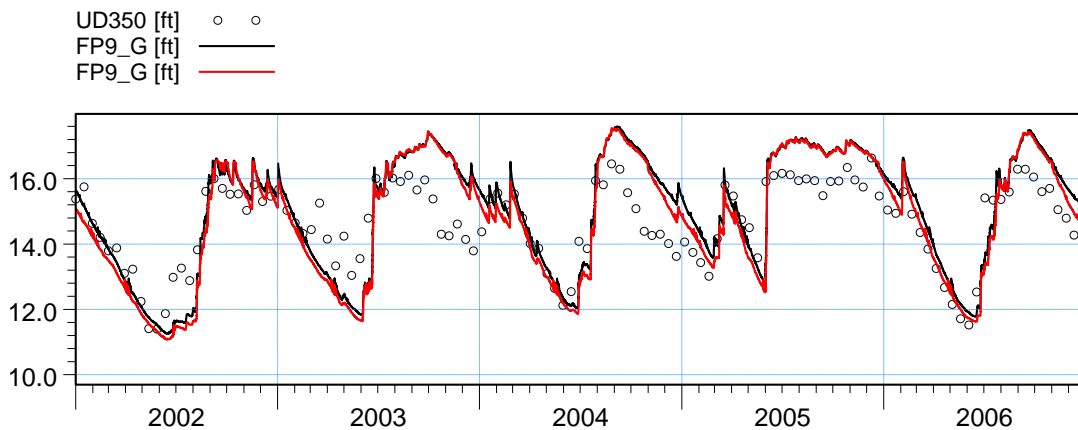


ME=-0.410671  
 MAE=0.838382  
 RMSE=1.02652  
 STDres=0.940798  
 R(Correlation)=0.863737  
 R2(Nash\_Sutcliffe)=0.36804

Figure C23. Groundwater elevation at wells FP6\_GW1 and FP7\_GW1. The black line corresponds to LS ECM result, and red line to the ECM result.

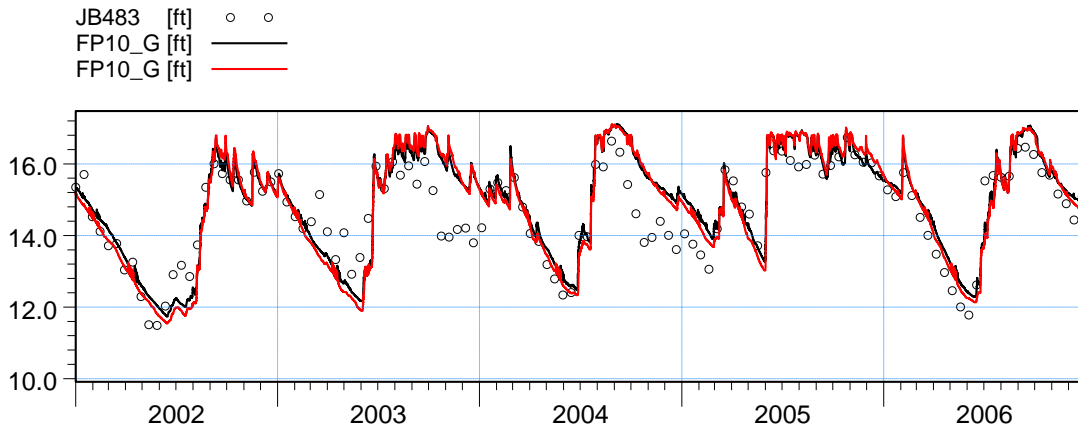


ME=-0.272483  
 MAE=0.702247  
 RMSE=0.854308  
 STDres=0.809688  
 R(Correlation)=0.883307  
 R2(Nash\_Sutcliffe)=0.625276

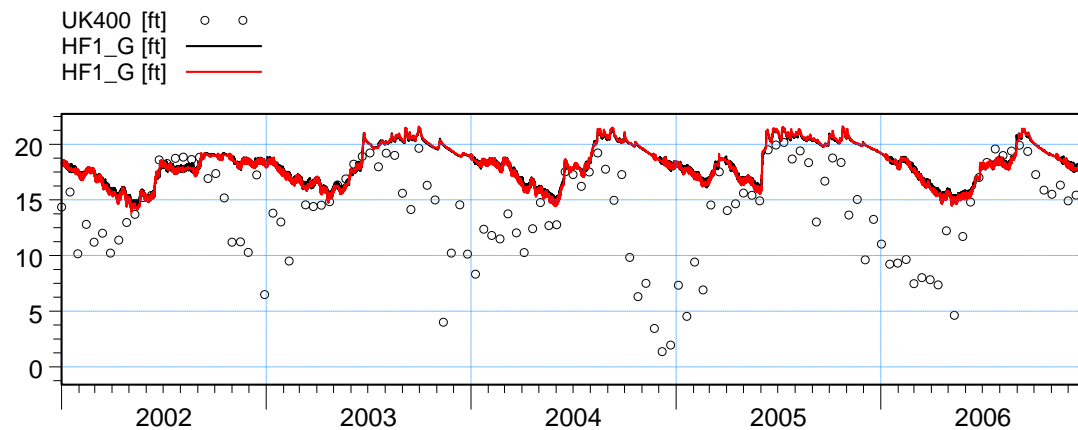


ME=-0.393952  
 MAE=0.825674  
 RMSE=1.01907  
 STDres=0.939844  
 R(Correlation)=0.85594  
 R2(Nash\_Sutcliffe)=0.363127

Figure C24. Groundwater elevation at wells FP8\_GW1 and FP9\_G. The black line corresponds to LS ECM result, and red line to the ECM result.

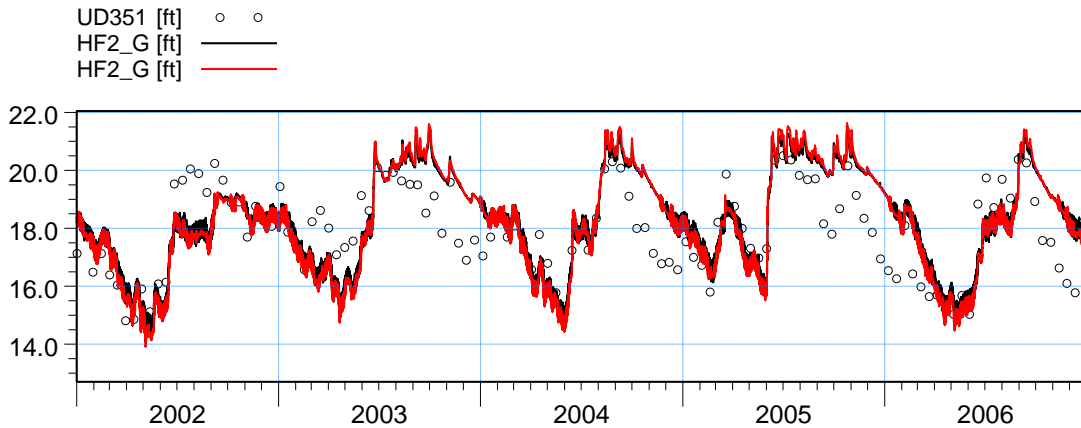


ME=-0.283452  
 MAE=0.546869  
 RMSE=0.729223  
 STDres=0.671879  
 R(Correlation)=0.877626  
 R2(Nash\_Sutcliffe)=0.678147

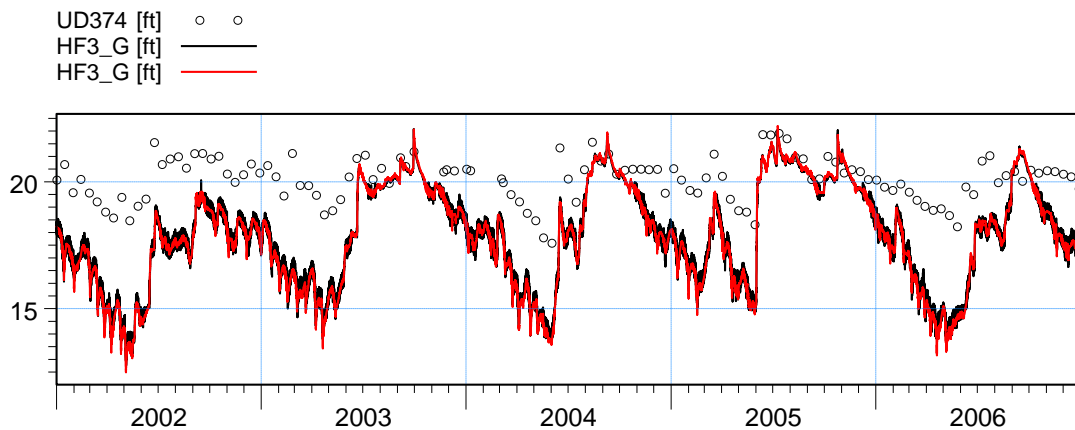


ME=-4.28368  
 MAE=4.43244  
 RMSE=5.98319  
 STDres=4.17716  
 R(Correlation)=0.27164  
 R2(Nash\_Sutcliffe)=-0.926593

Figure C25. Groundwater elevation at wells FP10\_G and HF1\_G. The black line corresponds to LS ECM result, and red line to the ECM result.

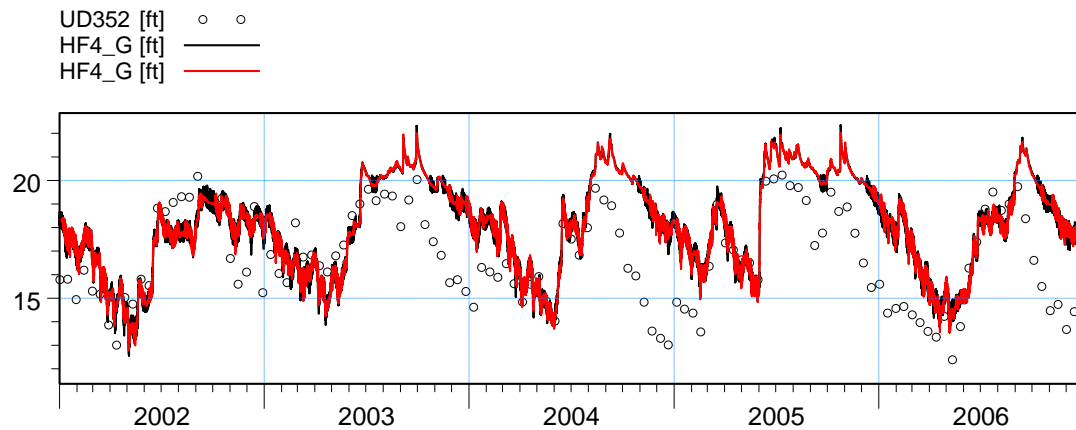


ME=-0.377051  
 MAE=1.04649  
 RMSE=1.24513  
 STDres=1.18667  
 R(Correlation)=0.714211  
 R2(Nash\_Sutcliffe)=0.306722

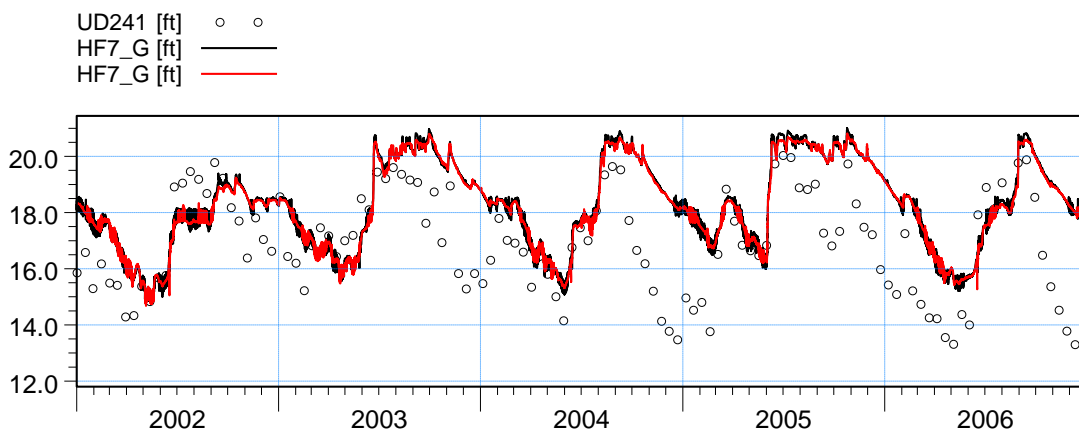


ME=2.23605  
 MAE=2.26786  
 RMSE=2.62156  
 STDres=1.36846  
 R(Correlation)=0.799221  
 R2(Nash\_Sutcliffe)=-8.43752

Figure C26. Groundwater elevation at wells HF2\_G and HF3\_G. The black line corresponds to LS ECM result, and red line to the ECM result.

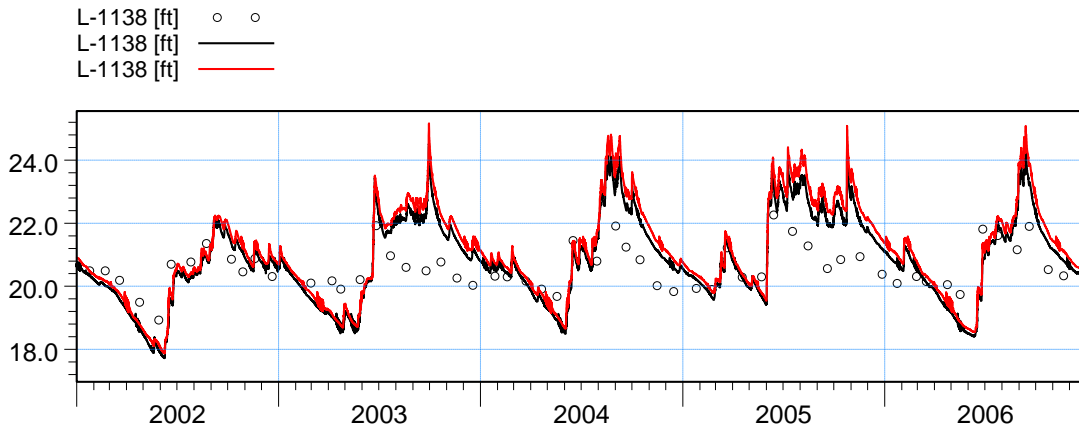


ME=-1.38327  
 MAE=1.79062  
 RMSE=2.20599  
 STDres=1.71842  
 R(Correlation)=0.622821  
 R2(Nash\_Sutcliffe)=-0.210921

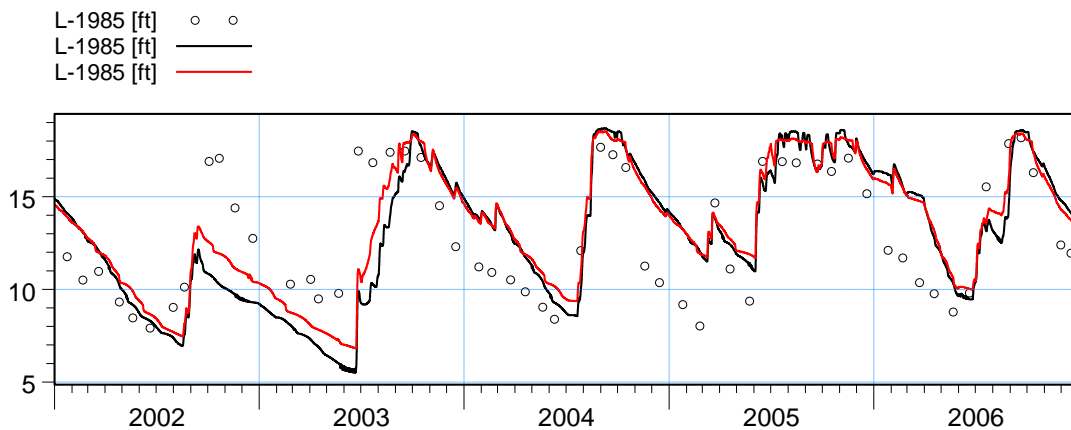


ME=-1.42468  
 MAE=1.69665  
 RMSE=2.08527  
 STDres=1.52271  
 R(Correlation)=0.594652  
 R2(Nash\_Sutcliffe)=-0.33131

Figure C27. Groundwater elevation at wells HF4\_G and HF7\_G. The black line corresponds to LS ECM result, and red line to the ECM result.

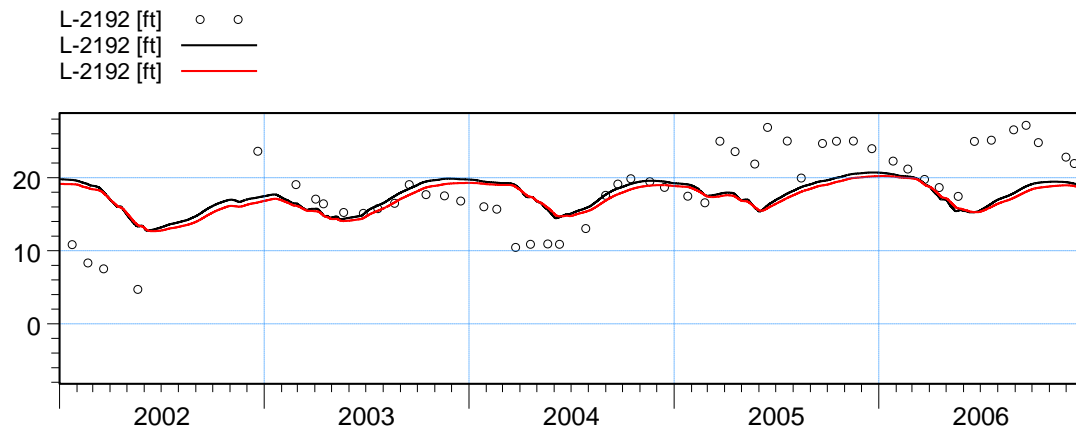


ME=-0.290586  
 MAE=0.77523  
 RMSE=0.891337  
 STDres=0.84264  
 R(Correlation)=0.805711  
 R2(Nash\_Sutcliffe)=-0.766072

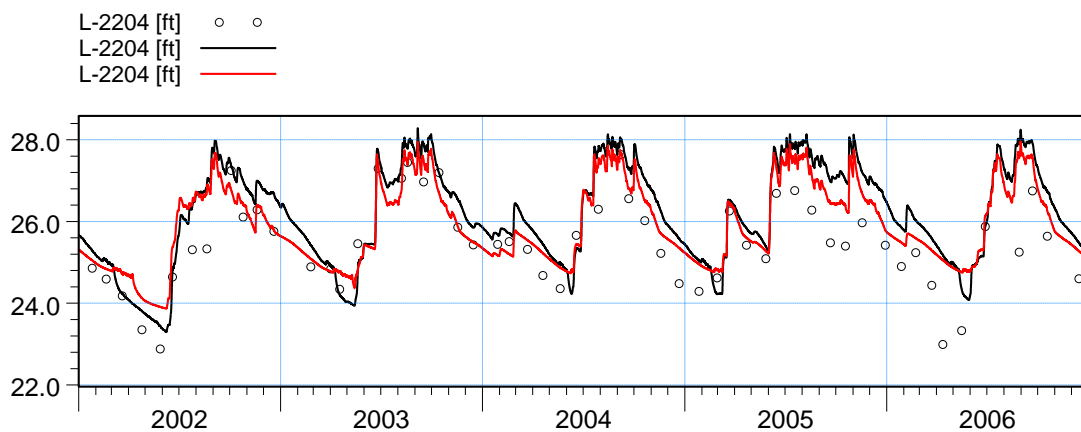


ME=-0.215227  
 MAE=2.46106  
 RMSE=2.97852  
 STDres=2.97073  
 R(Correlation)=0.620126  
 R2(Nash\_Sutcliffe)=0.195474

Figure C28. Groundwater elevation at wells L-1138 and L-1985. The black line corresponds to LS ECM result, and red line to the ECM result.

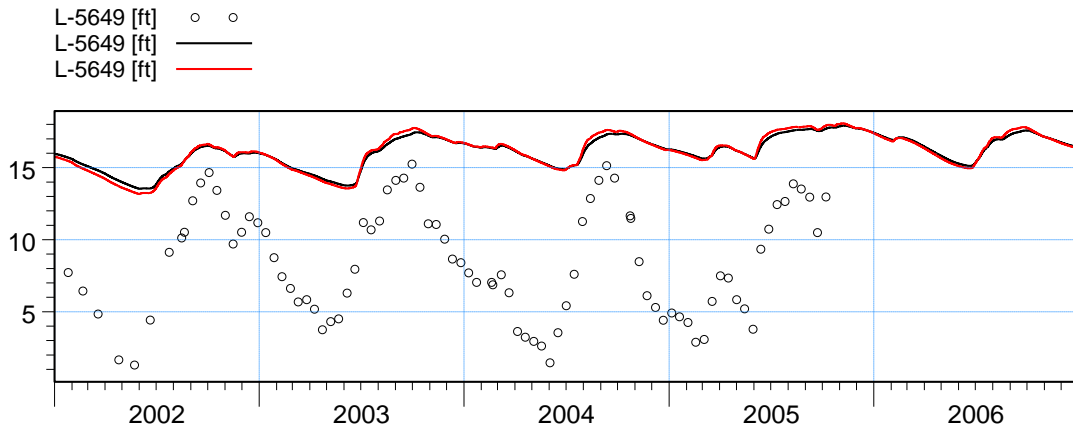


ME=0.778973  
 MAE=4.01338  
 RMSE=5.15608  
 STDres=5.09689  
 R(Correlation)=0.315689  
 R2(Nash\_Sutcliffe)=0.0779353

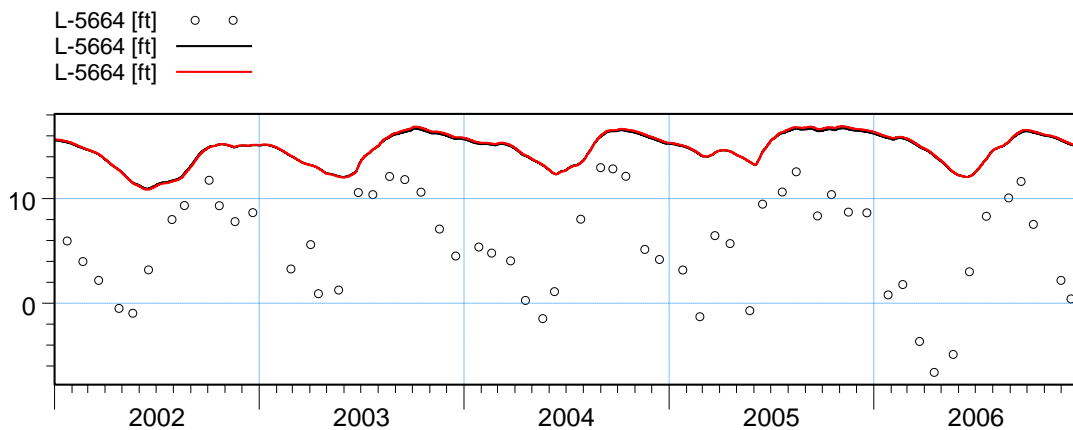


ME=-0.703268  
 MAE=0.756949  
 RMSE=0.922013  
 STDres=0.596257  
 R(Correlation)=0.867378  
 R2(Nash\_Sutcliffe)=0.286258

Figure C29. Groundwater elevation at wells L-2192 and L-2204. The black line corresponds to LS ECM result, and red line to the ECM result.

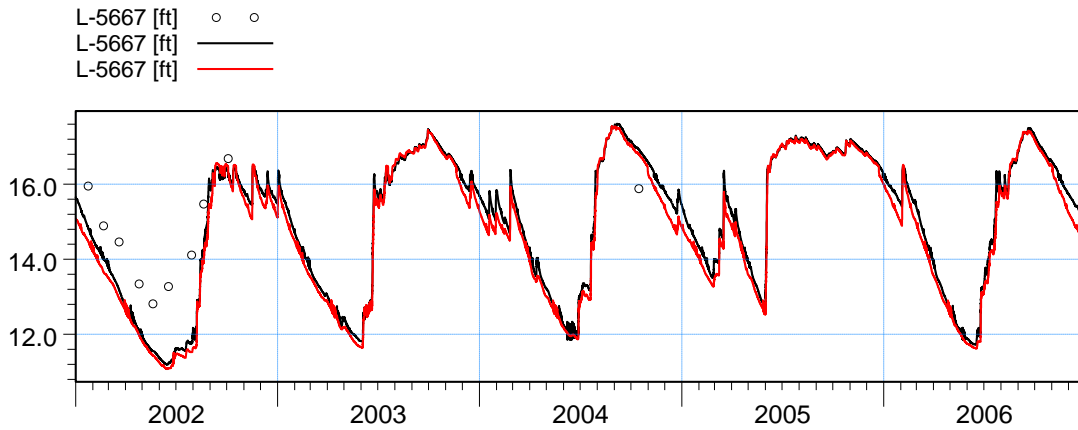


ME=-7.45185  
 MAE=7.45185  
 RMSE=8.14725  
 STDres=3.29356  
 R(Correlation)=0.631775  
 R2(Nash\_Sutcliffe)=-3.54896

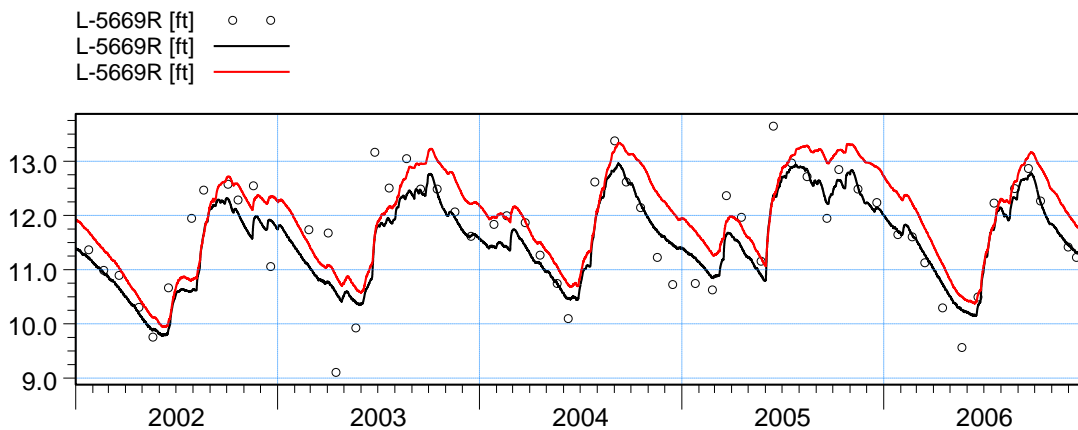


ME=-9.11431  
 MAE=9.11431  
 RMSE=10.068  
 STDres=4.27723  
 R(Correlation)=0.50387  
 R2(Nash\_Sutcliffe)=-3.34129

Figure C30. Groundwater elevation at wells L-5649 and L-5664. The black line corresponds to LS ECM result, and red line to the ECM result.

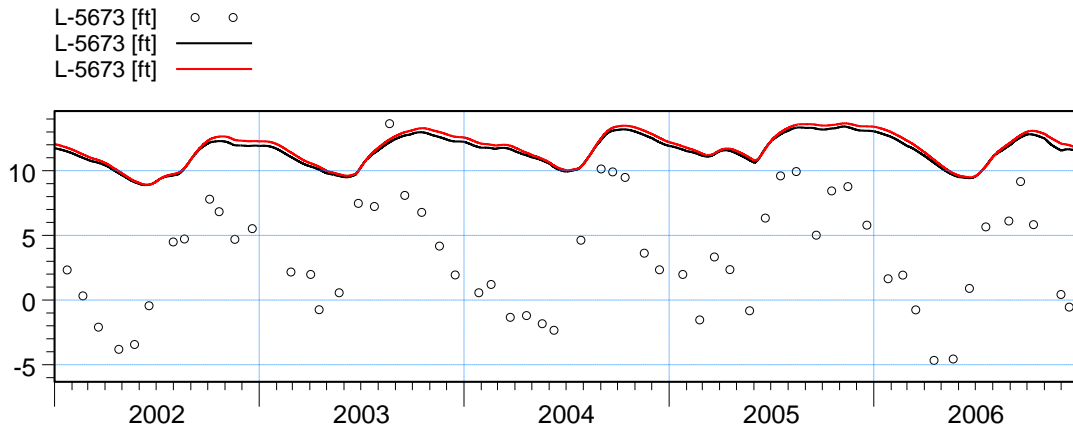


ME=1.08568  
 MAE=1.29351  
 RMSE=1.39415  
 STDres=0.874607  
 R(Correlation)=0.927497  
 R2(Nash\_Sutcliffe)=-0.264188

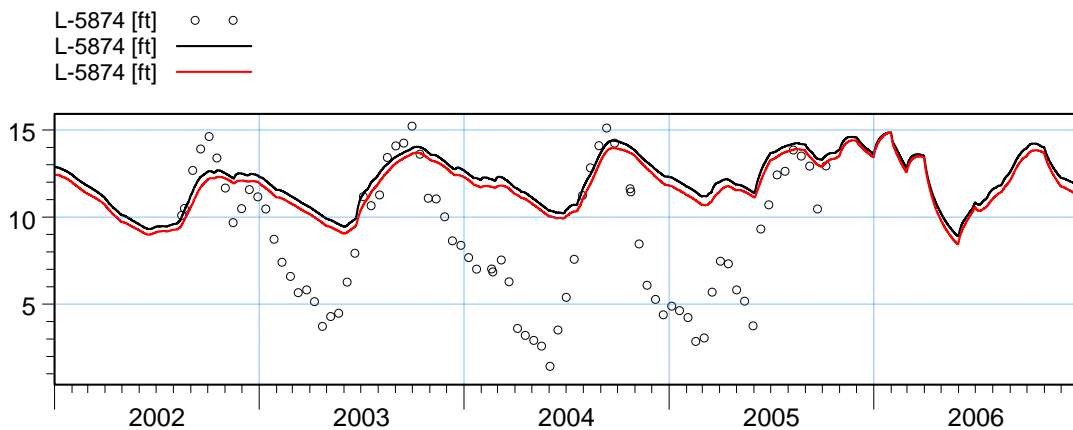


ME=0.15033  
 MAE=0.399392  
 RMSE=0.549613  
 STDres=0.528654  
 R(Correlation)=0.852318  
 R2(Nash\_Sutcliffe)=0.699264

Figure C31. Groundwater elevation at wells L-5667 and L-5669R. The black line corresponds to LS ECM result, and red line to the ECM result.

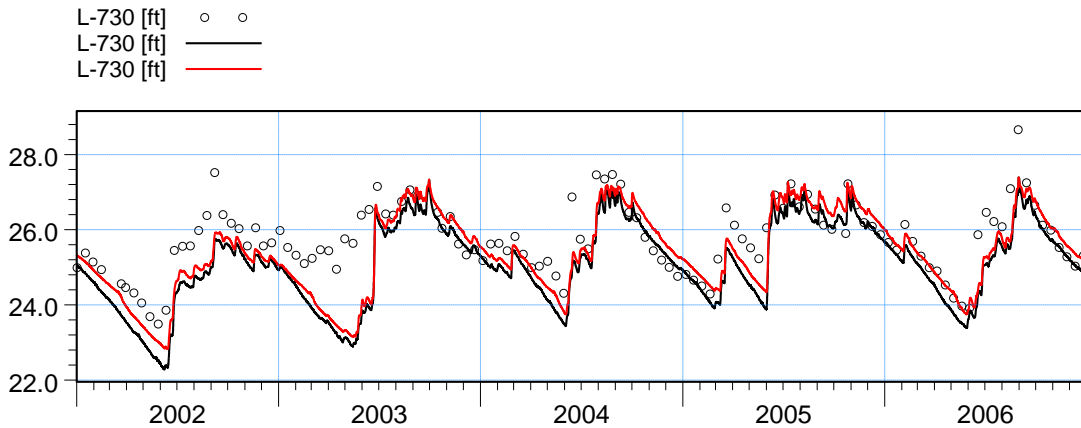


ME=-8.21043  
 MAE=8.25917  
 RMSE=8.97698  
 STDres=3.62974  
 R(Correlation)=0.631532  
 R2(Nash\_Sutcliffe)=-3.44054

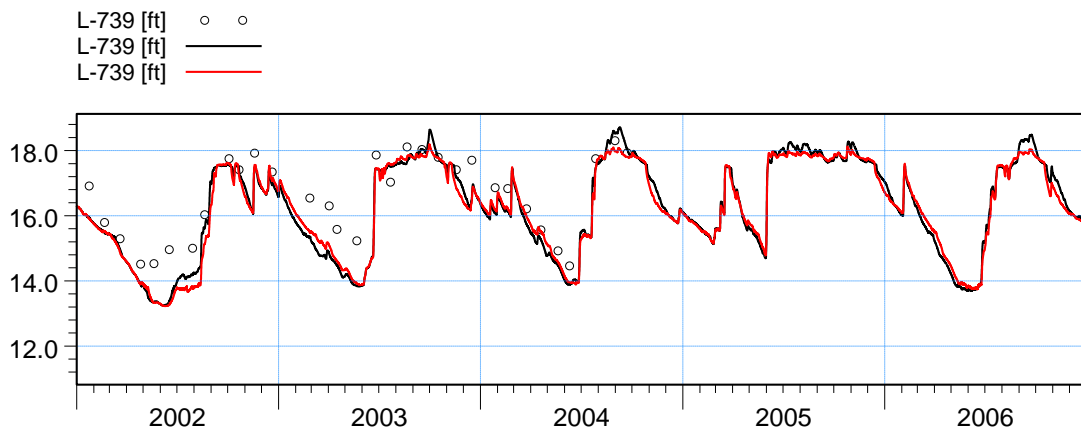


ME=-3.50002  
 MAE=3.76479  
 RMSE=4.64814  
 STDres=3.0586  
 R(Correlation)=0.71358  
 R2(Nash\_Sutcliffe)=-0.484398

Figure C32. Groundwater elevation at wells L-5673 and L-5874. The black line corresponds to LS ECM result, and red line to the ECM result.

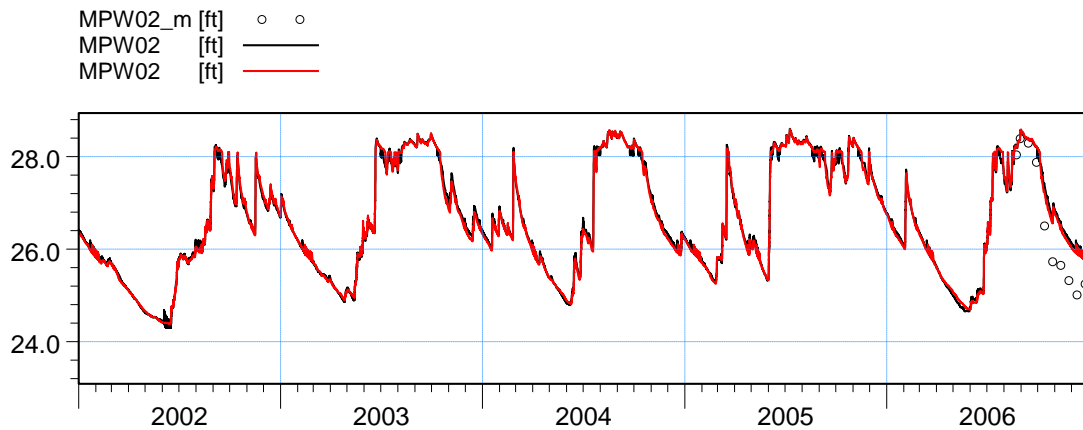


ME=0.653599  
 MAE=0.686917  
 RMSE=0.922452  
 STDres=0.650943  
 R(Correlation)=0.796161  
 R2(Nash\_Sutcliffe)=0.0242095

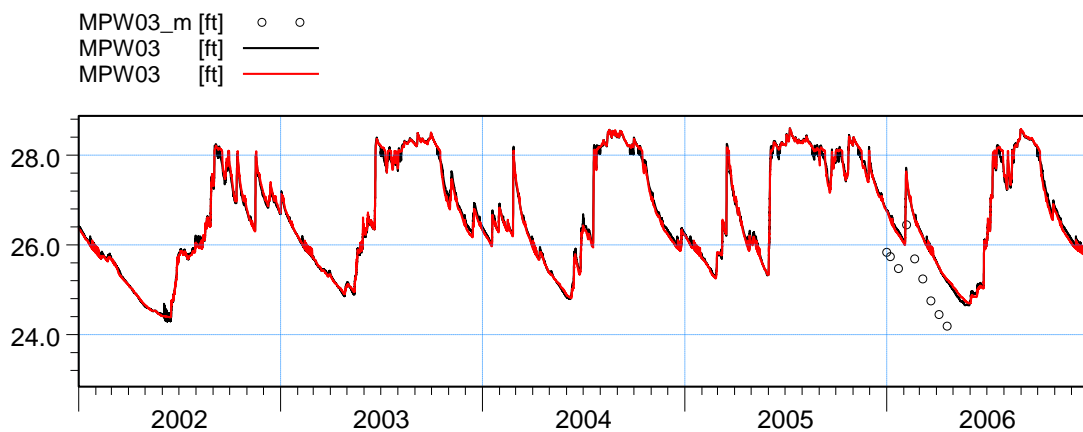


ME=0.548706  
 MAE=0.600805  
 RMSE=0.744771  
 STDres=0.503592  
 R(Correlation)=0.958899  
 R2(Nash\_Sutcliffe)=0.630479

Figure C33. Groundwater elevation at wells L-730 and L-739. The black line corresponds to LS ECM result, and red line to the ECM result.

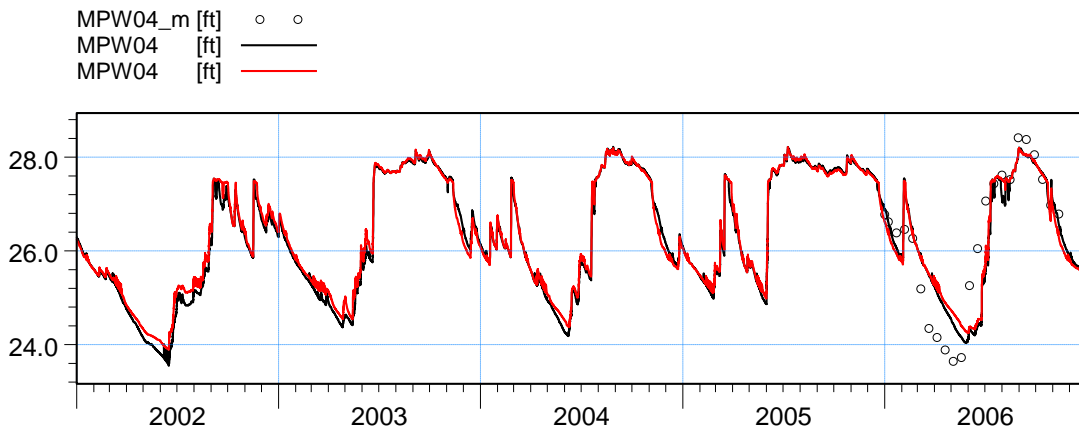


ME=-0.668428  
 MAE=0.672992  
 RMSE=0.776394  
 STDres=0.394958  
 R(Correlation)=0.978988  
 R2(Nash\_Sutcliffe)=0.634725

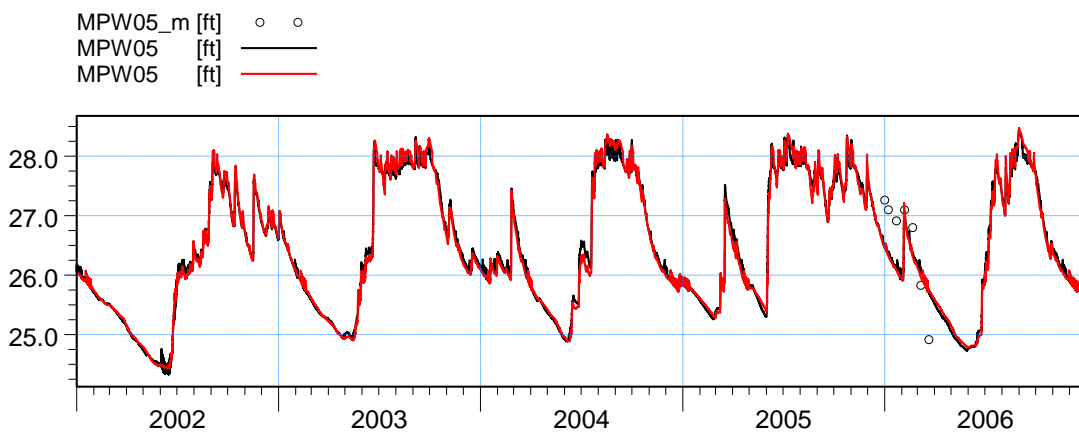


ME=-0.980798  
 MAE=0.980798  
 RMSE=0.985699  
 STDres=0.0981716  
 R(Correlation)=0.988933  
 R2(Nash\_Sutcliffe)=-1.53278

Figure C34. Groundwater elevation at wells MPW02 and MPW03. The black line corresponds to LS ECM result, and red line to the ECM result.

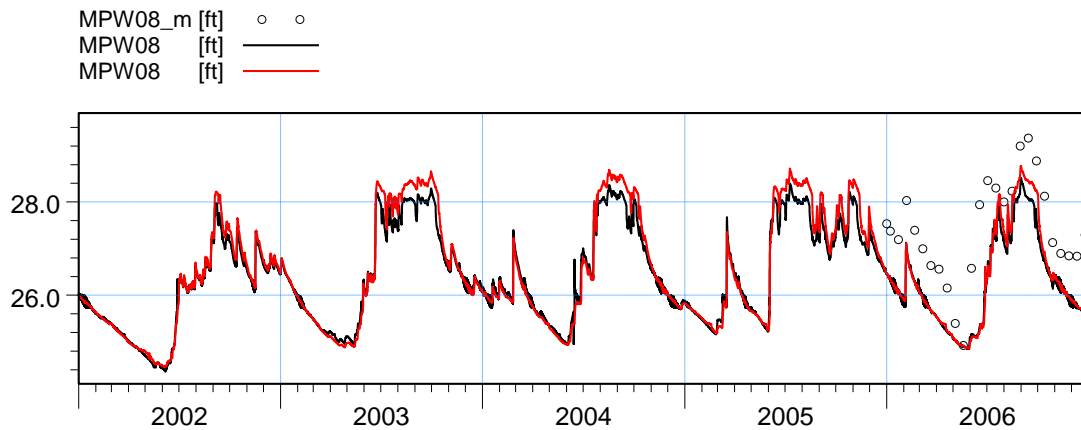


ME=-0.0141754  
 MAE=0.506182  
 RMSE=0.650089  
 STDres=0.649935  
 R(Correlation)=0.910588  
 R2(Nash\_Sutcliffe)=0.823336

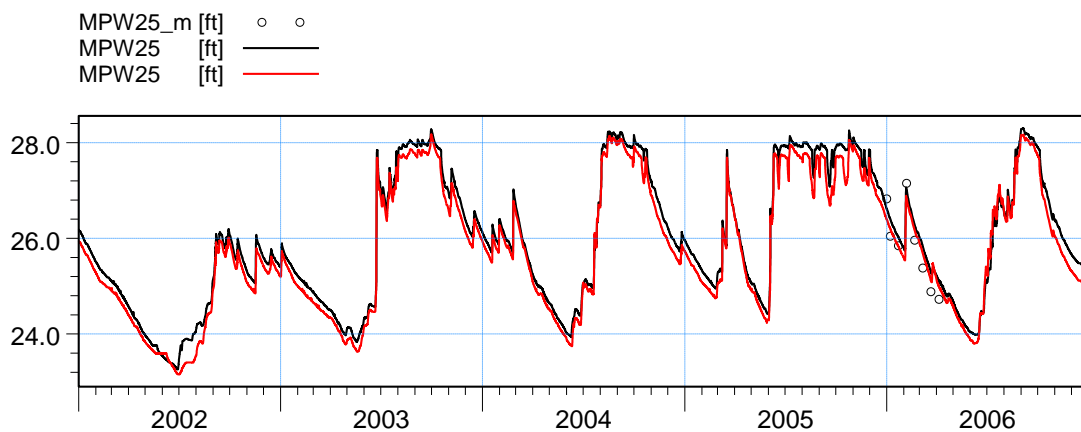


ME=0.245159  
 MAE=0.527312  
 RMSE=0.574793  
 STDres=0.519889  
 R(Correlation)=0.780856  
 R2(Nash\_Sutcliffe)=0.376076

Figure C35. Groundwater elevation at wells MPW04 and MPW05. The black line corresponds to LS ECM result, and red line to the ECM result.

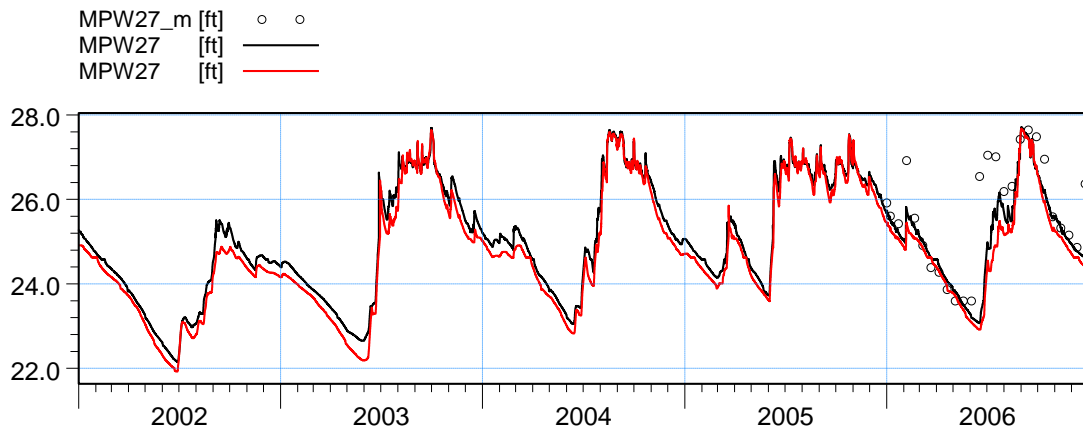


ME=1.06324  
 MAE=1.0663  
 RMSE=1.14865  
 STDres=0.434638  
 R(Correlation)=0.921404  
 R2(Nash\_Sutcliffe)=-0.0781867

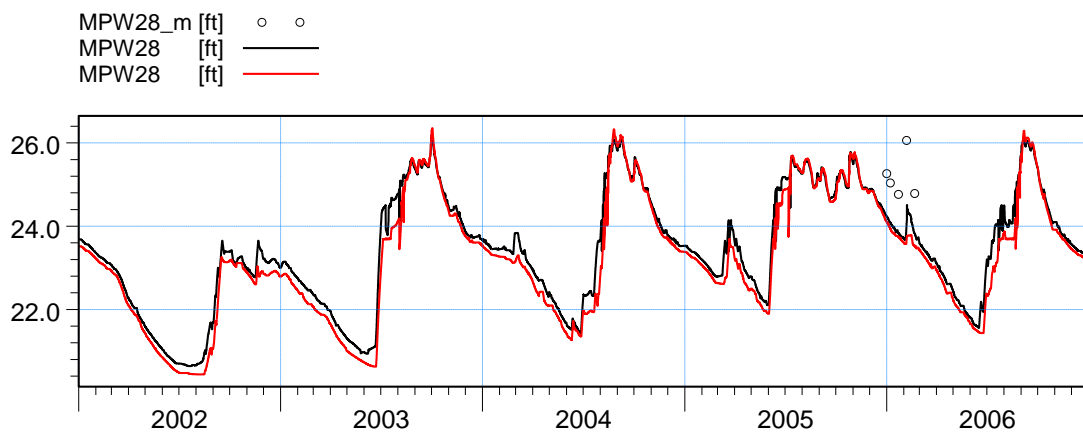


ME=-0.267954  
 MAE=0.353416  
 RMSE=0.385798  
 STDres=0.277563  
 R(Correlation)=0.951355  
 R2(Nash\_Sutcliffe)=0.736048

Figure C36. Groundwater elevation at wells MPW08 and MPW25. The black line corresponds to LS ECM result, and red line to the ECM result.

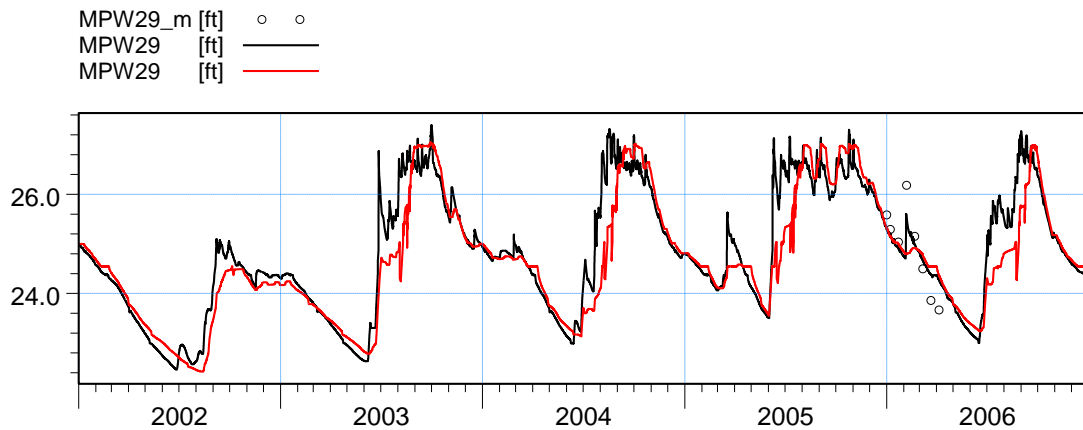


ME=0.462521  
 MAE=0.517404  
 RMSE=0.809541  
 STDres=0.664403  
 R(Correlation)=0.854764  
 R2(Nash\_Sutcliffe)=0.600076

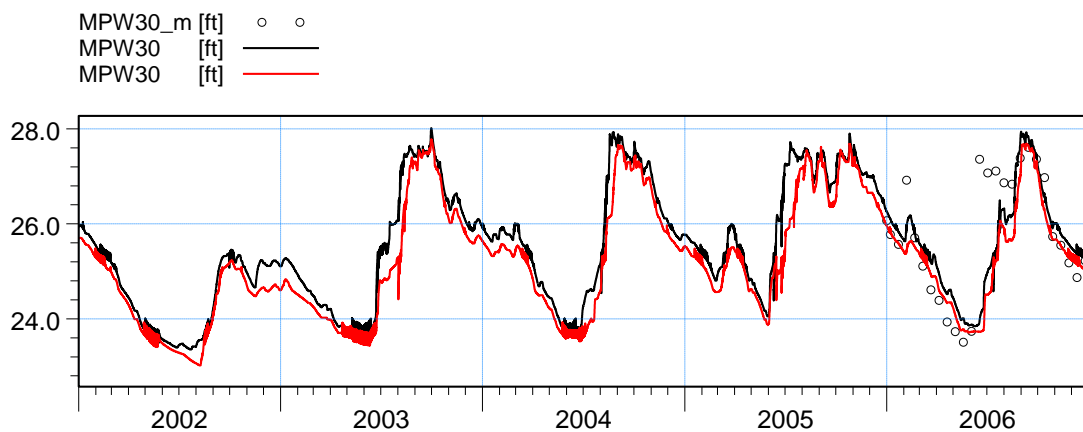


ME=0.948265  
 MAE=0.948265  
 RMSE=0.997715  
 STDres=0.310207  
 R(Correlation)=0.767206  
 R2(Nash\_Sutcliffe)=-3.95778

Figure C37. Groundwater elevation at wells MPW27 and MPW28. The black line corresponds to LS ECM result, and red line to the ECM result.

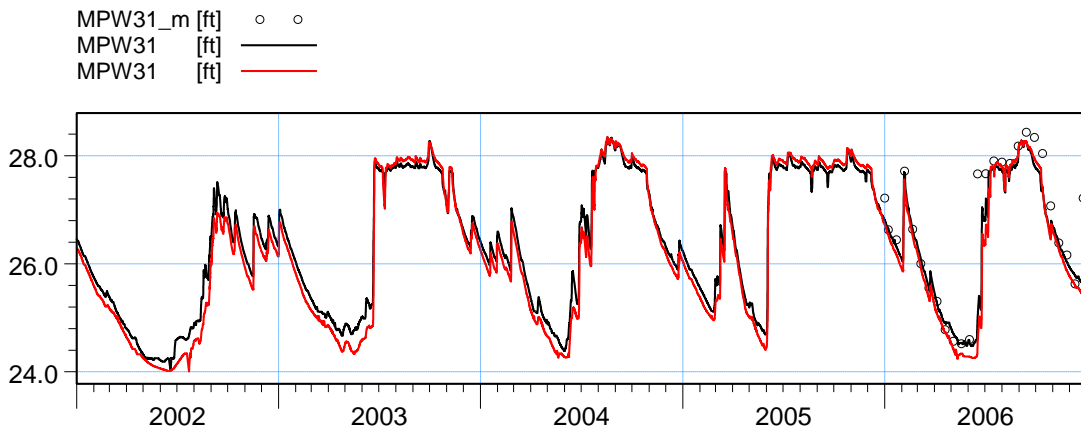


ME=-0.0837851  
 MAE=0.306204  
 RMSE=0.404929  
 STDres=0.396166  
 R(Correlation)=0.961765  
 R2(Nash\_Sutcliffe)=0.703925

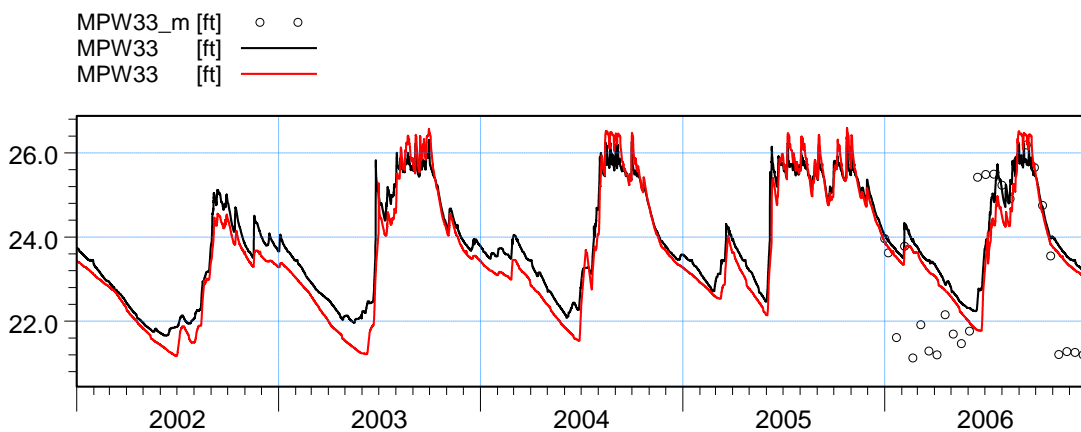


ME=0.100017  
 MAE=0.568356  
 RMSE=0.832724  
 STDres=0.826696  
 R(Correlation)=0.770217  
 R2(Nash\_Sutcliffe)=0.586053

Figure C38. Groundwater elevation at wells MPW29 and MPW30. The black line corresponds to LS ECM result, and red line to the ECM result.

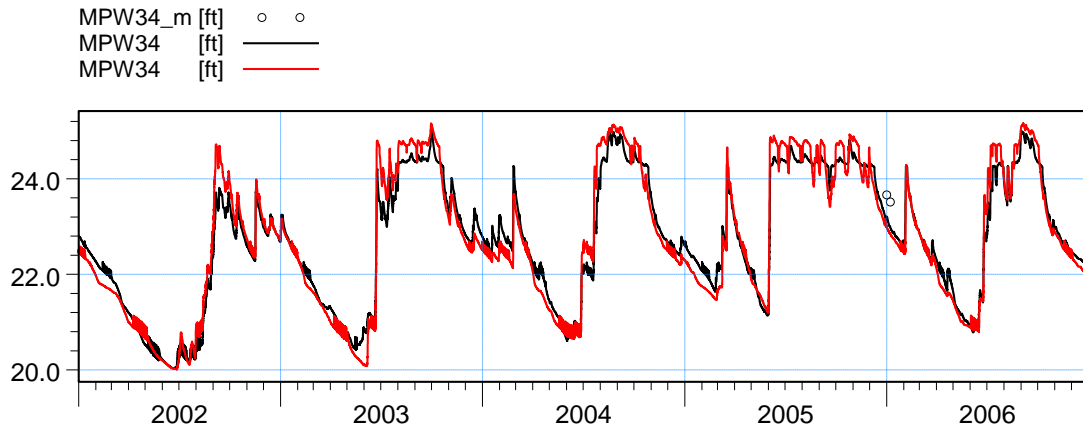


ME=0.252363  
 MAE=0.30479  
 RMSE=0.475714  
 STDres=0.403258  
 R(Correlation)=0.948259  
 R2(Nash\_Sutcliffe)=0.857437

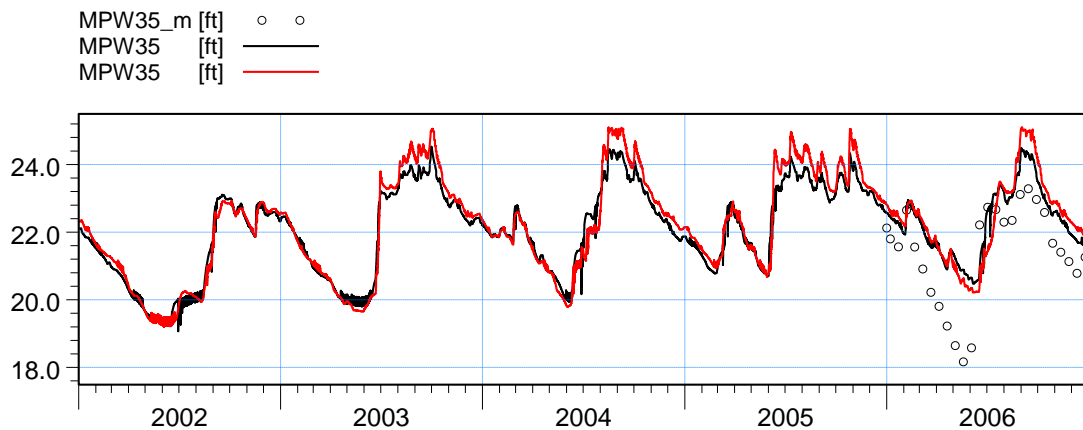


ME=-0.786936  
 MAE=1.20063  
 RMSE=1.50747  
 STDres=1.28576  
 R(Correlation)=0.767788  
 R2(Nash\_Sutcliffe)=0.37259

Figure C39. Groundwater elevation at wells MPW31 and MPW33. The black line corresponds to LS ECM result, and red line to the ECM result.

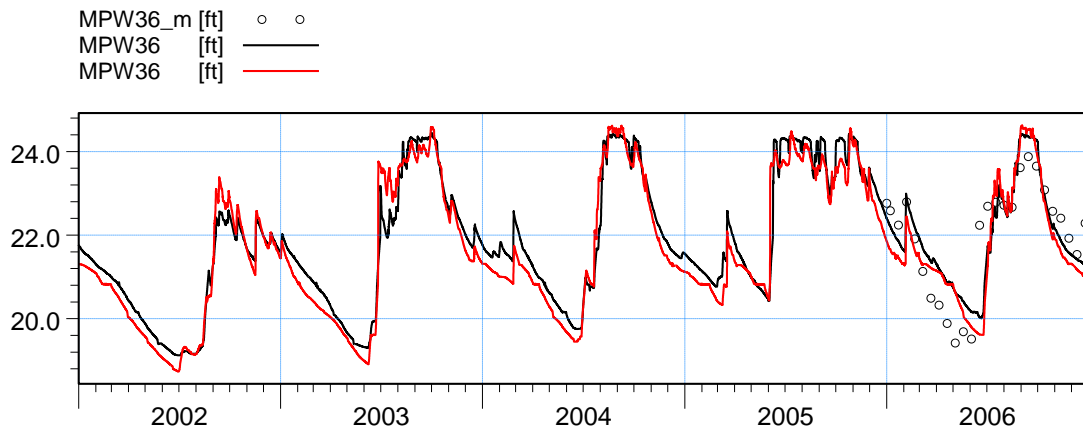


ME=0.484512  
 MAE=0.484512  
 RMSE=0.486411  
 STDres=0.0429319  
 R(Correlation)=0.968054  
 R2(Nash\_Sutcliffe)=-10.135

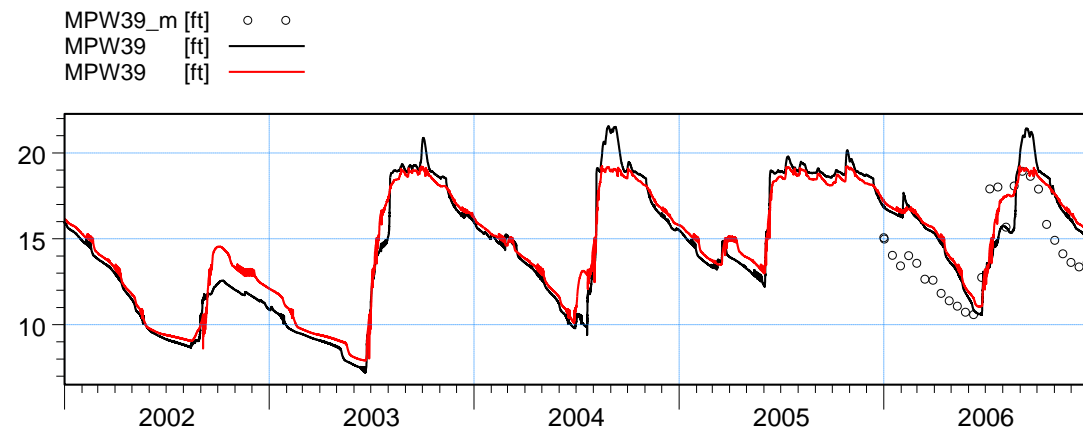


ME=-1.00822  
 MAE=1.05751  
 RMSE=1.24186  
 STDres=0.725048  
 R(Correlation)=0.900097  
 R2(Nash\_Sutcliffe)=0.28692

Figure C40. Groundwater elevation at wells MPW34 and MPW35. The black line corresponds to LS ECM result, and red line to the ECM result.

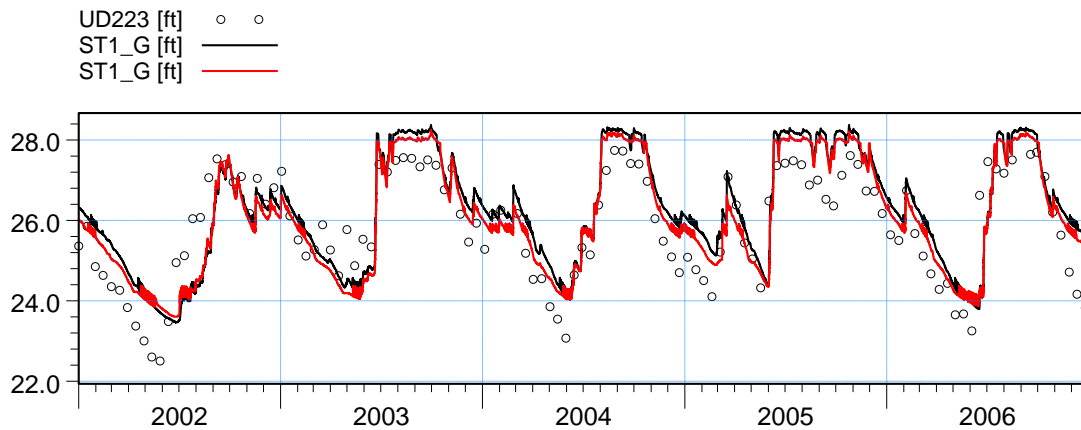


ME=-0.108337  
 MAE=0.528172  
 RMSE=0.658465  
 STDres=0.649492  
 R(Correlation)=0.873067  
 R2(Nash\_Sutcliffe)=0.755623

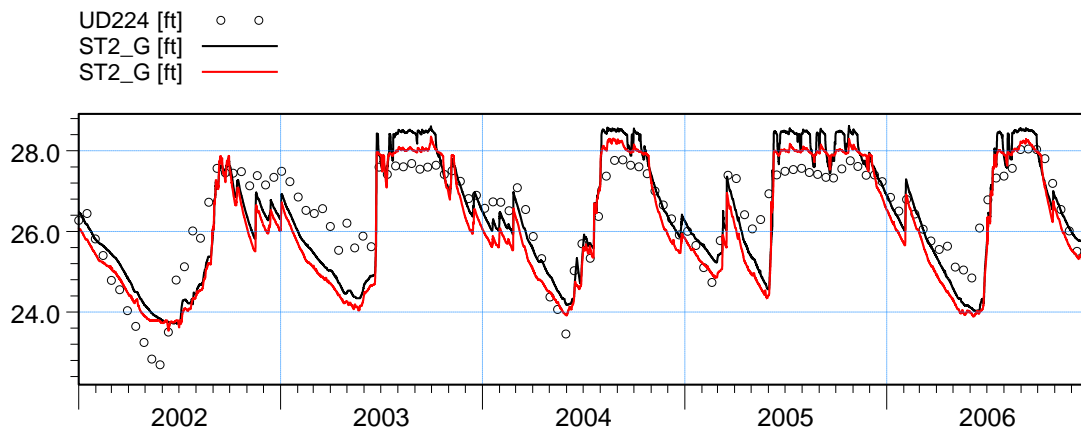


ME=-1.35057  
 MAE=2.34856  
 RMSE=2.51442  
 STDres=2.12092  
 R(Correlation)=0.6394  
 R2(Nash\_Sutcliffe)=-0.0135076

Figure C41. Groundwater elevation at wells MPW36 and MPW39. The black line corresponds to LS ECM result, and red line to the ECM result.

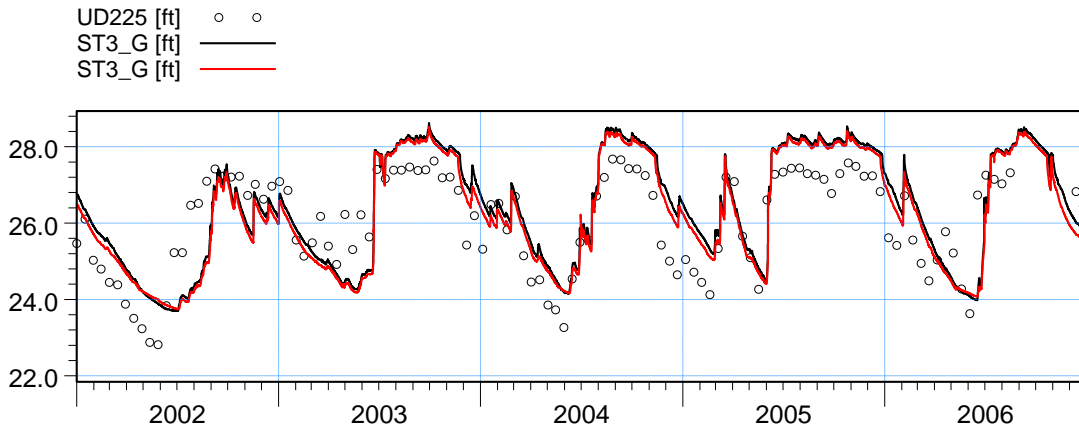


ME=-0.435901  
 MAE=0.725199  
 RMSE=0.846669  
 STDres=0.725837  
 R(Correlation)=0.856511  
 R2(Nash\_Sutcliffe)=0.612885

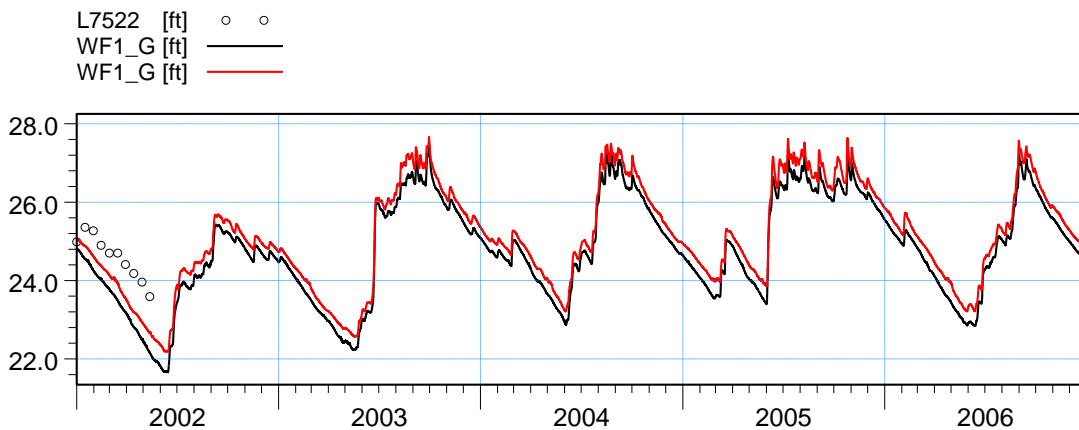


ME=0.0534259  
 MAE=0.607322  
 RMSE=0.729568  
 STDres=0.727609  
 R(Correlation)=0.858897  
 R2(Nash\_Sutcliffe)=0.639309

Figure C42. Groundwater elevation at wells ST1\_G and ST2\_G. The black line corresponds to LS ECM result, and red line to the ECM result.

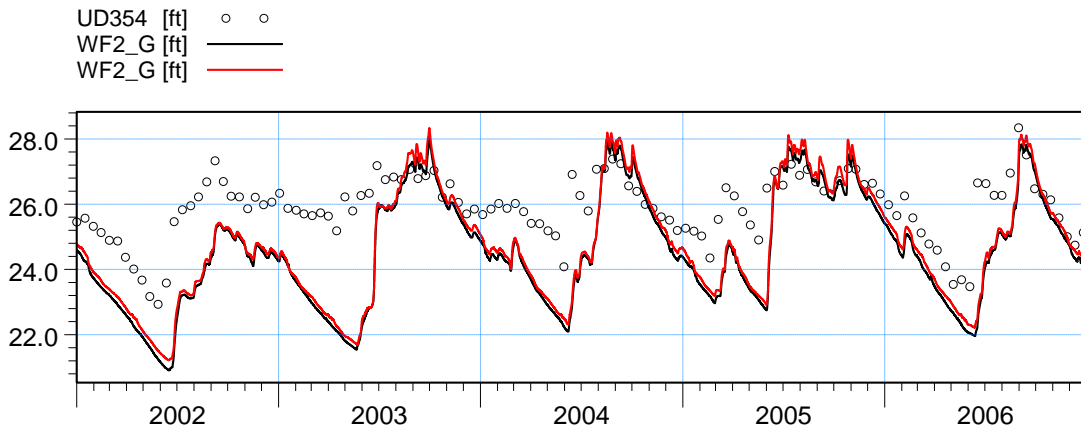


ME=-0.343846  
 MAE=0.798748  
 RMSE=0.916499  
 STDres=0.849553  
 R(Correlation)=0.803928  
 R2(Nash\_Sutcliffe)=0.488001

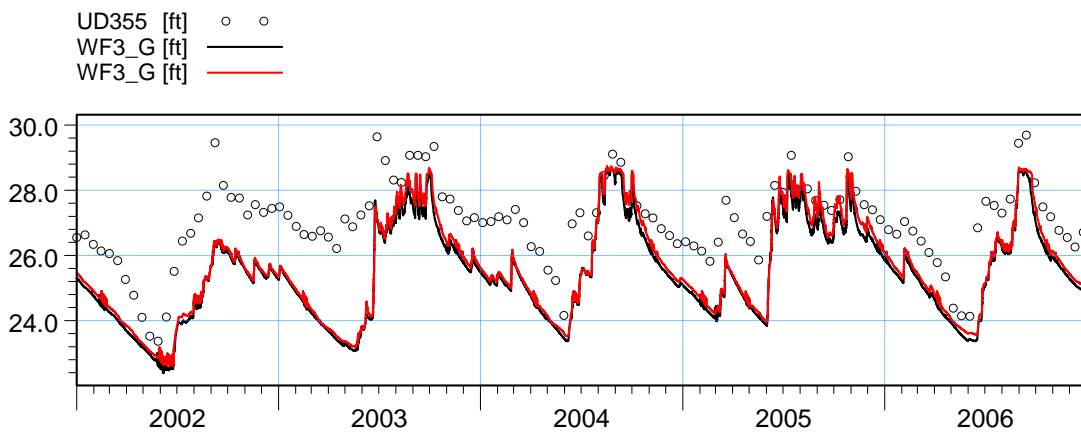


ME=1.05959  
 MAE=1.05959  
 RMSE=1.11813  
 STDres=0.357057  
 R(Correlation)=0.941571  
 R2(Nash\_Sutcliffe)=-3.97131

Figure C43. Groundwater elevation at wells ST3\_G and WF1\_G. The black line corresponds to LS ECM result, and red line to the ECM result.

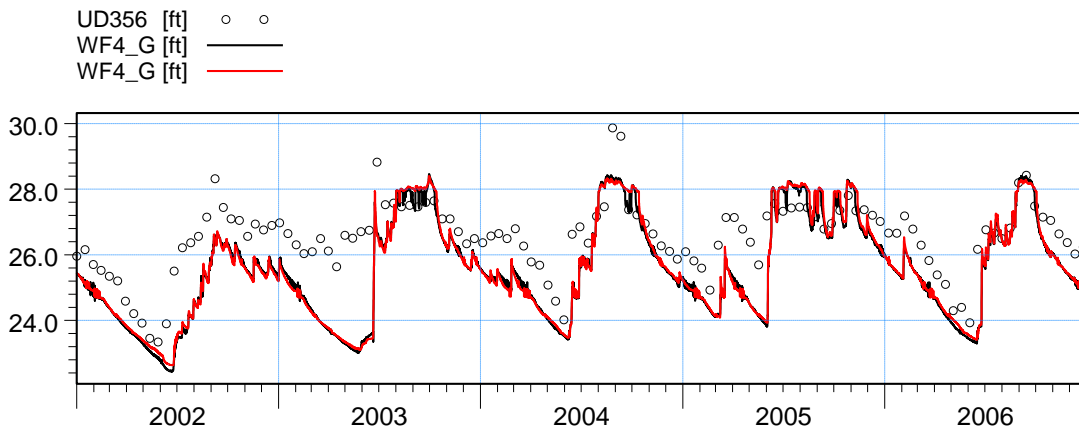


ME=1.31365  
 MAE=1.39004  
 RMSE=1.7284  
 STDres=1.12324  
 R(Correlation)=0.767344  
 R2(Nash\_Sutcliffe)=-2.05325

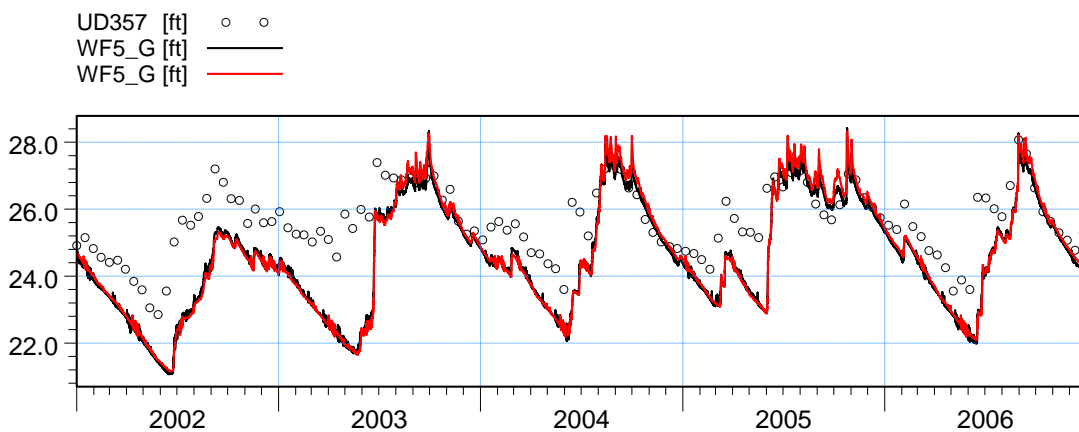


ME=1.54338  
 MAE=1.54524  
 RMSE=1.71127  
 STDres=0.739207  
 R(Correlation)=0.856086  
 R2(Nash\_Sutcliffe)=-0.860367

Figure C44. Groundwater elevation at wells WF2\_G and WF3\_G. The black line corresponds to LS ECM result, and red line to the ECM result.

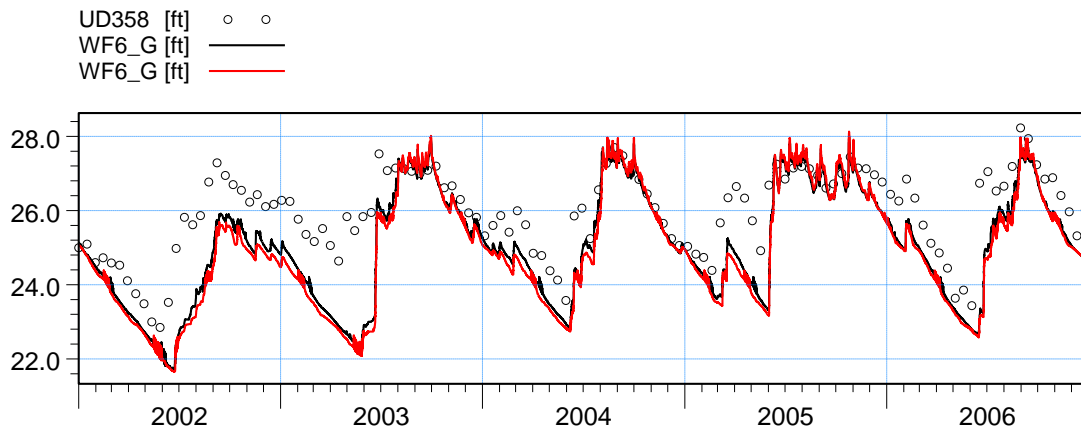


ME=0.946728  
 MAE=1.04964  
 RMSE=1.27143  
 STDres=0.848671  
 R(Correlation)=0.8258  
 R2(Nash\_Sutcliffe)=-0.284437

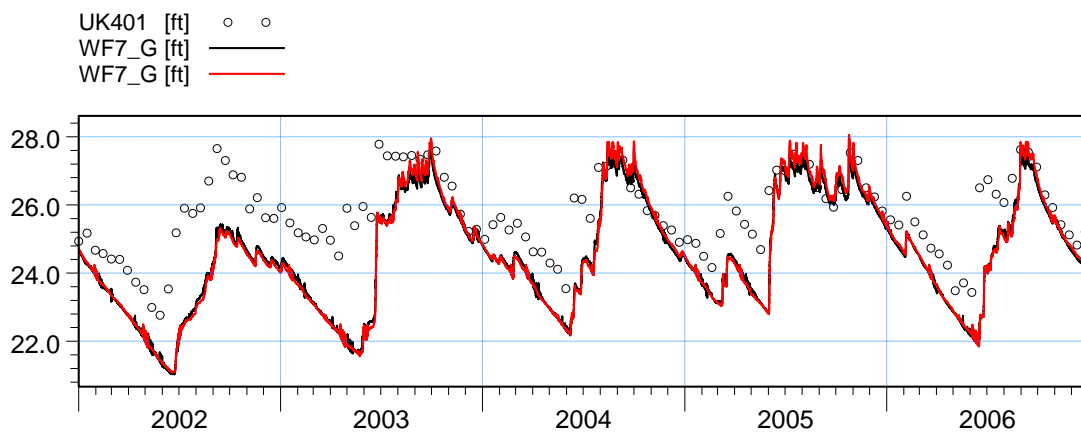


ME=1.02553  
 MAE=1.08209  
 RMSE=1.403  
 STDres=0.957437  
 R(Correlation)=0.809416  
 R2(Nash\_Sutcliffe)=-0.821041

Figure C45. Groundwater elevation at wells WF4\_G and WF5\_G. The black line corresponds to LS ECM result, and red line to the ECM result.

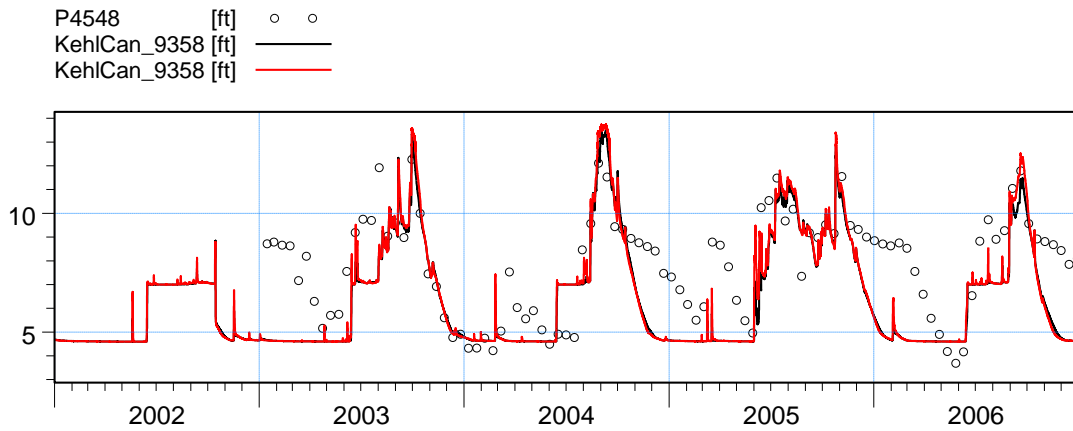


ME=0.872846  
 MAE=0.913201  
 RMSE=1.17882  
 STDres=0.792316  
 R(Correlation)=0.846484  
 R2(Nash\_Sutcliffe)=-0.0597566

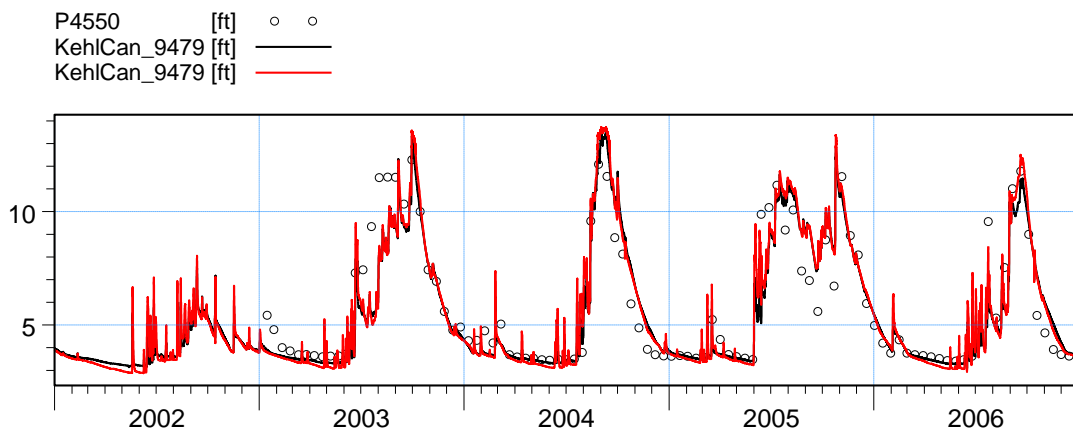


ME=1.16267  
 MAE=1.18116  
 RMSE=1.48744  
 STDres=0.927724  
 R(Correlation)=0.810341  
 R2(Nash\_Sutcliffe)=-0.602172

Figure C46. Groundwater elevation at wells WF6\_G and WF7\_G. The black line corresponds to LS ECM result, and red line to the ECM result.

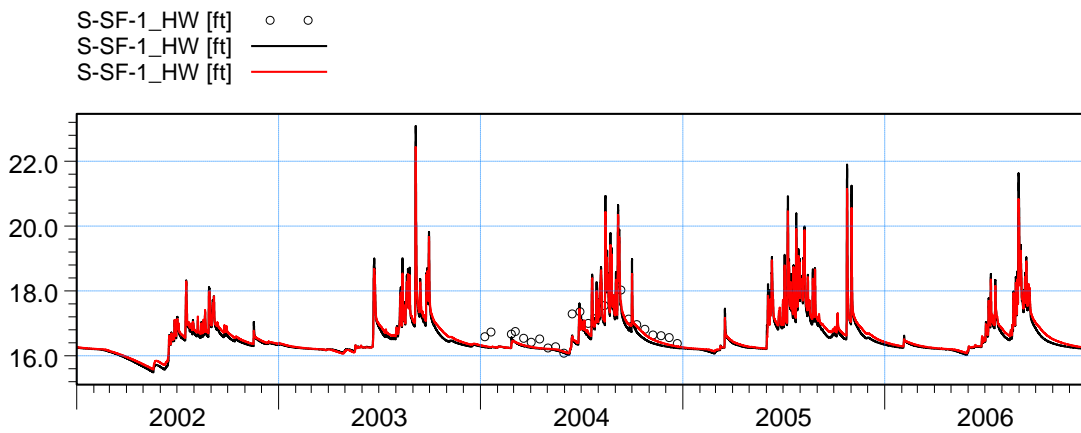


ME=1.33183  
 MAE=1.66753  
 RMSE=2.10264  
 STDres=1.62706  
 R(Correlation)=0.727239  
 R2(Nash\_Sutcliffe)=-0.0250685

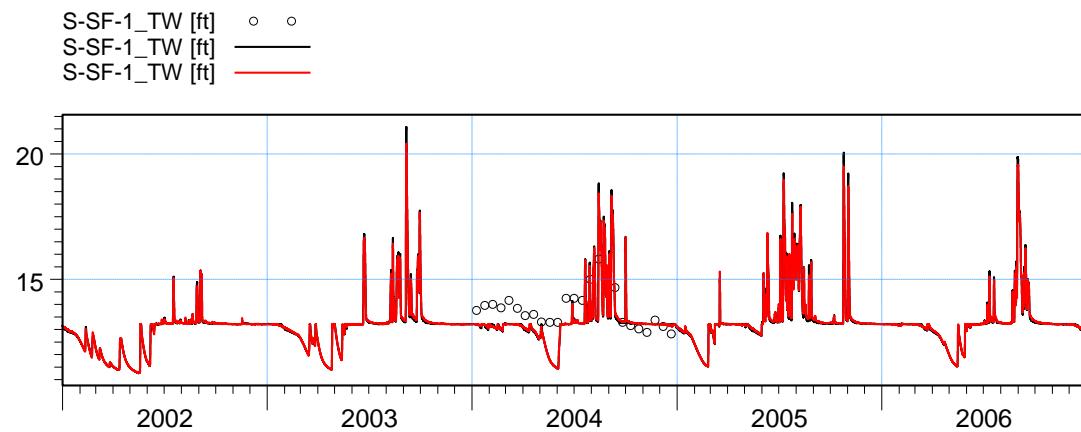


ME=0.100662  
 MAE=0.715742  
 RMSE=1.06258  
 STDres=1.05781  
 R(Correlation)=0.923102  
 R2(Nash\_Sutcliffe)=0.846087

Figure C47. Stage at surface stations KehlCan\_9358 and KehlCan\_9479. The black line corresponds to LS ECM result, and red line to the ECM result.

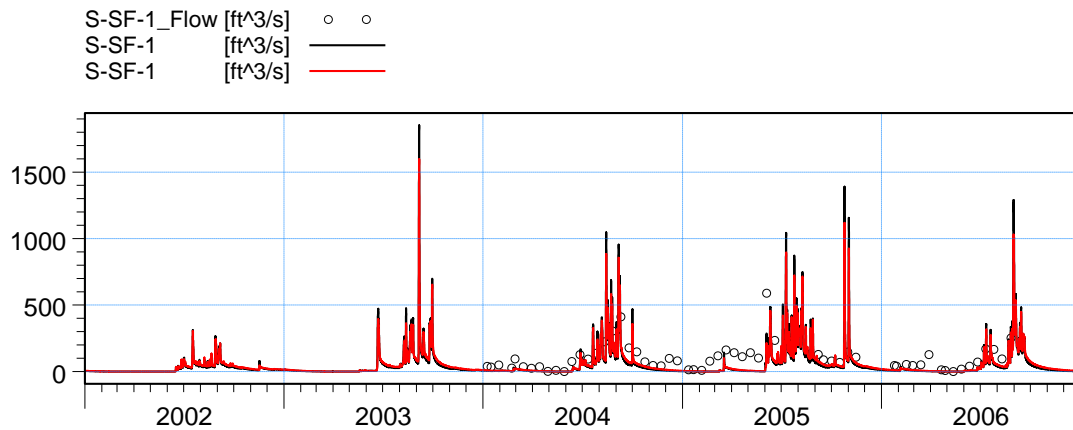


ME=0.232335  
 MAE=0.276605  
 RMSE=0.321776  
 STDres=0.222621  
 R(Correlation)=0.824989  
 R2(Nash\_Sutcliffe)=-0.224969

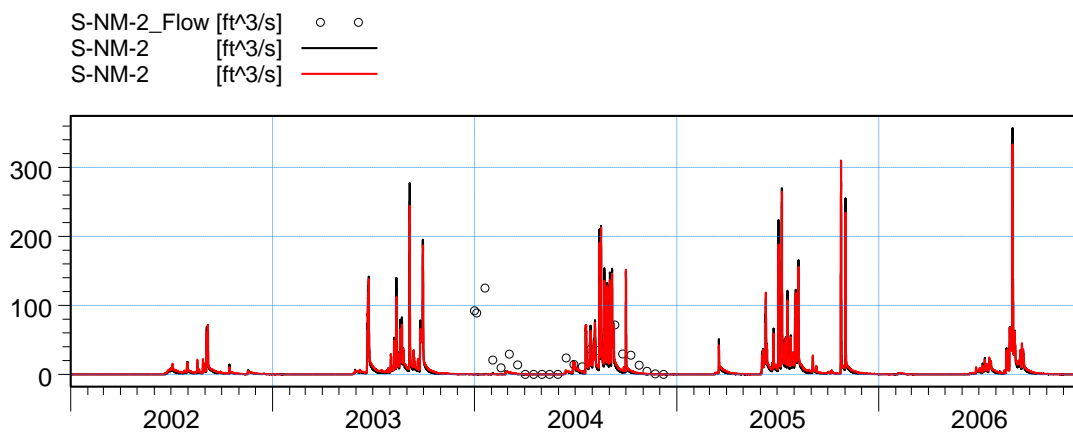


ME=-0.028889  
 MAE=0.305331  
 RMSE=0.479278  
 STDres=0.478407  
 R(Correlation)=0.432064  
 R2(Nash\_Sutcliffe)=-0.26904

Figure C48. Stage at surface stations S-SF-1\_HW and S-SF-1\_TW. The black line corresponds to LS ECM result, and red line to the ECM result.

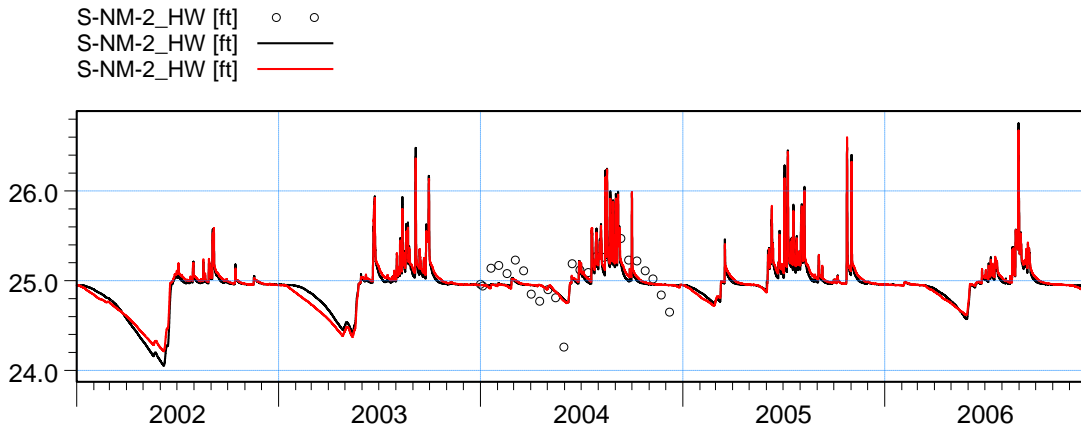


ME=68.4511  
 MAE=78.8351  
 RMSE=107.212  
 STDres=82.5152  
 R(Correlation)=0.705758  
 R2(Nash\_Sutcliffe)=-0.0686276

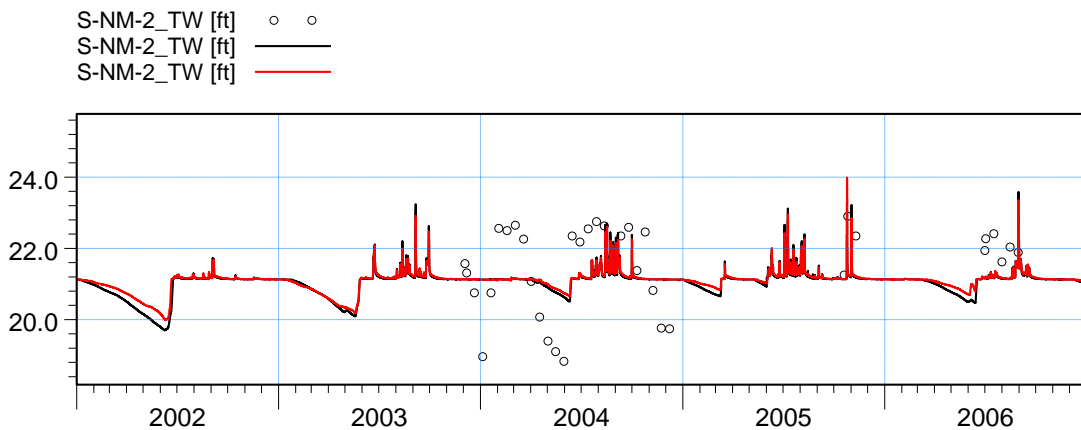


ME=17.2387  
 MAE=21.5971  
 RMSE=36.6679  
 STDres=32.363  
 R(Correlation)=0.414189  
 R2(Nash\_Sutcliffe)=-0.282121

Figure C49. Flow at surface stations S-SF-1 Q and S-NM-2 Q. The black line corresponds to LS ECM result, and red line to the ECM result.

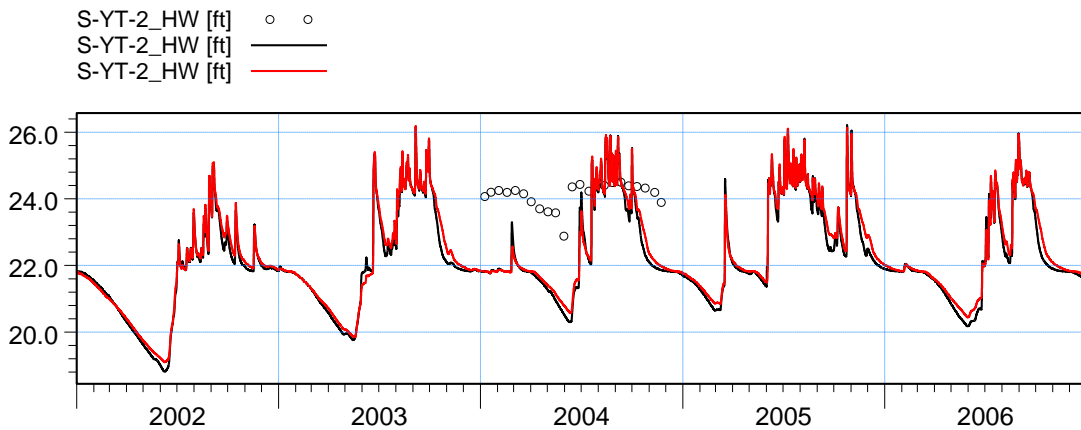


ME=-0.000162317  
 MAE=0.18776  
 RMSE=0.241697  
 STDres=0.241697  
 R(Correlation)=0.606554  
 R2(Nash\_Sutcliffe)=0.362795

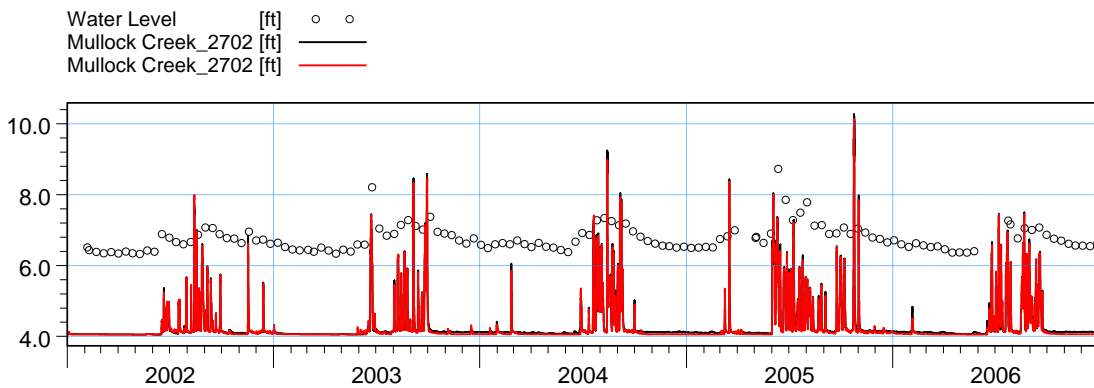


ME=0.804087  
 MAE=1.03932  
 RMSE=1.15916  
 STDres=0.834926  
 R(Correlation)=0.434092  
 R2(Nash\_Sutcliffe)=-0.574237

Figure C50. Stage at surface stations S-NM-2\_HW and S-NM-2\_TW. The black line corresponds to LS ECM result, and red line to the ECM result.



ME=1.63052  
 MAE=1.73938  
 RMSE=1.96508  
 STDres=1.09678  
 R(Correlation)=0.757756  
 R2(Nash\_Sutcliffe)=-21.2045



ME=2.47858  
 MAE=2.4837  
 RMSE=2.51273  
 STDres=0.412822  
 R(Correlation)=0.621358  
 R2(Nash\_Sutcliffe)=-50.603

Figure C51. Stage at surface stations S-YT-2\_HW and Mullock Creek\_2702. The black line corresponds to LS ECM result, and red line to the ECM result.



## ***APPENDIX D. LAND-USE MAPS FOR LOCAL SCALE MODELS***

Additional figures and tables related to the land-use maps for the different local scale models are presented in this appendix.

### **List of Tables**

|  |   |
|--|---|
| Table D1. Number of land-use grid cells inside the local scale domain area in different local scale models. .... | 2 |
| Table D2. Number of land-use grid cells inside the DR/GR Area in different local scale models. ....              | 3 |

### **List of Figures**

|  |    |
|--|----|
| Figure D1. Land-use map in the LS ECM. ....  | 4  |
| Figure D2. Land-use map in the LS FCM1.....  | 5  |
| Figure D3. Areas with land-use map changes in the LS FCM1, with respect to the LS ECM., with respect to the LS ECM. .... | 6  |
| Figure D4. Land-use map in the LS FCM2.....  | 7  |
| Figure D5. Areas with land-use map changes in the LS FCM2, with respect to the LS ECM..                                  | 8  |
| Figure D6. Land-use map in the LS FCM3.....  | 9  |
| Figure D7. Areas with land-use map changes in the LS FCM3, with respect to the LS ECM.                                   | 10 |
| Figure D8. Land-use map in the LS FCM4.....  | 11 |
| Figure D9. Areas with land-use map changes in the LS FCM4, with respect to the LS ECM.                                   | 12 |



| MIKE SHE |                      | Total number of 750-ft grid cells |      |      |      |      |       | Differences with the ECM |      |      |      |       |
|----------|----------------------|-----------------------------------|------|------|------|------|-------|--------------------------|------|------|------|-------|
| code     | Name                 | ECM                               | FCM1 | FCM2 | FCM3 | FCM4 | NSM   | FCM1                     | FCM2 | FCM3 | FCM4 | NSM   |
| 1        | Citrus               | 3222                              | 3098 | 2957 | 2871 | 2889 | 0     | -124                     | -265 | -351 | -333 | -3222 |
| 2        | Pasture              | 2628                              | 2505 | 2450 | 2386 | 2413 | 0     | -123                     | -178 | -242 | -215 | -2628 |
| 3        | Sugar Cane & Sod     | 24                                | 3    | 2    | 3    | 2    | 0     | -21                      | -22  | -21  | -22  | -24   |
| 5        | Truck (Row) Crops    | 1214                              | 1111 | 1074 | 983  | 1044 | 0     | -103                     | -140 | -231 | -170 | -1214 |
| 6        | Golf Course          | 678                               | 678  | 678  | 678  | 678  | 0     | 0                        | 0    | 0    | 0    | -678  |
| 7        | Bare Ground          | 209                               | 171  | 169  | 171  | 169  | 0     | -38                      | -40  | -38  | -40  | -209  |
| 8        | Mesic Flatwood       | 1864                              | 1844 | 1854 | 1850 | 1855 | 10317 | -20                      | -10  | -14  | -9   | 8453  |
| 9        | Mesic Hammock        | 182                               | 182  | 179  | 182  | 179  | 136   | 0                        | -3   | 0    | -3   | -46   |
| 10       | Xeric Flatwood       | 0                                 | 0    | 0    | 0    | 0    | 227   | 0                        | 0    | 0    | 0    | 227   |
| 11       | Xeric Hammock        | 0                                 | 0    | 0    | 0    | 0    | 173   | 0                        | 0    | 0    | 0    | 173   |
| 12       | Hydric Flatwood      | 2899                              | 2831 | 2822 | 2851 | 2851 | 6366  | -68                      | -77  | -48  | -48  | 3467  |
| 13       | Hydric Hammock       | 110                               | 110  | 110  | 110  | 110  | 1074  | 0                        | 0    | 0    | 0    | 964   |
| 14       | Wet Prairie          | 324                               | 316  | 312  | 314  | 312  | 1832  | -8                       | -12  | -10  | -12  | 1508  |
| 16       | Marsh                | 2486                              | 2474 | 2469 | 2462 | 2465 | 1384  | -12                      | -17  | -24  | -21  | -1102 |
| 17       | Cypress              | 2075                              | 2066 | 2055 | 2058 | 2055 | 4395  | -9                       | -20  | -17  | -20  | 2320  |
| 18       | Swamp Forest         | 1011                              | 1007 | 1000 | 1002 | 1003 | 1276  | 195                      | 318  | 393  | 492  | 265   |
| 19       | Mangrove             | 115                               | 115  | 115  | 115  | 115  | 105   | 0                        | 0    | 0    | 0    | -10   |
| 20       | Water                | 798                               | 798  | 798  | 798  | 798  | 147   | 347                      | 488  | 612  | 420  | -651  |
| 41       | Urban Low Density    | 3956                              | 3955 | 3950 | 3955 | 3953 | 0     | -1                       | -6   | -1   | -3   | -3956 |
| 42       | Urban Medium Density | 1745                              | 1744 | 1744 | 1744 | 1744 | 0     | 68                       | 68   | 68   | 68   | -1745 |
| 43       | Urban High Density   | 1924                              | 1841 | 1840 | 1848 | 1840 | 0     | -83                      | -84  | -76  | -84  | -1924 |

Table D1. Number of land-use grid cells inside the local scale domain area in different local scale models.



| MIKE SHE |                      | Total number of 750-ft grid cells |      |      |      |      |      | Differences with the ECM |      |      |      |      |
|----------|----------------------|-----------------------------------|------|------|------|------|------|--------------------------|------|------|------|------|
| code     | Name                 | ECM                               | FCM1 | FCM2 | FCM3 | FCM4 | NSM  | FCM1                     | FCM2 | FCM3 | FCM4 | NSM  |
| 1        | Citrus               | 668                               | 544  | 403  | 317  | 335  | 0    | -124                     | -265 | -351 | -333 | -668 |
| 2        | Pasture              | 946                               | 833  | 778  | 714  | 741  | 0    | -113                     | -168 | -232 | -205 | -946 |
| 3        | Sugar Cane & Sod     | 24                                | 3    | 2    | 3    | 2    | 0    | -21                      | -22  | -21  | -22  | -24  |
| 5        | Truck (Row) Crops    | 540                               | 437  | 400  | 309  | 370  | 0    | -103                     | -140 | -231 | -170 | -540 |
| 6        | Golf Course          | 11                                | 11   | 11   | 11   | 11   | 0    | 0                        | 0    | 0    | 0    | -11  |
| 7        | Bare Ground          | 58                                | 25   | 23   | 25   | 23   | 0    | -33                      | -35  | -33  | -35  | -58  |
| 8        | Mesic Flatwood       | 250                               | 246  | 243  | 239  | 244  | 895  | -4                       | -7   | -11  | -6   | 645  |
| 9        | Mesic Hammock        | 5                                 | 5    | 2    | 5    | 2    | 0    | 0                        | -3   | 0    | -3   | -5   |
| 10       | Xeric Flatwood       | 0                                 | 0    | 0    | 0    | 0    | 0    | 0                        | 0    | 0    | 0    | 0    |
| 11       | Xeric Hammock        | 0                                 | 0    | 0    | 0    | 0    | 0    | 0                        | 0    | 0    | 0    | 0    |
| 12       | Hydric Flatwood      | 1827                              | 1769 | 1753 | 1782 | 1782 | 1861 | -58                      | -74  | -45  | -45  | 34   |
| 13       | Hydric Hammock       | 9                                 | 9    | 9    | 9    | 9    | 851  | 0                        | 0    | 0    | 0    | 842  |
| 14       | Wet Prairie          | 169                               | 161  | 157  | 159  | 157  | 0    | -8                       | -12  | -10  | -12  | -169 |
| 16       | Marsh                | 262                               | 253  | 248  | 241  | 244  | 0    | -9                       | -14  | -21  | -18  | -262 |
| 17       | Cypress              | 813                               | 805  | 794  | 797  | 794  | 2355 | -8                       | -19  | -16  | -19  | 1542 |
| 18       | Swamp Forest         | 206                               | 401  | 524  | 599  | 698  | 443  | 195                      | 318  | 393  | 492  | 237  |
| 19       | Mangrove             | 0                                 | 0    | 0    | 0    | 0    | 0    | 0                        | 0    | 0    | 0    | 0    |
| 20       | Water                | 340                               | 654  | 815  | 939  | 747  | 0    | 314                      | 475  | 599  | 407  | -340 |
| 41       | Urban Low Density    | 108                               | 107  | 102  | 107  | 105  | 0    | -1                       | -6   | -1   | -3   | -108 |
| 42       | Urban Medium Density | 9                                 | 65   | 65   | 65   | 65   | 0    | 56                       | 56   | 56   | 56   | -9   |
| 43       | Urban High Density   | 160                               | 77   | 76   | 84   | 76   | 0    | -83                      | -84  | -76  | -84  | -160 |

Table D2. Number of land-use grid cells inside the DR/GR Area in different local scale models.

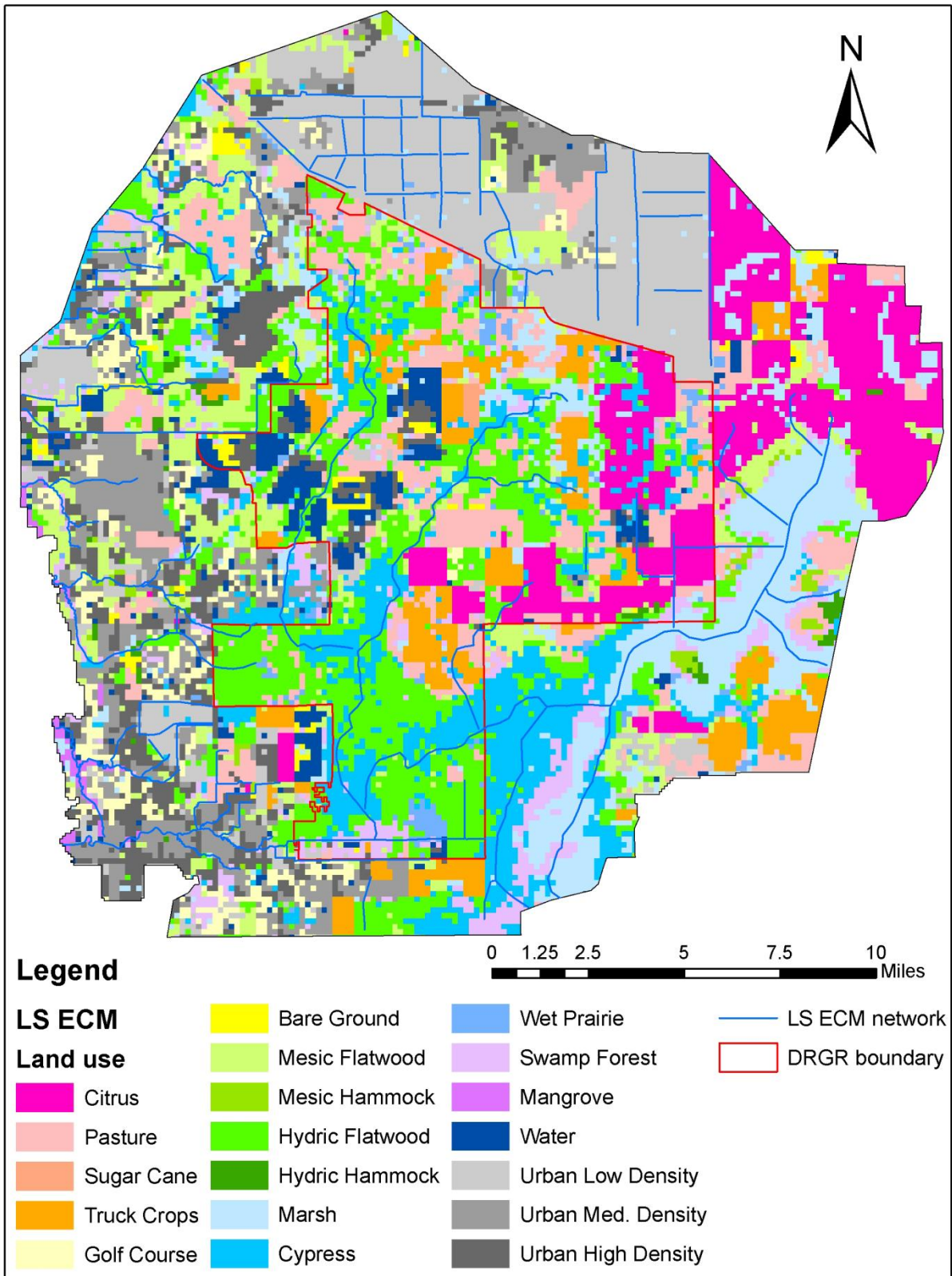


Figure D1. Land-use map in the LS ECM.

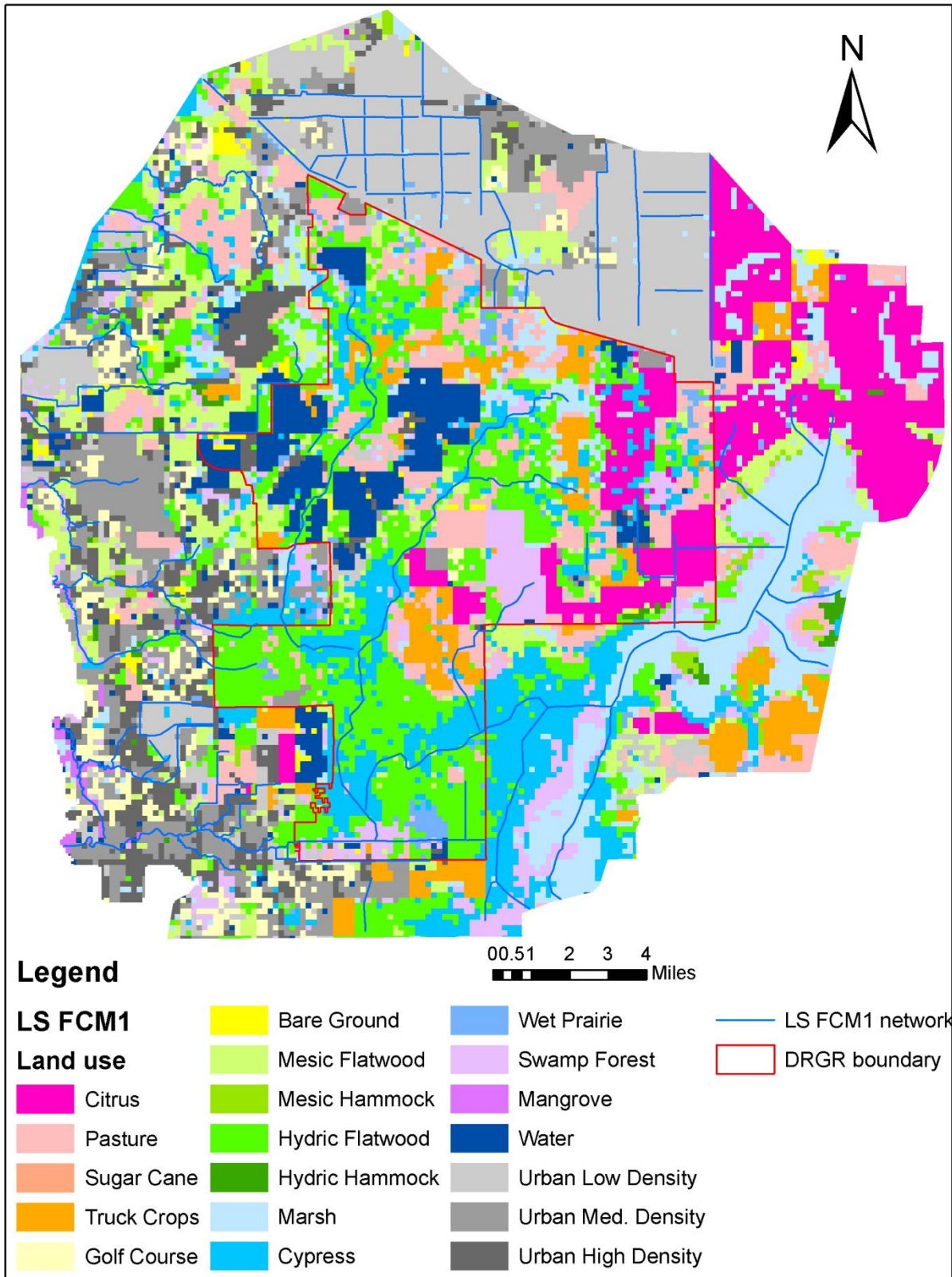


Figure D2. Land-use map in the LS FCM1.

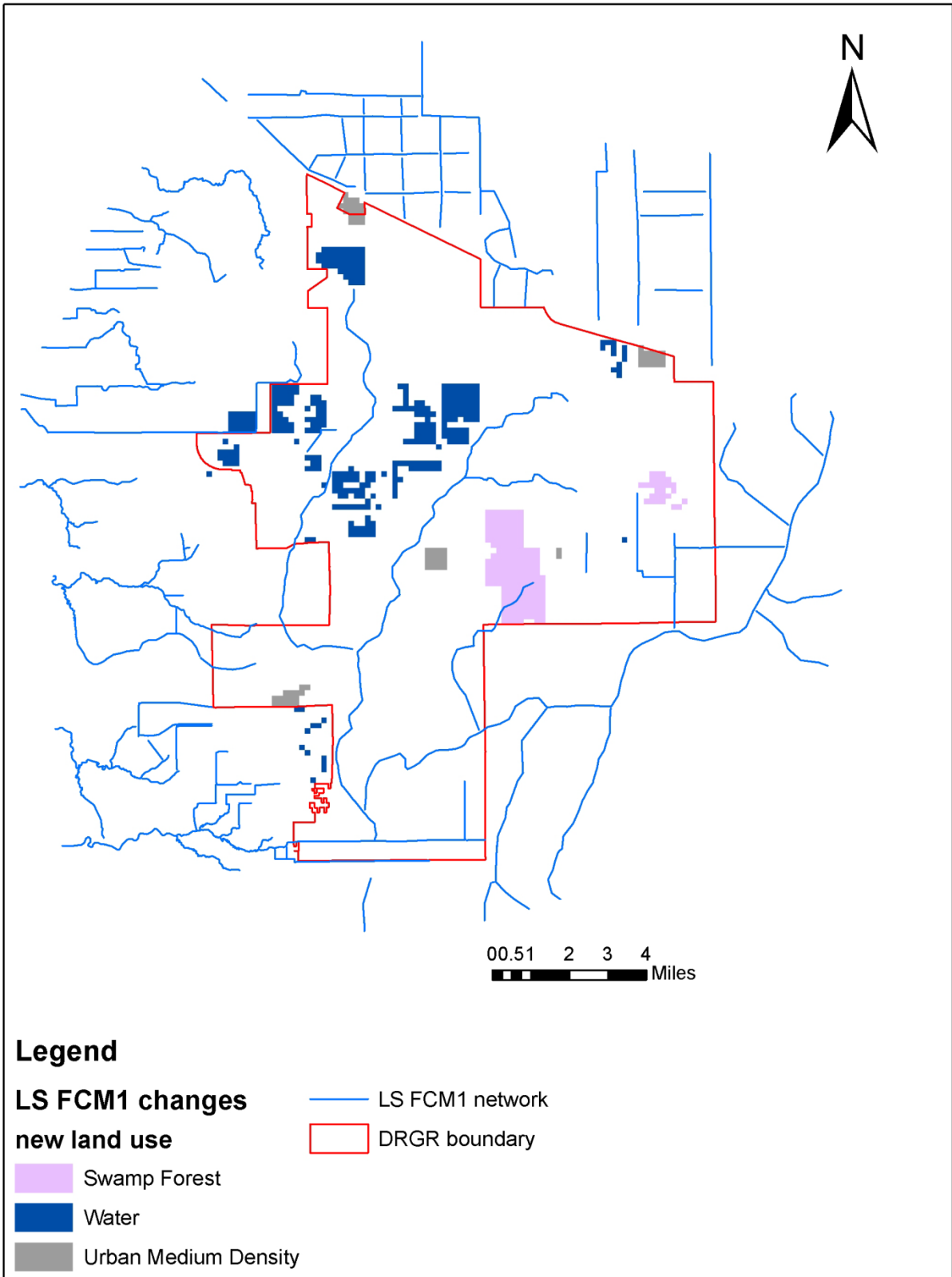


Figure D3. Areas with land-use map changes in the LS FCM1, with respect to the LS ECM., with respect to the LS ECM.

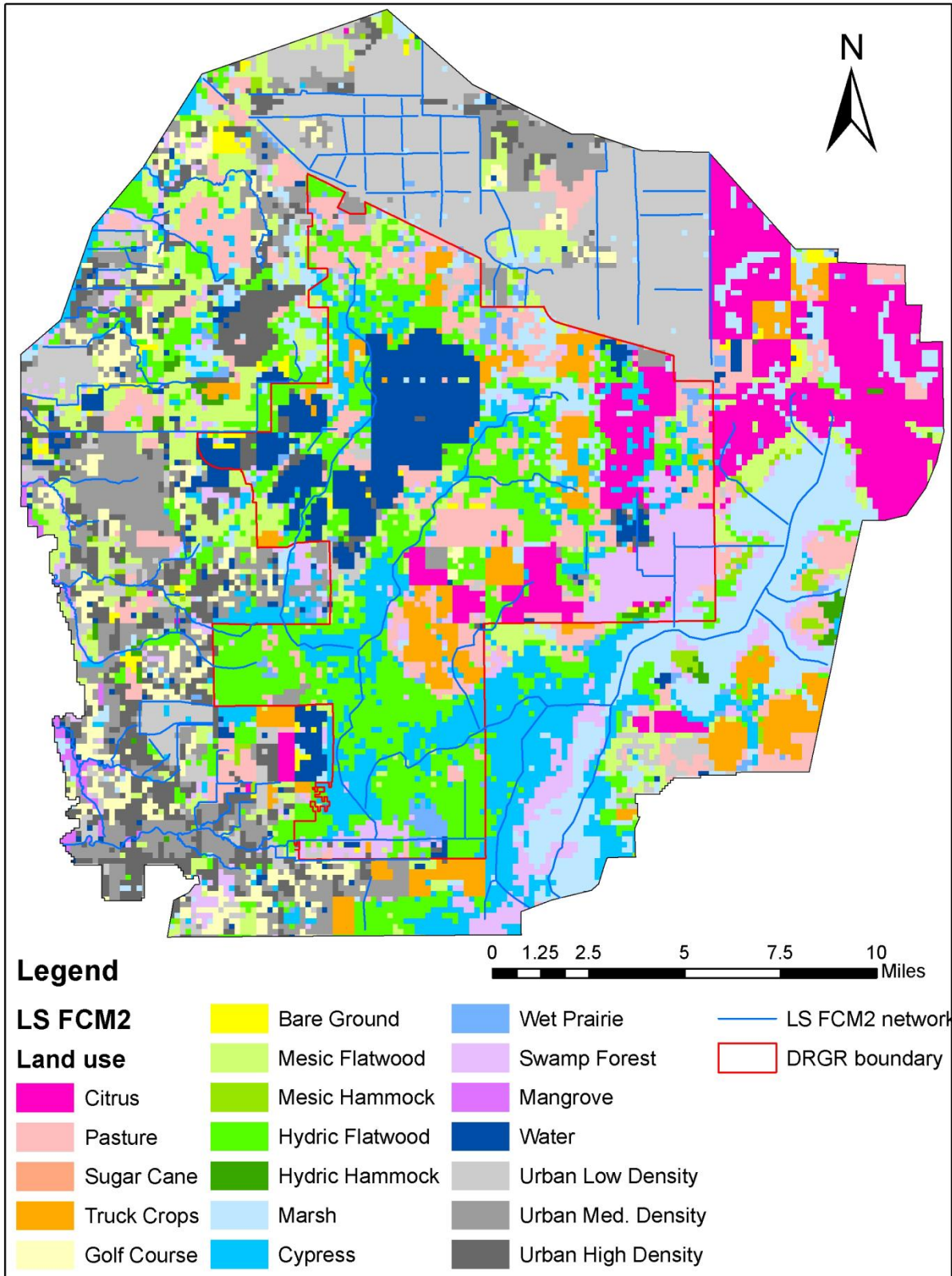


Figure D4. Land-use map in the LS FCM2.

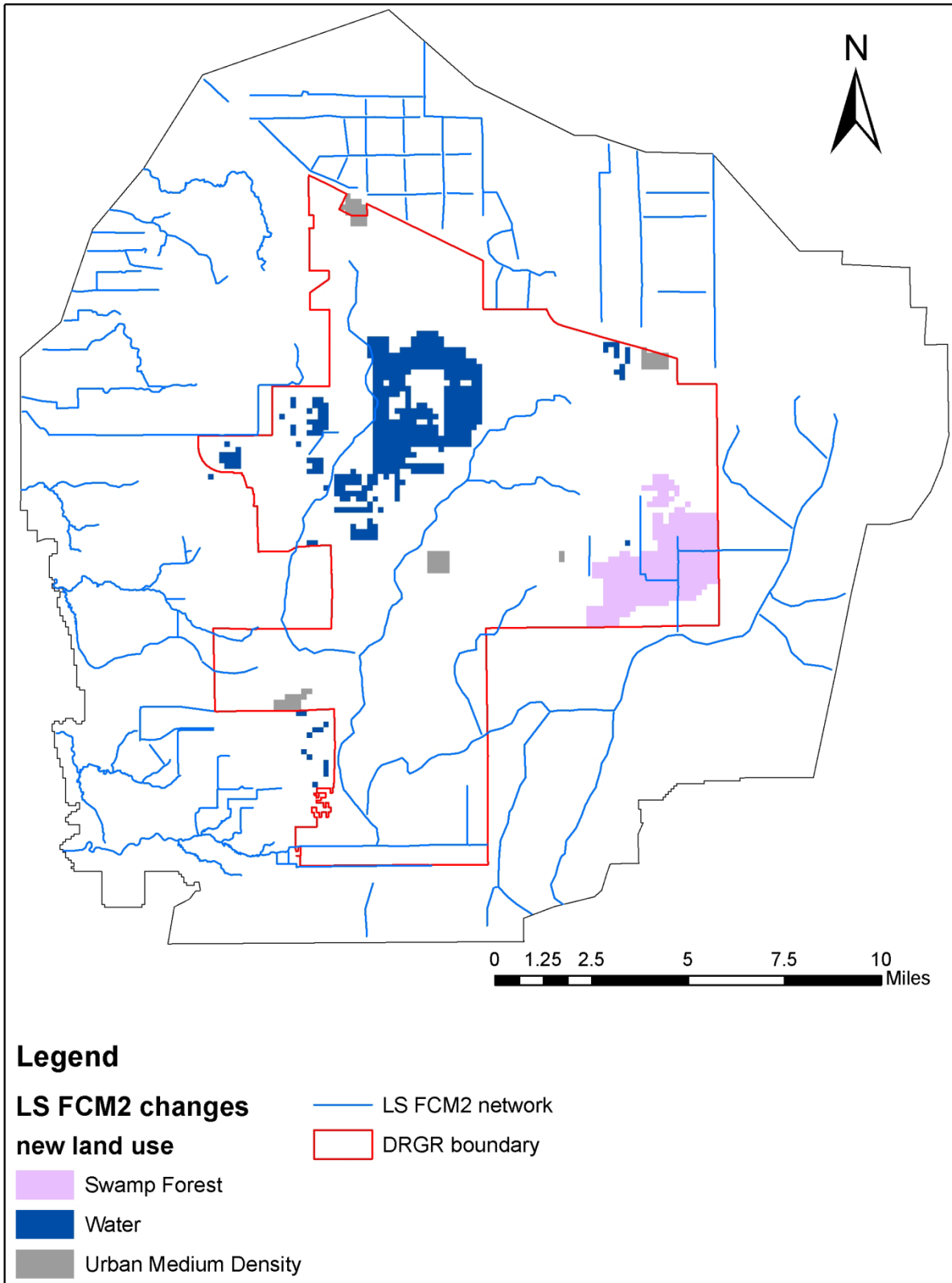


Figure D5. Areas with land-use map changes in the LS FCM2, with respect to the LS ECM.

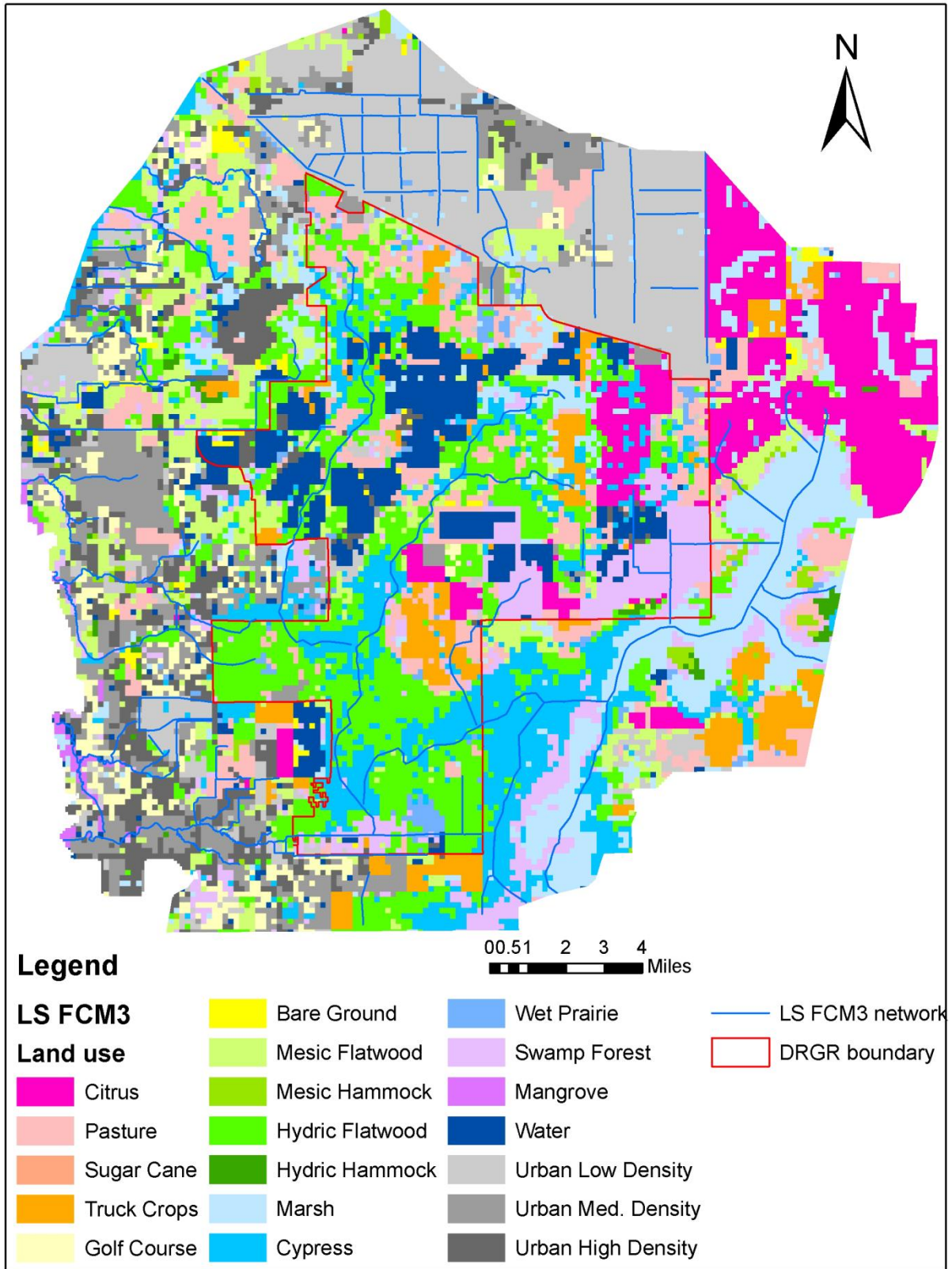


Figure D6. Land-use map in the LS FCM3.

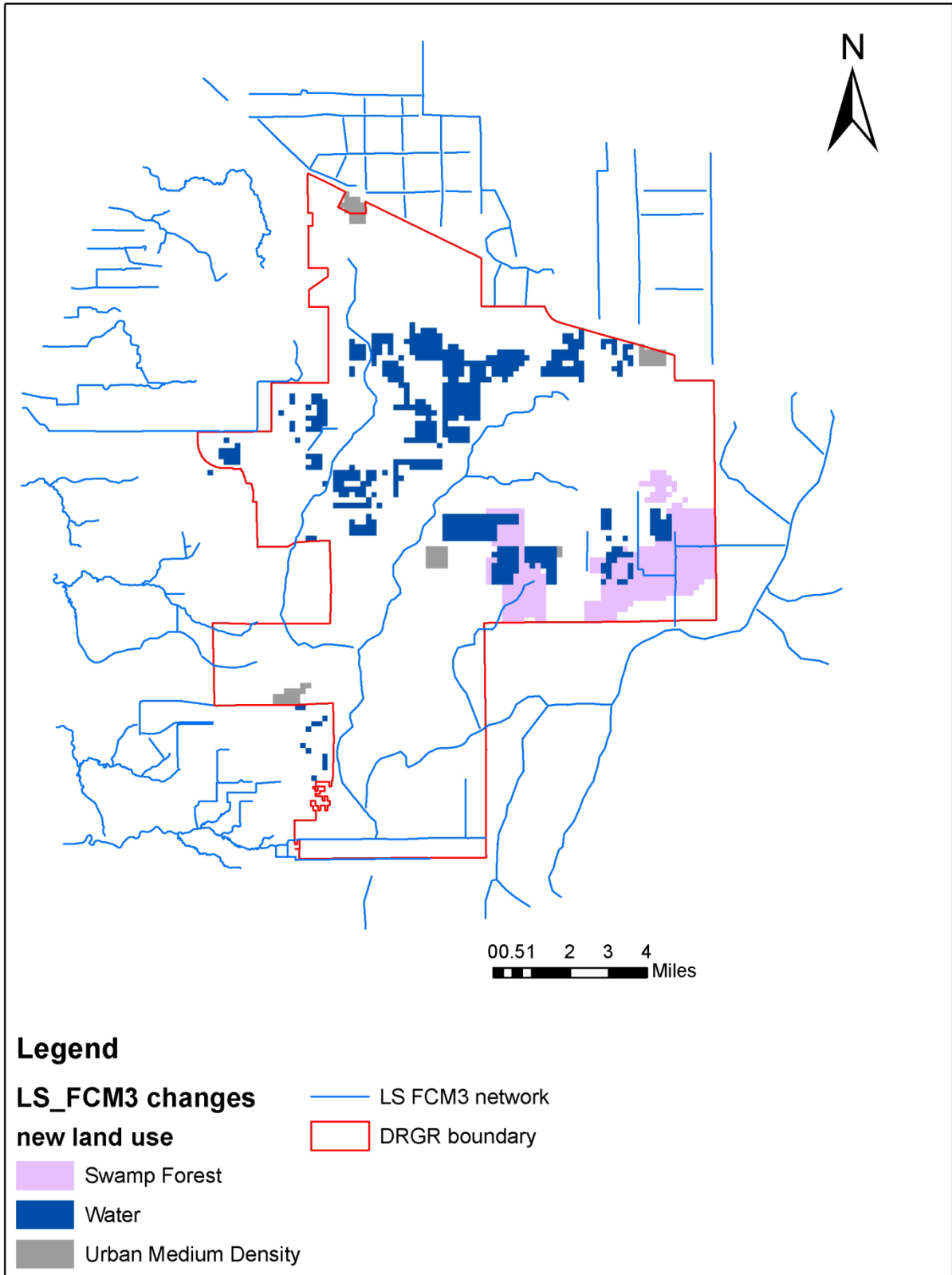


Figure D7. Areas with land-use map changes in the LS FCM3, with respect to the LS ECM.

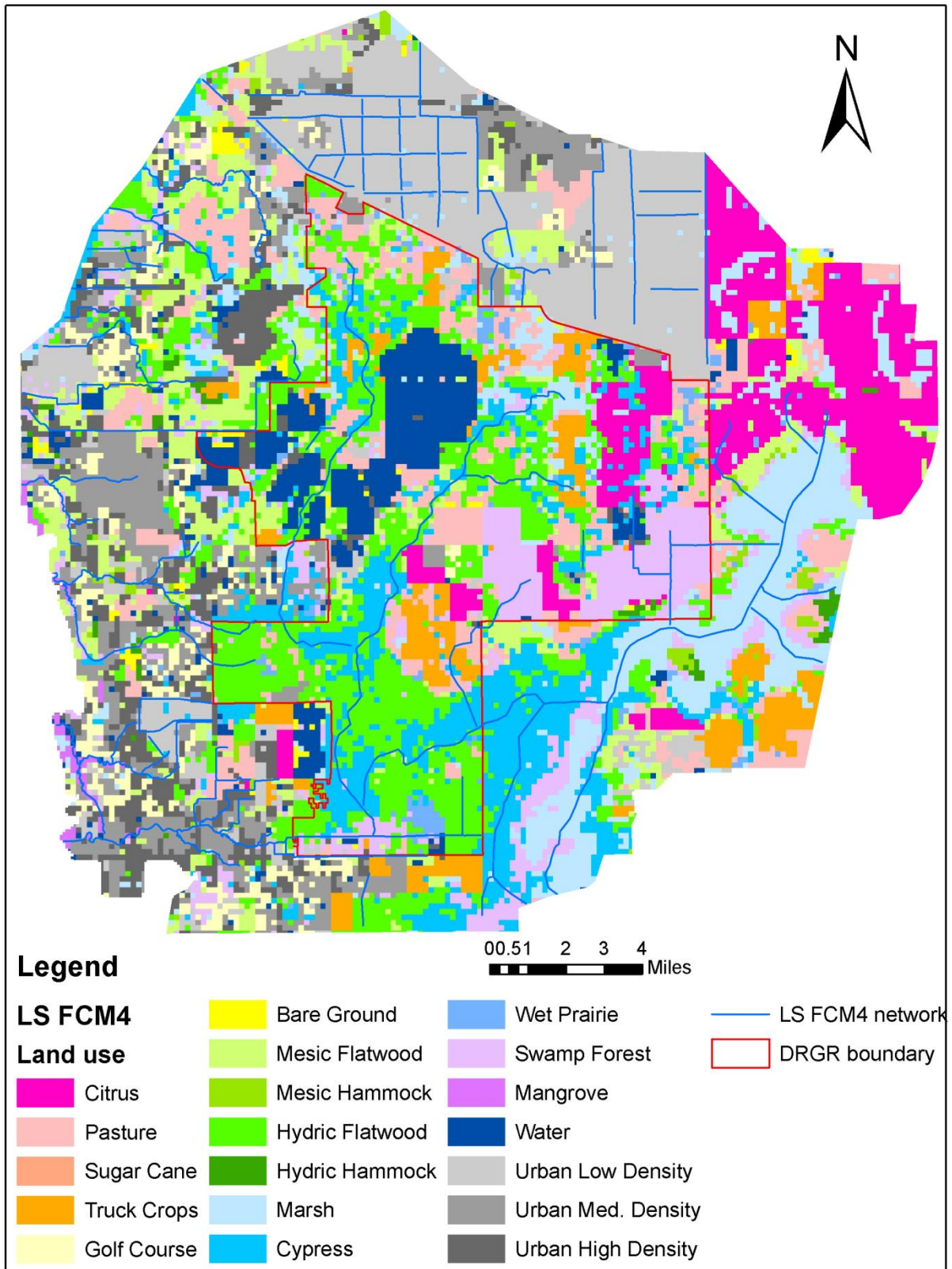


Figure D8. Land-use map in the LS FCM4.

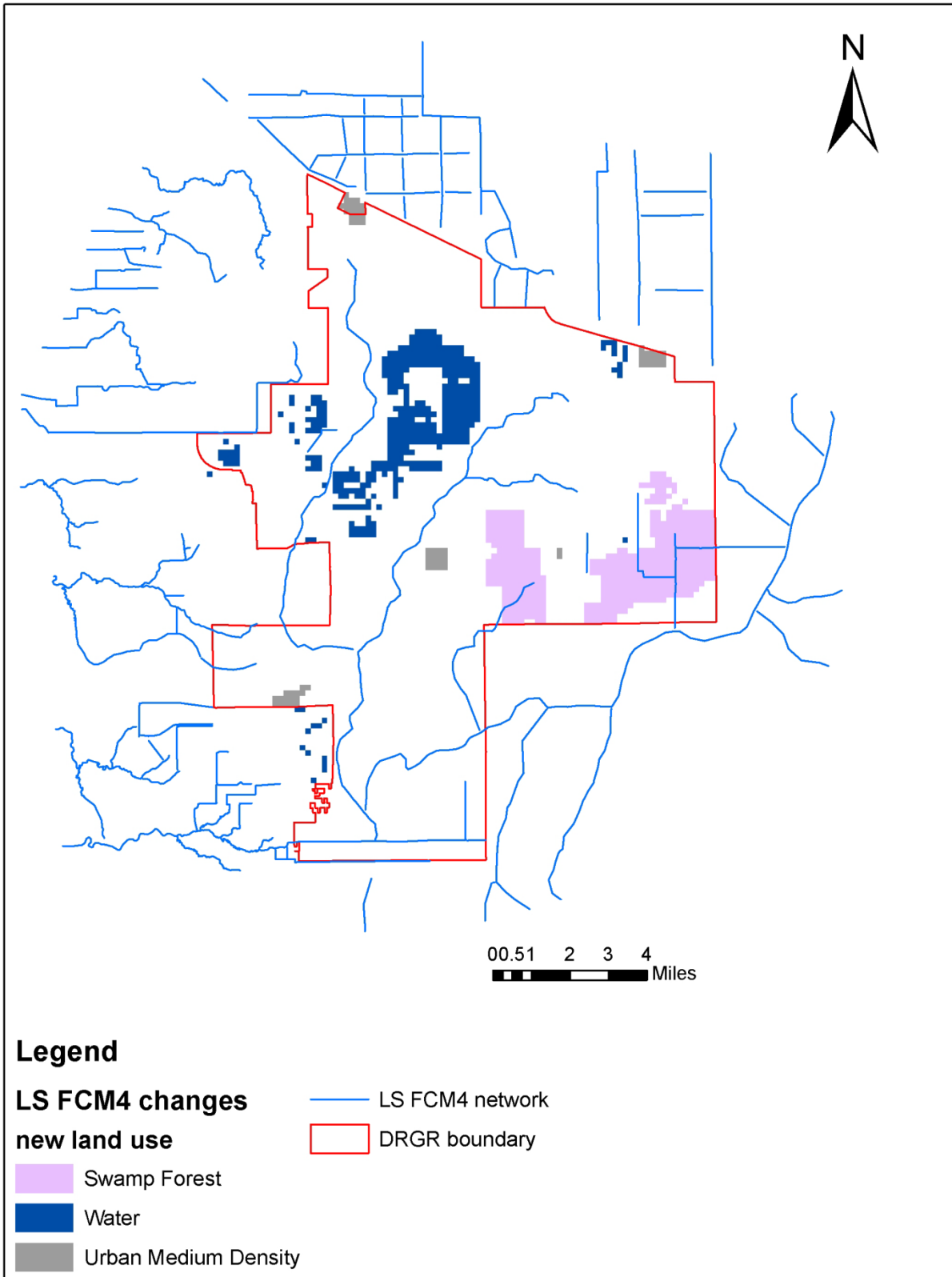


Figure D9. Areas with land-use map changes in the LS FCM4, with respect to the LS ECM.

## Appendix E. Open Water Evaporation around the DR/GR Area

This appendix contains a few comparisons between the spatially distributed ET data available from the USGS (<http://hdwp.er.usgs.gov/>) and the ET data from other sources. The objective is to find the best ET data to be applied as evaporation in open water bodies located in the DR/GR Area.

The spatially distributed ET data from USGS was obtained by using solar radiation obtained from Geostationary Operational Environmental Satellites (GOES) [Jacobs et al., 2008]. Reference ET (RET) and a potential ET (PET) were estimated at a 2 km spatial scale and a daily time scale from 1995 to 2004 for the entire state of Florida. The PET calculation used the Priestley-Taylor model that requires incoming solar radiation, air temperature and relative humidity data. Two different constant albedo values are used for land (0.149) and for water (0.062). Inland pixels were identified as water if 75% or more of the pixel contained water. RET calculation is based on the Penman-Monteith equation [Allen et al., 1998], considering short crop or grass reference on a daily basis. Besides incoming solar radiation, air temperature and relative humidity, this method also requires the wind speed.

The ET data from station FPWX (DBHYDRO key OH520) is compared to the USGS data. This station is located in Lee County, in the western boundary of the DR/GR area, and covers most of the DR/GR model domain area in the Thiessen polygon approach used in the previous model version. The ET rate calculation is based on total radiation multiplied by a constant coefficient established by W. Abteew at SFWMD [W. Qinglong, SFWMD, personal communication]. This simple method has been recommended when limited data is available, but it has been found less accurate than the Penman-Monteith method [Abteew, 1996]. **Figure E1** shows the location of this station regarding the distributed ET grid.

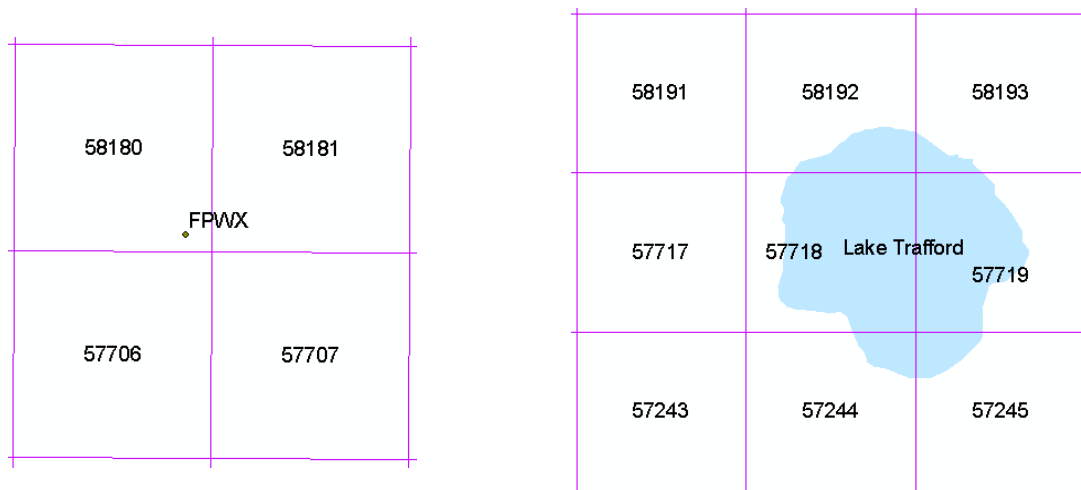


**Figure E1.** Distributed ET grid around station FPWX and Lake Trafford.

The pan evaporation data from station BCBNAPLE\_E (DBHYDRO key DJ227) is used also in the comparison. According to R. Woods [SFWMD, personal communication], this station uses a standard NWS Class A evaporation pan, which is made of unpainted galvanized steel or stainless steel, is 4 feet in diameter by 10 inches deep, and sits on a raised wood frame exposed beneath to let air circulate. The pan is filled to a depth of 8 inches, and is refilled when the depth falls to 7 inches. Water surface level is measured daily with a hook gauge in a stilling well. Evaporation is computed as the difference between observed levels, adjusted for any precipitation measured in a standard rain gauge. Alternatively, water is added each day to bring the level up to a fixed point in the stilling well. This method assures proper water level at all times. Depending on the water level measurement method and how water is supplied to the pan, the measurement accuracy can be varied. The ET data reported is the raw ET data measured at the pan, and there is no (pan) coefficient involved to convert to lake evaporation (LE). This coefficient usually varies between 0.6 and 0.8. A pan coefficient of 0.75 has been used for the estimation of Lake Okeechobee evaporation [Chandra Pathak, SFWMD, personal communication].

The lake evaporation was measured previously in Florida by energy budget methods [Sacks et al., 1994], [Lee and Swancar, 1997], [Swancar et al., 2000]. Here, the lake evaporation reported by Swancar et al. [2000] at Lake Starr (Polk County, FL) and the lake evaporation data at Reedy Lake (Orange County, FL) delivered by D. Sumner at USGS are also compared to the USGS data. **Figure E2** shows the positions of those two lakes regarding the distributed ET grid.

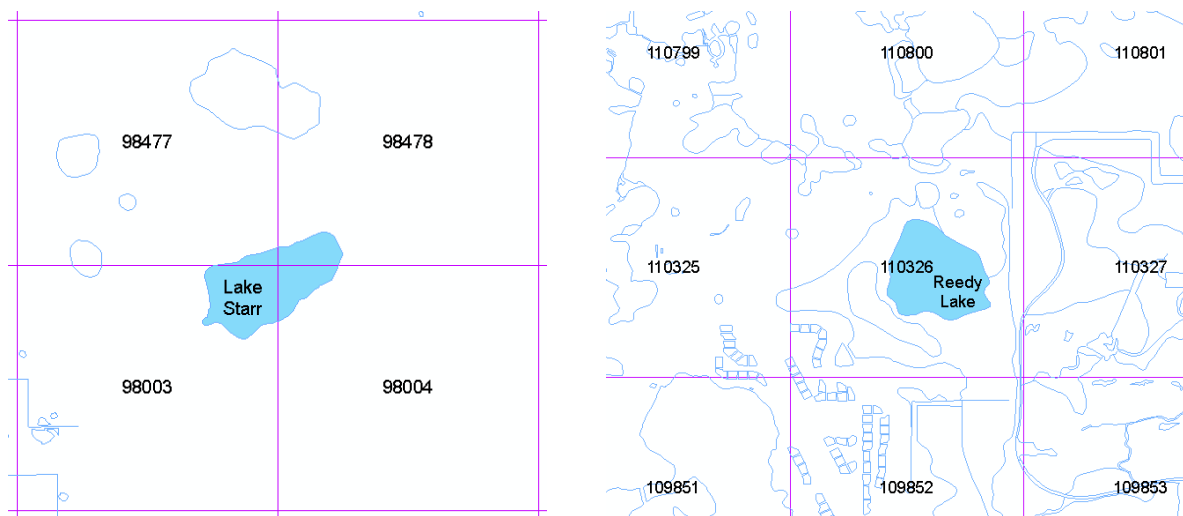


**Figure E2.** Distributed ET grid around Lake Starr and Reedy Lake.

Finally, a comparison between the PET estimated by the USGS in grid cells marked as “water” and the PET in grid cells marked as “land” and the RET is conducted. Unfortunately, there were not any grid cells marked as water in the model domain or close to it. Lake Trafford, located close to the east boundary of the model domain, was excluded by a slight distance (see Figure E1) from the water classification that required 75% water coverage

[Jacobs et al., 2008]. Thus, three grid cells marked as water west to Lake Okeechobee and shown in **Figure E3** are selected for this comparison.

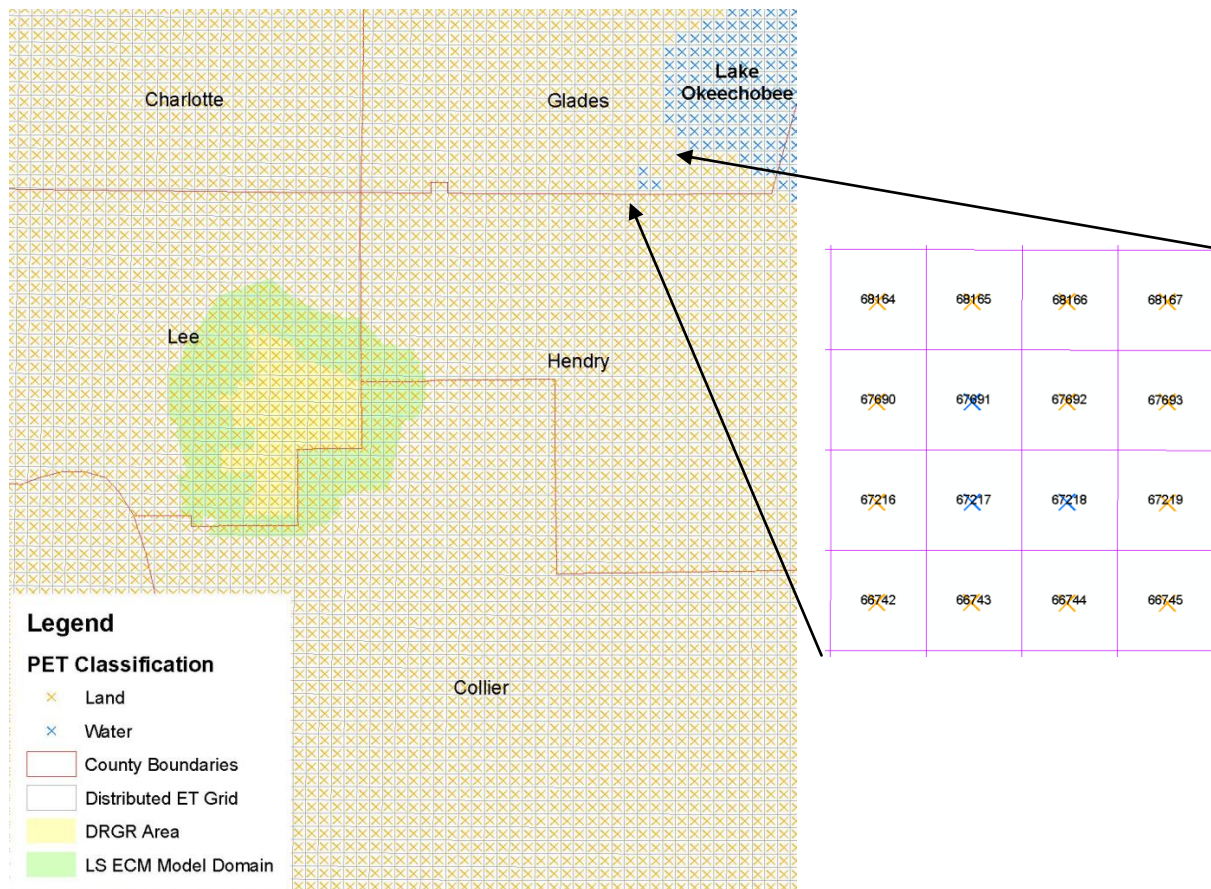


**Figure E3.** Distributed ET grid around the model domain showing the cells classified as “water” and as “Land”. The zoom-in view shows three “water” grid cells used in the ET comparison (see text for details).

The annual ET rates from alternative data and the corresponding RET and PET rates from the USGS are compared in **Table E1**. Comparative plots of the daily ET rates are presented in **Figure E4**. A map with all the site locations is shown in **Figure E5**.

In the four locations compared, PET data from the USGS for grid cells marked as land has higher seasonal amplitude than the corresponding RET data from the USGS. PET is higher during the middle of the year and lower at the end / beginning of the year. In annual averaged magnitudes, PET is lower than RET in a range from 0.2 to 3.1 inches (0.4% to 5.3% of RET).

At station FPWX, the simple method used to estimate ET from solar radiation produced daily ET values closer to the RET values from the USGS. The PET seasonal

oscillation has higher amplitude than the one from the station and the RET. In annual averaged magnitudes, that ET estimation underpredicts both PET and RET by about 3%.

The daily pan evaporation measured at the Naples station behaves closer to the RET data during the minimum ET period and closer to the PET (land) data during the maximum ET period (mid-year). In annual averaged magnitudes, the pan evaporation rate exceeds PET by 11.5% and RET by 8.0%. This is surprising since a coefficient to convert from pan evaporation to PET or RET would be of 0.90 or 0.93, respectively, which are above the range of 0.6 to 0.8 suggested for the pan coefficient that converts into lake evaporation. A pan evaporation of 0.9, for instance, would give a lake evaporation equal to 55.0 inches/year (RET- 2.8%). Possible lower values of measured pan evaporation than expected might be a consequence of the algae coverage existing in the pan water surface at the Naples station and also to a building nearby that may reduce the wind and produce some shadow late in the afternoon.

The lake evaporation at Lake Starr and Reedy Lake estimated from energy budget also behaves closer to the RET data during the minimum ET period and closer to the PET (land) data during the maximum ET period (middle of the year). In annual averaged magnitudes, the lake evaporation rate exceeds PET by 9.4% and 19.6%, and exceeds RET by 5.3% and 11.2%, respectively. Notice that Reedy Lake is located north of Lake Starr and the annual average PET and RET values decrease toward the north, as expected. The annual average lake evaporation estimation, however, increases unexpectedly by about 3 inches from Lake Starr to Reedy Lake.

**Table E1.** Annual ET rates obtained from USGS distributed data (PET and RET) and from alternative data (labeled as ET).

| Alternative Data for ET                | Pixels for PET and RET                          | period                 | ET (in/y) | PET (in/y) | RET (in/y) | ET-PET (% PET) | ET-RET (% RET) | PET-RET (% RET) |
|--|---|------------------------|-----------|------------|------------|----------------|----------------|-----------------|
| FPWX                                   | 57706, 57707, 58180, 58181                      | 1/1/2002<br>12/31/2006 | 52.4      | 53.8       | 54.0       | -2.7           | -3.1           | -0.4            |
| BCBNAPLE_E                             | 52488   | 1/1/2002<br>12/31/2006 | 61.1      | 54.8       | 56.6       | 11.5           | 8.0            | -3.2            |
| Lake Starr                             | 98477, 98478, 98003, 98004                      | 7/20/1996<br>7/19/1998 | 56.7      | 51.8       | 53.9       | 9.4            | 5.3            | -3.8            |
| Reedy Lake                             | 110326  | 1/1/2002<br>12/31/2006 | 59.6      | 49.8       | 53.5       | 19.6           | 11.2           | -7.0            |
| Water pixels at 67217, 67218 and 67691 | 66743, 66744, 67216, 67219, 67690, 67692, 68165 | 1/1/2002<br>12/31/2006 | 61.4      | 53.4       | 56.5       | 14.9           | 8.8            | -5.3            |

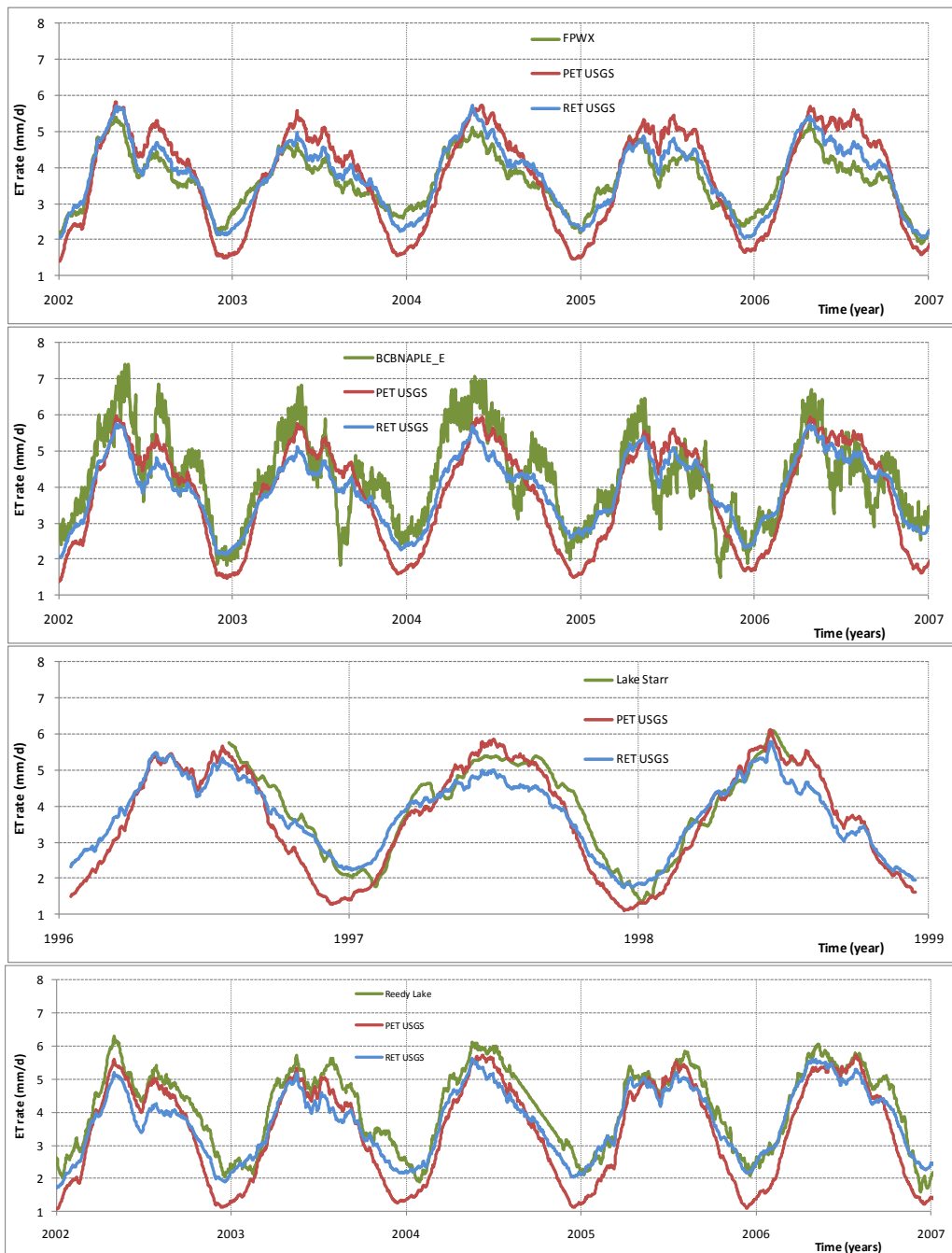


**Figure E4.** Comparative plot of the daily ET rates, which are running averaged with a 31 days windows. They are presented in the same order as in Table E1.

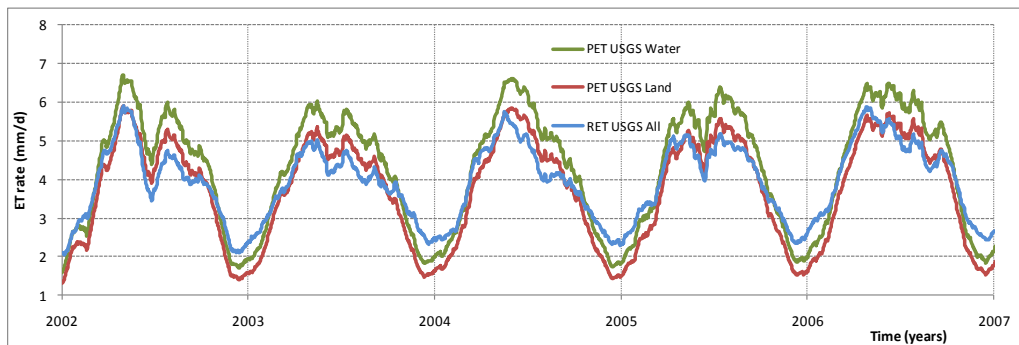


**Figure E4.** Comparative plot of the daily ET rates, which are running averaged with a 31 days windows. They are presented in the same order as in Table E1. Continuation.

The PET estimated in “water” pixels west of Lake Okeechobee is consistently higher than PET in neighboring “land” pixels through the year. At the same time, RET is higher than both PET estimations during the minimum period and lower during the maximum period (mid-year). In annual averaged magnitudes, the PET estimated in “water” pixels is 14.9% higher than PET in “land” pixels and 8.8% higher than RET. Thus, in this case, the annual PET estimated in water pixels is between the RET + 5.3% estimation at Lake Starr and the RET + 11.2% estimation at Reedy Lake.

In summary, the lake evaporation rates estimated by energy budget methods at Lake Starr and Reedy Lake suggest the use of an increment in the range of 5.3% and 11.2% to convert RET to lake evaporation. This range contains PET at water pixels estimated west of Lake Okeechobee as RET + 8.8%. The pan evaporation of RET + 8.0% measured at Naples seems to be low considering that a pan coefficient between 0.6 and 0.8 is typically applied to convert to lake evaporation. From all these results, the use of RET + 8.2% is recommended as a middle value of lake evaporation, with a possible range of variation of RET + 5.3% to RET + 11.2%.

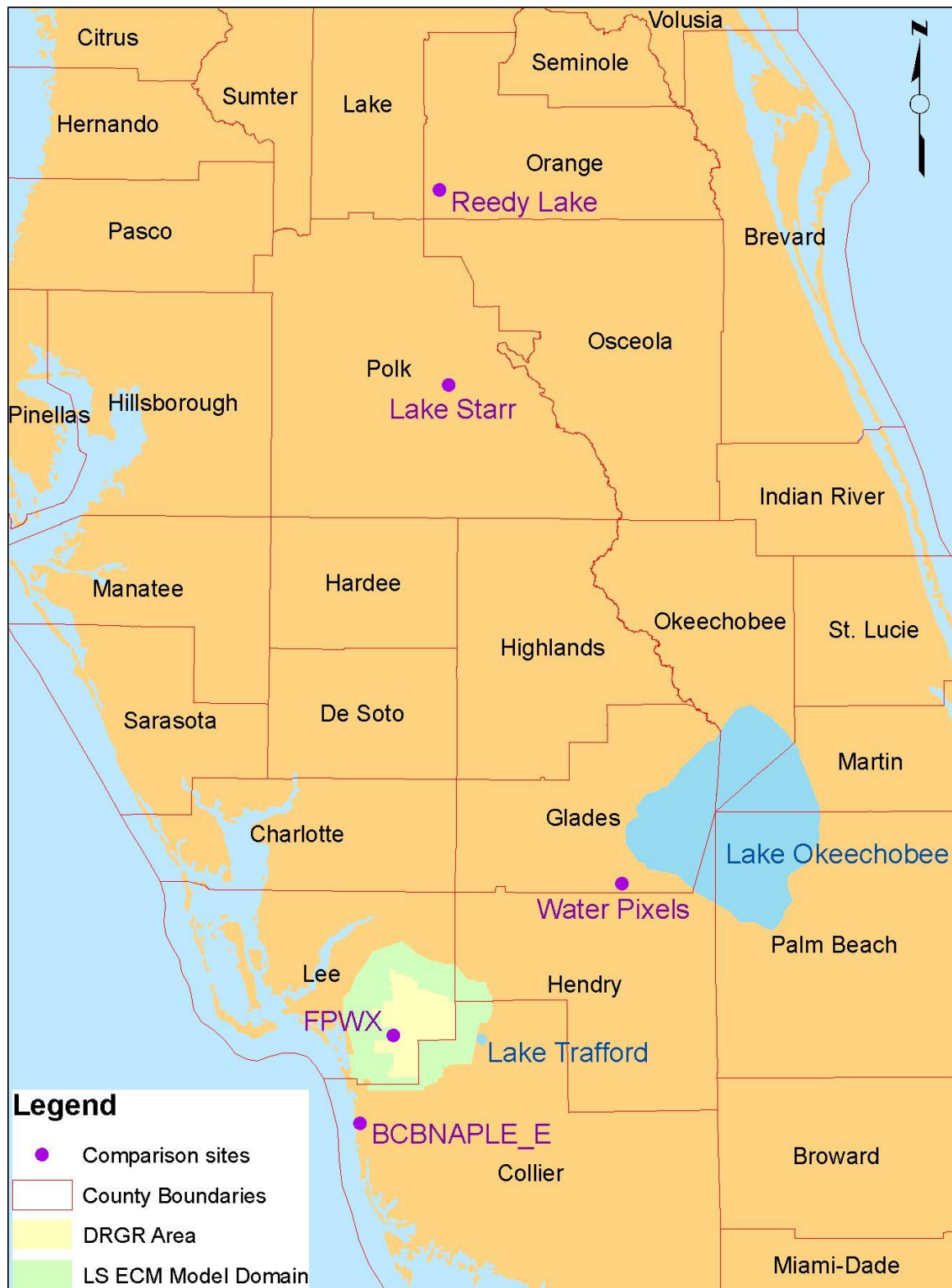


**Figure E5.** Location of the comparison sites.

## Appendix F. LS ECM V2 Results at Observation Stations

This appendix has additional tables and figures related to the LS ECM V2 results at observation stations. The statistical analysis was conducted in the period from Jan. 1, 2002 to Nov. 1, 2007, which is longer than the period considered in Appendixes B and C that ended in Jan 1, 2007. This may cause slight differences in the statistical parameters presented.

The meaning of symbols for the statistical parameter used in this appendix is

ME: mean error;

MAE: mean absolute error;

RMSE: root mean square error;

R: Correlation coefficient;

PL: average performance level, which is number in the range from 1.0 (high) to 3.0 (low).

### List of sections

|                              |    |
|------------------------------|----|
| Mining Pits .....            | 3  |
| Observation Wells .....      | 6  |
| Surface water stations ..... | 46 |

### List of Tables

|  |    |
|--|----|
| Table F1. Difference of the model results at mining pits and lakes. .... | 3  |
| Table F2. Statistical parameters at observation wells. ....              | 6  |
| Table F3. Statistic parameters at surface water stations.....            | 46 |

### List of Figures

|  |    |
|--|----|
| Figure F1. Water level differences (Lidar – model) in mining pits and lakes from previous (V1) model. .... | 4  |
| Figure F2. Water level differences (Lidar – model) in mining pits and lakes from new (V2) model.....       | 5  |
| Figure F3. Average performance levels in shallow wells (layer 1) from previous (V1) model.                 | 9  |
| Figure F4. Average performance levels in shallow wells (layer 1) from new (V2) model. ....                 | 10 |
| Figure F5. Average performance levels in deeper wells (layer> 1) from previous (V1) model. ....            | 11 |
| Figure F6. Average performance levels in deeper wells (layer> 1) from new (V2) model. ....                 | 12 |
| Figure F7. Water level at stations 49-GW3, 49-GW6 and 49-GW7.....  | 13 |
| Figure F8. Water level at stations 49-GW8, 49-GW9 and 49-GW10.....   | 14 |
| Figure F9. Water level at stations 49-GW11, 49-GW12 and 49-GW14.....                                       | 15 |

|   |    |
|---|----|
| Figure F10. Water level at stations 49-GW15, 49L-GW1 and L-1985.....                                | 16 |
| Figure F11. Water level at stations FP2_GW1, FP3_GW1 and FP4_GW1. ....                              | 17 |
| Figure F12. Water level at stations L-5874, FP5_GW1 and FP6_GW1.....                                | 18 |
| Figure F13. Water level at stations FP7_GW1, FP8_GW1 and FP9_G.....                                 | 19 |
| Figure F14. Water level at stations L-5667, FP10_G and 46A-GW3.....                                 | 20 |
| Figure F15. Water level at stations 46A-GW4, L-5649 and 46A-GW10. ....                              | 21 |
| Figure F16. Water level at stations 46A-GW11, 46A-GW12 and 46A-GW13. ....                           | 22 |
| Figure F17. Water level at stations 46A-GW14, 46A-GW15 and 46A-GW18. ....                           | 23 |
| Figure F18. Water level at stations 46A-GW21, 46A-GW25 and 46A-GW26. ....                           | 24 |
| Figure F19. Water level at stations 40-GW1, 40-GW2 and 40-GW3.....                                  | 25 |
| Figure F20. Water level at stations 40-GW4, 40-GW5 and 40-GW6.....                                  | 26 |
| Figure F21. Water level at stations 40-GW7, HF1_G and HF2_G.....                                    | 27 |
| Figure F22. Water level at stations HF3_G, HF4_G and HF7_G.....                                     | 28 |
| Figure F23. Water level at stations ST1_G, ST2_G and ST3_G. ....                                    | 29 |
| Figure F24. Water level at stations L-2192, WF1_G and L-730. ....                                   | 30 |
| Figure F25. Water level at stations WF2_G, WF3_G and WF4_G. ....                                    | 31 |
| Figure F26. Water level at stations WF5_G, WF6_G and WF7_G. ....                                    | 32 |
| Figure F27. Water level at stations Corkscrew Swamp, L-1138 and L-2204.....                         | 33 |
| Figure F28. Water level at stations L-5664., L-5669R and L-5673.....                                | 34 |
| Figure F29. Water level at stations L-739, MPW02 and MPW03.....                                     | 35 |
| Figure F30. Water level at stations MPW04, MPW05 and MPW08. ....                                    | 36 |
| Figure F31. Water level at stations MPW25, MPW27 and MPW28. ....                                    | 37 |
| Figure F32. Water level at stations MPW29, MPW30 and MPW31. ....                                    | 38 |
| Figure F33. Water level at stations MPW33, MPW34 and MPW35. ....                                    | 39 |
| Figure F34. Water level at stations MPW36, MPW39 and MW1. ....                                      | 40 |
| Figure F35. Water level at stations MW2, MW3 and MW4.....   | 41 |
| Figure F36. Water level at stations Lake, L-5844 and DEW-MW-1. ....                                 | 42 |
| Figure F37. Water level at stations DEW-MW-2, LM-1891 and LM-1892.....                              | 43 |
| Figure F38. Water level at stations LM-2290, LM-2993 and Section_11_W. ....                         | 44 |
| Figure F39. Water level at stations Section_11_E, and PWS-MW-1.....                                 | 45 |
| Figure F40. Average performance levels in surface water stations from previous (V1) model.<br>..... | 47 |
| Figure F41. Average performance levels in surface water stations from new (V2) model. ....          | 48 |
| Figure F42. Comparison plots at surface water stations KehlCan_HW, KehlCan_TW and S-SF-1_HW. ....   | 49 |
| Figure F43. Comparison plots at surface water stations S-SF-1 Q, S-SF-1_TW and S-NM-2_HW. ....      | 50 |

Figure F44. Comparison plots at surface water stations S-NM-2 Q, S-NM-2\_TW and S-YT-2\_HW. .... 51

Figure F45. Comparison plots at surface water stations Mullock Creek, EsteroRiv and EsteroRiv Q. .... 52

Figure F46. Comparison plots at surface water stations EsteroRivS, EsteroRivS Q and SpringCRSS. .... 53

Figure F47. Comparison plots at surface water stations SpringCRSS Q, Imperial and Imperial Q. .... 54

Figure F48. Comparison plots at surface water stations Halfway\_S HW, Halfway\_S TW and Copperleaf. .... 55

Figure F49. Comparison plots at surface water stations HalfwayCrDS HW, and HalfwayCrDS TW. .... 56

### Mining Pits

**Table F1.** Difference of the model results at mining pits and lakes.

| Lidar Point | D V1 (ft) | D V2 (ft) | Lidar Point | D V1 (ft) | D V2 (ft) | Lidar Point | D V1 (ft)    | D V2 (ft)    |
|-------------|-----------|-----------|-------------|-----------|-----------|-------------|--------------|--------------|
| 1           | 1.2       | 1.7       | 22          | -2.1      | -0.8      | 43          | -0.9         | 0.0          |
| 2           | 6.3       | 6.8       | 23          | -2.1      | -0.9      | 44          | -0.9         | -0.1         |
| 3           | -2.5      | -0.3      | 24          | -3.3      | -1.9      | 45          | 0.3          | 1.2          |
| 4           | -3.0      | -0.8      | 25          | -3.4      | -1.9      | 46          | -0.9         | 0.0          |
| 5           | -3.7      | -1.4      | 26          | 2.8       | 2.8       | 47          | -1.2         | -0.3         |
| 6           | -2.2      | -0.6      | 27          | 2.4       | 2.8       | 48          | -2.6         | -1.6         |
| 7           | -2.6      | -0.8      | 28          | -3.2      | -1.6      | 49          | -0.9         | 0.1          |
| 8           | -0.8      | 0.1       | 29          | -0.3      | 1.0       | 50          | -0.6         | 0.3          |
| 9           | -3.8      | -1.5      | 30          | -0.3      | 1.0       | 51          | 0.3          | 1.3          |
| 10          | -2.7      | -1.6      | 31          | 0.7       | 1.8       | 52          | -0.8         | 0.2          |
| 11          | -4.4      | -2.7      | 32          | -1.0      | -1.1      | 53          | -0.8         | 0.2          |
| 12          | -3.1      | -2.3      | 33          | 2.8       | 2.8       | 54          | 0.4          | 1.5          |
| 13          | -2.1      | -1.0      | 34          | 2.8       | 3.0       | 55          | -3.3         | -2.4         |
| 14          | -2.4      | -1.0      | 35          | 2.1       | 2.5       | 56          | -1.6         | -0.6         |
| 15          | -1.9      | -1.0      | 36          | 0.8       | 1.8       | 57          | -4.6         | -4.0         |
| 16          | -3.9      | -2.3      | 37          | -6.9      | -5.6      | 58          | -3.3         | -2.6         |
| 17          | -1.9      | -1.0      | 38          | 0.6       | 1.7       | 59          | -0.1         | 0.3          |
| 18          | -3.0      | -1.8      | 39          | 0.8       | 1.7       | 60          | -0.1         | 0.5          |
| 19          | -3.1      | -1.9      | 40          | 3.8       | 4.1       | 61          | -3.1         | -2.7         |
| 20          | -3.1      | -1.9      | 41          | 0.9       | 1.7       | 62          | 0.8          | 1.2          |
| 21          | -2.7      | -1.5      | 42          | 6.9       | 4.4       | <b>mean</b> | <b>-1.04</b> | <b>-0.07</b> |

Note: “D” stands for difference between Lidar elevation and water level from model, “V1” for LC ECM V1 and “V2” for LC ECM V2.

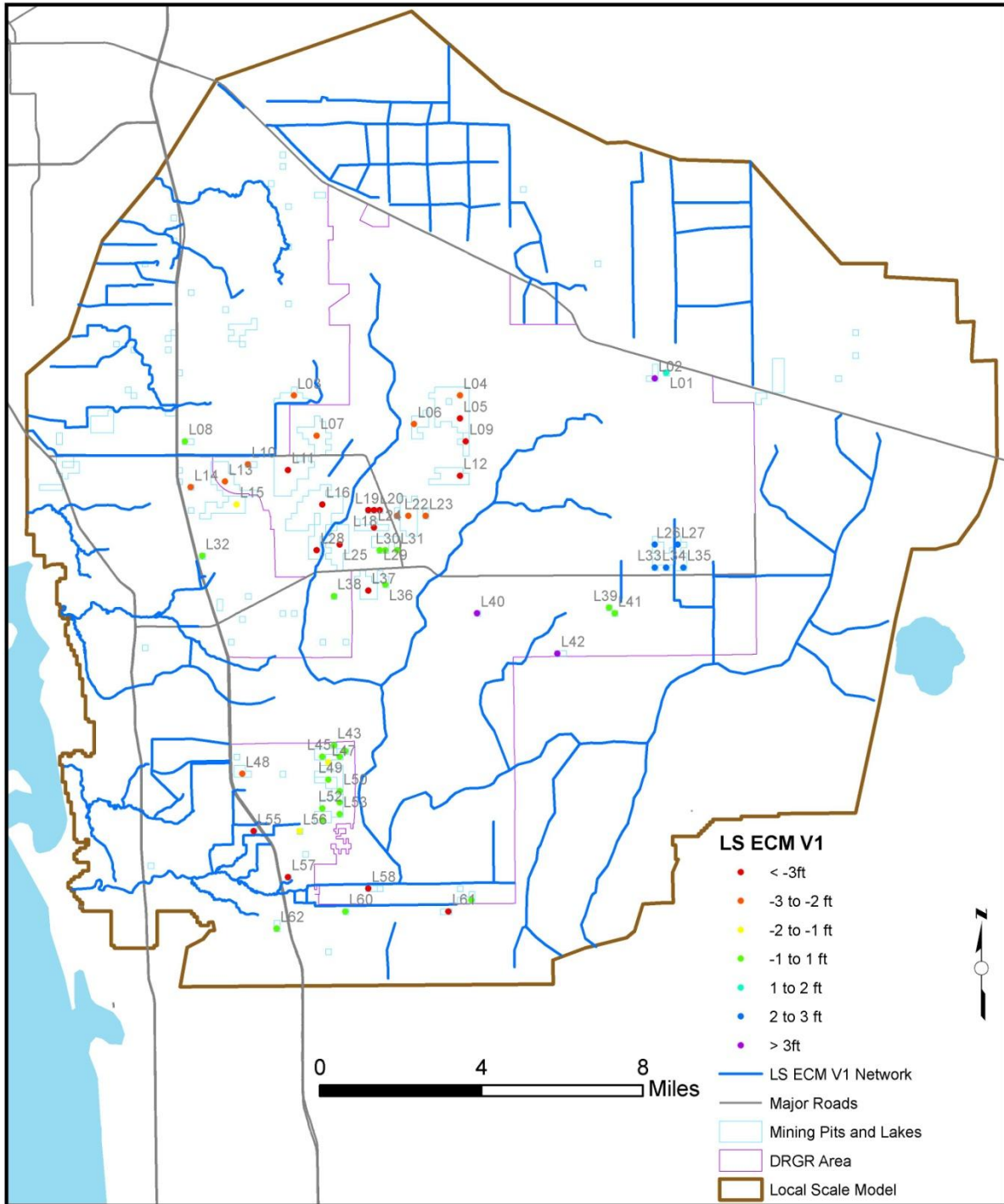


**Figure F1.** Water level differences (Lidar – model) in mining pits and lakes from previous (V1) model.

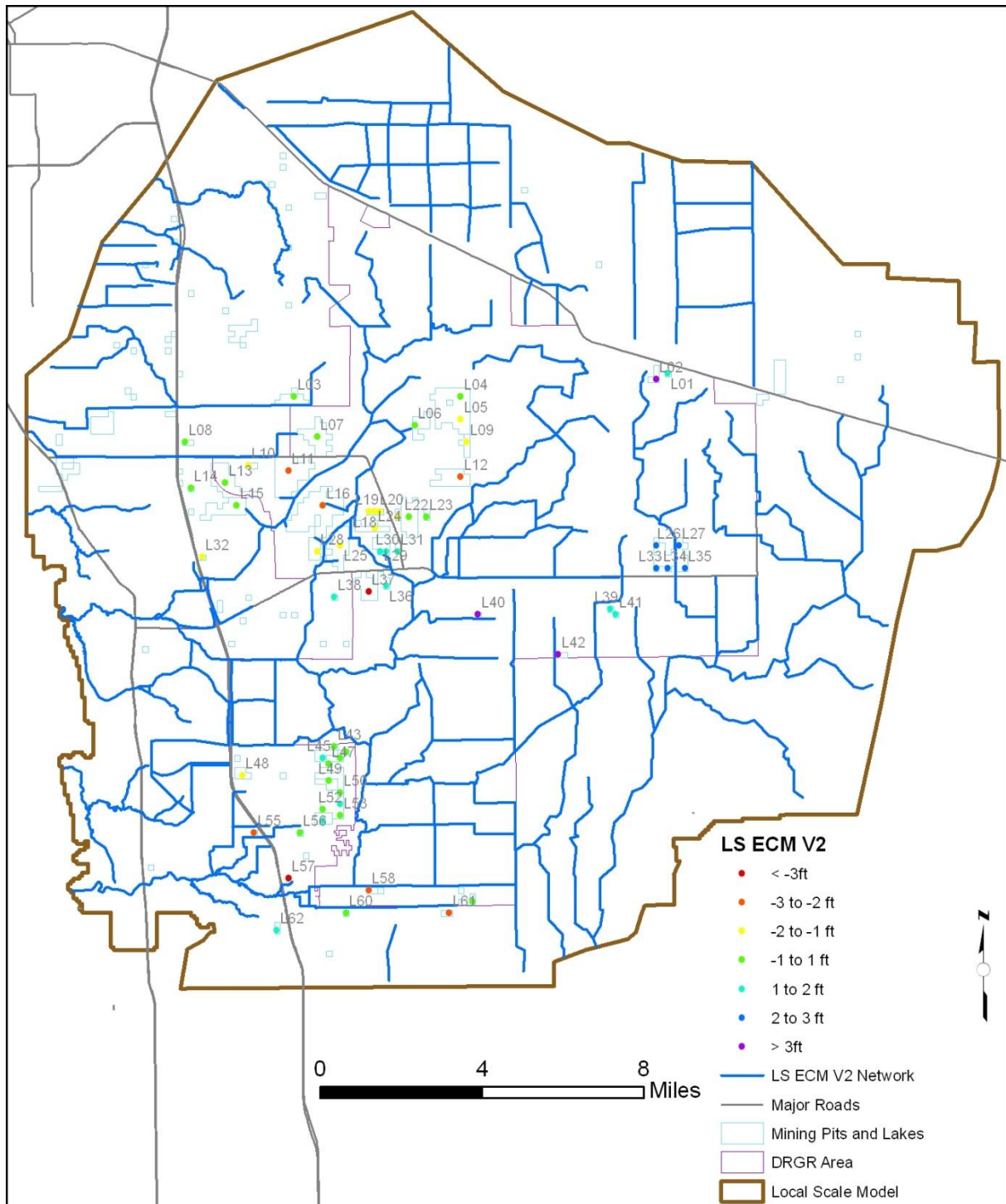


**Figure F2.** Water level differences (Lidar – model) in mining pits and lakes from new (V2) model.

## Observation Wells

**Table F2.** Statistical parameters at observation wells.

| Name     | Layer | LS ECM V1 |          |           |      |     | LS ECM V2 |          |           |      |     |
|----------|-------|-----------|----------|-----------|------|-----|-----------|----------|-----------|------|-----|
|          |       | ME (ft)   | MAE (ft) | RMSE (ft) | R    | PL  | ME (ft)   | MAE (ft) | RMSE (ft) | R    | PL  |
| 49-GW3   | 1     | 0.11      | 0.90     | 1.14      | 0.40 | 1.5 | 0.93      | 1.32     | 1.63      | 0.37 | 2.0 |
| 49-GW6   | 1     | 0.38      | 1.18     | 1.43      | 0.75 | 1.5 | 0.76      | 1.16     | 1.54      | 0.72 | 1.5 |
| 49-GW7   | 1     | 0.44      | 0.86     | 1.29      | 0.58 | 1.5 | 0.20      | 0.78     | 1.14      | 0.61 | 1.3 |
| 49-GW8   | 1     | 1.79      | 1.79     | 2.19      | 0.23 | 2.3 | 1.64      | 1.64     | 2.03      | 0.23 | 2.3 |
| 49-GW9   | 1     | 1.31      | 1.34     | 1.61      | 0.84 | 1.8 | 1.53      | 1.57     | 1.81      | 0.82 | 1.8 |
| 49-GW10  | 1     | -0.46     | 0.88     | 1.06      | 0.87 | 1.0 | -0.02     | 0.81     | 0.96      | 0.88 | 1.0 |
| 49-GW11  | 1     | 0.20      | 1.07     | 1.35      | 0.85 | 1.5 | 0.88      | 1.23     | 1.57      | 0.87 | 1.5 |
| 49-GW12  | 1     | 0.56      | 0.85     | 1.12      | 0.87 | 1.0 | 1.16      | 1.24     | 1.48      | 0.90 | 1.8 |
| 49-GW14  | 1     | -0.14     | 0.64     | 0.76      | 0.89 | 1.0 | 0.12      | 0.61     | 0.78      | 0.87 | 1.0 |
| 49-GW15  | 1     | 1.72      | 1.76     | 1.92      | 0.53 | 2.0 | 1.54      | 1.56     | 1.69      | 0.57 | 2.0 |
| 49L-GW1  | 1     | 0.23      | 0.78     | 0.96      | 0.77 | 1.0 | 0.85      | 0.99     | 1.21      | 0.81 | 1.0 |
| L-1985   | 2     | 0.19      | 2.51     | 3.04      | 0.61 | 2.3 | 1.19      | 2.66     | 3.57      | 0.52 | 2.5 |
| FP2_GW1  | 1     | 0.50      | 1.09     | 1.53      | 0.80 | 1.5 | 1.26      | 1.54     | 2.19      | 0.71 | 1.8 |
| FP3_GW1  | 1     | 0.28      | 0.60     | 0.73      | 0.86 | 1.0 | 0.82      | 0.86     | 1.10      | 0.85 | 1.0 |
| FP4_GW1  | 1     | -0.22     | 0.55     | 0.70      | 0.89 | 1.0 | 0.20      | 0.79     | 0.95      | 0.84 | 1.0 |
| L-5874   | 3     | -3.50     | 3.77     | 4.65      | 0.71 | 2.5 | -3.04     | 3.52     | 4.37      | 0.66 | 2.8 |
| FP5_GW1  | 1     | -0.33     | 0.60     | 0.76      | 0.88 | 1.0 | 0.01      | 0.75     | 0.95      | 0.82 | 1.0 |
| FP6_GW1  | 1     | -0.41     | 0.76     | 0.94      | 0.87 | 1.0 | 0.10      | 0.79     | 1.01      | 0.82 | 1.0 |
| FP7_GW1  | 1     | -0.41     | 0.84     | 1.03      | 0.86 | 1.0 | 0.25      | 0.80     | 1.03      | 0.84 | 1.0 |
| FP8_GW1  | 1     | -0.27     | 0.70     | 0.85      | 0.88 | 1.0 | 0.17      | 0.79     | 0.99      | 0.84 | 1.0 |
| FP9_G    | 1     | -0.39     | 0.83     | 1.02      | 0.86 | 1.0 | 0.27      | 0.81     | 1.05      | 0.83 | 1.0 |
| L-5667   | 1     | 1.08      | 1.28     | 1.39      | 0.93 | 1.8 | 1.80      | 1.88     | 2.02      | 0.89 | 1.8 |
| FP10_G   | 1     | -0.25     | 0.54     | 0.72      | 0.89 | 1.0 | 0.09      | 0.77     | 0.99      | 0.82 | 1.0 |
| 46A-GW3  | 1     | -2.14     | 2.14     | 2.39      | 0.72 | 2.3 | -1.97     | 1.98     | 2.20      | 0.77 | 1.8 |
| 46A-GW4  | 1     | -0.52     | 1.12     | 1.36      | 0.74 | 1.5 | 0.07      | 1.00     | 1.21      | 0.72 | 1.0 |
| L-5649   | 4     | -7.45     | 7.45     | 8.15      | 0.63 | 2.8 | -7.38     | 7.38     | 8.10      | 0.58 | 2.8 |
| 46A-GW10 | 1     | -0.25     | 0.53     | 0.70      | 0.81 | 1.0 | -0.63     | 0.74     | 0.91      | 0.81 | 1.0 |
| 46A-GW11 | 1     | -1.28     | 1.28     | 1.36      | 0.92 | 1.8 | -1.49     | 1.49     | 1.55      | 0.93 | 1.8 |
| 46A-GW12 | 1     | -1.69     | 1.78     | 2.10      | 0.69 | 2.0 | -1.64     | 1.65     | 2.00      | 0.83 | 1.8 |
| 46A-GW13 | 1     | -0.94     | 1.00     | 1.12      | 0.86 | 1.0 | -0.84     | 0.91     | 1.07      | 0.82 | 1.0 |
| 46A-GW14 | 1     | -0.96     | 1.21     | 1.39      | 0.58 | 1.8 | -0.63     | 1.05     | 1.18      | 0.54 | 1.5 |
| 46A-GW15 | 1     | -0.53     | 0.62     | 0.81      | 0.91 | 1.0 | 0.01      | 0.42     | 0.58      | 0.91 | 1.0 |
| 46A-GW18 | 1     | -1.05     | 1.22     | 1.40      | 0.85 | 1.8 | -0.58     | 0.92     | 1.07      | 0.86 | 1.0 |
| 46A-GW21 | 1     | -1.01     | 1.10     | 1.28      | 0.73 | 1.8 | -1.10     | 1.17     | 1.37      | 0.70 | 1.8 |



| Name         | Layer | LS ECM V1 |          |           |      |     | LS ECM V2 |          |           |      |     |
|--------------|-------|-----------|----------|-----------|------|-----|-----------|----------|-----------|------|-----|
|              |       | ME (ft)   | MAE (ft) | RMSE (ft) | R    | PL  | ME (ft)   | MAE (ft) | RMSE (ft) | R    | PL  |
| 46A-GW25     | 1     | 0.06      | 0.48     | 0.60      | 0.86 | 1.0 | -0.10     | 0.48     | 0.60      | 0.87 | 1.0 |
| 46A-GW26     | 1     | -0.27     | 0.47     | 0.61      | 0.78 | 1.0 | -0.37     | 0.53     | 0.67      | 0.79 | 1.0 |
| 40-GW1       | 1     | 0.21      | 0.82     | 1.11      | 0.67 | 1.3 | -1.17     | 1.34     | 1.65      | 0.67 | 2.0 |
| 40-GW2       | 1     | 0.86      | 1.36     | 1.65      | 0.45 | 2.0 | 0.80      | 1.28     | 1.65      | 0.46 | 2.0 |
| 40-GW3       | 2     | -0.65     | 0.86     | 1.03      | 0.80 | 1.0 | -0.73     | 0.94     | 1.09      | 0.81 | 1.0 |
| 40-GW4       | 2     | -3.86     | 3.86     | 3.97      | 0.78 | 2.5 | -4.65     | 4.65     | 4.74      | 0.80 | 2.5 |
| 40-GW5       | 1     | -0.74     | 1.11     | 1.37      | 0.77 | 1.5 | -2.49     | 2.49     | 2.69      | 0.75 | 2.5 |
| 40-GW6       | 1     | 0.38      | 1.24     | 1.67      | 0.44 | 2.0 | 0.42      | 1.27     | 1.68      | 0.46 | 2.0 |
| 40-GW7       | 1     | -0.42     | 0.79     | 1.12      | 0.69 | 1.3 | -0.45     | 0.86     | 1.20      | 0.63 | 1.3 |
| HF1_G        | 1     | -4.28     | 4.43     | 5.98      | 0.27 | 3.0 | -4.30     | 4.51     | 6.06      | 0.22 | 3.0 |
| HF2_G        | 1     | -0.37     | 1.04     | 1.24      | 0.71 | 1.3 | -0.38     | 1.10     | 1.30      | 0.69 | 1.8 |
| HF3_G        | 1     | 2.24      | 2.27     | 2.63      | 0.80 | 2.5 | 2.23      | 2.25     | 2.59      | 0.81 | 2.5 |
| HF4_G        | 1     | -1.37     | 1.78     | 2.20      | 0.62 | 2.0 | -1.40     | 1.83     | 2.24      | 0.60 | 2.0 |
| HF7_G        | 1     | -1.42     | 1.69     | 2.08      | 0.59 | 2.0 | -1.43     | 1.76     | 2.14      | 0.56 | 2.0 |
| ST1_G        | 1     | -0.44     | 0.72     | 0.85      | 0.86 | 1.0 | -0.44     | 0.78     | 0.91      | 0.82 | 1.0 |
| ST2_G        | 1     | 0.05      | 0.61     | 0.73      | 0.86 | 1.0 | 0.04      | 0.63     | 0.76      | 0.84 | 1.0 |
| ST3_G        | 1     | -0.34     | 0.80     | 0.92      | 0.80 | 1.0 | -0.12     | 0.75     | 0.91      | 0.76 | 1.0 |
| L-2192       | 3     | 1.64      | 4.35     | 5.53      | 0.14 | 2.8 | 0.76      | 4.27     | 5.50      | 0.06 | 2.5 |
| WF1_G        | 2     | 1.06      | 1.06     | 1.12      | 0.94 | 1.5 | -0.01     | 0.42     | 0.51      | 0.94 | 1.0 |
| L-730        | 2     | 0.72      | 0.75     | 0.99      | 0.80 | 1.0 | 0.02      | 0.86     | 1.09      | 0.65 | 1.3 |
| WF2_G        | 2     | 1.31      | 1.39     | 1.73      | 0.77 | 1.8 | 0.31      | 1.25     | 1.49      | 0.62 | 1.8 |
| WF3_G        | 1     | 1.54      | 1.54     | 1.71      | 0.86 | 1.8 | 0.42      | 1.09     | 1.36      | 0.70 | 1.8 |
| WF4_G        | 1     | 0.95      | 1.05     | 1.27      | 0.83 | 1.5 | -0.07     | 1.07     | 1.30      | 0.71 | 1.5 |
| WF5_G        | 1     | 1.02      | 1.08     | 1.40      | 0.81 | 1.8 | -0.10     | 1.30     | 1.52      | 0.64 | 1.8 |
| WF6_G        | 1     | 0.87      | 0.91     | 1.18      | 0.85 | 1.0 | -0.19     | 1.11     | 1.29      | 0.71 | 1.5 |
| WF7_G        | 1     | 1.16      | 1.18     | 1.49      | 0.81 | 1.8 | 0.07      | 1.25     | 1.48      | 0.64 | 1.8 |
| Corkscrew S. | 1     | -0.53     | 0.99     | 1.05      | 0.85 | 1.0 | -0.39     | 0.99     | 1.08      | 0.81 | 1.0 |
| L-1138       | 1     | -0.19     | 0.76     | 0.89      | 0.81 | 1.0 | -0.32     | 0.81     | 0.98      | 0.76 | 1.0 |
| L-2204       | 2     | -0.71     | 0.75     | 0.91      | 0.90 | 1.0 | -0.99     | 1.01     | 1.16      | 0.89 | 1.3 |
| L-5664       | 4     | -9.75     | 9.75     | 10.74     | 0.57 | 2.8 | -10.2     | 10.23    | 11.20     | 0.61 | 2.8 |
| L-5669R      | 3     | 0.14      | 0.37     | 0.52      | 0.88 | 1.0 | 1.72      | 1.82     | 2.26      | 0.88 | 1.8 |
| L-5673       | 3     | -8.69     | 8.73     | 9.46      | 0.68 | 2.8 | -7.61     | 7.66     | 8.34      | 0.70 | 2.8 |
| L-739        | 2     | 0.54      | 0.60     | 0.74      | 0.96 | 1.0 | 1.05      | 1.05     | 1.15      | 0.95 | 1.5 |
| MPW02        | 1     | -0.66     | 0.70     | 0.80      | 0.94 | 1.0 | -0.47     | 0.69     | 0.82      | 0.87 | 1.0 |
| MPW03        | 1     | -0.77     | 0.78     | 0.87      | 0.92 | 1.0 | -0.56     | 0.77     | 0.92      | 0.71 | 1.0 |
| MPW04        | 1     | -0.01     | 0.50     | 0.65      | 0.91 | 1.0 | -0.08     | 0.68     | 0.83      | 0.85 | 1.0 |
| MPW05        | 1     | 0.25      | 0.53     | 0.57      | 0.78 | 1.0 | -0.38     | 0.44     | 0.59      | 0.83 | 1.0 |
| MPW08        | 1     | 1.11      | 1.11     | 1.18      | 0.93 | 1.5 | 0.65      | 0.68     | 0.85      | 0.87 | 1.0 |



| Name         | Layer | LS ECM V1 |          |           |      |     | LS ECM V2 |          |           |      |     |
|--------------|-------|-----------|----------|-----------|------|-----|-----------|----------|-----------|------|-----|
|              |       | ME (ft)   | MAE (ft) | RMSE (ft) | R    | PL  | ME (ft)   | MAE (ft) | RMSE (ft) | R    | PL  |
| MPW25        | 1     | -0.27     | 0.35     | 0.39      | 0.95 | 1.0 | -0.82     | 0.82     | 0.86      | 0.94 | 1.0 |
| MPW27        | 1     | 0.45      | 0.50     | 0.79      | 0.86 | 1.0 | 0.40      | 0.65     | 0.96      | 0.72 | 1.0 |
| MPW28        | 1     | 0.95      | 0.95     | 1.00      | 0.77 | 1.0 | -0.03     | 0.14     | 0.17      | 0.93 | 1.0 |
| MPW29        | 1     | -0.08     | 0.31     | 0.40      | 0.97 | 1.0 | 0.07      | 0.33     | 0.42      | 0.96 | 1.0 |
| MPW30        | 1     | 0.39      | 0.79     | 1.16      | 0.61 | 1.3 | 0.08      | 1.00     | 1.22      | 0.57 | 1.3 |
| MPW31        | 1     | 0.23      | 0.27     | 0.43      | 0.96 | 1.0 | 0.17      | 0.45     | 0.68      | 0.86 | 1.0 |
| MPW33        | 1     | -0.94     | 1.21     | 1.48      | 0.72 | 1.5 | -0.93     | 1.26     | 1.51      | 0.69 | 1.8 |
| MPW34        | 1     | 0.49      | 0.49     | 0.49      | 0.98 | 1.0 | -0.16     | 0.16     | 0.17      | 0.98 | 1.0 |
| MPW35        | 1     | -1.02     | 1.05     | 1.21      | 0.91 | 1.5 | -0.22     | 0.58     | 0.76      | 0.88 | 1.0 |
| MPW36        | 1     | -0.20     | 0.62     | 0.75      | 0.85 | 1.0 | 0.16      | 0.53     | 0.66      | 0.88 | 1.0 |
| MPW39        | 1     | 0.47      | 2.74     | 3.18      | 0.48 | 2.5 | 1.61      | 2.96     | 3.81      | 0.31 | 2.8 |
| MW1          | 1     | -0.30     | 0.92     | 1.68      | 0.49 | 1.8 | -0.86     | 0.99     | 1.65      | 0.70 | 1.3 |
| MW2          | 1     | 0.79      | 0.90     | 1.40      | 0.55 | 1.5 | 0.35      | 1.40     | 1.77      | 0.18 | 2.0 |
| MW3          | 1     | 1.32      | 1.32     | 1.58      | 0.72 | 1.8 | 0.78      | 1.24     | 1.69      | 0.42 | 2.0 |
| MW4          | 1     | 0.17      | 0.81     | 0.94      | 0.81 | 1.0 | -0.12     | 0.58     | 0.81      | 0.87 | 1.0 |
| Lake         | 1     | 0.74      | 0.87     | 1.33      | 0.59 | 1.5 | 0.31      | 1.31     | 1.67      | 0.24 | 2.0 |
| L-5844       | 2     | -7.34     | 7.34     | 7.38      | 0.75 | 2.5 | -7.96     | 7.96     | 8.01      | 0.70 | 2.8 |
| DEW-MW-1     | 1     | -3.14     | 3.14     | 3.22      | 0.63 | 2.8 | -2.44     | 2.44     | 2.55      | 0.54 | 2.8 |
| DEW-MW-2     | 1     | -2.87     | 2.87     | 2.89      | 0.87 | 2.5 | -1.96     | 1.96     | 1.99      | 0.89 | 1.8 |
| LM-1891      | 1     | -2.55     | 2.55     | 2.64      | 0.77 | 2.5 | -1.53     | 1.53     | 1.66      | 0.69 | 2.0 |
| LM-1892      | 1     | -1.80     | 1.80     | 1.97      | 0.00 | 2.3 | -0.07     | 0.63     | 0.68      | 0.00 | 1.5 |
| LM-2290      | 1     | -3.66     | 3.66     | 3.73      | 0.88 | 2.5 | -1.79     | 1.79     | 2.04      | 0.37 | 2.3 |
| LM-2993      | 1     | -3.49     | 3.49     | 3.58      | 0.82 | 2.5 | -2.22     | 2.22     | 2.47      | 0.65 | 2.5 |
| Section_11_W | 1     | -0.09     | 0.46     | 0.55      | 0.89 | 1.0 | 0.79      | 0.79     | 0.90      | 0.86 | 1.0 |
| Section_11_E | 1     | -2.76     | 2.76     | 2.82      | 0.73 | 2.5 | -1.08     | 1.09     | 1.24      | 0.70 | 1.5 |
| PWS-MW-1     | 1     | -4.18     | 4.18     | 4.25      | 0.66 | 2.8 | -2.37     | 2.37     | 2.52      | 0.22 | 3.0 |

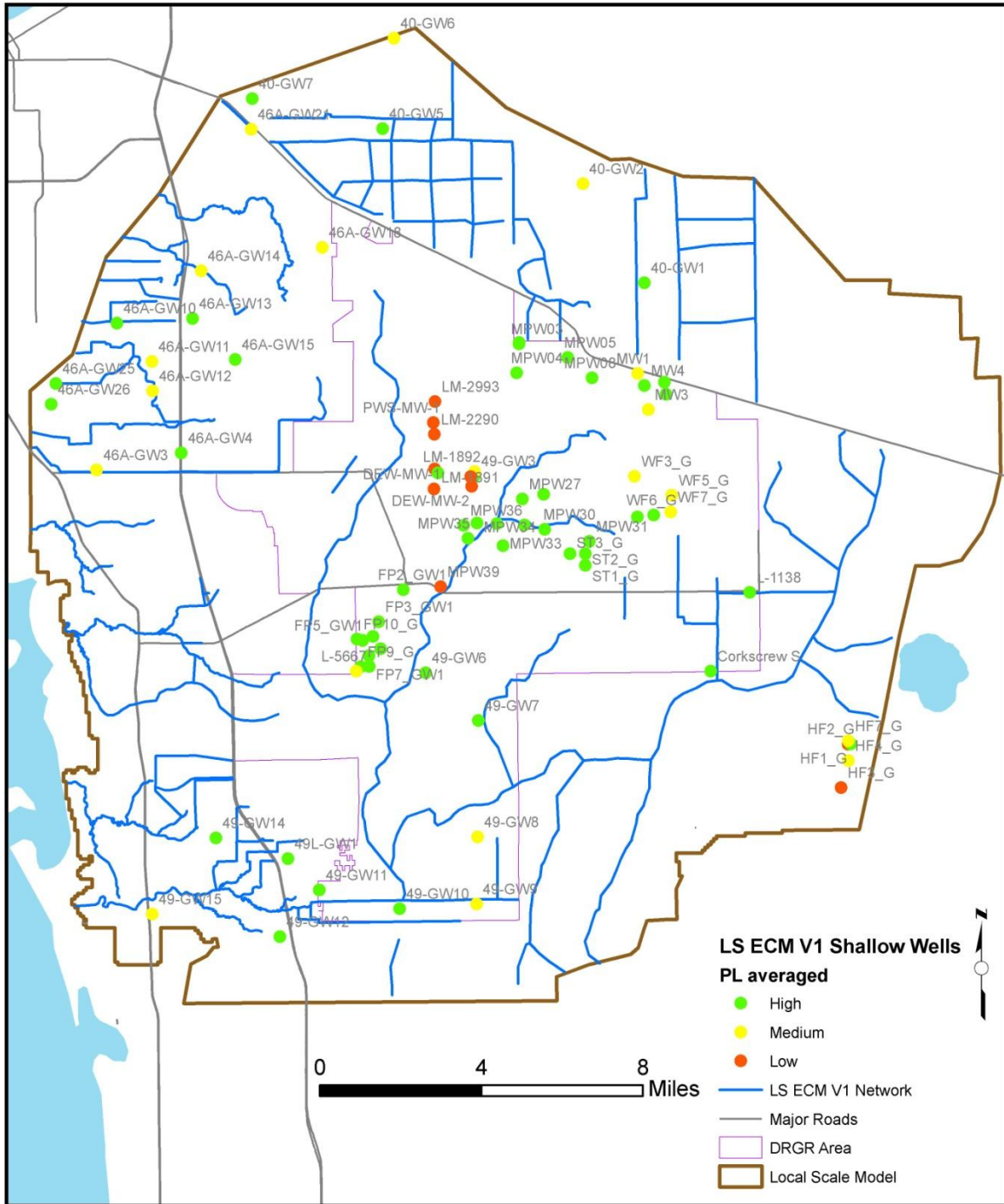


**Figure F3.** Average performance levels in shallow wells (layer 1) from previous (V1) model.

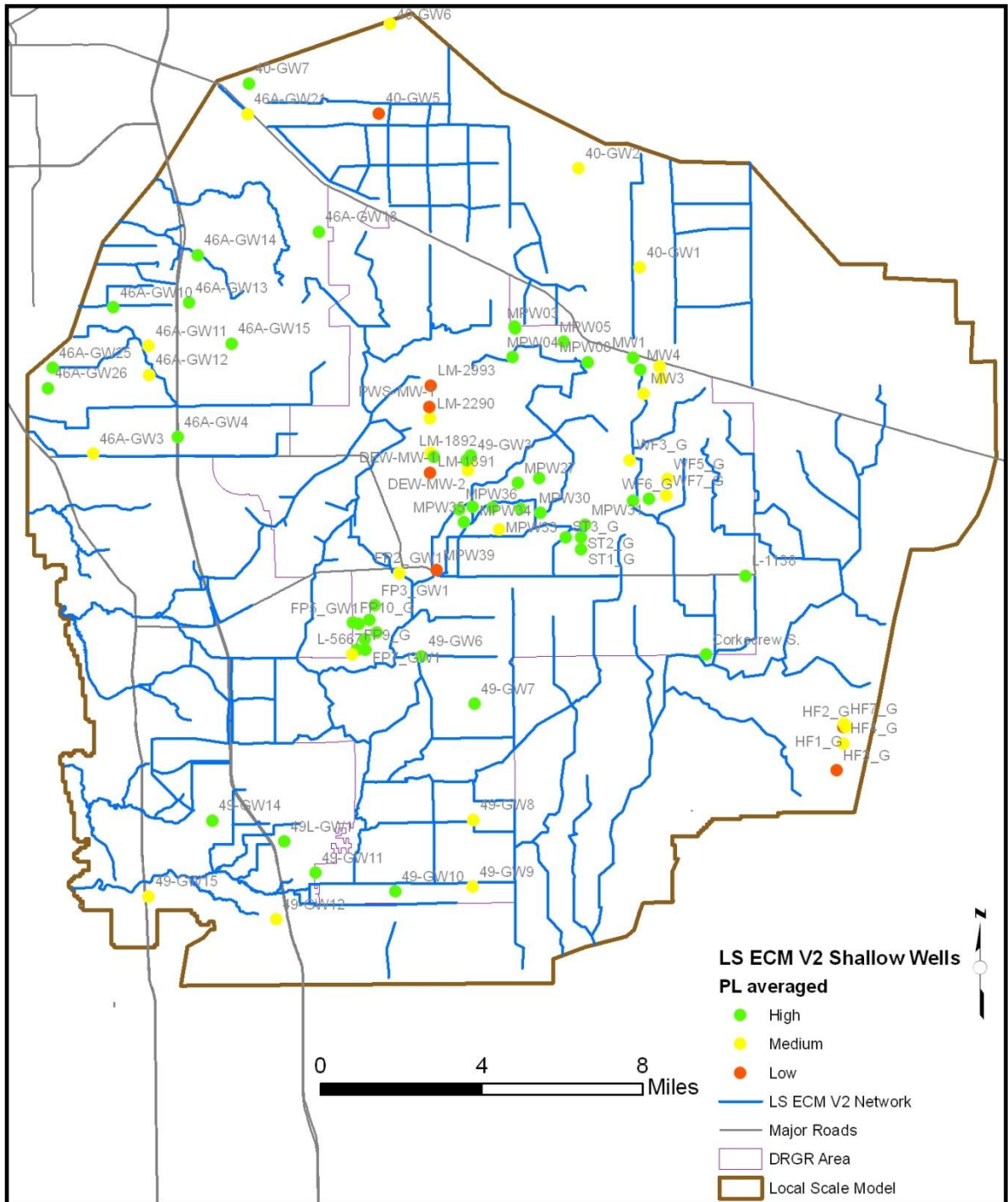


**Figure F4.** Average performance levels in shallow wells (layer 1) from new (V2) model.

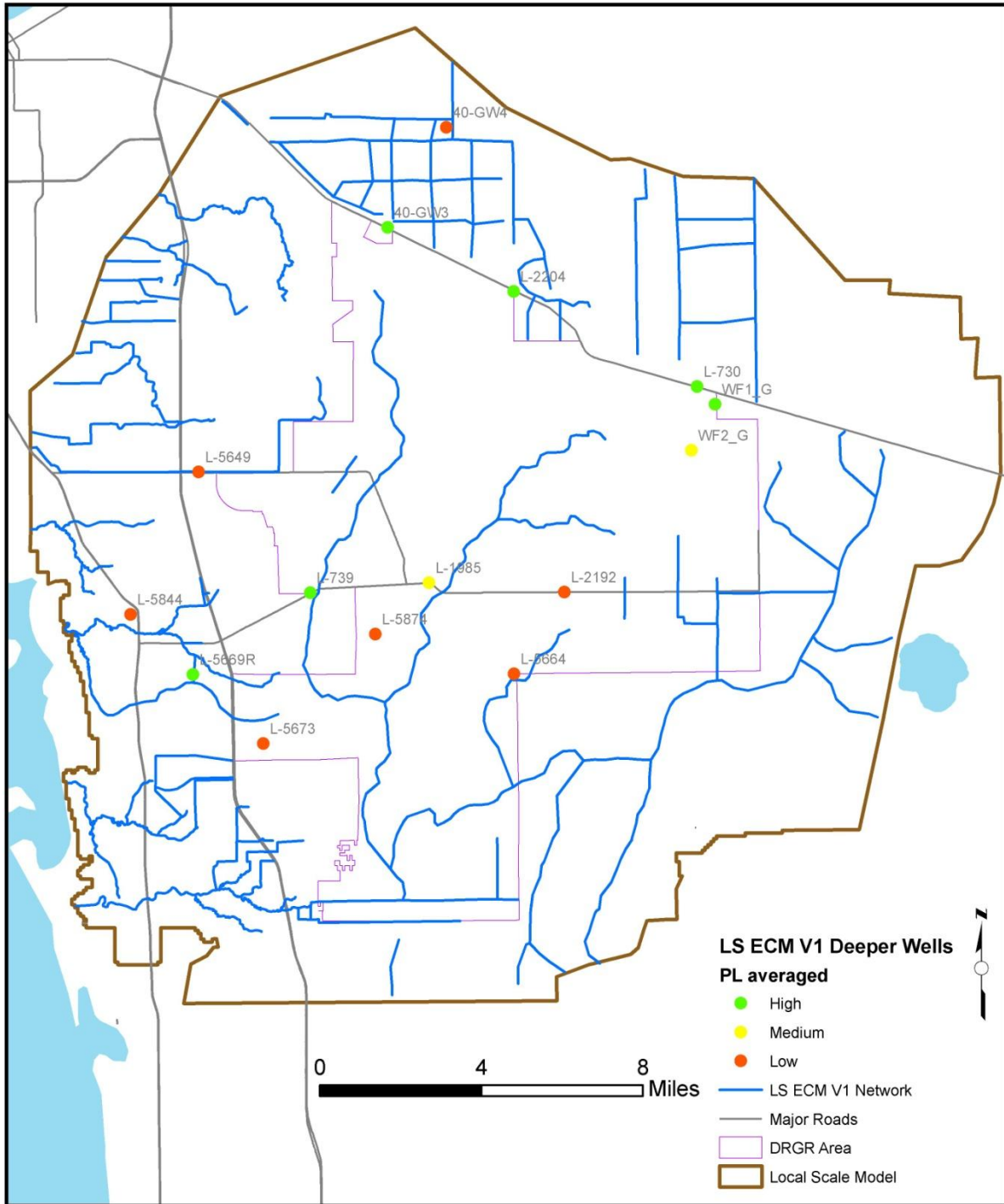


**Figure F5.** Average performance levels in deeper wells (layer > 1) from previous (V1) model.

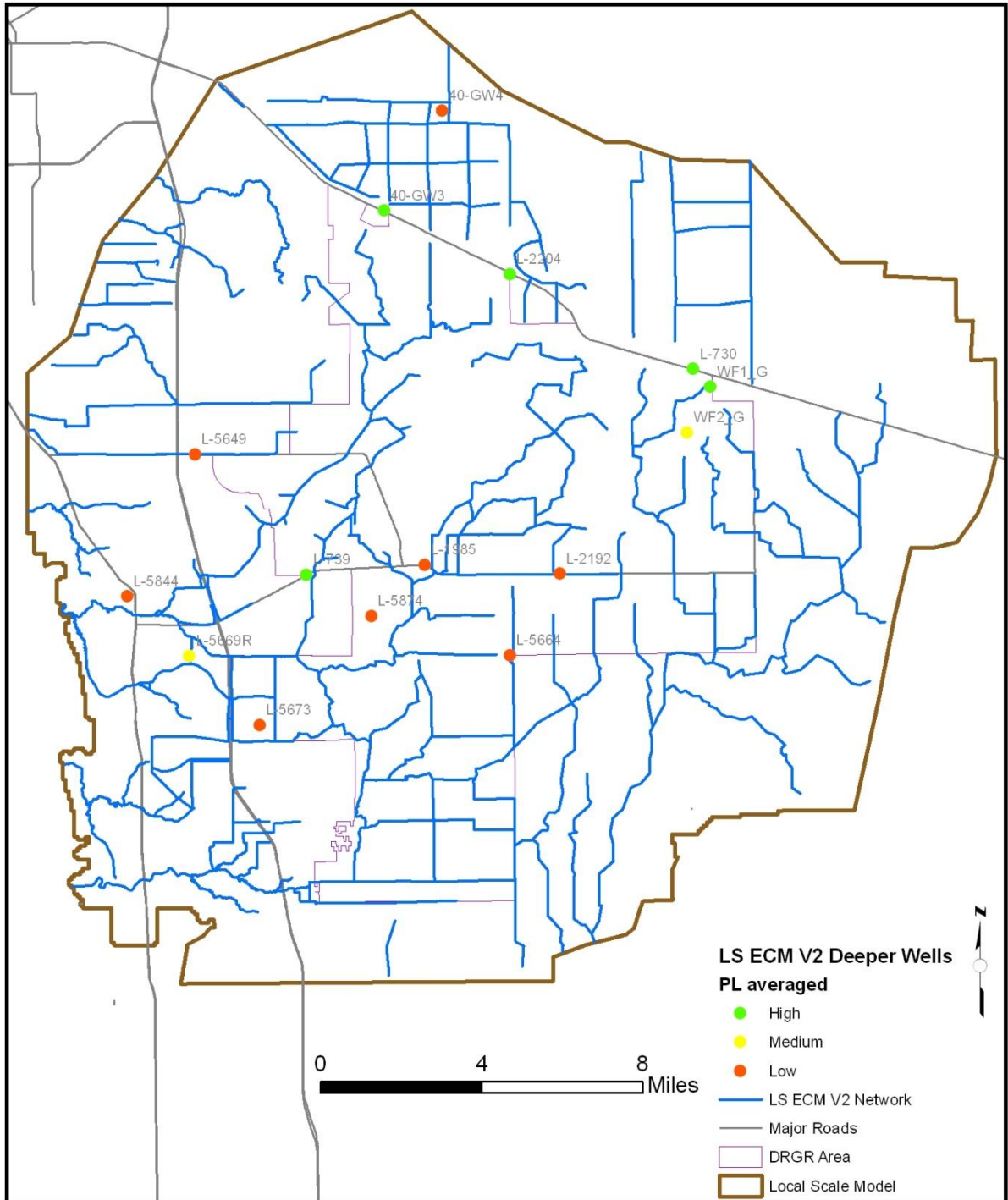
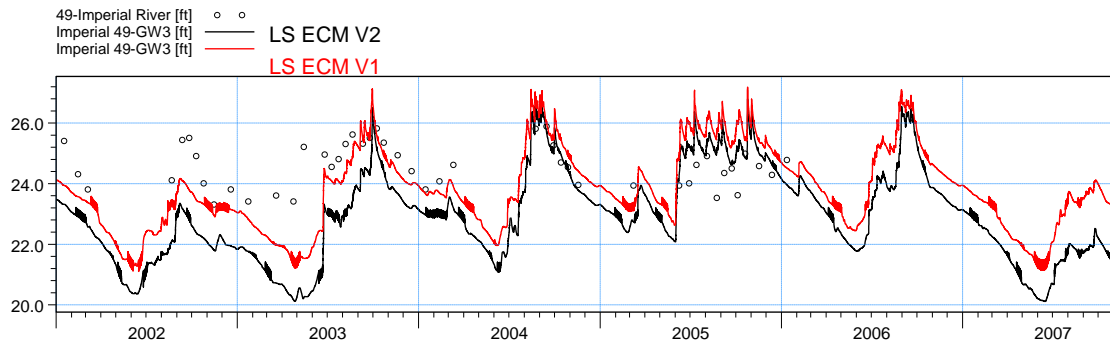
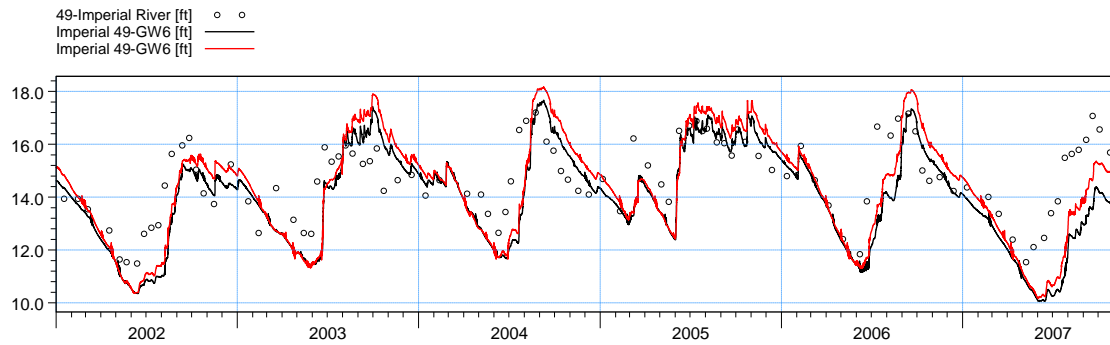


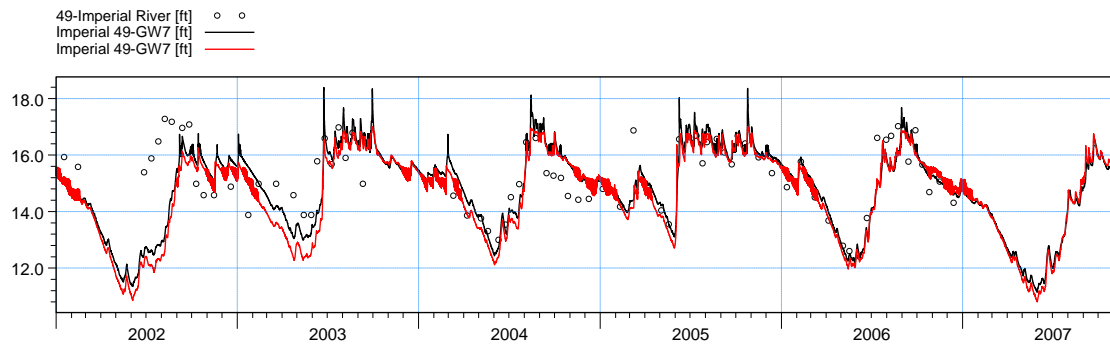
**Figure F6.** Average performance levels in deeper wells (layer > 1) from new (V2) model.



ME=0.928667  
 MAE=1.31542  
 RMSE=1.62539  
 STDres=1.33397  
 R(Correlation)=0.367991  
 R2(Nash\_Sutcliffe)=-4.11759

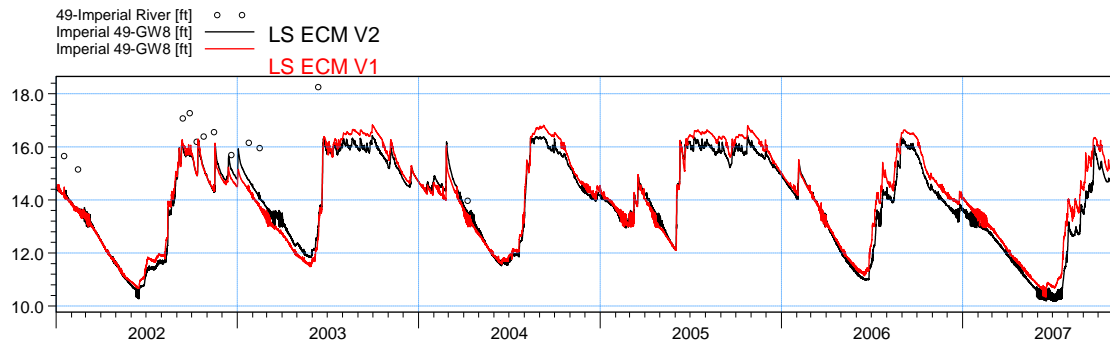


ME=0.760025  
 MAE=1.16258  
 RMSE=1.5387  
 STDres=1.3379  
 R(Correlation)=0.72251  
 R2(Nash\_Sutcliffe)=-0.11579

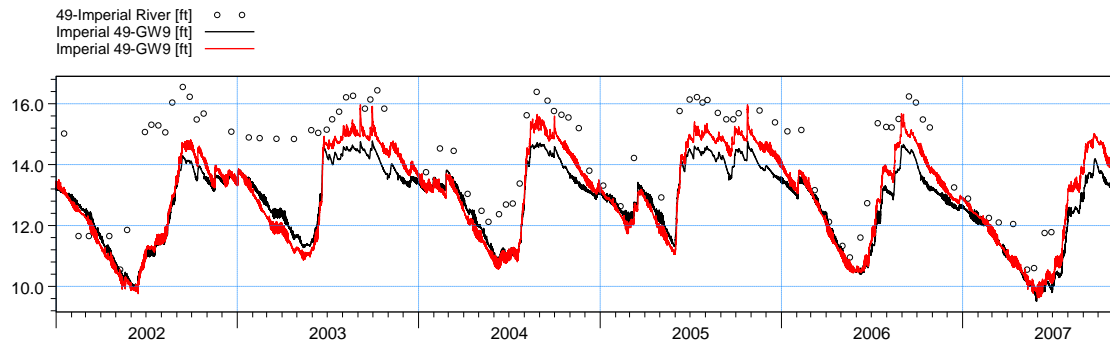


ME=0.195154  
 MAE=0.783466  
 RMSE=1.13887  
 STDres=1.12203  
 R(Correlation)=0.60994  
 R2(Nash\_Sutcliffe)=0.117423

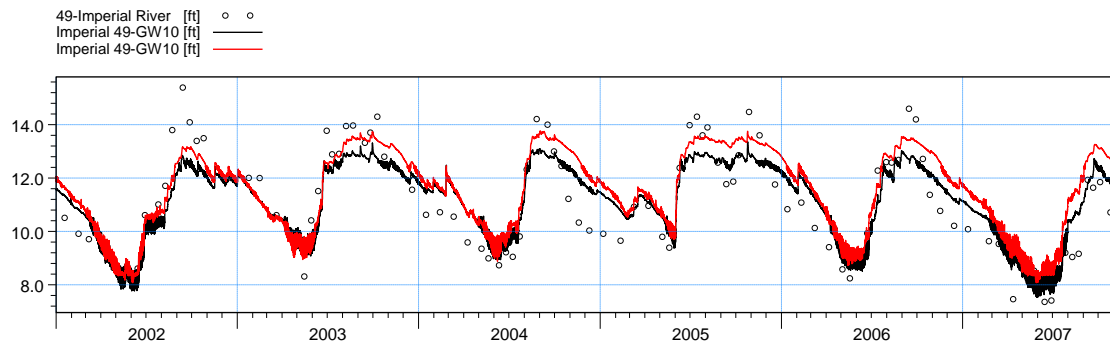
**Figure F7.** Water level at stations 49-GW3, 49-GW6 and 49-GW7.



ME=1.64345  
 MAE=1.64345  
 RMSE=2.02825  
 STDres=1.18864  
 R(Correlation)=0.234107  
 R2(Nash\_Sutcliffe)=-2.80765

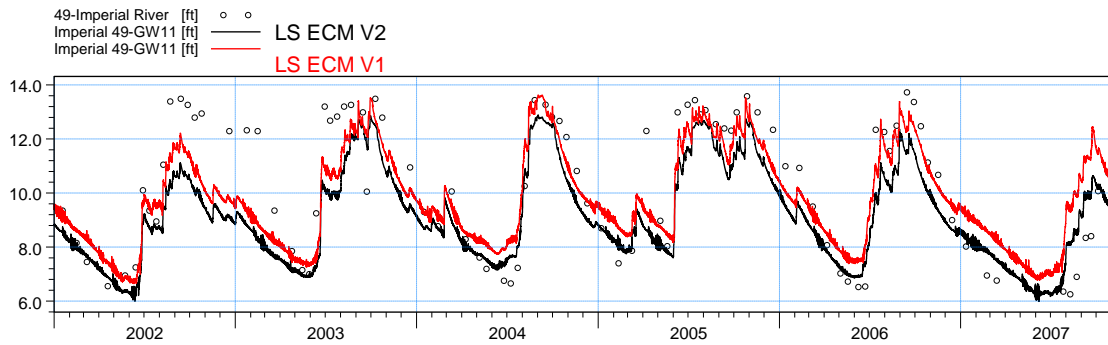


ME=1.53249  
 MAE=1.56704  
 RMSE=1.8135  
 STDres=0.969677  
 R(Correlation)=0.822169  
 R2(Nash\_Sutcliffe)=-0.135542

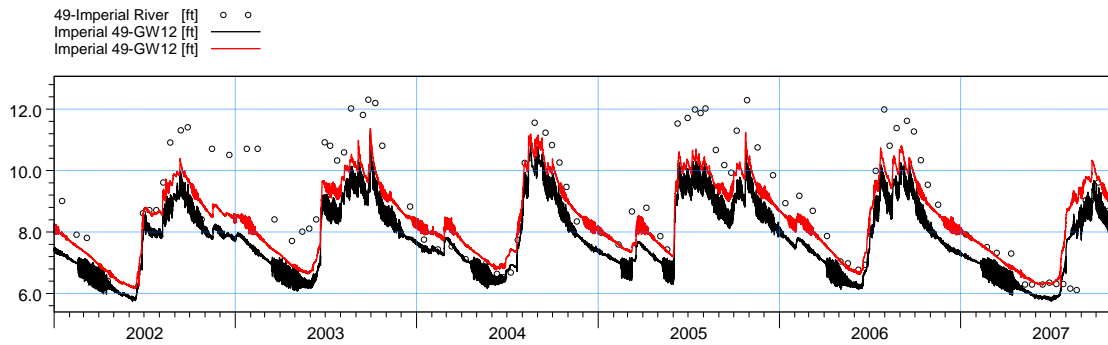


ME=-0.0185733  
 MAE=0.807532  
 RMSE=0.957893  
 STDres=0.957713  
 R(Correlation)=0.880488  
 R2(Nash\_Sutcliffe)=0.752261

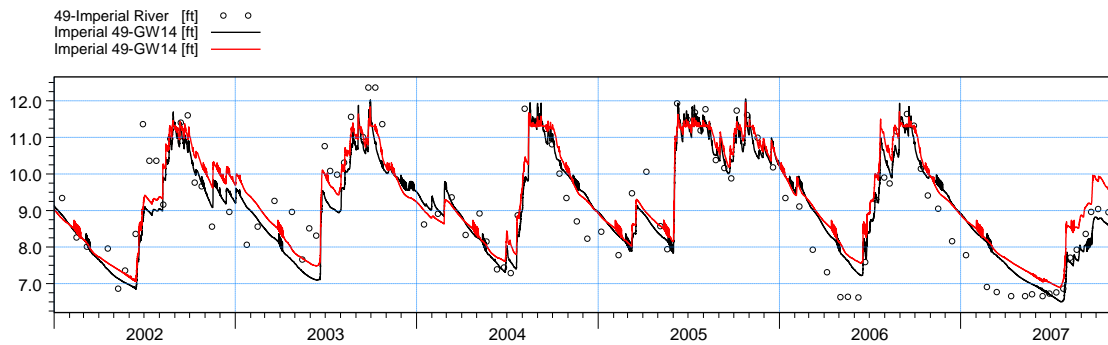
**Figure F8.** Water level at stations 49-GW8, 49-GW9 and 49-GW10.



ME=0.884991  
 MAE=1.23019  
 RMSE=1.56555  
 STDres=1.29141  
 R(Correlation)=0.86854  
 R2(Nash\_Sutcliffe)=0.598687



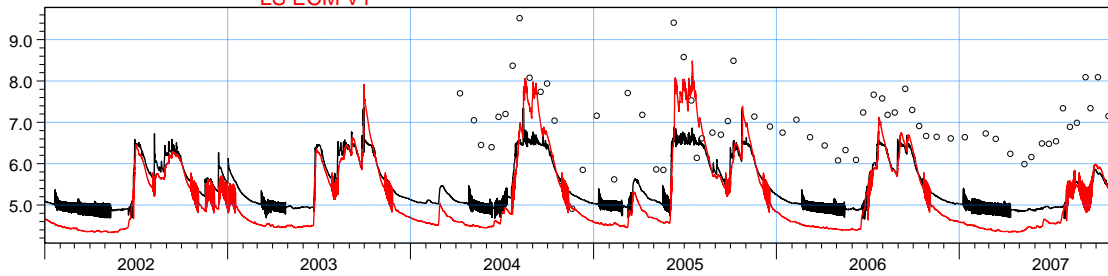
ME=1.161  
 MAE=1.24364  
 RMSE=1.47802  
 STDres=0.914669  
 R(Correlation)=0.901193  
 R2(Nash\_Sutcliffe)=0.330969



ME=0.116818  
 MAE=0.614708  
 RMSE=0.783266  
 STDres=0.774506  
 R(Correlation)=0.874479  
 R2(Nash\_Sutcliffe)=0.759295

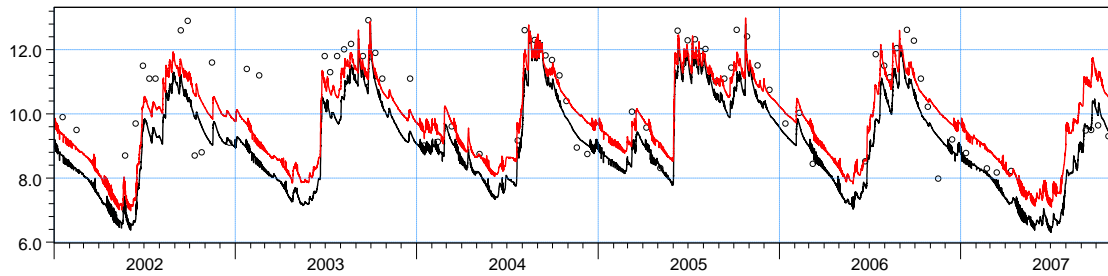
**Figure F9.** Water level at stations 49-GW11, 49-GW12 and 49-GW14.

49-Imperial River [ft] ○ ○  
 Imperial 49-GW15 [ft] — LS ECM V2  
 Imperial 49-GW15 [ft] — LS ECM V1



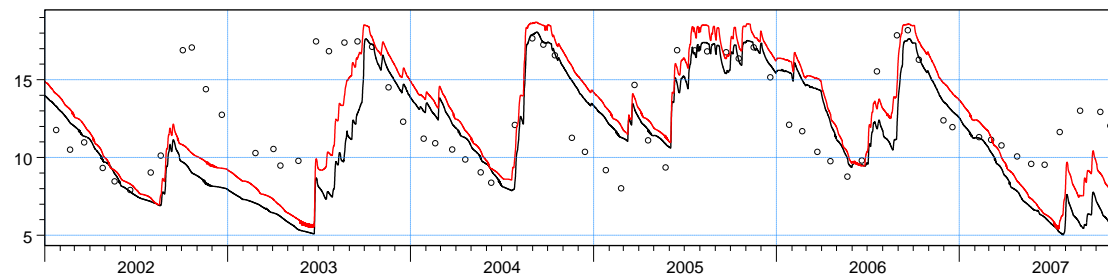
ME=1.54118  
 MAE=1.56087  
 RMSE=1.69222  
 STDres=0.698843  
 R(Correlation)=0.5745  
 R2(Nash\_Sutcliffe)=-3.01491

49L-Leitner Cr [ft] ○ ○  
 Leitner 49L-GW1 [ft] —  
 Leitner 49L-GW1 [ft] —



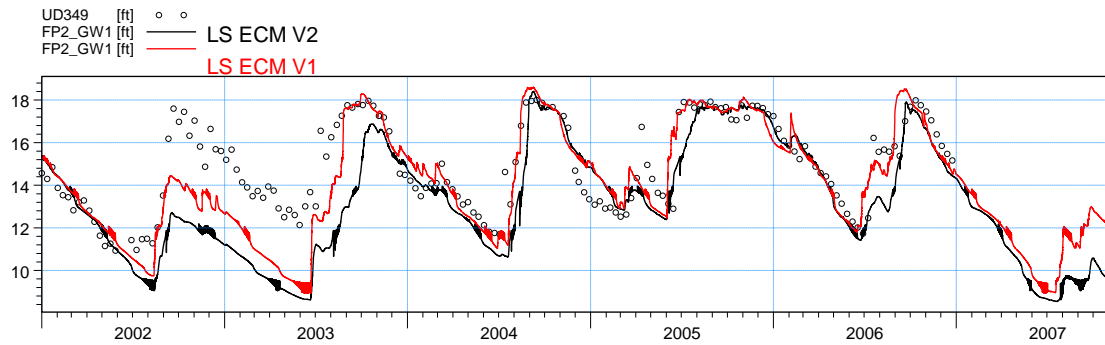
ME=0.852282  
 MAE=0.992982  
 RMSE=1.208  
 STDres=0.856081  
 R(Correlation)=0.807232  
 R2(Nash\_Sutcliffe)=0.306173

L-1985 [ft] ○ ○  
 L-1985 [ft] —  
 L-1985 [ft] —

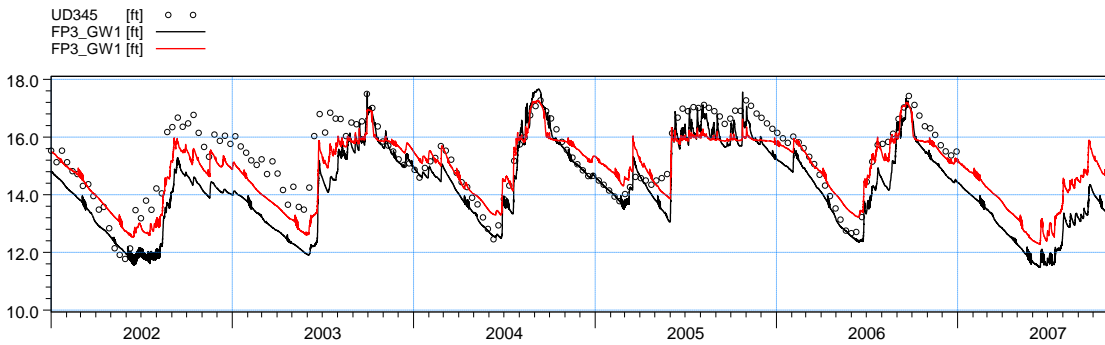


ME=1.19071  
 MAE=2.65966  
 RMSE=3.56893  
 STDres=3.36444  
 R(Correlation)=0.517265  
 R2(Nash\_Sutcliffe)=-0.275658

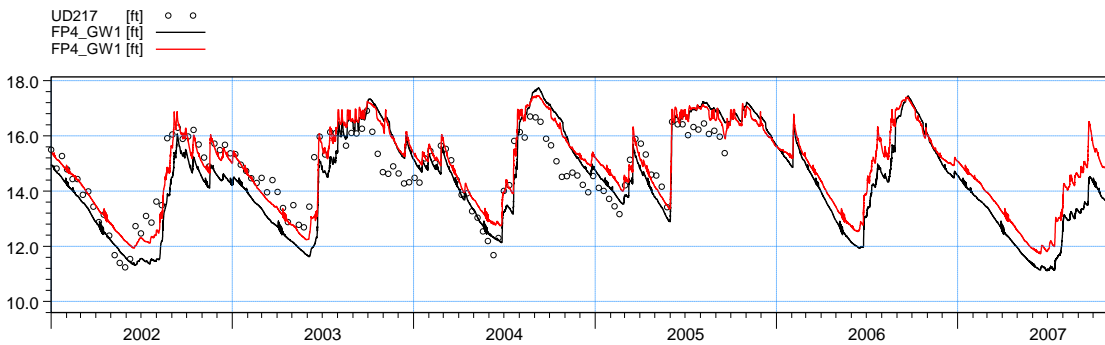
**Figure F10.** Water level at stations 49-GW15, 49L-GW1 and L-1985.



ME=1.2566  
 MAE=1.53616  
 RMSE=2.19289  
 STDres=1.79715  
 R(Correlation)=0.706801  
 R2(Nash\_Sutcliffe)=-0.125362

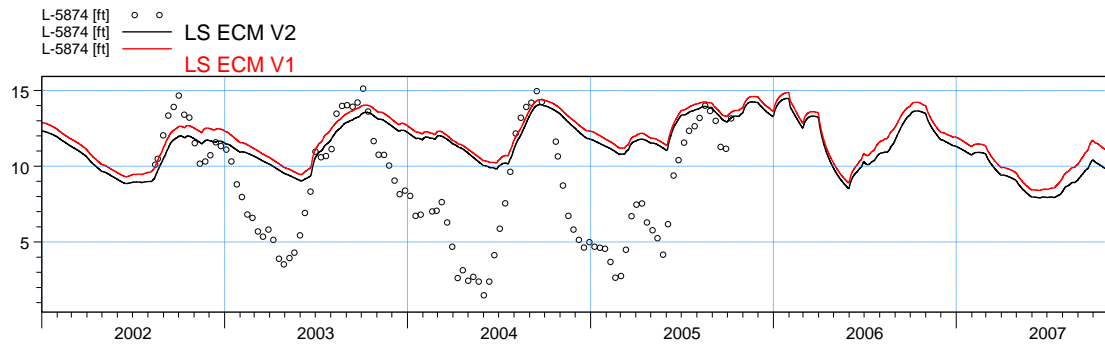


ME=0.820998  
 MAE=0.855789  
 RMSE=1.09537  
 STDres=0.725123  
 R(Correlation)=0.852103  
 R2(Nash\_Sutcliffe)=0.296092

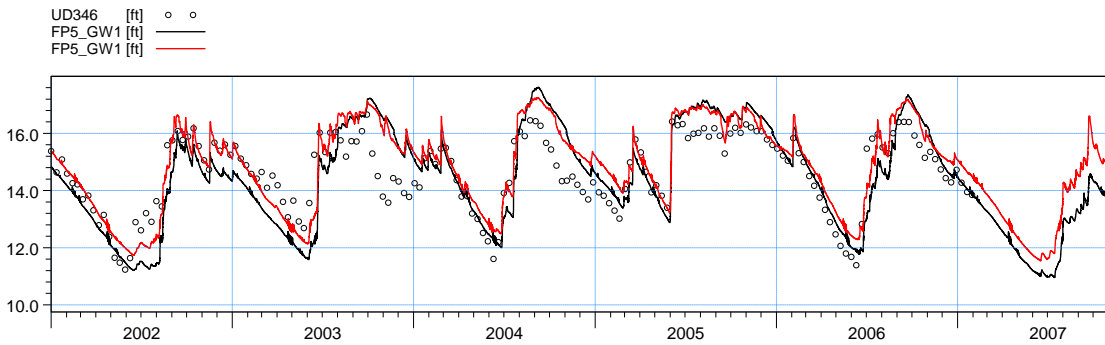


ME=0.196406  
 MAE=0.785355  
 RMSE=0.945135  
 STDres=0.924502  
 R(Correlation)=0.838132  
 R2(Nash\_Sutcliffe)=0.485834

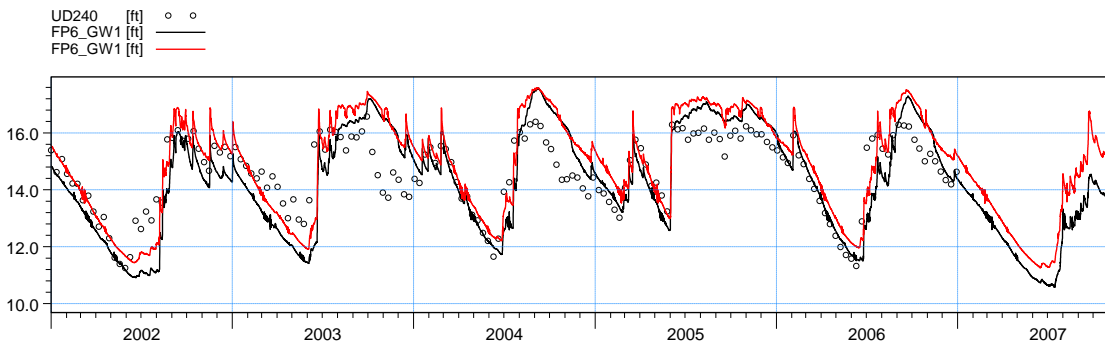
**Figure F11.** Water level at stations FP2\_GW1, FP3\_GW1 and FP4\_GW1.



ME=-3.03926  
 MAE=3.51852  
 RMSE=4.36571  
 STDres=3.13406  
 R(Correlation)=0.660625  
 R2(Nash\_Sutcliffe)=-0.30949

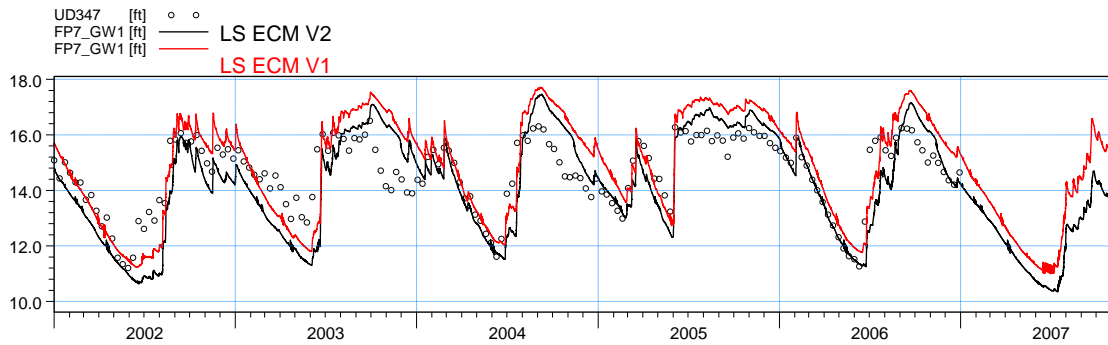


ME=0.00606229  
 MAE=0.74983  
 RMSE=0.946131  
 STDres=0.946112  
 R(Correlation)=0.821293  
 R2(Nash\_Sutcliffe)=0.464288

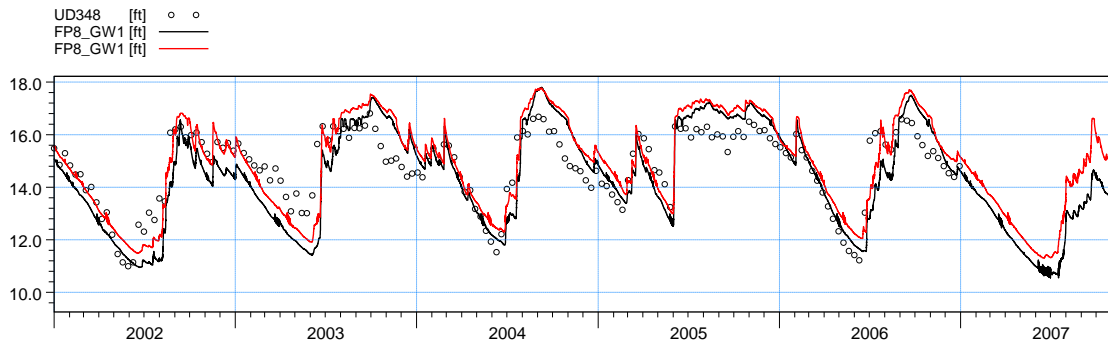


ME=0.0994867  
 MAE=0.790845  
 RMSE=1.01067  
 STDres=1.00576  
 R(Correlation)=0.824413  
 R2(Nash\_Sutcliffe)=0.385011

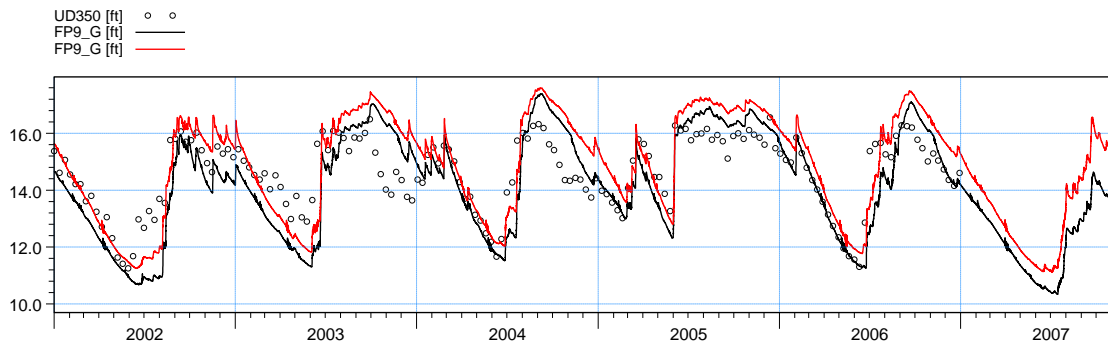
**Figure F12.** Water level at stations L-5874, FP5\_GW1 and FP6\_GW1.



ME=0.253485  
 MAE=0.801306  
 RMSE=1.03486  
 STDres=1.00333  
 R(Correlation)=0.835082  
 R2(Nash\_Sutcliffe)=0.357735

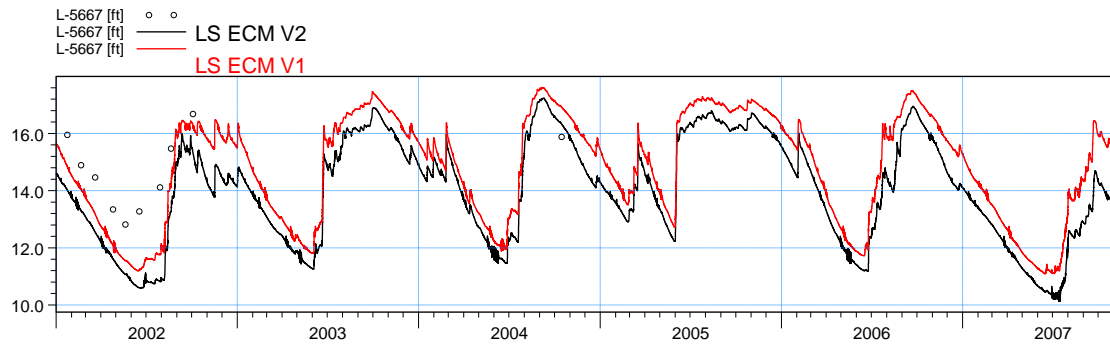


ME=0.171644  
 MAE=0.793099  
 RMSE=0.987878  
 STDres=0.972853  
 R(Correlation)=0.844639  
 R2(Nash\_Sutcliffe)=0.49894

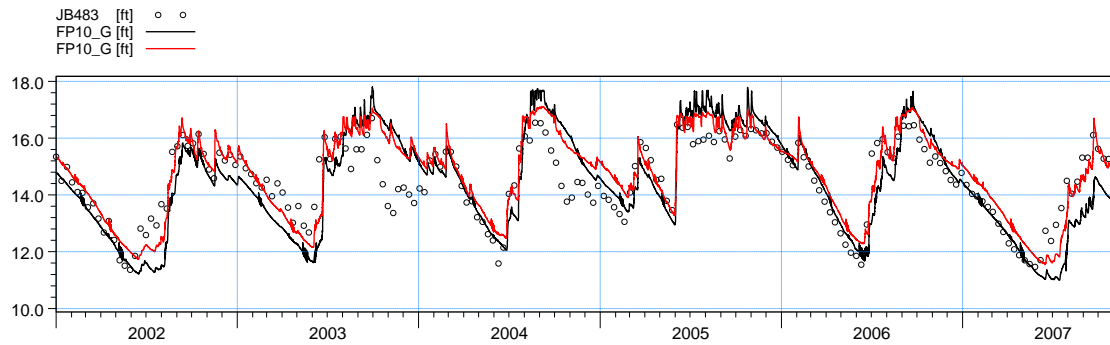


ME=0.268576  
 MAE=0.814621  
 RMSE=1.0513  
 STDres=1.01641  
 R(Correlation)=0.826398  
 R2(Nash\_Sutcliffe)=0.322206

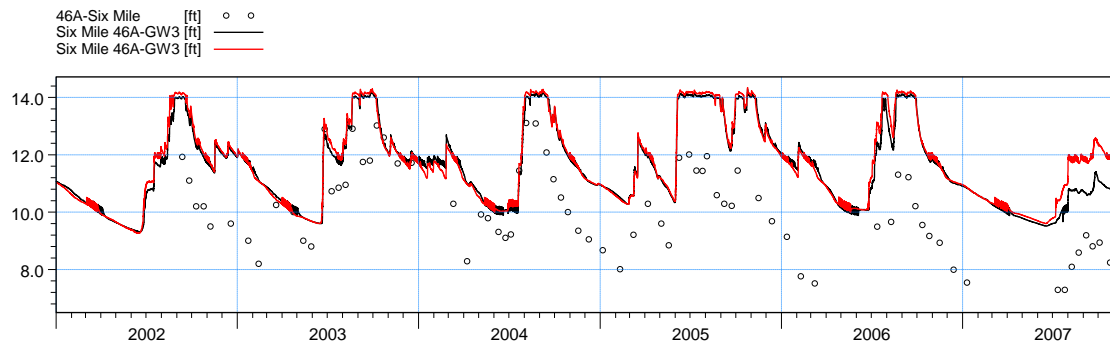
**Figure F13.** Water level at stations FP7\_GW1, FP8\_GW1 and FP9\_G.



ME=1.79898  
 MAE=1.88811  
 RMSE=2.02046  
 STDres=0.919754  
 R(Correlation)=0.893708  
 R2(Nash\_Sutcliffe)=-1.6552

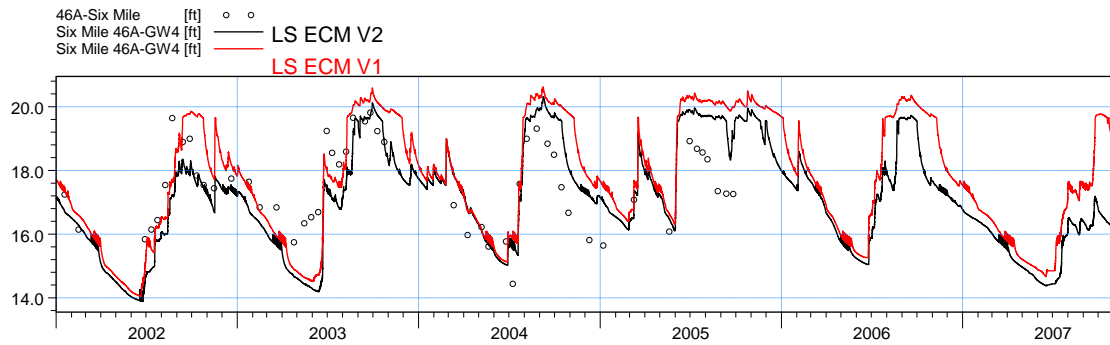


ME=0.0903254  
 MAE=0.767146  
 RMSE=0.990473  
 STDres=0.986345  
 R(Correlation)=0.820547  
 R2(Nash\_Sutcliffe)=0.458677

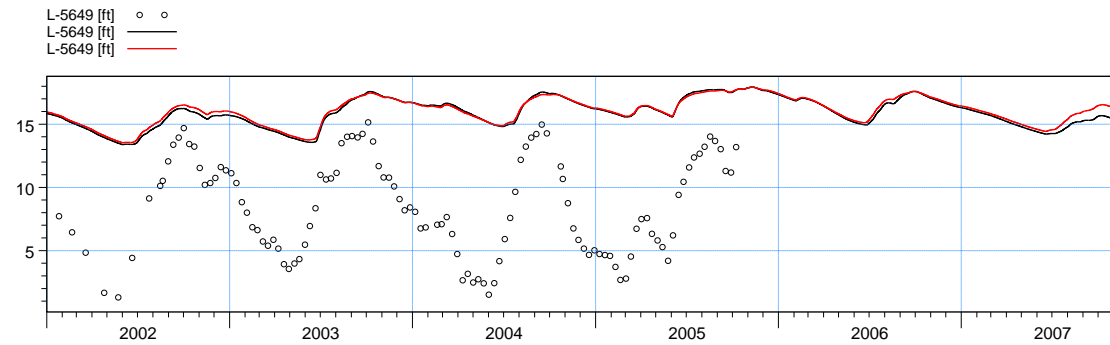


ME=-1.96547  
 MAE=1.9787  
 RMSE=2.19747  
 STDres=0.982751  
 R(Correlation)=0.76932  
 R2(Nash\_Sutcliffe)=-1.14887

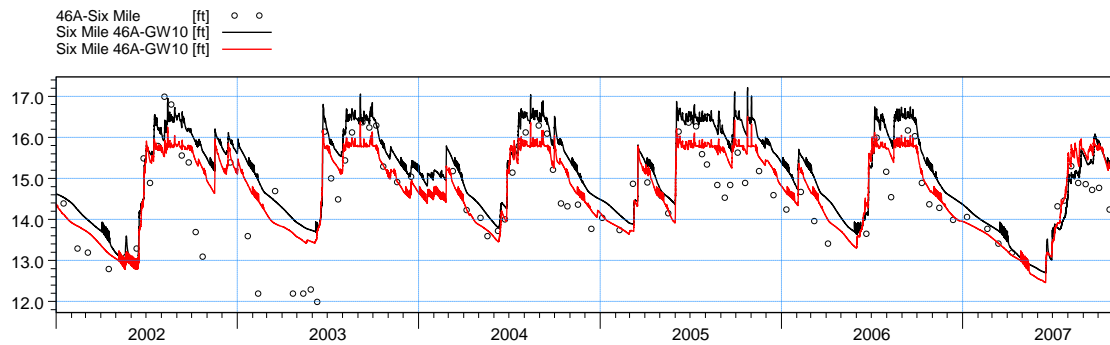
**Figure F14.** Water level at stations L-5667, FP10\_G and 46A-GW3.



ME=0.0693236  
 MAE=0.997836  
 RMSE=1.20518  
 STDres=1.20318  
 R(Correlation)=0.720727  
 R2(Nash\_Sutcliffe)=0.144251

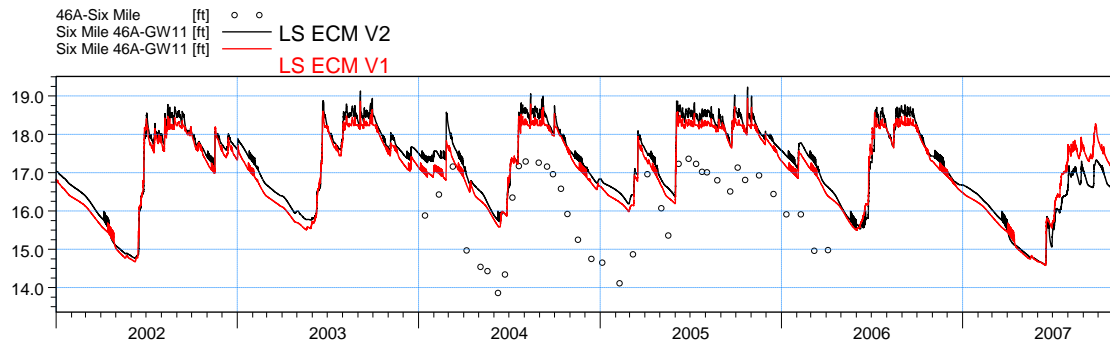


ME=-7.38298  
 MAE=7.38298  
 RMSE=8.09769  
 STDres=3.32631  
 R(Correlation)=0.576726  
 R2(Nash\_Sutcliffe)=-3.49379

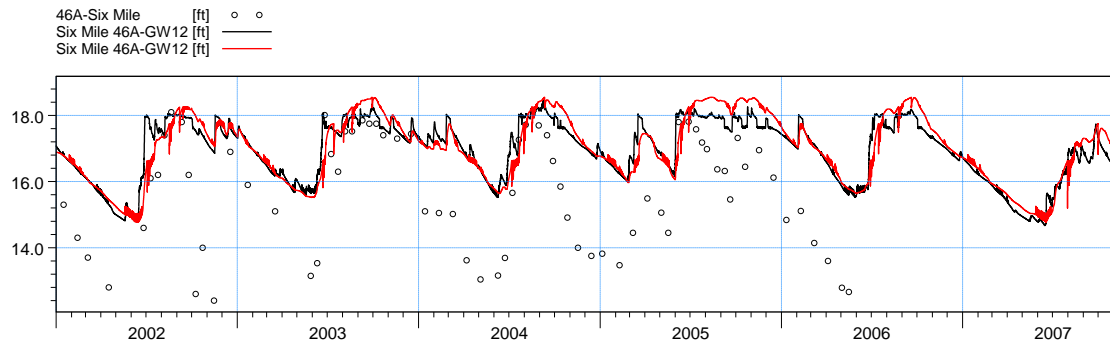


ME=-0.627015  
 MAE=0.735143  
 RMSE=0.90816  
 STDres=0.656967  
 R(Correlation)=0.810578  
 R2(Nash\_Sutcliffe)=0.333214

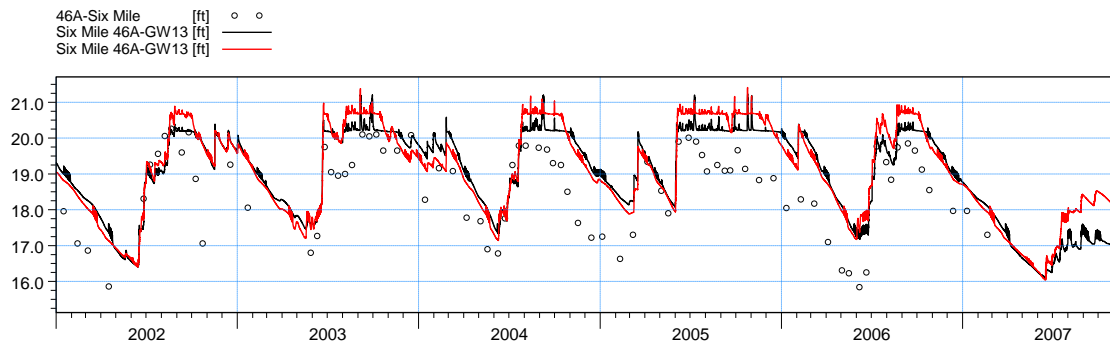
**Figure F15.** Water level at stations 46A-GW4, L-5649 and 46A-GW10.



ME=-1.48578  
 MAE=1.48578  
 RMSE=1.54828  
 STDres=0.435471  
 R(Correlation)=0.926756  
 R2(Nash\_Sutcliffe)=-1.08579

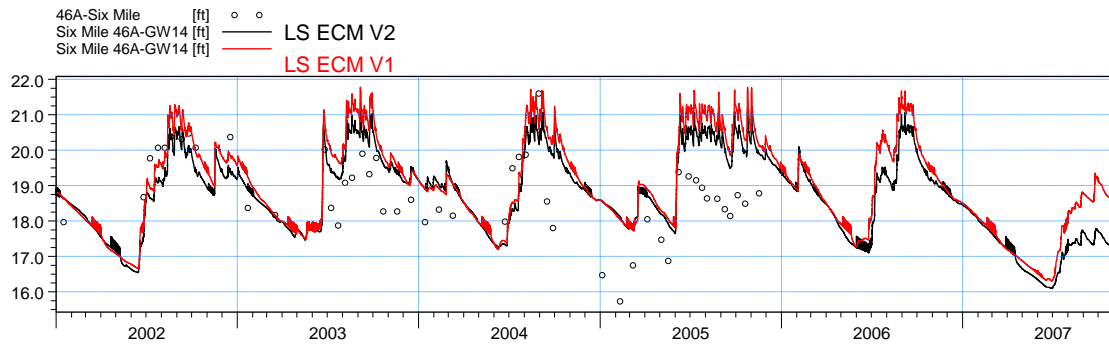


ME=-1.63555  
 MAE=1.6484  
 RMSE=2.00175  
 STDres=1.1541  
 R(Correlation)=0.832697  
 R2(Nash\_Sutcliffe)=-0.386939

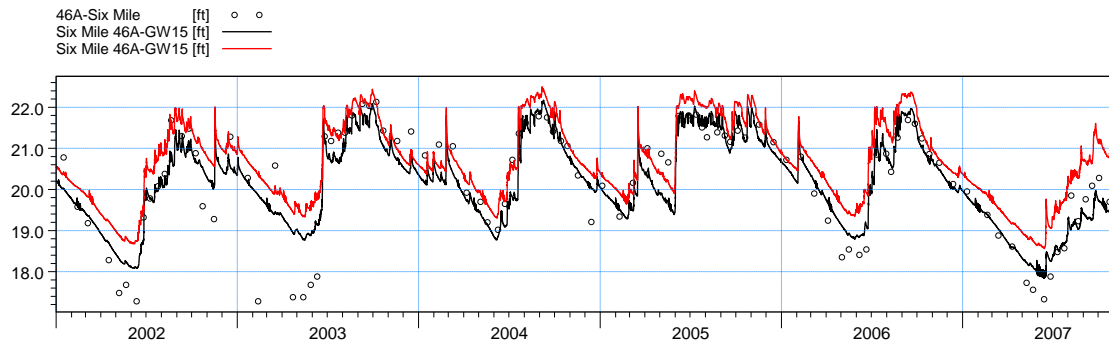


ME=-0.835668  
 MAE=0.907148  
 RMSE=1.07451  
 STDres=0.675454  
 R(Correlation)=0.82112  
 R2(Nash\_Sutcliffe)=0.172915

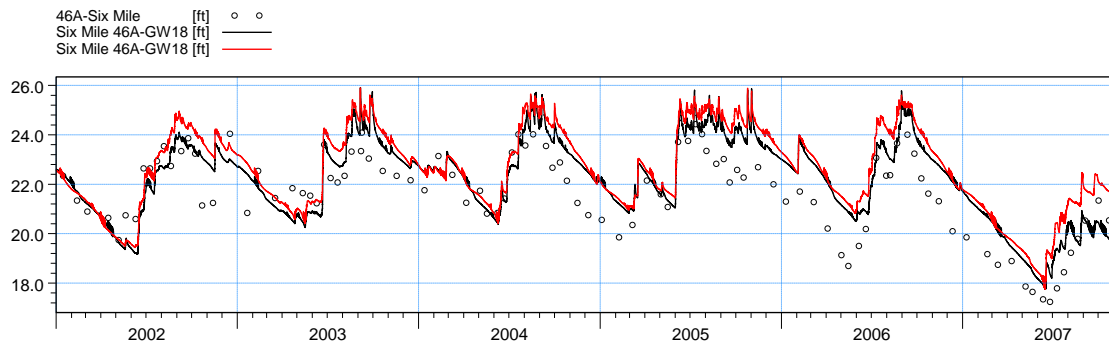
**Figure F16.** Water level at stations 46A-GW11, 46A-GW12 and 46A-GW13.



ME=-0.633166  
 MAE=1.04854  
 RMSE=1.17828  
 STDres=0.993704  
 R(Correlation)=0.536455  
 R2(Nash\_Sutcliffe)=-0.100747

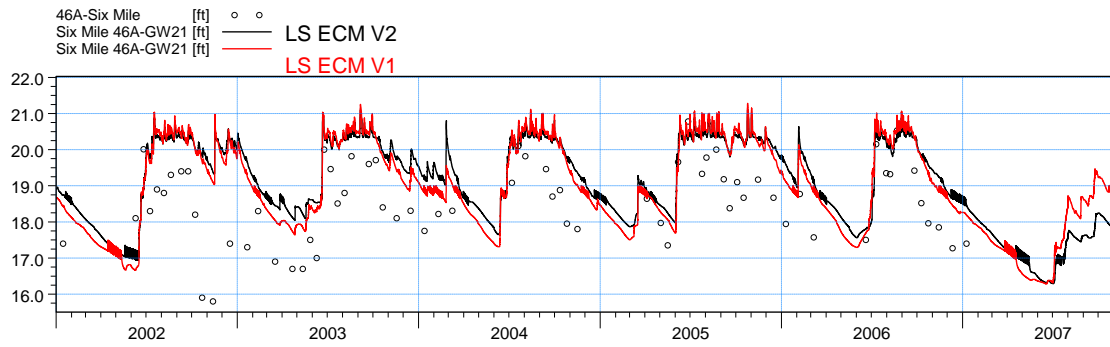


ME=0.0132922  
 MAE=0.420701  
 RMSE=0.579842  
 STDres=0.57969  
 R(Correlation)=0.910394  
 R2(Nash\_Sutcliffe)=0.817

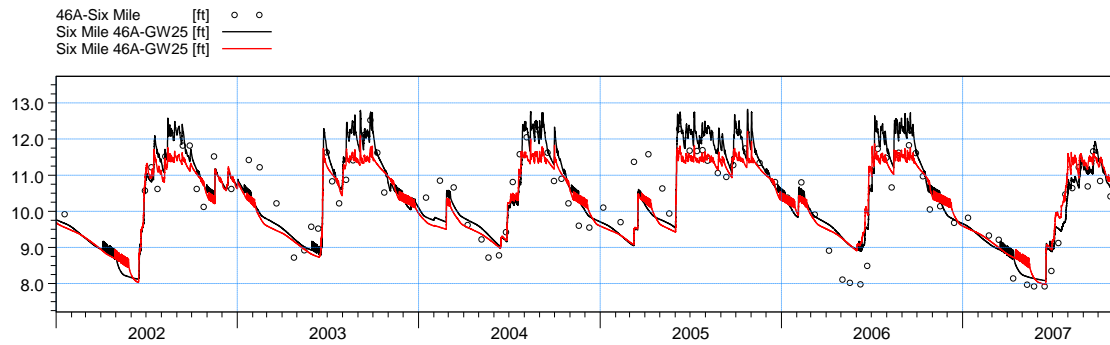


ME=-0.584637  
 MAE=0.918928  
 RMSE=1.07369  
 STDres=0.90056  
 R(Correlation)=0.857026  
 R2(Nash\_Sutcliffe)=0.58789

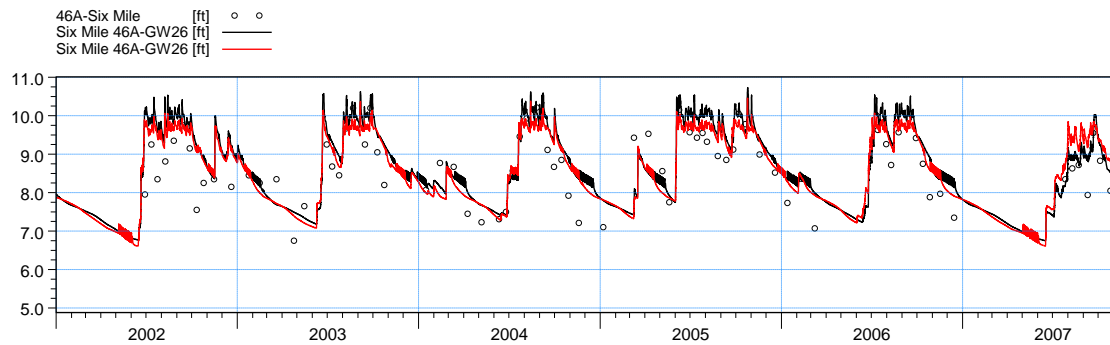
**Figure F17.** Water level at stations 46A-GW14, 46A-GW15 and 46A-GW18.



ME=-1.10457  
 MAE=1.17259  
 RMSE=1.36703  
 STDres=0.805412  
 R(Correlation)=0.702932  
 R2(Nash\_Sutcliffe)=-0.457639

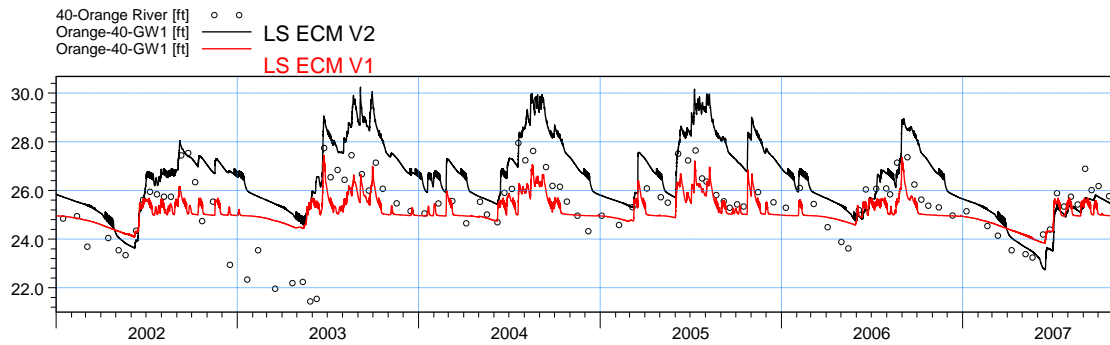


ME=-0.0967145  
 MAE=0.483999  
 RMSE=0.601889  
 STDres=0.594068  
 R(Correlation)=0.872256  
 R2(Nash\_Sutcliffe)=0.737757

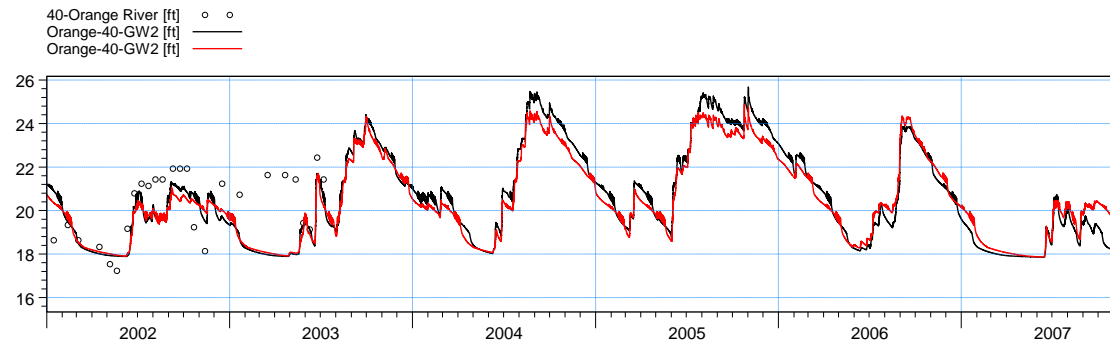


ME=-0.372104  
 MAE=0.526823  
 RMSE=0.667543  
 STDres=0.554213  
 R(Correlation)=0.786185  
 R2(Nash\_Sutcliffe)=0.384867

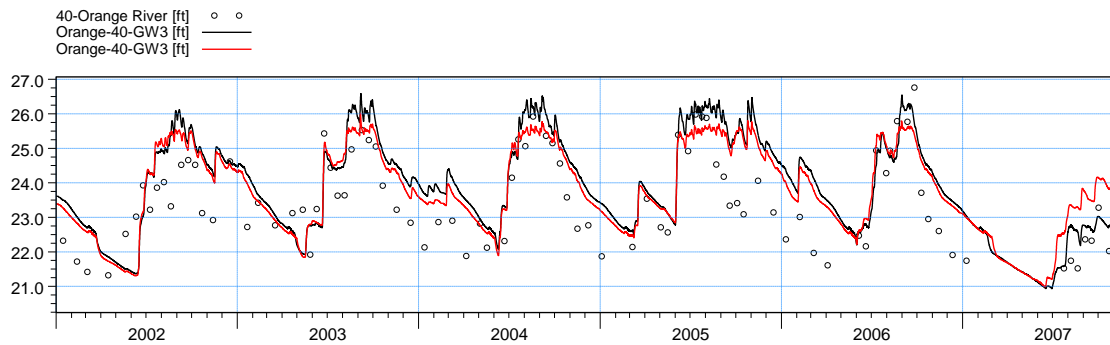
**Figure F18.** Water level at stations 46A-GW21, 46A-GW25 and 46A-GW26.



ME=-1.16861  
 MAE=1.34197  
 RMSE=1.64971  
 STDres=1.16443  
 R(Correlation)=0.672008  
 R2(Nash\_Sutcliffe)=-0.429208

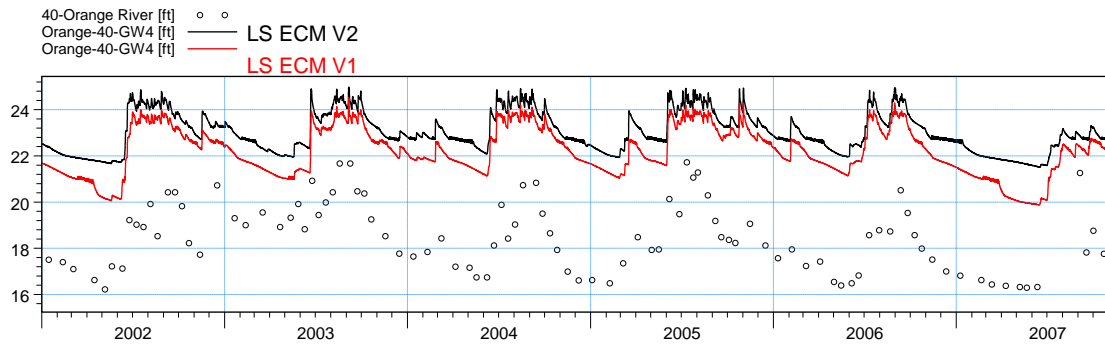


ME=0.800792  
 MAE=1.28491  
 RMSE=1.64867  
 STDres=1.44112  
 R(Correlation)=0.457632  
 R2(Nash\_Sutcliffe)=-0.163253

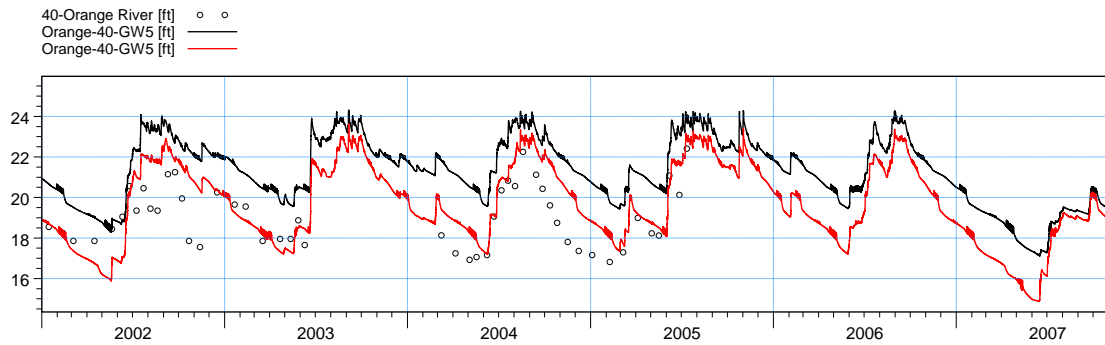


ME=-0.734208  
 MAE=0.938841  
 RMSE=1.09181  
 STDres=0.808072  
 R(Correlation)=0.805109  
 R2(Nash\_Sutcliffe)=0.312379

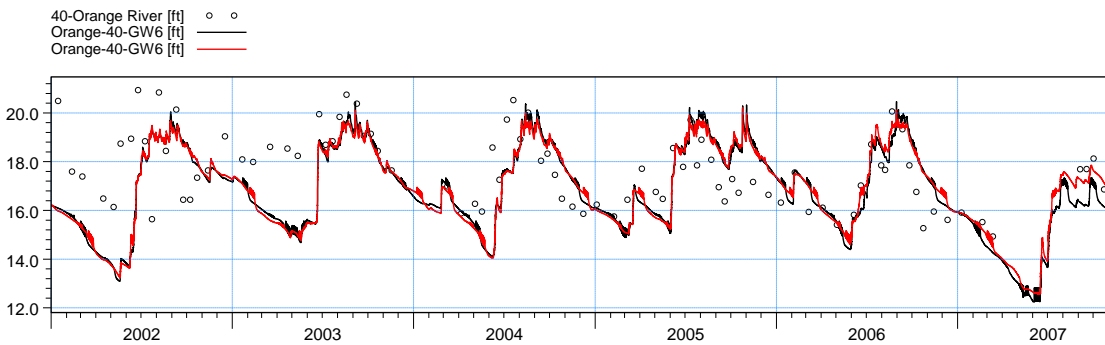
**Figure F19.** Water level at stations 40-GW1, 40-GW2 and 40-GW3.



ME=-4.64784  
 MAE=4.64784  
 RMSE=4.74232  
 STDres=0.941899  
 R(Correlation)=0.795238  
 R2(Nash\_Sutcliffe)=-9.35542

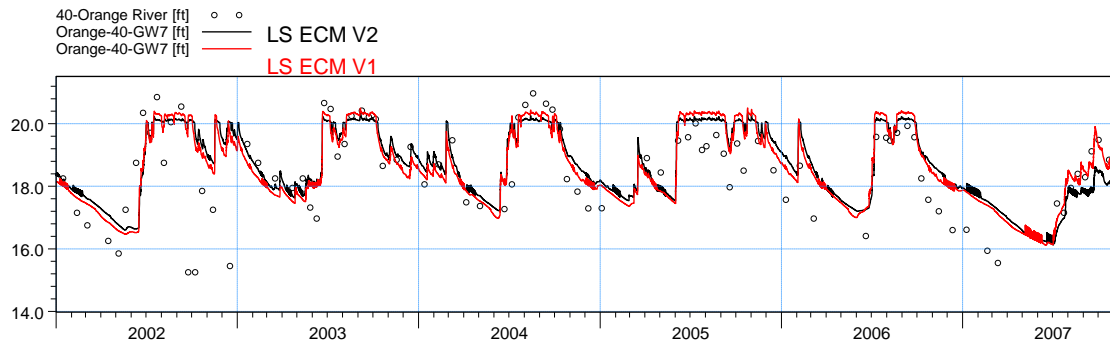


ME=-2.48622  
 MAE=2.49422  
 RMSE=2.68792  
 STDres=1.02157  
 R(Correlation)=0.75197  
 R2(Nash\_Sutcliffe)=-2.38502

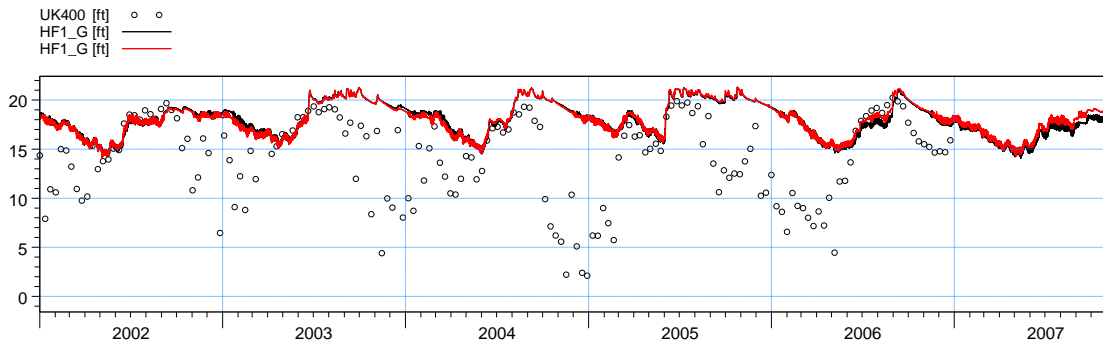


ME=0.416372  
 MAE=1.27452  
 RMSE=1.68279  
 STDres=1.63046  
 R(Correlation)=0.458984  
 R2(Nash\_Sutcliffe)=-0.278596

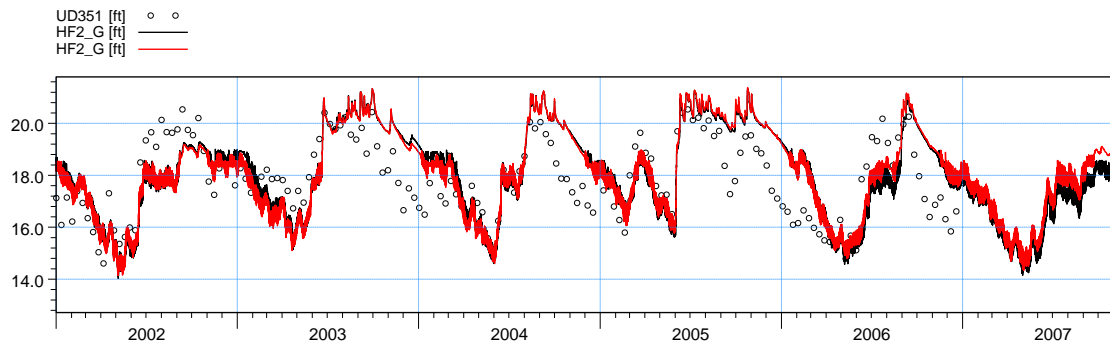
**Figure F20.** Water level at stations 40-GW4, 40-GW5 and 40-GW6.



ME=-0.453916  
 MAE=0.855878  
 RMSE=1.20032  
 STDres=1.11119  
 R(Correlation)=0.630409  
 R2(Nash\_Sutcliffe)=0.272248

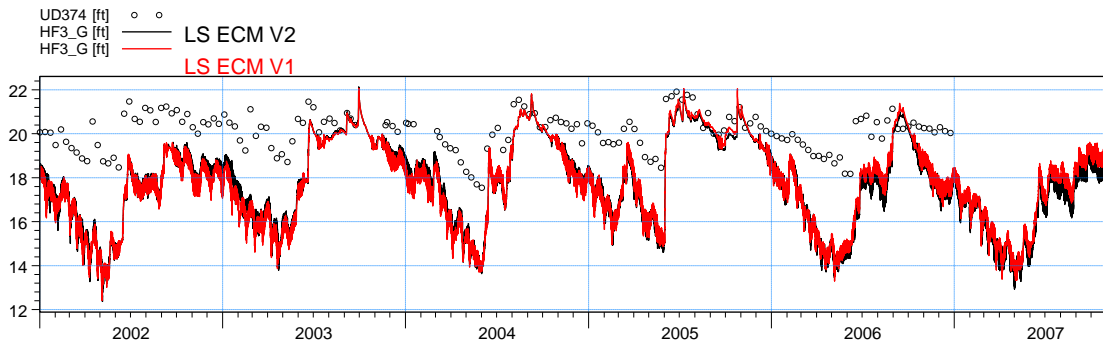


ME=-4.29685  
 MAE=4.50584  
 RMSE=6.05635  
 STDres=4.26807  
 R(Correlation)=0.217302  
 R2(Nash\_Sutcliffe)=-0.973993

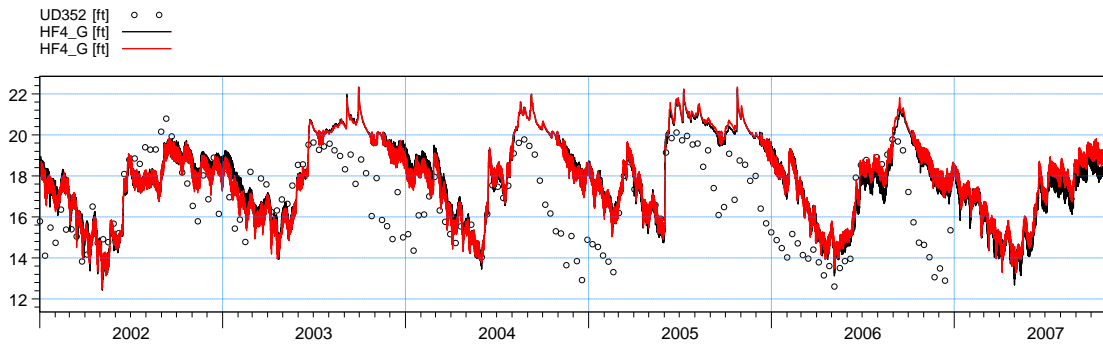


ME=-0.378918  
 MAE=1.10245  
 RMSE=1.30104  
 STDres=1.24464  
 R(Correlation)=0.686602  
 R2(Nash\_Sutcliffe)=0.243064

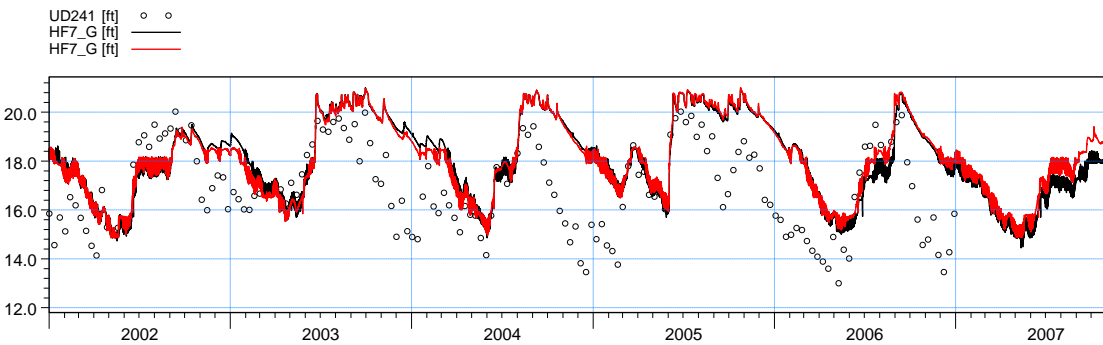
**Figure F21.** Water level at stations 40-GW7, HF1\_G and HF2\_G.



ME=2.224  
 MAE=2.24635  
 RMSE=2.58703  
 STDres=1.32157  
 R(Correlation)=0.807014  
 R2(Nash\_Sutcliffe)=-8.19052

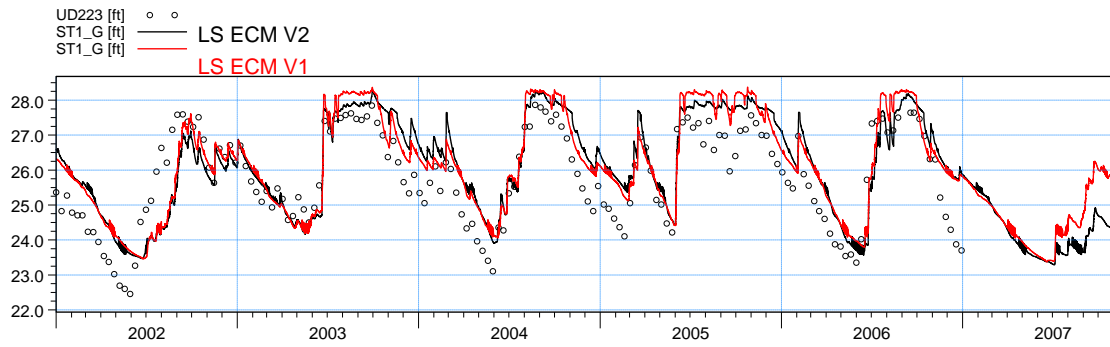


ME=-1.40059  
 MAE=1.83101  
 RMSE=2.23815  
 STDres=1.74575  
 R(Correlation)=0.604931  
 R2(Nash\_Sutcliffe)=-0.24648

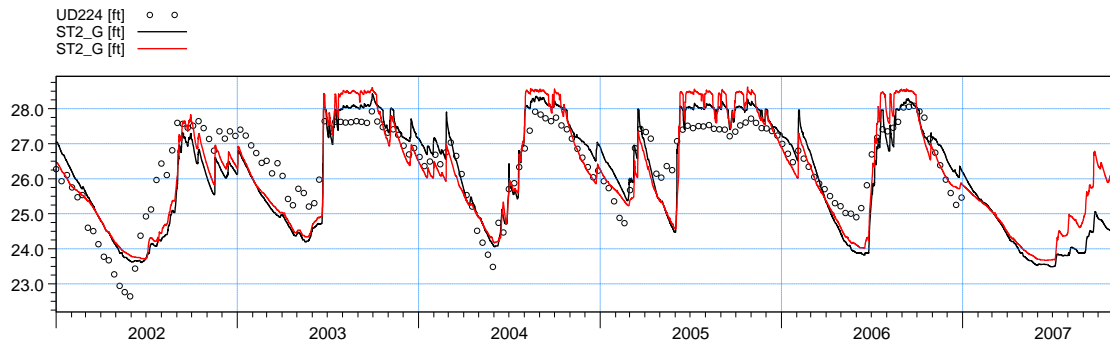


ME=-1.42636  
 MAE=1.75994  
 RMSE=2.14145  
 STDres=1.59728  
 R(Correlation)=0.556199  
 R2(Nash\_Sutcliffe)=-0.404011

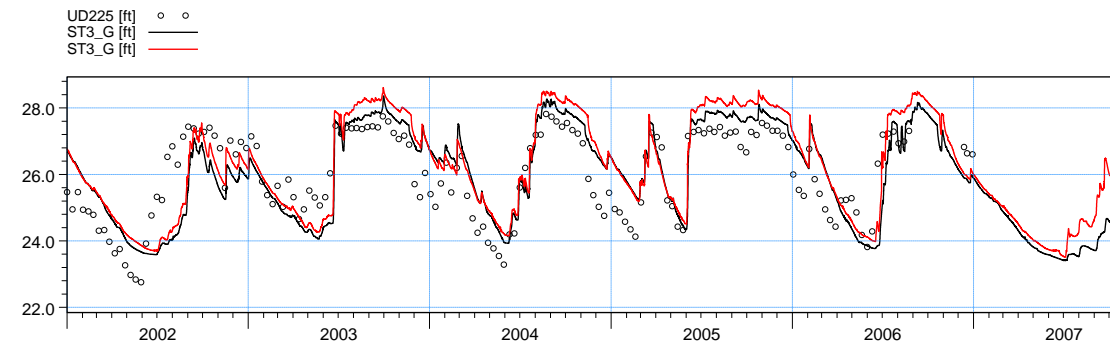
**Figure F22.** Water level at stations HF3\_G, HF4\_G and HF7\_G.



ME=-0.439627  
 MAE=0.779628  
 RMSE=0.912106  
 STDres=0.799165  
 R(Correlation)=0.82231  
 R2(Nash\_Sutcliffe)=0.550735

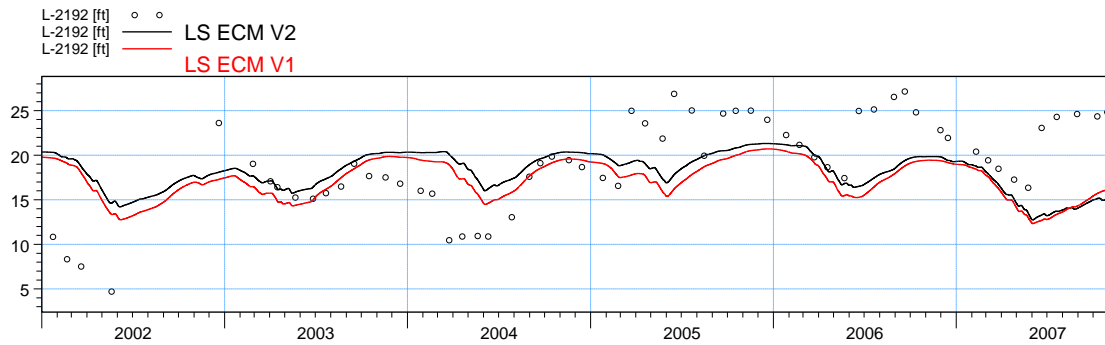


ME=0.0415042  
 MAE=0.633851  
 RMSE=0.756923  
 STDres=0.755784  
 R(Correlation)=0.838168  
 R2(Nash\_Sutcliffe)=0.611754

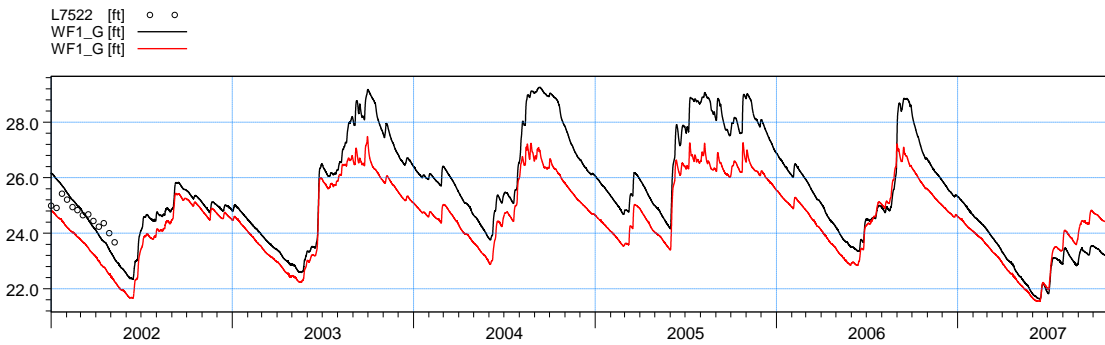


ME=-0.118018  
 MAE=0.747905  
 RMSE=0.908431  
 STDres=0.900733  
 R(Correlation)=0.762848  
 R2(Nash\_Sutcliffe)=0.496975

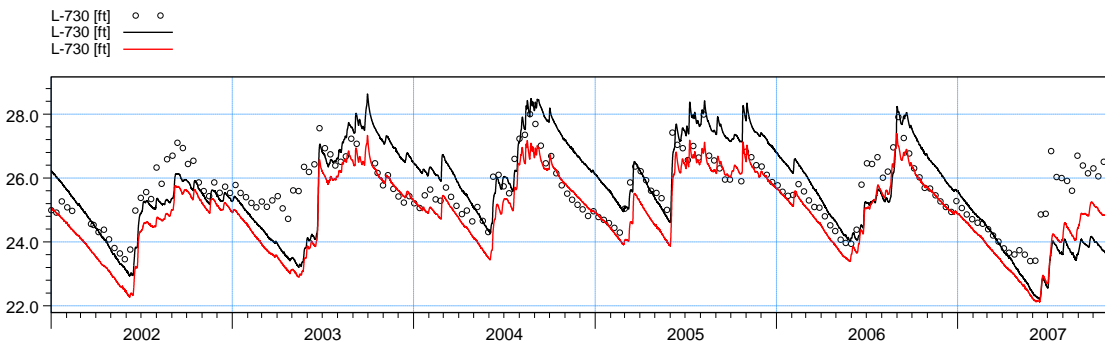
**Figure F23.** Water level at stations ST1\_G, ST2\_G and ST3\_G.



ME=0.757833  
 MAE=4.26817  
 RMSE=5.50089  
 STDres=5.44844  
 R(Correlation)=0.0637399  
 R2(Nash\_Sutcliffe)=-0.133474

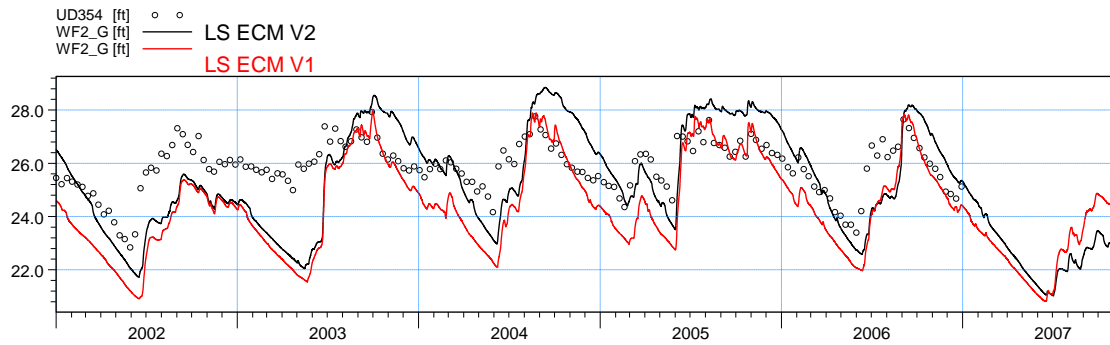


ME=-0.0147408  
 MAE=0.422168  
 RMSE=0.508144  
 STDres=0.507931  
 R(Correlation)=0.940139  
 R2(Nash\_Sutcliffe)=-0.0267335

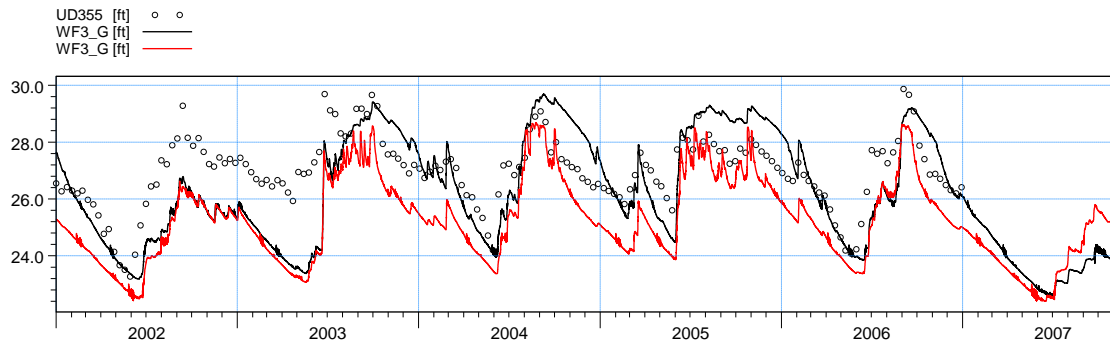


ME=0.0199252  
 MAE=0.862797  
 RMSE=1.08906  
 STDres=1.08888  
 R(Correlation)=0.645654  
 R2(Nash\_Sutcliffe)=-0.210692

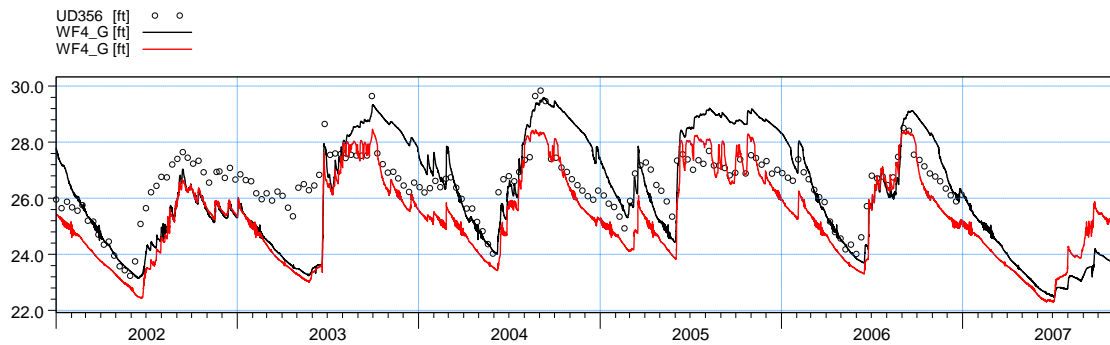
**Figure F24.** Water level at stations L-2192, WF1\_G and L-730.



ME=0.307578  
 MAE=1.24616  
 RMSE=1.48709  
 STDres=1.45494  
 R(Correlation)=0.623587  
 R2(Nash\_Sutcliffe)=-1.26022

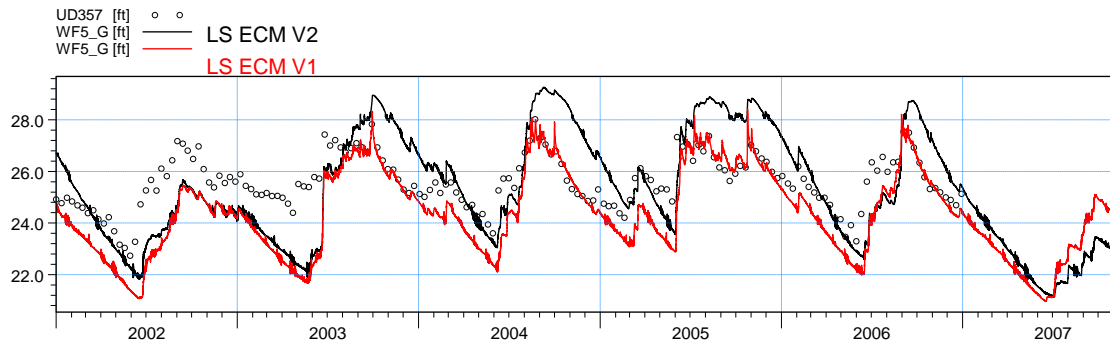


ME=0.417843  
 MAE=1.08771  
 RMSE=1.35914  
 STDres=1.29332  
 R(Correlation)=0.697686  
 R2(Nash\_Sutcliffe)=-0.173521

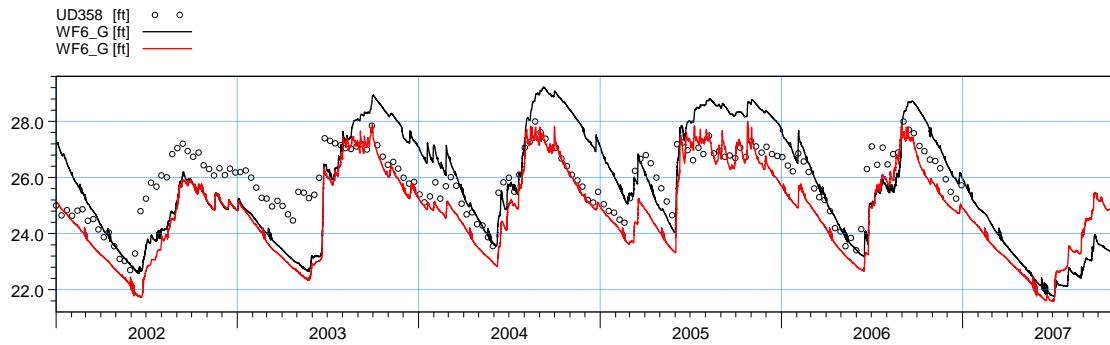


ME=-0.0678897  
 MAE=1.06785  
 RMSE=1.29757  
 STDres=1.29579  
 R(Correlation)=0.706617  
 R2(Nash\_Sutcliffe)=-0.33779

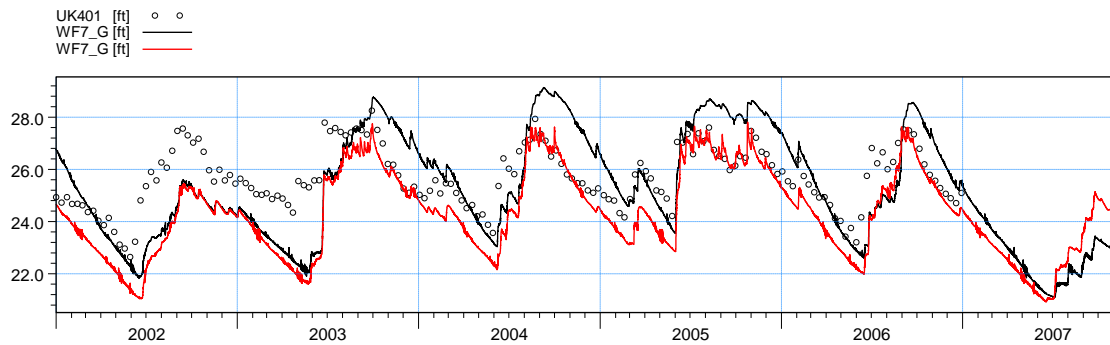
**Figure F25.** Water level at stations WF2\_G, WF3\_G and WF4\_G.



ME=-0.101636  
 MAE=1.29838  
 RMSE=1.52371  
 STDres=1.52032  
 R(Correlation)=0.640811  
 R2(Nash\_Sutcliffe)=-1.14789

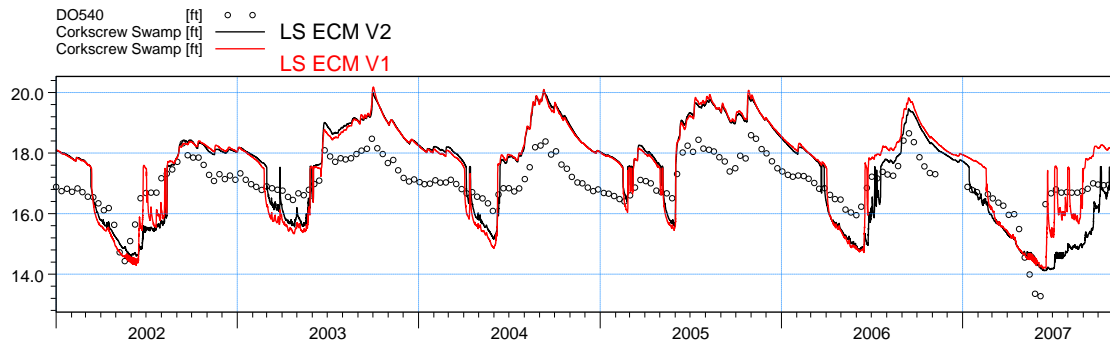


ME=-0.188608  
 MAE=1.1085  
 RMSE=1.29443  
 STDres=1.28062  
 R(Correlation)=0.705489  
 R2(Nash\_Sutcliffe)=-0.277809

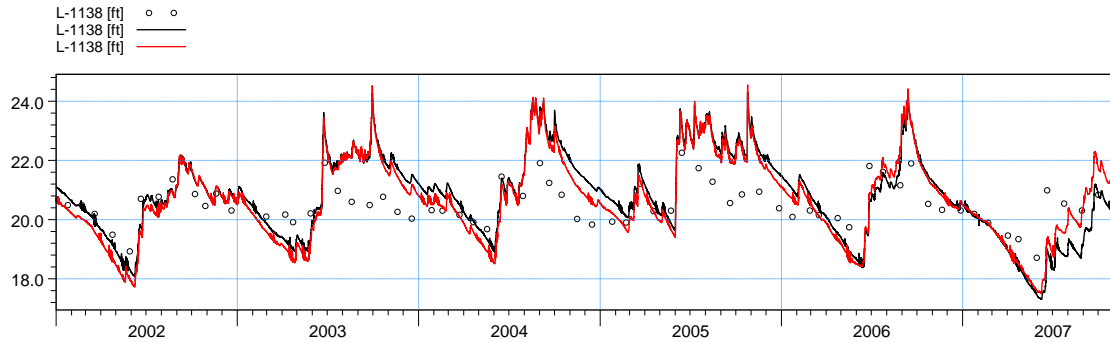


ME=0.0712018  
 MAE=1.2495  
 RMSE=1.47858  
 STDres=1.47687  
 R(Correlation)=0.637882  
 R2(Nash\_Sutcliffe)=-0.583145

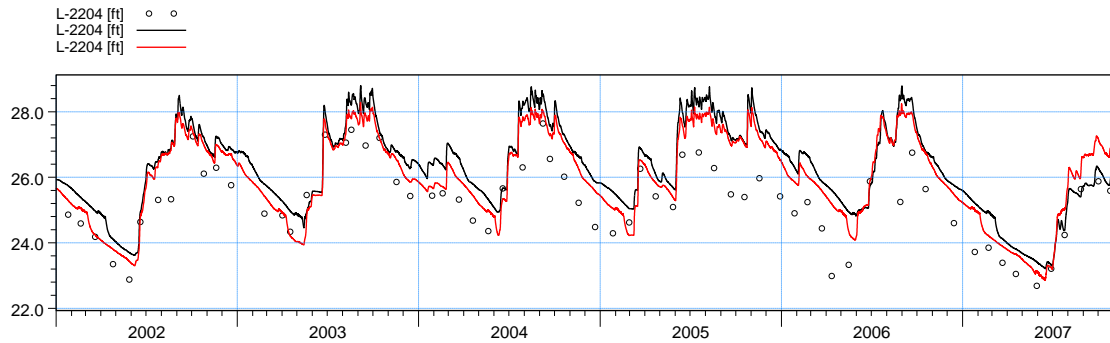
**Figure F26.** Water level at stations WF5\_G, WF6\_G and WF7\_G.



ME=-0.388986  
 MAE=0.989496  
 RMSE=1.08493  
 STDres=1.0128  
 R(Correlation)=0.809904  
 R2(Nash\_Sutcliffe)=-0.725558

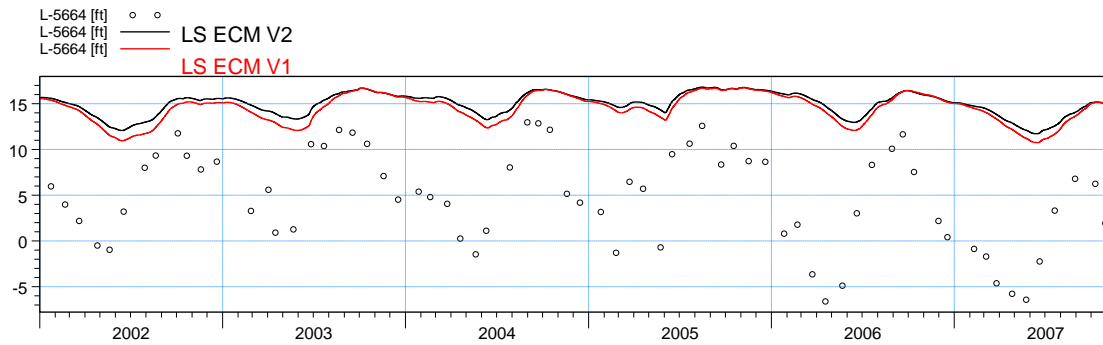


ME=-0.318008  
 MAE=0.807974  
 RMSE=0.973164  
 STDres=0.919739  
 R(Correlation)=0.758298  
 R2(Nash\_Sutcliffe)=-0.925606

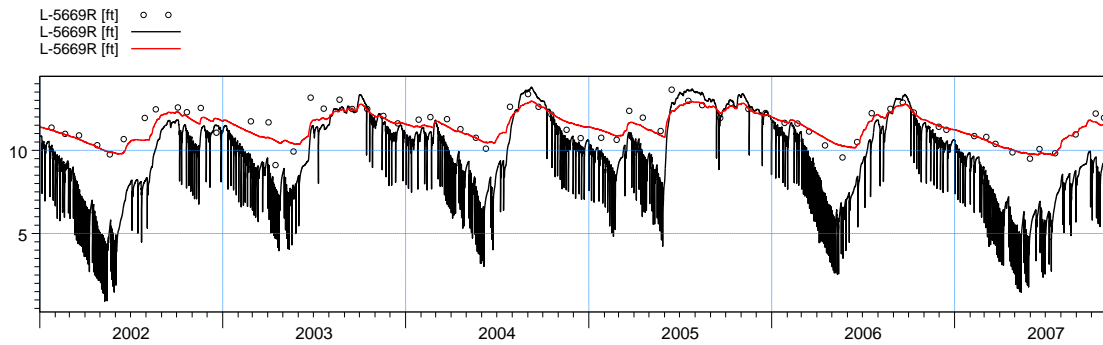


ME=-0.982822  
 MAE=1.00955  
 RMSE=1.15462  
 STDres=0.605971  
 R(Correlation)=0.887034  
 R2(Nash\_Sutcliffe)=0.0637709

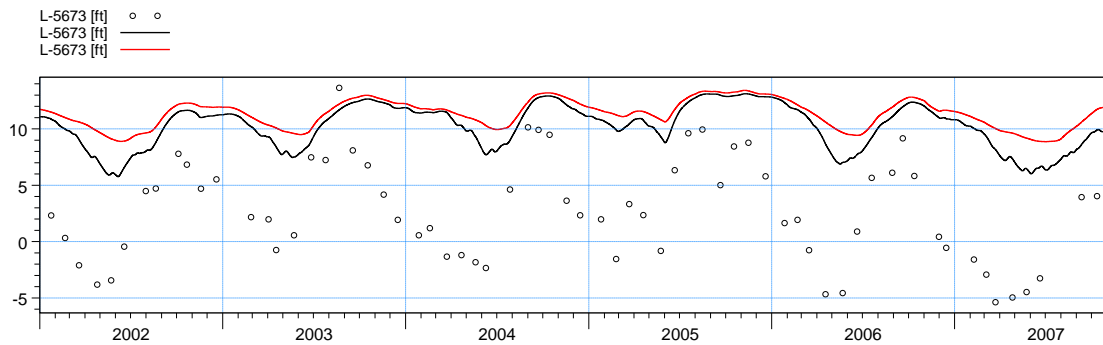
**Figure F27.** Water level at stations Corkscrew Swamp, L-1138 and L-2204.



ME=-10.2311  
 MAE=10.2311  
 RMSE=11.1984  
 STDres=4.55273  
 R(Correlation)=0.610895  
 R2(Nash\_Sutcliffe)=-3.60109

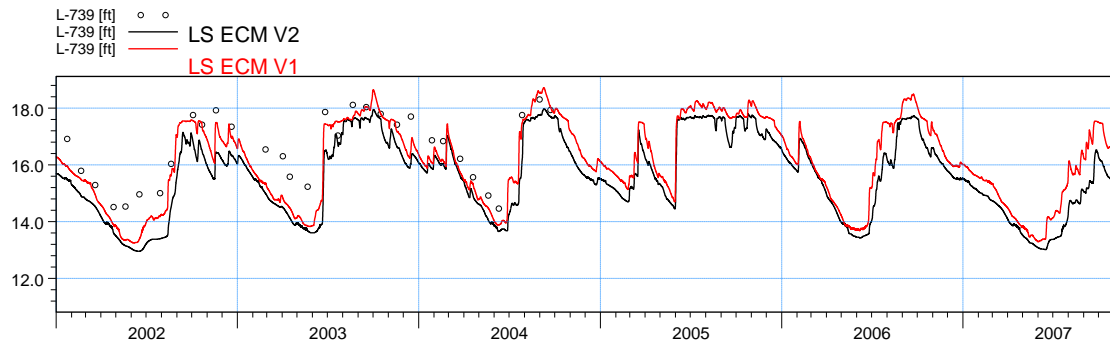


ME=1.72524  
 MAE=1.82986  
 RMSE=2.32578  
 STDres=1.55974  
 R(Correlation)=0.869257  
 R2(Nash\_Sutcliffe)=-3.90674

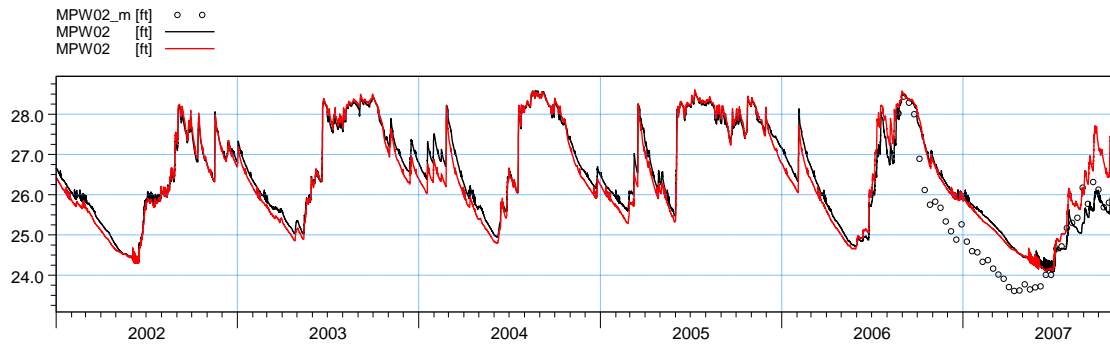


ME=-7.60688  
 MAE=7.66441  
 RMSE=8.3439  
 STDres=3.42869  
 R(Correlation)=0.69694  
 R2(Nash\_Sutcliffe)=-2.48487

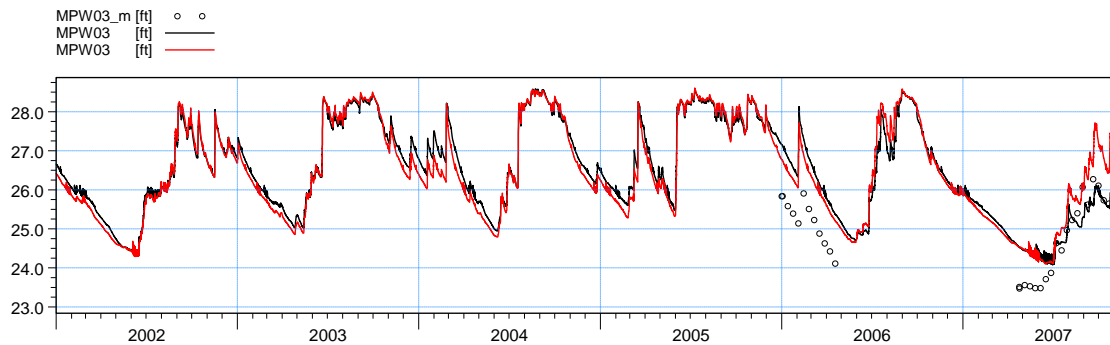
**Figure F28.** Water level at stations L-5664., L-5669R and L-5673.



ME=1.04864  
 MAE=1.04864  
 RMSE=1.15593  
 STDres=0.486325  
 R(Correlation)=0.947397  
 R2(Nash\_Sutcliffe)=0.109867

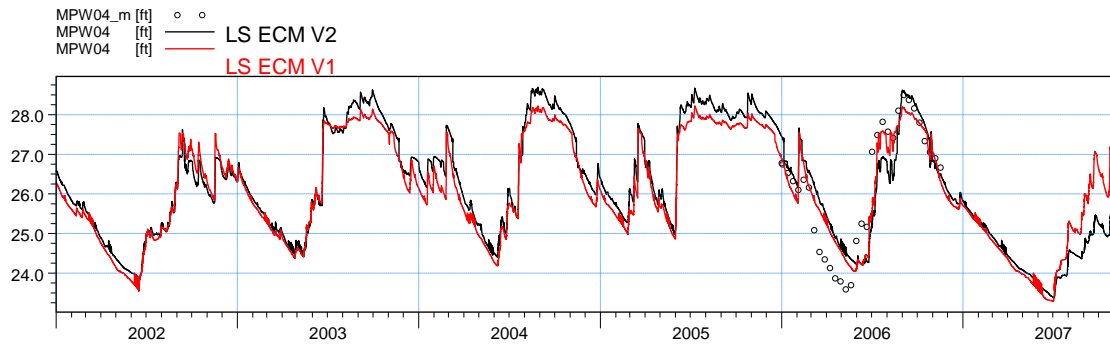


ME=-0.474392  
 MAE=0.690324  
 RMSE=0.817473  
 STDres=0.665743  
 R(Correlation)=0.865793  
 R2(Nash\_Sutcliffe)=0.622451

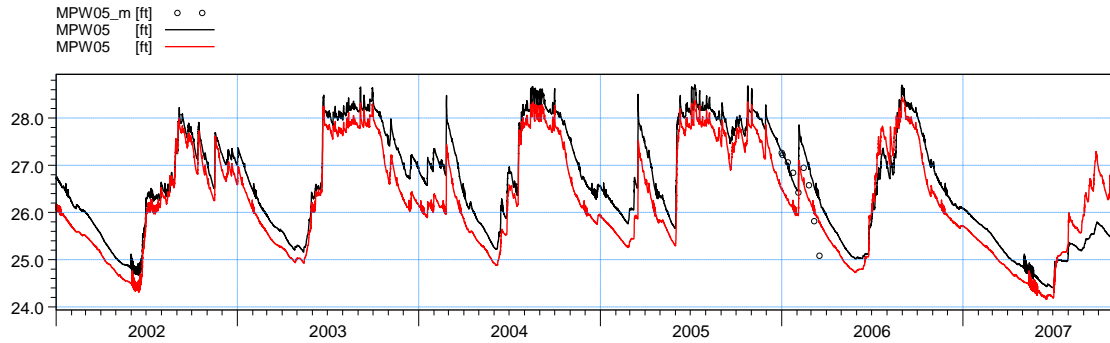


ME=-0.563431  
 MAE=0.774108  
 RMSE=0.917913  
 STDres=0.724644  
 R(Correlation)=0.708055  
 R2(Nash\_Sutcliffe)=0.0713091

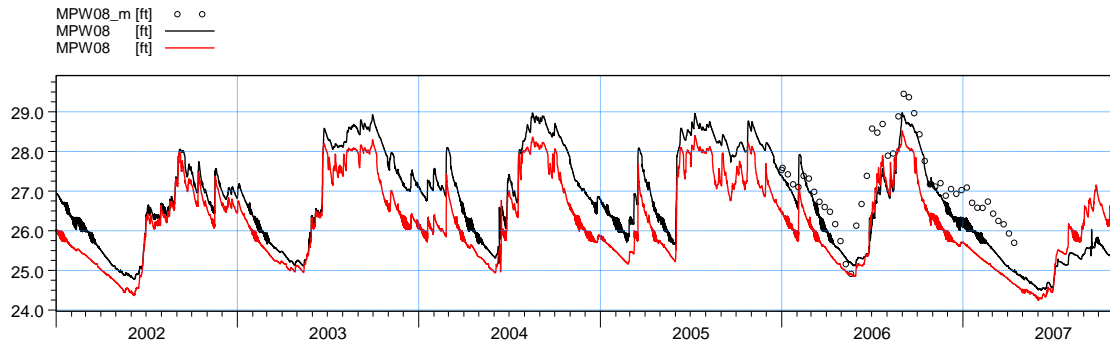
**Figure F29.** Water level at stations L-739, MPW02 and MPW03.



ME=-0.085591  
 MAE=0.68176  
 RMSE=0.83146  
 STDres=0.827043  
 R(Correlation)=0.845089  
 R2(Nash\_Sutcliffe)=0.711009

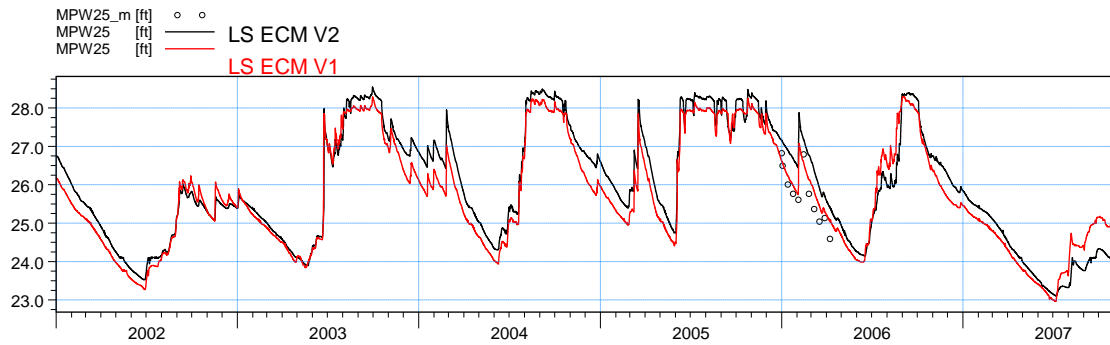


ME=-0.382236  
 MAE=0.434151  
 RMSE=0.586628  
 STDres=0.445004  
 R(Correlation)=0.832089  
 R2(Nash\_Sutcliffe)=0.350118

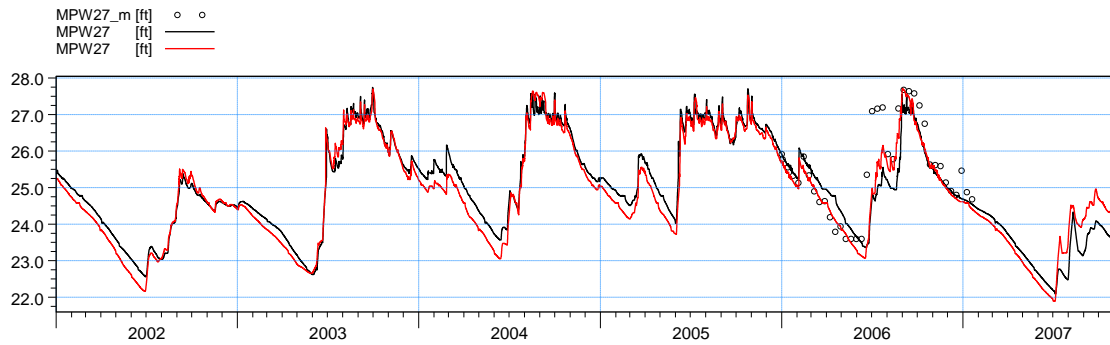


ME=0.655246  
 MAE=0.6819  
 RMSE=0.852676  
 STDres=0.545626  
 R(Correlation)=0.866049  
 R2(Nash\_Sutcliffe)=0.358498

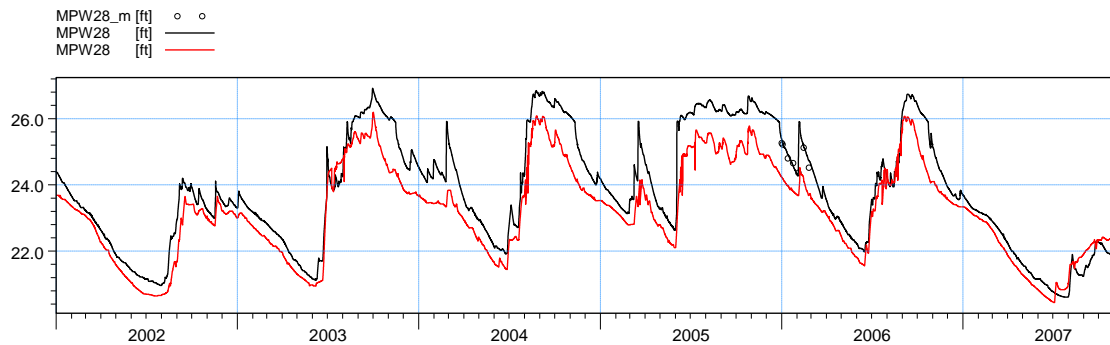
**Figure F30.** Water level at stations MPW04, MPW05 and MPW08.



ME=-0.818232  
 MAE=0.822706  
 RMSE=0.858243  
 STDres=0.258993  
 R(Correlation)=0.939809  
 R2(Nash\_Sutcliffe)=-0.306249

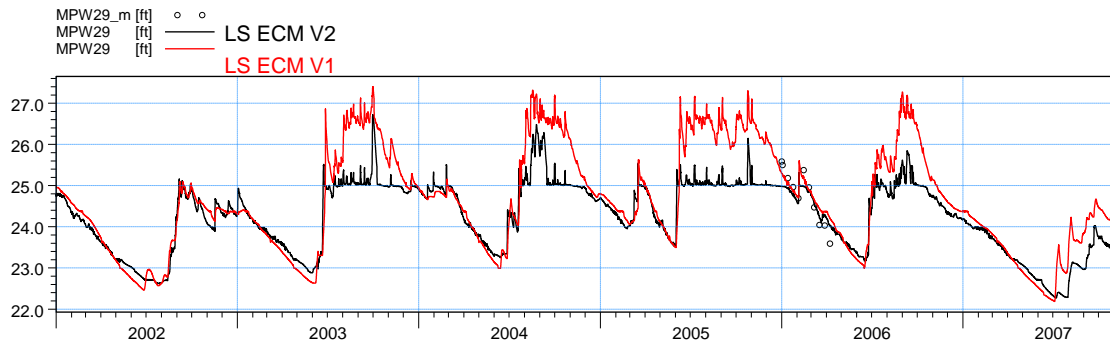


ME=0.401152  
 MAE=0.650942  
 RMSE=0.959506  
 STDres=0.871624  
 R(Correlation)=0.721175  
 R2(Nash\_Sutcliffe)=0.418404

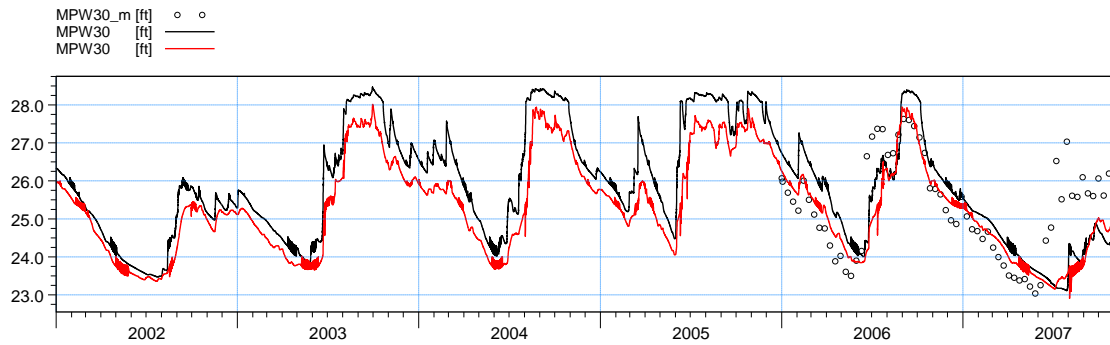


ME=-0.0327467  
 MAE=0.142218  
 RMSE=0.169961  
 STDres=0.166777  
 R(Correlation)=0.932394  
 R2(Nash\_Sutcliffe)=0.856129

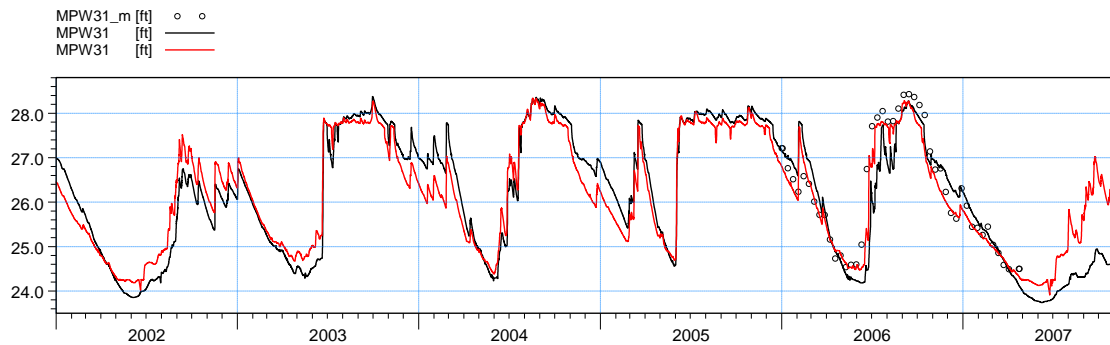
**Figure F31.** Water level at stations MPW25, MPW27 and MPW28.



ME=0.0656189  
 MAE=0.326192  
 RMSE=0.418012  
 STDres=0.41283  
 R(Correlation)=0.954564  
 R2(Nash\_Sutcliffe)=0.684484

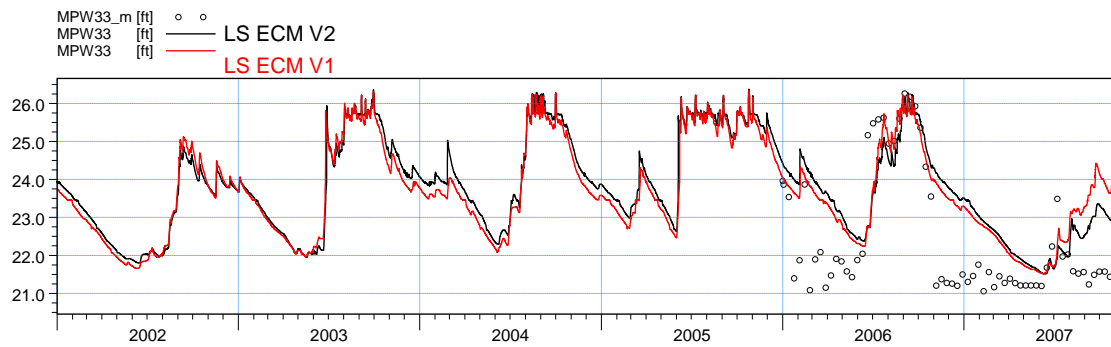


ME=0.0751656  
 MAE=0.997357  
 RMSE=1.21889  
 STDres=1.21657  
 R(Correlation)=0.568616  
 R2(Nash\_Sutcliffe)=0.132616

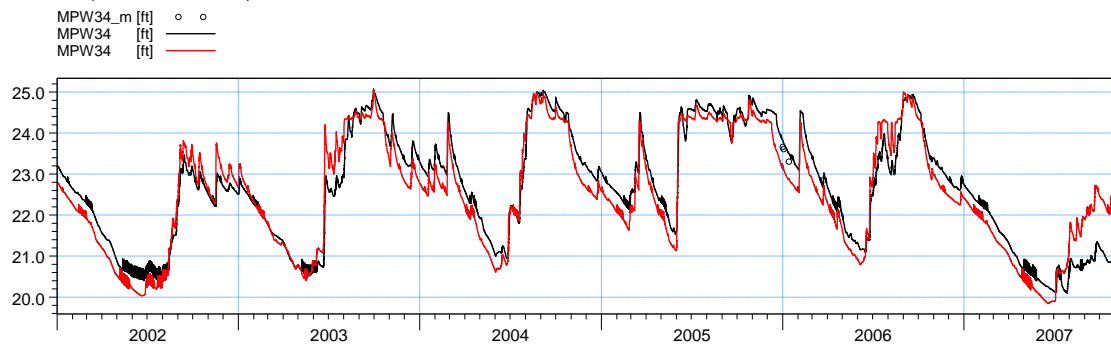


ME=0.174281  
 MAE=0.452815  
 RMSE=0.677352  
 STDres=0.654547  
 R(Correlation)=0.863579  
 R2(Nash\_Sutcliffe)=0.722141

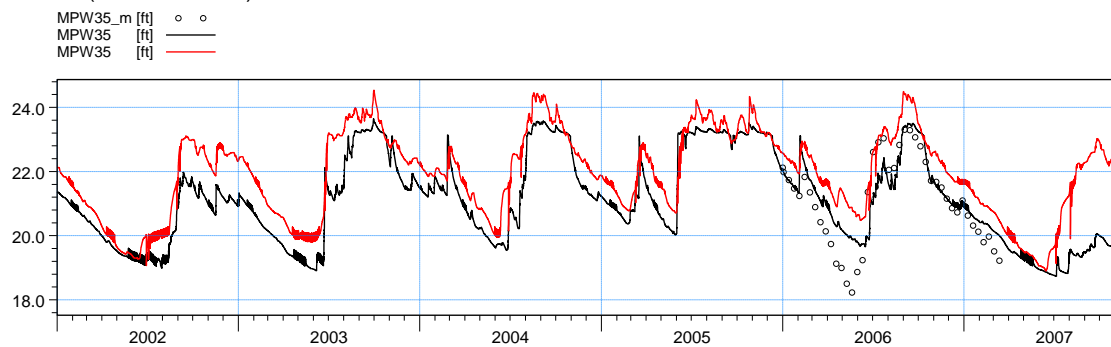
**Figure F32.** Water level at stations MPW29, MPW30 and MPW31.



ME=-0.927827  
 MAE=1.26371  
 RMSE=1.50598  
 STDres=1.18622  
 R(Correlation)=0.689761  
 R2(Nash\_Sutcliffe)=0.155017

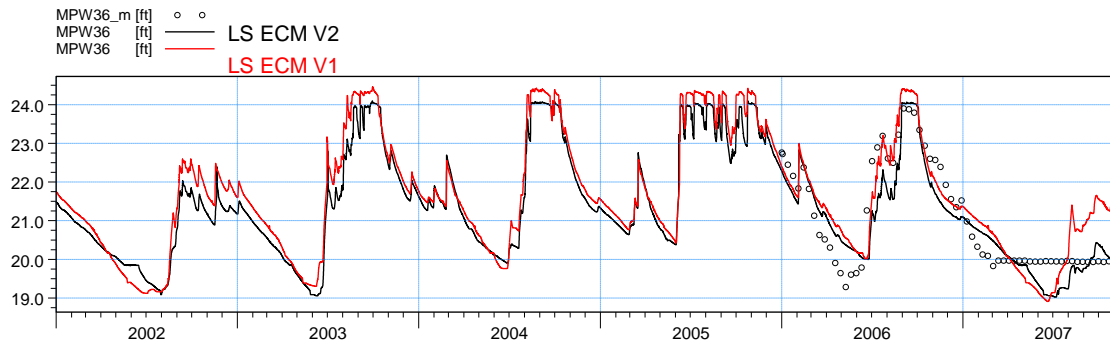


ME=-0.157151  
 MAE=0.157151  
 RMSE=0.160488  
 STDres=0.0325545  
 R(Correlation)=0.982522  
 R2(Nash\_Sutcliffe)=-0.21218

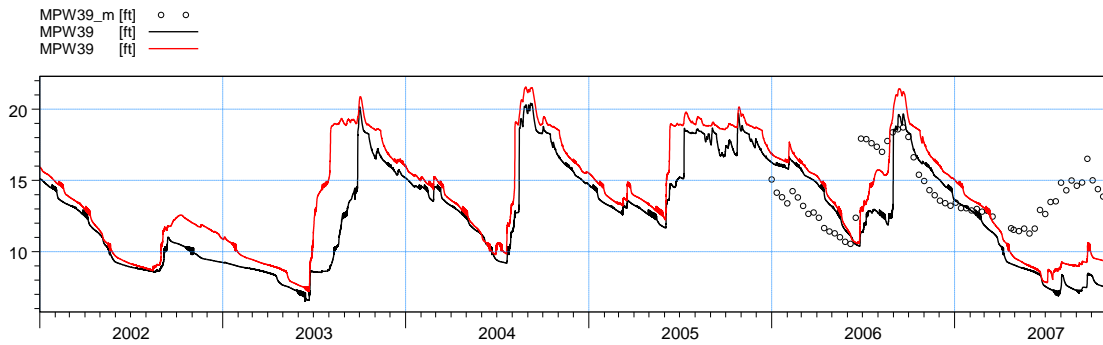


ME=-0.217088  
 MAE=0.57899  
 RMSE=0.761336  
 STDres=0.72973  
 R(Correlation)=0.877901  
 R2(Nash\_Sutcliffe)=0.720095

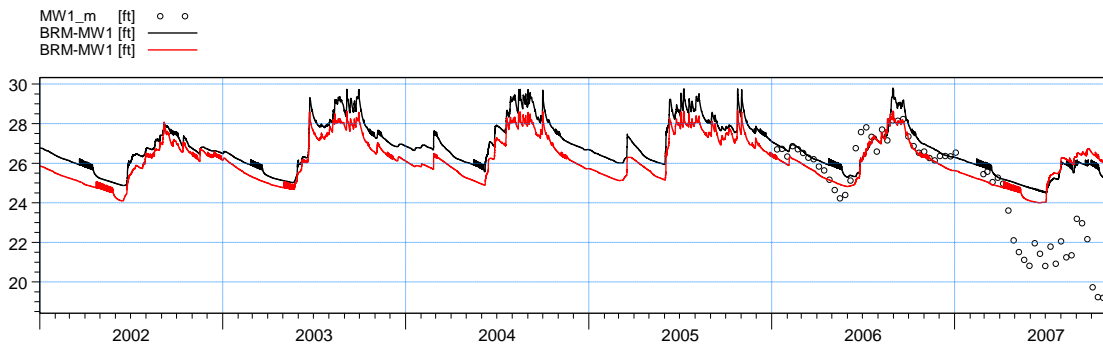
**Figure F33.** Water level at stations MPW33, MPW34 and MPW35.



ME=0.160134  
 MAE=0.531803  
 RMSE=0.660696  
 STDres=0.640996  
 R(Correlation)=0.879355  
 R2(Nash\_Sutcliffe)=0.758759

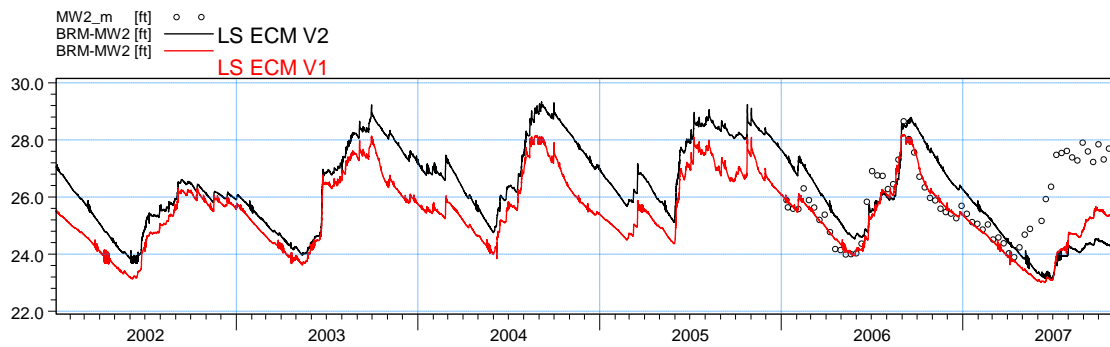


ME=1.60872  
 MAE=2.9622  
 RMSE=3.80712  
 STDres=3.45054  
 R(Correlation)=0.308197  
 R2(Nash\_Sutcliffe)=-2.15991

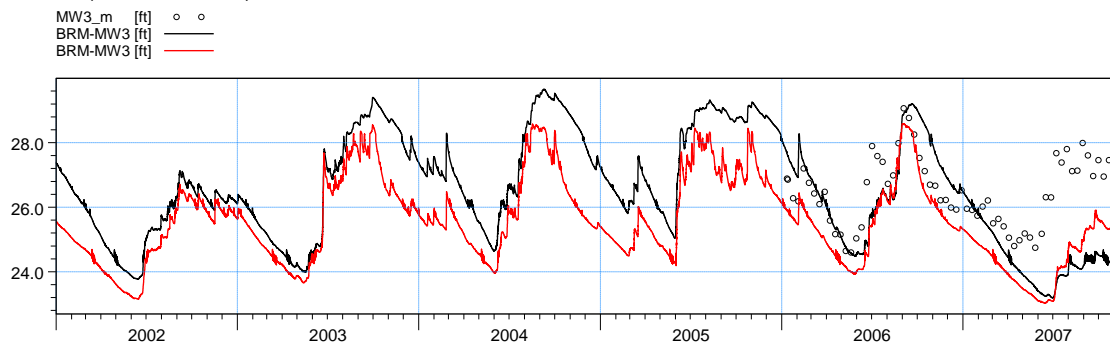


ME=-0.84697  
 MAE=0.980215  
 RMSE=1.64717  
 STDres=1.41273  
 R(Correlation)=0.699422  
 R2(Nash\_Sutcliffe)=0.241058

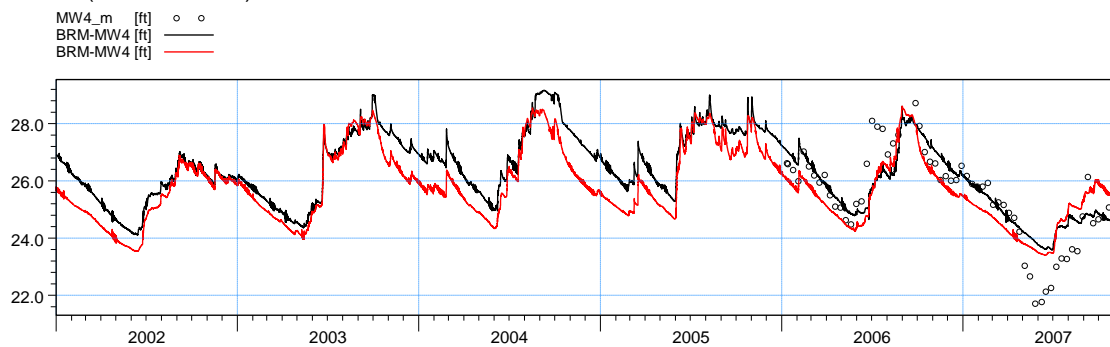
**Figure F34.** Water level at stations MPW36, MPW39 and MW1.



ME=0.354983  
 MAE=1.40266  
 RMSE=1.7749  
 STDres=1.73904  
 R(Correlation)=0.178412  
 R2(Nash\_Sutcliffe)=-0.899738

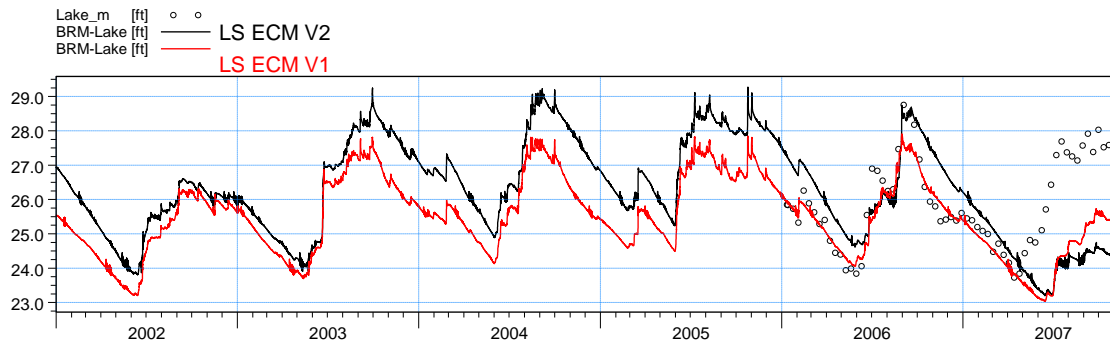


ME=0.77829  
 MAE=1.23914  
 RMSE=1.68884  
 STDres=1.49881  
 R(Correlation)=0.417489  
 R2(Nash\_Sutcliffe)=-1.39268

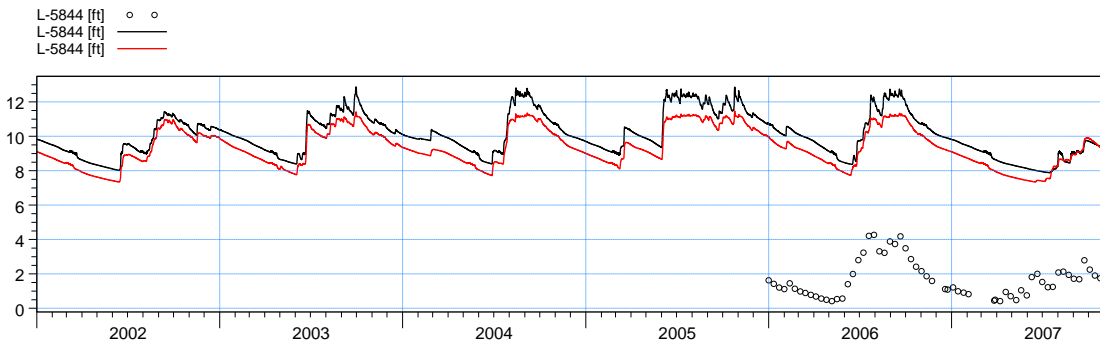


ME=-0.124469  
 MAE=0.5848  
 RMSE=0.811354  
 STDres=0.80175  
 R(Correlation)=0.865538  
 R2(Nash\_Sutcliffe)=0.712295

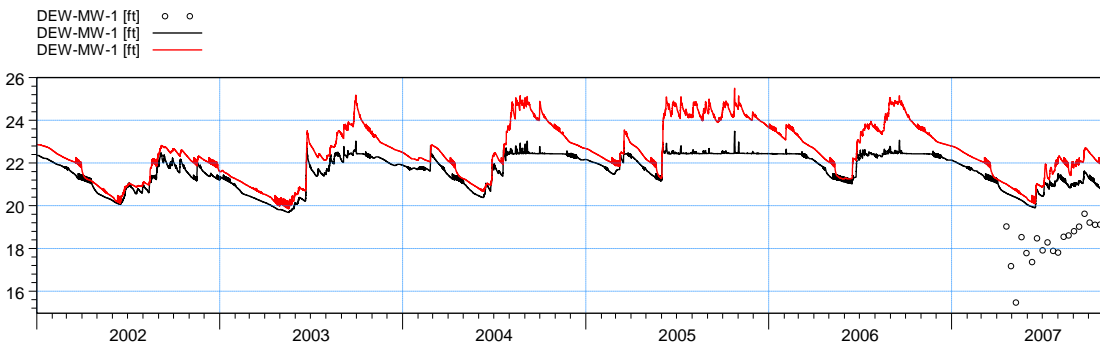
**Figure F35.** Water level at stations MW2, MW3 and MW4.



ME=0.313462  
 MAE=1.30658  
 RMSE=1.67343  
 STDres=1.64381  
 R(Correlation)=0.241735  
 R2(Nash\_Sutcliffe)=-0.584749

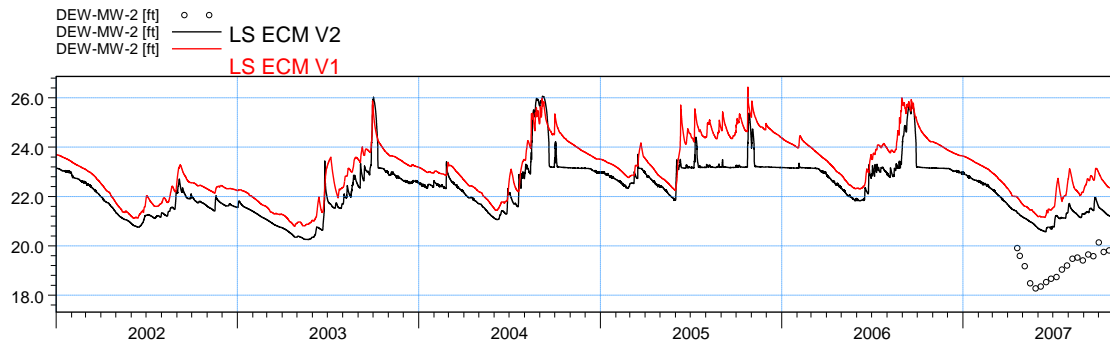


ME=-7.95745  
 MAE=7.95745  
 RMSE=8.01093  
 STDres=0.924117  
 R(Correlation)=0.698025  
 R2(Nash\_Sutcliffe)=-54.2434

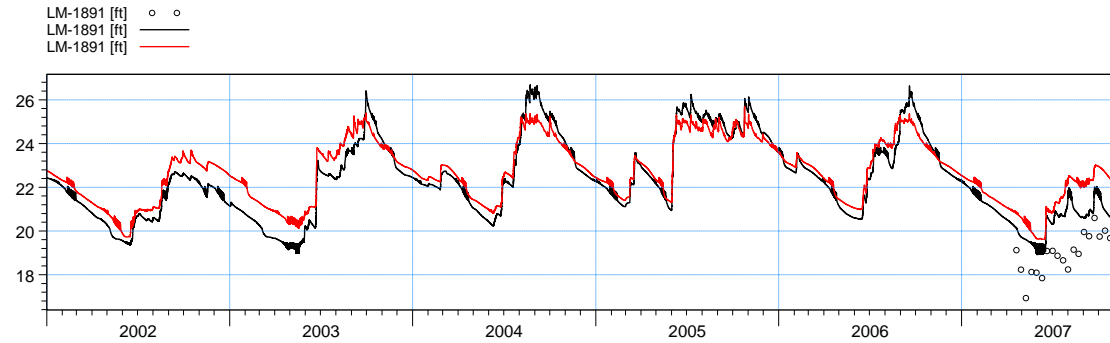


ME=-2.44421  
 MAE=2.44421  
 RMSE=2.54955  
 STDres=0.725271  
 R(Correlation)=0.543725  
 R2(Nash\_Sutcliffe)=-7.7192

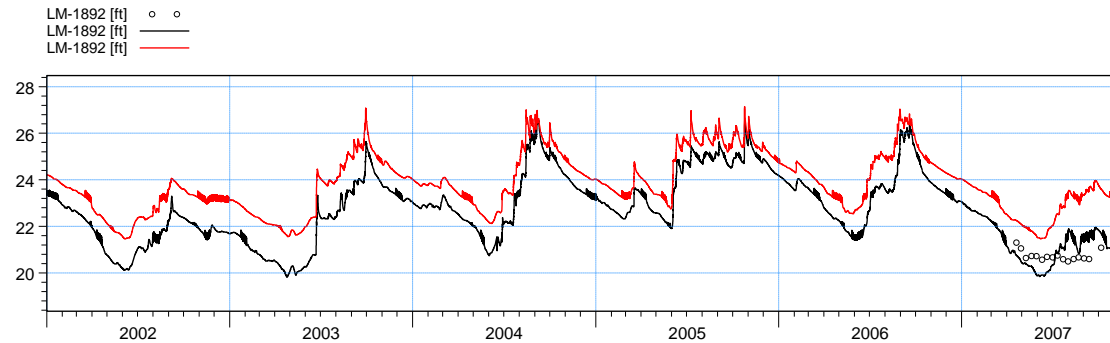
**Figure F36.** Water level at stations Lake, L-5844 and DEW-MW-1.



ME=-1.95976  
 MAE=1.95976  
 RMSE=1.99132  
 STDres=0.353081  
 R(Correlation)=0.88987  
 R2(Nash\_Sutcliffe)=-10.1697

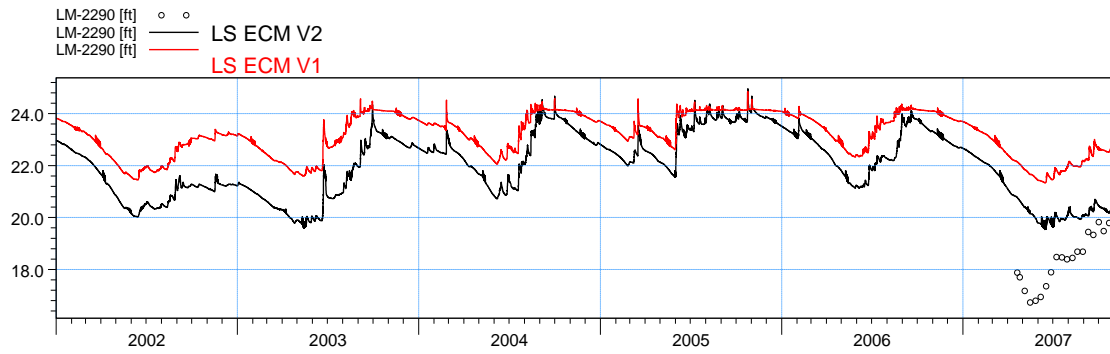


ME=-1.52895  
 MAE=1.52895  
 RMSE=1.65229  
 STDres=0.626419  
 R(Correlation)=0.691132  
 R2(Nash\_Sutcliffe)=-3.18463

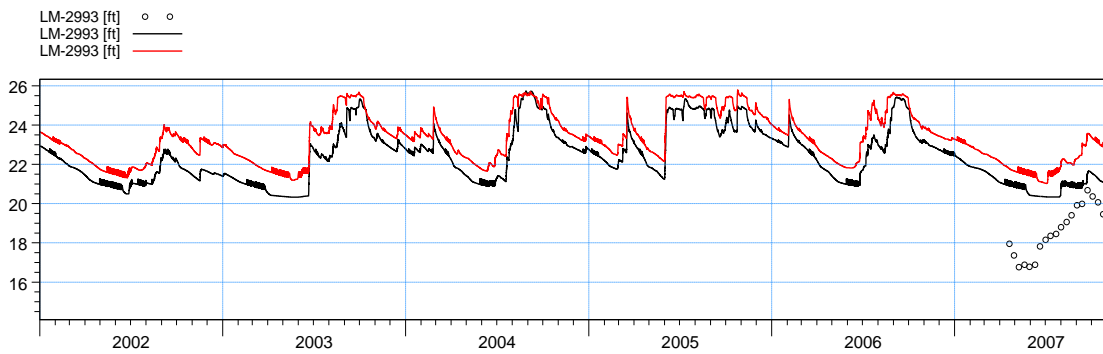


ME=-0.0692077  
 MAE=0.629409  
 RMSE=0.688247  
 STDres=0.684758  
 R(Correlation)=-0.218026  
 R2(Nash\_Sutcliffe)=-13.0404

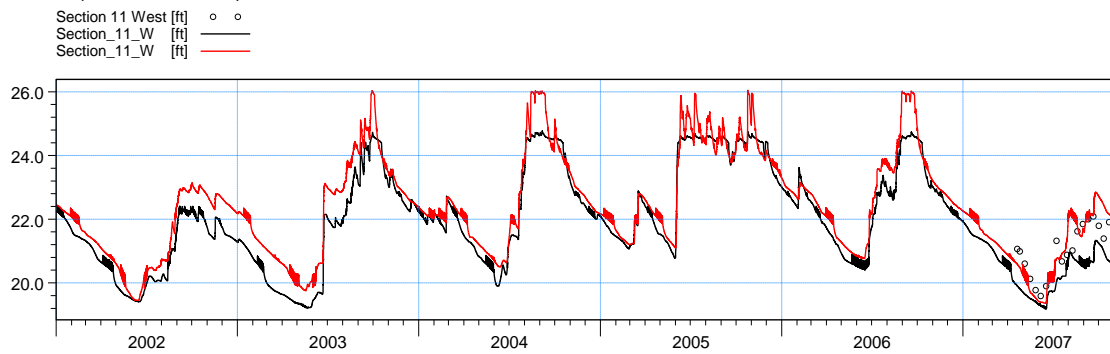
**Figure F37.** Water level at stations DEW-MW-2, LM-1891 and LM-1892.



ME=-1.7844  
 MAE=1.7844  
 RMSE=2.04109  
 STDres=0.990942  
 R(Correlation)=0.370224  
 R2(Nash\_Sutcliffe)=-2.72798

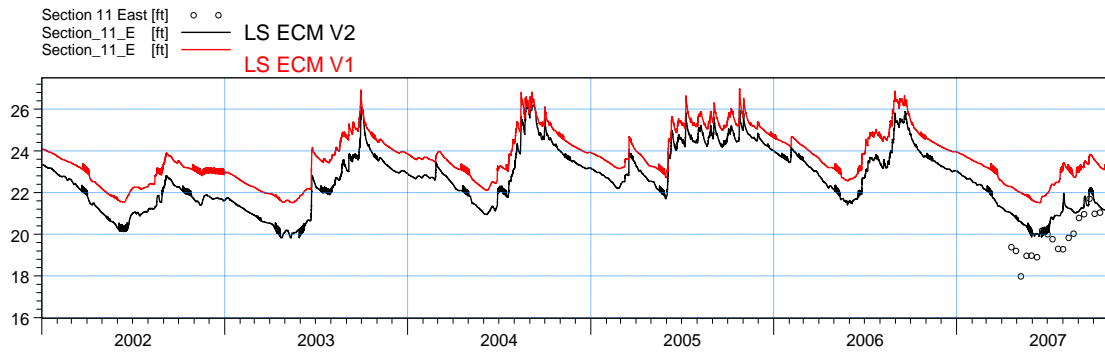


ME=-2.22414  
 MAE=2.22414  
 RMSE=2.47778  
 STDres=1.09205  
 R(Correlation)=0.627732  
 R2(Nash\_Sutcliffe)=-2.69222

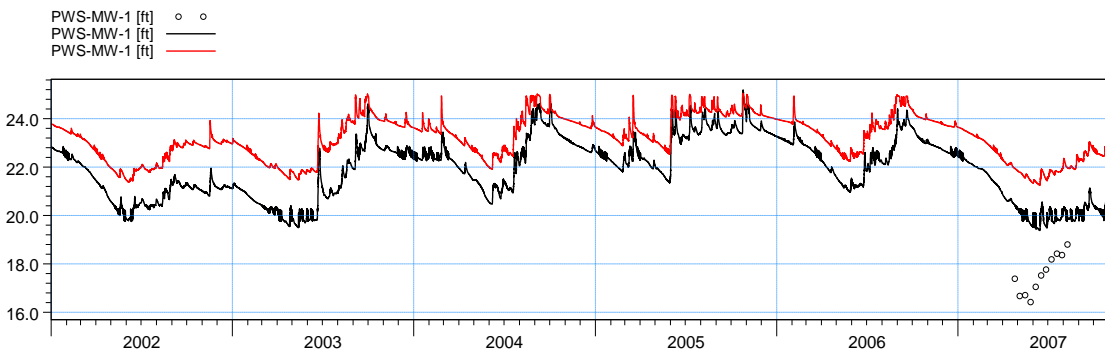


ME=0.789927  
 MAE=0.78931  
 RMSE=0.895454  
 STDres=0.421725  
 R(Correlation)=0.857483  
 R2(Nash\_Sutcliffe)=-0.224348

**Figure F38.** Water level at stations LM-2290, LM-2993 and Section\_11\_W.



ME=-1.06859  
 MAE=1.07931  
 RMSE=1.23839  
 STDres=0.625884  
 R(Correlation)=0.685332  
 R2(Nash\_Sutcliffe)=-1.07662



ME=-2.37652  
 MAE=2.37652  
 RMSE=2.53353  
 STDres=0.878016  
 R(Correlation)=0.18815  
 R2(Nash\_Sutcliffe)=-7.1626

**Figure F39.** Water level at stations Section\_11\_E, and PWS-MW-1.

## Surface water stations

**Table F3.** Statistic parameters at surface water stations.

| Name           | LS ECM V1 |          |           |      |     | LS ECM V2 |          |           |      |     |
|----------------|-----------|----------|-----------|------|-----|-----------|----------|-----------|------|-----|
|                | ME (ft)   | MAE (ft) | RMSE (ft) | R    | PL  | ME (ft)   | MAE (ft) | RMSE (ft) | R    | PL  |
| KehlCan_HW     | 1.05      | 1.66     | 2.07      | 0.68 | 2.5 | 1.57      | 1.78     | 2.21      | 0.75 | 2.5 |
| KehlCan_TW     | 0.08      | 0.64     | 0.98      | 0.93 | 1.0 | -0.34     | 0.81     | 0.95      | 0.96 | 1.3 |
| S-SF-1_HW      | 0.23      | 0.28     | 0.32      | 0.82 | 1.0 | 0.24      | 0.26     | 0.29      | 0.87 | 1.0 |
| S-SF-1 Q       | ---       | ---      | ---       | 0.70 | 1.0 | ---       | ---      | ---       | 0.74 | 2.0 |
| S-SF-1_TW      | -0.02     | 0.30     | 0.48      | 0.44 | 1.5 | -0.01     | 0.30     | 0.45      | 0.44 | 1.5 |
| S-NM-2_HW      | 0.00      | 0.19     | 0.24      | 0.60 | 1.3 | -0.01     | 0.19     | 0.25      | 0.57 | 1.5 |
| S-NM-2 Q       | ---       | ---      | ---       | 0.41 | 3.0 | ---       | ---      | ---       | 0.46 | 3.0 |
| S-NM-2_TW      | 0.80      | 1.04     | 1.16      | 0.43 | 2.3 | 0.84      | 1.07     | 1.20      | 0.43 | 2.3 |
| S-YT-2_HW      | 1.63      | 1.74     | 1.96      | 0.76 | 2.3 | 1.42      | 1.51     | 1.70      | 0.71 | 2.0 |
| Mullock Creek  | 0.78      | 0.83     | 0.86      | 0.65 | 1.5 | 0.81      | 0.84     | 0.88      | 0.66 | 1.8 |
| EsteroRiv      | 2.04      | 2.05     | 2.17      | 0.76 | 2.5 | -0.34     | 0.83     | 1.18      | 0.78 | 1.8 |
| EsteroRiv Q    | ---       | ---      | ---       | 0.67 | 2.0 | ---       | ---      | ---       | 0.80 | 2.0 |
| EsteroRivS     | 0.08      | 0.79     | 1.03      | 0.81 | 1.3 | -0.89     | 0.96     | 1.48      | 0.77 | 2.0 |
| EsteroRivS Q   | ---       | ---      | ---       | 0.77 | 1.0 | ---       | ---      | ---       | 0.75 | 2.0 |
| SpringCRSS     | 0.17      | 0.30     | 0.43      | 0.59 | 1.3 | 0.16      | 0.31     | 0.44      | 0.58 | 1.5 |
| SpringCRSS Q   | ---       | ---      | ---       | 0.69 | 2.0 | ---       | ---      | ---       | 0.74 | 2.0 |
| Imperial       | -0.06     | 0.74     | 1.16      | 0.88 | 1.3 | -0.38     | 1.18     | 1.35      | 0.92 | 1.5 |
| Imperial Q     | ---       | ---      | ---       | 0.79 | 1.0 | ---       | ---      | ---       | 0.83 | 1.0 |
| Halfway_S HW   | -1.24     | 1.24     | 1.36      | 0.78 | 1.8 | 0.78      | 0.89     | 1.01      | 0.48 | 2.0 |
| Halfway_S TW   | 0.27      | 0.27     | 0.28      | 0.56 | 1.3 | 0.96      | 0.96     | 1.28      | 0.00 | 2.3 |
| Copperleaf     | -0.88     | 0.88     | 0.98      | 0.84 | 1.5 | 1.69      | 1.70     | 1.84      | 0.66 | 2.5 |
| HalfwayCrDS HW | -0.96     | 0.96     | 1.05      | 0.91 | 1.8 | 1.71      | 1.72     | 1.84      | 0.79 | 2.5 |
| HalfwayCrDS TW | 0.13      | 0.27     | 0.31      | 0.81 | 1.0 | 1.75      | 1.77     | 1.97      | 0.00 | 2.8 |

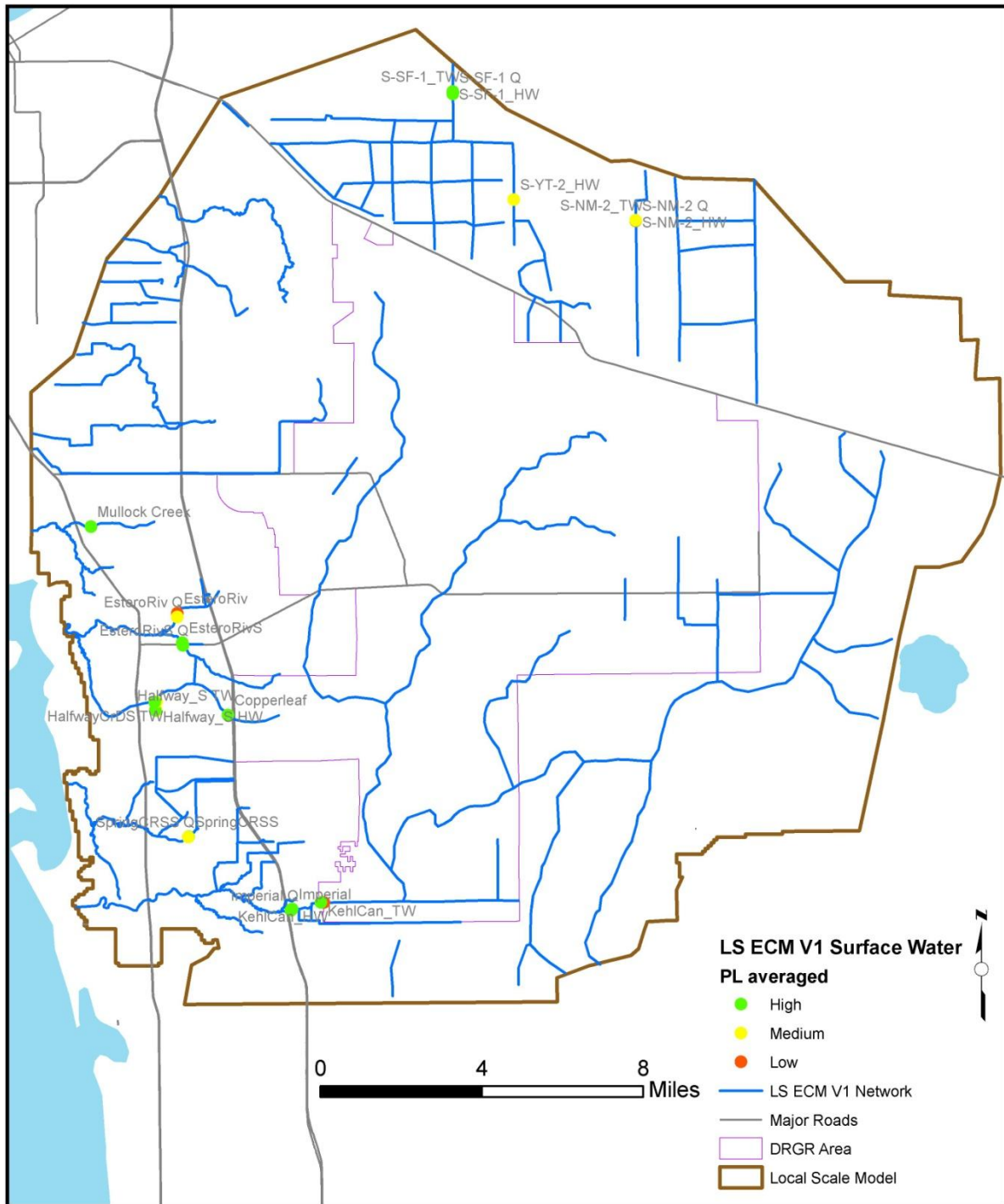


**Figure F40.** Average performance levels in surface water stations from previous (V1) model.

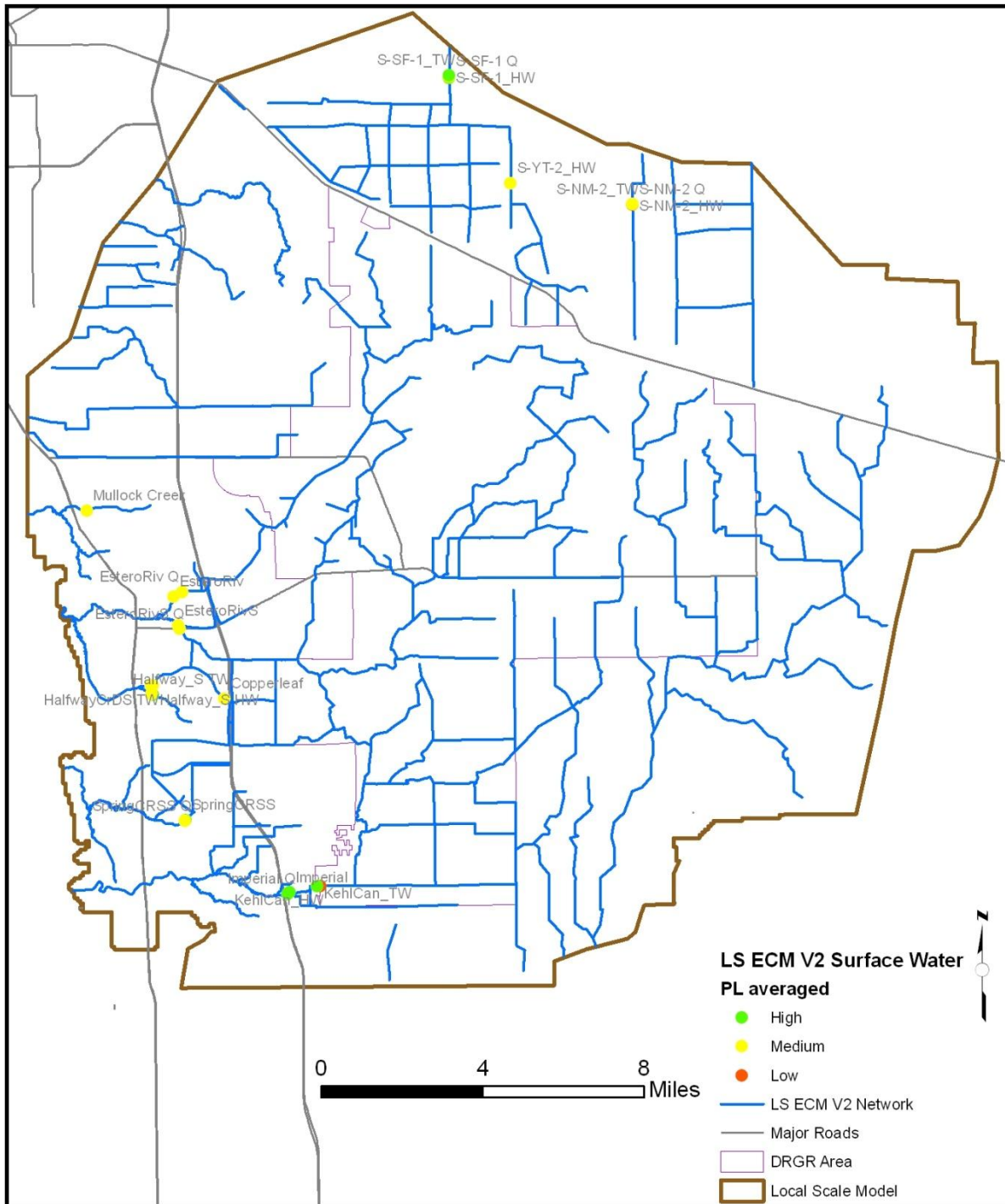
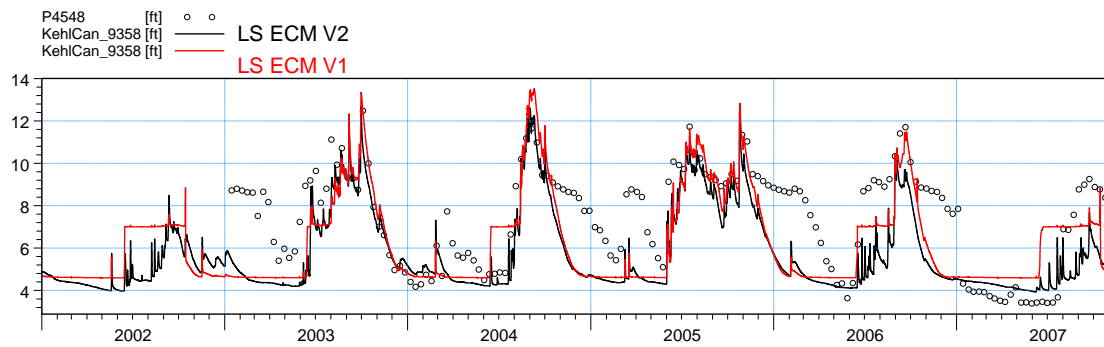
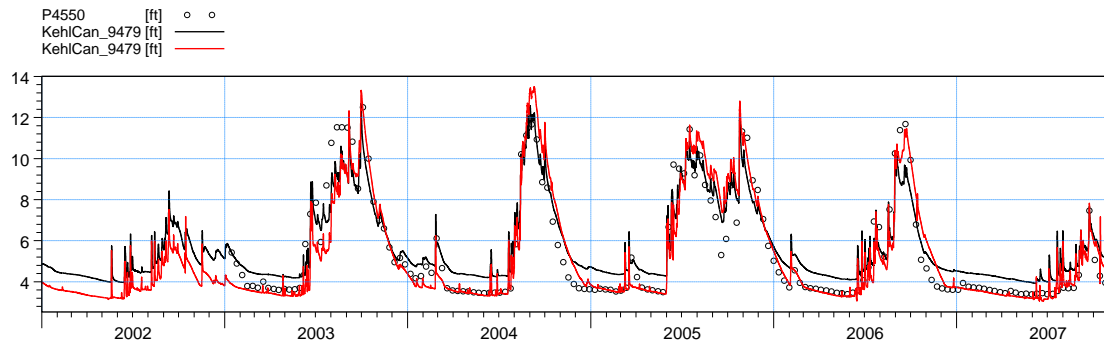


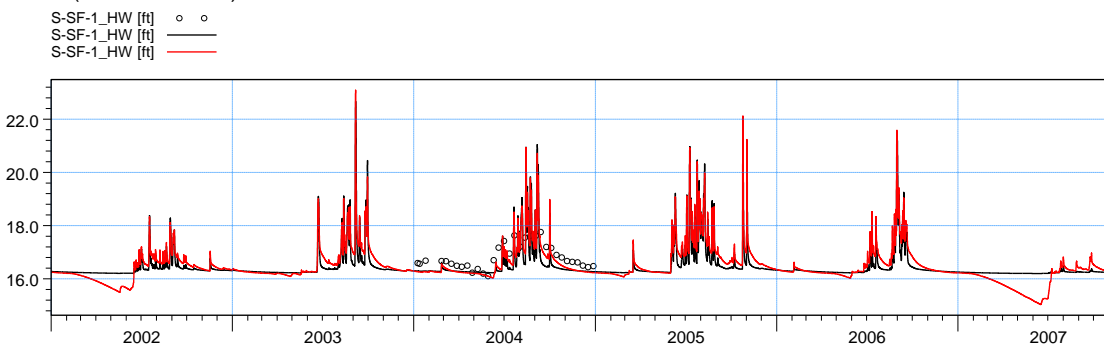
**Figure F41.** Average performance levels in surface water stations from new (V2) model.



ME=1.56669  
 MAE=1.78205  
 RMSE=2.2035  
 STDres=1.54948  
 R(Correlation)=0.751892  
 R2(Nash\_Sutcliffe)=0.09941

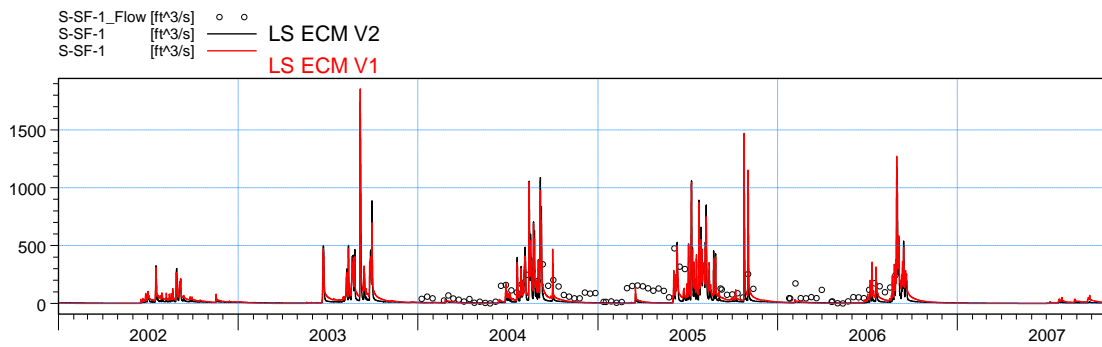


ME=-0.337993  
 MAE=0.838303  
 RMSE=0.973898  
 STDres=0.913366  
 R(Correlation)=0.956622  
 R2(Nash\_Sutcliffe)=0.858693

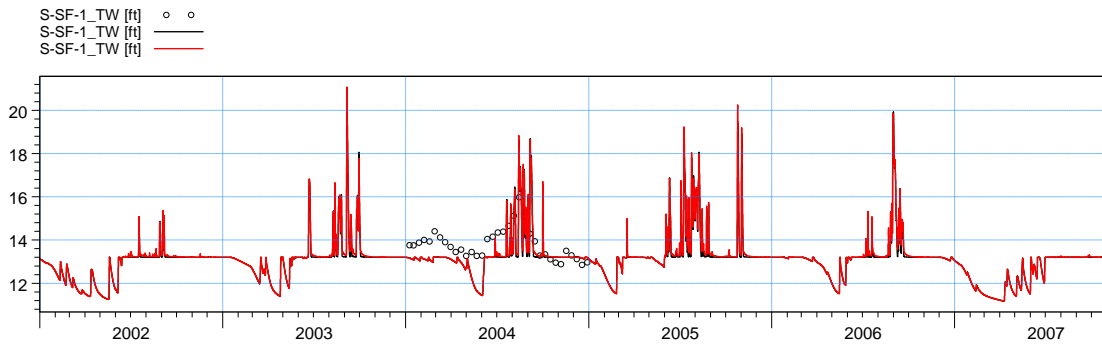


ME=0.31857  
 MAE=0.35693  
 RMSE=0.41375  
 STDres=0.264011  
 R(Correlation)=0.653733  
 R2(Nash\_Sutcliffe)=-1.02533

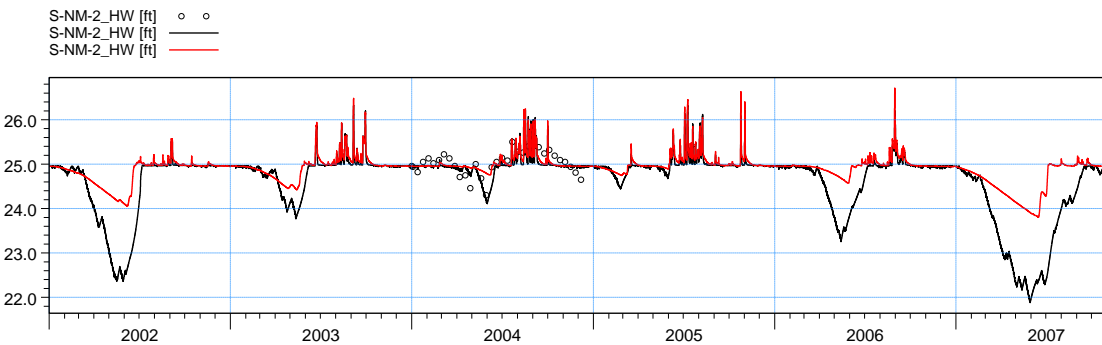
**Figure F42.** Comparison plots at surface water stations KehICan\_HW, KehICan\_TW and S-SF-1\_HW.



ME=78.6087  
 MAE=89.4908  
 RMSE=119.284  
 STDres=89.7182  
 R(Correlation)=0.649162  
 R2(Nash\_Sutcliffe)=-0.322842

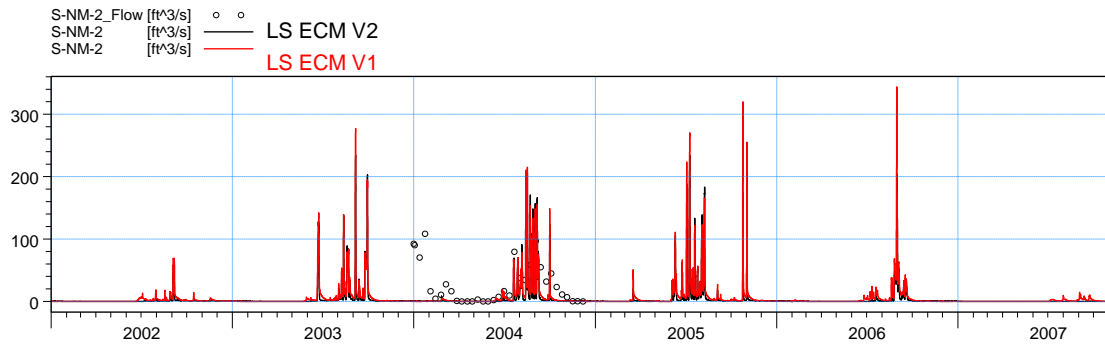


ME=-0.00204762  
 MAE=0.300898  
 RMSE=0.469909  
 STDres=0.469905  
 R(Correlation)=0.432146  
 R2(Nash\_Sutcliffe)=-0.21991

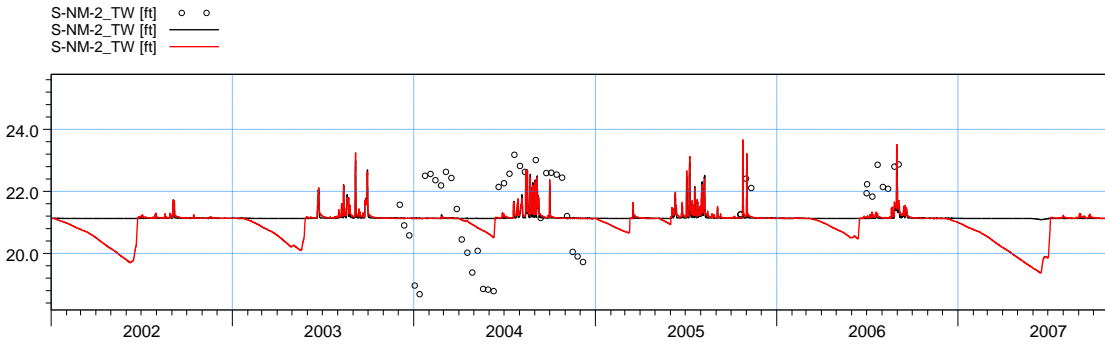


ME=0.0641465  
 MAE=0.187051  
 RMSE=0.234191  
 STDres=0.225235  
 R(Correlation)=0.694068  
 R2(Nash\_Sutcliffe)=0.401755

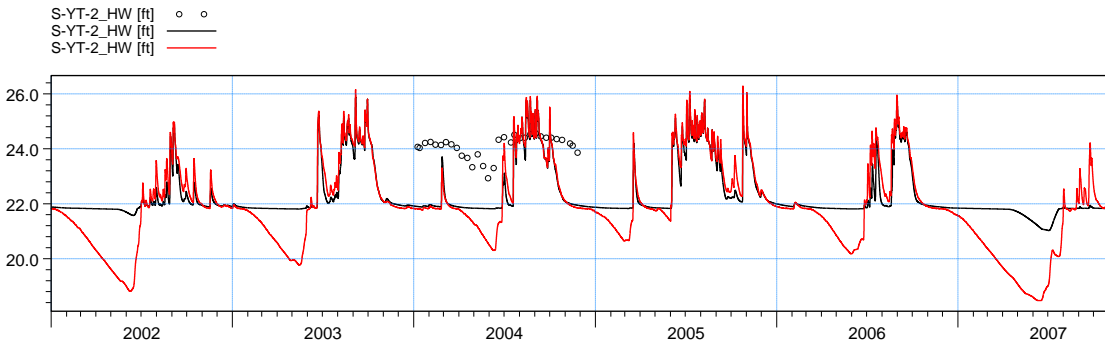
**Figure F43.** Comparison plots at surface water stations S-SF-1 Q, S-SF-1\_TW and S-NM-2\_HW.



ME=18.3076  
 MAE=22.832  
 RMSE=37.6788  
 STDres=32.9322  
 R(Correlation)=0.403244  
 R2(Nash\_Sutcliffe)=-0.35379

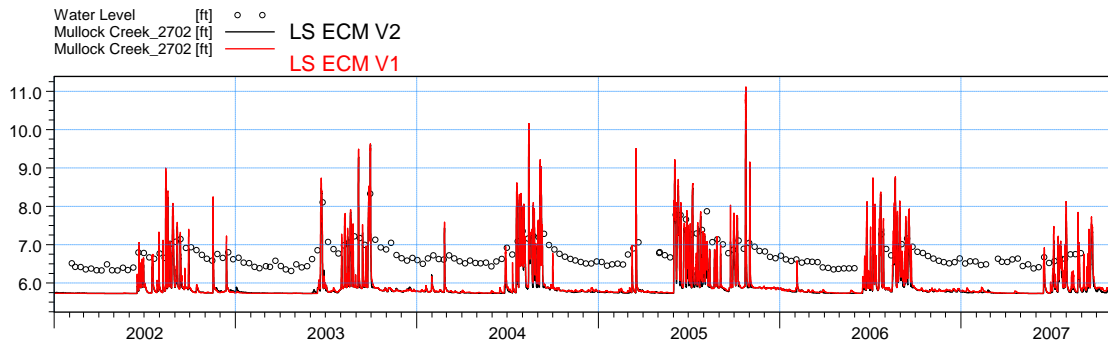


ME=0.849101  
 MAE=1.08698  
 RMSE=1.21366  
 STDres=0.867178  
 R(Correlation)=0.350905  
 R2(Nash\_Sutcliffe)=-0.72574

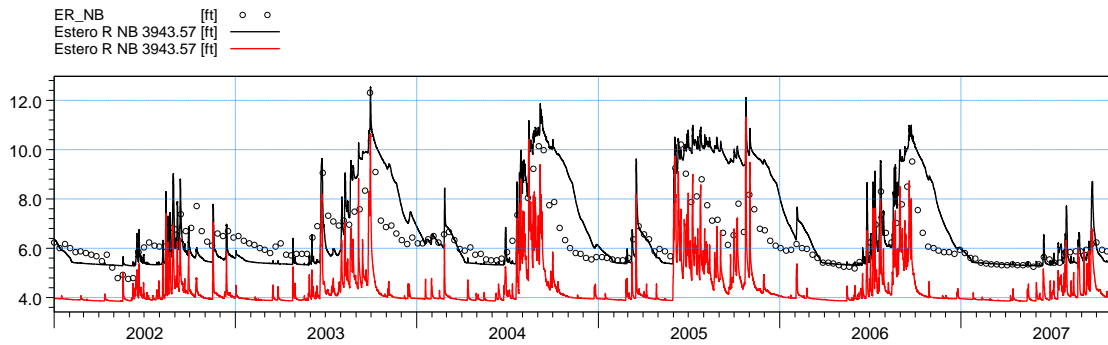


ME=1.45668  
 MAE=1.55253  
 RMSE=1.73205  
 STDres=0.937046  
 R(Correlation)=0.613843  
 R2(Nash\_Sutcliffe)=-16.2504

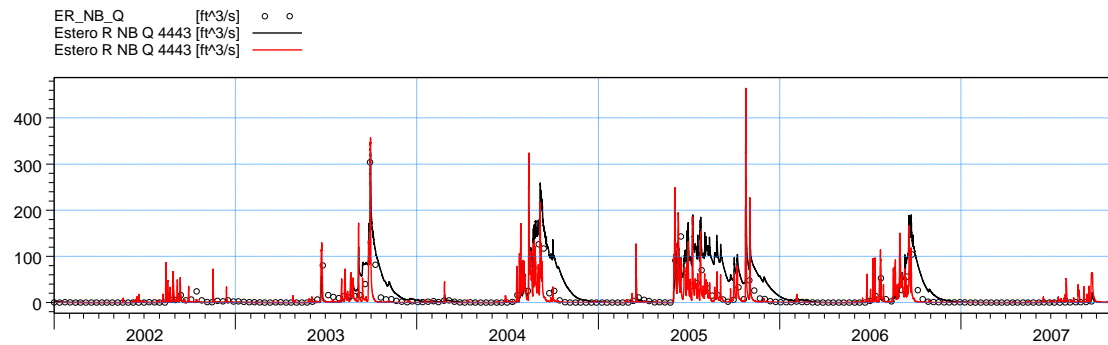
**Figure F44.** Comparison plots at surface water stations S-NM-2 Q, S-NM-2\_TW and S-YT-2\_HW.



ME=0.810328  
 MAE=0.841549  
 RMSE=0.877263  
 STDres=0.336094  
 R(Correlation)=0.662824  
 R2(Nash\_Sutcliffe)=-5.73976

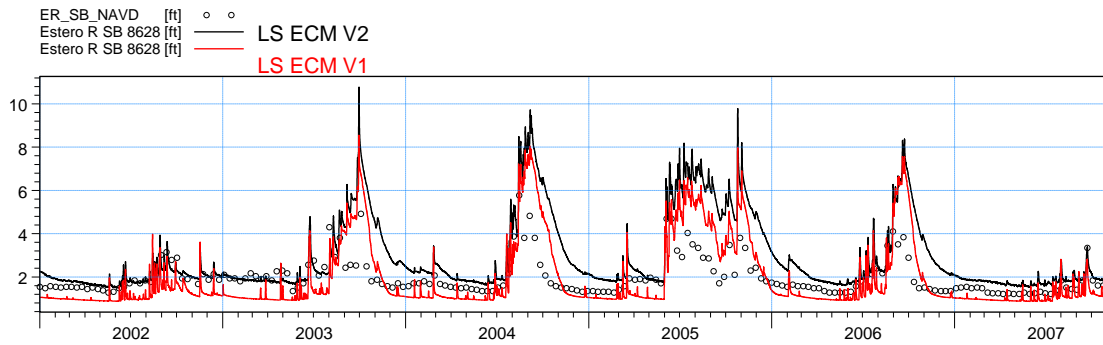


ME=-0.368303  
 MAE=0.832851  
 RMSE=1.19206  
 STDres=1.13374  
 R(Correlation)=0.779159  
 R2(Nash\_Sutcliffe)=-0.0823293

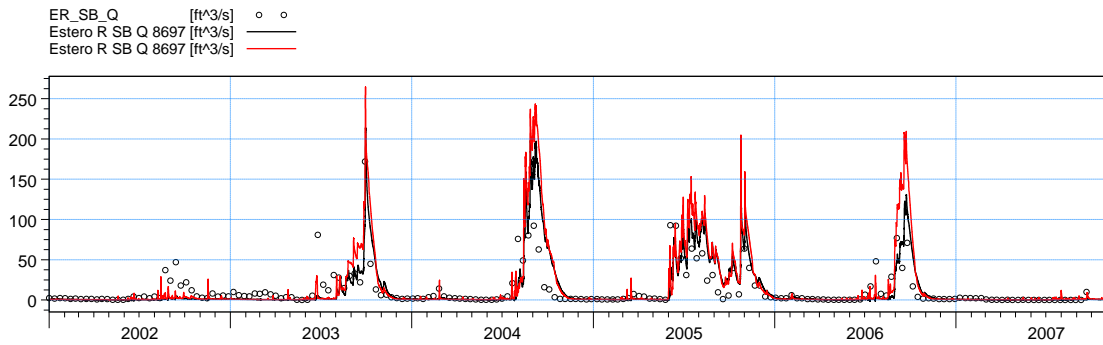


ME=-7.49791  
 MAE=12.1924  
 RMSE=24.9457  
 STDres=23.7922  
 R(Correlation)=0.797865  
 R2(Nash\_Sutcliffe)=0.4221

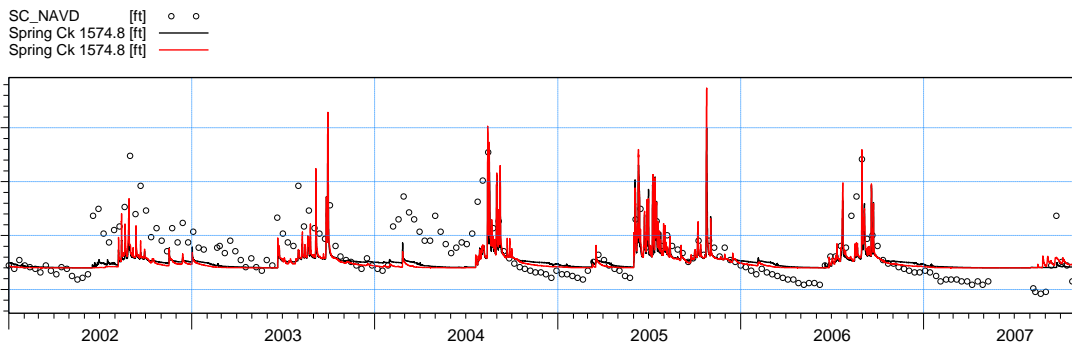
**Figure F45.** Comparison plots at surface water stations Mullock Creek, EsteroRiv and EsteroRiv Q.



ME=-0.925731  
 MAE=0.98899  
 RMSE=1.4937  
 STDres=1.17224  
 R(Correlation)=0.774002  
 R2(Nash\_Sutcliffe)=-2.09299

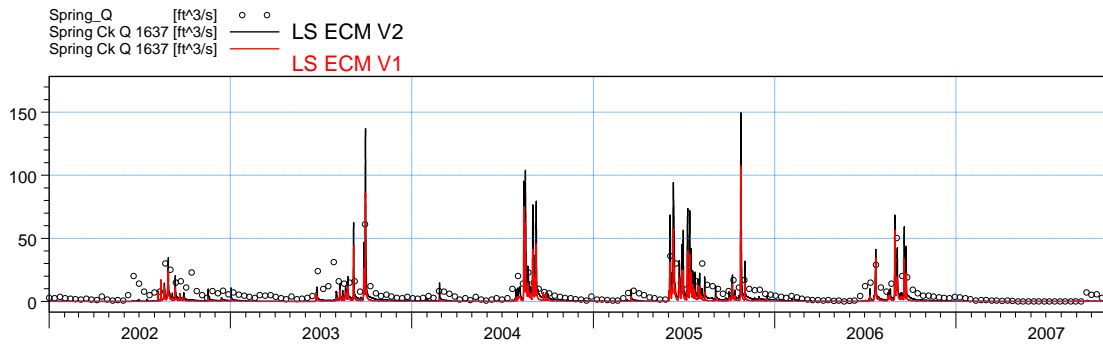


ME=-0.0426489  
 MAE=9.30175  
 RMSE=18.9981  
 STDres=18.9981  
 R(Correlation)=0.759021  
 R2(Nash\_Sutcliffe)=0.40971

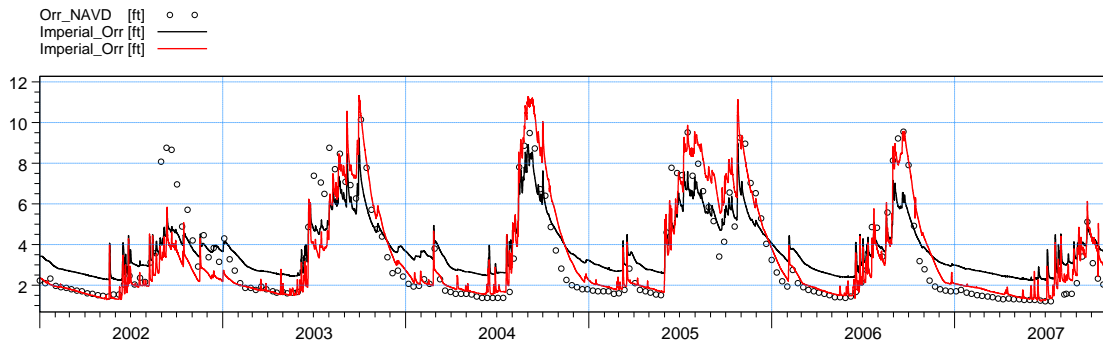


ME=0.157102  
 MAE=0.308744  
 RMSE=0.434797  
 STDres=0.405422  
 R(Correlation)=0.575771  
 R2(Nash\_Sutcliffe)=0.211537

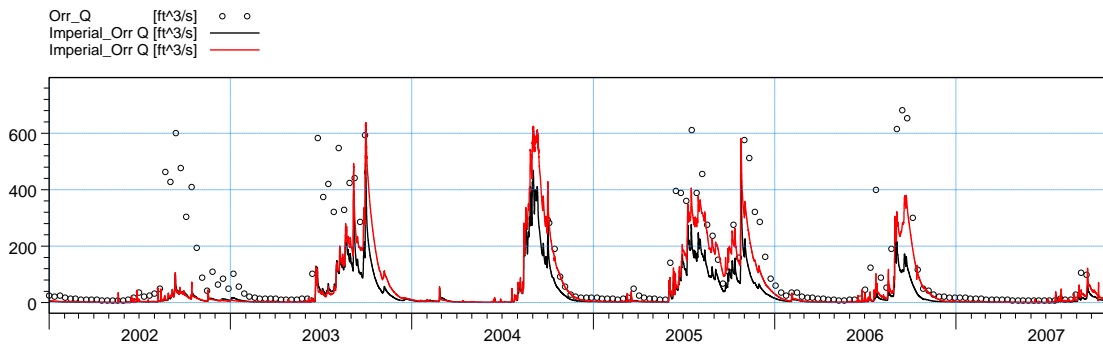
**Figure F46.** Comparison plots at surface water stations EsteroRivS, EsteroRivS Q and SpringCRSS.



ME=4.54128  
 MAE=4.99979  
 RMSE=8.00712  
 STDres=6.59475  
 R(Correlation)=0.730066  
 R2(Nash\_Sutcliffe)=0.299306

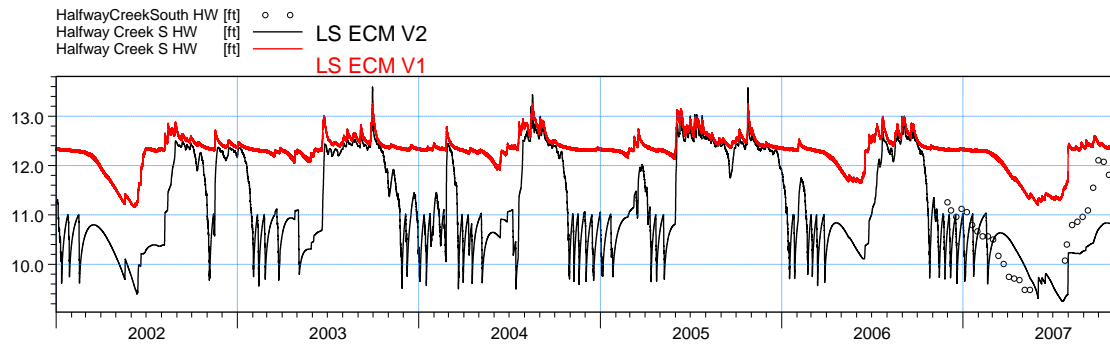


ME=-0.379481  
 MAE=1.20114  
 RMSE=1.37731  
 STDres=1.324  
 R(Correlation)=0.919475  
 R2(Nash\_Sutcliffe)=0.685333

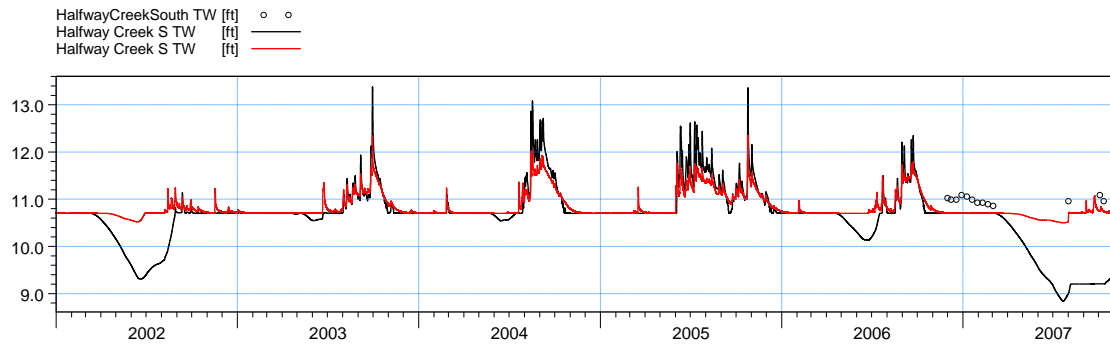


ME=87.778  
 MAE=87.8659  
 RMSE=156.134  
 STDres=129.123  
 R(Correlation)=0.817226  
 R2(Nash\_Sutcliffe)=0.147011

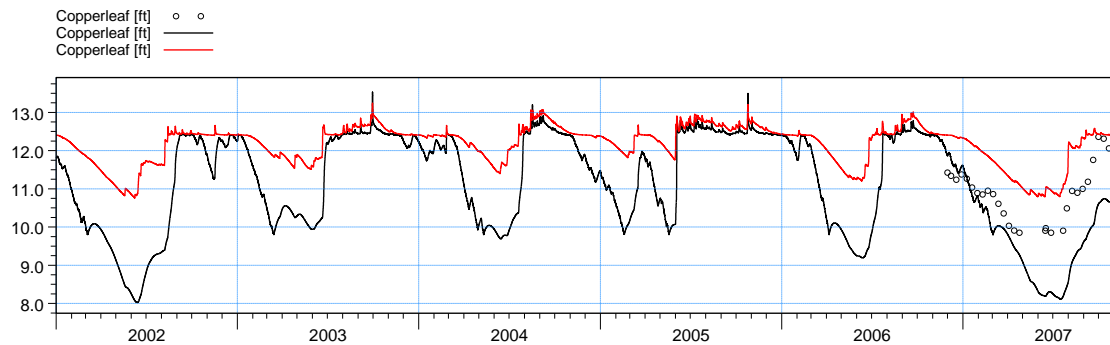
**Figure F47.** Comparison plots at surface water stations SpringCRSS Q, Imperial and Imperial Q.



ME=0.606666  
 MAE=0.767439  
 RMSE=0.848345  
 STDres=0.592997  
 R(Correlation)=0.594267  
 R2(Nash\_Sutcliffe)=-0.340278

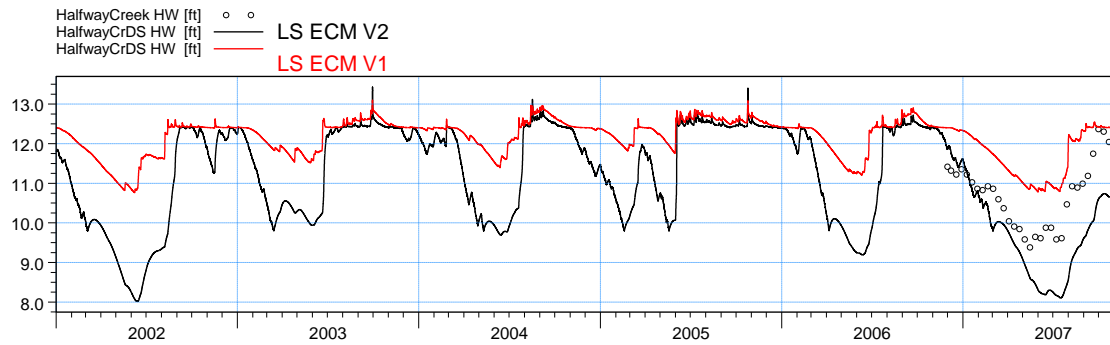


ME=0.903012  
 MAE=0.903012  
 RMSE=1.18691  
 STDres=0.770276  
 R(Correlation)=-0.213961  
 R2(Nash\_Sutcliffe)=-213.979

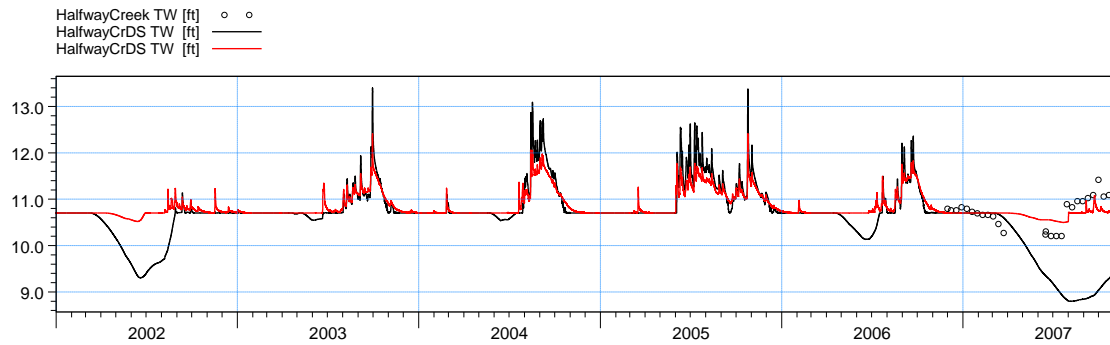


ME=1.26965  
 MAE=1.31116  
 RMSE=1.43999  
 STDres=0.679374  
 R(Correlation)=0.66763  
 R2(Nash\_Sutcliffe)=-2.72523

**Figure F48.** Comparison plots at surface water stations Halfway\_S HW, Halfway\_S TW and Copperleaf.



ME=1.26894  
 MAE=1.30463  
 RMSE=1.41574  
 STDres=0.627795  
 R(Correlation)=0.798173  
 R2(Nash\_Sutcliffe)=-1.38573



ME=1.50847  
 MAE=1.52967  
 RMSE=1.72303  
 STDres=0.832681  
 R(Correlation)=-0.226145  
 R2(Nash\_Sutcliffe)=-22.1851

**Figure F49.** Comparison plots at surface water stations HalfwayCrDS HW, and HalfwayCrDS TW.

## **APPENDIX G. WATER TABLE LEVEL MAPS**

The averaged water table level maps in the DR/GR Area are presented in this appendix. The maps are extracted from the different models at two different times of the year, commonly known as the end of the dry and the wet season. They were obtained by averaging the top-computational-layer heads for the last 10 days of the months of May and September, respectively, during the simulation period. The water table profiles along two transects through the mining pit complex area are also presented for all models and for the two times of the year.

### **List of Figures**

|  |    |
|--|----|
| Figure G1. Average water table level map for the DRGR Area at the end of the dry season as predicted by the ECM. ....          | 2  |
| Figure G2. Average water table level map for the DR/GR Area at the end of the wet season as predicted by the ECM. ....         | 3  |
| Figure G3. Average water table level map for the DR/GR Area at the end of the dry season as predicted by the LS ECM V1. ....   | 4  |
| Figure G4. Average water table level map for the DR/GR Area at the end of the wet season as predicted by the LS ECM V1. ....   | 5  |
| Figure G5. Average water table level map for the DR/GR Area at the end of the dry season as predicted by the LS FCM1 V2. ....  | 6  |
| Figure G6. Average water table level map for the DR/GR Area at the end of the wet season as predicted by the LS FCM1 V2. ....  | 7  |
| Figure G7. Average water table level map for the DR/GR Area at the end of the dry season as predicted by the LS FCM2 V2. ....  | 8  |
| Figure G8. Average water table level map for the DR/GR Area at the end of the wet season as predicted by the LS FCM2 V2. ....  | 9  |
| Figure G9. Average water table level map for the DR/GR Area at the end of the dry season as predicted by the LS FCM3 V2. ....  | 10 |
| Figure G10. Average water table level map for the DR/GR Area at the end of the wet season as predicted by the LS FCM3 V2. .... | 11 |
| Figure G11. Average water table level map for the DR/GR Area at the end of the dry season as predicted by the LS FCM4 V2. .... | 12 |
| Figure G12. Average water table level map for the DR/GR Area at the end of the wet season as predicted by the LS FCM4 V2. .... | 13 |

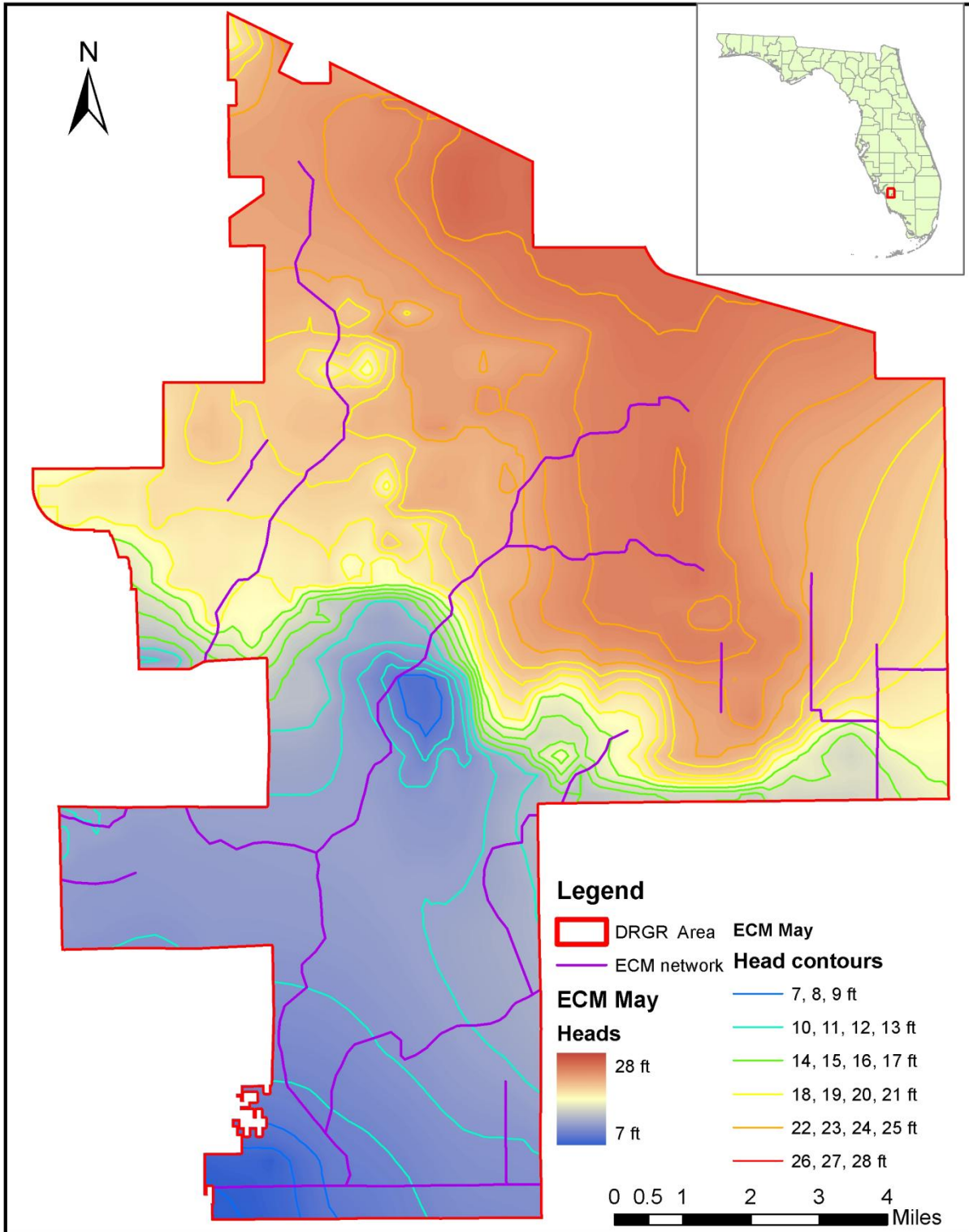


**Figure G1.** Average water table level map for the DRGR Area at the end of the dry season as predicted by the ECM.

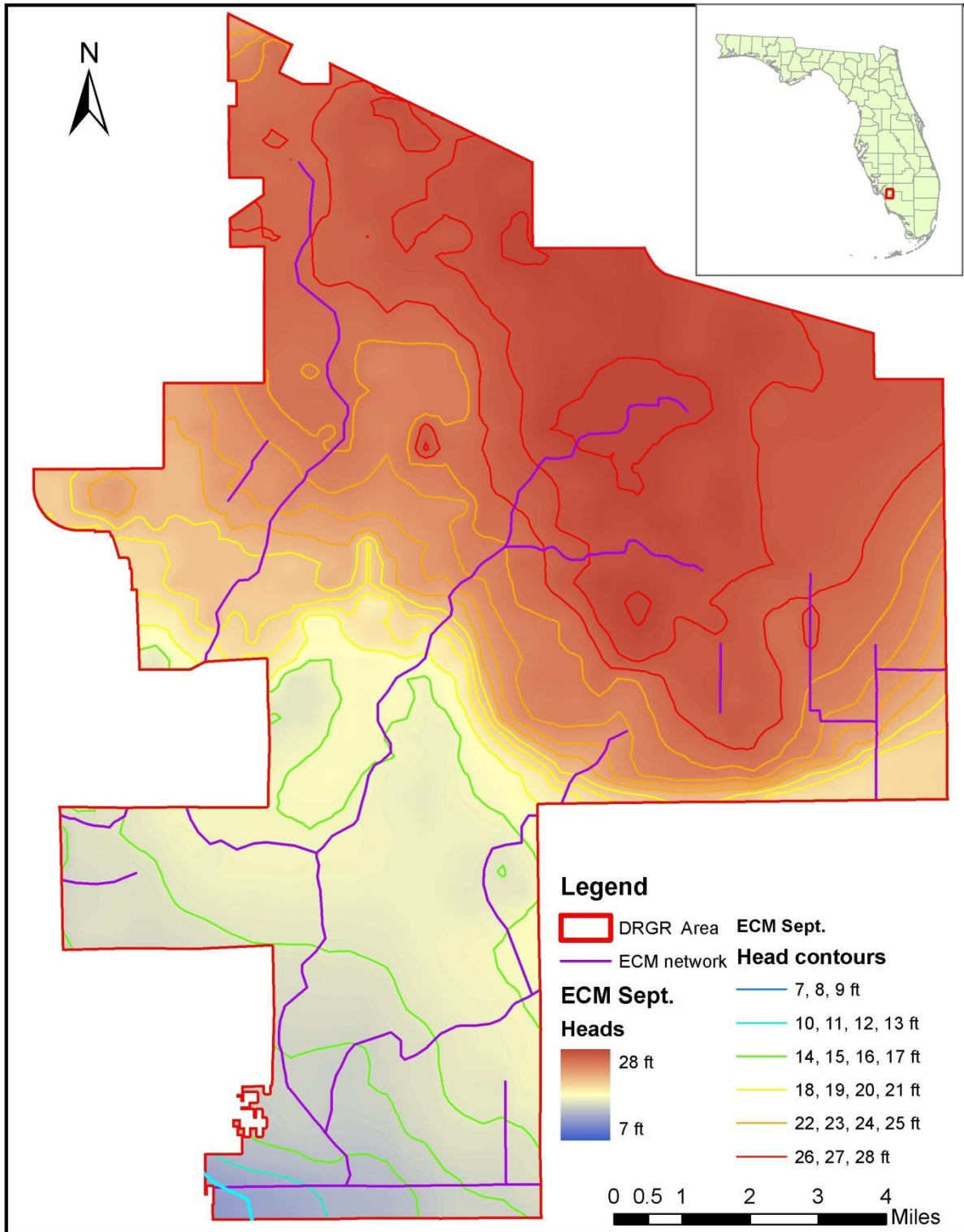


**Figure G2.** Average water table level map for the DR/GR Area at the end of the wet season as predicted by the ECM.

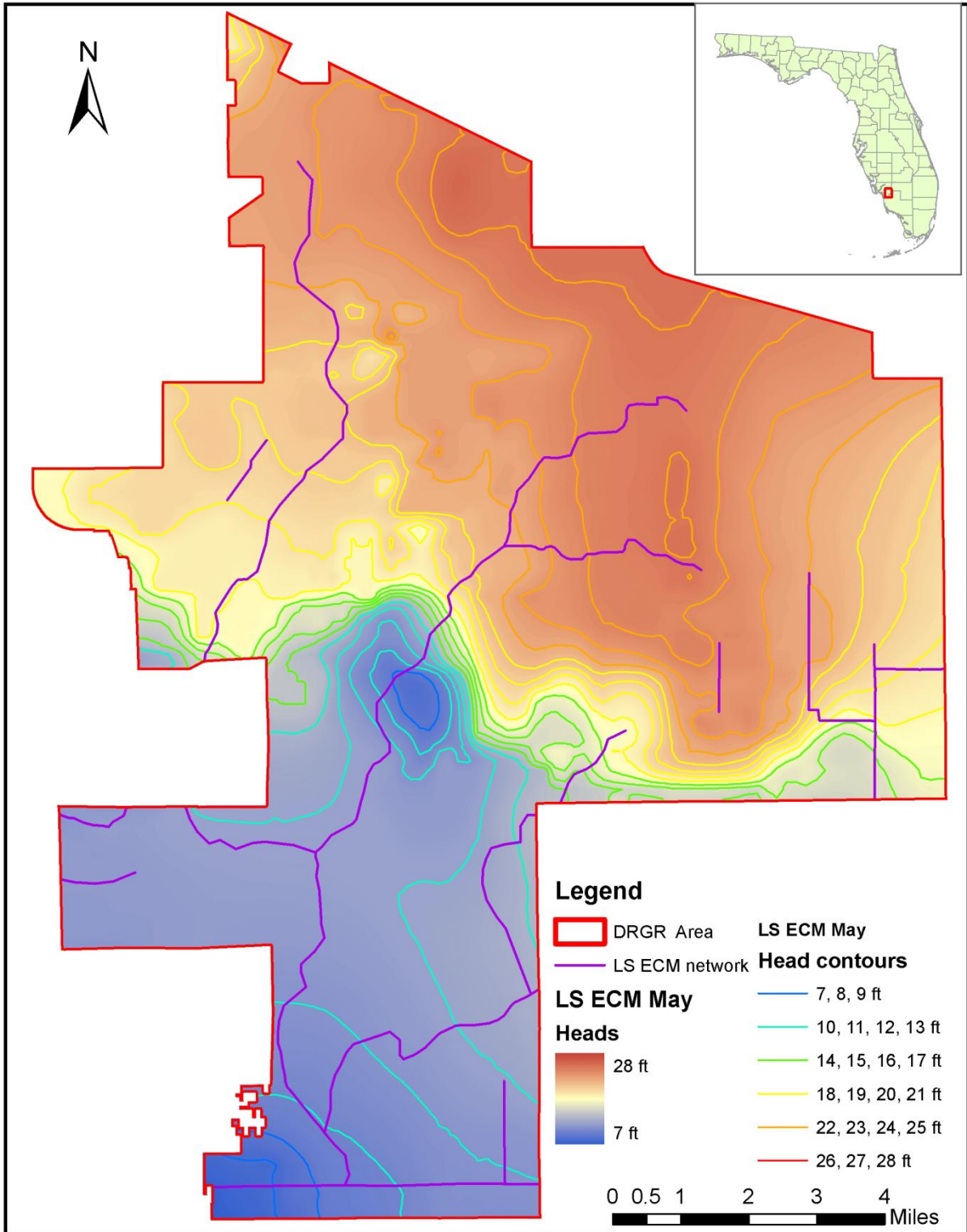


**Figure G3.** Average water table level map for the DR/GR Area at the end of the dry season as predicted by the LS ECM V1.

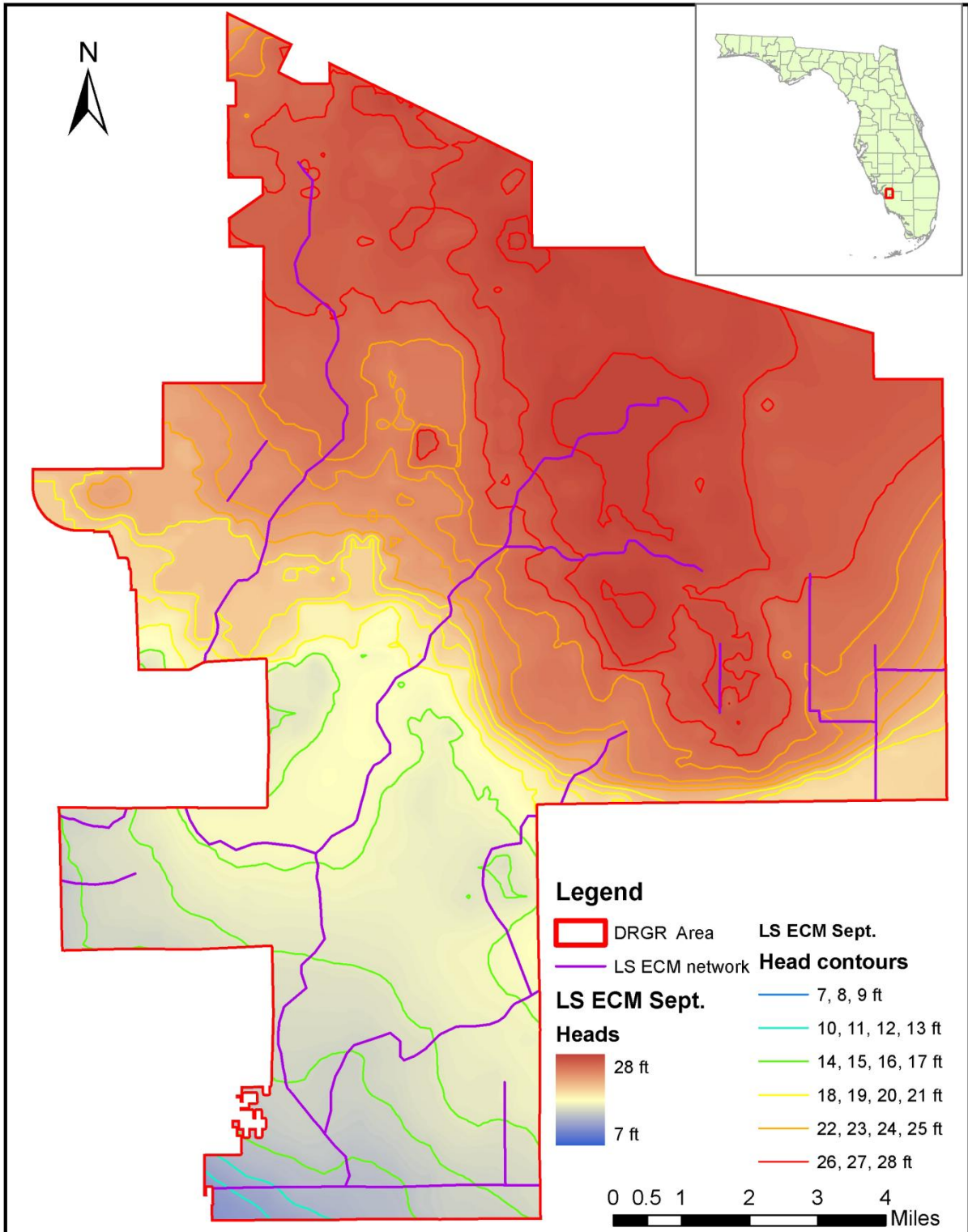


**Figure G4.** Average water table level map for the DR/GR Area at the end of the wet season as predicted by the LS ECM V1.

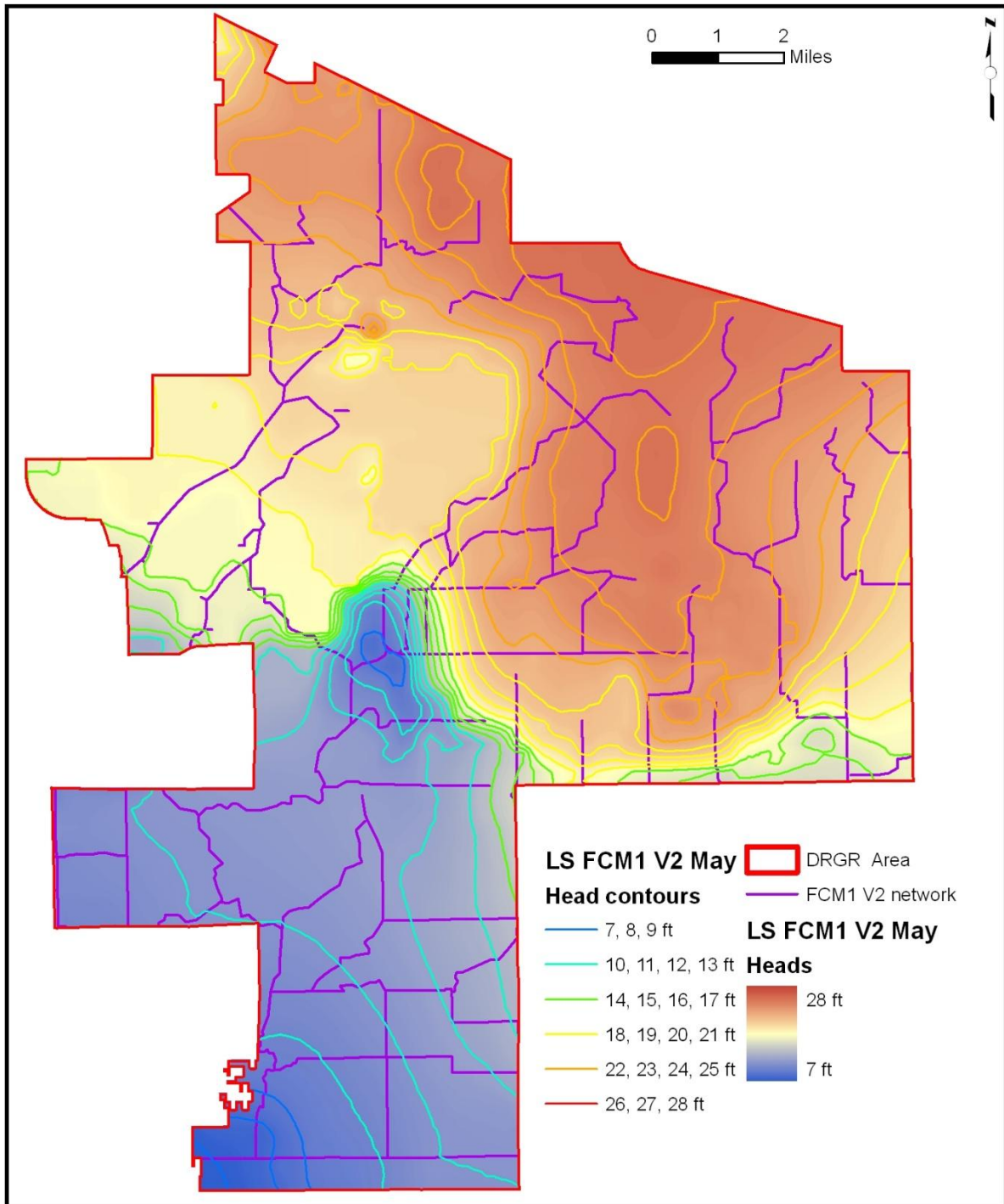


**Figure G5.** Average water table level map for the DR/GR Area at the end of the dry season as predicted by the LS FCM1 V2.

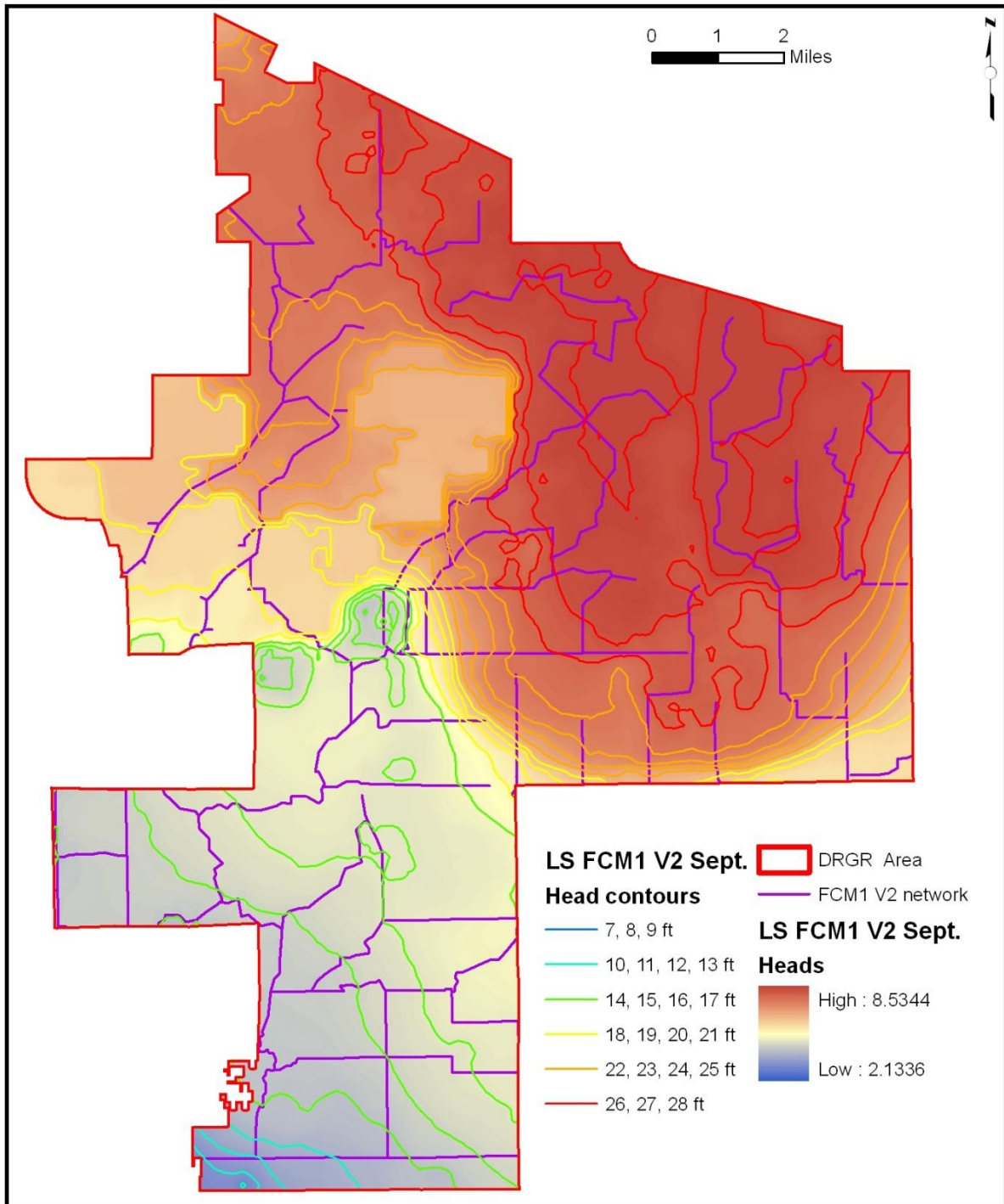


**Figure G6.** Average water table level map for the DR/GR Area at the end of the wet season as predicted by the LS FCM1 V2.

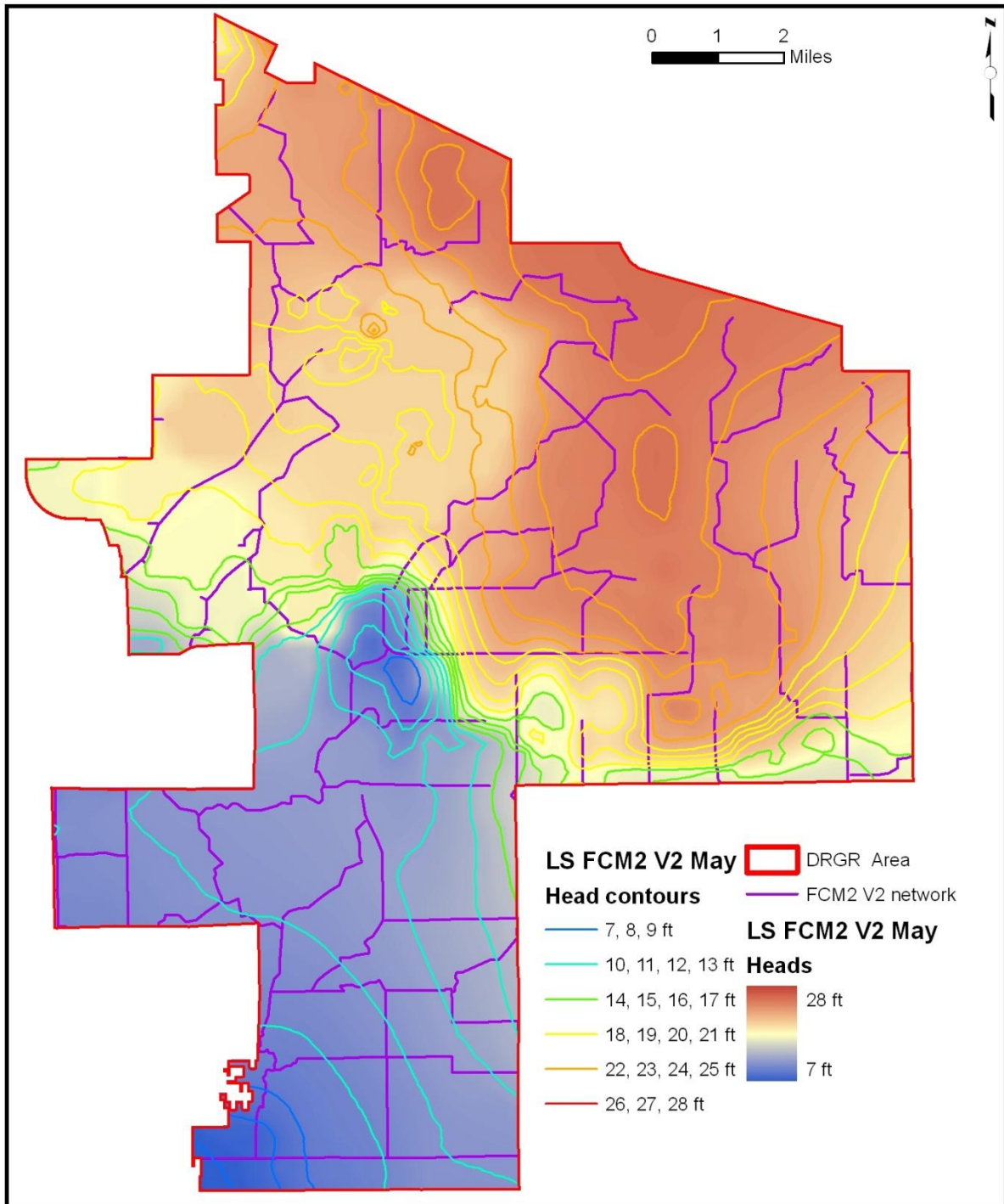


**Figure G7.** Average water table level map for the DR/GR Area at the end of the dry season as predicted by the LS FCM2 V2.

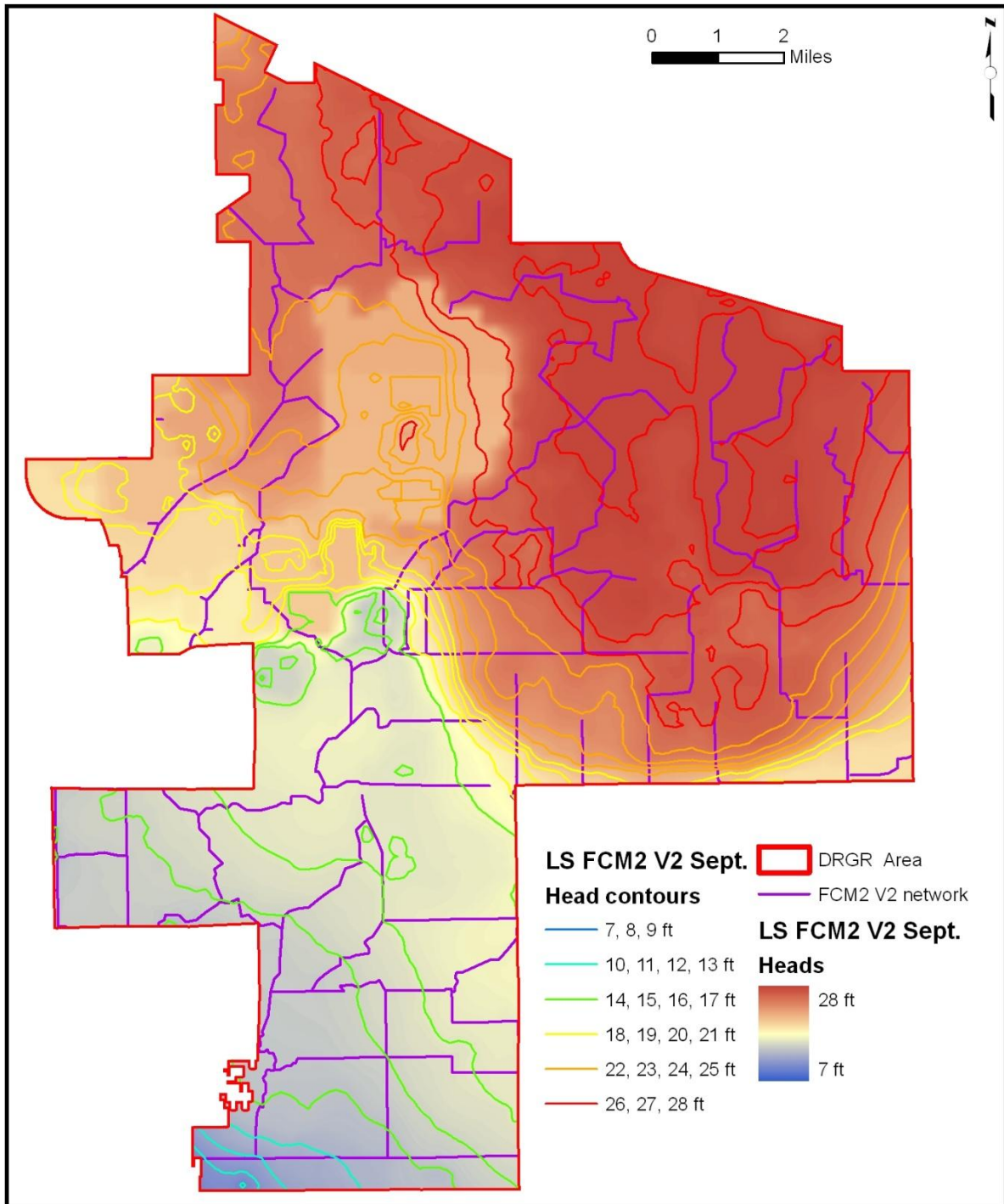


**Figure G8.** Average water table level map for the DR/GR Area at the end of the wet season as predicted by the LS FCM2 V2.

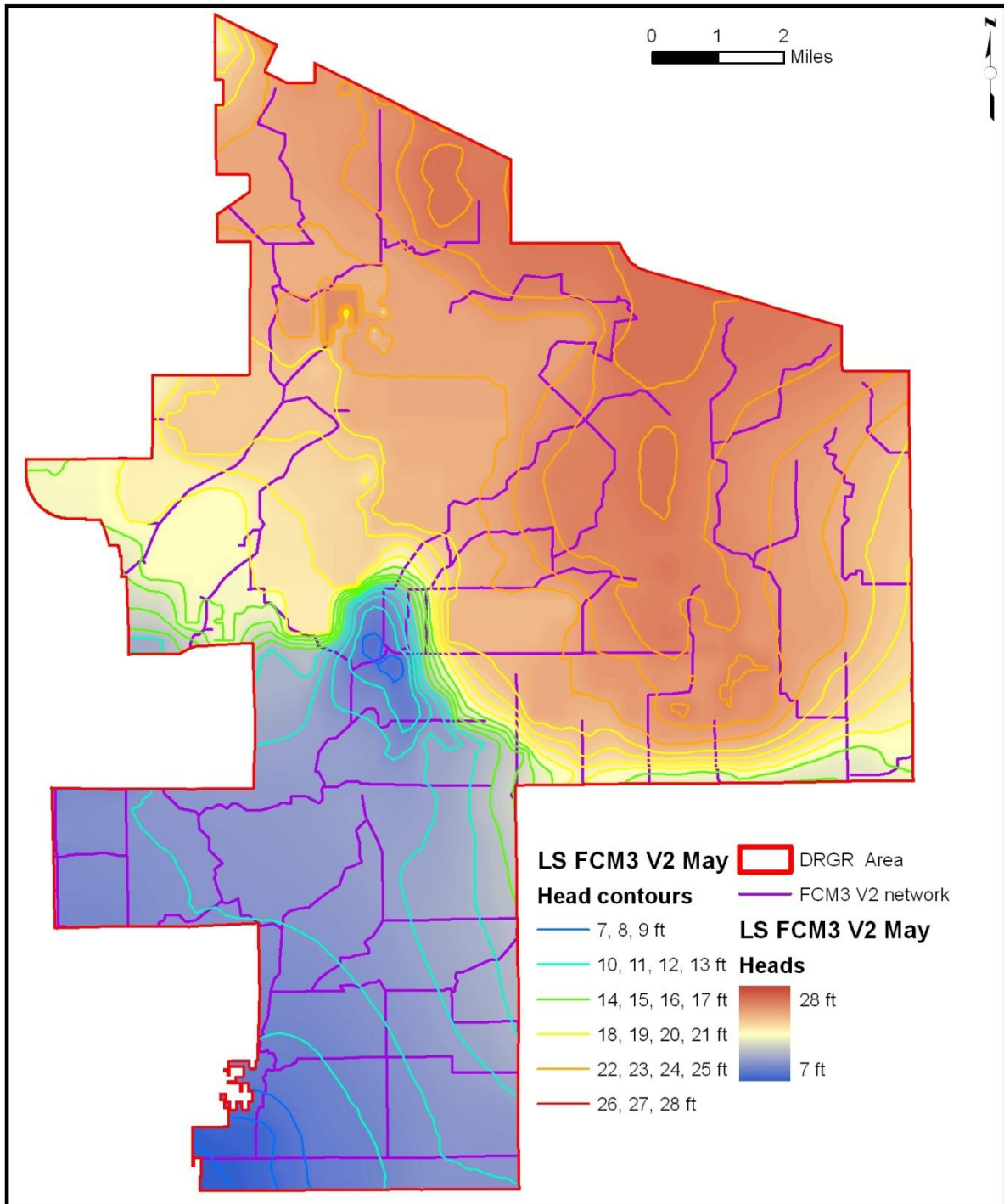


**Figure G9.** Average water table level map for the DR/GR Area at the end of the dry season as predicted by the LS FCM3 V2.

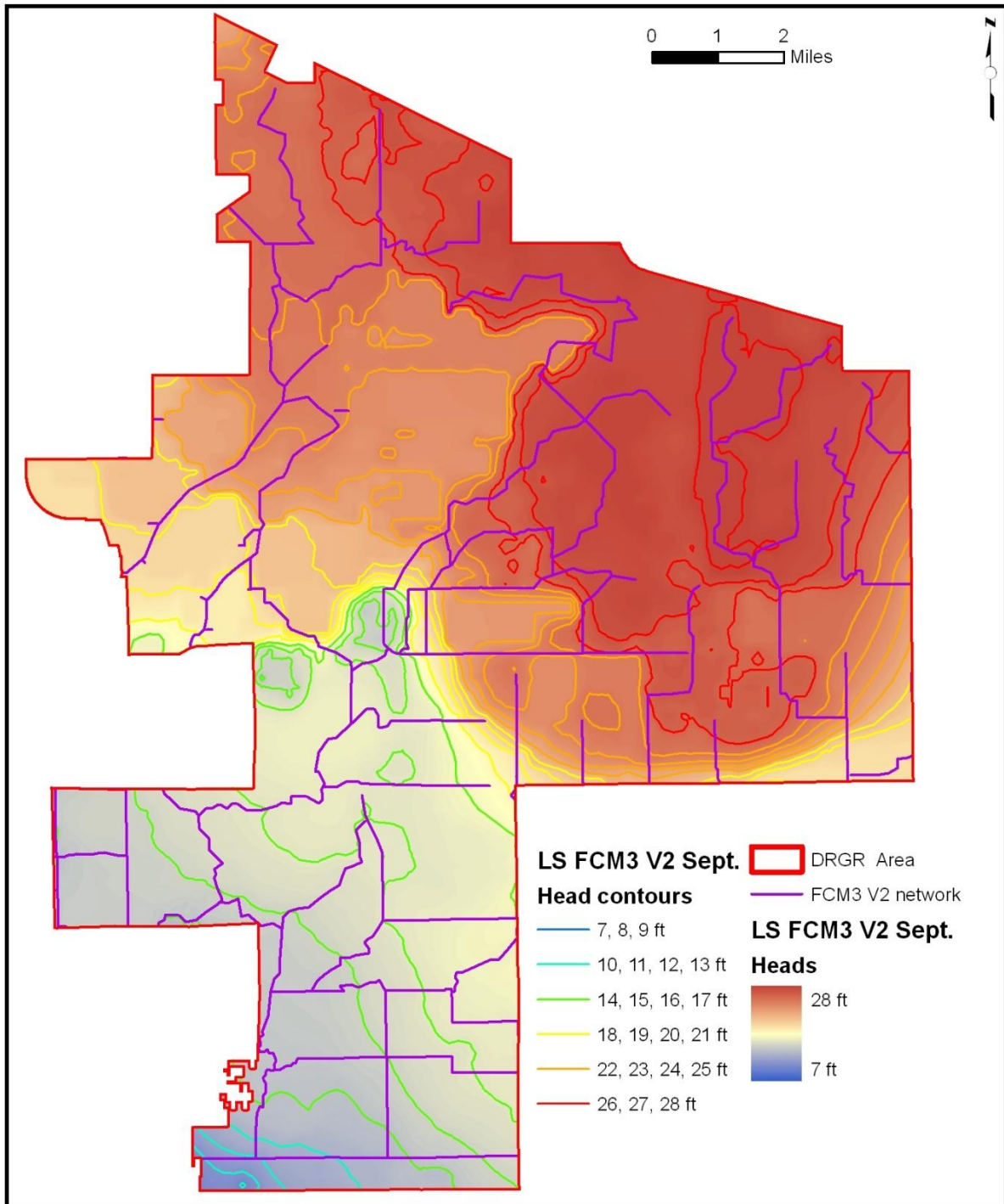


**Figure G10.** Average water table level map for the DR/GR Area at the end of the wet season as predicted by the LS FCM3 V2.

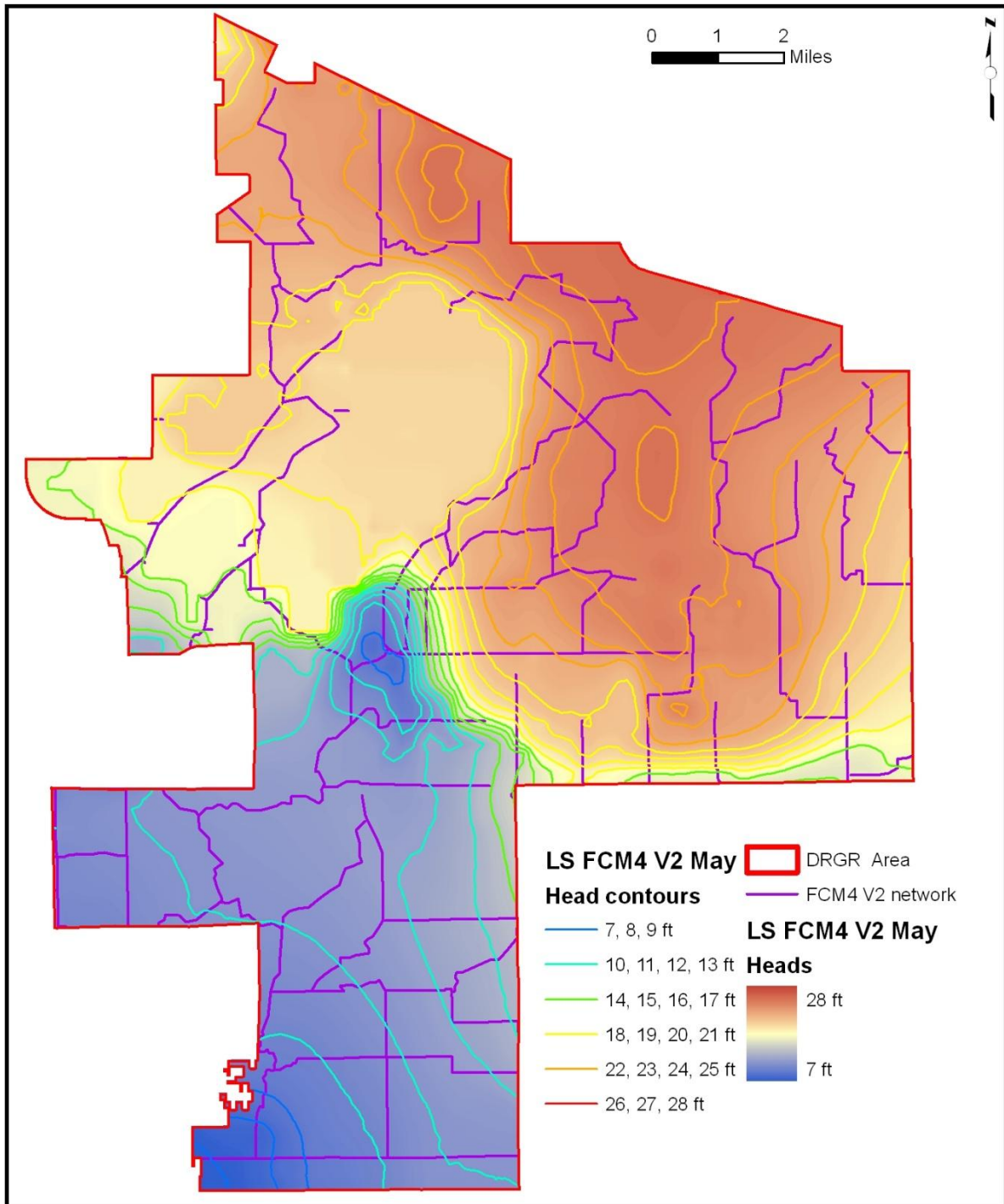


**Figure G11.** Average water table level map for the DR/GR Area at the end of the dry season as predicted by the LS FCM4 V2.

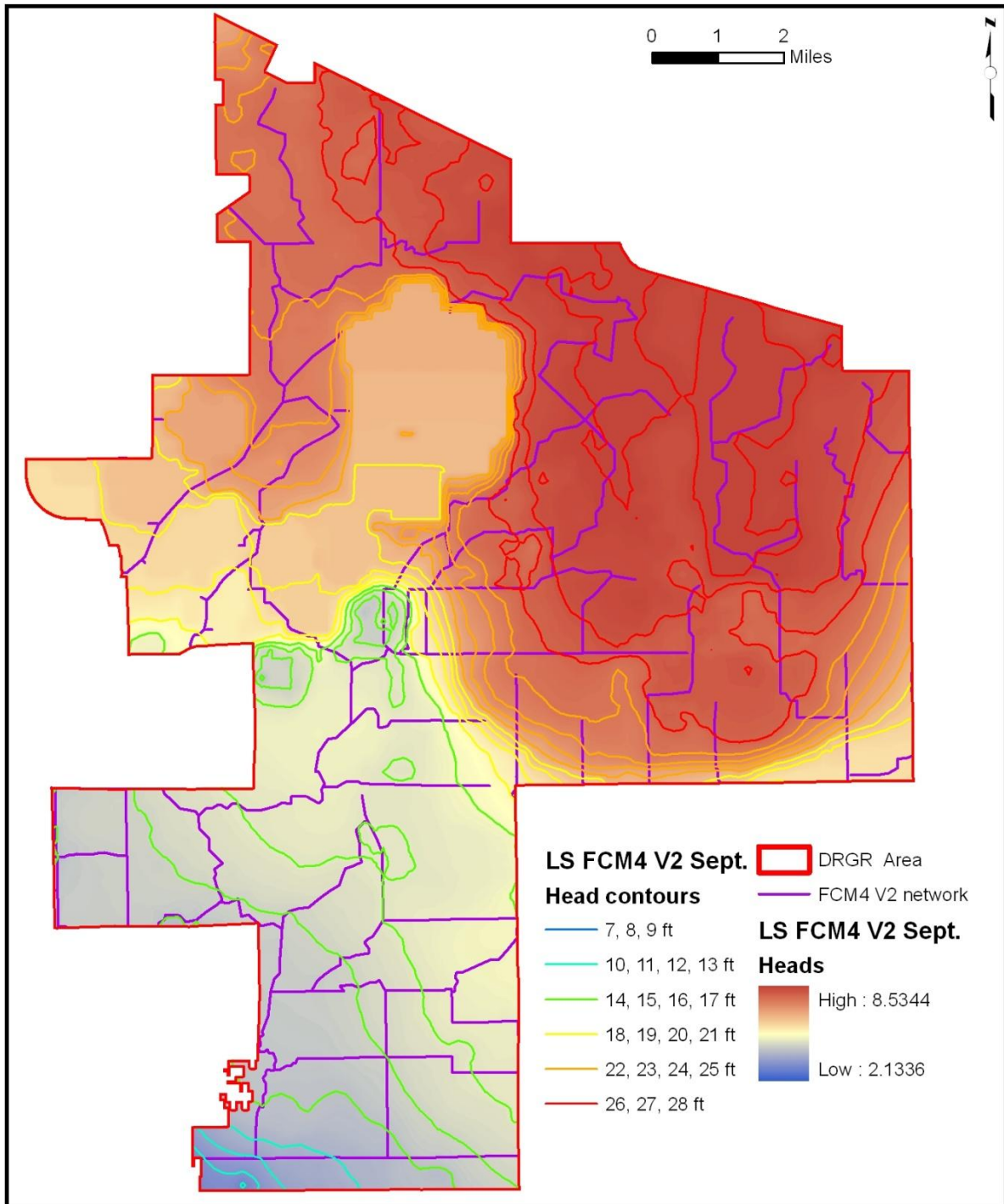


**Figure G12.** Average water table level map for the DR/GR Area at the end of the wet season as predicted by the LS FCM4 V2.

## **APPENDIX H. HYDROPERIOD MAPS**

Additional hydroperiod-related figures are presented in this appendix. This includes the hydroperiod maps in the DR/GR Area obtained from all the local scale models, as well as the mean water depth during the hydroperiod.

### **List of Figures**

|  |    |
|--|----|
| Figure H1. Average annual hydro-period map for the DR/GR Area as predicted by LS ECM V2* with LE = RET + 5.3%.....   | 2  |
| Figure H2. Average water depth during the hydro-period for the DR/GR Area as predicted by LS ECM V2* with LE = RET + 5.3%.....                                       | 3  |
| Figure H3. Average annual hydro-period map for the DR/GR Area as predicted by LS ECM V2* with LE = RET + 8.2%.....   | 4  |
| Figure H4. Average water depth during the hydro-period for the DR/GR Area as predicted by LS ECM V2* with LE = RET + 8.2%.....                                       | 5  |
| Figure H5. Average annual hydro-period map for the DR/GR Area as predicted by the LS FCM1 V2.....  | 6  |
| Figure H6. Average water depth during the hydro-period for the DR/GR Area as predicted by the LS FCM1 V2.....  | 7  |
| Figure H7. Difference in water depths during hydroperiod in FCM1 in relation to the ECM (Positive values indicate greater duration of water ponding in FCM1). .....  | 8  |
| Figure H8. Average annual hydro-period map for the DR/GR Area as predicted by the LS FCM2 V2.....  | 9  |
| Figure H9. Average water depth during the hydro-period for the DR/GR Area as predicted by the LS FCM2 V2.....  | 10 |
| Figure H10. Difference in water depths during hydroperiod in FCM2 in relation to the ECM (Positive values indicate greater duration of water ponding in FCM2). ..... | 11 |
| Figure H11. Average annual hydro-period map for the DR/GR Area as predicted by the LS FCM3 V2.....   | 12 |
| Figure H12. Average water depth during the hydro-period for the DR/GR Area as predicted by the LS FCM3 V2.....   | 13 |
| Figure H13. Difference in water depths during hydroperiod in FCM3 in relation to the ECM (Positive values indicate greater duration of water ponding in FCM3). ..... | 14 |
| Figure H14. Average annual hydro-period map for the DR/GR Area as predicted by the LS FCM4 V2.....   | 15 |
| Figure H15. Average water depth during the hydro-period for the DR/GR Area as predicted by the LS FCM4 V2.....   | 16 |
| Figure H16. Difference in water depths during hydroperiod in FCM4 in relation to the ECM (Positive values indicate greater duration of water ponding in FCM4). ..... | 17 |

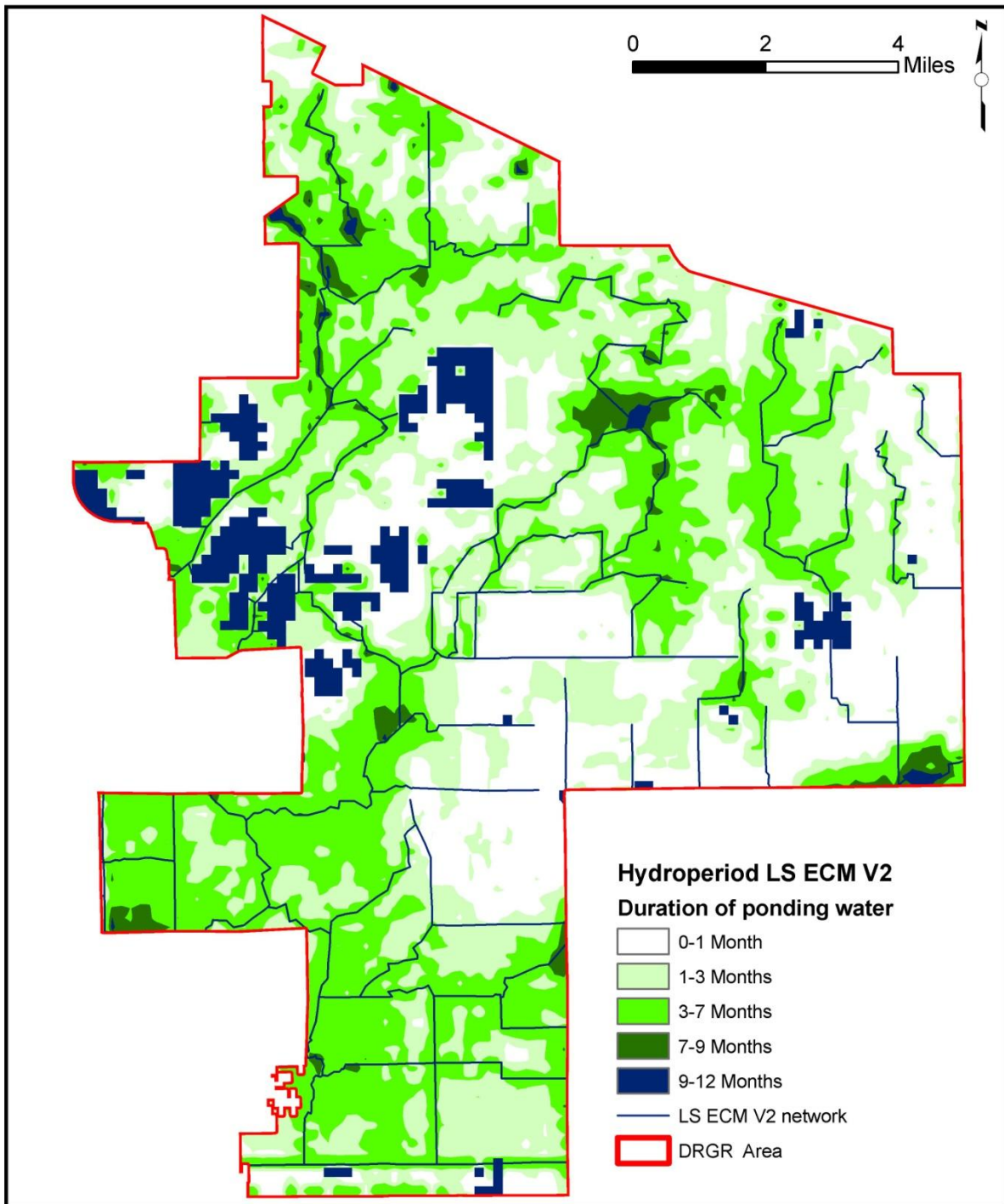


**Figure H1.** Average annual hydro-period map for the DR/GR Area as predicted by LS ECM V2\* with LE = RET + 5.3%.

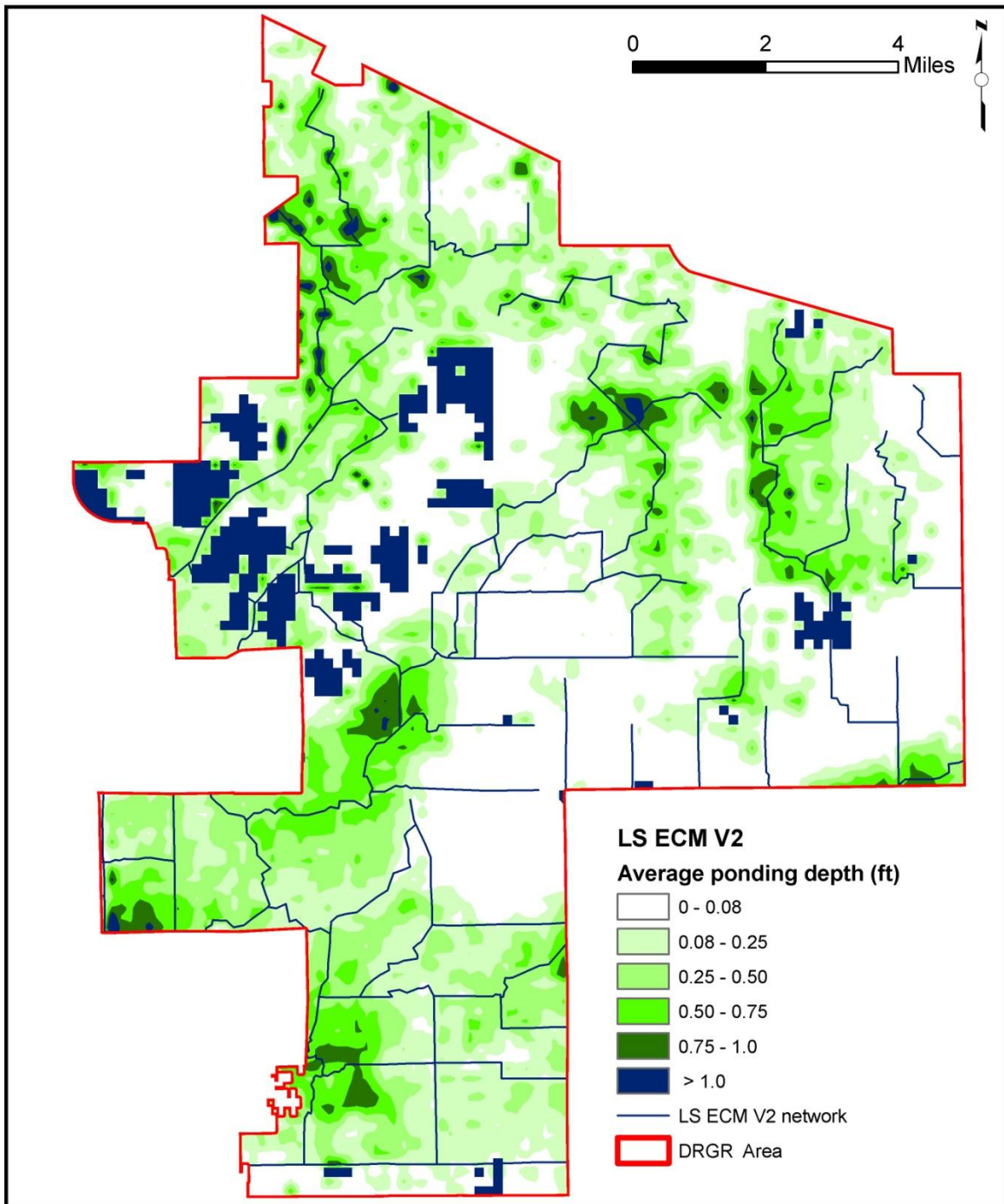


**Figure H2.** Average water depth during the hydro-period for the DR/GR Area as predicted by LS ECM V2\* with LE = RET + 5.3%.

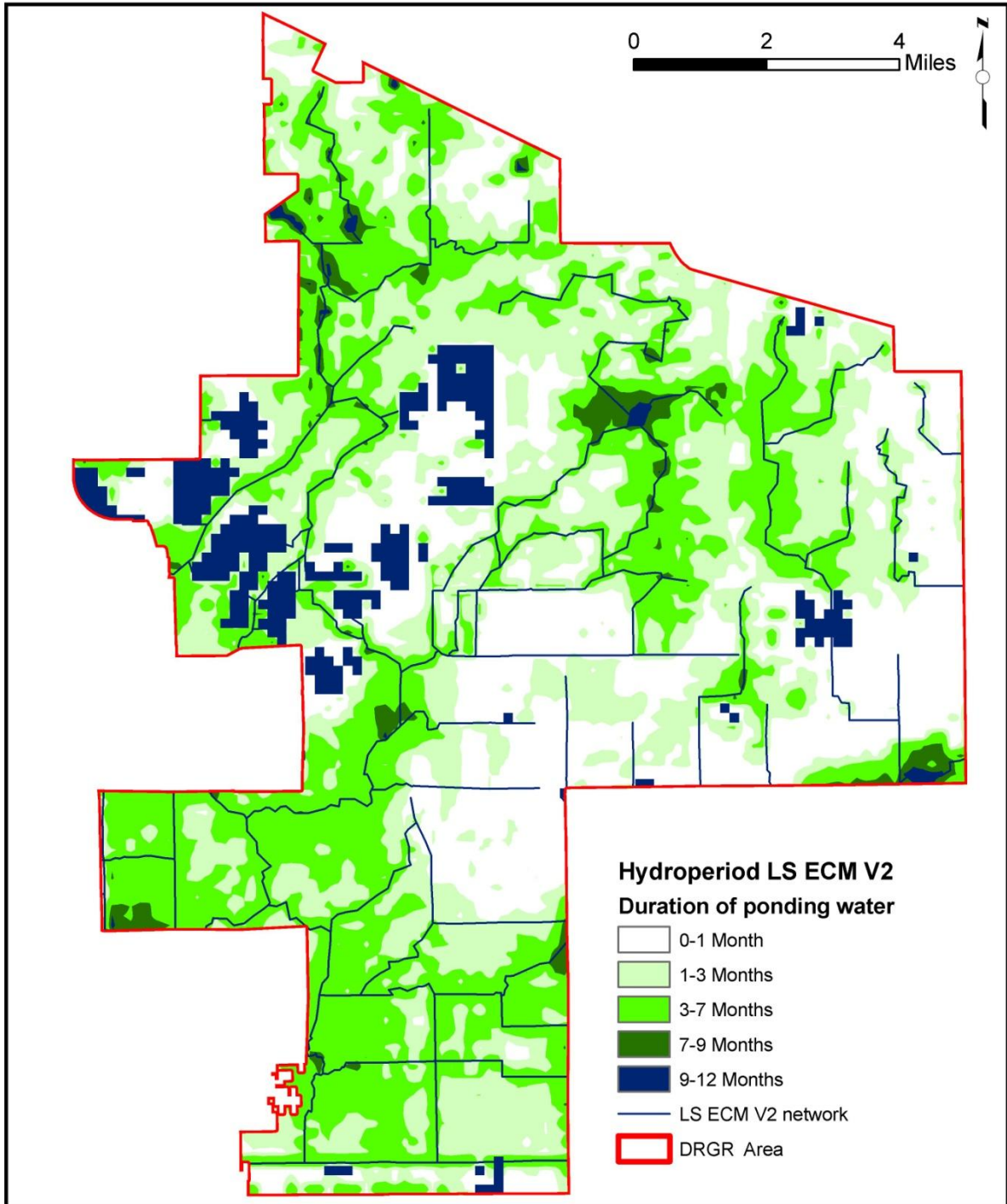


**Figure H3.** Average annual hydro-period map for the DR/GR Area as predicted by LS ECM V2\* with LE = RET + 8.2%.

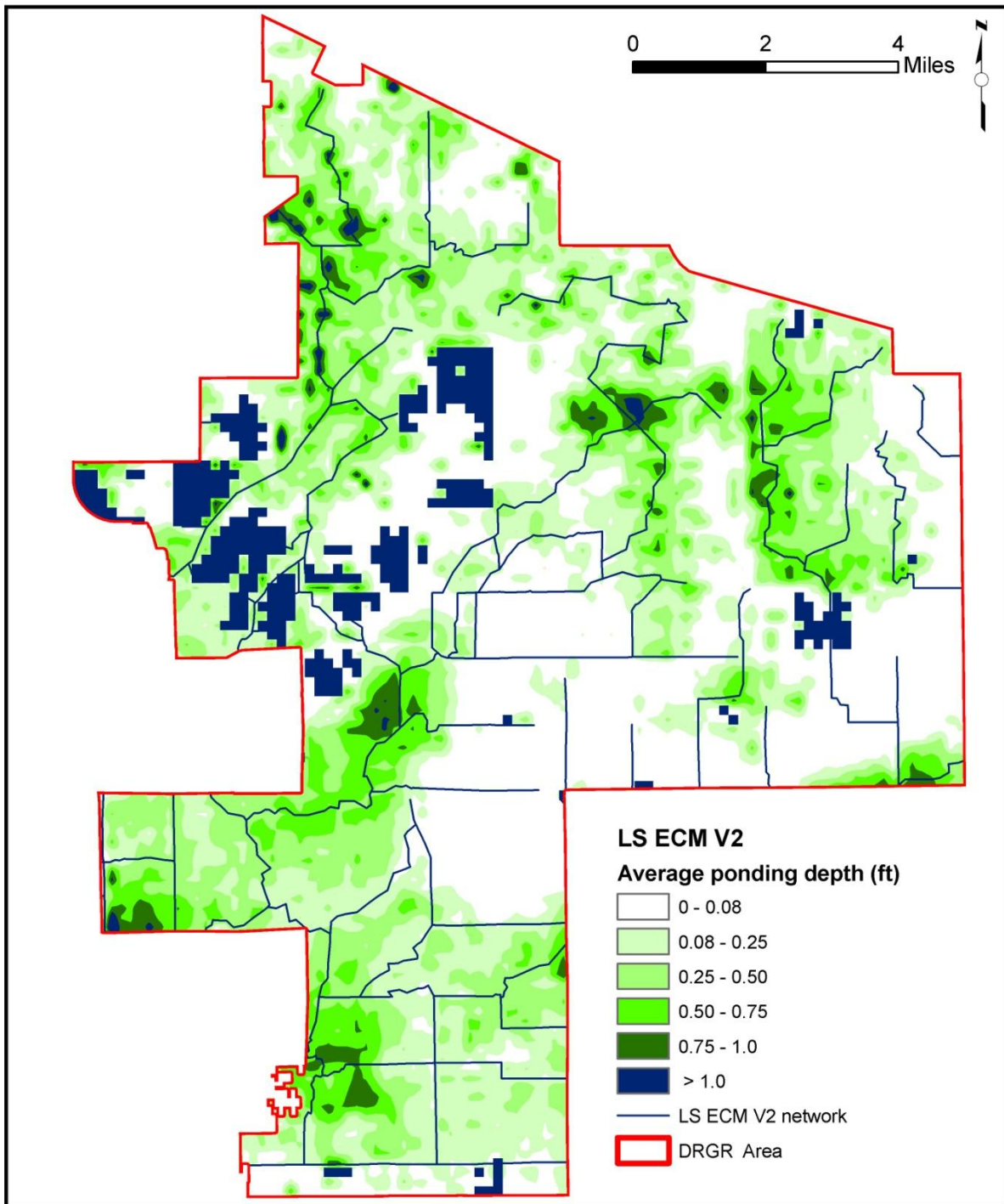


**Figure H4.** Average water depth during the hydro-period for the DR/GR Area as predicted by LS ECM V2\* with LE = RET + 8.2%.

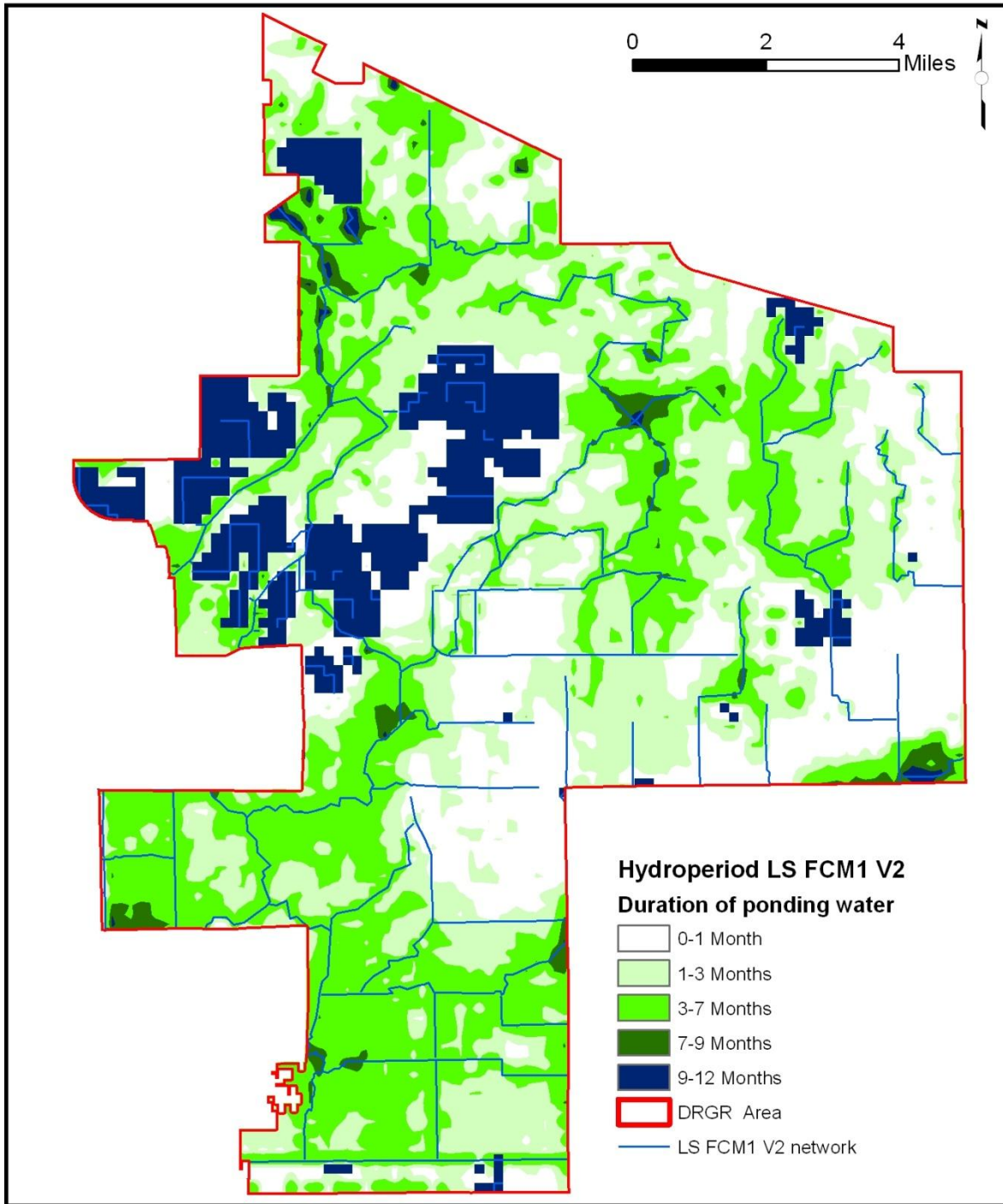


**Figure H5.** Average annual hydro-period map for the DR/GR Area as predicted by the LS FCM1 V2.

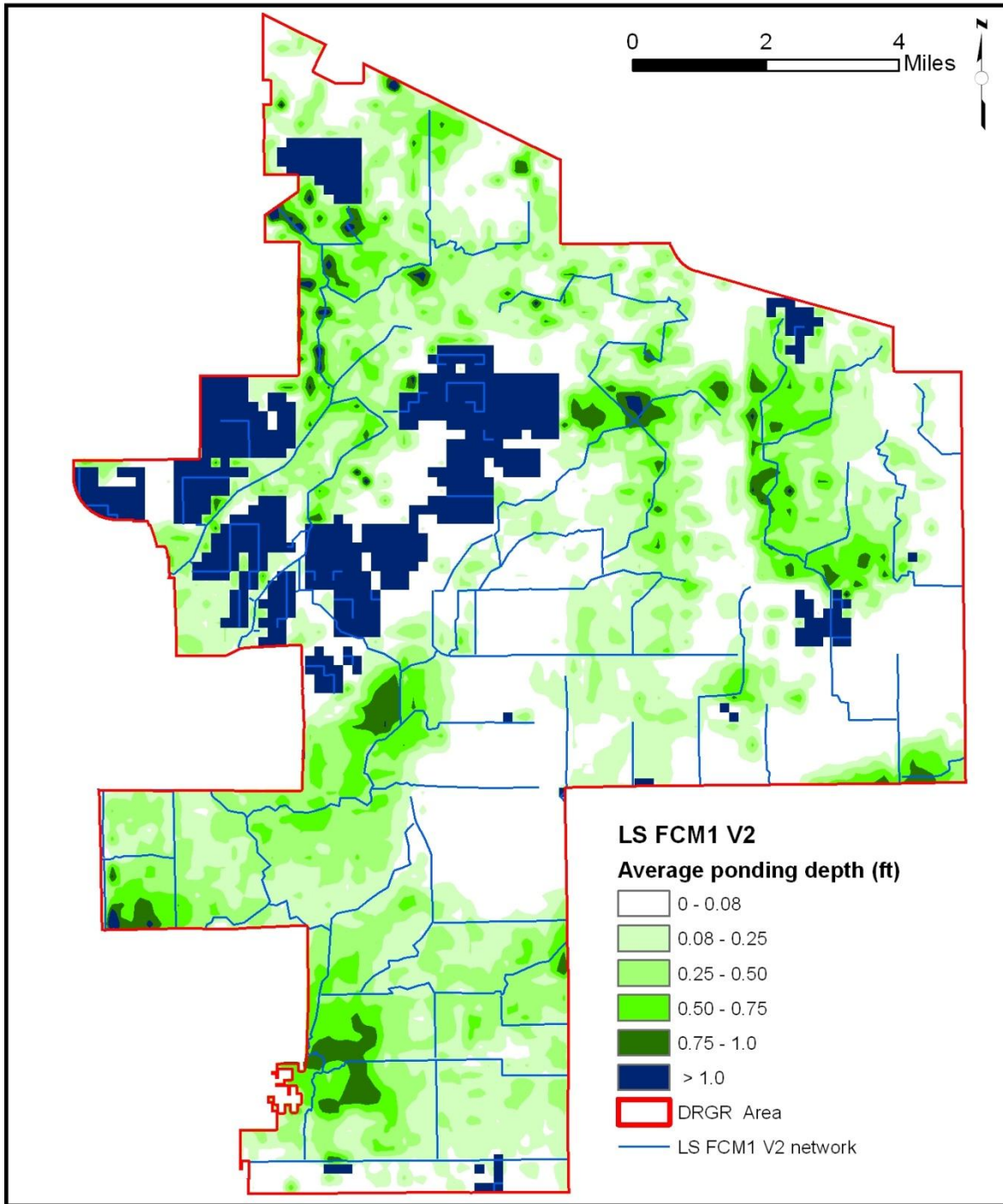


**Figure H6.** Average water depth during the hydro-period for the DR/GR Area as predicted by the LS FCM1 V2.

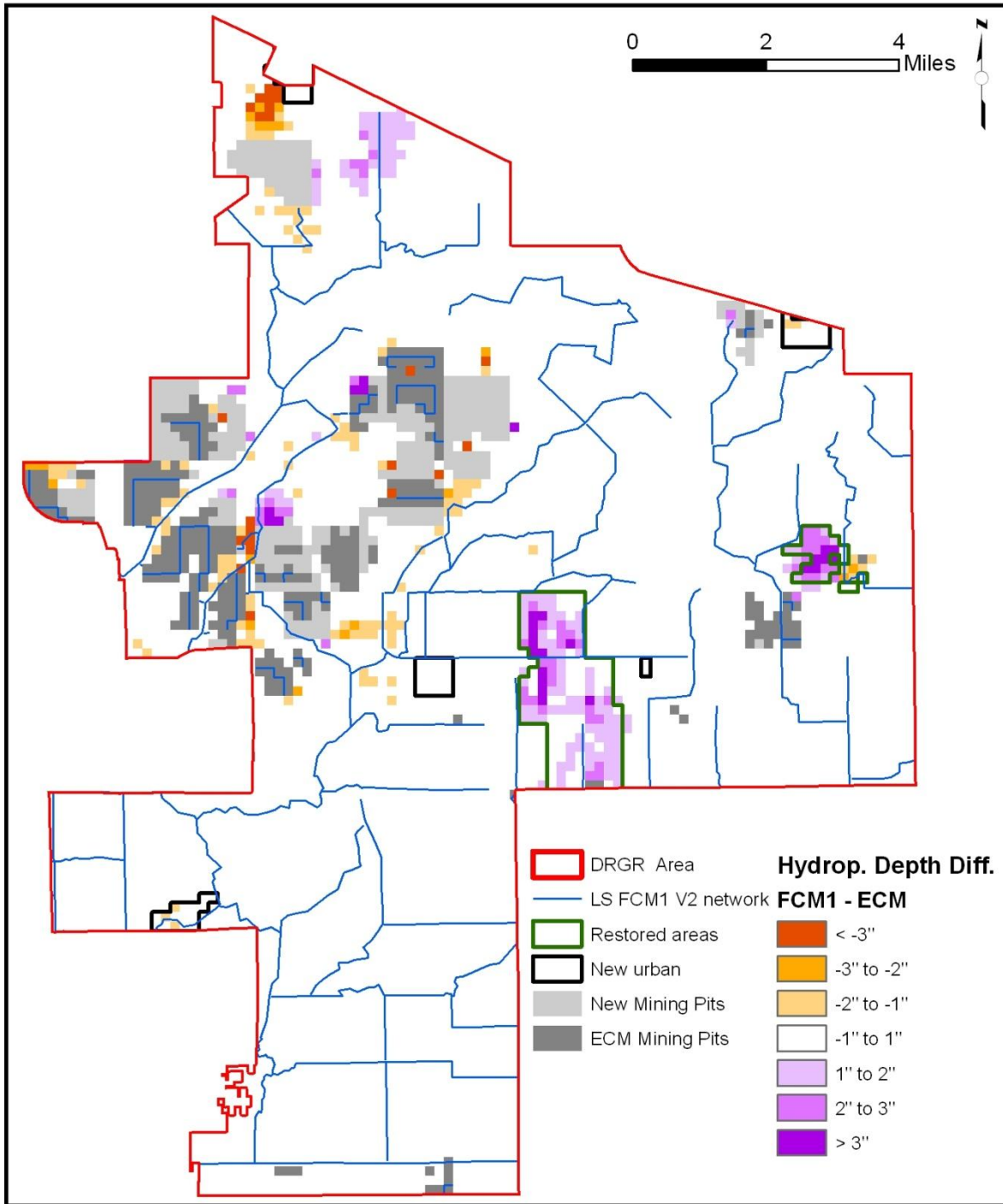


**Figure H7.** Difference in water depths during hydroperiod in FCM1 in relation to the ECM (Positive values indicate greater duration of water ponding in FCM1).

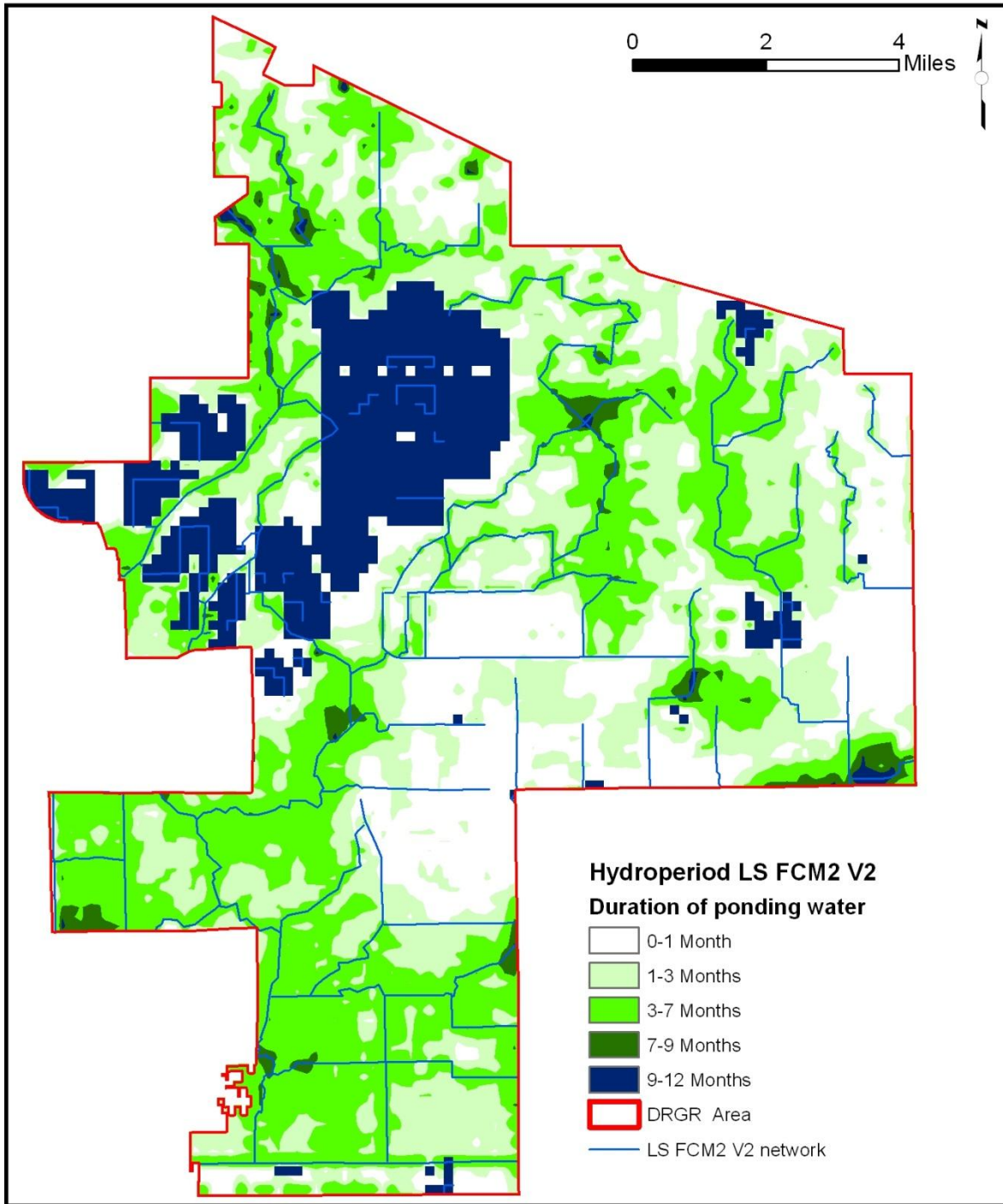


**Figure H8.** Average annual hydro-period map for the DR/GR Area as predicted by the LS FCM2 V2.

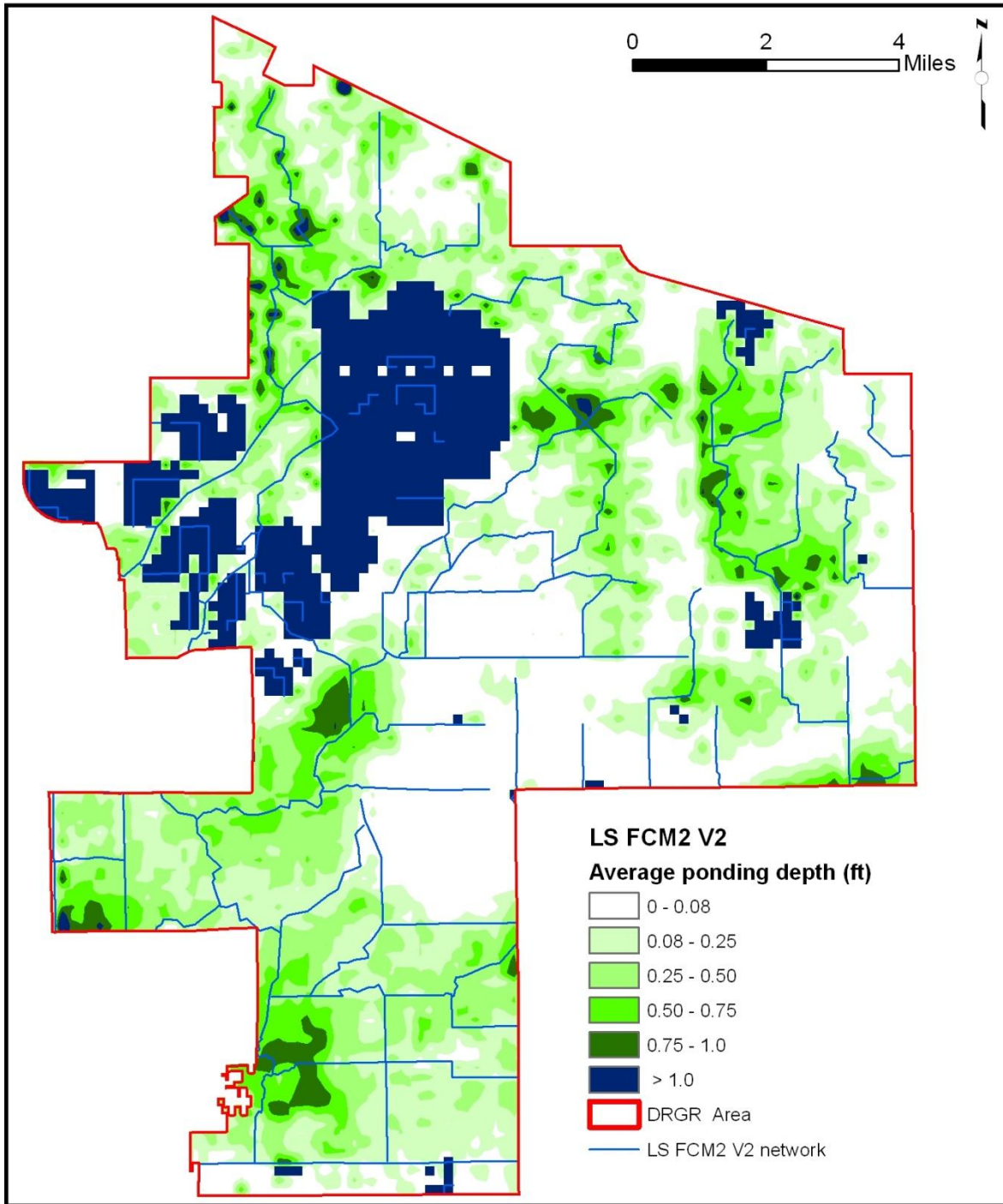


**Figure H9.** Average water depth during the hydro-period for the DR/GR Area as predicted by the LS FCM2 V2.

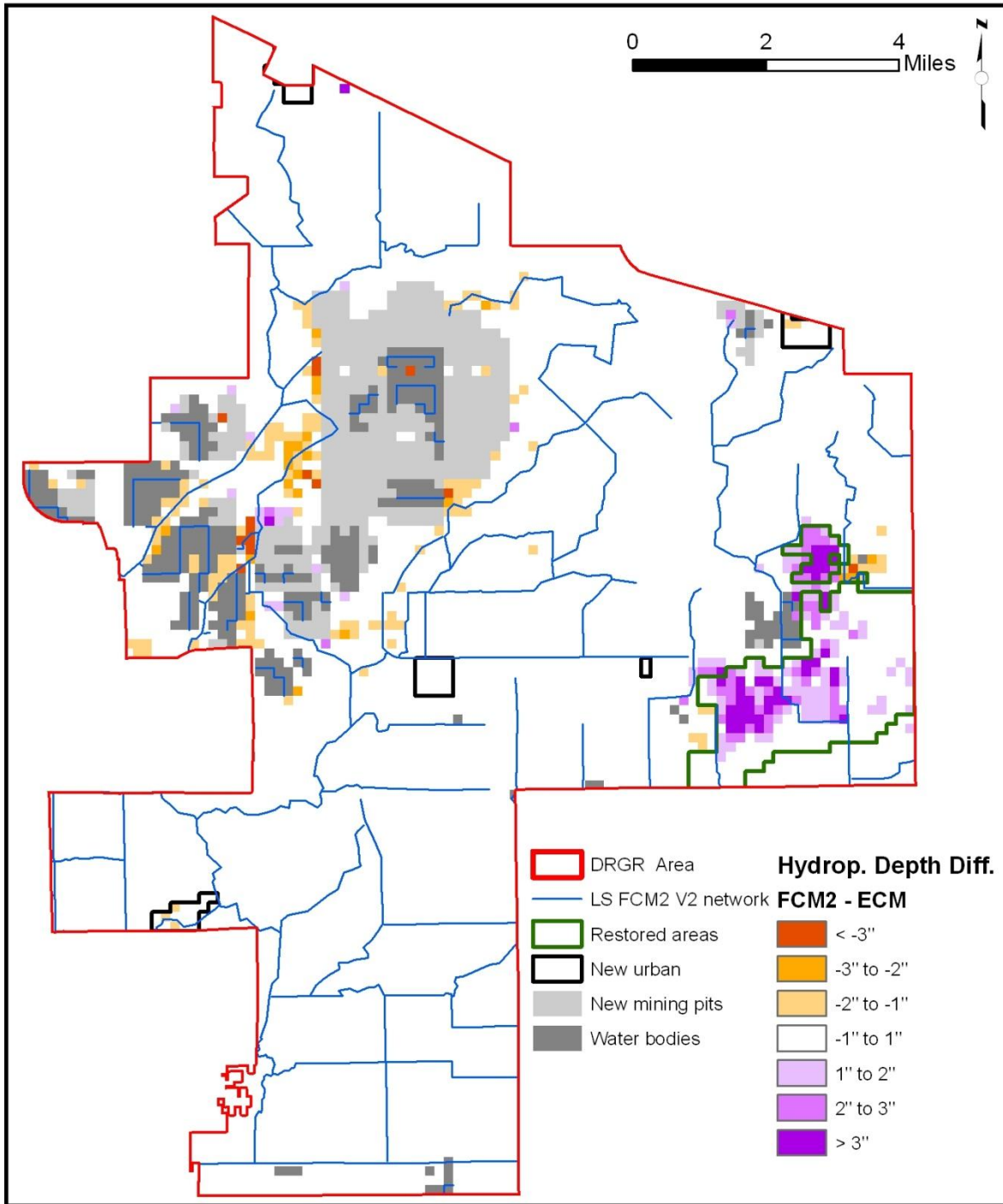


**Figure H10.** Difference in water depths during hydroperiod in FCM2 in relation to the ECM (Positive values indicate greater duration of water ponding in FCM2).

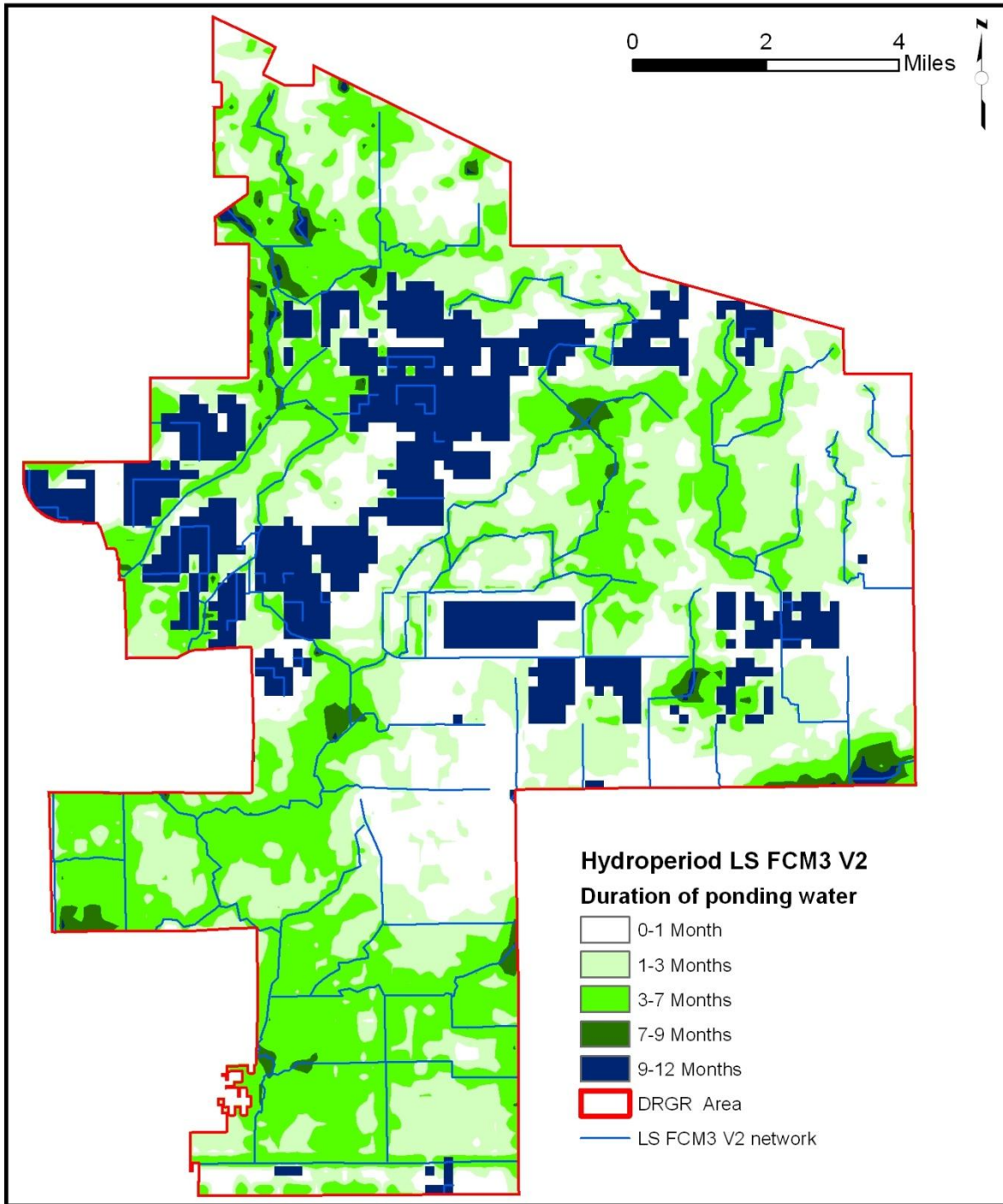


**Figure H11.** Average annual hydro-period map for the DR/GR Area as predicted by the LS FCM3 V2.

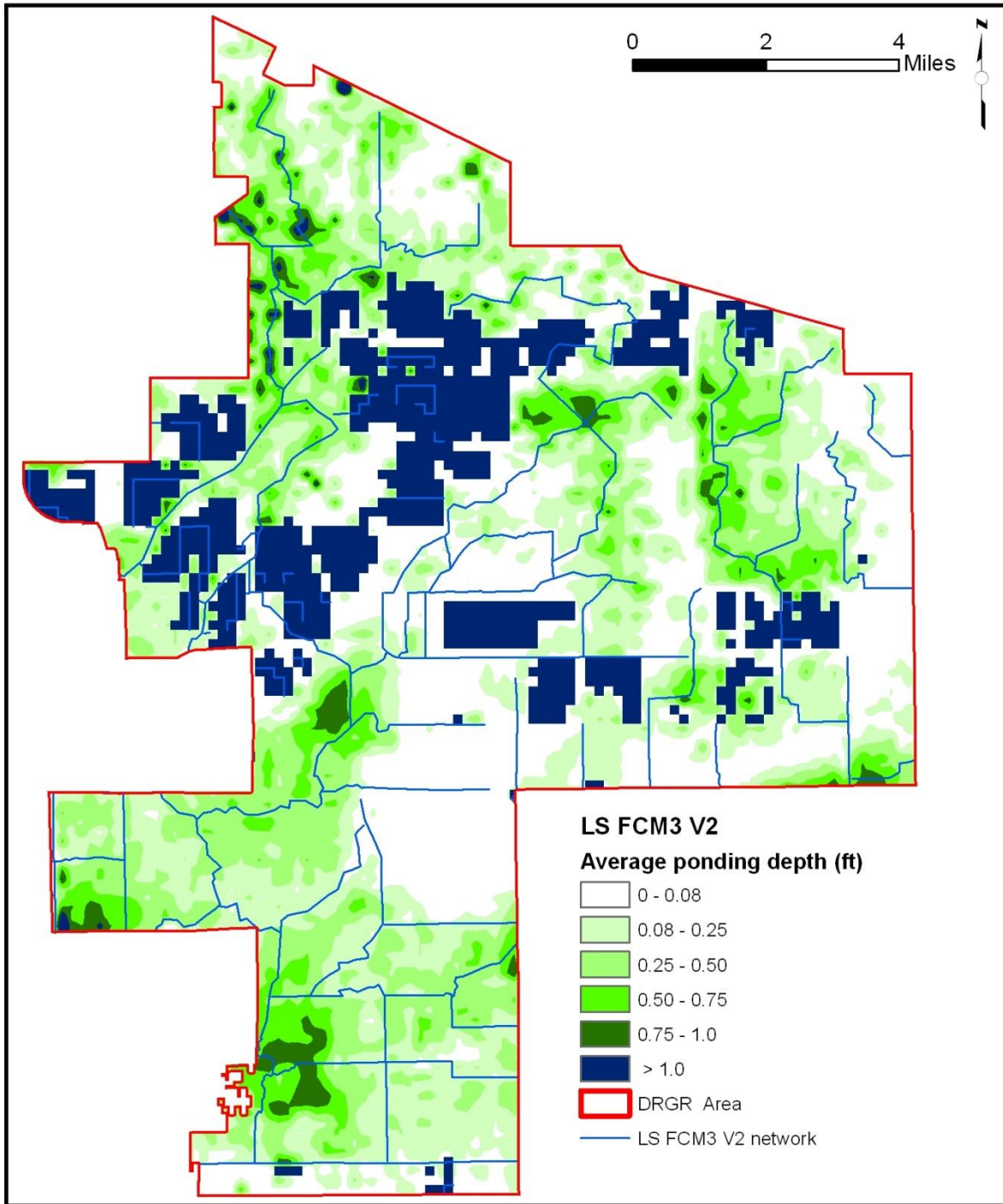


**Figure H12.** Average water depth during the hydro-period for the DR/GR Area as predicted by the LS FCM3 V2.

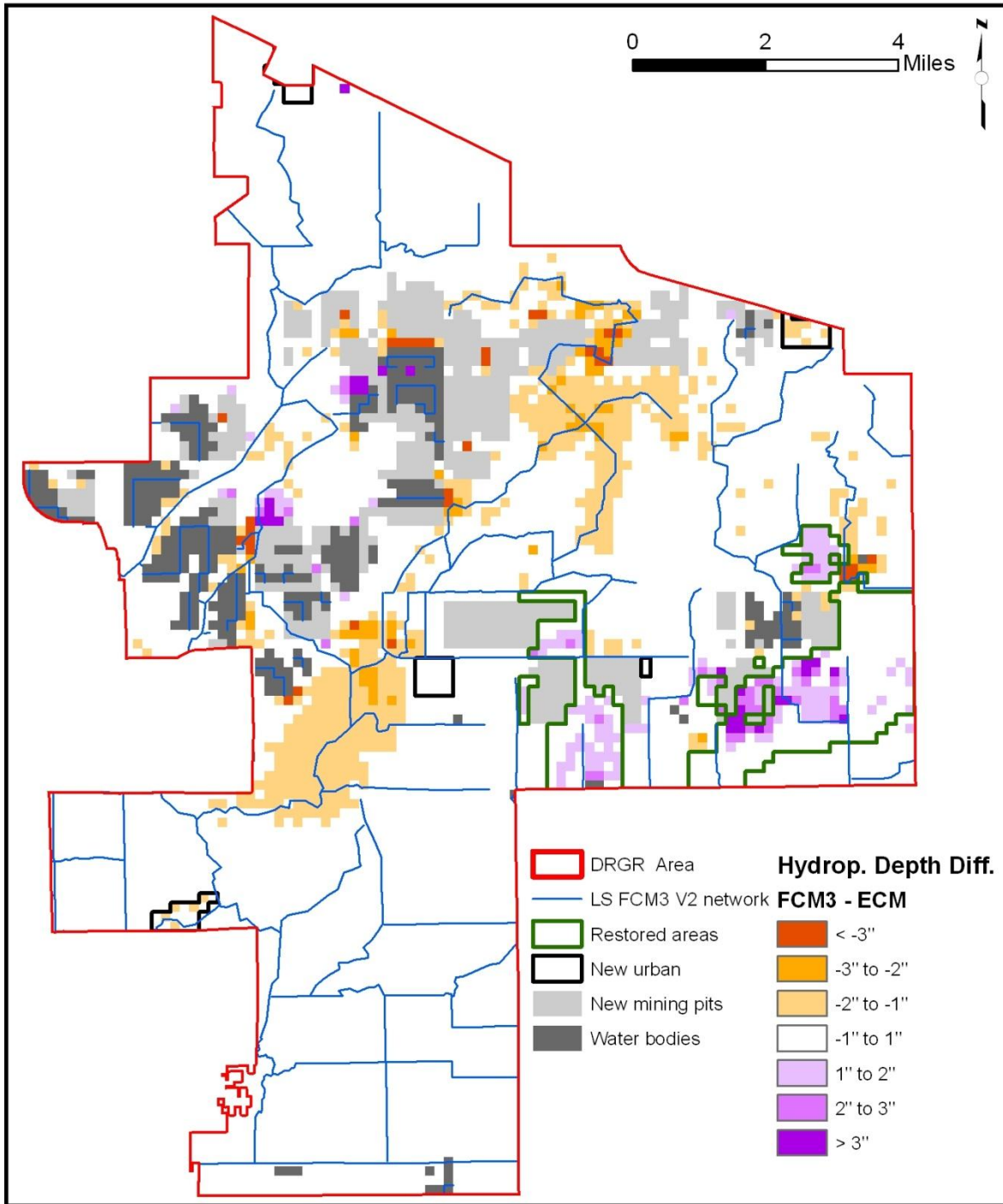


**Figure H13.** Difference in water depths during hydroperiod in FCM3 in relation to the ECM (Positive values indicate greater duration of water ponding in FCM3).

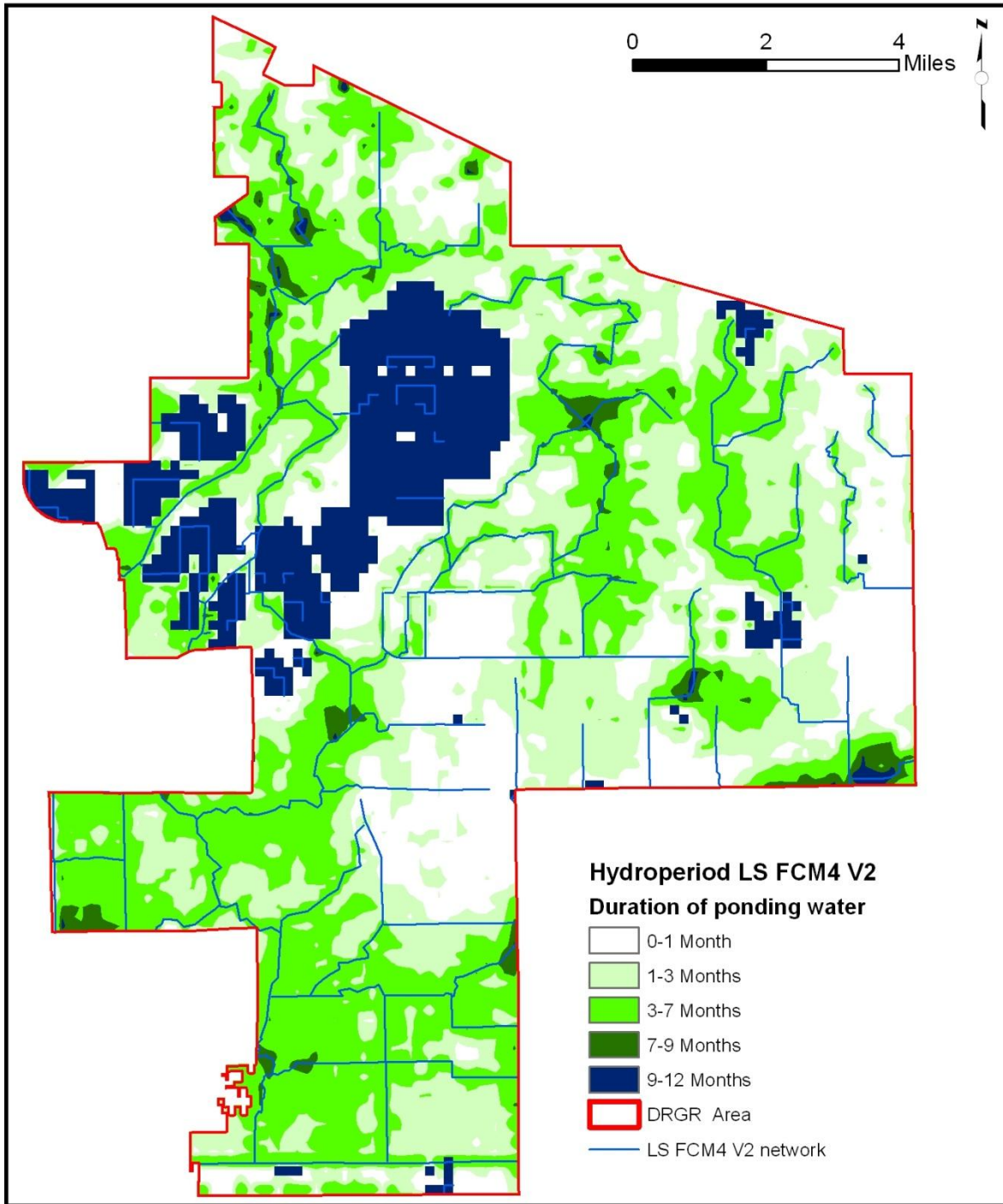


**Figure H14.** Average annual hydro-period map for the DR/GR Area as predicted by the LS FCM4 V2.

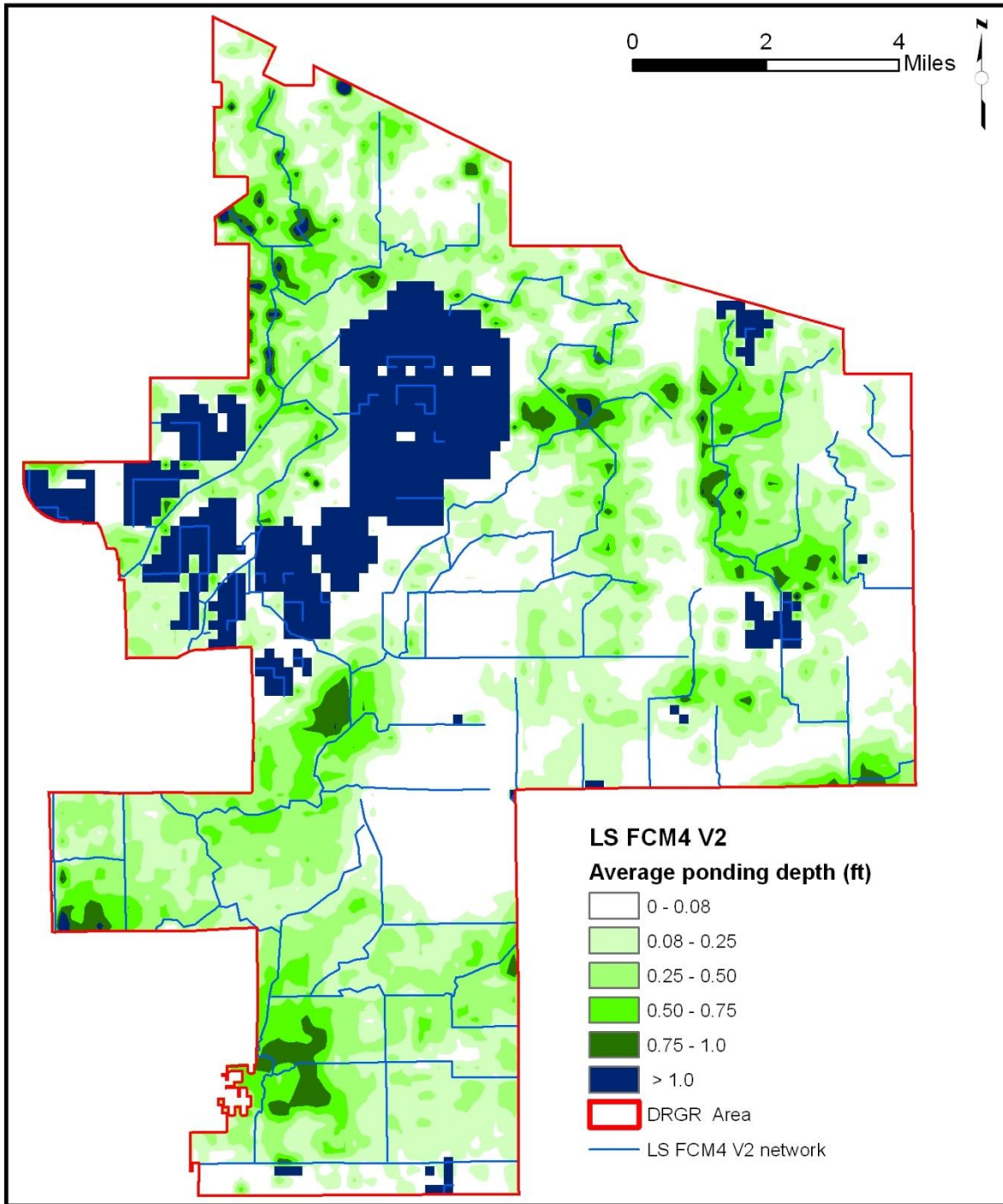


**Figure H15.** Average water depth during the hydro-period for the DR/GR Area as predicted by the LS FCM4 V2.

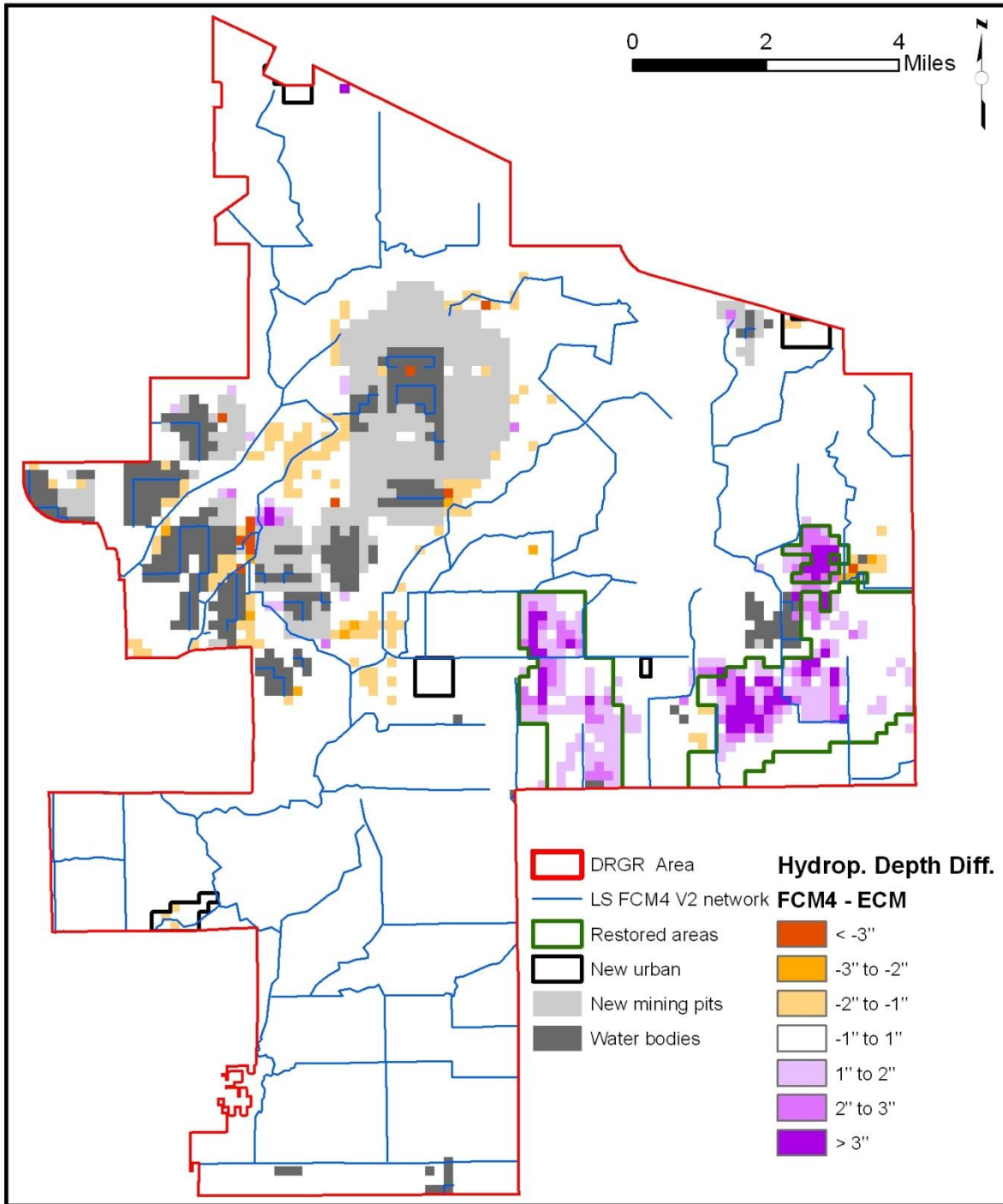


**Figure H16.** Difference in water depths during hydroperiod in FCM4 in relation to the ECM (Positive values indicate greater duration of water ponding in FCM4).



## **APPENDIX I. WATER BALANCE TABLES AND FIGURES**

Tables and figures from water balance calculations from the different models are presented in this appendix. The water balance has been made for the DR/GR Area and for the areas with water bodies, i.e., mining pits and other shallow water features (labeled as shallow holes) inside or close to the DR/GR Area.

### **List of Tables**

|  |   |
|--|---|
| Table I1. Annual average depth rates (mm/year) of the water balance components from the different (V2) models and in two different areas. .... | 3 |
|--|---|

### **List of Figures**

|  |    |
|--|----|
| Figure I1. Annual average water balance predicted from the ECM for the DR/GR Area in the years from 2002 to 2006. Magnitudes are volume rates per unit of horizontal area (mm/year). ....  | 5  |
| Figure I2. Annual average water balance predicted from the ECM for the mining pit areas in the years from 2002 to 2006. Magnitudes are volume rates per unit of horizontal area (mm/year). ....  | 6  |
| Figure I3. Annual average water balance predicted from the LS ECM V1 for the DR/GR Area in the years from 2002 to 2006. Magnitudes are volume rates per unit of horizontal area (mm/year). ....  | 7  |
| Figure I4. Annual average water balance predicted from the LS ECM V1 for the mining pits and other shallow water features close to the DR/GR Area in the years from 2002 to 2006. Magnitudes are volume rates per unit of horizontal area (mm/year). ....  | 8  |
| Figure I5. Annual average water balance predicted from the LS FCM1 V2 for the DR/GR Area in the years from 2002 to 2006. Magnitudes are volume rates per unit of horizontal area (mm/year). ....   | 9  |
| Figure I6. Annual average water balance predicted from the LS FCM1 V2 for the mining pits and other shallow water features close to the DR/GR Area in the years from 2002 to 2006. Magnitudes are volume rates per unit of horizontal area (mm/year). .... | 10 |
| Figure I7. Annual average water balance predicted from the LS FCM2 V2 for the DR/GR Area in the years from 2002 to 2006. Magnitudes are volume rates per unit of horizontal area (mm/year). ....   | 11 |
| Figure I8. Annual average water balance predicted from the LS FCM2 V2 for the mining pits and other shallow water features close to the DR/GR Area in the years from 2002 to 2006. Magnitudes are volume rates per unit of horizontal area (mm/year). .... | 12 |
| Figure I9. Annual average water balance predicted from the LS FCM3 V2 for the DR/GR Area in the years from 2002 to 2006. Magnitudes are volume rates per unit of horizontal area (mm/year). ....   | 13 |



Figure I10. Annual average water balance predicted from the LS FCM3 V2 for the mining pits and other shallow water features close to the DR/GR Area in the years from 2002 to 2006. Magnitudes are volume rates per unit of horizontal area (mm/year). ..... 14

Figure I11. Annual average water balance predicted from the LS FCM4 V2 for the DR/GR Area in the years from 2002 to 2006. Magnitudes are volume rates per unit of horizontal area (mm/year). ..... 15

Figure I12. Annual average water balance predicted from the LS FCM4 V2 for the mining pits and other shallow water features close to the DR/GR Area in the years from 2002 to 2006. Magnitudes are volume rates per unit of horizontal area (mm/year). ..... 16



| Depth rates (mm/year)                     | Area  | DR/GR      |            |            |            |            | Mining pits and other shallow holes<br>inside or close to DR/GR |             |             |             |             |
|---|-------|------------|------------|------------|------------|------------|---|-------------|-------------|-------------|-------------|
|   | Model | LS<br>ECM  | LS<br>FCM1 | LS<br>FCM2 | LS<br>FCM3 | LS<br>FCM4 | LS<br>ECM   | LS<br>FCM1  | LS<br>FCM2  | LS<br>FCM3  | LS<br>FCM4  |
| Rainfall                                  |       | 1496       | 1496       | 1496       | 1496       | 1496       | 1501  | 1514        | 1504        | 1494        | 1499        |
| ET  |       | 1220       | 1233       | 1236       | 1238       | 1231       | 1501  | 1502        | 1500        | 1498        | 1499        |
| <b>Rainfall - ET (A)</b>                  |       | <b>276</b> | <b>263</b> | <b>260</b> | <b>258</b> | <b>264</b> | <b>0</b>  | <b>12</b>   | <b>5</b>    | <b>-4</b>   | <b>0</b>    |
| OL storage change                         |       | -1         | -1         | 0          | -3         | 0          | -3  | -4          | 5           | -14         | 6           |
| UZ Storage change                         |       | 1          | 1          | 1          | 1          | 1          | 0   | 0           | 0           | 0           | 0           |
| Total SZ Storage change (BSZ)             |       | -10        | -9         | -9         | -9         | -9         | 0   | -1          | 0           | -1          | 0           |
| <b>Total storage (B)</b>                  |       | <b>-9</b>  | <b>-9</b>  | <b>-8</b>  | <b>-11</b> | <b>-8</b>  | <b>-4</b>   | <b>-4</b>   | <b>5</b>    | <b>-14</b>  | <b>6</b>    |
| Net OL Boundary outflow (COL)             |       | 5          | 4          | 4          | 4          | 5          | 1   | 0           | 0           | 4           | 0           |
| Drain to Boundary (CDR)                   |       | 0          | 0          | 0          | 0          | 0          | 0   | 0           | 0           | 0           | 0           |
| Net SZ Boundary outflow from SZ1          |       | 44         | 51         | 46         | 45         | 46         | -229  | -277        | -248        | -206        | -259        |
| Net SZ Boundary outflow from SZ2          |       | 1          | 2          | 2          | 3          | 3          | -53   | -12         | -15         | -4          | -17         |
| Net SZ Boundary outflow from SZ3          |       | -14        | -15        | -12        | -11        | -12        | 71  | 88          | 93          | 76          | 92          |
| Net SZ Boundary outflow from SZ4          |       | -10        | -11        | -9         | -9         | -9         | 3   | 10          | 19          | 9           | 16          |
| Net SZ Boundary outflow from all SZ (CSZ) |       | 22         | 28         | 27         | 28         | 28         | -208  | -191        | -150        | -125        | -167        |
| <b>Total Boundary outflow (C)</b>         |       | <b>27</b>  | <b>32</b>  | <b>31</b>  | <b>32</b>  | <b>33</b>  | <b>-208</b>   | <b>-191</b> | <b>-150</b> | <b>-121</b> | <b>-167</b> |
| Pumping from SZ1                          |       | 30         | 25         | 22         | 17         | 19         | 12  | 0           | 0           | 0           | 0           |
| Pumping from SZ2                          |       | 26         | 21         | 22         | 19         | 19         | 59  | 17          | 21          | 19          | 23          |

**Table I1.** Annual average depth rates (mm/year) of the water balance components from the different (V2) models and in two different areas.

| Area | DR/GR | Mining pits and other shallow holes |
|------|-------|-------------------------------------|
|------|-------|-------------------------------------|



| Depth rates (mm/year)             | Model                         |            |            |            |            |            | inside or close to DR/GR |            |            |           |            |
|-----------------------------------|-------------------------------|------------|------------|------------|------------|------------|--------------------------|------------|------------|-----------|------------|
|                                   |                               | LS ECM     | LS FCM1    | LS FCM2    | LS FCM3    | LS FCM4    | LS ECM                   | LS FCM1    | LS FCM2    | LS FCM3   | LS FCM4    |
| Pumping from SZ3                  |                               | 78         | 84         | 75         | 74         | 74         | 5                        | 3          | 4          | 4         | 5          |
| Pumping from SZ4                  |                               | 13         | 14         | 14         | 14         | 14         | 14                       | 9          | 12         | 11        | 13         |
| Pumping from all SZ               |                               | 147        | 144        | 133        | 124        | 127        | 90                       | 29         | 38         | 34        | 41         |
| Irrigation                        |                               | 65         | 53         | 42         | 33         | 36         | 0                        | 0          | 0          | 0         | 0          |
| <b>Pumping-Irrigation (D)</b>     |                               | <b>82</b>  | <b>91</b>  | <b>91</b>  | <b>91</b>  | <b>91</b>  | <b>90</b>                | <b>29</b>  | <b>38</b>  | <b>34</b> | <b>41</b>  |
| Infiltration from OL to SZ1       |                               | 708        | 614        | 569        | 501        | 569        | -119                     | -162       | -113       | -93       | -126       |
| Infiltration from SZ1 to SZ2      |                               | 94         | 95         | 92         | 88         | 89         | 98                       | 114        | 135        | 113       | 132        |
| Infiltration from SZ2 to SZ3      |                               | 67         | 72         | 68         | 67         | 67         | 92                       | 110        | 128        | 99        | 126        |
| Infiltration from SZ3 to SZ4      |                               | 3          | 4          | 5          | 5          | 5          | 17                       | 19         | 31         | 19        | 29         |
| OL->river                         |                               | -372       | -302       | -272       | -213       | -276       | 121                      | 177        | 112        | 98        | 120        |
| Drain to river                    |                               | 549        | 448        | 417        | 356        | 423        | 0                        | 0          | 0          | 0         | 0          |
| Drain to ext. river               |                               | 5          | 8          | 5          | 6          | 5          | 0                        | 0          | 0          | 0         | 0          |
| Base flow to River                |                               | -6         | -5         | -4         | -3         | -4         | 0                        | 0          | 0          | 0         | 0          |
| <b>Total flow to river (E)</b>    |                               | <b>176</b> | <b>149</b> | <b>146</b> | <b>145</b> | <b>148</b> | <b>121</b>               | <b>177</b> | <b>112</b> | <b>98</b> | <b>120</b> |
| Error (A-B-C-D-E)                 |                               | 0          | 0          | 0          | 0          | 0          | 0                        | 0          | 0          | 0         | 0          |
| Boundary surface outflow (runoff) | COL+CDR+E                     | 181        | 153        | 150        | 149        | 153        | ---                      | ---        | ---        | ---       | ---        |
|                                   | COL+CDR                       | ---        | ---        | ---        | ---        | ---        | 1                        | 0          | 0          | 4         | 0          |
| Net groundwater recharge          | A-(B-BSZ)-(C-CSZ)-E=BSZ+CSZ+D | 95         | 109        | 109        | 110        | 110        | ---                      | ---        | ---        | ---       | ---        |
|                                   | A= B+C+D+E                    | ---        | ---        | ---        | ---        | ---        | 0                        | 12         | 5          | -4        | 0          |

Table II. Annual average depth rates (mm/year) of the water balance components from the different (V2) models and in two different areas. (cont.)

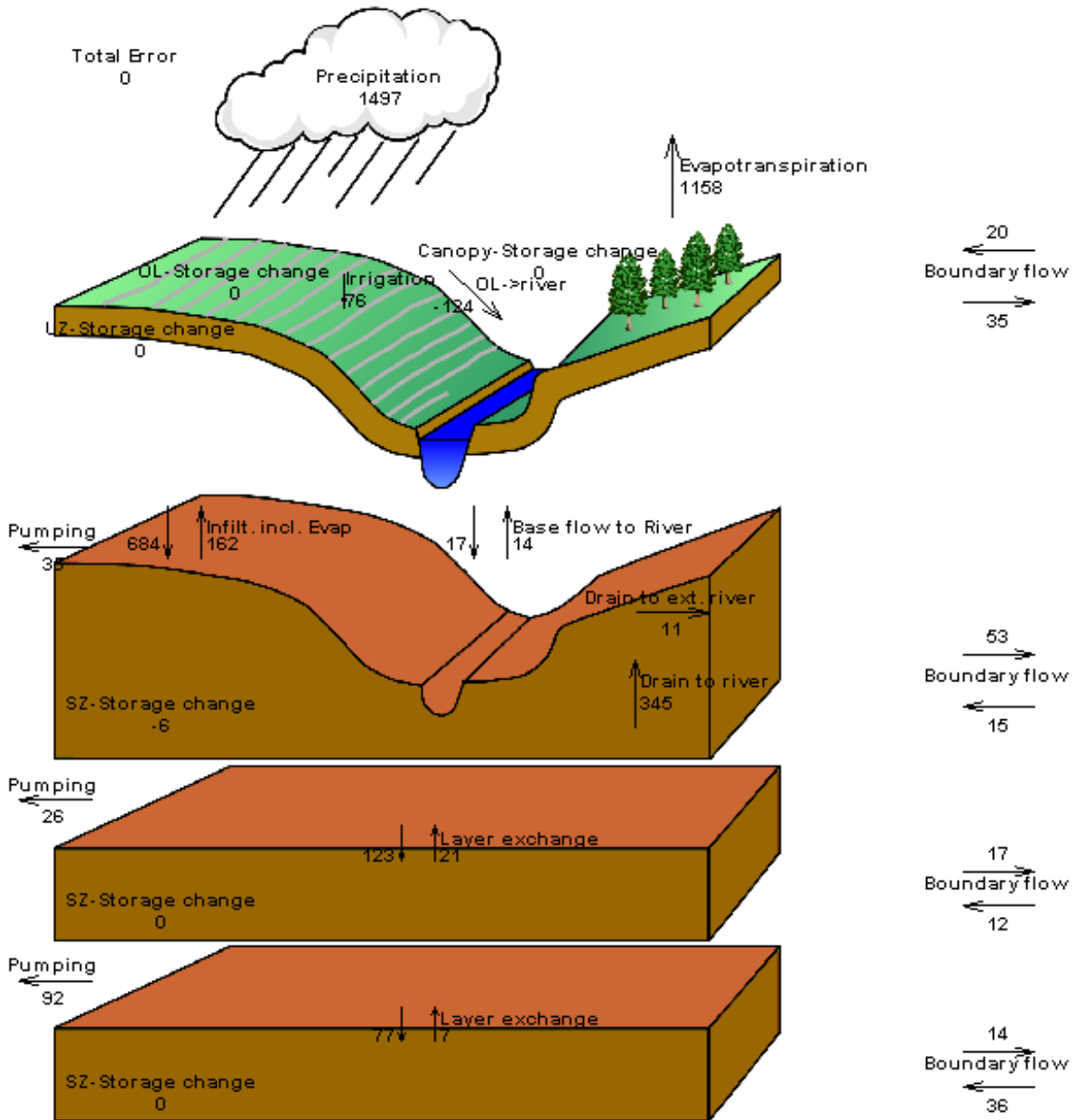


**Figure 11.** Annual average water balance predicted from the ECM for the DR/GR Area in the years from 2002 to 2006. Magnitudes are volume rates per unit of horizontal area (mm/year).

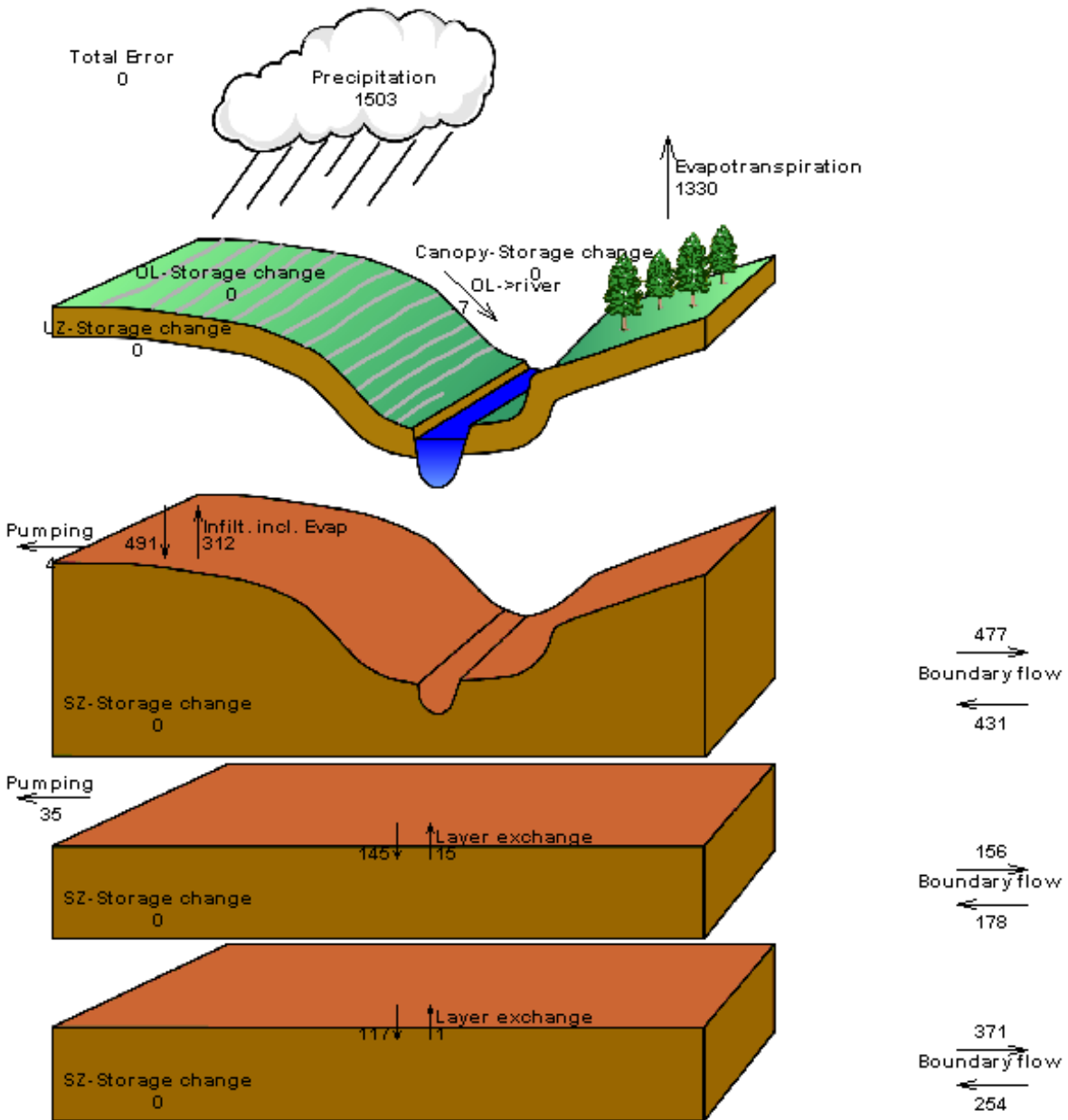


**Figure 12.** Annual average water balance predicted from the ECM for the mining pit areas in the years from 2002 to 2006. Magnitudes are volume rates per unit of horizontal area (mm/year).

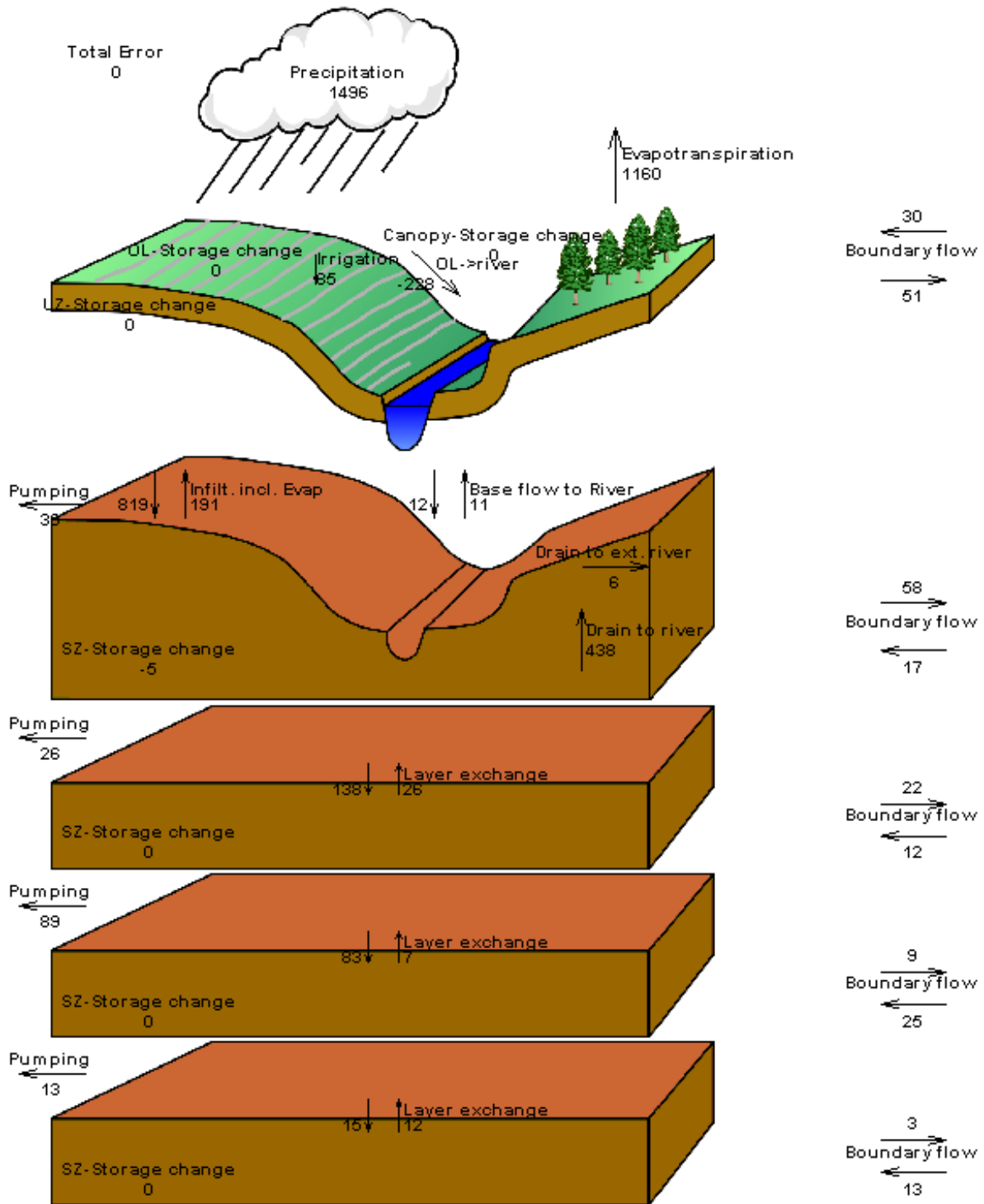


**Figure 13.** Annual average water balance predicted from the LS ECM V1 for the DR/GR Area in the years from 2002 to 2006. Magnitudes are volume rates per unit of horizontal area (mm/year).

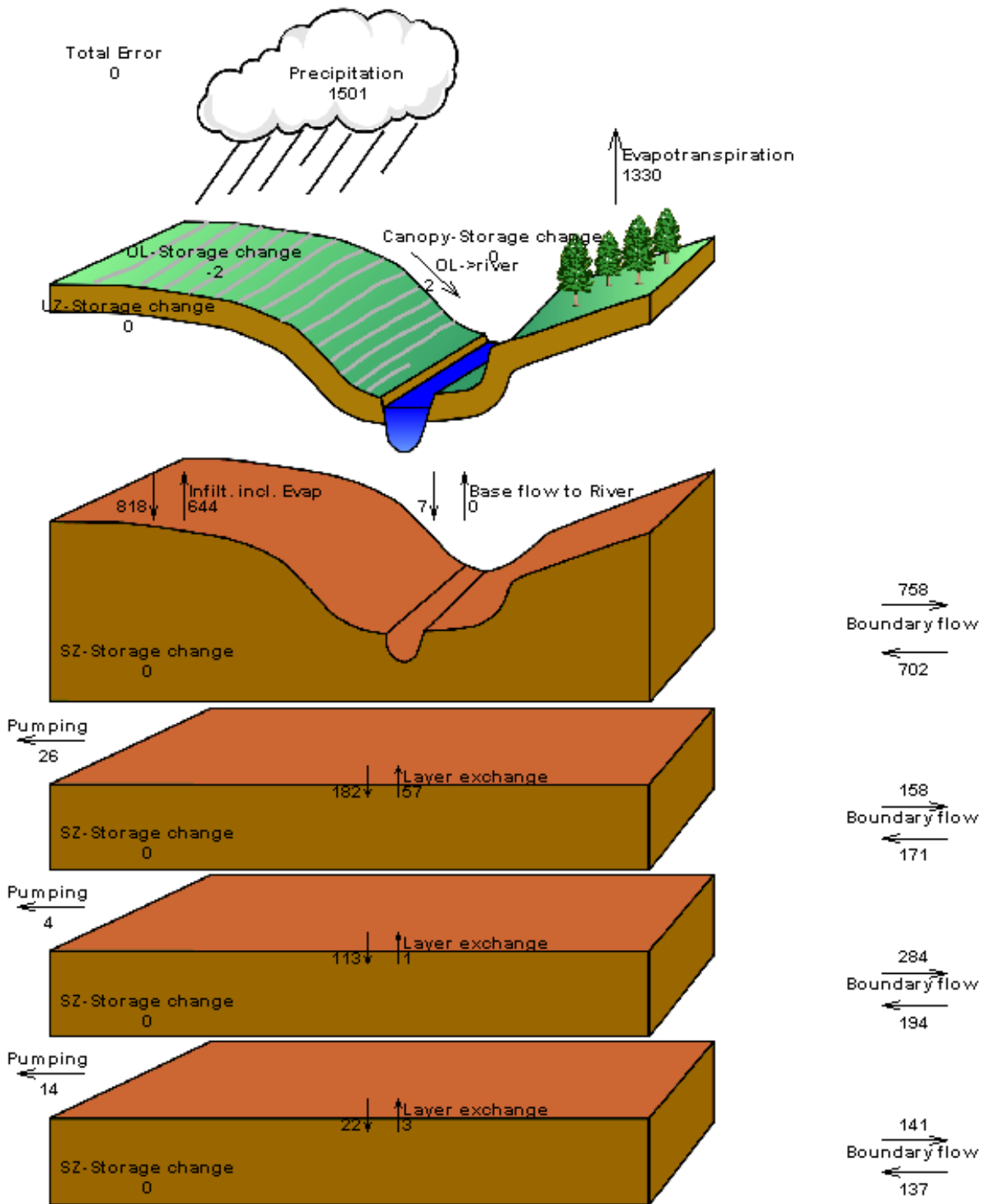


**Figure 14.** Annual average water balance predicted from the LS ECM V1 for the mining pits and other shallow water features close to the DR/GR Area in the years from 2002 to 2006. Magnitudes are volume rates per unit of horizontal area (mm/year).

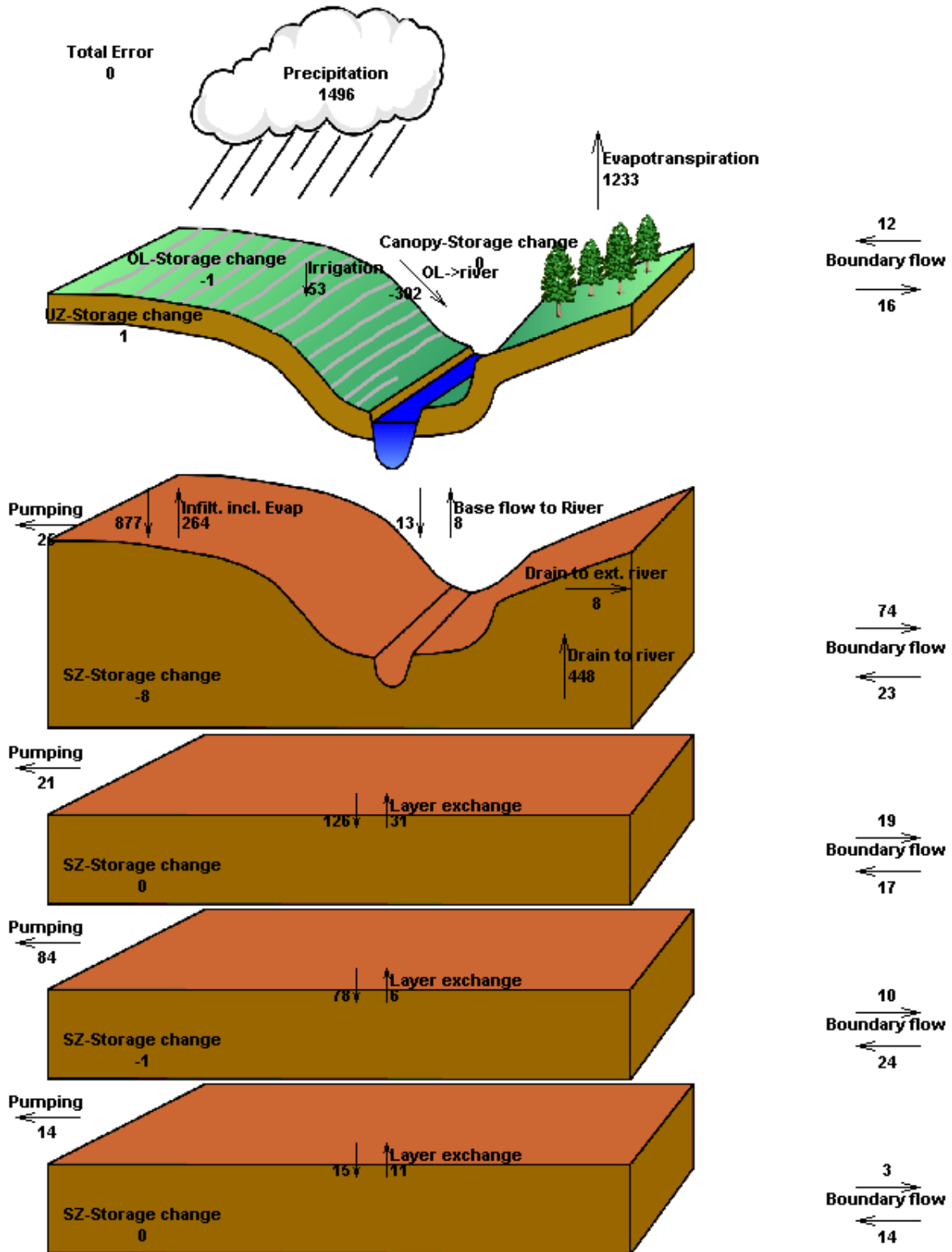


**Figure 15.** Annual average water balance predicted from the LS FCM1 V2 for the DR/GR Area in the years from 2002 to 2006. Magnitudes are volume rates per unit of horizontal area (mm/year).

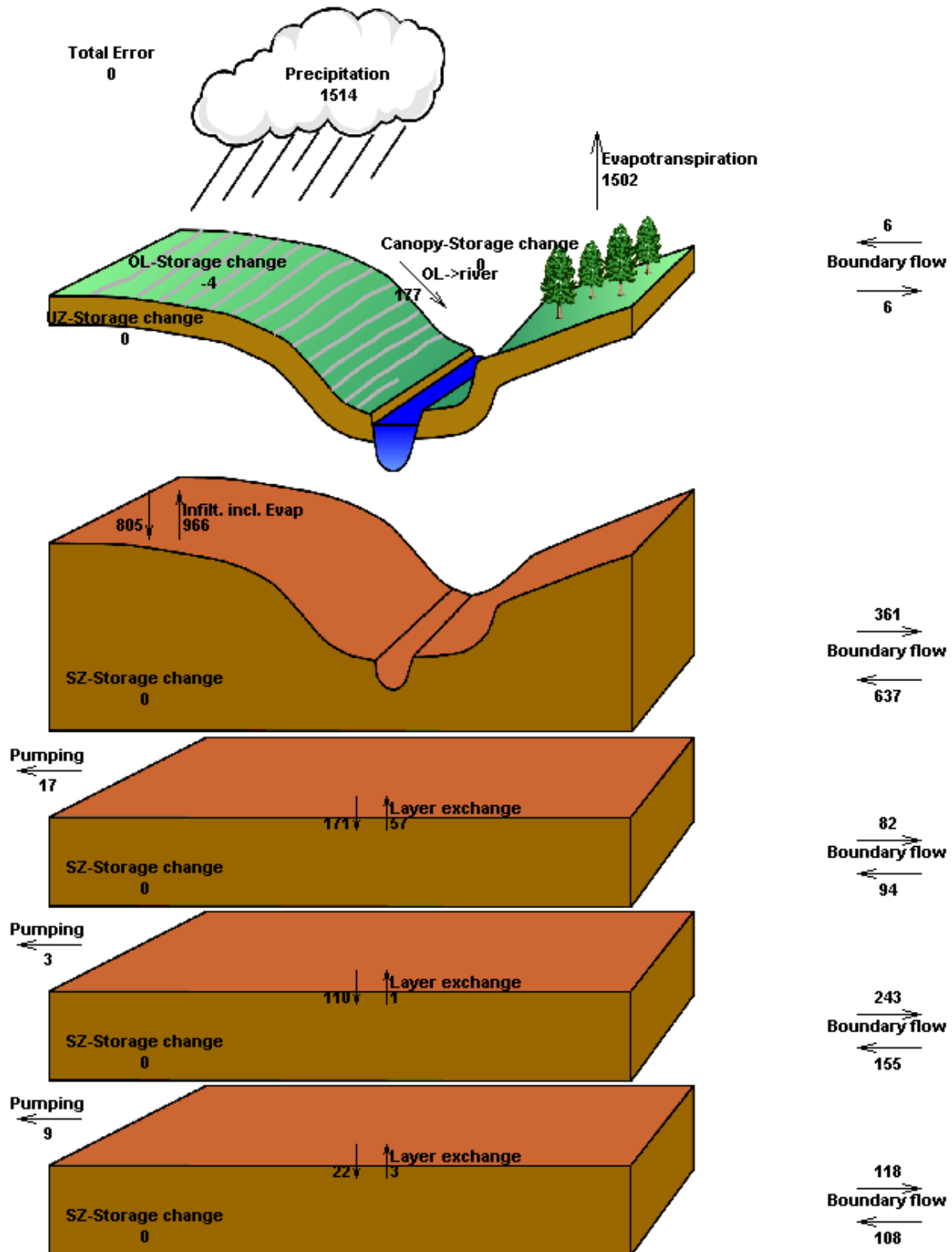


**Figure 16.** Annual average water balance predicted from the LS FCM1 V2 for the mining pits and other shallow water features close to the DR/GR Area in the years from 2002 to 2006. Magnitudes are volume rates per unit of horizontal area (mm/year).

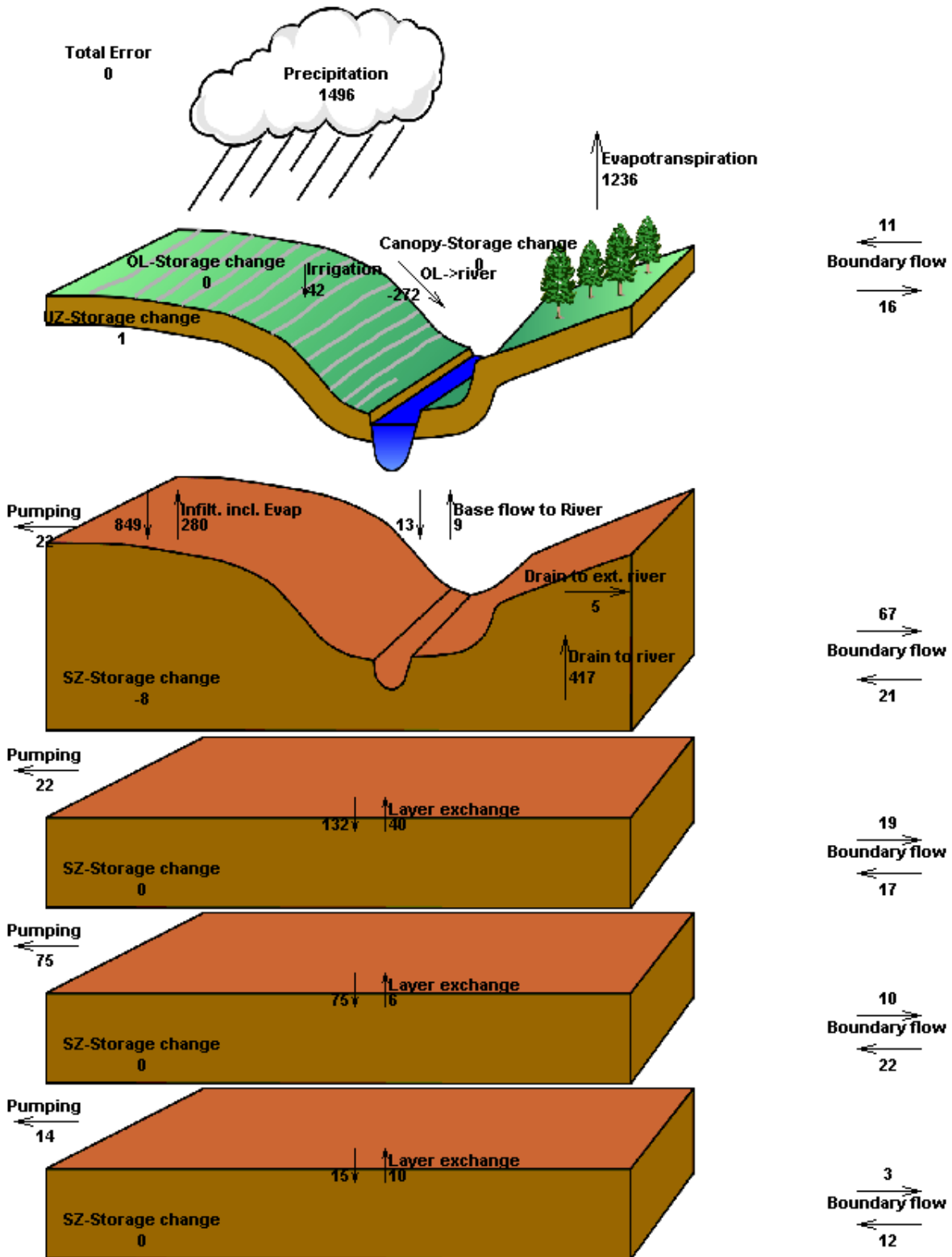


**Figure 17.** Annual average water balance predicted from the LS FCM2 V2 for the DR/GR Area in the years from 2002 to 2006. Magnitudes are volume rates per unit of horizontal area (mm/year).

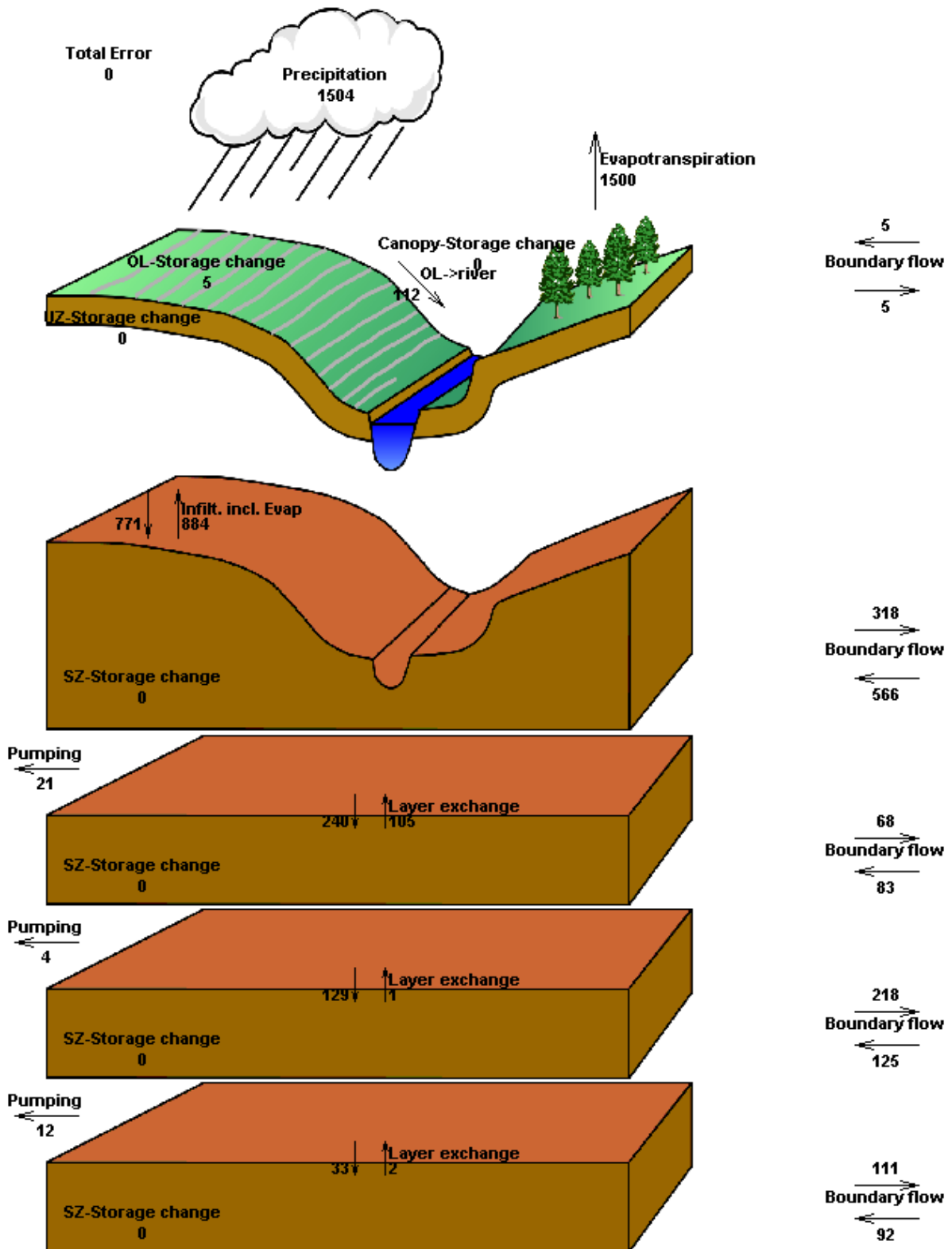


**Figure 18.** Annual average water balance predicted from the LS FCM2 V2 for the mining pits and other shallow water features close to the DR/GR Area in the years from 2002 to 2006. Magnitudes are volume rates per unit of horizontal area (mm/year).

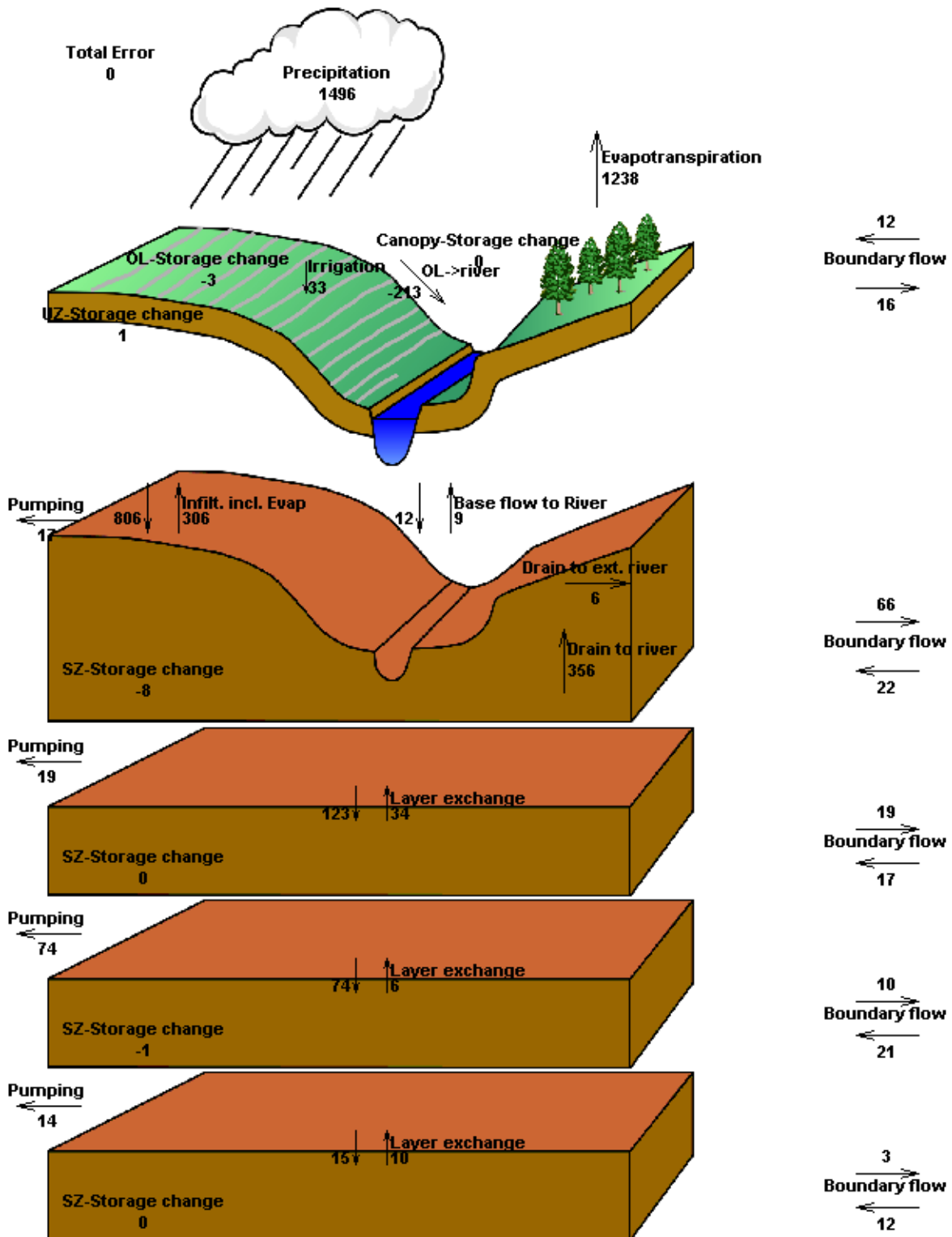


**Figure 19.** Annual average water balance predicted from the LS FCM3 V2 for the DR/GR Area in the years from 2002 to 2006. Magnitudes are volume rates per unit of horizontal area (mm/year).

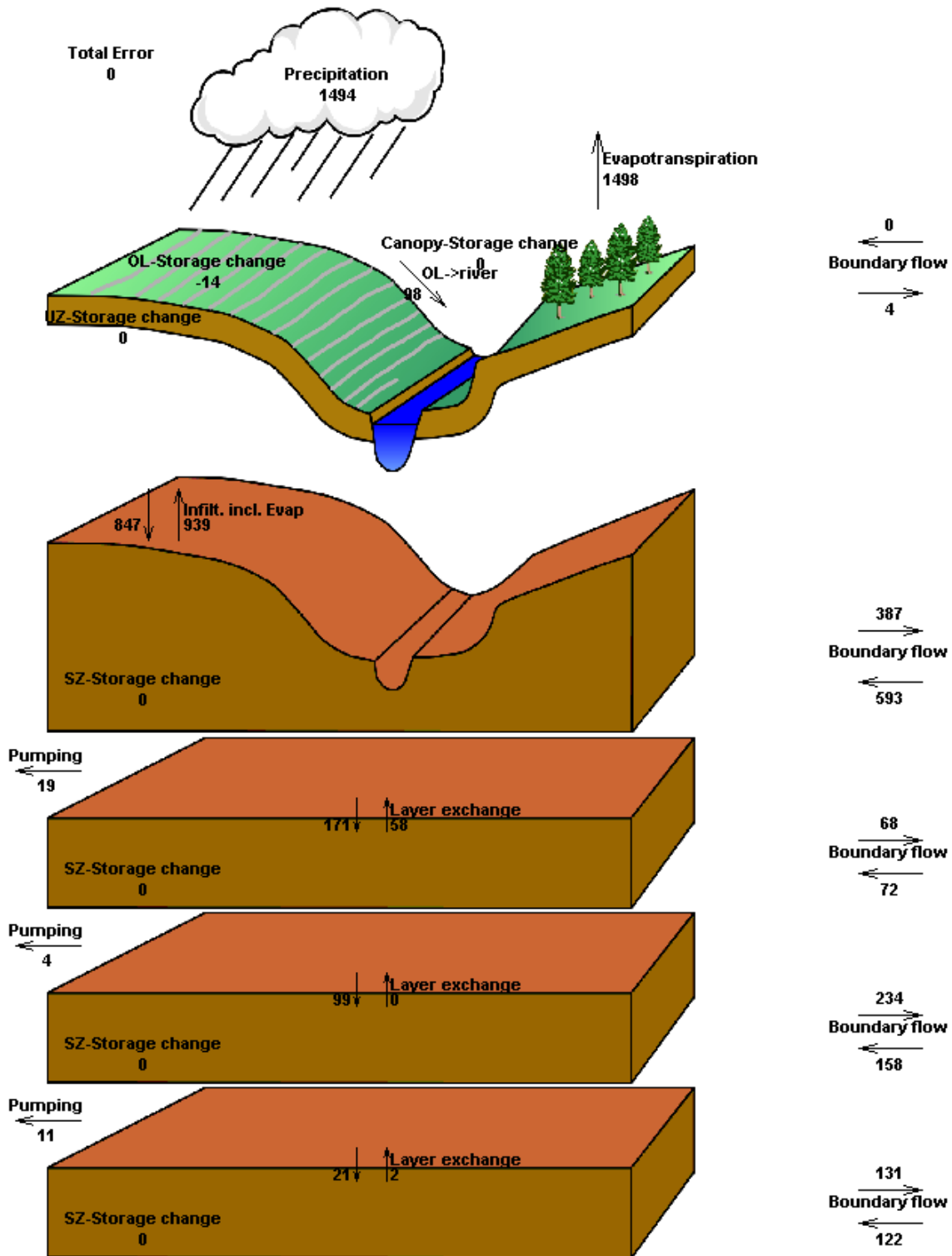


**Figure 110.** Annual average water balance predicted from the LS FCM3 V2 for the mining pits and other shallow water features close to the DR/GR Area in the years from 2002 to 2006. Magnitudes are volume rates per unit of horizontal area (mm/year).

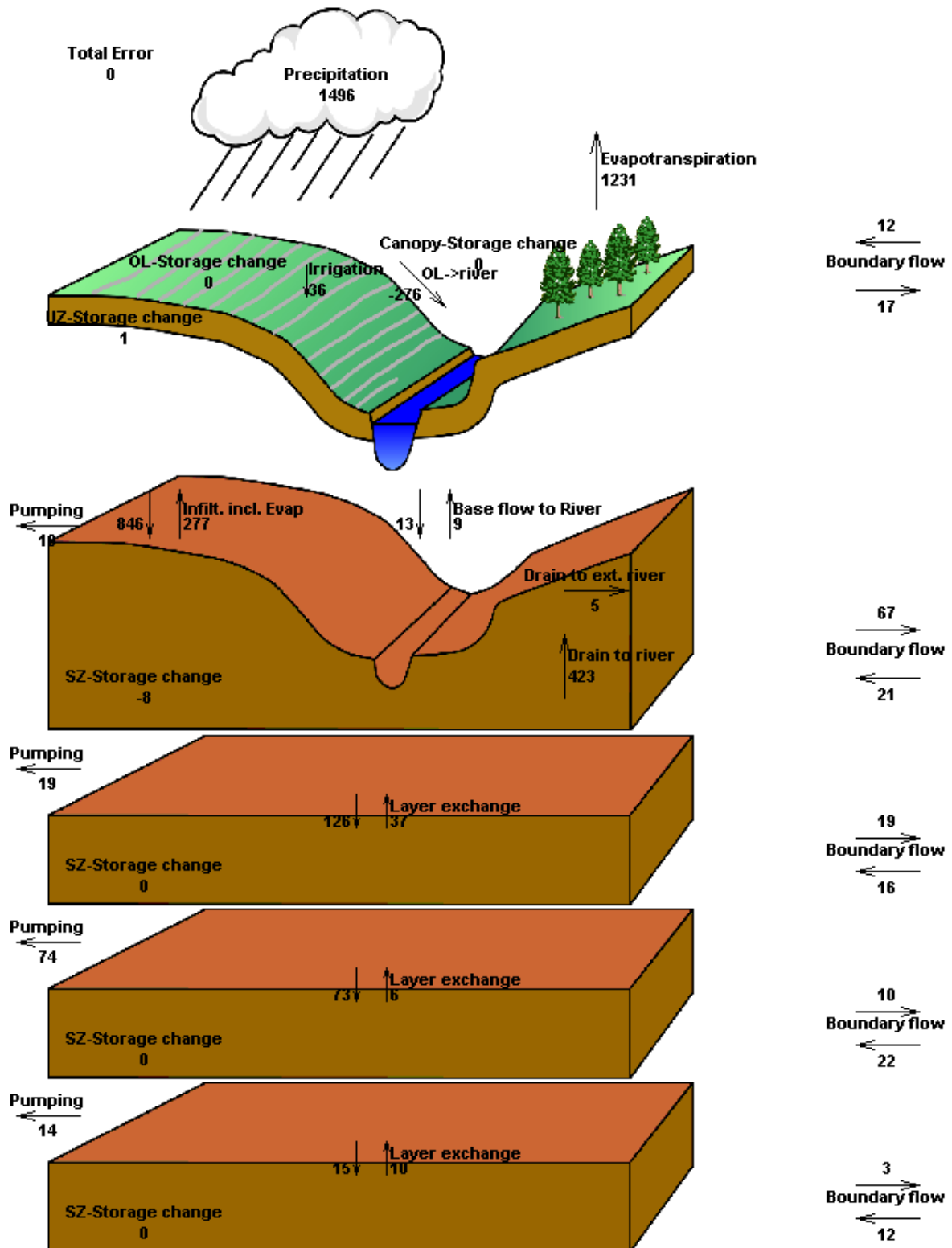


**Figure I11.** Annual average water balance predicted from the LS FCM4 V2 for the DR/GR Area in the years from 2002 to 2006. Magnitudes are volume rates per unit of horizontal area (mm/year).

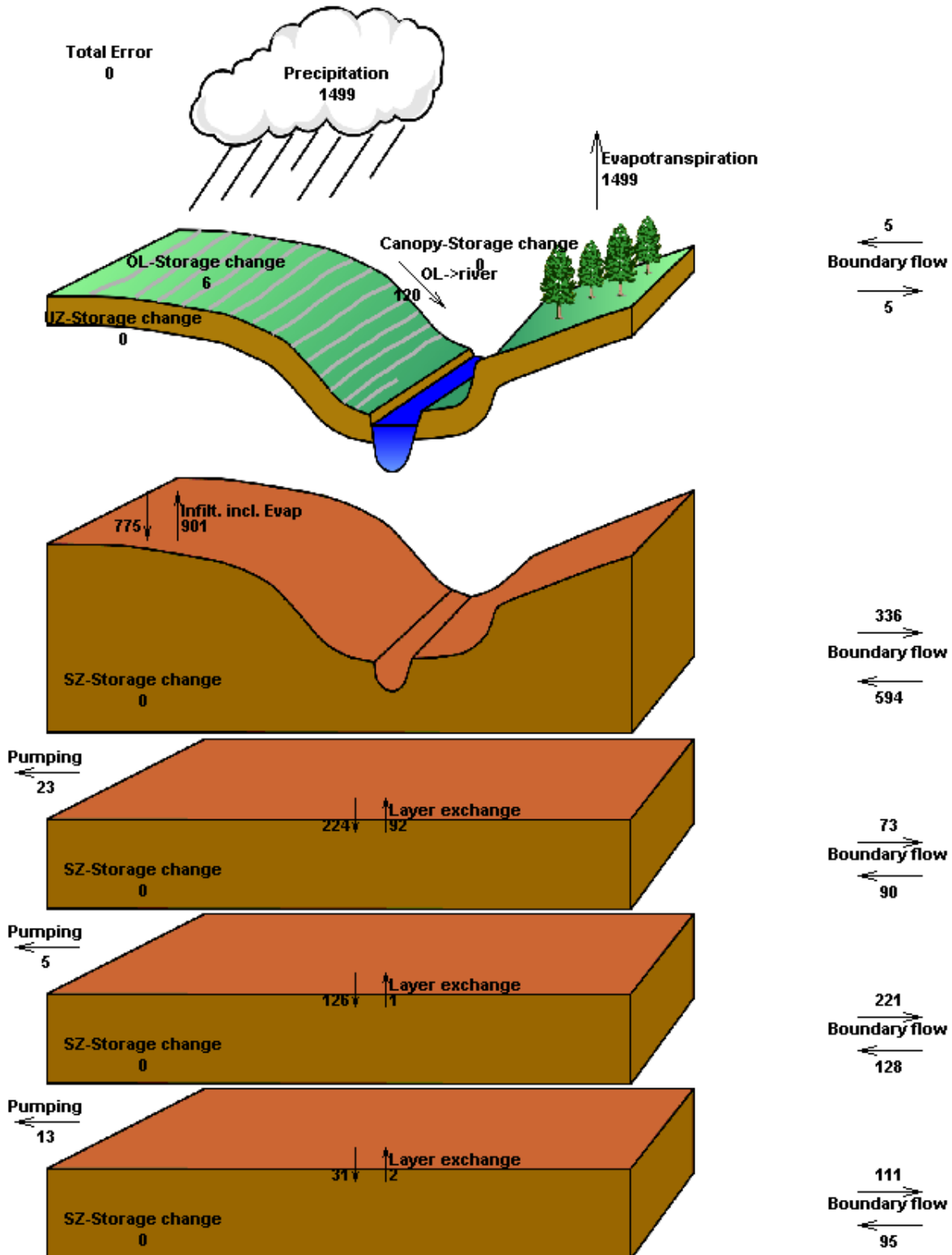


**Figure I12.** Annual average water balance predicted from the LS FCM4 V2 for the mining pits and other shallow water features close to the DR/GR Area in the years from 2002 to 2006. Magnitudes are volume rates per unit of horizontal area (mm/year).





## ***APPENDIX J. LS ECM VI CALIBRATION RESULTS***

The model calibration efforts improved the model results, especially in shallow wells within the DR/GR Area. Simulation of the deeper aquifer (computational layer 3) did not perform as well as the shallower layers, possibly due to the exclusion of the deeper Hawthorn Aquifer. Since the highest calibration priority was given to the DR/GR Area, the results presented in this section include the groundwater plots and statistics of the Water Table Aquifer (computational layer 1) in the DR/GR Area, the surface water plots and statistics for the Local Scale ECM, and hydroperiod maps for the DR/GR Area. All other calibration results, which include all of the output for the monitoring stations available for the Lee County ECM, are included in Appendices B and C. Appendix B contains the calibration results for the ECM and Appendix C includes the comparison between the ECM and the LS ECM.

### ***Water Table Elevations at Monitoring Well Stations***

**Figure J1** shows the water table monitoring stations within the Local Scale Model boundary. The color of the dots in the figure indicates the average statistical performance level of the LS ECM compared to observed data. **Table J1** shows the statistics for the water table stations within the DR/GR Area. The groundwater results for the Water Table Aquifer stations in the DR/GR Area (46 in total) showed that 85% of the calibration locations scored in the high performance range when compared to the observed data and the other 15% scored in the medium performance range. For these stations, the average mean error is 0.16 ft, average mean absolute error is 0.83 ft, and the average correlation coefficient is 0.84. Appendixes B and C display water elevation comparative graphs for stations throughout the model. In general, the model does a very good job in capturing the seasonality of the water table level variations. Some of the stations show a better match between the simulated and observed levels in the later years of the simulation (2004-2006). This could be a combination of both initial conditions and the model being a better representation of the land use conditions of the later period.

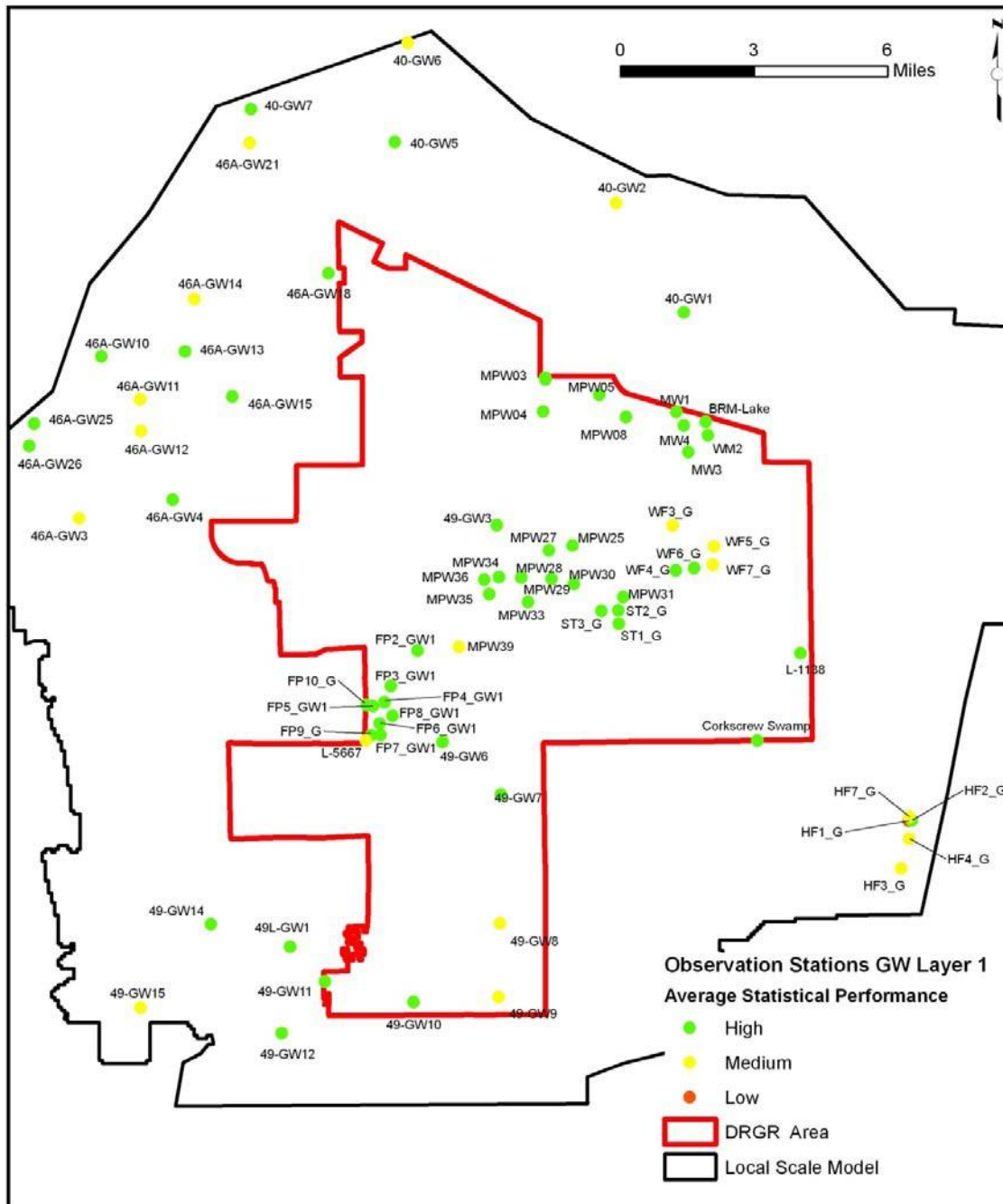


**Figure J1.** Groundwater Stations in the Local Scale Model.



**Table J1.** Groundwater Statistics for the DR/GR Area.

| Station Name    | ME (ft) | MAE (ft) | RMSE (ft) | R    | PL  |
|-----------------|---------|----------|-----------|------|-----|
| 49-GW7          | 0.43    | 0.87     | 1.29      | 0.57 | 1.5 |
| 49-GW8          | 1.78    | 1.78     | 2.17      | 0.26 | 2.3 |
| 49-GW9          | 1.35    | 1.38     | 1.66      | 0.80 | 1.8 |
| 49-GW10         | -0.32   | 0.81     | 0.97      | 0.87 | 1.0 |
| 49-GW11         | 0.43    | 0.97     | 1.23      | 0.89 | 1.0 |
| BRM-Lake        | 0.15    | 0.38     | 0.51      | 0.94 | 1.0 |
| BRM-MW1         | 0.28    | 0.47     | 0.59      | 0.86 | 1.0 |
| BRM-MW2         | 0.15    | 0.33     | 0.48      | 0.92 | 1.0 |
| BRM-MW3         | 0.85    | 0.85     | 0.99      | 0.91 | 1.0 |
| BRM-MW4         | 0.67    | 0.67     | 0.86      | 0.84 | 1.0 |
| Corkscrew Swamp | -0.61   | 1.01     | 1.06      | 0.87 | 1.3 |
| FP2_GW1         | 0.50    | 1.09     | 1.53      | 0.80 | 1.5 |
| FP3_GW1         | 0.28    | 0.60     | 0.73      | 0.86 | 1.0 |
| FP4_GW1         | -0.22   | 0.55     | 0.70      | 0.89 | 1.0 |
| FP5_GW1         | -0.33   | 0.60     | 0.76      | 0.88 | 1.0 |
| FP6_GW1         | -0.41   | 0.76     | 0.94      | 0.87 | 1.0 |
| FP7_GW1         | -0.41   | 0.84     | 1.03      | 0.86 | 1.0 |
| FP8_GW1         | -0.27   | 0.70     | 0.85      | 0.88 | 1.0 |
| FP9_G           | -0.39   | 0.83     | 1.02      | 0.86 | 1.0 |
| FP10_G          | -0.28   | 0.55     | 0.73      | 0.88 | 1.0 |
| L-1138          | -0.29   | 0.78     | 0.89      | 0.81 | 1.0 |
| L-5667          | 1.09    | 1.29     | 1.39      | 0.93 | 1.8 |
| MPW02           | -0.67   | 0.67     | 0.78      | 0.98 | 1.0 |
| MPW03           | -0.98   | 0.98     | 0.99      | 0.99 | 1.0 |
| MPW04           | -0.01   | 0.51     | 0.65      | 0.91 | 1.0 |
| MPW05           | 0.25    | 0.53     | 0.57      | 0.78 | 1.0 |
| MPW08           | 1.06    | 1.07     | 1.15      | 0.92 | 1.5 |
| MPW25           | -0.27   | 0.35     | 0.39      | 0.95 | 1.0 |
| MPW27           | 0.46    | 0.52     | 0.81      | 0.85 | 1.0 |
| MPW28           | 0.95    | 0.95     | 1.00      | 0.77 | 1.0 |
| MPW             | -0.08   | 0.31     | 0.40      | 0.96 | 1.0 |
| MPW30           | 0.10    | 0.57     | 0.83      | 0.77 | 1.0 |
| MPW31           | 0.25    | 0.30     | 0.48      | 0.95 | 1.0 |
| MPW33           | -0.78   | 1.20     | 1.51      | 0.77 | 1.5 |
| MPW             | 0.48    | 0.48     | 0.49      | 0.97 | 1.0 |
| MPW             | -1.01   | 1.06     | 1.24      | 0.90 | 1.5 |
| MPW             | -0.11   | 0.53     | 0.66      | 0.87 | 1.0 |
| MPW39           | -1.35   | 2.35     | 2.52      | 0.64 | 2.5 |
| ST1_G           | -0.44   | 0.73     | 0.85      | 0.86 | 1.0 |
| ST2_G           | 0.05    | 0.61     | 0.73      | 0.86 | 1.0 |
| ST3_G           | -0.34   | 0.80     | 0.92      | 0.80 | 1.0 |
| WF3_G           | 1.54    | 1.55     | 1.71      | 0.86 | 1.8 |
| WF4_G           | 0.95    | 1.05     | 1.27      | 0.83 | 1.5 |
| WF5_G           | 1.03    | 1.08     | 1.40      | 0.81 | 1.8 |
| WF6_G           | 0.87    | 0.91     | 1.18      | 0.85 | 1.0 |
| WF7_G           | 1.16    | 1.18     | 1.49      | 0.81 | 1.8 |



### *Surface Water Flow and Stage at Monitoring Stations*

**Figure J2** shows the surface water monitoring stations within the Local Scale Model boundary. **Table J2** shows the statistics and Appendixes B and C contain the stage and flow comparative graphs. There are only two stations within the DR/GR Area located at the southern boundary on the Kehl Canal. Simulated stages in these stations match observed data fairly well and are able to capture the highs and lows accurately. The other stations north of the DR/GR Area also perform within the acceptable statistical ranges.

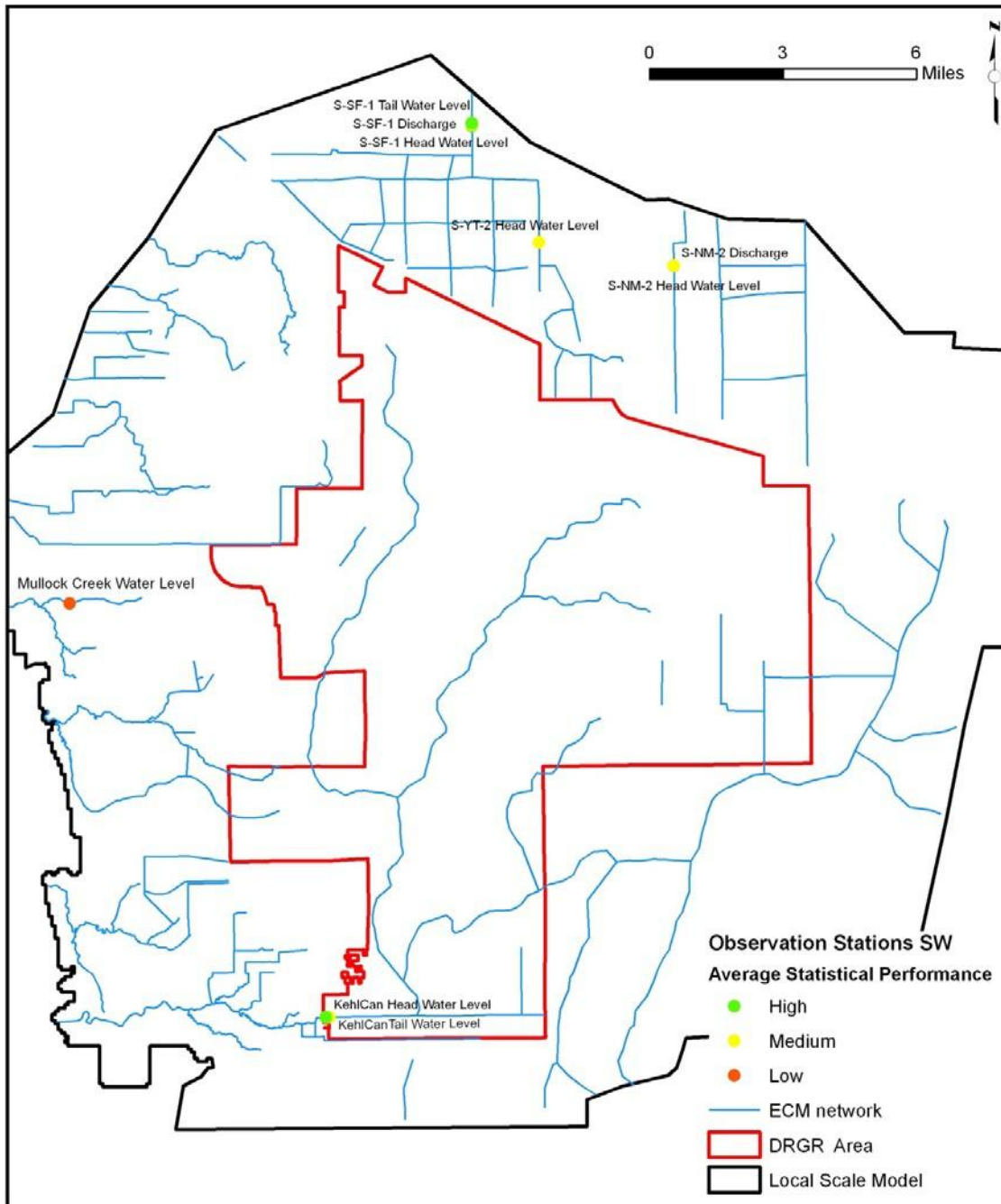


**Figure J2.** Surface Water Stations in the Local Scale Model.

**Table J2.** Surface Water Statistics for the Local Scale Model.

| Station Name  | ME (ft) | MAE (ft) | RMSE (ft) | R    | PL  |
|---------------|---------|----------|-----------|------|-----|
| S-SF-1 HW     | 0.23    | 0.28     | 0.32      | 0.83 | 1.0 |
| S-SF-1 Q      | ---     | ---      | ---       | 0.71 | 2.0 |
| S-SF-1 TW     | -0.03   | 0.31     | 0.48      | 0.43 | 1.5 |
| S-NM-2 HW     | 0.00    | 0.19     | 0.24      | 0.61 | 1.3 |
| S-NM-2 Q      | ---     | ---      | ---       | 0.41 | 3.0 |
| S-NM-2 TW     | 0.80    | 1.04     | 1.16      | 0.43 | 2.3 |
| S-YT-2 HW     | 1.63    | 1.74     | 1.97      | 0.76 | 2.5 |
| KehlCan 9358  | 1.33    | 1.67     | 2.10      | 0.73 | 2.5 |
| KehlCan 9479  | 0.10    | 0.72     | 1.06      | 0.92 | 1.3 |
| Mullock Creek | 2.48    | 2.28     | 2.51      | 0.62 | 2.8 |

### *Hydroperiod in the DR/GR Area*

The determination of the wetland hydroperiod has been an important indicator used in this study. A wetland hydroperiod has several definitions, but for this evaluation it is defined as the period during which water in the model is at least mm above the topographic surface. The simulated wetland hydroperiod for the DR/GR Area was qualitatively compared with hydroperiod maps generated based on data created by KLECE [2008]. The model follows similar general trends but the comparison is limited due to the coarser resolution of the model in comparison to the map from KLECE data. The scaling limitations are evident when comparing the results of the local higher resolution model hydroperiod map to the coarser regional model. Nevertheless, the hydroperiod output of the model together with the water table elevation and the water balance computation provide useful insight into the impact of the land use changes on wetland areas.

The hydroperiod data developed by KLECE is based on the vegetation communities, which have been mapped from GIS data and aerial photographs taken in 2007. This hydroperiod map was generated based on the estimated relationships among vegetation, hydroperiod, and water depth conditions. According to KLECE, the estimated water depths and hydroperiods are typical ranges of conditions for unaltered wetland systems in southwest Florida (KLECE 2008). These relationships have not been compared with measured water level data, though. Thus, a quantitative or direct comparison between this hydroperiod map and the one produced by the model is not appropriate.

The hydroperiod map shown in **Figure J3** was developed from results generated by the LS ECM. In general, the ECM hydroperiod map produces similar patterns to the map generated from KLECE data, particularly for larger wetland areas where the model resolution can capture the general topography and behavior of the system.

The map in **Figure J4** shows the average water depths above the surface, which produce similar patterns as in the hydroperiod map on Figure J3. These depths, however, are in general lower than those estimated by KLECE. This is probably due to the model resolution (750-ft cell) which is insufficient to capture the micro-topography.

In the ECM V2 section of this report, the positive impact of the more accurate topographic data on the hydroperiod prediction by the model is presented.

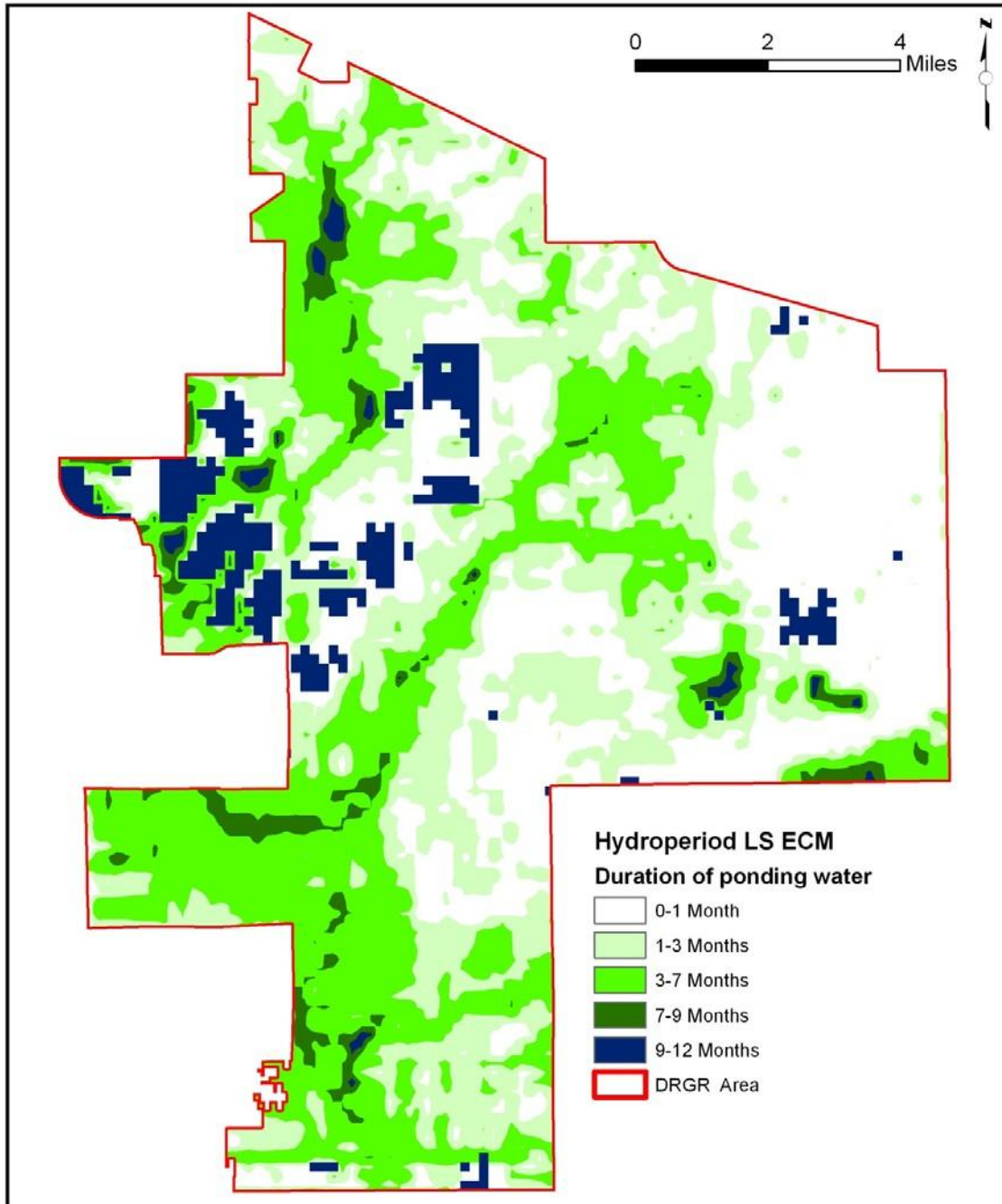


**Figure J3.** Average duration of water above ground surface from LS ECM.

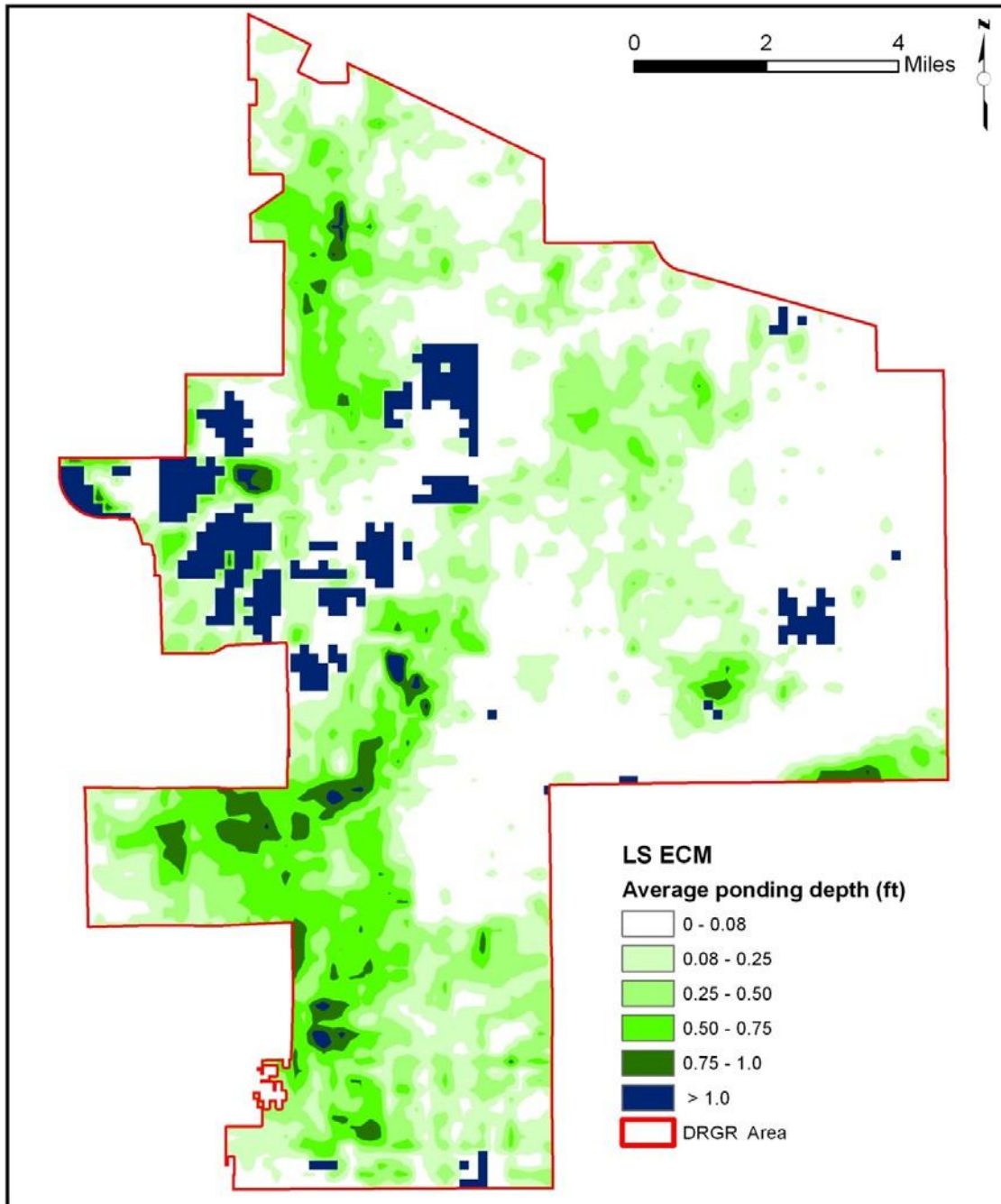


**Figure J4.** Average depth of water above ground surface from LS ECM.